MICROSCOPIC AND METABOLOMIC INVESTIGATION

OF *HEMATODINIUM* SP. INFECTIONS IN

NEWFOUNDLAND SNOW CRABS, *CHIONOECETES OPILIO*

A Thesis
Submitted to the Graduate Faculty
in Partial Fulfilment of the Requirements
for the Degree of

DOCTOR OF PHILOSOPHY

In the Department of Pathology and Microbiology
Faculty of Veterinary Medicine
University of Prince Edward Island

Melanie A. Buote
Charlottetown, P. E. I.
June, 2016

THESIS/DISSERTATION NON-EXCLUSIVE LICENSE

Family Name: Buote	Given Name, Middle Name (if applicable): Melanie Amber
Full Name of University: Atlantic Veterinary Collage at the University of Prince Edward Island	
Faculty, Department, School: Department of Pathology and Microbiology	
Degree for which thesis/dissertation was presented: PhD	Date Degree Awarded:
Thesis/dissertation Title: Microscopic and metabolomic investigation of *Hematodinium* sp. Infections in Newfoundland snow crabs, *Chionoecetes opilio*	

In consideration of my University making my thesis/dissertation available to interested persons, I, **Melanie Amber** Buote, hereby grant a non-exclusive, for the full term of copyright protection, license to my University, **the Atlantic Veterinary College at the University of Prince Edward Island**:

(a) to archive, preserve, produce, reproduce, publish, communicate, convert into any format, and to make available in print or online by telecommunication to the public for non-commercial purposes;
(b) to sub-license to Library and Archives Canada any of the acts mentioned in paragraph (a).

I undertake to submit my thesis/dissertation, through my University, to Library and Archives Canada. Any abstract submitted with the thesis/dissertation will be considered to form part of the thesis/dissertation.

I represent that my thesis/dissertation is my original work, does not infringe any rights of others, including privacy rights, and that I have the right to make the grant conferred by this non-exclusive license.

If third party copyrighted material was included in my thesis/dissertation for which, under the terms of the *Copyright Act*, written permission from the copyright owners is required I have obtained such permission from the copyright owners to do the acts mentioned in paragraph (a) above for the full term of copyright protection

I retain copyright ownership and moral rights in my thesis/dissertation, and may deal with the copyright in my thesis/dissertation, in any way consistent with rights granted by me to my University in this non-exclusive license.

I further promise to inform any person to whom I may hereafter assign or license my copyright in my thesis/dissertation of the rights granted by me to my University in this non-exclusive license.

Signature	**Date**

University of Prince Edward Island

Faculty of Veterinary Medicine

Charlottetown

CERTIFICATION OF THESIS WORK

We, the undersigned, certify that **Melanie A. Buote, BSc, DVM, DACVP**, candidate for the degree of **Doctor of Philosophy** has presented his/her thesis with the following title:

MICROSCOPIC AND METABOLOMIC INVESTIGATION OF *HEMATODINIUM* SP. INFECTIONS IN NEWFOUNDLAND SNOW CRABS, CHIONOECETES OPILIO

that the thesis is acceptable in form and content, and that a satisfactory knowledge of the field covered by the thesis was demonstrated by the candidate through an oral examination held on June 10th, 2016.

Examiners: Dr. Gary Conboy (Chair) _____

Dr. Spencer Greenwood _____

Dr. Rick Cawthorn _____

Dr. Dave Speare _____

Dr. Jeff Shields _____

Date: _____

Abstract

Bitter Crab Disease (BCD) is a fatal disease of crustaceans caused by parasitic syndinian dinoflagellates of the genus *Hematodinium*. Over forty species of crustaceans have been reported as hosts for *Hematodinium* or *Hematodinium*-like infections with a worldwide distribution concentrated in North Pacific and Atlantic oceans. In eastern Canada BCD was first reported in snow crabs *Chionoecetes opilio* from Conception Bay, Newfoundland in 1990 with very low disease prevalence (<0.11 – 3.7%). Subsequently, BCD has spread rapidly within the eastern and northeastern bays of Newfoundland and Labrador and has resulted in at least three epizootic disease outbreaks with prevalence up to 25% in some subpopulations of snow crabs.

Hematodinium infections can be presumptively diagnosed macroscopically via visual examination in many affected species, including snow crabs, due to characteristic discolorations of the carapace and/or arthrodial membranes. Specific detection of *Hematodinium* spp. via Polymerase Chain Reaction (PCR) assays is another diagnostic method used for the diagnosis of infection in various crustacean hosts. In our study, 100% of mild infections (1/1), 40% of infections with moderate infection intensity (2/5), 11-22% of advanced infections (1 or 2/9) had false negative test results while no very advanced infections (0/13) had false-negative test results for diagnosis by visual exam or PCR assay. These findings suggest that diagnosis by visual exam or PCR assay is less accurate in the early stages of BCD and both diagnostic tests underestimated the prevalence of *Hematodinium* infection in Atlantic Canadian snow crab by 1.25 – 1.76%.

Light microscopic examination of parasite life stages of *Hematodinium* sp. infections of varying intensity revealed changes in proportions of multinucleate plasmodia. In snow crabs with infections of mild intensity (early BCD infections) the parasitic life stages had a high proportion of multinucleate plasmodia and had enhanced cytoplasmic basophilia, changes suggestive of rapid cellular proliferation. Moderately intense infections were predominated by uninucleate cells. In advanced and very advanced infection intensities (late BCD infections) there appeared to be a progressive increase in proportion of multinucleate life stages, suggestive of a resurgence of parasitic proliferation and/or impaired cytokinesis (possibly due to reduced host resources).

The uninucleate and multinucleate life stages were most often amoeboid in shape; vermiform plasmodial life stages were also observed, typically in heavily infected animals. The vermiform plasmodia were often intimately associated with cell surfaces, most commonly in the heart and also rarely in the eyestalk, gill, and leg. Ultrastructural examination of these attached vermiform plasmodia revealed cytoplasmic extensions which interdigitated with host cell membranes and which occasionally appeared to form connections between parasite cell bodies. Comparison of the *in vivo* and *in vitro* life stages of *Hematodinium* isolated from snow crabs suggests that *in vitro* sheet-like and arachnoid plasmodia may represent exaggerations of amoeboid plasmodia and attached vermiform plasmodial life stages observed *in vivo*.

The rapid proliferation of the *Hematodinium* parasites in hemolymph and the parasites' high metabolic requirements during growth have been reported to decrease the hosts' protein and carbohydrate reserves and contribute to host morbidity and eventual mortality. Our research concurs with these findings and indicates that BCD is associated with depletion of protein (reduction in hemolymph refractive index) and carbohydrate (reduced reserve inclusion scores) metabolic reserves as well as potentially altering host lipid metabolism. Several BCD-associated phospholipids were identified in this study. These BCD-associated phospholipids could contribute to the bitter taste associated with this disease. Additionally, BCD-associated phospholipids could contribute to the apparent lack of a cellular immune response against *Hematodinium*.

A histopathologic study of Newfoundland snow crabs confirmed that BCD was the most significant infectious cause of internal disease in the populations examined. Two patterns of necrotizing and ulcerative enteritis were also observed in this study: focal ulcers at the level of the midgut-hindgut junction and more extensive areas of enteritis in the non-chitinized midgut epithelium. The cause of these lesions is unclear; hypoxia/ischemia and/or infection with pathogenic *Vibrio* bacteria are possible contributing factors in lesion development. There was no significant difference in the prevalence of hemocytic aggregates between *Hematodinium* infected snow crabs and uninfected snow crabs suggesting that the hemocytic aggregates were background lesions unrelated to *Hematodinium* infection. No significant difference in the prevalence of intestinal inflammation (midgut-hindgut junctional ulcers or midgut necrotizing enteritis) or in the prevalence of hemocytic aggregates between BCD- and BCD+ snow crabs was observed. When the data from both bays that contain cases of BCD were combined, higher prevalence of one pattern of inflammation (midgut-hindgut junctional ulcers) was seen in snow crabs without BCD. There was also no significant difference in the prevalence of hemocytic aggregates between *Hematodinium*-infected snow crabs and uninfected snow crabs, suggesting that hemocytic aggregates observed in animals with BCD were background lesions unrelated to *Hematodinium* infection.

This study confirms that BCD is associated with alterations in protein, glycogen, and lipid metabolism consistent with parasite-associated negative energy balance (i.e., starvation) in affected snow crabs. Histologic examination of BCD infected snow crabs revealed vacuolar degeneration in hepatopancreatic epithelium although there was no definitive evidence of parasite-associated inflammation or tissue necrosis. These findings indicate that the main pathologic effects of BCD are metabolic in nature.

Acknowledgements

First, I'd like to gratefully acknowledge my co-supervisors, Dr. Rick Cawthorn and Dr. Russ Kerr, and the other members of my supervisory committee, Dr. Spencer Greenwood, Dr. Glenda Wright, and Dr. Fred Kibenge. Your mentorship, guidance, and support throughout my program have been exceptional.

Second, I'd also like to thank all my colleagues who collaborated with us on this project. A large group of people contributed to this project including colleagues from the AVC Lobster Science Center (Peter Gaudet, Dr. Andrea Battison, Dr. Fraser Clark, Rachel Summerfield, Melanie Burton, Sarah Daley, Sarah Ramsey-Ogilvie, Dr. Janet Saunders), AVC Diagnostic Services (Ramona Taylor and Sarah Bernard), the Newfoundland Department of Fisheries and Oceans (Earl Dawe, Darrell Mullowney, and their collaborator Jan Negrin), NOAA (Dr. Frank Morado), the UPEI Department of Biology (Dr. Pedro Quijon), and the Kerr Lab (Dr. Malcolm McCulloch, Brad Haltli, Dr. David Overy, Dr. Fabrice Berrue). I'd also like to think Dr. Henrik Stryn for consulting in regards to statistical analysis of our data. We couldn't have completed this project without all of your expert assistance.

Third, I'd also like to thank Dr. Gary Conboy and Nicole Murphy. Rick, Spencer, Gary, and Nicole graciously allowed me to gain experience teaching parasitology during my PhD training. The experience working with you has been unforgettable - you have been fantastic colleagues and friends.

Next, I'd like to thank all my colleagues and friends in the Department of Pathology and Microbiology. I was able to work part-time in the department for the majority of my PhD program which allowed me to pursue this further education while still continuing to provide for my growing family. The group of pathologists, parasitologists, virologists, immunologists, and bacteriologists gathered in our department is amazing. It has been a privilege and a pleasure to work with every single one of you.

Finally, I'd like to thank my friends & family for all their patience, love, and support. You have been there for me and with me throughout my educational career, going from vet school to a residency to a part-time PhD. I couldn't have done it without you.

Every PhD project is a group effort made possible by collaborations with and support from colleagues, family, and friends. Thank you all for helping me with mine.

TABLE OF CONTENTS

List of Figures

Chapter 1:

Chapter 2:

Appendix 1:

Appendix 2:

Appendix 4:

Appendix 7:

Appendix 8:

List of Tables

List of Appendices

List of Abbreviations

Abbreviation	Definition
EC	Degrees Celsius
Hg	Multiplied by the acceleration caused by gravity (centrifugal force)
µl	microliter
µm	Micrometer (micron)
ACN	Acetonitrile
adj	Adjusted
AVC	Atlantic Veterinary College
BB	Bonavista Bay, Newfoundland
bp	Base pair
CL	Cardiolipin
DCM	Dichloromethane
dH_20	Distilled water
ddH_20	Double distilled water
DG	Diacylglycerol
EDTA	Ethylenediaminetetraacetic acid
EtOAc	Ethyl acetate
EtOH	Ethanol
ESI	Electrospray ionization
FA	Formic acid
g	Gram
GlcCer	Glucosylceramide
GuSCN	Guanidium thiocyanate
h	Hour
H&E	Hematoxylin and eosin stain
HRI	Hemolymph refractive index
kg	Kilograms
kV	Kilovolts
LacCer	Lactosylceramide
LCMS	Liquid chromatography-mass spectrometry
LysoPC	Lysophosphatidylcholine
m	Meter
M	Molar concentration
m/z	Mass-to-charge ratio
MeOH	Methanol
MG	Monoacylglycerol
min	Minute
ml	Milliliter
mm	Millimeter
mM	Millimolar concentration
mOsm	Milliosmoles

Abbreviation	Definition
ms	Millisecond
n	Number
NaCl	Sodium chloride
NDB	Notre Dame Bay, Newfoundland
NL	Newfoundland
nm	Nanometer
PA	Phosphatidic acid
PAS	Periodic acid shift
PC	Phosphatidylcholine
PCR	Polymerase chain reaction
PDA	Photodiode array detection
PE	Phosphatidylethanolamine
PEI	Prince Edward Island
PG	Phosphatidylglycerol
PI	Phosphatidylinositol
pred	Predicted
proPO	Prophenoloxidase
PS	Phosphatidylserine
RI	Reserve inclusion
RT	Room temperature
sec	Second
SM	Sphingomyelin
TAG	Triacylglycerol
TG	Triglycerides
Tris-HCl	Tris hydrochloride (tromethamine hydrochloride)
UPEI	University of Prince Edward Island
UPLC	Ultra-performance liquid chromatography
WB	White Bay, Newfoundland
x	Magnification level

1. GENERAL INTRODUCTION

1.1. Parasitic Dinoflagellates

Dinoflagellates (Greek *dinos* "whirling" and Latin *flagellum* "whip, scourge") are a large group of unicellular flagellate protists which exhibit great diversity of form. Most dinoflagellates are marine plankton many of which can produce “red tides” and other monospecific blooms. More than 2000 extant species have been described, of which more than 1,700 are marine, about 220 are from freshwater, and 5% to 7% (~140-150 species) are parasitic in aquatic organisms (Shields 1994, Levy et al 2007, Taylor 2006, Taylor et al 2008, Skovgaard et al 2012).

Dinoflagellate life styles include a variety of modes of nutrition: autotrophy (phototrophy), mixotrophy, osmotrophy, phagotrophy, and parasitic heterotrophy (Coats 1999, Leander and Keeling 2004, Gilbert and Legrand 2006). Species that rely strictly on photosynthesis as their carbon source and use inorganic nutrients for their nutrition are called autotrophs or phototrophs. Some phototropic species also use alternative pathways for acquiring carbon or nutrients: these are the mixotrophs. They use dissolved or particulate organic substances to renew their cellular reserves of carbon, macronutrients, amino acids, trace elements, or phospholipids (Gilbert and Legrand 2006). Mixotrophy encompasses several processes, including osmotrophy, phagotrophy, and heterotrophy. Osmotrophy is nutrition by direct absorption and uptake of organic molecules while phagotrophy is the ingestion of prey or other food particles (Gilbert and Legrand 2006, Stoecker et al 2006). When carbon is incorporated in osmotrophy or phagotrophy the process is called heterotrophy. Heterotrophic dinoflagellates are among the species that have lost the ability for autotrophy (i.e., are non-photosynthetic).

Approximately half of all dinoflagellates are capable of photosynthesis (autotrophs and mixotrophs) while the remaining half is composed of obligate heterotrophs (Smayda 1997, Gilbert and Legrand 2006). While some heterotrophs feed by simple phagotrophy, other dinoflagellates have more complex feeding mechanisms such as formation of a "feeding veil" (i.e., pallium) or peduncle-feeding (Gaines and Taylor 1984).

Parasitic dinoflagellates infect a wide variety of aquatic species including algae, protozoans, crustaceans, annelids, mollusks, salps, tunicates, rotifers, and fishes (Cachon and Cachon 1987, Shields 1994, Konovalova 2008). Parasitic dinoflagellates in the orders Blastodinida (Blastodiniales) and Syndinia (Syndiniales) together with the closely related Ellobiopsidae parasitize marine crustaceans including copepods, amphipods, mysids, euphausiids, and decapods (Shields 1994, Konovalova 2008). Blastodinians are extracellular, predominantly marine parasites of other protozoans, invertebrates, and fish. These parasites occur on the outside of the cell of a unicellular organism or on the surface of a multicellular organism. Most commonly, they have a specific host and site and usually attach by means of a simple spine or a complex organoid (Konovalova 2008). *Blastodinium* is a genus of parasites that inhabit the gut of marine planktonic copepods (Skovgaard et al 2012). Parasites within the genus *Oodinium* are ectoparasites of tunicate appendicularians, annelids, chaetognaths, ctenophores and cnidarians, and fish (Gomez and Skovgaard 2015). Parasitic dinoflagellates within the genera *Amyloodinium, Piscinoodinium* and *Crepidoodinium* infest the skin and/or gills of marine, brackish, or freshwater fish (Levy et al 2007). The life cycle of the fish blastodinophyceans has 3 stages: a parasitic pyriform trophont, a reproductive tomont, and a free-swimming infective

dinospore (Levy et al 2007). Virulent strains of these parasites can cause mass mortalities in affected fish (Cachon and Cachon 1987, Coats 1999, Noga and Levy 2006). *Ichthyodinium* is a dinoflagellate parasite of fish eggs which is lethal to the egg or newly hatched fish larvae that also has non-motile and motile flagellated (dinospore) life stages (Skovgaard et al 2009). Ellobiopsids are a small diverse group of protists which are closely related to the dinoflagellates and may be distantly related to some water molds (e.g., Saprolegniales; Silberman et al 2004). This family predominantly comprises ectoparasites of marine crustacean zooplankton, although it also includes commensal epibionts and parasites of freshwater copepods, cladocerans, and polychaete worms (Shields 1994, Konovalova 2008). The family Ellobiopsidae contains five genera, of which four (*Ellobiocystis, Parallobiopsis, Ellobiopsis*, and *Thalassomyces*) are chiefly ectoparasites of pelagic marine crustaceans (zooplankton) and one monotypic genus *Rhizellobiopsis* parasitizes a benthic polychaete worm (Konovalova 2008). Syndinians are heterotrophic endoparasitic dinoflagellates that are parasites of protozoans (including dinoflagellates), invertebrates, and the eggs of copepods and fish. They may be intracellular, intranuclear (i.e., *Amoebophyra*), or located extracellularly in the host's tissues or hemolymph (Shields 1994, Coats 1999, Konovalova 2008). Syndinians have two distinct life phases: a parasitic, multinucleate stage that lives intracellularly or extracellularly in crustaceans, tintinnids or other dinoflagellates, and a flagellated motile stage superficially similar to typical dinoflagellates (Coats 1999, Taylor et al 2008). The infectious life stage in this disease is most likely the dinospore since this life stage transmits infections of many other parasitic dinoflagellates (Coats 1999). Population-level effects of parasitic dinoflagellate infections can include sexual castration, mortality of hosts, and destruction of eggs (Shields 1994).

1.2. Systematics of *Hematodinium*

Dinoflagellates are unicellular eukaryotes that are grouped in the superphylum Alveolata with ciliates and apicomplexans. These protozoans are grouped together as alveolates because they all share a few derived morphological features, such as cortical amphiesmal vesicles and micropores. However, dinoflagellates have several unique features which separate them from other alveolates. First, dinoflagellates are biflagellate with a distinctive flagellar apparatus consisting of a coiled transverse flagellum within a cingular groove or girdle and a posterior flagellum within a sulcal groove (Taylor et al. 1987, Leander and Keeling 2003, 2004). Second, dinoflagellates contain a unique type of nucleus, the dinokaryon, with permanently condensed, "banded" or "beaded", V-shaped chromosomes which in most taxa lack typical eukaryotic histones but which may contain histone-like proteins (Hudson and Shields 1994, Rizzo 2003, Saldarriaga et al 2004). Dinomitosis, another unique feature of dinoflagellates, is a form of closed mitosis in which the nuclear envelope stays intact throughout the cell cycle and microtubules of the extranuclear mitotic spindle traverse the nucleus through tunnels or furrows (Rizzo 2003).

Only two species have been described within the genus *Hematodinium.* The type species, *Hematodinium perezi,* was first described from the common shore crab *Carcinus maenas* and the blue-legged swimming crab *Liocarcinus depurator* off the coast of Normandy, France (Chatton and Poisson 1931). The second species, *Hematodinium australis,* was described in Australian blue crabs *Portunus pelagicus* and was differentiated from the type species based on

life stage size and morphology, geographic location, and affected host (Hudson and Shields 1994).

More recently, sequencing of 18S ribosomal DNA (rDNA) and the adjacent internal transcribed spacer 1 (ITS1) regions of *Hematodinium* spp. suggest that at least two distinct clades exist among the sequenced isolates from different host species (Jensen et al 2010, Hamilton et al 2010a). Analysis of *Hematodinium* sp. ITS1 sequences isolated from decapod hosts in the North Pacific and North Atlantic oceans (*Chionoecetes* spp., *Hyas coarctatus, Lithodes couesi*, *Nephrops norvegicus*, and *Paralithodes camtschaticus*) indicated they be placed in one clade, whereas *Hematodinium* sp. sequences isolated from portunid crabs (*Callinectes sapidus, Liocarcinus depurator* and *Scylla serrata*) were placed in a second clade. Jensen et al (2010) suggested that variations identified between the clades suggested that these two clades may represent two different species of *Hematodinium.* Similar work by Hamilton et al (2010a) suggests that three *Hematodinium* clades may exist. The first clade, the Langoustine clade, includes sequences isolated from infections in Norway lobsters *Nephrops norvegicus*. Their second clade, the northeastern Atlantic clade, includes isolates from two portunid crabs, the common shore crab *Carcinus maenas* and the edible crab *Cancer pagurus.* Their largest clade, the northeastern and northwestern Atlantic (or "All") clade, includes isolates from all three species in their other two clades and isolates from snow crabs *Chionoecetes opilio* and three anomuran crustaceans - the hermit crabs *Pagurus bernhardus* and *Pagurus prideaux* and the rugose squat lobster *Munida rugosa*. The morphological and molecular characterization of *Hematodinium perezi* in *Liocarcinus depurator* from a similar geographical location to that of the type description has also been investigated. Analysis of the ITS1 rRNA region from

Hematodinium perezi infecting *Liocarcinus depurator*, *Portunus trituberculatus, Scylla serrata*, and *Callinectes sapidus* indicated that there were three distinct *H. perezi* genotypes (Small et al 2012). Furthermore, a recent study (Pagenkopp Lohan et al 2013) indicates that a single species and genotype of *Hematodinium*, *Hematodinium perezi* genotype III, infects blue crabs *Callinectes sapidus* from Virginia to Texas. Small et al (2012) also compared their SSU rRNA gene and ITS region sequences to those in GenBank and found differences that substantiate delineation of *H.* perezi from the species of *Hematodinium* sp. infecting other crustaceans in the northern hemisphere. These findings indicate that there are at least two (if not three or more) different species of *Hematodinium* parasites infecting crustacean hosts.

1.3. Hematodiniosis

Hematodiniosis is a fatal disease of crustaceans caused by parasitic syndinian dinoflagellates of the genus *Hematodinium*. *Hematodinium* sp. infection was first reported off the coast of Europe in common shore crabs *Carcinus maenas* and harbour crab *Liocarcinus depurator* (Chatton and Poisson 1931). Over forty species of crustaceans have been documented as hosts for *Hematodinium* or *Hematodinium*-like infections with distribution concentrated in the North Pacific and Atlantic oceans (reviewed in Morado 2011). Most affected hosts are brachyuran crabs; reports of disease have also been described in anomuran crabs, amphipods, and palaemonid prawns (Table 1.1). Most affected hosts are marine crustaceans; however, a recent report of *Hematodinium*-associated disease in tropical mud crabs *Scylla serrata* indicates that hematodiniosis can also occur in low salinity (<9 ppt) ponds (Li et al 2008). Numerous outbreaks of hematodiniosis have occurred that significantly impacted commercially important

crustaceans, with reports of epidemics in snow crabs *Chionoecetes opilio* (Meyers et al 1990, Taylor and Khan 1995, Dawe 2002, Shields et al 2005, 2007), Tanner crabs *Chionoecetes bairdi* (Meyers et al 1987, 1990; Morado 2011), blue crabs *Callinectes sapidus* (Newman and Johnson 1975, Messick 1994, Shields and Squyars, 2000, Messick and Shields 2000), and Norway lobsters *Nephrops norvegicus* (Field et al 1992, Stentiford et al 2001). The parasite has also affected crustaceans grown in aquaculture settings, including both cultured tropical mud crabs *Scylla serrata* (Li et al 2008) and cultured ridgetail white prawns *Exopalaemon carinicauda* (Xu et al 2010). Generally, diseased hosts appear lethargic or moribund with discolored carapaces and opaque milky hemolymph (Field et al 1992, Meyers et al 1987, Messick 1994, Wheeler et al 2007).

In several hosts, including Tanner crabs *Chionoecetes bairdi,* snow crabs *Chionoecetes opilio,* edible crabs *Cancer pagurus*, Norway lobsters *Nephrops norvegicus*, and red and blue king crabs *Paralithodes* spp*.,* anecdotal reports indicate that the disease alters the texture and taste of infected meat rendering the product unmarketable (Meyers et al 1987, Love et al 1996, Stentiford et al 2000, Ryazanova 2008, Ryazanova et al 2010). Affected meat in some hosts (i.e., snow crabs *Chionoecetes opilio* and Tanner crabs *Chionoecetes bairdi*) has been described as either watery or chalky, and the altered taste is typically described as bitter, astringent, or aspirin-like, and is reflected in one common name of hematodiniosis – Bitter Crab Disease (BCD). The cause of the bitter taste associated with this disease is currently unknown.

The essential taste components in snow crabs have been listed as a combination of amino acids (alanine, arginine, glutamate, and glycine), nucleic acid-related substances (adenylic acid and

guanylic acid), and minerals (sodium, chloride, and potassium) (Hayashi et al 1981). Increased bitterness of snow crab meat synthetic extracts was observed when minerals were omitted as a group or singly (sodium), and when amino acids were removed as a group (glycine, arginine, alanine, proline, and taurine) or singly (arginine) (Hayashi et al 1981). Sodium has been reported to enhance flavor by suppressing bitterness (Breslin and Beauchamp 1997, Liem et al 2011). Note, at high concentrations sodium chloride can stimulate bitter-sensing taste cells (Oka et al 2013, Roper 2015). Increased potassium (hyperkalemia) could also result in an astringent taste to the meat as the potassium cation tastes bitter at high concentrations (Bartoshuk et al 1988, Saavedra-Garcia et al 2015). Bitter taste can also result from oxidation of free fatty acids or oxidation of unsaturated fatty esters in protein-bound lipids (Stephan and Steinhart 2000, Rackis et al 1979, Usuki and Kaneda 1980). Amino acids and peptides, esters and lactones, phenols and polyphenols, flavonoids and terpenes, methylxanthines (caffeine), sulfimides (saccharin), organic and inorganic salts, plant-derived alkaloids, and other toxins are all among the compounds which may taste bitter in foods (Drewnowski and Gomez-Carneros 2000, Drewnowski 2001, Meyerhof 2005, Maehashi and Huang 2009). A toxin of dinoflagellate origin is one potential cause of the bitter aftertaste reported in snow crab with Bitter Crab Disease.

Table 1.1: Worldwide list of species reported to be infected with *Hematodinium* spp.

Host	Order	Infraorder	Family	Reference(s)
Carcinus maenas	Decapoda	Brachyura	Portunid	Chatton and Poisson 1931, Messick and Shields 2000, Hamilton et al 2007, 2009, 2010b
Liocarcinus depurator	Decapoda	Brachyura	Portunid	Chatton and Poisson 1931, Hamilton et al 2005, Stentiford et al 2005, Hamilton et al 2009, Eigemann et al 2010
Portumnus latipes	Decapoda	Brachyura	Portunid	Chatton and Poisson 1931, Gallien 1938, Chatton 1952
Callinectes sapidus	Decapoda	Brachyura	Portunid	Newman and Johnson 1975, Couch 1983, Messick 1994, Messick et al 1999, Messick and Shields 2000, Sheppard et al 2003, , Lee and Frischer 2004, Frischer et al 2006, Troedsson et al 2008b, Nagle et al 2009, Walker et al 2009
Ovalipes ocellatus	Decapoda	Brachyura	Portunid	MacLean and Ruddell 1978
Ovalipes australiensis	Decapoda	Brachyura	Portunid	Gornik et al 2013
Necora puber	Decapoda	Brachyura	Portunid	Wilhelm and Boulo 1988, Wilhelm and Mialhe 1996, Stentiford et al 2002, Stentiford et al 2003, Hamilton et al 2009, 2010b
Scylla serrata	Decapoda	Brachyura	Portunid	Shields 1992, Hudson and Lester 1994, Xu et al 2007, Li et al 2008
Portunus pelagicus	Decapoda	Brachyura	Portunid	Hudson and Shields 1994, Shields 1999
Callinectes similis	Decapoda	Brachyura	Portunid	Messick and Shields 2000, Sheppard et al 2003
Portunus trituberculatus	Decapoda	Brachyura	Portunid	Xu et al 2007, Li et al 2013, 2015
Chionoecetes bairdi	Decapoda	Brachyura	Oregonid (Majid)	Meyers et al 1987, Meyers et al 1990, Eaton et al 1991, Love et al 1993, Meyers et al 1996, Urban and Byersdorfer 2002, Bednarski et al 2010
Chionoecetes opilio	Decapoda	Brachyura	Oregonid (Majid)	Taylor and Khan 1995, Meyers et al 1996, Williams-Ryan 1997, Dawe 2002, Pestal et al 2003, Shields and Pickavance 2003, Shields et al 2005, Shields et al 2007, Wheeler et al 2007, Eigemann et al 2010, Dawe et al 2010, Mullowney et al 2011
Chionoecetes tanneri	Decapoda	Brachyura	Oregonid (Majid)	Bower et al 2003
Hyas araneus	Decapoda	Brachyura	Oregonid (Majid)	Hamilton et al 2005, Eigemann et al 2010
Chionoecetes angulatus	Decapoda	Brachyura	Oregonid (Majid)	Jensen et al 2010
Hyas coarctatus	Decapoda	Brachyura	Oregonid (Majid)	Jensen et al 2010
Leptomithrax gaimardii	Decapoda	Brachyura	Oregonid (Majid)	Gornik et al 2013
Libinia emarginata	Decapoda	Brachyura	Epialtid (Majid)	Sheppard et al 2003, Pagenkopp et al 2012
Libinia dubia	Decapoda	Brachyura	Epialtid (Majid)	Pagenkopp et al 2012
Menippe mercenaria	Decapoda	Brachyura	Menippid (Majid)	Sheppard et al 2003
Nephrops norvegicus	Decapoda	Brachyura	Nephropid	Field et al 1992, Taylor et al 1996, Field et al 1998, Tärnlund 2000, Stentiford et al 2001a,b,c,d, Briggs and McAliskey 2002, Small et al 2006a, Hamilton et al 2007, Eigemann et al 2010
Cancer irroratus	Decapoda	Brachyura	Cancrid	MacLean and Ruddell 1978
Cancer borealis	Decapoda	Brachyura	Cancrid	MacLean and Ruddell 1978
Cancer pagurus	Decapoda	Brachyura	Cancrid	Latrouite et al 1988, Stentiford et al 2002, 2003, Chualáin et al 2009, Hamilton et al 2009,2010b, Chualáin and Robinson 2011, Smith et al 2013
Metacarcinus magister	Decapoda	Brachyura	Cancrid	Meyers and Burton 2009
Hexapanopeus angustifrons	Decapoda	Brachyura	Panopeid	Messick and Shields 2000
Dyspanopeus sayi	Decapoda	Brachyura	Panopeid	Messick and Shields 2000, Sheppard et al 2003

Panopeus herbstii	Decapoda	Brachyura	Panopeid	Messick and Shields 2000, Pagenkopp et al 2012
Eurypanopeus depressus	Decapoda	Brachyura	Panopeid	Pagenkopp et al 2012
Trapezia areolata	Decapoda	Brachyura	Trapezid	Hudson et al 1993
Trapezia coerulea	Decapoda	Brachyura	Trapezid	Hudson et al 1993
Plagusia chabrus	Decapoda	Brachyura	Plagusiid (Grapsid)	Gornik et al 2013
Paralithodes platypus	Decapoda	Anomura	Lithodid	Ryazanova et al 2008
Paralithodes camtschaticus	Decapoda	Anomura	Lithodid	Ryazanova et al 2008
Lithodes couesi	Decapoda	Anomura	Lithodid	Jensen et al 2010
Munida rugosa	Decapoda	Anomura	Munidid	Hamiton et al 2009, 2010b
Pagurus prideaux	Decapoda	Anomura	Pagurid	Hamilton et al 2009, Eigemann et al 2010
Pagurus bernhardus	Decapoda	Anomura	Pagurid	Hamilton et al 2009, 2010b, Eigemann et al 2010
Pagurus pollicarus	Decapoda	Anomura	Pagurid	Pagenkopp et al 2012
Exopalaemon carinicauda	Decapoda	Caridea	Palaemonid	Xu et al 2010
Crangon crangon	Decapoda	Caridea	Crangonid	Stentiford et al 2012
Orchomene nanus	Amphipoda	Gammaridea	Amphipod	Small et al 2006
Caprella geometrica	Amphipoda	Gammaridea	Amphipod	Pagenkopp et al 2012
13 amphipod species	Amphipoda	Gammaridea	Amphipod	Johnson 1986

1.4. Parasite Life Stages

1.4.1. *In vitro*

In vitro culture findings from Appleton and Vickerman (1998) revealed a complex range of developmental forms of *Hematodinium* (Figure 1.1). When grown in culture, dinospores acquired from *Nephrops norvegicus* gave rise to non-motile rounded trophonts or filamentous trophonts which further developed into assemblages of filamentous forms called “Gorgonlocks” trophont colonies. Gorgonlocks trophont colonies developed either into interdigitated syncytia called “clump colonies” that formed more filamentous trophonts (uninucleate trophonts and/or multinucleate plasmodia) or developed into a syncytial network or plasmodial mass called an arachnoid trophont. The arachnoid sporont then enlarged and was referred to as an arachnoid sporont since it produced sporoblasts via sporogony. The sporoblasts were direct precursors for motile dinospores. Dinospores produced *in vitro* were uninucleate and of 2 types, macrodinospores and microdinospores. Each dinospore was biflagellate: the anterior flagellum encircled the anterior end of the body and provided the principle propulsive force while the posterior flagellum trailed behind the spore and acted as a rudder.

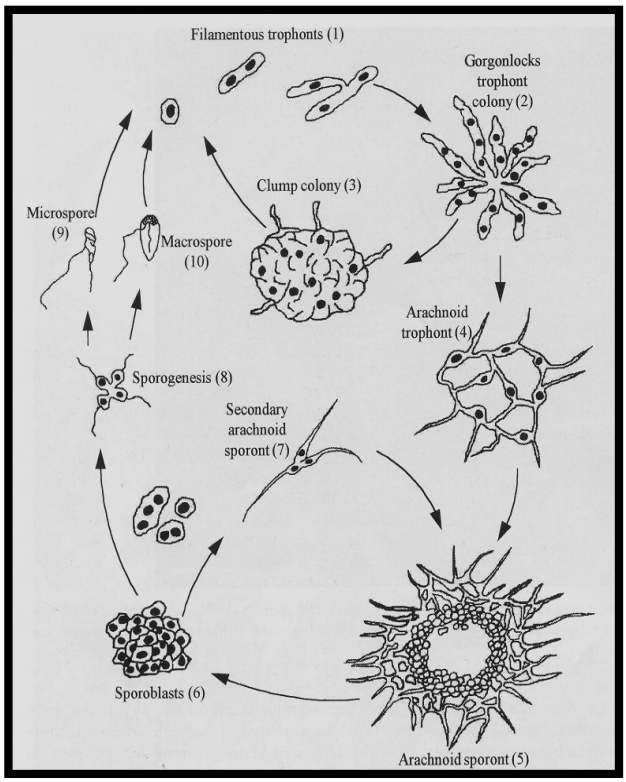

Figure 1.1. Schematic diagram of *in vitro* developmental cycle of *Hematodinium* sp. from the Norway lobster *Nephrops norvegicus* grown in culture (from Appleton and Vickerman, 1998).

In vitro culture of *Hematodinium perezi* isolated from the blue crab *Callinectes sapidus* has also recently been accomplished (Li et al 2011a). Their findings are very similar to those observed by Appleton and Vickerman (1998). In Li et al (2016), filamentous trophonts represented the initial stage of infection in a blue crab host. The filamentous trophont underwent merogony to form amoeboid trophonts. Arachnoid trophonts arose from the syncytial network laid down by the amoeboid trophonts and were the main proliferative stage of the parasite *in vitro*. Arachnoid sporonts developed as a mass within the arachnoid trophont and gave rise to schizonts or sporoblasts. Schizonts developed into gorgonlocks that underwent schizogony and developed into clump colonies. When the clump colonies were subcultured they developed into arachnoid trophonts. The sporoblasts occurred as single cells or aggregates of cells which were released

from the arachnoid sporonts when fully developed. Sporoblasts then went through a transitional stage called prespores and then progressed to become dinospores. Again, two types of biflagellate dinospores, the highly motile life stage, were described – microdinospores and macrodinospores.

Finally, *in vitro* culture of *Hematodinium* sp. isolated from snow crab *Chionoecetes opilio* with late stage disease has also been described (Gaudet et al 2015). Their findings were similar to those reported above in that amoeboid trophonts, arachnoid (plasmodial) sporonts, sporonts, and dinospore forms were all observed. Schizonts were also observed, although they were interpreted as an aberrant form of the life cycle. Unlike Appleton and Vickerman (1998) and Li et al (2011), gorgonlocks colonies, viable clump colonies, and arachnoid trophonts were not observed in the study by Gaudet et al (2015). Instead of arachnoid trophonts more cohesive sheet-like forms referred to as trophont plasmodia were noted. A similar sheet-like sporont plasmodial life stage was also described. In this study, the plasmodial sheets of trophont origin did not undergo further development into advanced life stages, whereas the sporont plasmodia transformed into sporonts and dinospores. Transition of the dinospores into trophonts (i.e., completion of the life cycle) was not observed.

1.4.2. *In vivo*

In most descriptions of *Hematodinium*-associated disease in crustaceans, the predominant life stage observed is typically referred to as the trophont, the vegetative or trophic stage of the life cycle (Table 1.2). Microscopically, uninucleate trophonts have moderate to abundant amounts

of vacuolated cytoplasm which contain many refractile granules. The term plasmodial trophont or plasmodium is often used to describe the multinucleate trophont life stage. In addition to multinucleate (plasmodial) forms of trophonts, elongated finger-like forms with nuclear rowing are occasionally described, often referred to as vermiform plasmodia. These vermiform plasmodia are often compared morphologically to the filamentous trophont life form described *in vitro* (by Appleton and Vickerman, 1998, and then later by Li et al 2011a). Vermiform plasmodia are not described in reports of infection uniformly in affected host species, and the reported life stage sizes vary between and within hosts (Table 1.2).

Vermiform plasmodia are occasionally reported to be attached to or intimately associated with tissue surfaces (Table 1.3). In addition, sheet-like plasmodial forms have been described in the hepatopancreatic interstitial tissues of snow crabs *Chionoecetes opilio* with advanced *Hematodinium* infections (Wheeler et al 2007). These plasmodial sheets were considered to resemble the syncytial life stages described *in vitro.* Similarly, network syncytial forms were observed in the heart and abdominal muscles of Norway lobsters (Field et al 1992, Vickerman et al 1993, Field and Appleton 1995).

In vivo studies in blue crabs *Callinectes sapidus* reported that vermiform plasmodial produced more plasmodia via budding (Figures 1.2 and 1.3; Stentiford and Shields 2005, Li et al 2011a). The plasmodia then underwent merogony to produce rounded vegetative trophonts, the trophonts transformed into sporonts, and the sporonts produced dinospores via sporogony. Similar studies in Tanner crab *Chionoecetes bairdi* described ovoid plasmodial trophonts which

produced vegetative cells (amoeboid trophonts). These infections then transformed into a smaller life stage referred to as prespores since that life stage later developed into dinospores. These prespores are approximately equivalent of the sporoblasts in the *in vitro* culture work described above (Meyers et al 1987). Similar life stages referred to as prespores or sporoblasts have also occasionally been seen in red and blue king crabs *Paralithodes* spp. and tropical mud crabs *Scylla serrata* (Li et al 2008, Ryazanova et al 2010). Dinospores are more infrequently reported, although dimorphic dinospores have been seen in natural infections in Tanner crabs *Chionoecetes bairdi,* snow crab *Chionoecetes opilio,* and red and blue king crabs *Paralithodes* spp. (Table 1.2; Meyers et al 1987, Wheeler et al 2007, Ryazanova et al 2010).

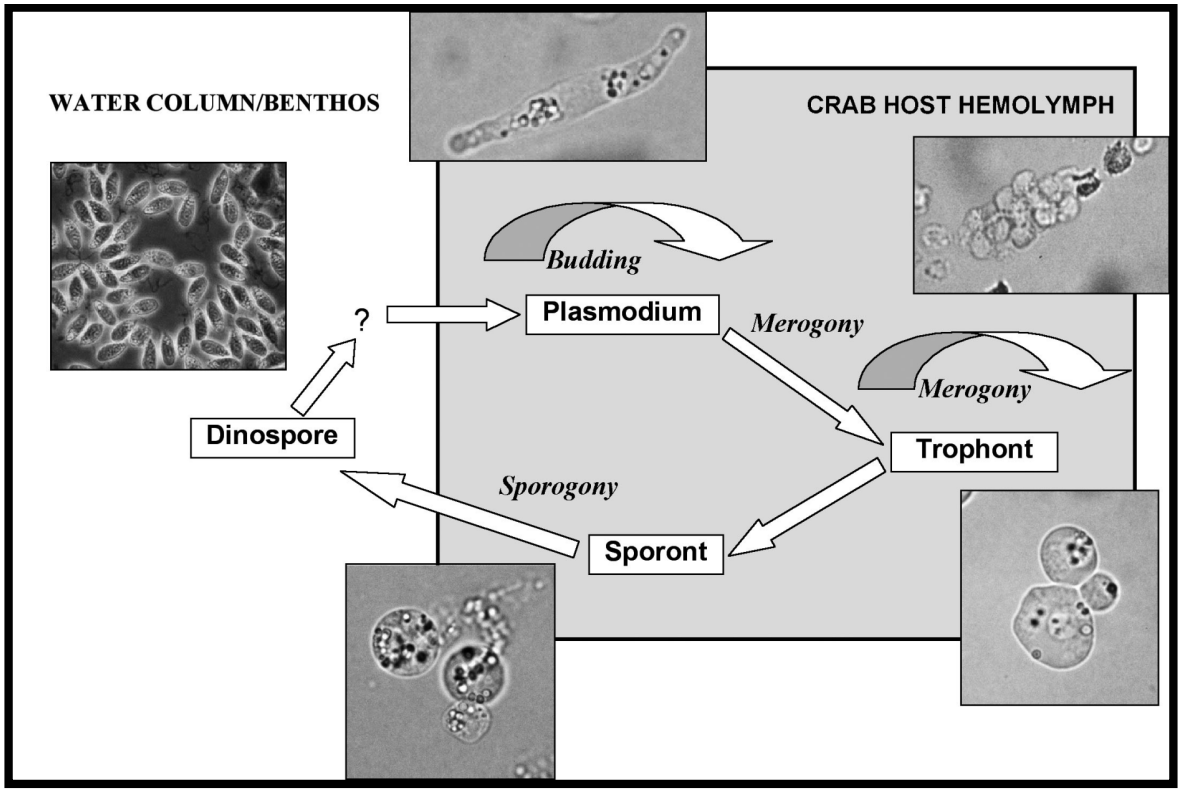

Figure 1.2. Proposed *in vivo* life cycle for *Hematodinium* sp. from the blue crab *Callinectes sapidus* (from Stentiford and Shields 2005).

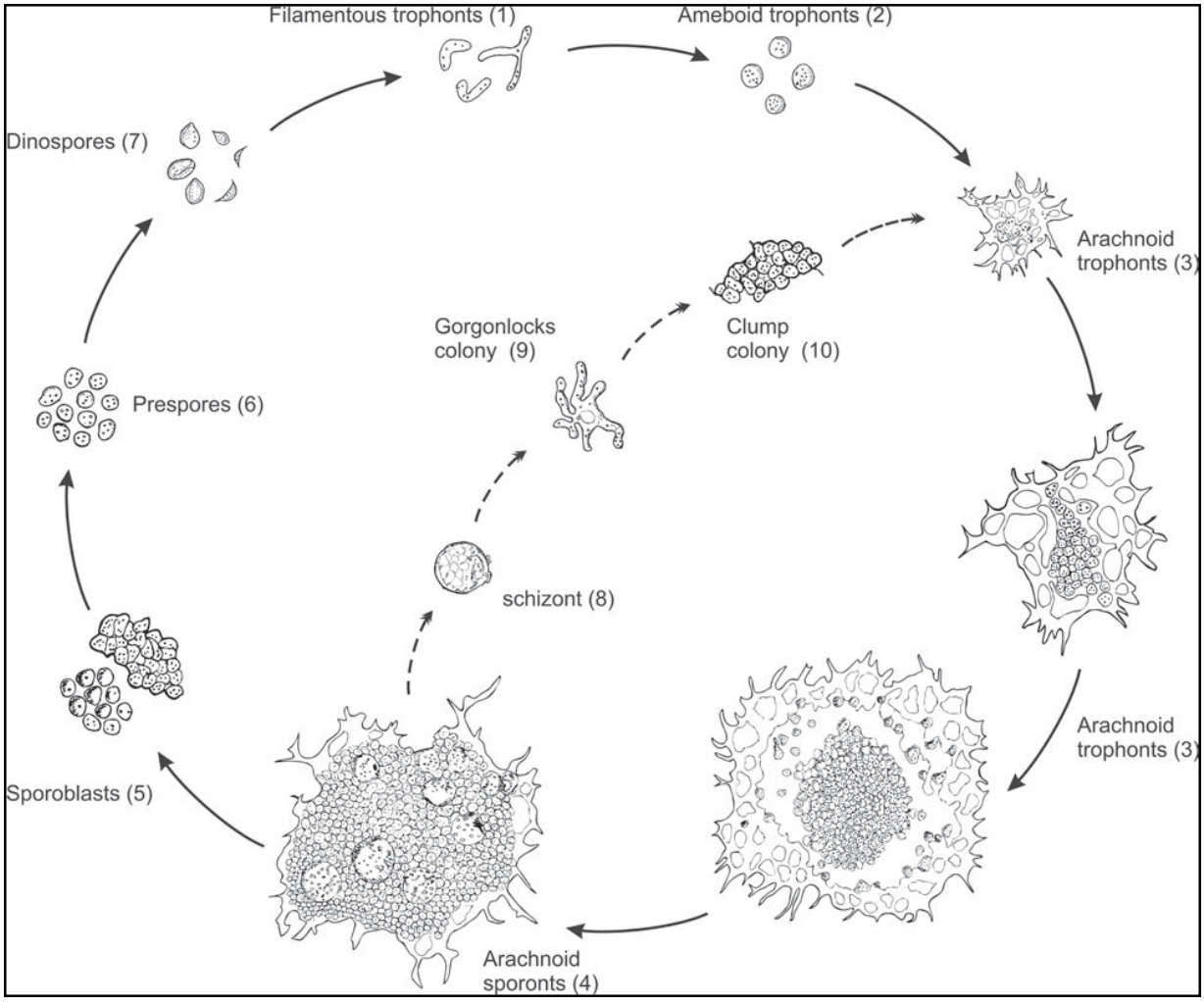

Figure 1.3. Schematic diagram of the *in vitro* life cycle of *Hematodinium* sp. from *Callinectes sapidus.* (1) Filamentous trophonts represent the initial stage of infection in a blue crab host. (2) Amoeboid trophonts arise from merogony of the filamentous trophont. This stage is often found in the circulating hemolymph of infected crabs. (3) Arachnoid trophonts arise from the syncytial network laid down by the amoeboid trophonts. They were the main proliferative stage of the parasite *in vitro*. (4) Arachnoid sporonts develop as a mass within the arachnoid trophont. They give rise to sporoblasts (5) which occur as single cells or aggregates of cells, which are released from the arachnoid sporonts when fully developed. (6) Prespores arise as the transition between sporoblasts and dinospores. (7) Dinospores, microdinospores or macrodinospores, arise from the prespores and represent the highly motile stage in the life cycle of the parasite. (8) Schizonts also developed from within arachnoid sporonts; they apparently represent an alternate pathway for proliferation of parasites in crab hosts (dashed arrows). The schizonts develop into gorgonlocks (9) that undergo schizogony (cf. segmentation) and develop into clump colonies (10). The clump colonies develop into arachnoid trophonts when subcultured *in vitro* (from Li et al 2011a).

Table 1.2: Morphologic characteristics of *Hematodinium* spp. life stages per host species (modified from Hudson and Shields 1994).

Host	Trophont Size (Φm)		Trophont Nucleus (Φm)		T	Plasmodial Shape	Dinospores (Φm)	Reference
	Range	0	Range	0	+/-			
Carcinus maenas	8.0-9.0				+	Vermiform		Chatton and Poisson 1931
Liocarcinus depurator	8.0-9.0				+	Vermiform		Chatton and Poisson 1931
Callinectes sapidus	6.4-10.4	8.1	4.6-8.1	6.2	+	Vermiform*		Newman and Johnson 1975
	10.5					Vermiform*		Messick 1994
	9-15 20-100 (length)					Round Vermiform*		Shields and Squyars 2000
	9 to 17 13 to 58 (length)	12.0 31.3				Round Vermiform*	14.3∀1.6; 9.2∀2.4	Li et al 2011
Ovalipes ocellatus	9.0-14.0					Round		MacLean and Ruddell 1978
Necora puber	12.0-25.0				-			Wilhelm and Mialhe 1996
Scylla serrata	9.9-11.9	10.7	5.9-9.9	8.1	-	Round		Li et al 2008
Portunus pelagicus	7.9-8.9 (early)	8.3	7.5-7.9	7.7	+	Round		Hudson and Shields 1994
	9.9-11.9 (late)	10.9	7.9-9.9	8.7	+	Round		Hudson and Shields 1994
Chionoecetes bairdi	15.6-12.8					Round	15.2 x 11.4; 12.0 x 4.4	Meyers et al 1987
	6.0-11.0 (early)					Round	Two types	Eaton et al 1991
	12.0-20.0 (late)					Round		Eaton et al 1991
Chionoecetes opilio	8.0-10.0				+		10.8 x 3.6	Williams-Ryan 1997
Nephrops norvegicus	6.0-10.0				+	Vermiform and Round		Field et al 1992
Cancer irroratus	9.0-14.0							MacLean and Ruddell 1978
Cancer borealis	9.0-14.0							MacLean and Ruddell 1978
Cancer pagurus	10.0-15.0				+			Latroite et al 1988
Trapezia areolata	6.9-12.8	11.0	8.0-9.6	8.5	+	Round		Hudson et al 1993
***Paralithodes* spp.**		10.7			+	Vermiform and Round	4.5+-0.4	Ryazanova et al 2010
Exopalaemon carinicauda					+	Round	7 to 9	Xu et al 2010

T = Trichocysts in trophont life stages; ~= Not described; *Vermiform plasmodia reported to be highly motile or exhibited amoeboid movement.

Table 1.3: Parasitic life stages of *Hematodinium* sp. observed via light microscopy in hemolymph, hemal spaces, and tissues of various host species.

Host	Hemolymph	Hemal spaces	Hepatopancreas	Muscle	Heart	Gill	Gonad	Midgut	Eyestalk	Antennal Gland
Callinectes sapidus	T, P, V^M, S	T, V	T, P, V^A		T, P V	T	—			
Ovalipes ocellatus	T, P	T, P								
Necora puber	T, P	T, P	T, P		T, P	T, P	T, P			
Scylla serrata	T, P, S, D	T, P	T, P		T, P	T, P				
Portunus pelagicus	T, P	T, P	T, P	T, P		T, P	T, P			
Chionoecetes bairdi	T, P	T, P	T,P	T,P				T,P	T, P	T, P
Chionoecetes opilio	T, P	T, P^S	T, P^S		T	T, S				
Libinia emarginata	T, P	T, P	T, P	T	T, P	T, P				
Menippe mercenaria	T>>P	T, P	T, P	T	T, P	T	—			
Nephrops norvegicus	T	T, P	T, P, V^A	T, P^S	T, P^S, V^A	T, P		T, P, V^A		T, V^A
Cancer irroratus	T, P	T, P								
Cancer borealis	T, P	T, P								
Cancer pagurus	T, P	T, P	T, P, P^A	T, P, P^A	T, P	T, P	T, P	T, P		
***Paralithodes* spp.**	T, P, S	T, P, V^A	T, P, V^A		T, P	T, P	T, P	T, P, V^A	T, P	T, P
Exopalaemon carinicauda	T, P									
13 amphipods species	T, P	T, P	T, P	T, P	T, P	T, P				

T = Uninucleate trophonts; P = Multinucleate plasmodia; P^S= Plasmodial syncytia or sheets; P^A = plasmodia in close association with surface;
V = vermiform plasmodia (filamentous syncytia); V^A = attached vermiform plasmodia; V^M = motile vermiform plasmodia;
S = Sporoblasts (sporonts or prespores); D = Dinospores;
— = Tissue was examined histologically and an absence of parasitic infiltration was noted;
~= Tissue was not examined histologically or parasites were not described.

1.5. Diagnosis of Infection

1.5.1. Macroscopic (Visual) Examination

In advanced stages of hematodiniosis, affected hosts are often externally recognized by discoloration of the carapace. This discoloration varies from pink to orange and is often compared to the "cooked" appearance of that species (Table 1.5). Less commonly the carapace coloration is described as chalky white as occurs in the Australian blue crab *Portunus pelagicus* (Hudson and Shields 1994). White lines on the underside of the merus or along arthrodial membranes (tanner crabs *Chionoecetes bairdi*) *or* yellow arthrodial membranes (edible crabs *Cancer pagurus* and red and blue king crabs *Paralithodes camtschaticus* and *P. platypus*) may also be seen (Love et al 1996, Stentiford et al 2002, Ryazanova et al 2010). In some hosts (including *Cancer borealis, Ovalipes ocellatus, Scylla serrata, Paralithodes* spp.), external examination of the crustacean may not reveal macroscopic evidence of disease (MacLean and Ruddell 1978, Hudson and Shields 1994, Ryazanova et al 2008).

When hemolymph is drawn from infected animals the parasitized blood is commonly opaque and "milky" in appearance; it can vary from cloudy to opalescent to creamy yellow (Table 1.5). The plasma of normal crustaceans is typically clear and colorless or blue-tinged. This blue hue is imparted by the presence of the oxygenated form of the copper-based respiratory pigment hemocyanin. The blue color is usually not apparent in the opaque, milky hemolymph of infected animals. The milky-white hemolymph is often clearly visible through the translucent cuticle of the ventral abdomen of Norway lobsters *Nephrops norvegicus* (Field et al 1992). Similarly, the ventrum of diseased snow crabs often is described as chalky white, and opaque internal tissues

can often be seen through the ventral carapace of blue crabs *Callinectes sapidus* with advanced infections (Messick 1994, Shields et al 2005, Wheeler et al 2007). At post mortem examination of affected hosts' organs, tissues were often described as having a similarly "milky" appearance. More rarely, the tissues were discolored pink similar to the carapace. In two species, tissue discoloration was due to milky to creamy yellow deposits on the tissues; occasionally affected tissues were described as friable (Table 1.4).

1.5.2. Pleopod Examination

One traditional technique of disease detection involved microscopic examination of pleopods. In this easy, accurate diagnostic method, dense aggregates of the parasite appeared as darkened areas when observed under transmitted light. This method was effective in identifying Norway lobsters *Nephrops norvegicus* with advanced disease. An early study suggested that the degree of cell aggregation visible in the pleopod was indicative of severity of infection (Field et al 1992). However, later investigations proved that dinoflagellate infections were often more severe than indicated by the observed degree of pleopod aggregation (Field and Appleton 1995). A modified method of pleopod examination was also used as a screening tool in the blue crab *Callinectes* sapidus; observation of the flattened portion of the 5th pleopod with an inverted microscope revealed hemal sinuses occluded by the numerous parasites, occasionally with no observable blood flow (Messick 1994).

Table 1.4: Macroscopic coloration alterations in advanced hematodiniosis in affected crustacean hosts, with specific tissue gross appearance details when available.

Host	Carapace color	Hemolymph	Tissues	Specific tissue details
Callinectes sapidus	Pink or orange	Milky or Opaque	Pink	Opaque skeletal muscles; Pink gills
Ovalipes ocellatus	**Normal**	Milky or opalescent	**Normal**	ND
Necora puber	Pale pink	Creamy and yellowish	Creamy to yellowish deposits	Deliquescent (friable) tissues
Scylla serrata	"Cooked"	Milky	Milky	ND
Portunus pelagicus	White chalky	Milky or chalky or cloudy	Milky	Cream-colored hepatopancreas; Cream-colored gills
Chionoecetes bairdi	Pink	Opalescent white to milky to cloudy white	Milky to "frosted"	Atrophied, soft and opaque skeletal muscle
Chionoecetes opilio	Pink, Orange or "Cooked"	Milky or chalky	Cream	Cream-colored heart ; Cream-colored gills
Nephrops norvegicus	Orange	Milky	Milky to thick creamy deposits	Green, shrunken hepatopancreas; Swollen and yellow heart Swollen, yellow, and enlarged hematopoietic tissue
Cancer irroratus	Pink	Milky or opalescent	Pink opalescent	ND
Cancer borealis	**Normal**	Milky or opalescent	**Normal**	ND
Cancer pagurus	Pink	Cream	Creamy to yellow	Friable skeletal muscle
***Paralithodes* spp.**	**Normal**	Creamy yellow	Creamy yellow	Creamy yellow heart; Creamy yellow gills
Exopalaemon carinicauda	"Cooked"	Milky	Milky	Whitish skeletal muscles

Normal= Macroscopically normal; ND = Not described

1.5.3. Direct Hemolymph Smears

The macroscopic milky-white appearance of the hemolymph is primarily due to increased total numbers of circulating cells, a combination of both host hemocytes and protistan cells. In early disease, the intensity of infection can be very light with only a small proportion of circulating dinoflagellates; only rare parasites are observed in direct hemolymph smears at this stage of disease. In more advanced stages of the disease, parasitic proliferation results in predominance of dinoflagellate parasites, with hundreds of parasites per field of view with rare or no host cells visible (Meyers et al 1987). Reduced intensity of the blue background-staining of hemolymph smears, suggestive of reduced plasma protein content, occurs in diseased snow crabs *Chionoecetes opilio* (personal observation). Pestal et al (2003) reported that microscopic examination of stained hemolymph smears detected almost twice as many infected snow crabs *Chionoecetes opilio* as did examinations for macroscopic signs of disease (estimated specificity of 100% and estimated sensitivity of only 52.7%).

1.5.4. Immunodiagnostics

Several immunodiagnostic techniques have been used to diagnose *Hematodinium* spp. infections. An indirect fluorescent antibody technique (IFAT) was developed with polyclonal rabbit antiserum raised against cultured vegetative forms of *Hematodinium* from Norway lobsters *Nephrops norvegicus* and showed that some individuals harbor infections outside the main infective season (Field and Appleton 1996). A Western blot method was also developed using polyclonal anti-*Hematodinium* antiserum and applied to study the occurrence and infection progression (Stentiford et al 2001c). In addition, an enzyme-linked immunosorbent

assay (ELISA) was developed to screen large numbers of samples in a short period without sophisticated analytical equipment. In comparison to the ELISA, the IFAT and Western blot are complex and time-consuming, and may not be able to detect all life stages of the disease in that host or in alternate hosts (Small et al 2002, 2006; Stentiford et al 2002).

1.5.5. Polymerase Chain Reaction Assays

Specific detection of *Hematodinium* spp. via Polymerase Chain Reaction (PCR) assays is often used for the diagnosis of infection in various crustacean hosts and for detection of the parasitic dinoflagellate in water and sediment samples (Bower et al 2003, Dyson et al 2009, Frischer et al 2006, Gornik et al 2013, Gruebl et al 2002, Hamilton et al 2009, Hudson and Adlard 1994, Jensen et al 2010; Li et al 2010, Lohan et al 2012, Pitula et al 2012, Shields et al 2015, Small et al 2007, Stentiford et al 2002). Use of PCR has become increasingly widespread in pathogen identification and disease detection and monitoring and is particularly useful in the diagnosis of cryptic organisms such as dinoflagellates and parasitic stages (Gruebl et al 2002, Lee and Frischer 2004, Small et al 2006). Ribosomal DNA (rDNA) has been used in many successful PCR-based diagnostic assays, including assays for *Hematodinium* in blue crabs (Gruebl et al 2002, Small et al 2007), Norway lobsters (Small et al 2006), and North Pacific Tanner crabs and snow crabs (Jensen et al 2010). Representative PCR amplicons can then be sequenced to confirm the identity of the parasites (Sheppard et al 2003). Furthermore, a quantitative real-time PCR-based (qPCR) assay has been developed for detection and enumeration of *Hematodinium* sp. in blue crab *Callinectes sapidus,* which can detect as few as 10 copies of the amplified gene per reaction (Nagle et al 2009). qPCR has also been used to detect and quantify *Hematodinium* sp.

in water and sediment samples with a level of detection of 1 parasitic cell in 100 ml of environmental water or one gram of sediment (Li et al 2010). Troedsson et al (2008a, 2008b) have also described a new technique using a novel denaturing high-performance liquid chromatography (DHPLC) approach useful for initial detection and identification of crustacean parasites. In addition to parasitic detection, their DHPLC approach has the potential for detecting unknown or unsuspected parasites and parasitoids during disease investigations (Troedsson et al 2008b).

1.6. Histopathologic Changes

Histologic examination of tissues of infected animals reveals multisystemic infiltration of hemal spaces by proliferating parasites. Changes associated with the parasitic infection vary with the host and infiltrated tissue but include disruption of tissue architecture; degeneration, attenuation, atrophy, or loss; tissue necrosis; inflammation; and increased mitotic activity (summarized in Table 1.5).

Table 1.5: Histopathologic changes characterized by disrupted tissue architecture, epithelial or muscular degeneration, epithelial or muscular necrosis, increased mitotic activity, and inflammation described in advanced stages of hematodiniosis in various crustacean hosts.

Host	Hepato-pancreas	Muscle	Heart	Gill	Midgut	Hematopoietic Tissue	Eyestalk	Antennal gland
Nephrops norvegicus	A, D, N	N	A	I	A	M		D
Chionoecetes bairdi	A, N	A			A		A	I
Callinectes sapidus	A, D, N, I	A, N	I	I				
Chionoecetes opilio	A		D	D, N				
Libinia emarginata	A	A						
Menippe mercenaria	A							
***Paralithodes* spp.**	A, N	A				M, I		I
Portunus pelagicus	A, D	D						
Cancer pagurus	A, D	D, I	D, I		I			
Scylla serrata	A, D		N	D				
Exopalaemon carinicauda	A	A	D	N				

A = disrupted tissue architecture (i.e., marked parasitic interstitial infiltrates);
D = epithelial vacuolar degeneration or attenuation, myodegeneration, tissue atrophy, or loss of density;
N = necrosis, lytic necrosis, or markedly disrupted tissue structure;
I = inflammation (hemocytic aggregates, hemocytic encapsulation, or melanized nodules);
M = mitotically active;
~= Tissue was not examined histologically or histopathologic changes (not including parasitic interstitial infiltrates) were not described. (Not marked in table.)

1.6.1. Hepatopancreas

In every host in which the hepatopancreas was examined histologically, dinoflagellate parasites infiltrated the hepatopancreatic interstitium and typically expanded the interstitium, increasing the space between the hepatopancreatic tubules (Field and Appleton 1995, Meyers et al 1987, Sheppard et al 2003). In snow crabs *Chionoecetes opilio*, edible crabs *Cancer pagurus*, tropical mud crabs *Scylla serrata*, and ridgetail white prawns *Exopalaemon carinicauda*, the infiltrate was associated with reduction or loss of interstitial spongy connective tissue (Stentiford et al 2002, Wheeler et al 2007, Li et al 2008, Xu et al 2010). In snow crab *Chionoecetes opilio* and edible crabs *Cancer pagurus*, the parasitic infiltrate was also associated with loss of reserve inclusion (RI) cells (Stentiford et al 2002, Wheeler et al 2007). In the Norway lobster *Nephrops norvegicus*, Tanner crab *Chionoecetes bairdi*, blue crab *Callinectes sapidus*, Australian blue crab

Portunus pelagicus, and edible crab *Cancer pagurus*, vacuolation of the hepatopancreatic epithelium was often observed and was often interpreted as evidence of cellular degeneration (Meyers et al 1987, Field et al 1992, Messick 1994).

In fewer species, including the Norway lobster *Nephrops norvegicus*, blue crab *Callinectes sapidus* and red and blue King crabs *Paralithodes* spp., similar changes were interpreted as epithelial lysis (lytic necrosis; Field et al 1992). Very rarely, such degenerative or lytic changes accompanied by observations of parasitic dinoflagellates within the lumina of hepatopancreatic tubules as reported in the Norway lobster *Nephrops norvegicus*, Tanner crab *Chionoecetes bairdi*, and edible crab *Cancer pagurus* (Meyers et al 1987, Field and Appleton 1995). In the tropical mud crab *Scylla serrata* hepatopancreatic tubular atrophy with luminal dilation was observed, rather than vacuolar degeneration or necrosis (Li et al 2008).

The marked interstitial expansion observed in the hepatopancreas was often the most severe change noted in affected crustaceans; thus it has been suggested that the hepatopancreas may be the initial site of infection in this disease (Stentiford et al 2002). Field et al (1995) also showed filamentous trophonts which appeared to be intimately associated with or attached to the outer wall of hepatopancreatic tubules. Evidence of immune system recognition of the parasitic infection is limited. In Norway lobster *Nephrops norvegicus* and in snow crabs *Chionoecetes opilio*, interstitial fixed phagocytes were described as enlarged and vacuolated, morphological alterations interpreted as reactive changes in response to the parasitic infection (Field and Appleton 1995, Wheeler et al 2007). In blue crabs *Callinectes sapidus* with

experimentally induced infections, hemocytic aggregates were seen in the hepatopancreas early in the course of the infection (within hours of experimental exposure; Walker et al 2009).

1.6.2. Skeletal Muscle

Another histopathologic lesion often reported in affected crustaceans was alteration of striated skeletal muscle. In the skeletal muscle, parasitic dinoflagellates typically infiltrated the interstitial connective tissues between the skeletal muscle myofibers which resulted in myofiber separation (Chualain and Robinson 2011, Field and Appleton 1995, Hudson and Shields 1994, Meyers et al 1987, Sheppard et al 2003, Stentiford et al 2002, Walker et al 2009). Reduction of interstitial connective tissue similar to that seen in the hepatopancreas was reported in red and blue king crabs *Paralithodes* spp. (Ryazanova et al 2008). In regards to the myofibers alterations, the mildest change noted was association of parasitic dinoflagellates with the sarcolemma of myocytes (Stentiford et al 2002). In many host species, the interstitial infiltrate was associated with fragmentation, degeneration, or disrupted structure of the muscle (Field and Appleton 1995, Meyers et al 1987, Ryazanova et al 2008, Sheppard et al 2003, Stentiford et al 2002, Walker et al 2009, Xu et al 2010). In the Norway lobster *Nephrops norvegicus* and blue crab *Callinectes sapidus*, myonecrosis was reported (Field et al 1992, Walker et al 2009). Breaching of the sarcolemma with parasitic dinoflagellates observed within myofibrils was only reported in red and blue king crabs *Paralithodes* spp. (Ryazanova et al 2008).

In edible crabs *Cancer pagurus*, conflicting results have been reported in the degree of severity of muscular disease. In a recent report by Chualain and Robinson (2011) muscle tissue was the least affected tissue examined, with light infections in the interstices of the muscle despite heavy populations in other tissues examined. Even in advanced infections where the hemal sinuses were dilated by the proliferating parasites, the muscle fibers only appeared atrophied, without evidence of degeneration and necrosis. This is in contrast to an earlier study where the claw muscle was markedly affected, with the claw muscle being almost completely replaced by large numbers of plasmodia with only small islands of identifiable muscle fibers remaining (Stentiford et al 2002). This is also the only report which described a host immune response in the skeletal muscle with intense multifocal inflammatory granulomas (encapsulations) in the claw tissue of heavily infected crabs (Stentiford et al 2002).

1.6.3. Heart

Intraluminal parasites with mild interstitial myocardial infiltrates were the most commonly reported findings in hearts of infected crustaceans. In Norway lobsters *Nephrops norvegicus*, Field et al (1992) described vermiform plasmodia attached to the luminal surfaces of the myocardium, similar to those described above attached to the outer surface of hepatopancreatic tubules by the same authors (Field et al 1995). Vermiform plasmodia have also been reported in the hearts of blue crabs *Callinectes sapidus* (Walker et al 2009). Vermiform multinucleate trophonts were observed to be attached to the outer wall of hemolymph vessels in *Callinectes sapidus* (Small et al 2012).

In snow crabs *Chionoecetes opilio* and white ridgetail prawns *Exopalaemon carinicauda*, a loss of myofiber density was reported in affected heart and atrophy of myocardial bundles was reported in the edible crab *Cancer pagurus* (Stentiford et al 2002, Wheeler et al 2007, Xu et al 2010). Coagulative necrosis of myocardium was only reported for one host species, the tropical mud crab *Scylla serrata* (Li et al 2008). In snow crab *Chionoecetes opilio*, the infection was associated with RI cell loss and enlarged (reactive) fixed phagocytes, changes similar to those described previously in the hepatopancreas of this host species (Wheeler et al 2007). Hemocytic aggregates were reported in early stages of experimentally induced infections in blue crabs *Callinectes sapidus* (as seen in their hepatopancreas), and encapsulation reactions were observed in some edible crabs *Cancer pagurus* (as seen in their claw muscle; Stentiford et al 2002, Walker et al 2009).

1.6.4. Gill

In late hematodiniosis, the hemal canals of the gills are typically congested with intraluminal parasitic dinoflagellates. In the gills of infected snow crabs *Chionoecetes opilio*, tropical mud crabs *Scylla serrata*, and white ridgetail prawns *Exopalaemon carinicauda*, attenuation (flattening or squamous metaplasia) of the lining epithelium was observed (Wheeler et al 2007, Li et al 2008, Xu et al 2010). In addition, loss or necrosis of trabecular cells and podocytes were reported in snow crabs *Chionoecetes opilio* and white ridgetail prawns *Exopalaemon carinicauda* (Wheeler et al 2007, Xu et al 2010). At sporulation, marked gill filament changes were observed in snow crabs *Chionoecetes opilio* with formation of club-like dilations of the distal filament margins. Rupture of these terminally-located lesions was considered associated

with release of spores into the environment (Wheeler et al 2007). Hemocytic aggregates within the gill hemal canals were reported in Norway lobsters *Nephrops norvegicus* and in early stages of experimentally induced infections in blue crabs *Callinectes sapidus* (as seen in their hepatopancreas and heart; Field et al 1992, Walker et al 2009).

1.6.5. Midgut

Interstitial parasitic infiltration of the muscular layers of the midgut wall have been reported in several affected hosts, including Norway lobster *Nephrops norvegicus*, Tanner crabs *Chionoecetes bairdi*, red and blue king crabs *Paralithodes* spp., and edible crabs *Cancer pagurus* (Field et al 1992, Meyers et al 1987, Ryazanova et al 2008, Stentiford et al 2002). In Norway lobsters *Nephrops norvegicus* and Tanner crabs *Chionoecetes bairdi,* this interstitial infiltrate was associated with significant disruption of the muscular layers of the midgut wall (Field et al 1992, Meyers et al 1987). Granuloma-like encapsulations within the midgut wall were reported in the edible crab *Cancer pagurus* (as reported in their skeletal muscles and heart; Stentiford et al 2002).

1.6.6. Gonad

Interstitial gonadal infiltrates have been reported for several hosts affected with hematodiniosis, including red and blue king crabs *Paralithodes* spp., Australian blue crabs *Portunus pelagicus*, velvet swimming crabs *Necora puber*, and edible crabs *Cancer pagurus* (Hudson and Shields 1994, Ryazanova et al 2008, Stentiford et al 2002, Stentiford et al 2003). Gonadal tissues were infrequently examined in infected crabs, thus information in regards to

reproductive tract involvement is generally scanty. Expansion of the gonadal interstitium by the parasitic infiltrate was reported in the edible crab *Cancer pagurus* (Stentiford et al 2002). No reports of invasion of ova themselves were noted in this or any other reports of infection. A lack of gonadal interstitial infiltration despite extensive parasitic infiltrates in other organs was noted in blue crab *Callinectes sapidus* and stone crab *Menippe mercenaria* (Sheppard et al 2003).

1.6.7. Antennal Gland

Parasitic infiltration of the antennal gland was reported in Norway lobsters *Nephrops norvegicus*, Tanner crabs *Chionoecetes bairdi*, and red and blue king crabs *Paralithodes* spp. (Field and Appleton 1995, Meyers et al 1987, Ryazanova et al 2008). In Norway lobsters *Nephrops norvegicus*, the infection was associated with vacuolation of the labyrinthine epithelium and intraluminal parasites were observed (Field and Appleton 1995). Host responses of hemocytic aggregates and melanized nodules were reported in Tanner crabs *Chionoecetes bairdi* and red and blue king crabs *Paralithodes* spp., respectively (Meyers et al 1987, Ryazanova et al 2008).

1.6.8. Hematopoietic Tissue

Hematopoietic tissue changes were only noted in reports describing hematodiniosis in two affected host genera, Norway lobster *Nephrops norvegicus* and red and blue king crabs *Paralithodes* spp. (Field and Appleton 1995, Ryazanova et al 2008). In both reports, the hematopoietic tissue was described as mitotically active despite concurrent hemocytopenia. In

the Norway lobster *Nephrops norvegicus*, the hematopoietic tissue was noted to be grossly swollen and enlarged and melanized nodules were reported in the hematopoietic tissue of the red and blue king crabs *Paralithodes* spp. (Field and Appleton 1995, Ryazanova et al 2008).

1.6.9. Eyestalk

Infiltration of hemal spaces in the eyestalk was reported in Tanner crabs *Chionoecetes bairdi* and red and blue king crabs *Paralithodes* spp. (Field and Appleton 1995, Meyers et al 1987). In those reports parasites appeared to infiltrate into eyestalk glial elements in Tanner crabs *Chionoecetes bairdi*, while no such infiltration was observed in the red and blue king crabs *Paralithodes* spp.

1.7. Co-infections

1.7.1. Bacterial Co-infections

In the advanced or terminal stages of disease, bacteria were the most frequently reported co-infections (Table 1.6; Meyers et al 1987, Field et al 1992, Love et al 1993, Sheppard et al 2003, Stentiford et al 2003). In Tanner crabs *Chionoecetes bairdi*, bacteremia was most commonly seen in hemolymph collected post mortem, but similar bacteremia was also observed in several crabs prior to death supporting a diagnosis of antemortem bacterial infection (Meyers et al 1987). Experimental co-infection with *Bacillus subtilis* was investigated in early stage *Hematodinium* infections in juvenile edible crabs C*ancer pagurus*, with effective hemolymph bacterial clearance as indicated by standard plate counts (Rowley et al 2015).

1.7.2. Protozoal Co-infections

The hosts with ciliate infections in advanced *Hematodinium* infections overlapped with those reported to have bacteremia (Field et al 1992, Messick 1994, Meyers et al 1987). In one report of such ciliate infections in blue crabs *Callinectes sapidus*, infections with the amoeba *Paramoeba perniciosa* (the causative agent of Paramoebiasis in that host) was specified in addition to infections with unidentified ciliates. In Norway lobsters *Nephrops norvegicus*, gregarine infections were noted in the midgut lumen of a single lobster with late-stage *Hematodinium* infection (Field and Appleton 1995). Microsporidian co-infections were noted in one report describing late hematodiniosis in blue crabs *Callinectes sapidus* (Messick 1994). Similarly, haplosporidian infections were noted only in heart tissue smears of velvet swimming crabs *Necora puber*. Haplosporidian infection in the velvet swimming crab *Necora puber* was the only infection that was seen in both crabs with and without *Hematodinium* infections and was thought to be non-pathogenic in affected hosts (Wilhelm and Mialhe 1996).

1.7.3. Fungal Co-infections

In a study examining edible crabs *Cancer pagurus* and velvet swimming crabs *Necora puber* from the English Channel, co-infections with yeast-like organisms were commonly observed (25 to 100% prevalence) in crabs with advanced *Hematodinium* infections (Stentiford et al 2003). Despite apparent hemocytopenia, hemocyte encapsulation of the yeast-like cells was evident. In contrast, no such response was observed to the dinoflagellate plasmodia (Stentiford et al 2003). Co-infection of *Hematodinium* and an emerging fungal disease caused by a fungus of the *Ophiocordycepes* clade has also been reported in edible crabs *Cancer pagurus* (Smith et al

2013). The majority (94%) of crabs with natural fungal infections were co-infected with *Hematodinium.* Conversely, only a relatively small percentage (9%) of crabs infected with *Hematodinium* were also infected with the fungus. In a co-infection trial, apparently the presence of *Hematodinium* suppressed the development of the fungus and that rapid mortality of the co-infected animals was caused by multiplication of the dinoflagellate parasite alone. The authors suggested that the additional stress imposed by the invading fungus may have allowed *Hematodinium* to overwhelm its host. Fungal infections were also identified in two infected amphipods which were co-infected by *Hematodinium*- like dinoflagellates (Johnson 1986). Among all the amphipods screened (>7000 amphipods), only 2 amphipods having heavy syndinid infections had systemic fungal infections. Fungi were being phagocytized by hemocytes and fixed phagocytes or encapsulated in melanized nodules. The host's immune cells were actively destroying fungi; there was no evidence that the accompanying syndinids were recognized as foreign (Johnson 1986).

Table 1.6: Co-infections reported in crustaceans with hematodiniosis.

Host	**Co-infection**	**Immune responses observed**[1]
Nephrops norvegicus	Bacteria, ciliates, gregarines	Hemocytic aggregates
Chionoecetes bairdi	Bacteria, ciliates	Hemocytic aggregates
Callinectes sapidus	Bacteria, ciliates, microsporidians	Hemocytic aggregates
Libinia emarginata	Bacteria	ND
Menippe mercenaria	Bacteria	ND
Cancer pagurus	Bacteria (*Bacillus subtilis*)	ND
Necora puber	Yeast-like, Haplosporidian	Encapsulation (intralesional yeasts)
Cancer pagurus	Yeast-like	Encapsulation (with and without intralesional yeasts)
Cancer pagurus	*Ophiocordycepes* clade fungus	Encapsulation (intralesional fungi)
Benthic amphipods	Fungus	Phagocytosis (intralesional fungi)

[1]No definitive evidence of parasitic dinoflagellates reported within immune response in any report;
ND = Not determined.

1.8. Hemolymph Total Cell Counts and Biochemistry

Crabs and lobsters infected with *Hematodinium* exhibit hemocytopenia (Shields 1994, Field and Appleton 1995, Shields and Squyars 2000, Stentiford and Shields 2005, Rowley et al 2015). Experimentally infected *Callinectes sapidus* showed a significant and rapid decline in absolute densities of circulating hemocytes (48% decline) within 3 days and an even more dramatic decline (70 to 80%) within 21 days of inoculation (Shields and Squyars 2000). Relative declines were noted primarily in hyalinocytes, hemocytes that function in coagulation and clot formation. Similar changes were noted in the hemograms of naturally infected crabs. Crustacean hemocytes normally function in wound repair, clotting, phagocytosis, nodulation and encapsulation of foreign material, tanning of the cuticle, carbohydrate transport, glucose regulation, hemocyanin synthesis, and possibly osmotic regulation (Johansson et al 2000, Jiravanichpaisal et al 2006). The cause of this hemocytopenia is unknown. Possible causes include reduced production, sequestration, or destruction of hemocytes. No evidence of parasitic phagocytosis of host hemocytes has been noted. Starvation results in altered total hemocyte counts (THCs) in crustacean hosts, causing decreased THCs in white shrimp *Litopenaeus vannamei* and decreased THCs in American lobsters *Homarus americanus* but increased THCs in the green crab *Carcinus aestuarii* (Stewart et al 1967, Matozzo et al 2011, Lin et al 2012). Thus, host metabolic exhaustion due to parasitic acquisition of host resources is also a possible cause of the hemocytopenia (Rowley et al 2015). Declines in hemocytes may facilitate development of secondary infections, contribute to the loss of clotting ability since hyalinocytes regulate coagulation, and are highly correlated with imminent host death (Meyers et al 1987, Field et al 1992, Shields and Squyars 2000, Shields et al 2003, Stentiford et al 2003).

The hemolymph of heavily infected crabs often loses its ability to clot (Meyers et al 1987, Hudson and Shields 1994, Shields and Squyars 2000). The clotting mechanisms may be specifically suppressed and/or reduced via hyalinocyte depletion (Shields and Squyars 2000). *Paramoeba* infections in the blue crab also result in coagulopathy that was hypothesized to result from parasite-modulated proteolytic activity or from the loss of serum fibrinogen as a component of the total serum protein (Pauley et al 1975). *Hematodinium* spp. infections often result in marked hypoproteinemia (Love et al 1996, Taylor et al 1996, Shields et al 2003). Hemocyanin is the primary protein in crustacean hemolymph and reduction in hemocyanin concentration occurs in infected Norway lobsters *Nephrops norvegicus*, Tanner crabs *Chionoecetes bairdi* and male blue crabs *Callinectes sapidus* (Field et al 1992, Love et al 1996, Shields et al 2003). Decreased hemocyanin levels most likely have significant impacts on infected hosts as hemocyanin is a multifunctional protein that acts in oxygen transportation, protein storage, osmotic regulation, ecdysone transportation, and anti-microbial defense (Paul and Pirow 1998, Jaenicke et al 1999, Destoumieux-Garzón et al 2001). Mechanisms behind this reduction in serum proteins are not known. Direct uptake of proteins from the plasma by micropores on circulating hemocytes, disturbance in hemocyanin synthesis in the hepatopancreas, and/or degradation of the metabolism of the host (e.g., starvation) may be contributing factors in its pathogenesis (Appleton and Vickerman 1996, Field et al 1992, Taylor et al 1996, Stentiford and Shields 2005). Proteases have been detected in extracellular products from parasite culture supernates or lysates, suggesting they may play a role in protein loss (Stentiford and Shields 2005).

The metabolic demand of rapidly proliferating parasites reduces the protein constituents of the host and contributes to host morbidity (Stentiford et al 2000, 2001a, Shields et al 2003). The metabolic demands of the proliferating parasite are most likely compounded by cessation of feeding associated with morbidity (starvation; Uglow 1969a,b, Stewart et al 1972,Taylor et al 1996, Stentiford et al 2000, Stentiford and Shields 2005). Starvation and hypoproteinemia can also impair crustacean innate immunity via reduction in hemolymph antimicrobial protein levels. Antimicrobial peptides and proteins are important components of the host defense system with broad ability to kill microbes, and with functions in inflammation, wound repair and regulation of the adaptive immune system (Fredrick and Ravichandran, 2012). Antimicrobial peptides are present in cell-free hemolymph and have been identified in the hemocyte membrane and cytoplasmic granules (Hauton et al 2006). Stentiford et al (1999, 2000) recorded disturbance of the free amino acid profiles of plasma and muscle. Tissue and hemocyte degradation and the induction of a generalized host stress response were associated with an increase in the concentration of taurine during infection. Increases in serine and phenylalanine were also observed. Free amino acids significantly affect the taste of crustacean meat (Hayashi et al 1981, Shirari et al 1996, Stentiford 2000). The increased taurine may be from leakage of skeletal muscles or due to upregulation as part of a stress reaction (Stentiford et al 1999, 2000).

The metabolic demands of the disease process and/or starvation also result in significant reductions in tissue reserves of glycogen in infected crabs and lobsters (Love et al 1996,

Stentiford et al 2000, 2001, Shields et al 2003). Altered glycogenesis, alteration of the host's hormonal regulation, and/or carbohydrate uptake by the parasitic dinoflagellates may also contribute to loss of the hosts' glycogen stores (Stentiford et al 2000). In *Chionoecetes opilio*, tissue glycogen was depleted by 50%, whereas in *Nephrops norvegicus*, the glycogen in the abdominal muscles was reduced by up to 80% and was concomitant with increasing parasite burden (Stentiford et al 2000, Shields et al 2003, Stentiford et al 2005). In blue crabs *Callinectes sapidus* males were more depleted than females with tissue glycogen depletion of 50% in females and 70% in males with advanced infections (Shields et al 2003).

The metabolic impairment caused by Bitter Crab Disease (BCD) on its host may also impair cuticular hardening. The multilayered crustacean cuticle is composed of chitin-protein fibers (chitin nanofibrils wrapped with proteins) in a mineral-protein matrix (Nikolov et al 2010). Glycogen depletion would most likely impair the ability of heavily infected animals to molt as glycogen is a significant precursor to chitin (Stevenson 1985, Stentiford and Shields 2005). Systemic hypoproteinemia would most likely impact protein supply for cuticular synthesis and hardening in affected new-shelled animals. More specifically, hemocyanin has been found within the cuticle of *Penaeus japonicus* where it was hypothesized to play a role in cuticular sclerotization and in antimicrobial defense (Adachi et al 2005). Also, the phenoloxidase activity present in hemocytes may participate in the sclerotization of the initial shell-hardening process in new-shelled crustaceans (Vacca and Fingerman 1983, Terwilliger and Ryan 2006, Alvarez and Chung 2013). Thus, hemocytopenia may also impair cuticular sclerotization in crustaceans with hematodiniosis.

Respiratory dysfunction is evident by the decline in hemocyanin levels, the loss of oxygen binding capacity of the hemocyanin, and the magnitude of parasitic congestion with disruption of the gills and other tissues (Meyers et al 1987, Field et al 1992, Field and Appleton 1995, Hudson and Shields 1994, Messick 1994, Taylor et al 1996, Stentiford et al 2002, Shields et al 2003). Changes in osmoregulation resulting from shifts in plasma proteins, amino acids and other compounds, leading to osmotic collapse, likely contribute to the cause of death (Stentiford et al 1999). Moribund animals may suffer from tissue hypoxia and ischemia as metabolic effects of parasitism due to tissue destruction (Taylor et al 1996). Lactate is the main end product of anaerobiosis in crustaceans (Maciel et al 2008) and lactate levels show significant increases in the late stages of disease in infected Norway lobsters (Taylor et al 1996).

1.9. Seasonality

The occurrence of hematodiniosis in many affected species is described as markedly seasonal, with the season of highest prevalence varying among affected hosts. In Norway lobsters *Nephrops norvegicus,* disease prevalence is highest in the Spring and early Summer (Field et al 1992, Field and Appleton 1995). Highest disease prevalence is also seen in the late Spring and Summer in Tanner crabs *Chionoecetes bairdi* (Eaton et al 1991, Love et al 1993). In blue crabs *Callinectes sapidus* highest disease prevalence occurs in the Fall (Newman and Johnson 1975, Messick 1994, Messick and Shields 2000) or with bimodal distribution with disease peaks in both the Spring and Fall (Messick 1994, Messick and Shields 2000, Sheppard et al 2003). Seasonal peak disease prevalence in each host species tends to occur over a relatively narrow

period followed by a longer period of subclinical or low-level prevalence (Field et al 1992, 1998; Shields 1994, Messick and Shields 2000, Stentiford et al 2002).

In Norway lobster *Nephrops norvegicus* and Tanner crabs *Chionoecetes bairdi*, disease seasonality coincides with the host's main annual molting period, suggesting an association with molting (Eaton et al 1991, Field et al 1992, Messick 1994, Field et al 1998, Messick and Shields 2000, Stentiford et al 2002, Stentiford and Shields 2005, Hamilton et al 2009). An association with molting is also supported by the finding of highest disease prevalence in smaller individuals, since smaller (younger) individuals molt more frequently than larger ones (Field et al 1992, Field et al 1998, Messick 1994, Messick and Shields 2000, Mullowney et al 2011). The disease is also most commonly seen in new-shelled animals, animals which have molted within the last year or two, than in old-shelled animals (Meyers et al 1987, Wilhelme and Mialhe 1996, Dawe 2002, Shields et al 2005, Shields et al 2007, Mullowney et al 2011). Furthermore, females tend to have higher disease prevalence in several affected species including Norway lobsters *Nephrops norvegicus,* and snow crabs *Chionoecetes opilio* (Field et al 1992, 1998; Pestal et al 2003, Shields et al 2005). In Norway lobsters *N. norvegicus*, this sex distribution of disease could be associated with molting since molting times differ for females and males. Female animals molt earlier in the Spring so that they have soft cuticles to allow mating with hard shelled males. Small males then molt in late Spring to early Summer and larger males molt in the Autumn. This indicates that in Norway lobsters *N. norvegicus* the majority of females are molting at the time of peak disease prevalence, while fewer males are molting at that time (Field et al 1992).

1.10. Transmission

The association with molting remains unclear as the natural mode and route of infection in hematodiniosis is unclear. Field et al (1998) suggest that dinospores may enter new hosts through cuticular lesions directly after ecdysis. Host defense mechanisms may be compromised during ecdysis, rendering new-shelled organisms more susceptible to invading organisms (Messick 1994). The disease can be spread experimentally by injecting naïve hosts with vegetative (trophic) stages of the disease (Meyers et al 1987, Hudson and Shields 1994) and with variable success via cannibalism (Walker et al 2009. Li et al 2011b). In addition, sexual transmission and involvement of intermediate host(s) also cannot be ruled out as contributing to disease spread (Meyers et al 1999, Coats 1999).

The intermediate size of affected snow crabs could be linked to cannibalism and with molting. Cannibalism is most frequently practiced in intermediate-sized crabs and it is also observed more frequently in females than males (Squires and Dawe 2003). Size of crabs and molt status also impacts the diet of crabs. In larval stages, snow crabs feed on plankton. As juveniles and adults they become generalists, feeding on gastropods, bivalves, shrimp/prawns, polychaete worms, and decapod crustaceans including snow crabs (Pinfold 2006). In one study, the most frequently occurring prey items for snow crab off the coast of Newfoundland were polychaetes (81–90%) and bivalves (43–48%). With respect to prey biomass, shrimp (22–65%) and fish (capelin *Mallotus villosus,* Atlantic spiny lumpsucker *Eumicrotremus spinosus,* redfish *Sebastes* spp.; 5–35%) were most important. Crabs, mostly small *Chionoecetes opilio,* were also

frequently consumed (Lovrich 1997, Squires and Dawe 2003). Differences in size affected the diet, with large crabs more likely to scavenge on dead fish (e.g. discarded bait) and smaller crabs more likely to ingest shrimp (Wieczorek and Hooper 1995). In addition, significant differences were seen in the diet of crabs with old carapaces versus those with new carapaces: crabs with old carapaces were more likely to ingest fish and more annelids than crabs with new carapaces (Wieczorek and Hooper 1995). *Hematodinium* infections occur in Pandalid and Caprellid shrimp (which are included in the diet of snow crabs), and in rock crabs and green crabs. Interestingly, Japanese skeleton shrimp (*Caprella mutica*) and green crab (*Carcinus maenas*) are both invasive species and their worldwide distribution maps overlap those of Hematodiniosis (Figures 1.4-1.6; Carlton and Cohen 2003, Ashton et al 2007). Although these invasive species could be involved in the worldwide dissemination of this parasitic infection, this shared distribution may simply represent overlap of the physiologic ranges of susceptible crustacean hosts.

The impact of other environmental and host factors on disease transmission and progression of hematodiniosis is also unknown. Outbreaks of Bitter Crab Disease in snow crabs (*Chionoecetes opilio*) off Newfoundland have been associated with warmer temperatures (Shields et al 2007). Marcogliese (2008) suggested that climate change will have important effects on parasitism and disease in marine ecosystems. Altered environmental variables associated with global warming can impact host-pathogen interactions through alterations of host range, parasite range, host immunocompetence, parasite virulence, and parasite transmission rates. In general, transmission rates of parasites and pathogens are expected to increase with increasing

temperature, and virulence of those organisms may also increase (Marcogliese 2008). Recently, Mullowney et al (2011) investigated the influences and interactions of several biotic and abiotic factors over hematodiniosis in snow crabs *Chionoecetes opilio* and found that the density of small to medium-sized snow crabs was directly related to prevalence and distribution of hematodiniosis, while temperature, salinity, and depth had either indirect or no effect.

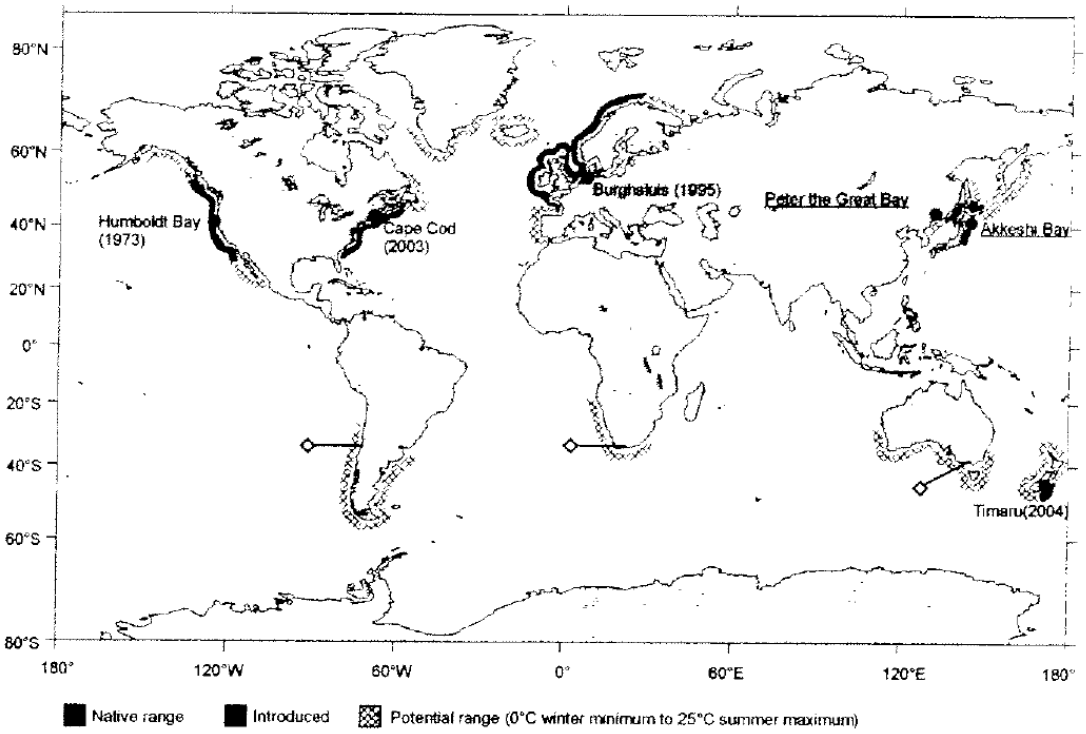

Figure 1.4. Current global distribution of *Caprella mutica*. Solid black: the native range and introduced areas. Hatched regions: potential range of *C. mutica.* Labels with underline show the native distribution; normal text labels show dates of first record on each coastline. Diamonds indicate locations of surveys which have not found *C. mutica* (from Ashton 2007).

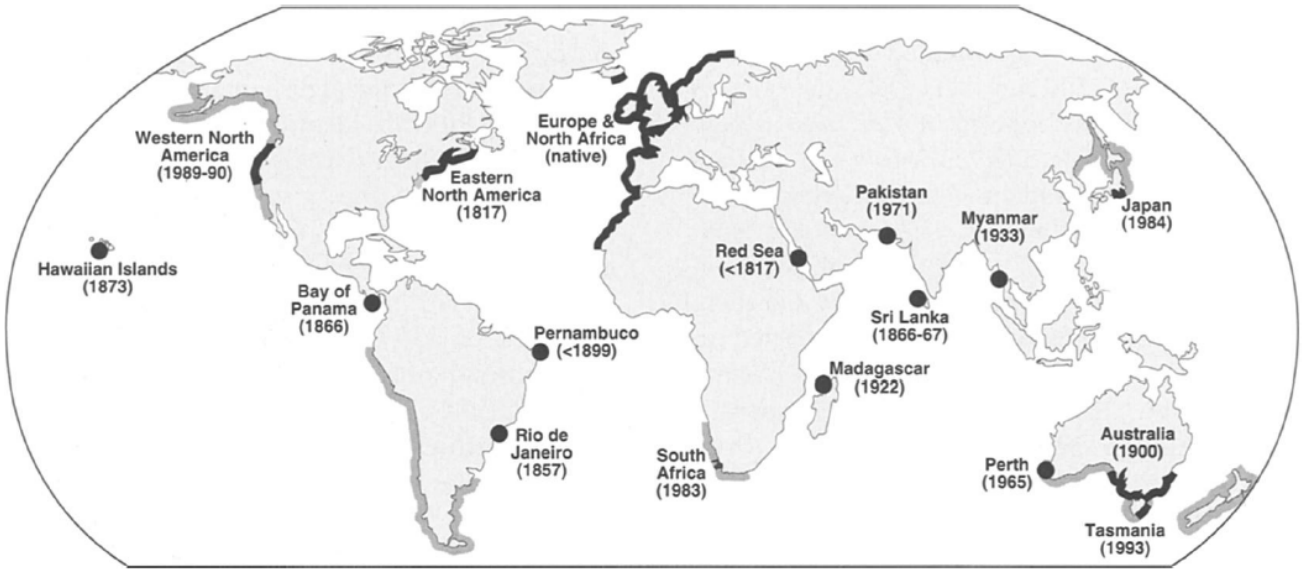

Figure 1.5. Occupied and potential range of *Carcinus maenas*. Black bands: occupied range of *C. maenas* or populations with *C. maenas* genes. Gray bands: potential range of *C. maenas*. Black circles: one-time collections of *Carcinus* species in regions without established populations. First or one-time collection dates are given (from Carlton and Cohen 2003).

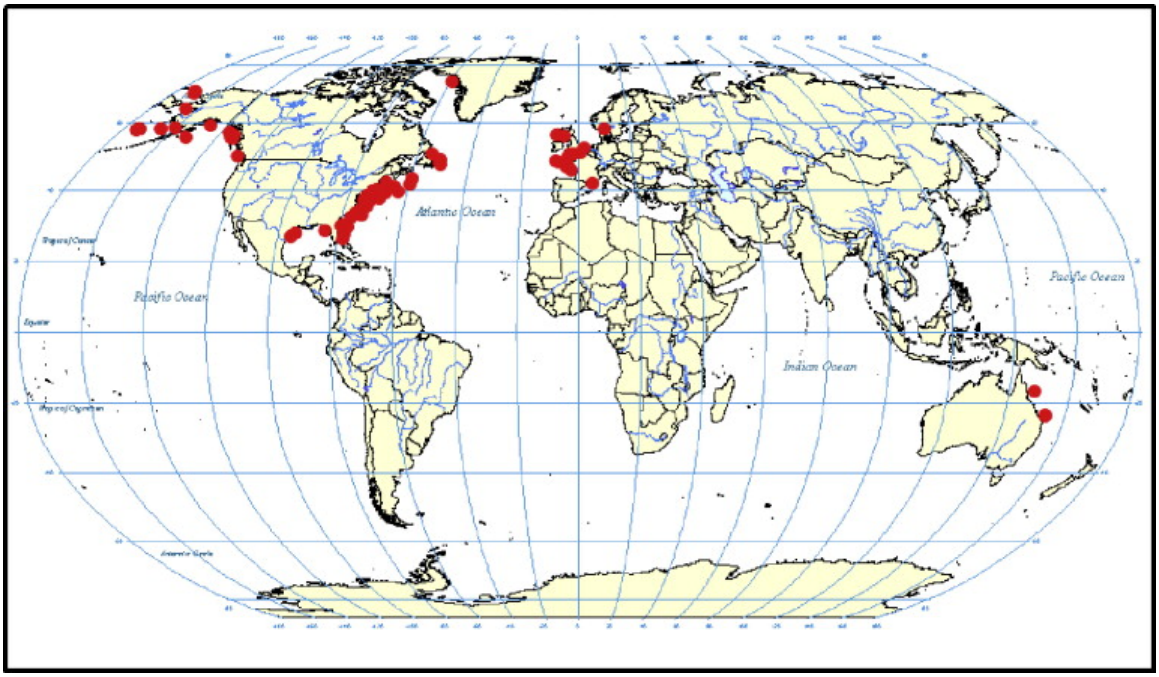

Figure 1.6. Worldwide distribution of *Hematodinium* and *Hematodinium*-like organisms (red dots) in various crustaceans (from Morado 2011).

1.11. Research Objectives and Rationale

The current study investigates the histopathology of *Hematodinium in vivo* in Newfoundland snow crabs *Chionoecetes opilio*. Snow crab *Chionoecetes opilio* are marine crustaceans found in the North Atlantic and North Pacific oceans. Canada is the world's largest producer of snow crab accounting for approximately two-thirds of the global supply with total landings in 2013 of 98,065 tonnes. Snow crab is the second most valuable Canadian fishery export product, with exports valued at $434.2 million in 2013 (www.dfo-mpo.gc.ca). Newfoundland and Labrador support the largest fishery for snow crab and the snow crab fishery is considered to be a lynchpin of the rural economy (Hermann and Greenberg 2007, Davis and Korneski 2012, Mullowney et al 2014).

Bitter Crab Disease (BCD) is one of the three main diseases of *Chionoecetes* crabs; the remaining two principle diseases of snow crabs are the shell diseases black mat syndrome (BMS), caused by the ascomycete fungus *Trichomaris invadens*, and black spot (or brown, rust, or burn spot) which is caused by chitinolytic bacteria (Kon et al 2011). The incidence of late-stage BCD (i.e., macroscopically visible BCD) in this host is generally low (0.11 – 3.7%) but is higher within subpopulations of snow crabs (i.e., those with intermediate carapace width) and several outbreaks of disease have occurred in this region with mortalities up to 24% in trapped males (Taylor and Khan 1995, Pestal et al 2003, Shields et al 2005, Shields et al 2007, Wheeler et al 2007, Mullowney et al 2011). The pathology of the late stages of disease was described in this host (Wheeler et al 2007). However, histologic screening of snow crabs without

macroscopic evidence of (late-stage) hematodiniosis in an attempt to identify and describe early stages of BCD in snow crabs has not previously been pursued. Although co-infections with other pathogens have been reported in other species of crustaceans with hematodiniosis, no such co-infections have been reported in snow crabs.

The *in vitro* life stages for *Hematodinium* sp. had previously been described in other crustacean hosts (Norway lobsters and blue crabs; Appleton and Vickerman 1998, Li et al 2011). More recently our research described the *in vitro* life stages of *Hematodinium* sp. isolated from snow crabs with late stage BCD and compared to them to those observed in other crustacean hosts (Gaudet et al 2015). However, comparisons of those *in vivo* and *in vitro* life stages of *Hematodinium* in snow crabs have not been thoroughly investigated.

The metabolic demand of BCD and/or starvation reduces the protein constituents of the host and results in significant reductions in tissue glycogen reserves contributing to host morbidity and mortality (Love et al 1996, Stentiford et al 2000, 2001a, Shields et al 2003). Alterations in targeted metabolites (such as hemocyanin, lactate, and free amino acids) have been noted in association with BCD (Field et al 1992, Love et al 1996, Taylor et al 1996, Stentiford et al 1999, Stentiford et al 2000, Shields et al 2003). Untargeted evaluation of the hemolymph metabolome of crustaceans with BCD has not previously been attempted, an investigation which could elucidate the cause of the bitter taste associated with the disease.

The main objectives of this study were: 1) to identify (if possible) and describe the early stages of *Hematodinium* sp. via histologic examination of Atlantic Canadian snow crabs, 2) compare the *in vivo* life stages of *Hematodinium* infection to life stages described *in vitro* from Atlantic Canadian snow crabs, 3) describe any co-infections seen in BCD-infected animals, and 4) screen snow crab hemolymph for metabolic changes associated with BCD. These aims would aid in our understanding of the pathogenesis of Bitter Crab Disease in snow crabs, one of the major diseases affecting snow crab in our region.

1.12. References

Adachi K, Endo H, Watanabe T, Nishioka T, Hirata T. 2005. Hemocyanin in the exoskeleton of crustaceans: enzymatic properties and immunolocalization. Pigment Cell Res 18(2):136-143.

Alvarez JV, Chung JS. 2013. Cloning of prophenoloxidase from hemocytes of the blue crab, *Callinectes sapidus* and its expression and enzyme activity during the molt cycle. Fish Shellfish Immunol 35(5):1349-1358.

Appleton PL, Vickerman K. 1998. *In vitro* cultivation and developmental cycle in culture of a parasitic dinoflagellate (*Hematodinium* sp.) associated with mortality of the Norway lobster (*Nephrops norvegicus*) in British waters. Parasitology 116(2):115-130.

Ashton GV, Willis KJ, Cook EJ, Burrows M. 2007. Distribution of the introduced amphipod, *Caprella mutica* Schurin, 1935 (Amphipoda: Caprellida: Caprellidae) on the west coast of Scotland and a review of its global distribution. Hydrobiologia 590(1): 31-41.

Bartoshuk LM, Rifkin B, Marks LE, Hooper JE. 1988. Bitterness of KCl and benzoate: related to genetic status for sensitivity to PTC/PROP. Chem Senses 13(4):517-528.

Bednarski, J., C. Siddon, G. Bishop, and J. F. Morado. 2010. Overview of bitter crab disease in Tanner crabs, *Chionoecetes bairdi*, in Southeast Alaska from 2001 to 2008. Biology and Management of Exploited Crab Populations under Climate Change. Alaska Sea Grant, University of Alaska Fairbanks. Anchorage, AK. Pp 317-333.

Bower SM, Meyer GR, Phillips A, Workman G, Clark D. 2003. New host and range extension of bitter crab syndrome in *Chionoecetes* spp. caused by *Hematodinium* sp. Bulletin of the European Association of Fish Pathologists 23(2):86-91.

Bower SM, Carnegie RB, Goh B, Jones SRM, Lowe GJ, Mak MWS. 2004. Preferential PCR amplification of parasitic protistan small subunit rDNA from metazoan tissues. J Eukaryot Microbiol 51(3):325-332.

Breslin PA, Beauchamp GK. 1997. Salt enhances flavor by suppressing bitterness. Nature 387(6633): 563.

Briggs RP, McAliskey M. 2002. The prevalence of *Hematodinium* in *Nephrops norvegicus* from the western Irish sea. J Mar Biol Assoc UK 82(3):427-433.

Cachon J, Cachon M. 1987. Parasitic dinoflagellates. *The biology of dinoflagellates.* Oxford: Blackwell Scientific. Pp.571-610.

Carlton JT, Cohen AN. 2003. Episodic global dispersal in shallow water marine organisms: the case history of the European shore crabs *Carcinus maenas* and *C. aestuarii*. J Biogeogr 30(12):1809-1820.

Chatton É, Poisson R. 1931. Sur l'existence dans le sang des crabes, de péridiniens parasites: *Hematodinium perezi* n.g., n.sp. (Syndinidae). C R Seances Soc Biol Paris 105: 553–557.

Chualáin CN, Hayes M, Allen B, Robinson M. 2009. *Hematodinium* sp. in Irish *Cancer pagurus* fisheries: infection intensity as a potential fisheries management tool. Dis Aquat Org 83(1):59-66.

Chualáin CN, Robinson M. 2011. Comparison of assessment methods used to diagnose *Hematodinium* sp. infections in *Cancer pagurus*. ICES J Mar Sci 68(3):454-462.

Coats DW. 1999. Parasitic life styles of marine dinoflagellates. J Eukaryot Microbiol 46(4): 402-409.

Couch JA. 1983. Diseases caused by Protozoa. The Biology of Crustacea, Pathobiology. 6:79-111.

Davis R, Korneski K. 2012. In a pinch: snow crab and the politics of crisis in Newfoundland. Labour-Le Travail 69(1):119-145.

Dawe EG. 2002. Trends in prevalence of Bitter Crab Disease caused by *Hematodinium* sp. in snow crabs (*Chionoecetes opilio*) throughout the Newfoundland and Labrador continental shelf. *In* Crabs in Cold Water Regions: Biology, Management and Economics. Alaska Sea Grant College Program, AK-SG-02-02: 385-400.

Dawe E, Mullowney D, Colbourne E, Han G, Morado JF, Cawthorn R. 2010. Relationship of oceanographic variability with distribution and prevalence of bitter crab syndrome in snow crab (*Chionoecetes opilio*) on the Newfoundland–Labrador shelf. *In:* Biology and management of exploited crab populations under climate change. Alaska Sea Grant College Program, AK-SG-10-01:175-198.

Destoumieux-Garzón D, Saulnier D, Garnier J, Jouffrey C, Bulet P, Bachère E. 2001. Crustacean immunity antifungal peptides are generated from the c terminus of shrimp hemocyanin in response to microbial challenge. J Biol Chem 276(50):47070-47077.

Drewnowski A. 2001. The science and complexity of bitter taste. Nutr Rev 59(6):163-169.

Drewnowski A, Gomez-Carneros C. 2000. Bitter taste, phytonutrients, and the consumer: a review. Am J Clin Nutr 72(6):1424-1435.

Dyson W, Schott E, Pitula JS, Hanif A. 2009. A PCR-based assay for detection of *Hematodinium* sp. in sediment from the Maryland coastal bays. The Fifth Education and Science Forum, abstract.

Eaton WD, Love DC, Botelho C, Meyers TR, Imamura K, Koeneman T. 1991. Preliminary results on the seasonality and life cycle of the parasitic dinoflagellate causing Bitter Crab Disease in Alaskan Tanner crabs (*Chionoecetes bairdi*). J Invertebr Pathol 57(3): 426-434.

Eigemann F, Burmeister A, Skovgaard A. 2010. *Hematodinium* sp. (Alveolata, Syndinea) detected in marine decapod crustaceans from waters of Denmark and Greenland. Dis Aquat Org 92(1):59-68.

Field RH, Appleton PL. 1995. A *Hematodinium* -like dinoflagellate infection of the Norway lobster *Nephrops norvegicus*: Observations on pathology and progression of infection. Dis Aquat Org 22(2):115-128.

Field RH, Appleton PL. 1996. An indirect fluorescent antibody technique for the diagnosis of *Hematodinium* sp. infection of the Norway lobster *Nephrops norvegicus*. Dis Aquat Org 24(3):199-204.

Field RH, Hills JM, Atkinson RJA, Magill S, Shanks AM. 1998. Distribution and seasonal prevalence of *Hematodinium* sp. infection of the Norway lobster (*Nephrops norvegicus*) around the west coast of Scotland. ICES J Mar Sci 55(5):846-858.

Field RH, Chapman CJ, Taylor AC, Neil DM, Vickerman K. 1992. Infection of the Norway lobster *Nephrops norvegicus* by a *Hematodinium*-like species of dinoflagellate on the west coast of Scotland. Dis Aquat Org 13(1):1-15.

Fredrick WS, Ravichandran S. 2012. Hemolymph proteins in marine crustaceans. Asian Pac J Trop Biomed 2(6):496-502.

Frischer ME, Lee RF, Sheppard MA, Mauer A, Rambow F, Neumann M, Brofft JE, Wizenmann T, Danforth JM. 2006. Evidence for a free-living life stage of the blue crab parasitic dinoflagellate, *Hematodinium* sp. Harmful Algae 5(5):548-557.

Gaines G, Taylor FJR. 1984. Extracellular digestion in marine dinoflagellates. J Plankton Res 6(6): 1057-1061.

Gaudet PH, Cawthorn RJ, Buote MA, Morado JF, Wright GM, Greenwood SJ. 2015. In vitro cultivation of *Hematodinium* sp. isolated from Atlantic snow crab, *Chionoecetes opilio*: partial characterization of late developmental stages. Parasitology 142(4):598-611.

Gilbert PM, Legrand C. 2006. The diverse nutrient strategies of harmful algae: focus on osmotrophy. Pp 163-175. *In* E. Graneli and JT Turner (Eds.) Ecology of Harmful Algae. Ecological studies 189.

Gomez F, Skovgaard A. 2015. The molecular phylogeny of the type-species of *Oodinium* Chatton, 1912 (Dinoflagellata: Oodiniaceae), a highly divergent parasitic dinoflagellate with non-dinokaryotic features. Syst Parasitol 90(2):125-135.

Gornik SG, Cranenburgh A, Waller RF. 2013. New host range for *Hematodinium* in southern Australia and new tools for sensitive detection of parasitic dinoflagellates. PLoS One 8(12):e82774.

Gruebl T, Frischer ME, Sheppard M, Neumann M, Maurer AN, Lee RF. 2002. Development of an 18S rRNA gene-targeted PCR-based diagnostic for the blue crab parasite *Hematodinium* sp. Dis Aquat Org 49(1):61-70.

Hamilton KM, Morritt D, Shaw PW. 2010a. Genetic diversity of the crustacean parasite *Hematodinium* (Alveolata, Syndinea). Eur J Protistol 46(1):17-28.

Hamilton KM, Shaw PW, Morritt D. 2009. Prevalence and seasonality of *Hematodinium* (Alveolata: Syndinea) in a Scottish crustacean community. ICES J Mar Sci 66(9):1837-1845.

Hamilton KM, Shaw PW, Morritt D. 2010b. Physiological responses of three crustacean species to infection by the dinoflagellate-like protist *Hematodinium* (Alveolata: Syndinea). J Invertebr Pathol 105(2):194-196.

Hamilton KM, Morritt D, Shaw PW. 2007. Molecular and histological identification of the crustacean parasite *Hematodinium* sp. (Alveolata, Syndinea) in the shore crab *Carcinus maenas*. Acta Protozool 46(3):183-192.

Hauton C, Brockton V, Smith VJ. 2006. Cloning of a crustin-like, single whey-acidic-domain, antibacterial peptide from the haemocytes of the European lobster, *Homarus gammarus*, and its response to infection with bacteria. Mol Immunol 43(9):1490-1496.

Hayashi T, Yamaguchi K, Konosu S. 1981. Sensory analysis of taste-active components in the extract of boiled snow crab meat. J Food Sci 46(2):479-483.

Hermann M, Greenberg J. 2007. The demand and allocation of Alaskan and Canadian snow crab. Can J Agr Econ 55(1):27-48.

Hudson DA, Adlard RD. 1996. Nucleotide sequence determination of the partial SSU rDNA gene and ITS1 region of *Hematodinium* cf. *perezi* and *Hematodinium* -like dinoflagellates. Dis Aquat Org 24(1):55-60.

Hudson DA, Hudson NB, Shields JD. 1993. Infection of *Trapezia* spp. (Decapoda: Xanthidae) by *Hematodinium* sp. (Duboscquodinida: Syndinidae): a new family record of infection. J Fish Dis 16(3):273-276.

Hudson DA, Lester RJ. 1994. Parasites and symbionts of wild mud crabs *Scylla serrata* (Forskal) of potential significance in aquaculture. Aquaculture 120(3-4):183-99.

Hudson DA, Shields JD. 1994. *Hematodinium australis* n. sp., a parasitic dinoflagellate of the sand crab *Portunus pelagicus* from Moreton Bay, Australia. Dis Aquat Org 19(2):109-119.

Jaenicke E, Föll R, Decker H. 1999. Spider hemocyanin binds ecdysone and 20-OH-ecdysone. J Biol Chem 274(48):34267-34271.

Jensen PC, Califf K, Lowe V, Hauser L, Morado JF. 2010. Molecular detection of *Hematodinium* sp. in northeast Pacific *Chionoecetes* spp. and evidence of two species in the northern hemisphere. Dis Aquat Org 89(2):155-166.

Jiravanichpaisal P, Lee BL, Söderhäll K. 2006. Cell-mediated immunity in arthropods: hematopoiesis, coagulation, melanization and opsonization. Immunobiology 211(4): 213-236.

Johansson MW, Keyser P, Sritunyalucksana K, Söderhall K. 2000. Crustacean hemocytes and hematopoiesis. Aquaculture 191(1-3):45-52.

Johnson PT. 1986. Parasites of benthic amphipods: dinoflagellates (Duboscquodinida: Syndinidae). Fish Bull 84(3):605-614.

Kon T, Isshiki T, Miyadai T, Honma Y. 2011. Milky hemolymph syndrome associated with an intranuclear bacilliform virus in snow crab *Chionoecetes opilio* from the Sea of Japan. Fisheries Sci 77(6):999-1007.

Konovalova GV. 2008. Parasitic dinoflagellates and ellobiopsids (Ellobiopsidae) of the coastal waters of the Sea of Japan. Russian J Mar Biol 34(1): 28-37.

Latrouite D, Morizur Y, Noel P, Chagot D, Wilhelm G. 1988. Mortalité du tourteau *Cancer pagurus* provoquée par le dinoflagelle parasite: *Hematodinium* sp. ICES: Comité des Mollusques et Crustacés 1988.

Leander BS, Keeling PJ. 2003. Morphostasis in alveolate evolution. Trends Ecol Evolution 18(8):395-402.

Leander BS, Keeling PJ. 2004 Early evolutionary history of dinoflagellates and apicomplexans (Alveolata) as inferred from HSP90 and actin phylogenies. J Phycol 40(2):341-350.

Lee RR, Frischer ME. 2004. The decline of the blue crab. Am Sci 92(6):548-553.

Levy MG, Litaker RW, Goldstein RJ, Dykstra MJ, Vandersea MW, Noga EJ. 2007. *Piscinoodinium*, a fish-ectoparasitic dinoflagellate, is a member of the class Dinophyceae, subclass Gymnodiniphyceae: convergent evolution with *Amyloodinium*. J Parasitol 93(5):1006-1015.

Li YY, Xia XA, Wu QY, Liu WH, Lin YS. 2008. Infection with *Hematodinium* sp. in mud crabs *Scylla serrata* cultured in low salinity water in southern China. Dis Aquat Org 82(2):145-150.

Li C, Shields JD, Miller TL, Small HJ, Pagenkopp KM, Reece KS. 2010. Detection and quantification of the free-living stage of the parasitic dinoflagellate *Hematodinium* sp. in laboratory and environmental samples. Harmful Algae 9(5):515-521.

Li C, Miller TL, Small HJ, Shields JD. 2011a. *In vitro* culture and developmental cycle of the parasitic dinoflagellate *Hematodinium* sp. from the blue crab *Callinectes sapidus*. Parasitology 138(14):1924-1934.

Li C, Song S, Liu Y, Chen T. 2013. Hematodinium infections in cultured Chinese swimming crab, *Portunus trituberculatus*, in northern China. Aquaculture 396(2013):59-65.

Li C, Wheeler KN, Shields JD. 2011b. Lack of transmission of *Hematodinium* sp. in the blue crab *Callinectes sapidus* through cannibalism. Dis Aquat Org 96(3):249-258.

Li M, Wang J, Song S, Li C. 2015. Early transcriptional response to the parasitic dinoflagellate *Hematodinium* in hepatopancreas of *Portunus trituberculatus*. J Invertebr Pathol 130:28-36.

Liem DG, Miremadi F, Keast RSJ. 2011. Reducing sodium in foods: the effect on flavor. Nutrients 3(6):694-711

Lin YC, Chen JC, Man SNC, Morni WZW, Suhaili ASNA, Cheng SY, Hsu CH. 2012. Modulation of innate immunity and gene expressions in white shrimp *Litopenaeus vannamei* following long-term starvation and re-feeding. Results Immunol 2:148-156.

Lohan KM, Reece KS, Miller TL, Wheeler KN, Small HJ, Shields JD. 2012. The role of alternate hosts in the ecology and life history of *Hematodinium* sp., a parasitic dinoflagellate of the blue crab (*Callinectes sapidus*). J Parasitol 98(1):73-84.

Love DC, Rice SD, Moles DA, Eaton WD. 1993. Seasonal prevalence and intensity of Bitter Crab dinoflagellate infection and host mortality in Alaskan Tanner crabs *Chionoecetes bairdi* from Auke Bay, Alaska, USA. Dis Aquat Org 15(1): 1-7.

Love D, Thomas T, Moles A. 1996. Bitter crab hemolymph studies: indications of host physiological condition. High Latitude Crabs: Biology Management and Economics. Alaska Sea Grant College Program. AK-SG-96-02:549-562.

Lovrich GA, Sainte-Marie B. 1997. Cannibalism in the snow crab, *Chionoecetes opilio* (O. Fabricius) (Brachyura: Majidae), and its potential importance to recruitment. J Exp Mar Biol Ecol 211(2):225-245.

Maciel JES, Souza F, Valle S, Kucharski LC, da Silva RS. 2008. Lactate metabolism in the muscle of the crab *Chasmagnathus granulatus* during hypoxia and post-hypoxia recovery. Comp Biochem Physiol A Mol Integr Physiol 151(1):61-65.

MacLean SA, Ruddell CL. 1978. Three new crustacean hosts for the parasitic dinoflagellate *Hematodinium perezi* (Dinoflagellata: Syndinidae). J Parasitol 64(1):158-160.

Maehashi K, Huang L. 2009. Bitter peptides and bitter taste receptors. Cell Mol Life Sci 66(10):1661-1671.

Marcogliese DJ. 2008. The impact of climate change on the parasites and infectious diseases of aquatic animals. Rev Sci Tech 27(2):467-484.

Matozzo V, Gallo C, Marin MG. 2011. Can starvation influence cellular and biochemical parameters in the crab *Carcinus aestuarii*? Mar Environ Res 71(3):207-212.

Messick GA. 1994. *Hematodinium perezi* infections in adult and juvenile blue crabs *Callinectes sapidus* from coastal bays of Maryland and Virginia, USA. Dis Aquat Org 19(1):77-82.

Messick GA and Shields JD. 2000. Epizootiology of the parasitic dinoflagellate *Hematodinium* sp. in the American blue crab *Callinectes sapidus*. Dis Aquat Org 43(2):139-152.

Meyerhof W. 2005. Elucidation of mammalian bitter taste. *Reviews of physiology, biochemistry and pharmacology*. Springer Berlin Heidelberg. pp 37-72.

Meyers TR, Botelho C, Koeneman TM, Short S, Imamura K. 1990. Distribution of bitter crab dinoflagellate syndrome in southeast Alaskan Tanner crabs *Chionoecetes bairdi*. Dis Aquat Org 9(1):37-43.

Meyers TR, Burton T. 2009. Diseases of wild and cultured shellfish in Alaska. Alaska Department of Fish & Game, Anchorage, AK.

Meyers TR, Lightner DV, Redman RM. 1994. A dinoflagellate-like parasite in Alaskan spot shrimp *Pandalus platyceros* and pink shrimp *P. borealis.* Dis Aquat Org 18(1):71-76.

Meyers TR, Koeneman TM, Botelho C, Short S. 1987. Bitter crab disease: a fatal dinoflagellate infection and marketing problem for Alaskan tanner crabs *Chionoecetes bairdi*. Dis Aquat Org 3(3):195-216.

Morado JF. 2011. Protistan diseases of commercially important crabs: a review. J Invert Pathol 106(1): 27-53.

Mullowney DR, Dawe EG, Morado JF, Cawthorn RJ. 2011. Sources of variability in prevalence and distribution of bitter crab disease in snow crab (*Chionoecetes opilio*) along the northeast coast of Newfoundland. ICES J Mar Sci 68(3):463-471.

Mullowney DR, Dawe EG, Colbourne EB, Rose GA. 2014. A review of factors contributing to the decline of Newfoundland and Labrador snow crab (*Chionoecetes opilio*). Rev Fish Biol Fisher 24(2):639-657.

Nagle L, Place AR, Schott EJ, Jagus R, Messick G, Pitula JS. 2009. Real-time PCR-based assay for quantitative detection of *Hematodinium* sp. in the blue crab *Callinectes sapidus*. Dis Aquat Org 84(1):79-87.

Newman MW, Johnson CA. 1975. A disease of blue crabs (*Callinectes sapidus*) caused by a parasitic dinoflagellate, *Hematodinium* sp. J Parasitol 61(3):554-557.

Nikolov S, Petrov M, Lymperakis L, Friak M, Sachs C, Fabritius HO, Raabe D, Neugebauer J. 2010 Revealing the design principles of high-performance biological composites using *ab initio* and multiscale simulations: the example of lobster cuticle. Adv Mater 22(4):519-526.

Noga EJ, Levy MG. 2006. Dinoflagellida (Phylum Sarcomastigophora). Pp 116-153. *In* PTK Woo (Ed) Fish Diseases and Disorders. Volume 1: protozoan and metazoan infections. 2nd Edition. CABI, Wallingford, UK.

Oka Y, Butnaru M, von Buchholtz L, Ryba NJ, Zuker CS. 2013. High salt recruits aversive taste pathways. Nature 494(7438):472–475.

Pagenkopp Lohan KM, Reece KS, Miller TL, Wheeler KN, Small HJ, Shields JD. 2012. The role of alternate hosts in the ecology and life history of Hematodinium sp., a parasitic dinoflagellate of the blue crab (Callinectes sapidus). J Parasitol 98(1):73-84.

Paul RJ, Pirow R. 1998. The physiological significance of respiratory proteins in invertebrates. Zoology 100(4):298-306.

Pauley GB, Newman MW, Gould ED. 1975. Serum changes in the blue crab, *Callinectes sapidus*, associated with *Paramoeba perniciosa*, the causative agent of gray crab disease. Mar Fish Rev 37:34-38.

Pestal GP, Taylor DM, Hoenig JM, Shields JD, Pickavance R. 2003. Monitoring the prevalence of the parasitic dinoflagellate *Hematodinium* sp. in snow crabs *Chionoecetes opilio* from Conception Bay, Newfoundland. Dis Aquat Org 53(1):67-75.

Pinfold, G. 2006. Overview of the Atlantic snow crab industry. Department of Fisheries and Oceans, Atlantic Council of Fisheries and Aquaculture Ministers. http://www.dfo-mpo.gc.ca/fm-gp/peches-fisheries/reports-rapports/sc-cn_e.pdf

Pitula JS, Dyson WD, Bacht HB, Njoku I, Chen F. 2012. Temporal distribution of genetically homogenous "free-living" *Hematodinium* sp. in a Delmarva costal ecosystem. Aquat Biosyst. 8(1):16.

Rackis JJ, Sessa DJ, Honig DH. 1979. Flavor problems of vegetable food proteins. J Am Oil Chem Soc 56(3):262-271.

Rizzo PF. 2003. Those amazing dinoflagellate chromosomes. Cell Research 13(4):215-217.

Rowley AF, Smith AL, Davies CE. 2015. How does the dinoflagellate parasite *Hematodinium* outsmart the immune system of its crustacean hosts? PLoS Pathog 11(5):e1004724.

Roper SD. 2015. The taste of table salt. Pflugers Arch 467(3):457-463.

Ryazanova TV. 2008. Bitter Crab Syndrome in Two Species of King Crabs from the Sea of Okhotsk. Russian J Mar Biol 34(6):411-414.

Ryazanova TV, Eliseikina MG, Kukhlevsky AD, Kharlamenko VI. 2010. *Hematodinium* sp. infection of red *Paralithodes camtschaticus* and blue *Paralithodes platypus* king crabs from the Sea of Okhotsk, Russia. J Invertebr Pathol 105(3):329-334.

Saavedra-Garcia L, Bernabe-Ortiz A, Gilman RH, Diez-Canseco F, Cardenas MK, Sacksteder KA, Miranda JJ. 2015. Applying the triangle taste test to assess the differences between low sodium salts and common salt: evidence from Peru. PLoS One 10(7):e0134700.

Saldarriaga JF, Taylor FJR, Cavalier-Smith T, Menden-Deuer S, Keeling PJ. 2004. Molecular data and the evolutionary history of dinoflagellates. J Protistol 40(1):85-111.

Sheppard M, Walker A, Frischer ME, Lee RF. 2003. Histopathology and prevalence of the parasitic dinoflagellate, *Hematodinium* sp., in crabs (*Callinectes sapidus, Callinectes similis, Neopanope sayi, Libinia emarginata, Menippe mercenaria*) from a Georgia estuary. J Shellfish Res 22(3):873-880.

Shields JD. 1992. Parasites and symbionts of the crab *Portunus pelagicus* from Moreton Bay, eastern Australia. J Crust Biol 12(1):94-100.

Shields JD. 1994. The parasitic dinoflagellates of marine crustaceans. Ann Rev Fish Dis 4:241-271.

Shields JD, Pickavance R. 2003. Monitoring the prevalence of the parasitic dinoflagellate *Hematodinium* sp. in snow crabs *Chionoecetes opilio* from Conception Bay, Newfoundland. Dis Aquat Org 53(1):67-75.

Shields JD, Scanlon C, Volety A. 2003. Aspects of the pathophysiology of blue crabs, *Callinectes sapidus*, infected with the parasitic dinoflagellate *Hematodinium perezi*. Bull Mar Sci 72(2):519-535.

Shields JD, Squyars CM. 2000. Mortality and hematology of blue crabs, *Callinectes sapidus,* experimentally infected with the parasitic dinoflagellate *Hematodinium perezi*. Fish Bull 98(1):139-152.

Shields JD, Sullivan SE, Small HJ. 2015. Overwintering of the parasitic dinoflagellate *Hematodinium perezi* in dredged blue crabs *Callinectes sapidus* from Wachapreague Creek, Virginia. J Invertebr Pathol 130(2015):124-132.

Shields JD, Taylor DM, Sutton SG, O'Keefe PG, Ings DW, Pardy AL. 2005. Epidemiology of Bitter Crab Disease (*Hematodinium* sp.) in snow crabs *Chionoecetes opilio* from Newfoundland, Canada. Dis Aquat Org 64(3):253-264.

Shields JD, Taylor DM, O'Keefe PG, Colbourne E, Hynick E. 2007. Epidemiological determinants in outbreaks of Bitter Crab Disease (*Hematodinium* sp.) in snow crabs *Chionoecetes opilio* from Conception Bay, Newfoundland, Canada. Dis Aquat Org 77(1):61-72.

Silberman JD, Collins AG, Gershwin LA, Johnson PJ, Roger AJ. Ellobiopsids of the genus *Thalassomyces* are alveolates. J Euk Microbiol 51(2):246-52.

Skovgaard A, Karpov SA, Guillou L. 2012. The parasitic dinoflagellates *Blastodinium* spp. inhabiting the gut of marine, planktonic copepods: morphology, ecology, and unrecognized species diversity. Front Microbiol 3:305.

Small HJ, Shields JD, Hudson KL, Reece KS. 2007a. Molecular detection of *Hematodinium* sp. infecting the blue crab, *Callinectes sapidus.* J Shellfish Res 26(1):131-139.

Small HJ, Shields JD, Moss A, Reece KS. 2007b. Conservation in the first internal transcribed spacer region (ITS1) in *Hematodinium* species infecting crustacean hosts found in the UK and Newfoundland. Dis Aquat Org 75(3):251-258.

Small HJ, Shields JD, Neil DM, Taylor AC, Coombs GH. 2007c. Differences in enzyme activities between two species of *Hematodinium*, parasitic dinoflagellates of crustaceans. J Invertebr Pathol 94(3):175-183.

Small HJ, Shields JD, Reece KS, Bateman K, Stentiford GD. 2012. Morphological and molecular characterization of *Hematodinium perezi* (Dinophyceae: Syndiniales), a dinoflagellate parasite of the harbour crab, *Liocarcinus depurator*. J Eukaryot Microbiol 59(1):54-66.

Small HJ, Neil DM, Taylor AC, Atkinson RJA, Coombs GH. 2006. Molecular detection of *Hematodinium* spp. in Norway lobster *Nephrops norvegicus* and other crustaceans. Dis Aquat Org 69(2):185-195.

Small HJ, Wilson S, Neil DM, Hagan P, Coombs GH. 2002. Detection of the parasitic dinoflagellate *Hematodinium* in the Norway lobster *Nephrops norvegicus* by ELISA. Dis Aquat Org 52(2):175-177.

Smith AL, Hamilton KM, Hirschle L, Wootton EC, Vogan CL, Pope EC, Eastwood DC, Rowley AF. 2013. Characterization and molecular epidemiology of a fungal infection of edible crabs (*Cancer pagurus*) and interaction of the fungus with the dinoflagellate parasite *Hematodinium*. Appl Environ Microbiol 79(3):783-793.

Smayda TJ. 1997. Harmful algal blooms: their ecophysiology and general relevance to phytoplankton blooms in the sea. Limnol Oceanogr 42(5):1137-1153.

Squires HJ, Dawe EG. 2003. Stomach contents from snow crab (*Chionoecetes opilio,* Decapoda, Brachyura) from the northeast Newfoundland Shelf. J Northw Atl Fish Sci 32(2003):27-38.

Stentiford GD, Bateman KS, Small HJ, Pond M, Ungfors A. 2012. *Hematodinium* sp. and its bacteria-like endosymbiont in European brown shrimp (*Crangon crangon*). Aquat Biosyst. 8(1):1.

Stentiford GD, Chang ES, Chang SA, Neil DM. 2001a. Carbohydrate dynamics and the crustacean hyperglycemic hormone (CHH): Effects of parasitic infection in Norway lobsters (*Nephrops norvegicus*). Gen Comp Endocrinol 121(1):13-22.

Stentiford GD, Evans M, Bateman K, Feist SW. 2003. Co-infection by a yeast-like organism in *Hematodinium* -infected European edible crabs *Cancer pagurus* and velvet swimming crabs *Necora puber* from the English Channel. Dis Aquat Org 54(3):195-202.

Stentiford GD, Feist SW. 2005. A histopathological survey of shore crab (*Carcinus maenas*) and brown shrimp (*Crangon crangon*) from six estuaries in the United Kingdom. J Invert Pathol 88(2):136–146

Stentiford GD, Green M, Bateman K, Small HJ, Neil DM, Feist SW. 2002. Infection by a *Hematodinium* -like parasitic dinoflagellate causes Pink Crab Disease (PCD) in the edible crab *Cancer pagurus*. J Invertebr Pathol 79(3):179-191.

Stentiford GD, Neil DM. 2011. Diseases of *Nephrops* and *Metanephrops*: a review. J Invert Path 106(1):92-109.

Stentiford GD, Neil DM, Atkinson RJA. 2001b. Alteration of burrow-related behaviour of the Norway lobster, *Nephrops norvegicus,* during infection by the parasitic dinoflagellate *Hematodinium*. Mar Freshwat Behav Physiol 34(3):139-156.

Stentiford GD, Neil DM, Atkinson RJ, Bailey N. 2000b. An analysis of swimming performance in the Norway lobster, *Nephrops norvegicus* L. infected by a parasitic dinoflagellate of the genus *Hematodinium*. J Exp Mar Biol Ecol 247(2):169-181.

Stentiford GD, Neil DM, Coombs GH. 1999. Changes in the plasma free amino acid profile of the Norway lobster *Nephrops norvegicus* at different stages of infection by a parasitic dinoflagellate (genus *Hematodinium*). Dis Aquat Org 38(2):151-157.

Stentiford GD, Neil DM, Coombs GH. 2000a. Alterations in the biochemistry and ultrastructure of the deep abdominal flexor muscle of the Norway lobster *Nephrops norvegicus* during infection by a parasitic dinoflagellate of the genus *Hematodinium*. Dis Aquat Organ 42(2):133-141.

Stentiford GD, Neil DM, Coombs GH. 2001c. Development and application of an immunoassay diagnostic technique for studying *Hematodinium* infections in *Nephrops norvegicus* populations. Dis Aquat Org 46(3):223-229.

Stentiford GD, Shields JD. 2005. A review of the parasitic dinoflagellates *Hematodinium* species and *Hematodinium* -like infections in marine crustaceans. Dis Aquat Org 66(1):47-70.

Stephan A, Steinhart H. 2000. Bitter taste of unsaturated free fatty acids in emulsions: contribution to the off-flavour of soybean lecithins. Eur Food Res Technol 212(1):17-25.

Stevenson JR. 1985. Dynamics of the integument. *The biology of the crustacea: integument, pigments, and hormonal processes, Vol. 9.* Academic Press, Orlando FL. Pp. 1-42.

Stewart JE, Cornick JW, Dingle JR. 1967. An electronic method for counting lobster (*Homarus americanus* Milne Edwards) hemocytes and the influence of diet on hemocyte numbers and hemolymph proteins. Can J Zool 5(3):291-304.

Stewart JE, Zwicker BM, Arie B, Horner GW. 1972. Food and starvation as factors affecting the time to death of the lobster *Homarus americanus* infected with *Gaffkya homari*. J Fish Res Board Can 29(4):461–464.

Stoecker D, Tillman U, Graneli E. 2006. Phagotrophy in harmful algae. Pp 177-187. *In* E. Graneli and JT Turner (Eds.) Ecology of Harmful Algae. Ecological studies 189. Springer-Verlag Berlin Heidelberg.

Tärnlund S. 2000. A comparison of two methods for identifying and assessing the parasitic dinoflagellate *Hematodinium* sp. in Norway lobster (*Nephrops norvegicus*). MSc Thesis.

Taylor FJR. 1987. *The biology of dinoflagellates.* Botanical Monographs, Vol. 21. Oxford: Blackwell Scientific. Pp 1-785.

Taylor FJR. 2006. Dinoflagellates. eLS.

Taylor AC, Field RH, Parslow-Williams PJ. 1996. The effects of *Hematodinium* sp.-infection on aspects of respiratory physiology of the Norway lobster, *Nephrops norvegicus* (L.). J Exp Mar Biol Ecol 207(1): 217-228.

Taylor DM, Khan RA. 1995. Observations on the occurrence of *Hematodinium* sp. (Dinoflagellata: Syndinidae), the causative agent of Bitter Crab Disease in Newfoundland snow crab (*Chionoecetes opilio*). J Invertebr Pathol 65(3):283-288.

Taylor FJR, Hoppenrath M, Saldarriaga JF. 2008. Dinoflagellate diversity and distribution. Biodivers Conserv 17(2):407-418.

Terwilliger NB, Ryan MC. 2006. Functional and phylogenetic analyses of phenoloxidases from brachyuran (*Cancer magister*) and branchiopod (*Artemia franciscana, Triops longicaudatus*) crustaceans. Biol Bull 210(1):38-50.

Troedsson C, Lee RF, Stokes V, Walters TL, Simonelli P, Frischer ME. 2008a. Development of a denaturing high-performance liquid chromatography method for detection of protist parasites of metazoans. Appl Environ Microbiol 74(14):4336-4345.

Troedsson C, Lee RF, Walters T, Stokes V, Brinkley K, Naegele V, Frischer ME. 2008b. Detection and discovery of crustacean parasites in blue crabs (*Callinectes sapidus*) by using 18S rRNA gene-targeted denaturing high-performance liquid chromatography. Appl Environ Microbiol 74(14):4346-4353.

Uglow RF. 1969a. Haemolymph protein concentrations in portunid crabs. I. Studies on adult *Carcinus maenas*. Comp Biochem Physiol 30(6):1083–1090.

Uglow RF. 1969b. Haemolymph protein concentrations in portunid crabs. II. The effects of imposed fasting on *Carcinus maenas*. Comp Biochem Physiol 31(6):959–967.

Urban D, Byersdorfer SC. 2002. Bitter crab syndrome in Tanner crab (*Chionoecetes bairdi*), Alitak Bay, Kodiak, Alaska 1991-2000. Crabs in Cold Water Region: Biology, Management, and Economics. Alaska Sea Grant Prog. AK-SG-02-01. 2002:401-403.

Usuki R, Kaneda T. 1980. Bitter taste of oxidized fatty acids. Agric Biol Chem 44(10):2477-2481.

Vacca LL, Fingerman M. 1983. The roles of hemocytes in tanning during the molting cycle: A histochemical study of the fiddler crab, *Uca pugilator*. Biol Bull 65(3):758-777.

Walker AN, Lee RF, Frischer ME. 2009. Transmission of the parasitic dinoflagellate *Hematodinium* sp. infection in blue crabs *Callinectes sapidus* by cannibalism. Dis Aquat Org 85(3):193-197.

Wheeler K, Shields JD, Taylor DM. 2007. Pathology of *Hematodinium* infections in snow crabs (*Chionoecetes opilio*) from Newfoundland, Canada. J Invertebr Pathol 95(2):93-100.

Wieczorek SK, Hooper RG. 1995. Relationship between diet and food availability in the snow crab *Chionoecetes opilio* (O. Fabricius) in Bonne Bay, Newfoundland. J Crust Biol 15(2):236-247.

Wilhelm G, Boulo V. 1988. Infection de l'etrille *Liocarcinus puber* (L.) par un dinoflagellate parasite de type *Hematodinium* sp. Int Counc Explor Sea CM-ICES/K:41.

Wilhelm G, Mialhe E. 1996. Dinoflagellate infection associated with the decline of *Necora puber* crab populations in France. Dis Aquat Org 26(3):213-219.

Williams-Ryan KA. 1997. Occurrence, histopathology and fine structural studies on *Hematodinium* sp. (Dinoflagellida: Syndinidae) parasitizing the snow crab (*Chionoecetes opilio*). Doctoral dissertation, Memorial University of Newfoundland.

Xu WJ, Shi H, Xu HX, Small HJ. 2007. Preliminary study on the *Hematodinium* infection in cultured *Portunus trituberculatus*. Acta Hydrobiologica Sinica 31(5):637-642.

Xu W, Xie J, Shi H, Li C. 2010. *Hematodinium* infections in cultured ridgetail white prawns, *Exopalaemon carinicauda,* in eastern China. Aquaculture 300(1-4):25-31.

2. DIAGNOSIS OF BCD IN NEWFOUNDLAND SNOW CRABS, *CHIONOECETES OPILIO*, BY MACROSCOPIC, MICROSCOPIC, AND MOLECULAR METHODS: A COMPARISON.

2.1. Introduction

Bitter Crab Disease (BCD) is a fatal disease of crustaceans caused by parasitic syndinian dinoflagellates of the genus *Hematodinium*. Infection with *Hematodinium* sp. was first reported off the coast of Europe in common shore crabs *Carcinus maenas* and blue-leg swimming crabs *Liocarcinus depurator* (Chatton and Poisson 1931). Over forty species of crustaceans have been reported as hosts for *Hematodinium* or *Hematodinium*-like infections with worldwide distribution concentrated in the North Pacific and Atlantic oceans (reviewed in Morado et al 2011; see Chapter 1, Table 1.1). In eastern Canada BCD was first reported in snow crabs *Chionoecetes opilio* from Conception Bay, Newfoundland in 1990 with very low disease prevalence (<0.11 – 3.7%; Taylor and Khan 1995). Subsequently, BCD has spread rapidly within the eastern and northeastern bays of Newfoundland and Labrador and has resulted in at least three epizootic disease outbreaks with prevalence up to 25% in some subpopulations of snow crabs (Shields et al 2005, 2007).

Hematodinium infections can be presumptively diagnosed macroscopically via visual examination in many affected species, due to characteristic discolorations of the carapace and/or arthrodial membranes which vary from pink to orange to chalky white (Hudson and Shields 1994, Messick 1994, Love et al 1996, Stentiford et al 2002, Wheeler et al 2007, Xu et al 2007, Li et al 2008). However, in some crustacean hosts *Hematodinium* spp. infections may not be associated with external discoloration (MacLean and Ruddell 1978, Hudson and Shields

1994, Ryazanova et al 2008). In snow crabs the advanced stages of BCD are associated with orangish-pink discoloration of the carapace, an opaque white appearance to the ventrum, and opaque white ("milky") hemolymph (Wheeler et al 2007).

Microscopically the late stages of disease are characterized by multisystemic infiltration of proliferating parasites within hemal sinuses and hemal spaces in interstitial tissues (Meyers et al 1987, Field et al 1992, Hudson and Shields 1994, Messick 1994, Field and Appleton 1995, Stentiford et al 2002, Sheppard et al 2003, Stentiford and Shields 2005, Wheeler et al 2007, Xu et al 2010, Li et al 2013). Methods for diagnosis of BCD include pleopod examination, stained hemolymph direct smears, indirect fluorescent antibody technique (IFAT), western blot, enzyme-linked immunosorbent (ELISA), and polymerase chain reaction (PCR) assays in a variety of crustacean hosts (Meyers et al 1987, Field et al 1992, Hudson and Adlard 1994, Field and Appleton 1995, Stentiford et al 2001,2002, Gruebl et al 2002, Small et al 2002,2006,2007, Bower et al 2003, Pestal et al 2003, Frischer et al 2006, Dyson et al 2009, Jensen et al 2010, Li et al 2010, Lohan et al 2012, Pitula et al 2012, Gornik et al 2013, Shields et al 2015; reviewed in Chapter section 1.5).

In this study we compared the diagnosis of BCD in Newfoundland snow crab, *C. opilio*, by visual gross macroscopic examination, light microscopic examination of histopathologic sections, and PCR assay. The intensity of infection in relation to diagnostic test success was also examined.

2.2. Materials and Methods

2.2.1. Snow Crab Collection

Atlantic snow crabs (*C. opilio*) were collected during annual Fall surveys in Notre Dame Bay (NDB) and White Bay (WB), Newfoundland, during September, 2010 and 2011. In Notre Dame Bay crabs were caught on the grounds of strata 610 and 611 (200-400 m in depth). In White Bay crabs were caught in strata 614 and 615 (200-400 m in depth) and the very deep stratum 613 (401-500m). NDB is an open ocean-type environment that becomes deeper with distance from shore while WB is a deep fjord-type environment protected at the mouth by a shallow sill and which is deepest inland (see Figure 2.1).

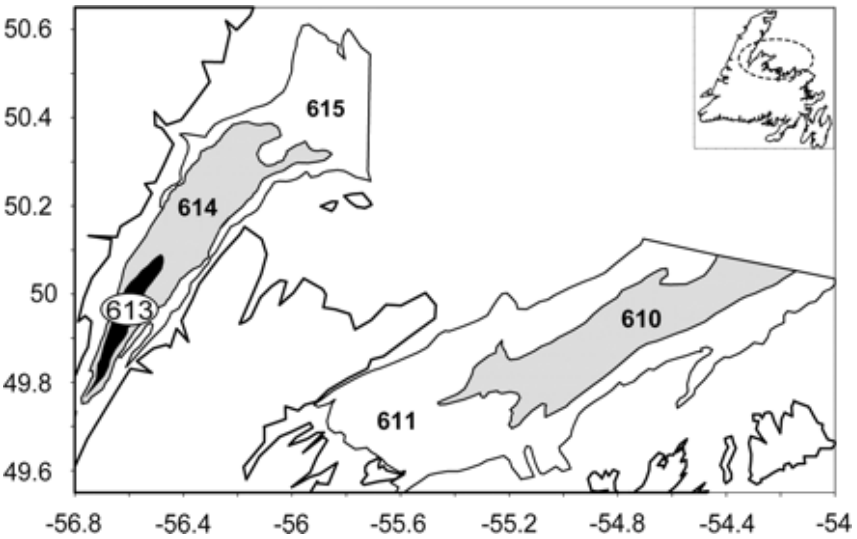

Figure 2.1. Map of the study area showing the depth strata in White Bay (WB) and Notre Dame Bay (NDB). Strata 615, 614, and 613 are in WB, and Strata 611 and 610 in NDB. White strata are 200–300 m, grey strata are 301–400 m, and the black stratum is 401–500 m (from Mullowney et al 2011).

The Fall survey had a target of 8 trap sets per stratum. Each set included 6 conical crab traps baited with squid. Crabs were sampled from two large-meshed (commercial, 135 mm) and two

small-meshed (27 mm) traps. Small-mesh trap positions alternated with those of large-meshed traps along each long line, and soak times were generally 24 h (weather permitting). Within each crab management area surveyed, the depth range and actual area sampled corresponded approximately to the commercial fishery area.

Shell condition was classified as soft, new, intermediate and old (Fonesca et al 2008, Dawe et al 2010; see section 2.2.5). New-shelled snow crabs are assumed to have molted during the most recent Spring whereas intermediate-shelled crabs are assumed to have molted in the previous year and old-shelled snow crabs two or more years previously (soft-shelled snow crabs were not collected). New-shelled snow crabs were selectively chosen for collection for this study as BCD is typically observed in new-shelled animals (Dawe 2002; Shields et al 2005, 2007; Wheeler et al 2007, Mullowney et al 2011).

Crabs were kept in coolers layered between seawater-soaked burlap, and placed on saltwater ice until reaching shore. On shore, coolers were transported to St. John's, Newfoundland, where they were sent via air cargo to the Atlantic Veterinary College (AVC) at University of Prince Edward Island (UPEI). The interval between snow crab harvest and their arrival at the AVC was usually 24-48 h. Snow crabs were held in 34 ppt artificial seawater which was aerated with air stones and maintained at 0-2 °C until processing. The interval between snow crab arrival at AVC and processing ranged from 15 min to ~4 h.

2.2.2. **Snow crab Processing and Sample Collection**

Crabs were evaluated for gross morphologic evidence of Bitter Crab Disease which is characterized by an orangish-pink or "cooked" appearance to the carapace and/or white discoloration of their arthrodial membranes. All snow crabs that survived shipping to AVC at UPEI and any snow crabs with macroscopic evidence of BCD were processed. In addition, 10 shipping mortalities per shipment (n = 30) were processed from WB.

Each snow crab was photographed (dorsal and ventral digital images), gender was noted and carapace width (mm) was measured. Hemolymph from each animal was collected aseptically from the base of the first walking leg using a 3 ml or 5 ml syringe with a 22 gauge needle. For each animal the gross appearance of the hemolymph was noted and hemolymph refractive index was measured using a digital refractometer (Reichert r^2mini digital refractometer; Reichert Analytical Instruments). A 200 µl sample of hemolymph was placed in a 96-well ethanol block containing 800 µl 100% ethanol per well for DNA extraction. These DNA samples were examined using a polymerase chain reaction (PCR) assay with *Hematodinium*-specific primers (Appendix 1). This assay was used for the molecular detection of *Hematodinium* spp. infection in a larger survey of Newfoundland snow crabs, and was used as a molecular method of disease detection for this project. The remaining hemolymph was placed on ice, incubated at 1°C for ~24 h, pooled in 50 ml Falcon tubes and frozen at -80°C for untargeted metabolomics evaluation (see Chapter 4).

The crab was then euthanized via nerve cord disruption via decapitation (i.e., removal of the carapace). Euthanasia via potassium chloride injection resulted in a large streak of tissue disruption and thus this alternative method of euthanasia was not employed (Appendix 2). Upon removal of the carapace, a digital image of the crab's internal organs was taken and tissue samples were collected. These included: heart, hepatopancreas, gill (1^{st} and 4^{th} gills on the right), gonad, midgut, eyestalks (left and right), a cross-section of the abdomen, and a cross-section of leg (1^{st} merus on the right). The tissues were immediately placed in Davidson's seawater fixative for 24 h (Appendix 3). After 24 h, the tissue samples were transferred into containers of 70% ethanol for storage until routine processing for histology.

2.2.3. **Tissue Trimming and Processing for Histology**

Sections of all soft tissues (heart, hepatopancreas, gill (x2), gonad, and midgut) were trimmed and placed into one cassette per individual snow crab for processing. A second cassette of sections lined by a thick cuticular layer (eyestalk, leg, and abdomen) was also processed. The eyestalk was bisected along the frontal plane as this plane was found to consistently result in optimal sections of internal neuroendocrine tissues (Appendix 4).

The blocks of trimmed tissues were processed routinely for histology (Leica processor), sectioned at 5 µm thickness, and stained with hematoxylin and eosin (H&E). In 2010, the tissue sections were all placed in a single large holding container until processing. Tissue sections were collected from this container daily until all blocks were processed. In 2011, all samples from animals with macroscopic evidence of BCD were placed in a separate holding container that was not submitted until all other blocks were processed and slides were prepared and

delivered. Then, the samples known to contain dinoflagellates were processed separately. This additional step was instituted after a tissue processing trial undertaken to mimic the conditions of 2010 indicated that a single large holding container can introduce cross-contamination of snow crab tissues with *Hematodinium* (Appendix 5). Stained sections were examined on a VistaVision compound microscope (VWR) and digital images were captured using an Axioplan 2 imaging microscope with an Axiocam HRc camera and AxioVision 4.8.2.0 software (Zeiss).

2.2.4. Histologic Examination of H&E Stained Tissue Slides

Each tissue on each slide was examined in a systematic manner for evidence of *Hematodinium* infection. *Hematodinium* sp. organisms have a characteristic nuclear condensation pattern which makes their nucleus stain more darkly than host hemocytes, and thus are relatively easily identified at low magnification (100x magnification). *Hematodinium* sp. organisms also contain numerous intracellular vacuoles (PAS bodies or accumulation bodies) which contain lipofuscin-like material resulting in the parasitic dinoflagellates having a vacuolated cytoplasmic appearance distinct from the agranular or granular appearance of host hemocytes. If no evidence of infection was observed during the 100x magnification examination, the tissues were screened again at higher magnification (400x magnification). The degree of bacterial gill fouling (minimal, mild, moderate, or marked) was noted. The histologic sections were then screened for histologic evidence of gill fouling, carapace fouling (eyestalk, leg, and abdominal cross sections), tissue glycogen stores, and histopathologic changes within soft tissues (see Chapters 3-5).

As reported in Wheeler et al (2007), relative intensity of the parasite within the tissue was used as the key indicator for severity of infection. The intensity of the parasitic infection (light, moderate, advanced, and very advanced) was assessed by evaluating parasitic infiltration of interstitial connective tissues per high power field (HPF, 400x magnification) using a modified version of the rating system from Wheeler et al (2007). The intensity of infection was rated as follows: light infection (1-25 parasites per HPF), moderate infection (25 -50 parasites per HPF, advanced infection (>50 to 100 parasites per HPF), and very advanced (>100 to too numerous to count). In moderate infection intensities the parasites infiltrated but did not completely fill or expand the interstitial connective tissues. With advanced and very advanced infection intensities, the parasitic infiltrates filled and expanded the interstitial connective tissue spaces.

2.2.5. Morphological Examination of Digital Images

Digital images of the dorsal carapace were screened for the presence of epibionts and the shell condition category of the snow crab was assessed as previously reported (modified from Fonseca *et al.*, 2008; Table 2.1). Soft-shelled and new-shelled snow crabs (Figure 2.2a) have molted in the spring of the current year, intermediate-shelled snow crabs (Figure 2.2b) had molted in spring of the previous year, old-shelled snow crabs (Figure 2.2c) last molted at least 2 years prior, and very old-shelled snow crabs have soft carapaces due to decalcification and decay in some joints (Dawe *et al.* 2010). External and internal digital images were also assessed for macroscopic evidence of *Hematodinium* sp. infections in animals that had evidence of BCD histologically but that were not diagnosed with the disease by initial visual exam.

Table 2.1: Criteria used to determine shell condition category.

Shell condition category	Epizoites	Carapace and Chelae	Ventrum	Hardness
Soft-shelled	None	Iridescent with sharp spines	Immaculate white	Chelae are soft or buckle when pressed with thumb
New-shelled	None or very few small (spirorbids, serpulids)	Iridescent with sharp spines	White	Chelae do not buckle when pressed with thumb
Intermediate-shelled	Epizoites present but of small to intermediate size (spirorbids, serpulids, barnacles, bryozoans, hydroids, sponges)	Partially iridescent or dull, spines snow some wear	Dull, yellowish or brownish, scarred	Chelae hard
Old-shelled	Numerous epizoites, often of large size	Yellow or brown, dirty, scarred; spines eroded	Yellow or brown, dirty, scarred	Chelae hard
Very old-shelled	Numerous epizoites and decaying spirorbid or serpulid shells	Yellow or brown, dirty, scarred, spongy	Yellow or brown, dirty, scarred	Chelae likely to buckle when pressed with thumb

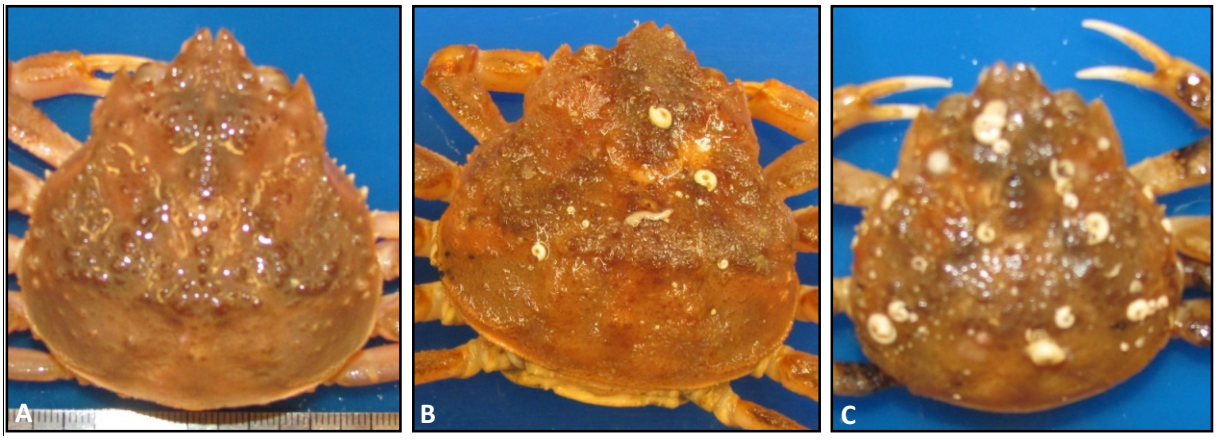

Figure 2.2. Examples of the gross morphological appearance of new-shelled (A), intermediate-shelled (B), and old-shelled (C) snow crabs.

2.3. Results

2.3.1. Shipping Mortality

In September 2010 a total of 354 snow crabs was shipped to the AVC at UPEI in 5 separate shipments. In 2011 a total of 281 snow crabs was shipped to the AVC at UPEI in 3 separate

shipments. The survival rate for shipment varied per shipment (Table 2.2)**.** The first shipment in 2010 had the highest mortality rate with no apparent survival of any crab. When received, the crabs in this first shipment were dry and warm with no visible activity and no response when mouthparts were touched. However, our collaborators at DFO indicated that the snow crabs may have been in stasis (hypobiosis) after transport at low temperatures. Thus, in subsequent shipments snow crabs were recovered in tanks of artificial seawater. If the first snow crab shipment (with 100% mortality) is removed from the data, the shipping mortality rate in the remaining shipments was positively correlated (Pearson correlation = 0.971, p-value = 0.000) with increased shipment stocking density (Figure 2.3).

In year 2010 a total 160 snow crabs, which were shipped to AVC at UPEI, was processed for the study. The only dead crabs processed were crabs with macroscopic evidence of BCD. The snow crabs had a ~50:50 male to female ratio (see Table 2.3). In 2011 a total of 174 snow crabs which were shipped to AVC at UPEI, was processed for the study. This total included all live crabs and 10 dead crabs per shipment (i.e., a total of 30 dead snow crabs). These dead crabs were added to the collection protocol to determine if crabs that died during shipping had evidence of subclinical *Hematodinium* infection. The processed snow crabs had an ~80:20 ratio of male to female crabs (Table 2.2). A significantly higher number of female intermediate-shelled snow crabs was collected in 2010 than in 2011 (Pearson Chi-Square = 5.567, DF=1, P-value = 0.018; Figure 2.4).

Table 2.2: Shipping mortalities in snow crab shipped from White Bay (WB) and Notre Dame Bay (NDB), Newfoundland. (Note: The mortality rate does not include deaths due to BCD.)

Shipment	NFLD Bay	Crabs Shipped (n)	Dead BCD- Crabs† (n)	Dead BCD+ Crabs† (n)	Mortality rate* (%)
2010 – 1 (Sept. 10)	WB	70	70	0	100%
2010 – 2 (Sept. 14)	WB	20	2	0	10%
2010 – 3 (Sept. 17)	NDB	23	4	3	17.4%
2010 – 4 (Sept. 19)	NDB	84	37	6	36.9%
2010 – 5 (Sept. 21)	NDB	157	87	5	55.4%
2011 – 1 (Sept. 3)	WB	161	99	0	68.8%
2011 – 2 (Sept. 5)	WB	58	10	8	17.2%
2011 – 3 (Sept. 9)	WB	62	16	4	25.8%

*Does not include BCD-related deaths.

†BCD- and BCD+ status in this table is based on macroscopic evidence of disease.

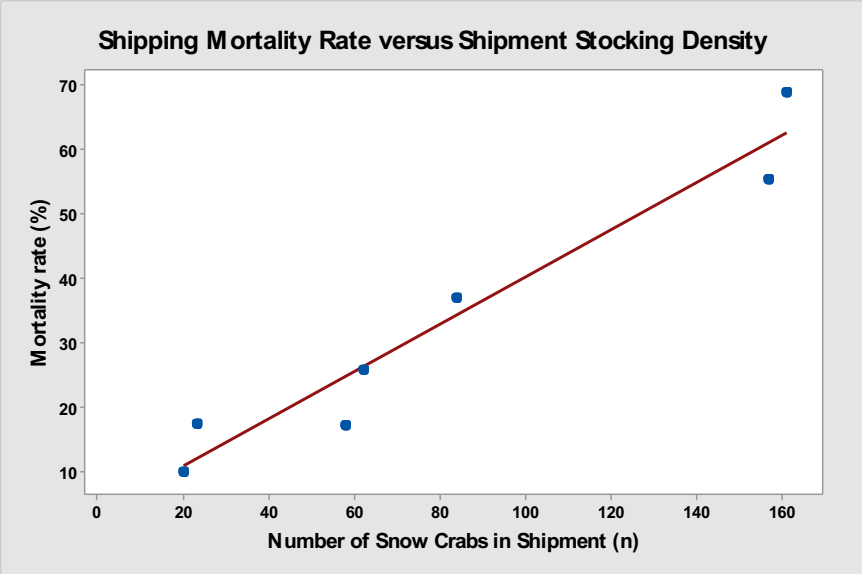

Figure 2.3. Scatterplot of mortality rate versus stocking density for snow crab shipments (Pearson correlation = 0.971, p-value = 0.000).

Table 2.3. Gender distribution, carapace width range and mean, and prevalence of BCD for year 1 (2010) and year 2 (2011) of the study.

	September 2010		**September 2011**	
n	**160**		**174 crabs (includes 30 dead crabs)**	
Gender Distribution	51% males (n=81)	49% females (n = 79)	81 % males (n=141)	19% females (n=33)
Carapace width Range (mm)	53-110	27-69	46 -108	40-68
Carapace width Mean (mm)	80.2	54.4	79.0	46.6
Macroscopic BCD+ (processed)	12.34% (10/81)	2.53% (2/79)	8.51% (12/141)	0% (0/32)
Macroscopic BCD+ (processed)	7.50% (12/160)		6.90% (12/174)	
Macroscopic BCD+ (all shipped)	3.39% (12/354)		4.27% (12/281)	

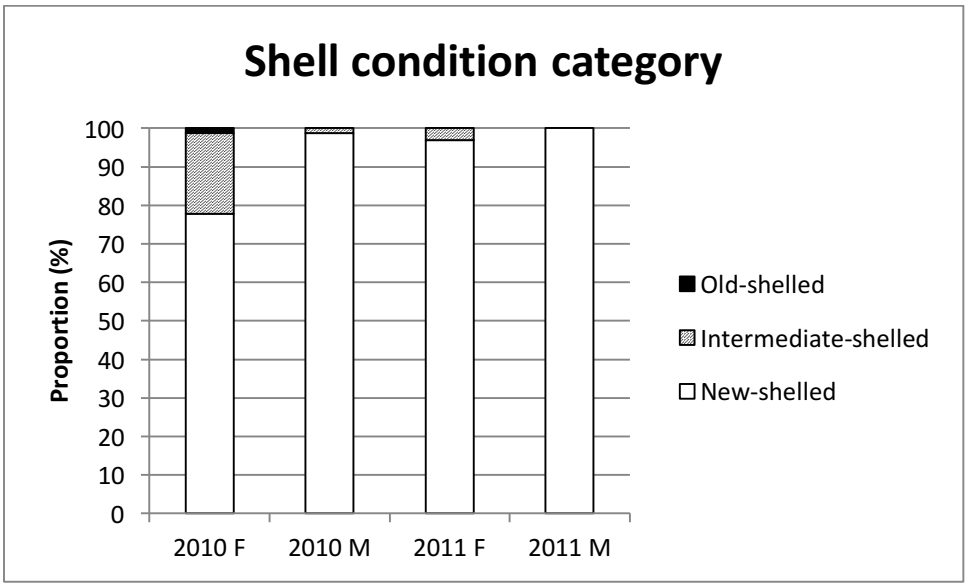

Figure 2.4. Comparison of shell condition indices by year of collection and gender (F = female, M = male). Note higher proportion of intermediate-shelled snow crabs in 2010 female snow crabs. This same subgroup was the only group that contained old-shelled snow crabs.

2.3.2. Gross Findings

2.3.2.1. Snow Crabs Collected in Fall 2010

In September 2010 BCD was diagnosed via visual examination (macroscopic BCD+) in 12 of the 160 snow crabs. BCD+ snow crabs were all new-shelled animals with no spirorbid worm tubes

or a single spirorbid worm tube (n=2); no serpulids or barnacles were observed on their dorsal carapaces. Among the 12 BCD+ animals, 9 were male and 3 were female (Table 2.4). All three BCD+ female snow crabs were mature gravid females (i.e., carrying a clutch of eggs under her abdomen or "berried") with a rounded (convex) abdomen (Figure 2.5). All 12 infected snow crabs had characteristic opacity of the ventral carapace (Figures 2.6A), opaque "milky" hemolymph (Figures 2.6B), and a similar "milky" appearance to their internal organs (Figures 2.7C and 2.7D) when compared to uninfected snow crab tissues (Figures 2.7A and 2.7B).

One additional snow crab (snow crab 2010-#26) was recorded as having milky hemolymph. However this snow crab had a normal appearance to its ventral carapace (Figure 2.8) and did not have discolored internal tissues. (Note: Photograph of the internal organs of this snow crab is missing from the data set.) This snow crab was interpreted as BCD- via visual exam despite being recorded as having milky hemolymph (incorrectly recorded due to human error, presumably).

Table 2.4: Snow crabs diagnosed with BCD via macroscopic (visual examination) diagnosis in Fall 2010.

Crab	BCD Status (macroscopic)	Gender	Carapace Width	Hemolymph appearance	Spirorbid Worm Tubes on Carapace
2010-19	+	Male	90	Milky	None
2010-20	+	Male	96	Milky	None
2010-38	+	Male	83	Milky	None
2010-39	+	Male	80	Milky	None
2010-40	+	Male	54	Milky	None
2010-59	+	Male	75	Milky	None
2010-60	+	Male	80	Milky	None
2010-106	+	Female (gravid)	56	Milky	None
2010-117	+	Male	65	Milky	None
2010-119	+	Male	78	Milky	None
2010-120	+	Female (gravid)	60	Milky	None
2010-131	+	Female (gravid)	60	Milky	1

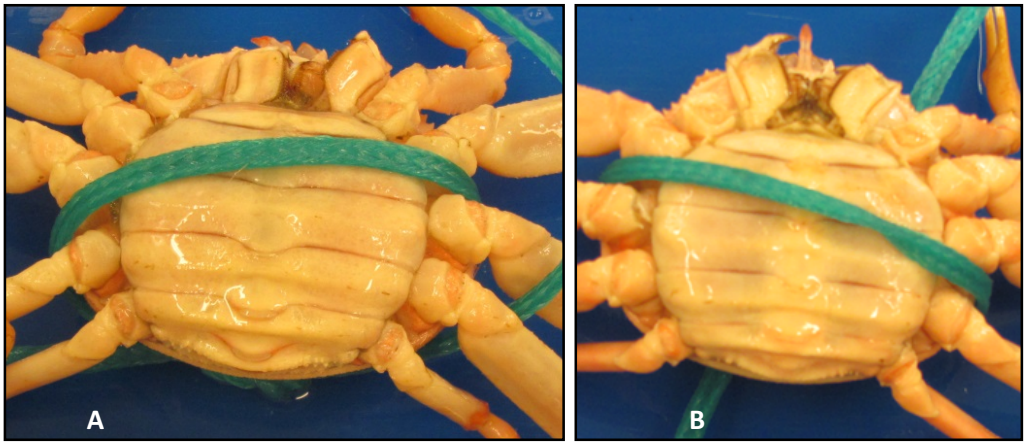

Figure 2.5. BCD+ mature berried female snow crabs (A and B). Note the opaque appearance of the ventral carapace with a rounded (convex) abdominal profile.

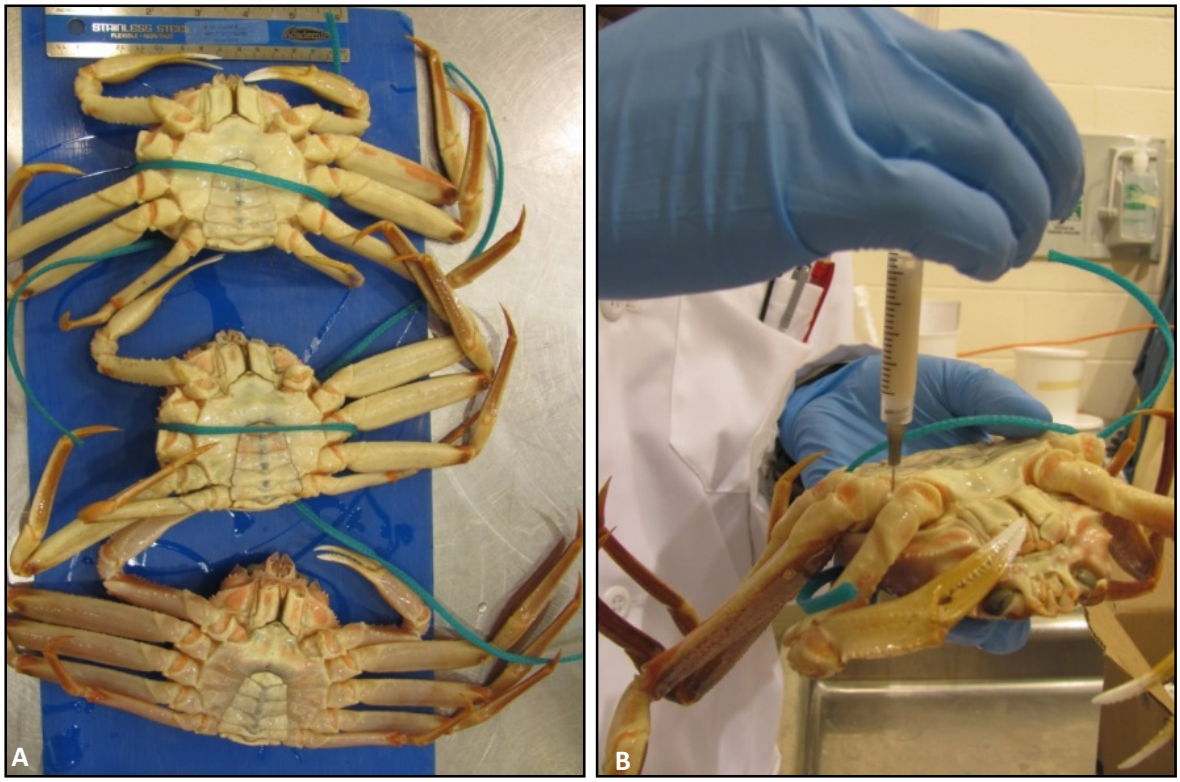

Figure 2.6. Characteristic macroscopic appearance BCD infected crabs and hemolymph. **A)** Male snow crabs with BCD (top 2) as compared to a snow crab without BCD (bottom). Note the opaque appearance of the ventral carapace as compared to the more translucent appearance of the unaffected snow crab. **B)** Opaque white ("milky") hemolymph of a BCD+ snow crab.

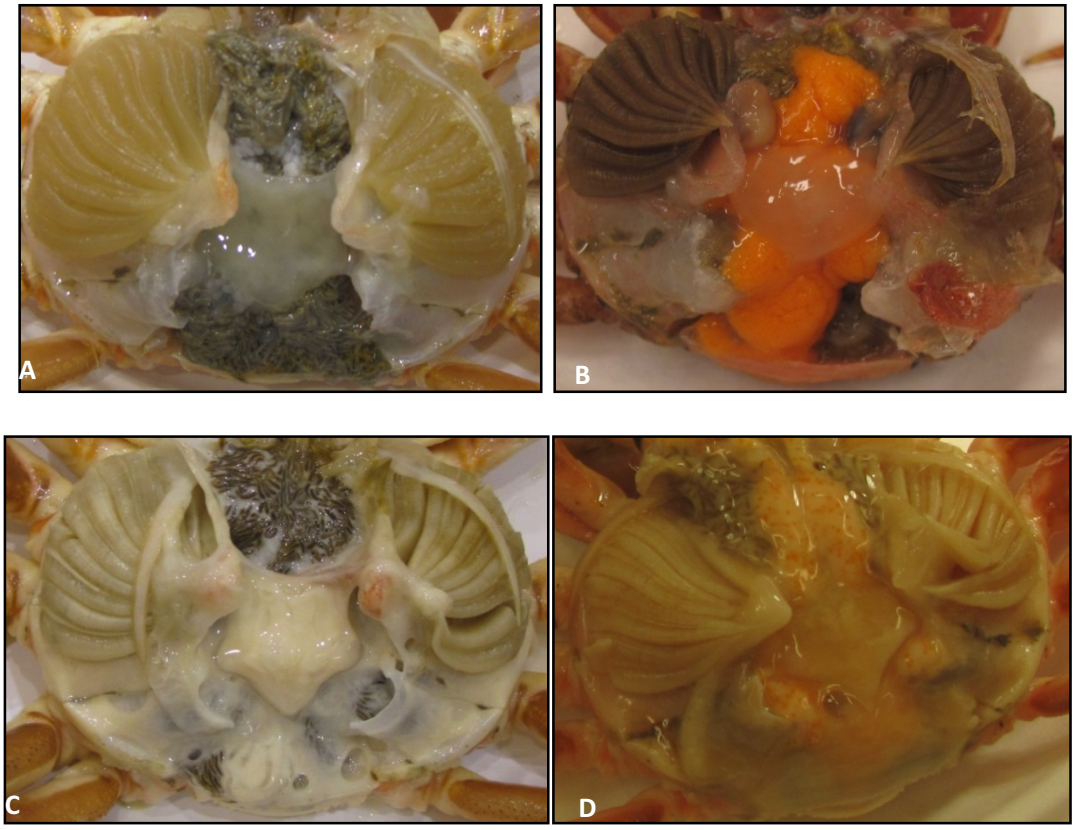

Figure 2.7. Macroscopic appearance male and female snow crabs with and without BCD. **A & B)** Examples of a male (A) and female (B) snow crabs without BCD. **C & D)** Examples of a male (C) and female (D) with BCD. Note opaque, white, "milky" appearance of internal organs in BCD+ snow crabs.

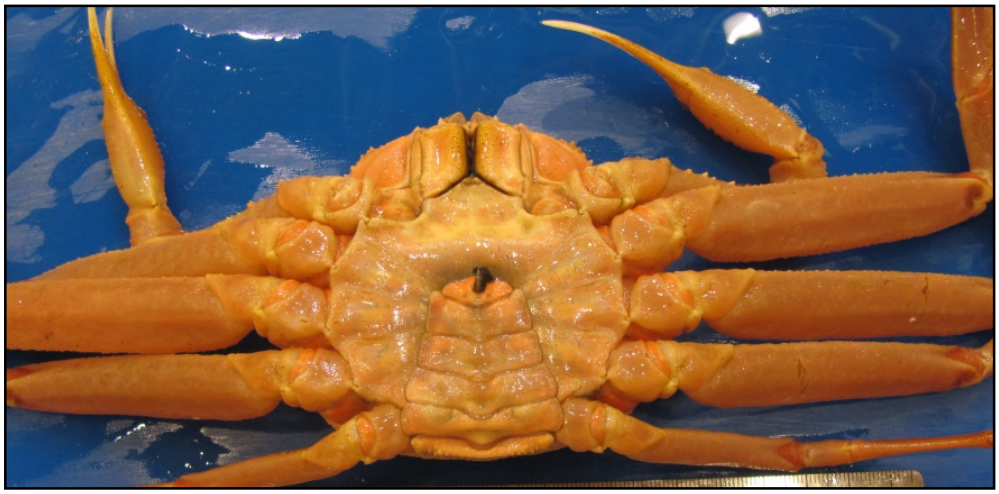

Figure 2.8. Appearance of the ventral carapace of snow crab 2010-#26. This snow crab was recorded as having milky hemolymph, a macroscopic feature of BCD.

2.3.2.2. Snow Crabs Collected in Fall 2011

In September 2011, BCD was diagnosed via visual examination in 12 of 174 crabs. All crabs with macroscopic evidence of BCD were new-shelled male crabs. All 12 affected snow crabs had macroscopic evidence of late-stage BCD with opaque ventral carapaces, opaque white hemolymph, and "milky" internal organs similar to that described and shown above (Table 2.5). In addition, a single dead female snow (crab 2011-#163) which did not have external macroscopic evidence of BCD (i.e., lacked characteristic gross characteristics of BCD such as a cooked or opaque appearance to the carapace) had hemolymph that was discolored but instead of being cloudy white was reddish-orange and opaque (Figures 2.9 and 2.10). Gross examination of this crab's tissues revealed a pale orange appearance of the ovaries, pale hepatopancreas, and pale streaks in her gills (Figure 2.11).

Table 2.5. Snow crabs diagnosed with BCD via macroscopic (visual examination) diagnosis in Fall 2011.

Crab	BCD Status (macroscopic)	Gender	Carapace Width	Hemolymph appearance	Spirurid Worm Tubes on Carapace
2011-61	+	Male	80	Milky	None
2011-62	+	Male	99	Milky	None
2011-63	+	Male	65	Milky	None
2011-64	+	Male	87	Milky	None
2011-65	+	Male	101	Milky	1
2011-66	+	Male	107	Milky	None
2011-67	+	Male	67	Milky	None
2011-98	+	Male	67	Milky	None
2011-99	+	Male	74	Milky	None
2011-100	+	Male	79	Milky	None
2011-155	+	Male	72	Milky	None
2011-156	+	Male	85	Milky	None

Figure 2.9. Flat abdomen of female snow crab 2011-#163 (as opposed to rounded abdomen in mature gravid female snow crabs shown above in Figure 2.5).

Figure 2.10. Reddish-orange hemolymph sampled from snow crab 2011-163.

Figure 2.11. Internal organs of snow crab 2011-#163. Note pale orange ovaries, pale hepatopancreas, and pale streaky gills.

2.3.3. Histologic Diagnosis of *Hematodinium* spp. Infections

2.3.3.1. Histologic Diagnosis of BCD - Fall 2010 Snow Crabs

All 12 snow crabs with macroscopic evidence of BCD exhibited multisystemic intravascular and interstitial infiltration of *Hematodinium*-like organisms upon examination via histology. All twelve infections were late-stage in nature and intensity of the infections ranged from moderate to very advanced (see Chapter 3). One additional snow crab (#2010-26) was recorded as having milky hemolymph; this snow crab did not have convincing macroscopic evidence of BCD as its carapace was not discolored and its internal tissues were not discolored white or opaque (did not have a "milky" appearance). And, two additional 2010 snow crabs had microscopic evidence of BCD that were not recorded as having macroscopic evidence of BCD infection (false negatives via visual exam diagnosis; see Table 2.6).

Moderate infection intensity was noted in both snow crabs that were negative for BCD via visual exam but positive for BCD via histologic examination of tissues (i.e., false negative diagnoses via visual exam). The first snow crab with a false negative visual exam diagnostic test was snow crab #2010-30. This snow crab had hemolymph and ventral carapace which were normal in gross appearance (Figure 2.12) and the internal organs were not "milky" in appearance. However, this snow crab's gills were pale and the spongy connective tissue of the heart had a mild increase in tissue opacity with an irregularly mottled appearance (Figure 2.13). The second snow crab from 2010 with false negative diagnosis via visual exam was a female snow crab #2010-133. This snow crab had normal hemolymph appearance. Her ventral abdominal carapace was intermediate in appearance (Figure 2.14A) between the normal translucent appearance and the opaque appearance associated with BCD (Figures 2.14B and 2.14C). This snow crab's heart had a very mild increase in opacity and the ovarian interstitium was very mildly expanded by edematous stroma (Figure 2.15A) when compared to an uninfected female of similar size (Figure 2.15B).

In 2010 snow crabs without late-stage BCD (n=145) histologic tissue sections often contained rare individual *Hematodinium*-like organisms or very small clusters of *Hematodinium* organisms (2-6 dinoflagellates) within interstitial hemal spaces or along tissue surfaces. These rare sightings of dinoflagellates were observed in a large proportion (140 out of 145) of the BCD- individuals (87.5% of all 160 snow crabs). These clusters of dinoflagellates were most commonly associated with the hepatopancreas (90/140), gonad (70/140), and eyestalk (36/140; Figures 2.16 and Figure 2.17). No *Hematodinium*-like organisms were observed in 5 individuals. Three

of the five uninfected crabs were from cooler 4 (n=53, 5 BCD+ individuals in this shipment) and

2 of the uninfected crabs were from cooler 5 (n=70, 6 BCD+ individuals in this shipment).

Table 2.6: Comparison of histologic and macroscopic (visual examination) diagnosis of BCD in Fall 2010 snow crabs with definitive histologic evidence of BCD infection. False negatives via visual exam diagnosis are noted in bold.

Crab	BCD Status (histologic)	BCD Status (macroscopic)	Gender	Carapace Width	Spirorbid Worm Tubes on Carapace	Infection intensity
2010-19	+	+	Male	90	None	Advanced
2010-20	+	+	Male	96	None	Very advanced
2010-30	**+**	**-**	**Male**	**93**	**None**	**Moderate**
2010-38	+	+	Male	83	None	Very Advanced
2010-39	+	+	Male	80	None	Advanced
2010-40	+	+	Male	54	None	Very Advanced
2010-59	+	+	Male	75	None	Very Advanced
2010-60	+	+	Male	80	None	Advanced
2010-106	+	+	Female	56	None	Moderate
2010-117	+	+	Male	65	None	Very Advanced
2010-119	+	+	Male	78	None	Very Advanced
2010-120	+	+	Female	60	None	Very Advanced
2010-131	+	+	Female	60	1	Very Advanced
2010-133	**+**	**-**	**Female**	**49**	**None**	**Moderate**

Figure 2.12. Appearance of the ventral carapace of snow crab 2010-#30.

Figure 2.13. Appearance of the internal organs of snow crab 2010-#30. The gills were pale and the spongy connective tissue of the heart had mildly increased opacity.

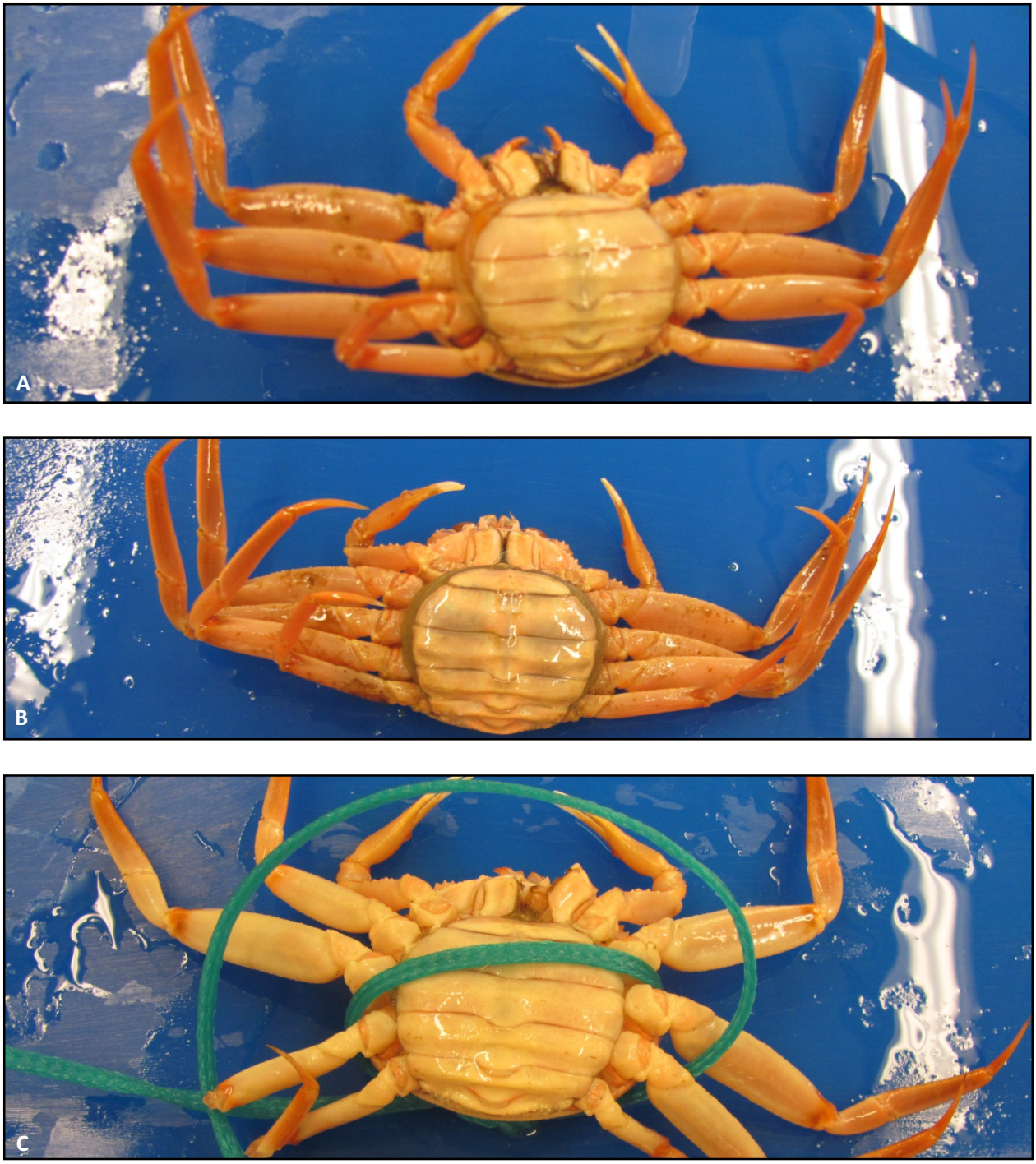

Figure 2.14. Comparison of subclinical BCD infection with a BCD- snow crab and a snow crab with macroscopic evidence of BCD. **A)** Appearance of the ventral carapace of snow crab snow crab 2010-133, a subclinical infection with BCD. **B)** A similar sized BCD- female (snow crab #2010-136). **C)** A similar sized BCD+ female (snow crab #2010-106).

Figure 2.15. Comparison of the appearance of internal organs of a snow crab with a subclinical BCD infection and a BCD- snow crab. **A)** Appearance of the internal organs of snow crab 2010-133, a snow crab with subclinical BCD infection (blurry). The myocardium had a mild increase in tissue opacity and the ovarian interstitium was very mildly expanded. **B)** Appearance of the internal organs of a similarly sized BCD- mature female snow crab (snow crab #2010-136).

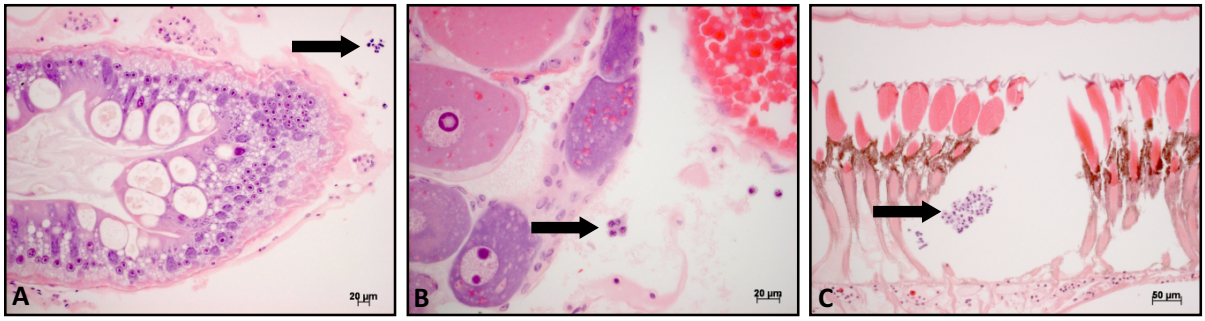

Figure 2.16. Clusters of *Hematodinium* sp. parasites in snow crabs without multisystemic infections (arrows). **A)** Cluster of *Hematodinium* sp. parasites adjacent to a hepatopancreatic tubule (crab #2010-107; 200x, H&E). **B)** Individualized and clusters of *Hematodinium* sp. parasites adjacent to the ovary (crab #2010-109; 200x, H&E). **C)** Cluster of *Hematodinium* sp. parasites within an eyestalk located above the retinal basement membrane between the ommatidia of the retina (crab #2010-103; 200x, H&E).

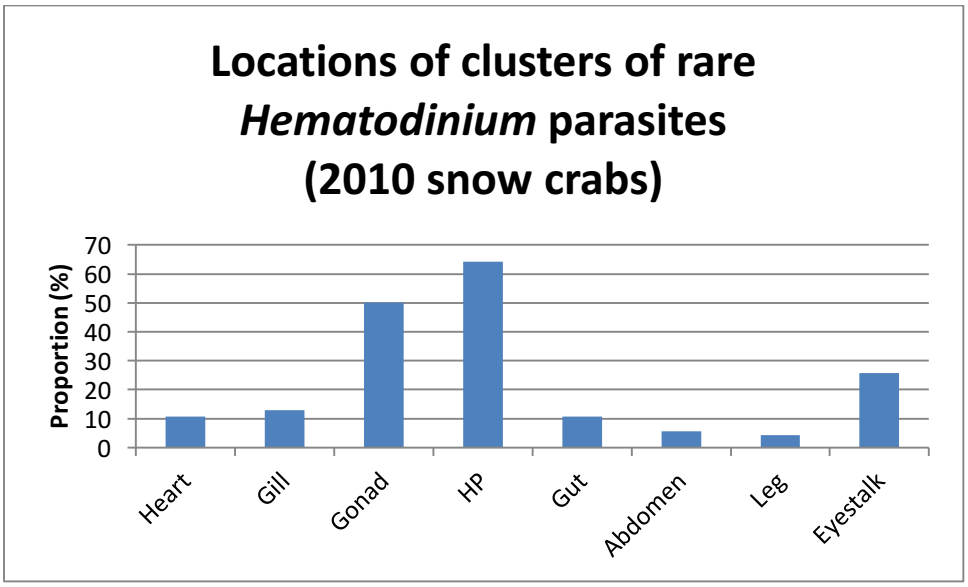

Figure 2.17. Tissue distribution of rare clusters and individual parasites observed in snow crabs collected in year 1 of the study. (Note: Clusters of parasites were often seen in more than one tissue location in an individual snow crab.)

2.3.3.2. Histologic diagnosis of BCD - Fall 2011 Snow Crabs

All 12 snow crabs with macroscopic evidence of BCD exhibited multisystemic intravascular and interstitial infiltration of *Hematodinium*-like organisms upon examination via histology. All infections were late-stage in nature with expansion of interstitial hemal spaces by the parasitic

infection. In addition, two additional snow crabs had microscopic evidence of BCD (false negatives by visual examination diagnosis, Table 2.7).

The two snow crabs with false negative diagnoses via visual examination had mild (n=1) and advanced (n=1) infection intensities. The snow crab with mild infection intensity (#2011-147) had normal appearances to both the hemolymph and the ventral carapace (Figure 2.18). Gross examination of the gills reveals small white streaks in the gill lamellae (Figure 2.19). The 2011 snow crab with a false negative diagnostic test result via visual exam and advanced infection intensity was the female snow crab described above with a normal (iridescent) ventral carapace appearance (Figure 2.9), opaque reddish-orange hemolymph (Figure 2.10), and internally had pale orange ovaries, variable pallor in the gills, and mild diffuse hepatopancreatic pallor (Figure 2.11).

No individual *Hematodinium*-like organisms or very small clusters of *Hematodinium* organisms (2-6 dinoflagellates) were observed in histologic sections of any of the remaining BCD- individuals (n=160). The absence of this finding was a major difference when compared to the 2010 results.

Table 2.7: Comparison of histologic and macroscopic (visual examination) diagnosis of BCD in Fall 2011 snow crabs with definitive histologic evidence of BCD infection. False negatives via visual exam diagnosis are noted in bold.

Crab	Histologic BCD Status	Macroscopic BCD Status	Gender	Carapace Width	Spirorbid Worm Tubes on Carapace	Infection Intensity
2011-61	+	+	Male	80	None	Advanced
2011-62	+	+	Male	99	None	Very advanced
2011-63	+	+	Male	65	None	Advanced
2011-64	+	+	Male	87	None	Advanced
2011-65	+	+	Male	101	1	Advanced
2011-66	+	+	Male	107	None	Very advanced
2011-67	+	+	Male	67	None	Very advanced
2011-98	+	+	Male	67	None	Very advanced
2011-99	+	+	Male	74	None	Very advanced
2011-100	+	+	Male	79	None	Advanced
2011-147	**+**	**-**	**Male**	**67**	None	**Mild**
2011-155	+	+	Male	72	None	Moderate
2011-156	+	+	Male	85	None	Moderate
2011-163	**+**	**-**	**Female**	**48**	None	**Advanced**

Figure 2.18: External appearance of Crab 2011-147 (Dead 3). The ventrum has a normal iridescent appearance (i.e., no apparent discoloration of the carapace or arthrodial membranes).

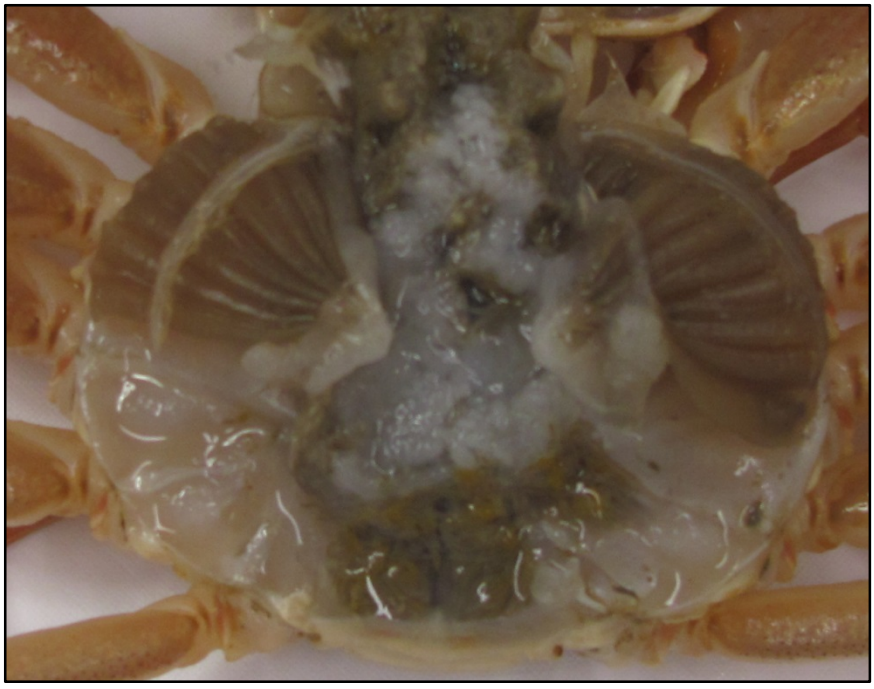

Figure 2.19: Appearance of internal organs of Crab 2011-147 (Dead 3). Note the small white streaks within the gill lamellae.

2.3.4. Carapace Width

2.3.4.1. Carapace Width: Gender and Year Effects

In 160 snow crabs were sampled and processed in Fall 2010 and 174 snow crabs that were processed in Fall 2011. When the data from both years were combined, a total of 334 snow crabs was sampled. Male snow crabs (n=221, carapace width mean = 79.4 ± 0.85 SEM) were significantly larger than female snow crabs (n=113, carapace width mean = 52.0 ± 0.66 SEM; two-sample T-test: T-value = 25.42, DF = 330, p-value = 0.000; Figure 2.20). 2010 male snow crabs (n = 79, mean = 80.2 ± 1.5 SEM) were larger than 2010 female snow crabs (n=81, mean = 54.42 ± 0.73 SEM; two-sample T-test: T-value = 15.18, DF = 112, p-value = 0.000). 2011 male snow crabs (n=142, mean = 78.9 ± 1.0 SEM) were larger than 2011 female snow crabs (n=32, mean = 45.94 ± 0.59 SEM; two-sample T-test: T-value = 28.08, DF = 166, p-value = 0.000). Mean

carapace width did not vary significantly between years for male snow crabs (two-sample T-test: T-value = -0.70, DF = 146, p-value = 0.488; Figure 2.21). Female snow crabs were significantly larger in 2010 than in 2011 (two-sample T-test: T-value = 9.03, DF = 104, p-value = 0.000). The gender proportions differed significantly between years (Pearson Chi-Square = 38.688, DF=1, P-value = 0.000) with fewer females collected in year 2 than in year 1 of the study (Table 2.1).

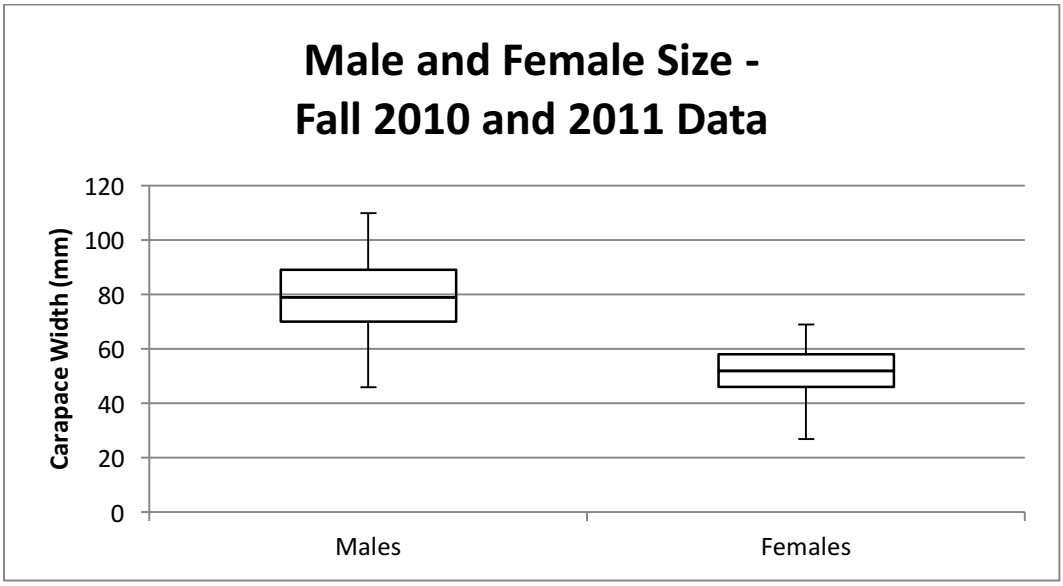

Figure 2.20. Box and whisker plots of average carapace widths of all processed Fall 2010 and 2011 male and female snow crabs showing sexual dimorphism.

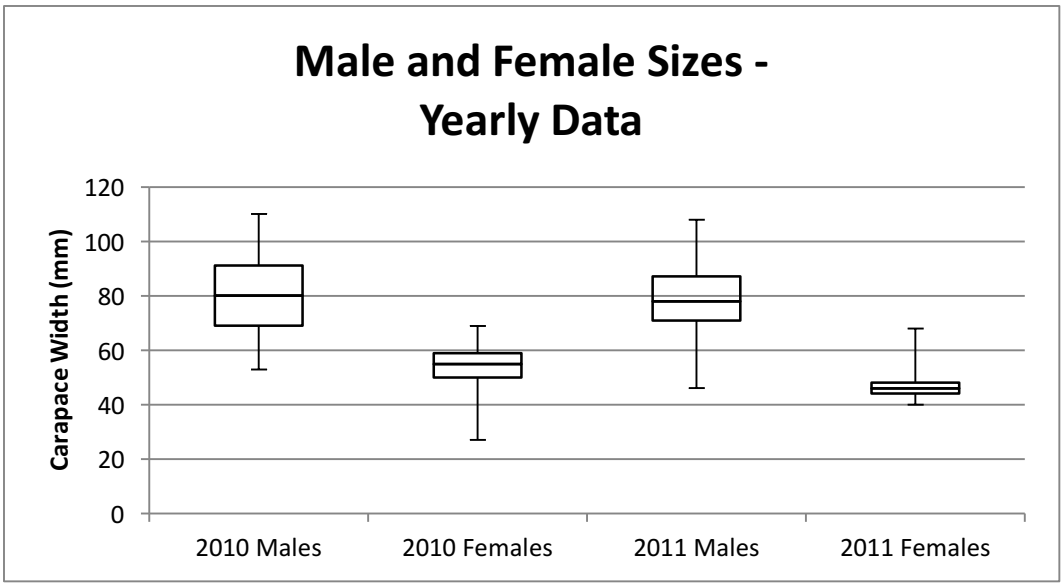

Figure 2.21. Box and whisker plots of average carapace widths of all processed Fall 2010 and 2011 male and female snow crabs separated by year.

2.3.4.2. Carapace Width: Effect of BCD Status

When the data were not separated by gender BCD+ snow crabs (n=29, mean = 75.9 ± 2.9 SEM) appeared to have larger mean carapace widths than BCD- snow crabs (n = 305, mean = 69.6 ± 0.98 SEM; two-sample T-test: T-value = 2.07, DF = 34, p-value = 0.046; Figure 2.22). When the data were separated by gender there were no significant differences in mean carapace widths between BCD+ females (n=5, mean = 54.60 ± 2.6 SEM) and BCD- females (n=108, mean = 51.90 ± 0.68 SEM; two-sample T-test: T-value = -0.101, DF = 4, p-value = 0.372) or between BCD+ males (n = 24, mean = 80.3 ± 2.7 SEM) and BCD- males (n = 197, mean = 79.3 ± 0.90 SEM; two-sample T-test: T-value = 0.38, DF = 28, p-value = 0.707; Figure 2.23).

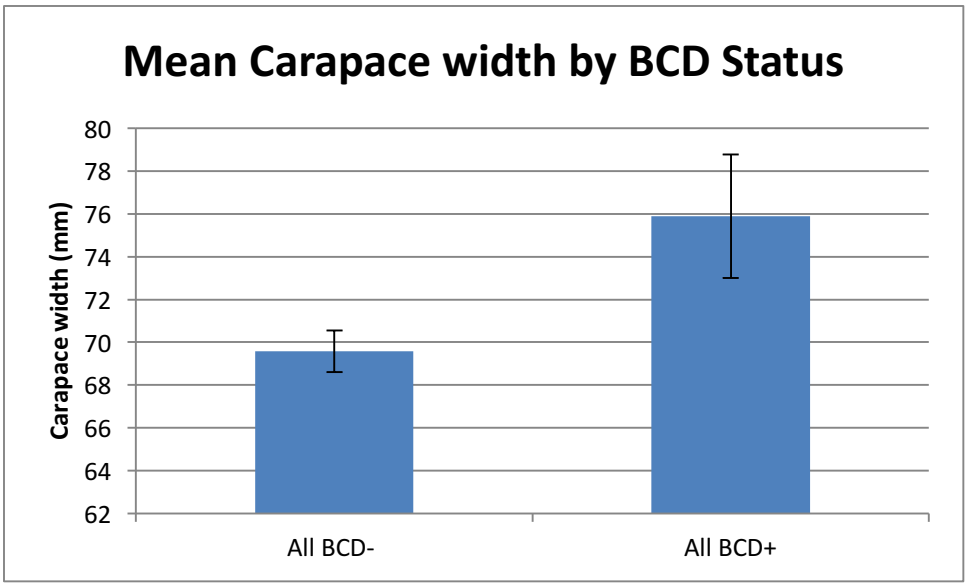

Figure 2.22. Graph of average carapace widths of all BCD- and BCD+ snow crabs (mean ± SEM). Note that gender effect on carapace width was not included in this comparison.

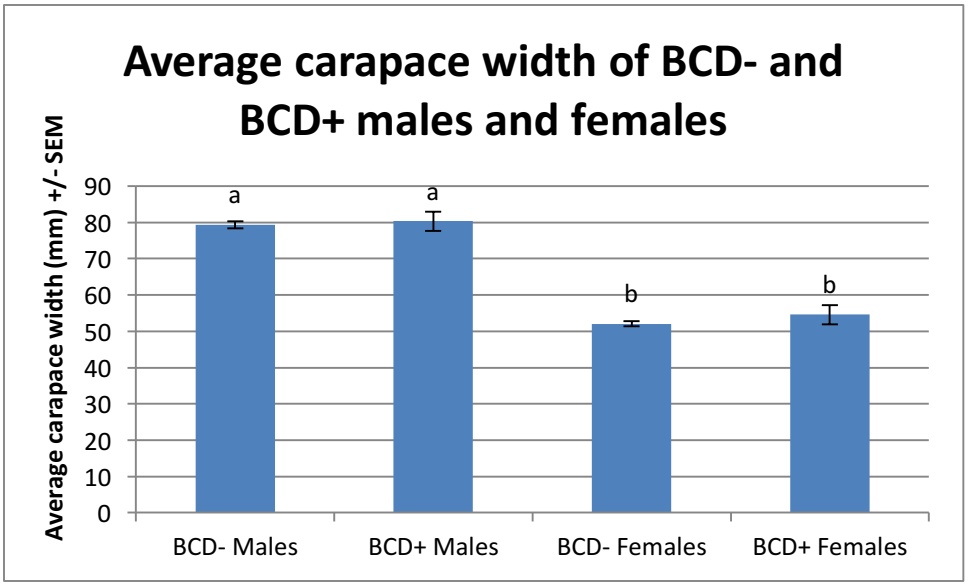

Figure 2.23. Graph of average carapace widths of all snow crabs by gender and BCD status (mean ± SEM). No significant difference in carapace width (size) was evident between BCD+ and BCD- crabs within either male or female snow crabs. Groups with different letters above the data bar were statistically significant ($p<0.05$).

2.3.5. BCD Diagnosis by PCR Assay

PCR assay of snow crab hemolymph for molecular evidence of *Hematodinium* sp. infection revealed 12 PCR-positive animals in 2010 and 11 PCR-positive animals in 2011 (see Tables 2.8 and 2.9). In both years all PCR+ animals also had macroscopic evidence of BCD infection with only a single exception: snow crab #2011-100 had macroscopic evidence of BCD but the PCR assay was negative. Hemolymph collection from this snow crab was poor with only a very small amount of hemolymph collected suggesting that the false-negative PCR result in this animal was due to sampling error (i.e., insufficient hemolymph).

In 2010 and 2011 there were six false negative PCR assay tests: two female and four male snow crabs with definitive histologic evidence of BCD. The average carapace width of animals that had false negative PCR assay results was 68 mm (range from 48 to 93 mm). Five of the six animals which had false negative PCR assay results also had false negative test results via diagnosis by visual exam (i.e., also did not have macroscopic evidence of BCD). The intensity of infection within the snow crabs with false negative results ranged from mild to moderate to advanced; no false negative PCR assay test results were from snow crabs with very advanced BCD infections.

Table 2.8: Comparison of histologic and macroscopic (visual examination) diagnosis of BCD in Fall 2010 snow crabs with definitive histologic evidence of BCD infection. False negatives via visual exam diagnosis and diagnosis via PCR are noted in bold.

Crab	Histologic BCD Status	Macroscopic BCD Status	PCR Assay BCD Status	Gender	Carapace Width	Infection Intensity
2010-19	+	+	+	Male	90	Advanced
2010-20	+	+	+	Male	96	Very advanced
2010-30	**+**	**-**	**-**	**Male**	**93**	**Moderate**
2010-38	+	+	+	Male	83	Very Advanced
2010-39	+	+	+	Male	80	Advanced
2010-40	+	+	+	Male	54	Very Advanced
2010-59	+	+	+	Male	75	Very Advanced
2010-60	+	+	+	Male	80	Advanced
2010-106	+	+	+	Female	56	Moderate
2010-117	+	+	+	Male	65	Very Advanced
2010-119	+	+	+	Male	78	Very Advanced
2010-120	+	+	+	Female	60	Very Advanced
2010-131	+	+	+	Female	60	Very Advanced
2010-133	**+**	**-**	**-**	**Female**	**49**	**Moderate**

Table 2.9: Comparison of histologic and macroscopic (visual examination) diagnosis of BCD in Fall 2011 snow crabs with definitive histologic evidence of BCD infection. False negatives via visual exam diagnosis and/or diagnosis via PCR are noted in bold.

Crab	Histologic BCD Status	Macroscopic BCD Status	PCR Assay BCD Status	Gender	Carapace Width	Infection Intensity
2011-61	+	+	+	Male	80	Advanced
2011-62	+	+	+	Male	99	Very advanced
2011-63	+	+	+	Male	65	Advanced
2011-64	+	+	+	Male	87	Advanced
2011-65	+	+	+	Male	101	Advanced
2011-66	+	+	+	Male	107	Very advanced
2011-67	+	+	+	Male	67	Very advanced
2011-98	+	+	+	Male	67	Very advanced
2011-99	+	+	+	Male	74	Very advanced
2011-100	**+**	**+**	**-***	**Male**	**79**	**Advanced**
2011-147	**+**	**-**	**-**	**Male**	**67**	**Mild**
2011-155	+	+	+	Male	72	Moderate
2011-156	+	+	+	Male	85	Moderate
2011-163	**+**	**-**	**-**	**Female**	**48**	**Advanced**

*Very little hemolymph was collected from this snow crab.

2.3.6. Comparison of Diagnostic Tests

When diagnosis via visual exam was compared to definitive diagnosis via histology (gold standard of diagnosis), one false positive and six false negative results were observed (see Tables 2.8 and 2.9). When diagnosis via PCR assay was compared to diagnosis via histology, no false positives and seven false negatives were observed (see Tables 2.8 and 2.9). The specificity of diagnosis via visual exam and by PCR was excellent (100%; confidence levels: 98.8-100%). The sensitivity of diagnosis via visual exam was 85.7% (67.3 – 96.0%), which was slightly greater than the sensitivity of diagnosis by PCR which was 82.1 5 (63.1 – 93.9%). No significant difference in test performance was observed (Fisher Exact Test p-value = 1.000).

2.4. Discussion

2.4.1. Shipping Mortality Rate

The first shipment of snow crabs 2010 had the highest mortality rate with no apparent survival of any crabs. When received, the crabs in this first shipment were dry and warm with no visible activity and no response when mouthparts were touched. After discussions with our collaborators, we determined that the crabs were most likely in a state of stasis (hypobiosis) rather than dead. Subsequently all crabs were recovered in chilled seawater tanks prior to processing. Mortality rate was positively correlated with increased stocking density of the shipments (Figure 2.2). High animal stocking density during transport is one of the most important stressors on live-shipped crustaceans (Barrento et al 2008, 2010). The snow crabs were shipped in a cold and humid environment; however, the snow crabs were emersed (air-exposed). Capture and aerial exposure in crustaceans results in hypoxia, alterations in acid-base

status (acidosis), altered carbohydrate storage and release, and hormonal disruption (reviewed in Ridgway et al 2006).

2.4.2. Shell Condition of BCD+ Snow Crabs

BCD+ snow crabs were observed exclusively in new-shelled animals in this study. The vast majority of snow crabs collected in this study was new-shelled snow crabs (as specified in our selection criteria) and thus our results were heavily biased towards new-shelled animals. However, the selection criterion for new-shelled snow crabs was chosen as BCD occurs predominantly in new-shelled crabs that have molted in the immediately-preceding Spring with one study reporting 91-96% of BCD snow crabs as new-shelled (Dawe et al 2002).

2.4.3. Histologic Findings

Infection intensity ranged from moderate to very advanced and mild to very advanced in each of the two years of the study. The range of infection intensities observed within the snow crabs collected suggests that *Hematodinium* infections in snow crabs are not tightly synchronous whereas synchronous infections have been reported in disease outbreaks in mud crabs *Scylla serrata* and ridgetail white prawns *Exopalaemon carinicauda* (Li et al 2008, Xu et al 2010).

In the samples collected in the Fall of 2010, rare clusters of *Hematodinium* parasites were observed in crabs that lacked gross evidence of BCD infection. These rare clusters of parasites had predilection sites including the eyestalk, hepatopancreas, and gonad. These rare clusters of parasites were initially interpreted as evidence of subclinical infection. However, the very high

rate of subclinical infection observed (88%) was very surprising and was not expected given the low prevalence of BCD observed in the Fall and thus it was suspected that these rare clusters of parasites could represent tissue cross-contamination. Thus, a small trial to determine if cross-contamination could be induced during the histology process was conducted which confirmed that cross-contamination could easily be induced by co-mingling trimmed tissues from BCD+ animals with tissues from BCD- animals (Appendix 5). Thus, in the light of these findings, these rare clusters of *Hematodinium* parasites within tissues of snow crabs were reinterpreted as probable cross-contamination during storage of trimmed tissue cassettes in a common container.

Given the likelihood that cross-contamination was a significant problem in the Fall 2010 samples processed for histology, the processing protocol was modified for processing of samples collected in Fall 2011 such that samples from BCD+ snow crabs were held in separate containers from samples from crabs that did not have macroscopic evidence suggestive of BCD. Furthermore, samples from dead BCD- snow crabs were also held in separate containers from live BCD- snow crabs. Using this modified processing method, no rare clusters of *Hematodinium* parasites were evident in any 2011 snow crabs. The single snow crab with mild infection intensity had diffuse hemal and interstitial infection with light infection load, not rare scattered clusters of parasites as seen with cross-contamination. This suggests that the true subclinical infection rates were 2/160 (1.25%) and 2/174 (1.15%) in the first and second years of this study, respectively. However, this subclinical infection rate is most likely artificially inflated due to shipping mortalities as histology was not performed on the vast majority of snow crabs that

died during shipment. The ratio of subclinical infections to clinical infections in this study is 1:6, confirming that diagnosis of BCD by visual examination underestimates disease prevalence in Newfoundland snow crabs.

One omission from this study was sampling of the antennal gland. This organ was originally omitted from the sampling plan as we planned to concentrate our sampling on small snow crabs (27-55 mm) in which this organ is very difficult to extract off the anterior carapace wall. This organ should have been included in our sampling regime after we discovered that the collected snow crab size range was noted to be larger than expected and after we determined that collection of carapace-lined tissues would be included in the study. The stomach was also not included in our sampling. The stomach was not included to reduce the potential for cross-contamination of tissues with stomach contents. To be included in the study the stomachs could have been saved in a separate container, washed, and then processed separately from the rest of the tissues. Collection of the stomachs would have allowed us to evaluate the snow crabs' hematopoietic tissue which is typically located along the dorsal wall of the stomach.

2.4.4. Carapace Width

BCD was seen in 28 snow crabs: 23 male and 5 female snow crabs. No significant difference in disease prevalence was observed between male and female snow crabs. In contrast, Dawe et al (2002) reported that BCD prevalence in females was consistently twice that seen in males. In addition, no significant difference in mean carapace width was observed between snow crabs with or without BCD in each gender in this study. BCD is seen in snow crabs of all size categories

but prevalence is highest in intermediate-sized males (41-59 mm in Dawe et al 2002, 47-74 mm carapace width in Mullowney et al 2011) and lowest in large-sized males (Dawe et al 2002, Mullowney et al 2011). Low prevalence at large host size is commonly observed in *Hematodinium*-like infections (Stentiford and Shields, 2005). The snow crabs collected in this study were a convenience sample taken during DFO's Fall trap surveys. This convenience sample contained a very small number of small to intermediate-sized snow crabs, the size range of snow crabs thought to have highest disease prevalence and the size range of most female snow crabs (Dawe et al 2002, Dawe et al 2010, Mullowney et al 2011). Inefficient capture and small sample sizes of these smaller size classes of crabs most likely biased these results. Also, collection of snow crabs by traps (versus trawl) resulted in greater prevalence of BCD in male snow crabs with carapace widths greater than or equal to 40 mm, suggesting an increased catchability of some size classes of infected snow crabs by traps (Dawe et al 2010, Mullowney et al 2011).

2.4.5. Comparison of Diagnostic Tests

Diagnosis via visual examination and diagnosis via PCR both had high specificity and good sensitivity. Snow crabs that had gross evidence of BCD had infection intensities that varied from moderate (n=3) to advanced (n=8) and very advanced (n=13). Diagnosis via visual examination diagnosed BCD in one more animal than PCR, but this difference may have been due to a sampling error (insufficient hemolymph) rather than an indicator of test performance. Thus, the tests appeared to perform equally well. Both tests gave false negative test results for snow crabs with mild, moderate, and advanced infection intensities; no false negative test results

occurred in snow crabs with very advanced infections. One of the two advanced intensity infections that had a false negative test result (PCR assay only) was the animal from which only a small amount of hemolymph was collected. Thus, the false negative PCR assay test in this case may reflect sampling error (i.e., low amount of template DNA in the sample).

The second snow crab with an advanced infection intensity in which false negative test results (PCR and visual diagnosis) were seen, was the non-gravid female snow crab with a normal iridescent (rather than opaque) appearance to her ventral carapace opaque reddish-orange hemolymph. The reason for this reddish-orange discoloration is unclear. However, the discoloration may be due to carotenoid-containing hemolymph lipoproteins. Ovarian maturation in crustaceans is characterized by an important accumulation of carotenoids (Linan-Cabello et al 2002). Crustacean yolk proteins, referred to as lipovitellin, are complex molecules comprised of high-density lipoprotein conjugated to carbohydrates and carotenoid pigments including beta-carotene, astaxanthin, canthaxanthin, and *cis*-canthaxanthin, among other minor intermediary metabolites (Subramoniam 2011). Crustacean lipoprotein II (also known as vitellogenin) is the precursor to ovarian lipovitellin and is considered to be an important transporter of lipids to the ovary from the hemolymph during vitellogenesis (Lee and Puppione 1988, Subramoniam 2011). Lipovitellin (lipoprotein II) in the blue crab *Callinectes sapidus* was reported to be yellow to orange in color due to a mixture of carotenoids (Lee and Puppione 1988). Carotenoids vary from almost colorless to yellow and dark red because of their "chromophore" – a conjugated double bond system which absorbs particular wavelengths of light and gives color to the molecules based on the degree of conjugation in the hydrocarbon

chain and end-rings (molecules with more conjugated double bonds absorb more shorter wavelengths of light and thus are redder in color; McGraw 2006).

Carotenoids are biologically active pigments which are potent antioxidants which deactivate reactive chemical species such as singlet oxygen, triplet photochemical sensitizers, and free radicals (Matsuno 2001). One potent effector of invertebrate humoral responses is the prophenoloxidase (proPO) enzymatic cascade. This cascade involves stepwise proteolytic activation or phenoloxidase enzyme which produces melanin accompanied by release of cytotoxic compounds including quinoid intermediates of melanin and reactive oxygen species (Nappi and Ottaviani 2000). Cornet et al (2007) found higher concentrations of hemolymph carotenoids in populations of *Gammarus* crustaceans with activated immune systems and that carotenoid concentration in individuals co-varied positively with both total immune activity and phenoloxidase (PO) activity. They suggested that carotenoids may play a role as immunostimulants and/or antioxidants by scavenging free radicals produced during the proPO cascade thus allowing upregulation of the prophenoloxidase (proPO) system while avoiding self-harm (Cornet et al 2007). Increased hemolymph carotenoid concentration associated with vitellogenesis and/or an activated immune system could explain why this snow crab's hemolymph was reddish-orange. Interestingly, the infected hemolymph and tissues of marine crustaceans infected with *Hematodinium* spp. vary from white to yellow to (more rarely) pink and the carapace of infected species is often discolored pink to orange (MacLean and Ruddell 1978, Field et al 1992, Hudson and Shields 1994, Messick 1994, Taylor and Khan 1995, Love et al

1996, Stentiford et al 2002, Shields et al 2005, Wheeler et al 2007, Ryazanova et al 2010, Xu et al 2010). Altered carotenoid levels could play a role in these discolorations.

Most microorganisms and algae synthesize beta-carotene *de novo* (Matsuno 2001). Carotenoids including beta-carotene and xanthophylls (such as peridinin, dinoxanthin, and diadinoxanthin) are often present in photosynthetic dinoflagellates (Hackett et al 2004, Taylor 2006). Non-photosynthetic species may contain these pigments but exploit a wide range of modes of nutrition such as phagotrophy, saprotrophy, and parasitism suggesting that the origin of the pigments in heterotrophic dinoflagellates may be nutritional (Loeblich 1976). Thus, although the discoloration could be from a dinoflagellate-origin carotenoid, this is less likely than altered host carotenoids.

The reddish-orange color discoloration in the hemolymph masked an underlying parasitemia which in BCD is normally characterized by milky hemolymph, resulting in a false negative diagnosis via visual examination of hemolymph. This discoloration of the hemolymph also impacted the gross appearance of the ventral carapace. These findings suggest that altered hemolymph constituents (lipoproteins and/or carotenoids) during vitellogenesis may mask gross macroscopic changes of BCD in immature female snow crabs. Further investigation into this possibility is warranted. The PCR assay on this snow crab also yielded a false-negative result. The cause of the false negative molecular test result is unclear. False negative test results may be attributable to many factors, including low amount of template DNA in the test sample, inadequate removal of PCR inhibitors, ineffective release of DNA content from the host

cells, and poor DNA recovery after extraction and purification steps (da Cunha Gonçalves-de-Albuquerque et al 2014). In this case PCR inhibition due to hemolymph factors may have played a role in the false negative test results. A variety of chemical substances can act as PCR inhibitors including, but not limited to, calcium ions, urea, phenol, ethanol, glycogen, polysaccharides, tannic acid, humic acid, melanin, collagen, and proteinases (reviewed in Schrader et al 2012).

In regards to infection intensity, 100% of mild infections (1/1), 40% of infections with moderate infection intensity (2/5), 11% of advanced infections (1/9) had false negative test results while no very advanced infections (0/13) had false-negative test results. This suggests that diagnosis by visual exam and diagnosis by PCR assay are less accurate in the early stages of BCD. However, the sample numbers in each category are quite low; thus the proportions of false negative rates are not statistically significant among different infection intensities. These findings indicate that diagnosis of BCD by both visual examination and PCR underestimate the true prevalence of *Hematodinium* infection in Atlantic Canadian snow crab. In this study the diagnosis by visual exam or PCR assay resulted in false negative test results in 14.3-21.4% of diseased animals, resulting in underestimation of disease prevalence by 1.25 – 1.76%.

2.5. References

Barrento S, Marques A, Pedro S, Vaz-Pires P, Nunes ML. 2008. The trade of live crustaceans in Portugal: space for technological improvements. ICES J Mar Sci 65(4):551-559.

Barrento S, Marques A, Vaz-Pires P, Nunes ML. 2010. Live shipment of immersed crabs *Cancer pagurus* from England to Portugal and recovery in stocking tanks: stress parameter characterization. ICES J Mar Sci 67(3):435-443.

Bower SM, Meyer GR, Phillips A, Workman G, Clark D. 2003. New host and range extension of bitter crab syndrome in *Chionoecetes* spp. caused by *Hematodinium* sp. Bulletin of the European Association of Fish Pathologists 23(2):86-91.

Chatton É, Poisson R. 1931. Sur l'existence dans le sang des crabes, de péridiniens parasites: *Hematodinium perezi* n.g., n.sp. (Syndinidae). C R Seances Soc Biol Paris 105: 553–557.

Cornet S, Biard C, Moret Y. 2007. Is there a role for antioxidant carotenoids in limiting self-harming immune response in invertebrates? Biol Lett 3(3):284-288.

Dawe EG, Drew HJ, Warren RT. 2002. Trends in prevalence of Bitter Crab Disease (*Hematodinium* spp.) in snow crab (*Chionoecetes opilio*) throughout the Newfoundland and Labrador continental shelf. Crabs in Cold Water Regions: Biology, Management, and Economics. Alaska Sea Grant College Program 2002:385-400.

Dawe E, Mullowney D, Colbourne E, Han G, Morado JF, Cawthorn R. 2010. Relationship of oceanographic variability with distribution and prevalence of bitter crab syndrome in snow crab (*Chionoecetes opilio*) on the Newfoundland–Labrador shelf. Biology and management of exploited crab populations under climate change. Alaska Sea Grant College Program 2010:175-198.

da Cunha Gonçalves-de-Albuquerque S, e Silva RP, de Morais RC, Trajano-Silva LA, Régis-da-Silva CG, Brandão-Filho SP, de Paiva-Cavalcanti M. 2014. Tracking false-negative results in molecular diagnosis: proposal of a triplex-PCR based method for leishmaniasis diagnosis. J Venom Anim Toxins 20(1):1.

Dyson W, Schott E, Pitula JS, Hanif A. 2009. A PCR-based assay for detection of *Hematodinium* sp. in sediment from the Maryland coastal bays. The Fifth Education and Science Forum, abstract.

Field RH, Appleton PL. 1995. A *Hematodinium* -like dinoflagellate infection of the Norway lobster *Nephrops norvegicus*: Observations on pathology and progression of infection. Dis Aquat Org 22(2):115-128.

Field RH, Chapman CJ, Taylor AC, Neil DM, Vickerman K. 1992. Infection of the Norway lobster *Nephrops norvegicus* by a *Hematodinium*-like species of dinoflagellate on the west coast of Scotland. Dis Aquat Org 13(1):1-15.

Fonseca DB, Sainte-Marie B, Hazel F. 2008. Longevity and change in shell condition of adult male snow crab *Chionoecetes opilio* inferred from dactyl wear and mark-recapture data. T Am Fish Soc 137(4):1029-1043.

Frischer ME, Lee RF, Sheppard MA, Mauer A, Rambow F, Neumann M, Brofft JE, Wizenmann T, Danforth JM. 2006. Evidence for a free-living life stage of the blue crab parasitic dinoflagellate, *Hematodinium* sp. Harmful Algae 5(5):548-557.

Gornik SG, Cranenburgh A, Waller RF. 2013. New host range for *Hematodinium* in southern Australia and new tools for sensitive detection of parasitic dinoflagellates. PLoS One 8(12):e82774.

Gruebl T, Frischer ME, Sheppard M, Neumann M, Maurer AN, Lee RF. 2002. Development of an 18S rRNA gene-targeted PCR-based diagnostic for the blue crab parasite *Hematodinium* sp. Dis Aquat Org 49(1):61-70.

Hackett JD, Anderson DM, Erdner DL, Bhattacharya D. 2004. Dinoflagellates: a remarkable evolutionary experiment. Am J Botany 91(10):1523-1534.

Hudson DA, Adlard RD. 1996. Nucleotide sequence determination of the partial SSU rDNA gene and ITS1 region of *Hematodinium* cf. *perezi* and *Hematodinium* -like dinoflagellates. Dis Aquat Org 24(1):55-60.

Hudson DA, Shields JD. 1994. *Hematodinium australis* n. sp., a parasitic dinoflagellate of the sand crab *Portunus pelagicus* from Moreton Bay, Australia. Dis Aquat Org 19(2):109-119.

Jensen PC, Califf K, Lowe V, Hauser L, Morado JF. 2010. Molecular detection of *Hematodinium* sp. in northeast Pacific *Chionoecetes* spp. and evidence of two species in the northern hemisphere. Dis Aquat Org 89(2):155-166.

Lee RF, Puppione DL. 1988. Lipoproteins I and II from the hemolymph of the blue *crab Callinectes sapidus*: lipoprotein II associated with vitellogenesis. J Exp Zool 248(3):278-289.

Li C, Shields JD, Miller TL, Small HJ, Pagenkopp KM, Reece KS. 2010. Detection and quantification of the free-living stage of the parasitic dinoflagellate *Hematodinium* sp. in laboratory and environmental samples. Harmful Algae 9(5):515-521.

Li C, Song S, Liu Y, Chen T. 2013. *Hematodinium* infections in cultured Chinese swimming crab, *Portunus trituberculatus*, in northern China. Aquaculture 396(2013):59-65.

Li YY, Xia XA, Wu QY, Liu WH, Lin YS. 2008. Infection with *Hematodinium* sp. in mud crabs *Scylla serrata* cultured in low salinity water in southern China. Dis Aquat Org 82(2):145-50.

Liñán-Cabello MA, Paniagua-Michel J, Hopkins PM. 2002. Bioactive roles of carotenoids and retinoids in crustaceans. Aquac Nutr 8(4):299-309.

Loeblich AR. 1976. Dinoflagellate evolution: speculation and evidence. J Protozool 23(1):13-28.

Lohan KM, Reece KS, Miller TL, Wheeler KN, Small HJ, Shields JD. 2012. The role of alternate hosts in the ecology and life history of *Hematodinium* sp., a parasitic dinoflagellate of the blue crab (*Callinectes sapidus*). J Parasitol 98(1):73-84.

Love D, Thomas T, Moles A. 1996. Bitter crab hemolymph studies: indications of host physiological condition. High Latitude Crabs: Biology Management and Economics. Alaska Sea Grant College Program. AK-SG-96-02:549-562.

MacLean SA, Ruddell CL.1978. Three new crustacean hosts for the parasitic dinoflagellate *Hematodinium perezi* (Dinoflagellata: Syndinidae). J Parasitol 64(1):158-160.

Matsuno T. 2001. Aquatic animal carotenoids. Fisheries Sci 67(5):771-783.

McGraw KJ. 2006. Mechanics of carotenoid-based coloration. Bird coloration. Volume 1. Mechanisms and measurements. 1:177-242. Retrieved from http://books.google.com.

Messick GA. 1994. *Hematodinium perezi* infections in adult and juvenile blue crabs *Callinectes sapidus* from coastal bays of Maryland and Virginia, USA. Dis Aquat Org 19(1):77-82.

Meyers TR, Koeneman TM, Botelho C, Short S. 1987. Bitter crab disease: a fatal dinoflagellate infection and marketing problem for Alaskan tanner crabs *Chionoecetes bairdi*. Dis Aquat Org 3(3):195-216

Morado FJ. 2011. Protistan diseases of commercially important crabs: a review. J Invert Pathol 106(1): 27-53.

Mullowney DR, Dawe EG, Morado JF, Cawthorn RJ. 2011. Sources of variability in prevalence and distribution of bitter crab disease in snow crab (*Chionoecetes opilio)* along the northeast coast of Newfoundland. ICES J Mar Sci 68(3):463-471.

Nappi AJ, Ottaviani E. 2000. Cytotoxicity and cytotoxic molecules in invertebrates. BioEssays 22(5):469-480.

Pestal GP, Taylor DM, Hoenig JM, Shields JD, Pickavance R. 2003. Monitoring the prevalence of the parasitic dinoflagellate *Hematodinium* sp. in snow crabs *Chionoecetes opilio* from Conception Bay, Newfoundland. Dis Aquat Org 53(1):67-75.

Pitula JS, Dyson WD, Bacht HB, Njoku I, Chen F. 2012. Temporal distribution of genetically homogenous "free-living" *Hematodinium* sp. in a Delmarva costal ecosystem. Aquat Biosyst. 8(1):16.

Ridgway ID, Taylor AC, Atkinson RJ, Stentiford GD, Chang ES, Chang SA, Neil DM. 2006. Morbidity and mortality in Norway lobsters, *Nephrops norvegicus*: physiological, immunological and pathological effects of aerial exposure. J Exp Mar Biol and Ecol 328(2):251-264.

Ryazanova TV. 2008. Bitter Crab Syndrome in Two Species of King Crabs from the Sea of Okhotsk. Russian J Mar Biol 34(6):411-414.

Schrader C, Schielke A, Ellerbroek L, Johne R. 2012. PCR inhibitors–occurrence, properties and removal. J Appl Microbiol 113(5):1014-1026.

Sheppard M, Walker A, Frischer ME, Lee RF. 2003. Histopathology and prevalence of the parasitic dinoflagellate, *Hematodinium* sp., in crabs (*Callinectes sapidus, Callinectes similis, Neopanope sayi, Libinia emarginata, Menippe mercenaria*) from a Georgia estuary. J Shellfish Res 22(3):873-880.

Shields JD, Sullivan SE, Small HJ. 2015. Overwintering of the parasitic dinoflagellate *Hematodinium perezi* in dredged blue crabs *Callinectes sapidus* from Wachapreague Creek, Virginia. J Invertebr Pathol 130(2015):124-132.

Shields JD, Taylor DM, Sutton SG, O'Keefe PG, Ings DW, Pardy AL. 2005. Epidemiology of Bitter Crab Disease (*Hematodinium* sp.) in snow crabs *Chionoecetes opilio* from Newfoundland, Canada. Dis Aquat Org 64(3):253-264.

Shields JD, Taylor DM, O'Keefe PG, Colbourne E, Hynick E. 2007. Epidemiological determinants in outbreaks of Bitter Crab Disease (*Hematodinium* sp.) in snow crabs *Chionoecetes opilio* from Conception Bay, Newfoundland, Canada. Dis Aquat Org 77(1):61-72.

Small HJ, Shields JD, Hudson KL, Reece KS. 2007. Molecular detection of *Hematodinium* sp. infecting the blue crab, *Callinectes sapidus.* J Shellfish Res 26(1):131-139.

Small HJ, Neil DM, Taylor AC, Atkinson RJA, Coombs GH. 2006. Molecular detection of *Hematodinium* spp. in Norway lobster *Nephrops norvegicus* and other crustaceans. Dis Aquat Org 69(2):185-195.

Small HJ, Wilson S, Neil DM, Hagan P, Coombs GH. 2002. Detection of the parasitic dinoflagellate *Hematodinium* in the Norway lobster *Nephrops norvegicus* by ELISA. Dis Aquat Org 52(2):175-177.

Stentiford GD, Green M, Bateman K, Small HJ, Neil DM, Feist SW. 2002. Infection by a *Hematodinium* -like parasitic dinoflagellate causes Pink Crab Disease (PCD) in the edible crab *Cancer pagurus*. J Invertebr Pathol 79(3):179-191.

Stentiford GD, Neil DM, Coombs GH. 2001. Development and application of an immunoassay diagnostic technique for studying *Hematodinium* infections in *Nephrops norvegicus* populations. Dis Aquat Org 46(3):223-229.

Stentiford GD, Shields JD. 2005. A review of the parasitic dinoflagellates *Hematodinium* species and *Hematodinium* -like infections in marine crustaceans. Dis Aquat Org 66(1):47-70.

Subramoniam T. 2011. Mechanisms and control of vitellogenesis in crustaceans. Fisheries Sci 77(1):1-21.

Taylor FJR. 1987. *The biology of dinoflagellates.* Botanical Monographs, Vol. 21. Oxford: Blackwell Scientific. Pp 1-785.

Taylor FJR. 2006. Dinoflagellates. eLS.

Taylor DM and Khan RA. 1995. Observations on the occurrence of *Hematodinium* sp. (Dinoflagellata: Syndinidae), the causative agent of Bitter Crab Disease in Newfoundland snow crab (*Chionoecetes opilio*). J Invertebr Pathol 65(3):283-8.

Wheeler K, Shields JD, Taylor DM. 2007. Pathology of *Hematodinium* infections in snow crabs (*Chionoecetes opilio*) from Newfoundland, Canada. J Invertebr Pathol 95(2):93-100.

Xu WJ, Shi H, Xu HX, Small HJ. 2007. Preliminary study on the *Hematodinium* infection in cultured *Portunus trituberculatus*. Acta Hydrobiologica Sinica 31(5):637-642.

Xu W, Xie J, Shi H, Li C. 2010. *Hematodinium* infections in cultured ridgetail white prawns, *Exopalaemon carinicauda,* in eastern China. Aquaculture 300(1-4):25-31.

3. LIGHT AND ELECTRON MICROSCOPIC EXAMINATION OF ATLANTIC CANADIAN SNOW CRABS, *CHIONOECETES OPILIO*, WITH BITTER CRAB DISEASE INCLUDING COMPARISONS OF *IN VIVO* AND *IN VITRO* LIFE STAGES

3.1. Introduction

Bitter Crab Disease (BCD) is an emerging disease in decapod crustaceans caused by dinoflagellates of the genus *Hematodinium*. To date over forty species of crustaceans are infected by *Hematodinium* species world-wide, primarily in the North Pacific and Atlantic Oceans. This includes several commercially important decapods: snow crabs (*Chionoecetes opilio*), Tanner crabs (*C. bairdi*), grooved Tanner crabs (*C. tanneri*), blue crabs (*Callinectes sapidus*), Norway lobsters (*Nephrops norvegicus*), velvet crabs (*Necora puber*), and edible crabs (*Cancer pagurus*; Stentiford and Shields 2005, Morado et al 2011). Infections of *Hematodinium* spp. are thought to be fatal in most host species. Over the past two decades, the prevalence of BCD has increased worldwide (Stentiford and Shields 2005). In eastern Canada, BCD was first reported in snow crabs from Conception Bay, Newfoundland in 1990 with very low prevalence (<0.11 – 3.7%; Taylor and Khan 1995). Subsequently, BCD has spread rapidly within the eastern and northeastern bays of Newfoundland and Labrador and has resulted in at least three epizootics (Shields et al 2005, 2007).

Macroscopically, late stage infections are characterized by an opaque discoloration of the cuticle which gives snow crabs a “cooked” appearance and milky white hemolymph associated with large numbers of circulating parasites (Meyers et al 1987). This parasitemia is associated with hemocytopenia and with respiratory malfunction which may contribute to the host’s death (Shields 1994, Field and Appleton 1995, Shields and Squyars 2000, Shields et al 2003,

Wheeler et al 2007). Microscopically, the parasite proliferates within the hemolymph and multisystemically infiltrates hemal spaces (Stentiford and Shields, 2005). In some host species parasites occur in intimate association with various tissues surfaces, including the outer basal lamina of the hepatopancreatic tubule epithelial cells in Norway lobsters *Nephrops norvegicus*, the wall of hemolymph vessels in harbor crabs *Liocarcinus depurator*, and the myocardial lumina in snow crabs *C. opilio*, but tissue invasion beyond the level of hemal spaces is typically not observed (Field and Appleton 1995, Stentiford and Shields 2005, Wheeler et al 2007, Small et al 2012).

In most descriptions of *Hematodinium*-associated disease in crustaceans, the predominant life stage observed is typically referred to as the trophont, the vegetative or trophic stage of the life cycle. Microscopically, uninucleate trophonts have moderate to abundant amounts of vacuolated or "foamy" cytoplasm and are irregularly round to ovoid or amoeboid in shape (Eaton et al 1991, Appleton and Vickerman 1998, Morado 2007, Ryazanova 2008). The term plasmodial trophont or plasmodium is used to describe the multinucleate trophont life form. In addition to these amoeboid multinucleate (plasmodial) forms of trophonts, elongated finger-like forms with nuclear rowing referred to as vermiform plasmodia or filamentous trophonts are occasionally described. Vermiform plasmodia are occasionally attached to or intimately associated with tissue surfaces (Chatton and Poisson 1931, Newman and Johnson 1975, Field et al 1992, Messick 1994 Ryazanova 2010; see Chapter 1, Table 1.3). In addition, sheet-like plasmodial forms have been described in the hemal spaces, heart, muscle, and

hepatopancreatic interstitial connective tissues (Field and Appleton 1995, Wheeler et al 2007, Chualáin and Robinson 2011; see Chapter 1, Table 1.3).

Sporont life stages (uninucleate sporonts and multinucleate plasmodial sporonts) arise from trophonts and are indistinguishable from trophont life stages by light microscopy (Appleton and Vickerman 1998, Stentiford and Shields 2005, Ryazanova 2008, Li et al 2011). The ultrastructural presence of trichocysts within these parasitic life stages has been used as a defining feature to distinguish between trophonts (trichocysts absent) and sporonts (trichocysts present) in some host species including snow crabs *C. opilio*, Tanner crabs *C. bairdi*, Norway lobsters *N. norvegicus*, and tropical mud crabs *Scylla serrata* (Meyers et al 1987, Appleton and Vickerman, 1998, Hudson and Shields 1994, Gaudet et al 2015). However, this may not hold true for *Hematodinium* infections in all species as developing and mature trichocysts were described in vegetative (trophont) life stages in harbor crabs *Liocarcinus depurator* and blue swimming crabs *Portunus pelagicus* (Hudson and Shields 1994, Small et al 2012).

In some species (blue crabs *Callinectes sapidus,* and Tanner crab *Chionoecetes bairdi,* red and blue king crabs *Paralithodes* spp. and tropical mud crabs *Scylla serrata*) a smaller life stage referred to as a prespore or sporoblast was described *in vivo* (Meyers et al 1987, Taylor and Khan 1995, Ryazanova et al 2010, Coffey et al 2012). This life stage has also been seen *in vitro* in *Hematodinium* cultures derived from Norway lobsters *Nephrops norvegicus*, blue crabs *Callinectes sapidus,* and snow crab *Chionoecetes opilio* (Appleton and Vickerman 1998, Li et al 2011, Gaudet et al 2015). Sporoblasts have less cytoplasm (higher N:C ratio) and more

condensed nucleus than sporonts and are considered to be the direct precursors for motile dinospores. Dinospores, the final described life stage, are rarely seen. Dimorphic dinospores develop in natural infections in Tanner crabs *Chionoecetes bairdi,* snow crab *Chionoecetes opilio* red and blue king crabs *Paralithodes* spp., and blue crabs *Callinectes sapidus* (Meyers et al 1987, Wheeler et al 2007, Ryazanova et al 2010, Li et al 2011). Dinospores have been observed in some crustacean hosts to exit the host through the mouth and gills in 'plumes' at very high densities (1.6×10^8 cell/ml) in the terminal stage of the disease (Shields and Squyars 2000, Stentiford and Shields, 2005).

Three studies have investigated *Hematodinium* life stages *in vitro*: Appleton and Vickerman (1998) isolated *Hematodinium* sp. from the Norway lobster *Nephrops norvegicus*, Li et al (2011) isolated *Hematodinium perezi* from the blue crab *Callinectes sapidus*, and Gaudet et al (2015) isolated *Hematodinium* sp. from late stage infection in snow crabs *Chionoecetes opilio*. All three studies used light microscopy, and Appleton and Vickerman (1998) and Gaudet et al (2015) supplemented their life stage descriptions with electron microscopic findings. In addition to uninucleate and multinucleate trophont and sporont life stages, assemblages of filamentous forms known as "Gorgonlocks" trophont colonies, interdigitated syncytia called "clump colonies", and syncytial plasmodia called arachnoid plasmodia and sheet-like plasmodia have been described *in vitro* (Appleton and Vickerman 1998, Li et al 2011, Gaudet et al 2015).

Snow crabs with macroscopic evidence of BCD were collected off the northern coasts of Newfoundland and the northeastern coast of Nova Scotia. Light microscopic and ultrastructural examination of selected tissues were performed in an attempt to confirm infection with

Hematodinium sp. and compare the *in vivo* life stages with those described from *in vitro* culture of *Hematodinium* sp. from snow crabs (see Gaudet et al 2015).

3.2. Materials and Methods

3.2.1. Snow Crab Collection

Atlantic snow crabs (*C. opilio*) were collected during annual Fall surveys in Notre Dame Bay and White Bay, Newfoundland during September 2010 and 2011. In Notre Dame Bay, crabs were caught by pot trap on the grounds of strata 610 and 611 (200-400 m in depth). In Notre Dame Bay, stratum 611 is shallow (200-300m) and stratum 610 is deep (301-400 m). Deep stratum 610 was missed in 2011 due to inclement weather. Water temperatures for strata 610 and 611 range between -1°C and 3°C in early Fall (Mullowney et al 2011). In White Bay, crabs were caught by pot trap on the grounds of stratum 614 (300-401 m in depth). The water temperatures for stratum 614 normally ranged between 0-1°C in early Fall (Mullowney *et al*., 2011). The salinity in these bays ranges from 31-35 ppt, with BCD-positive crabs typically not found in regions with salinity <33 ppt (Dawe et al 2010).

Traps were separated by 45 m within each set and were baited using squid or mackerel. Soak time was usually about 24 h, depending on weather conditions. Within each crab management area surveyed, the depth range and actual area sampled corresponded approximately to the commercial fishery area. Minimum depth for sampling was 170 m for all survey areas. The survey has consistently occurred in September and occupies 5 of the inshore Fall multi-species

survey strata with a target of 8 sets per stratum. Each set includes 6 traps, with crabs sampled from two large-meshed (commercial, 135 mm) and two small-meshed (27 mm) traps.

Crabs were kept in coolers layered between seawater-soaked burlap, and placed on saltwater ice until reaching shore. On shore, coolers were transported to St. John's, Newfoundland, where they were sent via air cargo to the Atlantic Veterinary College (AVC) at University of Prince Edward Island (UPEI). The interval between snow crab harvest and their arrival at the AVC was usually 24-48 h. After the first shipment (100% mortality, see below) snow crabs were recovered in 34 ppt artificial seawater which was aerated with air stones and maintained at 0-2 °C until processing. The interval between snow crab arrival at AVC and processing ranged from 15 min to ~4 h.

In addition, one female BCD+ snow crab (*C. opilio*) was collected off the northeastern coast of Nova Scotia (position 44° 23.23N, 63° 28.11W) by DFO Nova Scotia during its 2010 annual Fall survey. The water depth was ~ 100 m and bottom temperatures ranged between 0-3°C at this location (Tremblay 1997). The crab was kept in chilled seawater in a cooler packed with saltwater ice and transported by land to the AVC, University of Prince
Edward Island. The time between snow crab harvest and arrival at AVC was ~24 h and the snow crab was processed immediately upon arrival at AVC.

3.2.2. Snow Crab Processing and Sample Collection

Each snow crab was photographed (dorsal and ventral digital images), gender was noted and recorded, and carapace width (mm) was measured and recorded. Hemolymph from each animal was collected aseptically from the base of the first walking leg using a 3 ml or 5 ml syringe with a 22 gauge needle. For each animal the gross appearance of the hemolymph was noted, hemolymph refractive index was measured using digital refractometer (Reichert r^2mini digital refractometer; Reichert Analytical Instruments) and the measured value was recorded, and two direct smears of hemolymph were made on glass slides. Air-dried smears were later stained with Wright-Giemsa in a Hema-Tek 1000 automated slide stainer (Miles Scientific). In addition, a 200 µl sample of hemolymph was placed in an ethanol block (96 well block) containing 800 µl 100% ethanol per well for DNA extraction. These DNA samples were examined using a polymerase chain reaction (PCR) assay with *Hematodinium*-specific primers (Appendix 1). This assay was used for the molecular detection of *Hematodinium* sp. infection in a larger survey of Newfoundland snow crabs, and was used as a molecular method of disease detection for this project.

Crabs were evaluated for gross morphologic evidence of Bitter Crab Disease, which is characterized by an orangish-pink or “cooked” appearance to the carapace and/or white discoloration of arthrodial membranes. Crabs with macroscopic evidence of BCD were exsanguinated, with the remaining hemolymph stored on ice and used for the *in vitro* cultivation (Gaudet *et al* 2015). The crab was then humanely euthanized via nerve cord disruption via decapitation (i.e., removal of the carapace) as it was previously determined that

euthanasia via potassium chloride injection resulted in a large streak of tissue disruption (Appendix 2). After removal of the carapace, a digital image of the crab's internal organs was taken and tissue samples were collected. The tissue samples collected included: heart, hepatopancreas, gill (1st and 4th gills on the right), gonad, midgut, eyestalks (left and right), a cross-section of the abdomen, and a cross-section of leg (1st merus on the right). The tissues were immediately placed in Davidson's seawater (Appendix 3) fixative for 24 hours. After 24 h, tissue samples were transferred into containers of 70% ethanol for storage until routine processing for histology.

Fixed samples were routinely processed (Leica processor) into paraffin-embedded tissue blocks. Sections were cut at 3-5 µm thickness on a rotary microtome, mounted on glass slides, and stained with hematoxylin and eosin (H&E) on an automated stainer (Leica). Stained sections were examined on a VistaVision light microscope (VWR) and digital images were captured using an Axioplan 2 imaging microscope with an Axiocam HRc camera and AxioVision 4.8.2.0 software (Zeiss).

Sections of all soft tissues (heart, hepatopancreas, gill (x2), gonad, and midgut) were trimmed and placed into one cassette per individual snow crab for processing. A second cassette of sections lined by a thick cuticular layer (eyestalk, leg, and abdomen) was also submitted. The eyestalk was bisected along the frontal plane which consistently resulted in optimal sections of internal neuroendocrine tissues (see Appendix 4).

3.2.3. Histologic Examination

As reported in Wheeler et al (2007), relative intensity of the parasite within the tissue was used as the key indicator for severity of infection. The intensity of the parasitic infection (light, moderate, advanced, and very advanced) was assessed by evaluating parasitic infiltration of interstitial connective tissues per high power field (HPF, 400x magnification) using a modified version of the rating system from Wheeler et al (2007). The intensity of infection was rated as follows: light infection (1-25 parasites per HPF), moderate infection (25 -50 parasites per HPF, advanced infection (>50 to 100 parasites per HPF), and very advanced (>100 to too numerous to count). In moderate infection intensities the parasites infiltrated but did not completely fill or expand the interstitial connective tissues. With advanced and very advanced infection intensities, the parasitic infiltrates filled and expanded the interstitial connective tissue spaces.

The morphologic appearance of *Hematodinium* sp. parasites within each tissue was then assessed. The morphologic appearance of the dinoflagellates was consistent with trophonts (histologically identical to sporonts) or sporoblasts. If the animal had trophont life stages, a 100 cell count of parasitic life stages within the hepatopancreatic interstitium was done to determine what proportion of cells were uninucleate versus multinucleate (plasmodial). The plasmodial cells were further divided by number of nuclei (2 nuclei, 3 nuclei, 4-8 nuclei, or 9-12 nuclei). For life stages other than trophoblastic life stages the morphologic appearance of the life stages was described. Dimensions of uninucleate life stages were measured using FIJI (FIJI is a freeware program based on Image J and can be downloaded at http://fiji.sc). Each tissue was also examined for evidence of hemocytic inflammation.

Samples of eight tissues were processed for transmission electron microscopy (TEM) from one Nova Scotian BCD+ female snow crab: gill, heart, stomach, midgut, leg muscle, hepatopancreas, ovary, and spermatheca. For TEM, the selected tissues were cut at 1 mm^3, fixed in 2% glutaraldehyde in artificial seawater (ASW) at 4°C for 24 h, washed in ASW, post-fixed in 1% osmium tetroxide in double-strength ASW at room temperature (~22 EC) for 1 h, and washed again in ASW. After dehydration in an ascending ethanol series followed by propylene oxide, the tissue fragments were embedded in Epon 812/Araldite and placed in a vacuum desiccator overnight to degas. The resin-embedded samples were then placed in Better Equipment for Electron Microscopy, Inc. (BEEM) capsules and polymerized in a 65EC oven for 24 h. Semi-thin (0.5 µm) sections were cut with a Reichert-Jung Ultracut E ultramicrotome, stained with 1% toluidine blue in 1% sodium tetraborate solution for viewing with a light microscope, and suitable areas identified for examination under TEM. The blocks were trimmed to <1 mm^2 areas of interest and ultrathin sections (90 nm) of these areas were cut on a Reichert-Jung Ultracut E ultramicrotome, mounted on uncoated 200 supermesh copper grids, and stained with 5% uranyl acetate in 50% ethanol followed by Sato lead stain. Thin sections were examined using a Hitachi Bio TEM 7500 transmission electron microscope operated at 80 kV. Images were captured using an Advance Microscopy Techniques (AMT) XR40 side mount digital camera.

3.3. Results

3.3.1. Light Microscopy

Histologic examination of 29 BCD+ snow crabs from NFLD (n=29) revealed 1 male snow crab with mild infection intensity, 5 individuals with moderate BCD infections (4 male crabs and 1 female crab), 10 individuals with advanced BCD infections (1 female crab), and 13 individuals with very advanced BCD infections (3 female crabs). The single female snow crab from NS had an advanced BCD infection (Table 3.1).

Table 3.1 Gender, carapace width, infection intensity, and predominant life stage observed in Atlantic Canadian snow crabs with BCD. The predominant life stage observed via light microscopy was noted with the life stage observed via TEM in parentheses if performed for that snow crab.

Crab	Gender	Carapace Width	Infection intensity	Uninucleate life stage [Light microscopy (TEM)]
2010-19	Male	90	Advanced	Trophont/sporont
2010-20	Male	96	Very advanced	Trophont/sporont
2010-30	Male	93	Moderate	Sporoblast
2010-38	Male	83	Very Advanced	Trophont/sporont
2010-39	Male	80	Advanced	Trophont/sporont
2010-40	Male	54	Very Advanced	Trophont/sporont
2010-59	Male	75	Very Advanced	Trophont/sporont
2010-60	Male	80	Advanced	Trophont/sporont
2010-106	Female	56	Moderate	Trophont/sporont
2010-117	Male	65	Very Advanced	Trophont/sporont
2010-119	Male	78	Very Advanced	Trophont/sporont
2010-120	Female	60	Very Advanced	Trophont/sporont
2010-131	Female	60	Very Advanced	Trophont/sporont
2010-133	Female	49	Moderate	Trophont/sporont
2011-61	Male	80	Advanced	Trophont/sporont (trophont)
2011-62	Male	99	Very advanced	Trophont/sporont (trophont)
2011-63	Male	65	Advanced	Trophont/sporont (trophont)
2011-64	Male	87	Advanced	Trophont/sporont (trophont)
2011-65	Male	101	Advanced	Trophont/sporont (sporont)
2011-66	Male	107	Very advanced	Trophont/sporont (trophont)
2011-67	Male	67	Very advanced	Trophont/sporont (trophont)
2011-98	Male	67	Very advanced	Trophont/sporont
2011-99	Male	74	Very advanced	Trophont/sporont
2011-100	Male	79	Advanced	Trophont/sporont
2011-147	Male	67	Mild	Trophont/sporont
2011-155	Male	72	Moderate	Trophont/sporont
2011-156	Male	85	Moderate	Trophont/sporont
2011-163	Female	48	Advanced	Trophont/sporont
2010-NS1	Female	50	Advanced	Trophont/sporont (sporont)

3.3.1.1. Parasitic Life Stages

3.3.1.1.1. Trophont/Sporont Life Stages

In most (28/29) infections, the predominant parasitic life stage observed was the trophont (trophont or sporont, which are indistinguishable in light microscopy). In the snow crabs with trophont life stages, the trophonts varied from uninucleate to multinucleate, with multinucleate forms having 2 to 12 visible nuclei. In most (27/28) snow crabs with trophont life stages, the uninucleate trophonts and plasmodial trophonts had foamy, vacuolated cytoplasm. In the single lightly infected snow crab, the trophonts had pale basophilic cytoplasm (Figure 3.1A) and lacked the foamy vacuolated cytoplasmic appearance typical of trophont life stages (Figure 3.1B). This mildly infected snow had 50% uninucleate life stages and 50% plasmodial life stages (Figure 3.2).

In snow crabs with moderate infections the uninucleate life stage predominated (range of 74 – 94% uninucleate trophonts/100 cell count; Figure 3.3). These trophont life stages all had foamy vacuolated cytoplasm (Figure 3.1B). In snow crabs with advanced infections the proportions of uninucleate life stages varied more widely (range of 43 to 93% uninucleate trophonts/100 cell count; Figures 3.1C and 3.4). The average proportion in the uninucleate life stage in advanced intensity infections (63.3 +/- 5.5 %) was significantly lower than that in moderate infections (84.75 +/- 4.5 %; two-sample t-test assuming equal variances p-value of 0.040221). (Two sample F-test for variances P (F<=f) value of 0.151549, indicating equal population variances.) In snow crabs with very advanced infection the proportions of multinucleate (plasmodial) life stages tended to increase (range of 34 to 69% uninucleate trophonts/100 cell count) and with

increased proportions of multinucleate trophonts with 4 or more nuclei (Figures 3.1D and 3.5). The average proportion of cells in the uninucleate life stage (54.5 +/- 2.8 %) was lower than that observed in advanced infections, but this difference was not statistically significant (two-sample t-test assuming unequal variances p-value 0f 0.178385). (Two-sample F-test for variances P(F<=f) value of 0.039574, indicating unequal population variances.)

In light and moderate infections vermiform life stages were not observed in any tissue examined. Vermiform life stages were observed in most (9/10) advanced intensity infections and in all (13/13) very advanced life stages. Vermiform life stages were not seen in one crab with an advanced infection (2010-163). In these advanced and very advanced intensity infections, vermiform life stages varied from rare to occasional to frequent. When vermiform plasmodia were frequently observed, attached forms were occasionally to frequently observed in the heart (Figure 3.7). When vermiform plasmodia were only occasionally observed, attached forms were rare in the heart. If vermiform plasmodia were rare in the tissues, attached forms were not observed. Attached vermiform plasmodia were rarely observed in tissues other than the heart. They were seen in the eyestalk, gill, and leg in 2 snow crabs with very advanced infections which had frequent attached vermiform plasmodia in the heart. The attached vermiform plasmodia were observed in the eyestalk and gill in the first crab, and in the eyestalk, gill, and leg of the second crab. When in these tissues the attached vermiform plasmodia were intimately associated with the cell surfaces of skeletal muscles (see Figure 3.8).

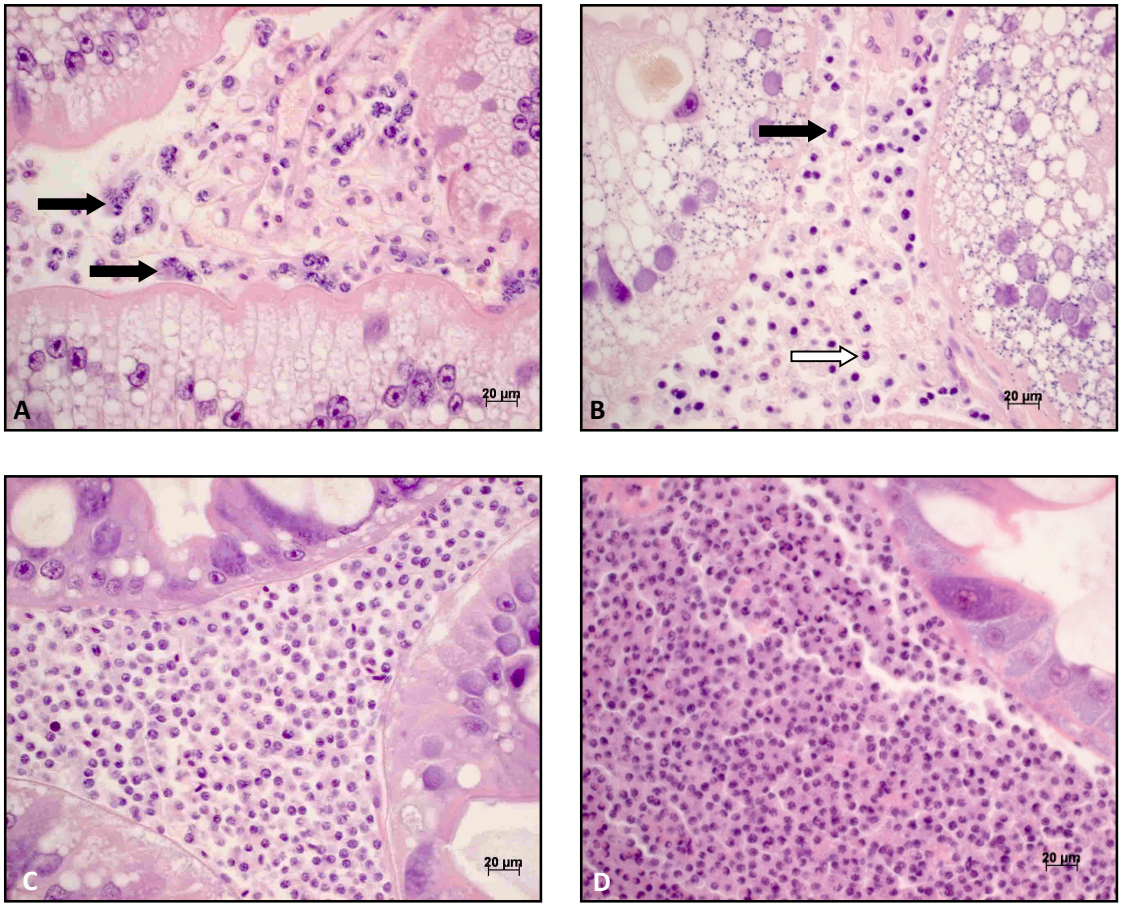

Figure 3.1. Trophont life stages in snow crabs with varying infection intensities. **A)** Trophont life stages with mild infection intensity (snow crab #2011-147). Note small to moderate amount of basophilic cytoplasm that is not foamy or vacuolated (black arrows). **B)** Trophont life stages in a moderately intense infection (snow crab #2011-155). Note moderate to abundant amounts of foamy, vacuolated cytoplasm in both uninucleate (white arrow) and multinucleate (black arrow) life stages. **C)** Vacuolated trophont life stages in an advanced infection (snow crab #2011-163). **D)** Dense sheets of trophont life stages in a very advanced infection (snow crab #2010-40).

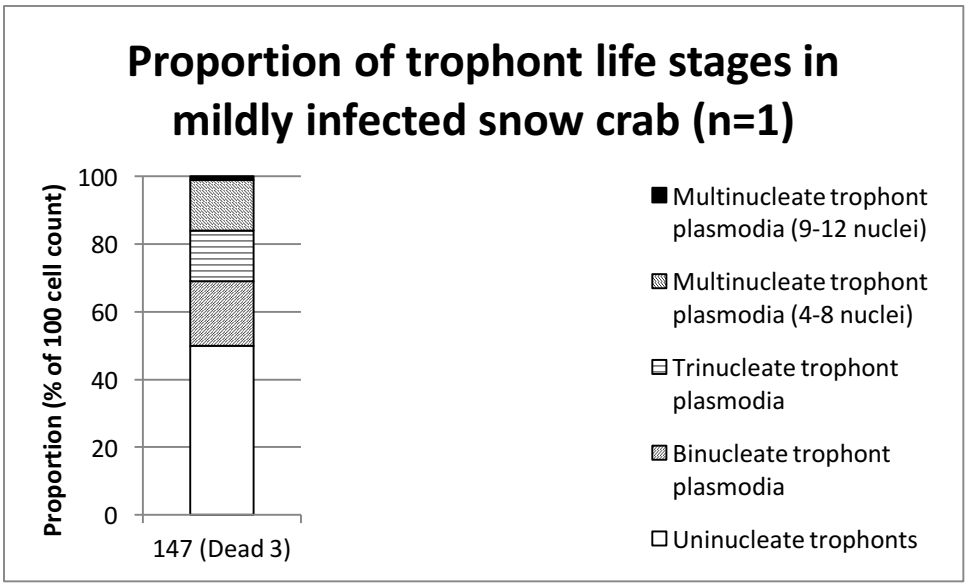

Figure 3.2. Uninucleate and multinucleate life stage proportions in the single snow crab with mild infection intensity. Note 50:50 ratio of uninucleate trophonts to multinucleate trophonts.

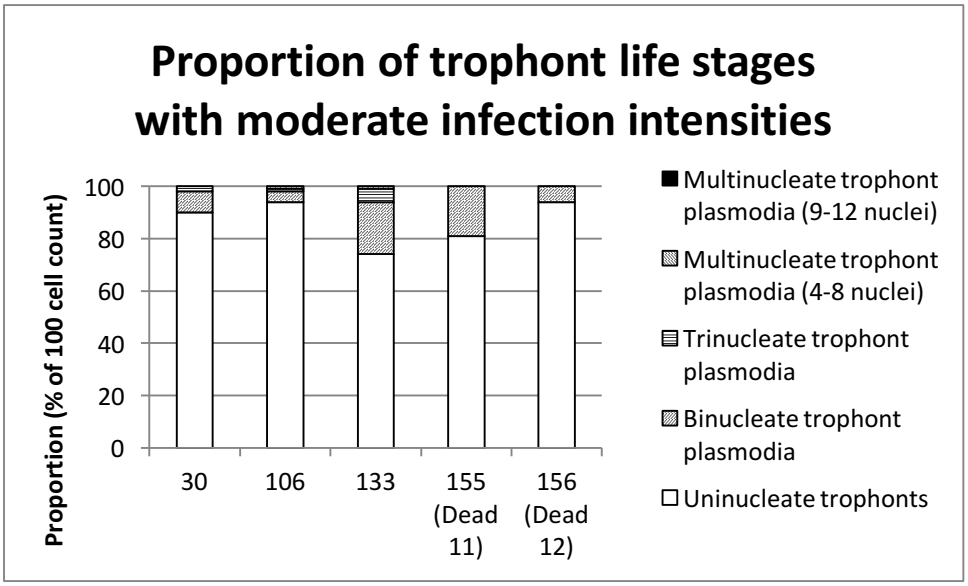

Figure 3.3. Uninucleate and multinucleate life stage proportions in snow crabs with moderate infection intensities. Uninucleate trophonts predominated.

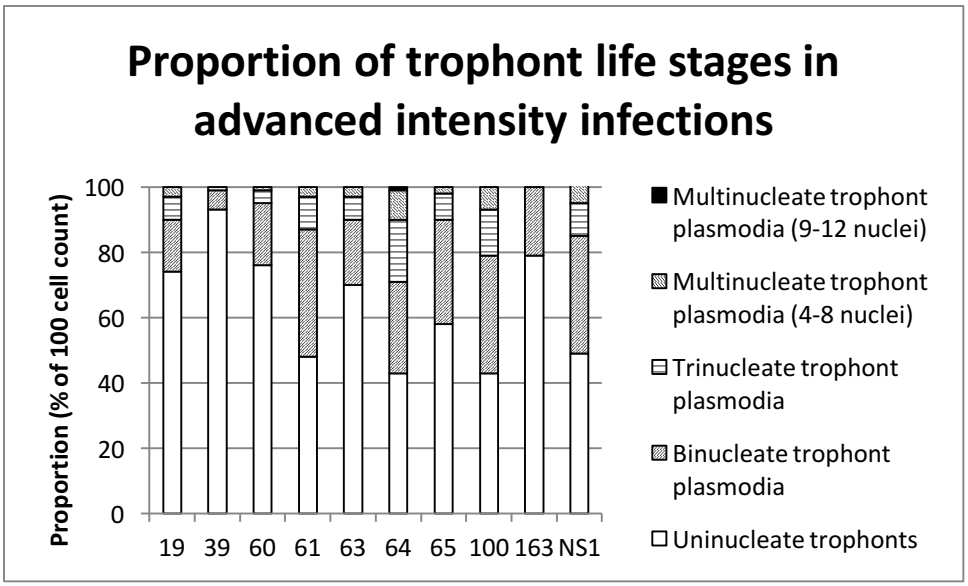

Figure 3.4. Uninucleate and multinucleate life stage proportions in advanced infection intensities. Uninucleate trophonts predominated, with increased proportions of multinucleate plasmodia.

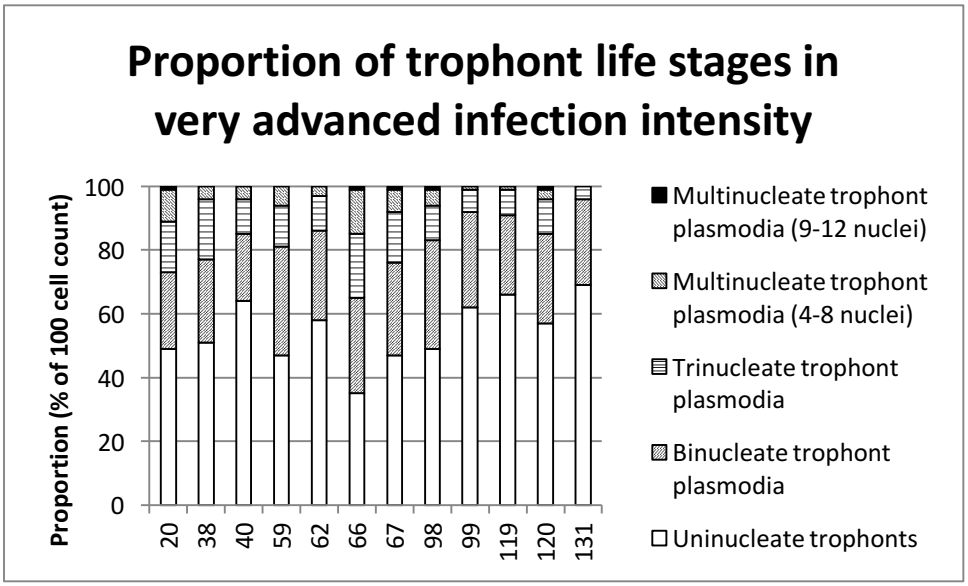

Figure 3.5. Uninucleate and multinucleate life stage proportions in snow crabs with very advanced infection intensities. Note increased proportions of multinucleate life stages and higher numbers of nuclei within plasmodia.

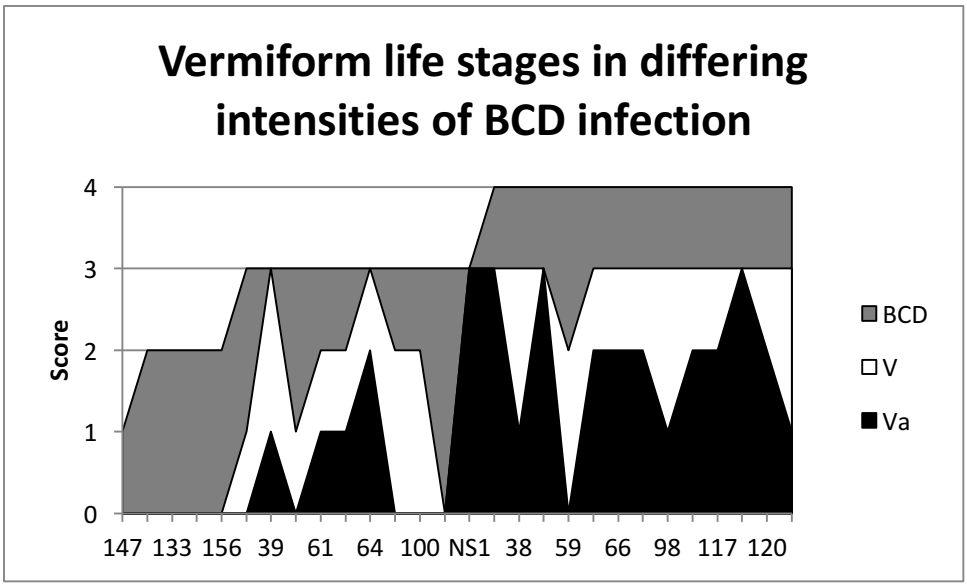

Figure 3.6. Intensity scores of vermiform plasmodia and attached vermiform plasmodia within the heart of snow crabs with mild, moderate, advanced, and very advanced infection intensities. BCD infection intensity scores: mild = 1, moderate = 2, advanced = 3, and very advanced= 4. Scores of vermiform plasmodia: absent = 0, rare = 1, occasional = 2, frequent = 3. Scores for attached vermiform plasmodia: absent = 0, rare = 1, occasional =2, frequent = 3.

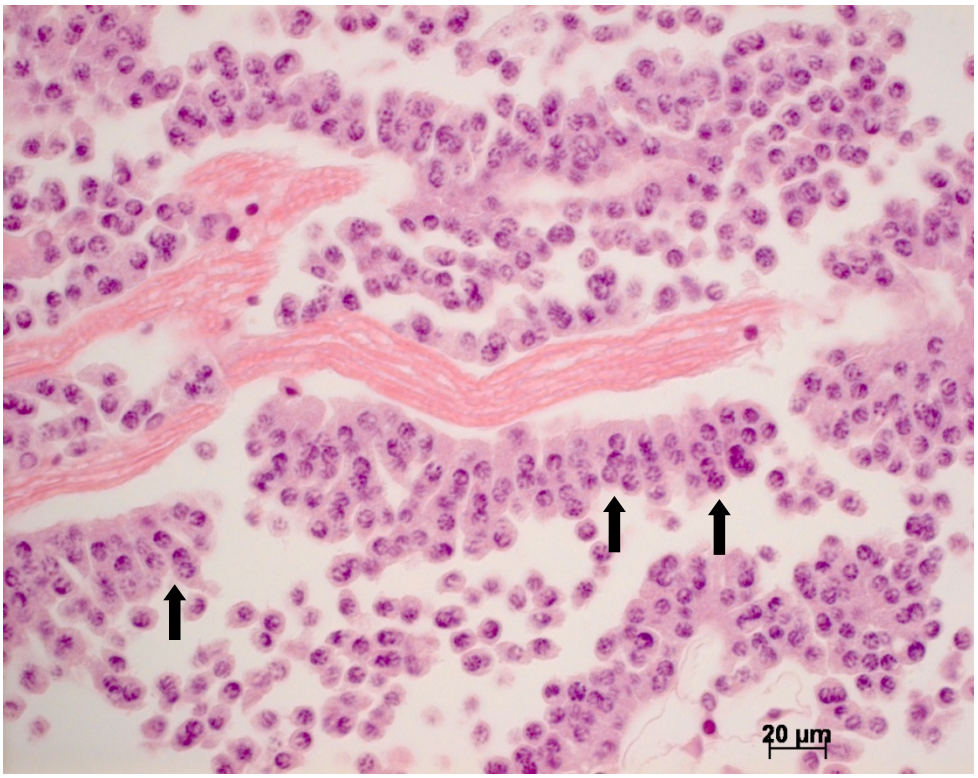

Figure 3.7. Histologic section of attached vermiform plasmodia in the heart (snow crab #2010-119). Note the attached vermiform plasmodia were intimately associated with and oriented perpendicularly to the sarcolemmal surface of the cardiomyocytes (black arrows; H&E, 400x).

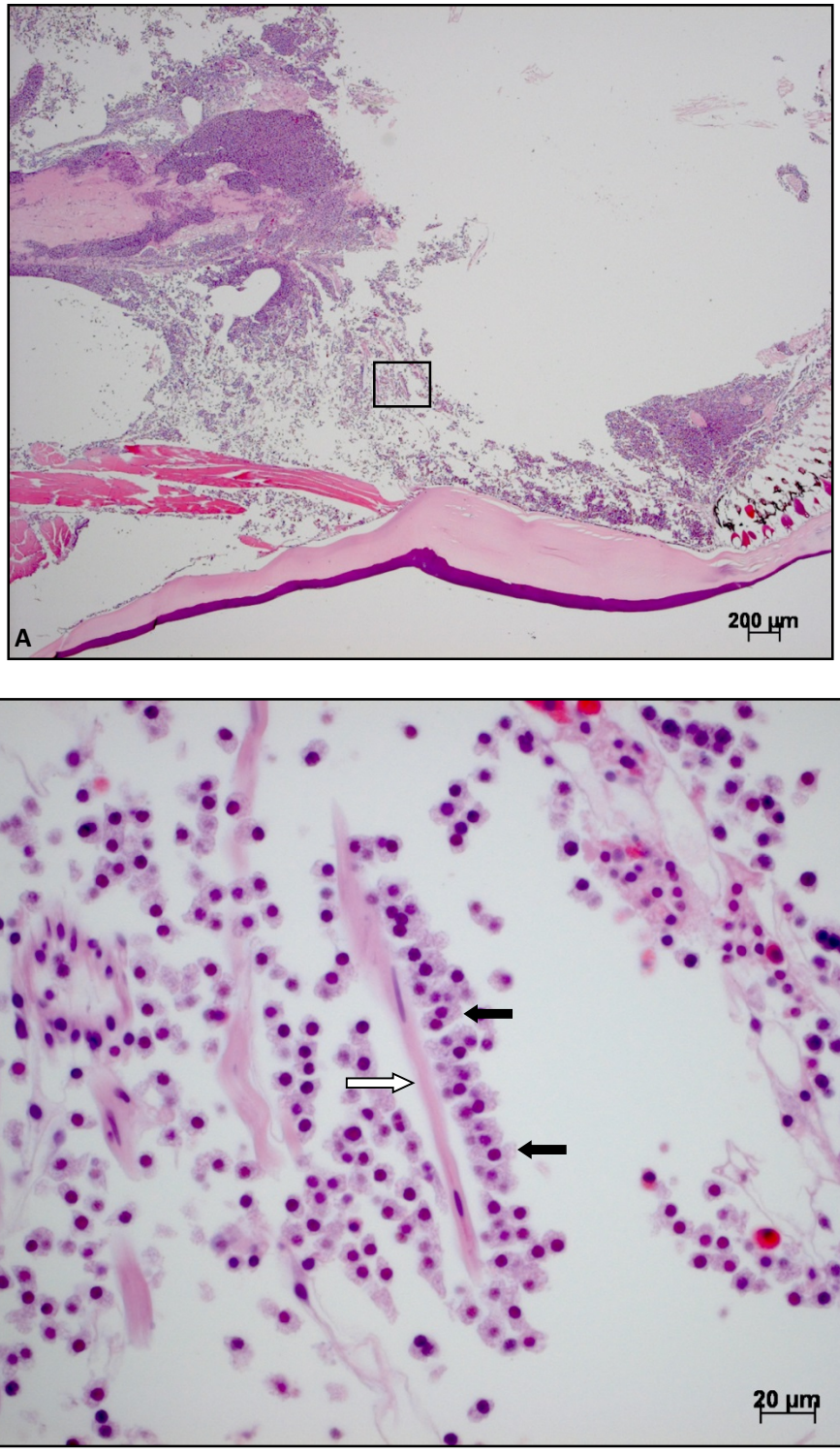

Figure 3.8. Sections of an eyestalk (snow crab #2010-20) infiltrated by trophont life stages at progressive magnifications. **A)** Eyestalk at low magnification for orientation. Note band of skeletal muscle (H&E, 25x). **B)** Boxed area of eyestalk at high magnification (H&E, 400x). Note attached vermiform plasmodia (black arrows) intimately associated with the surface of a fine skeletal muscle or connective tissue fiber (white arrow).

3.3.1.1.2. Sporoblastic Life Stage

The remaining snow crab (#2010-117) had sporoblastic parasites. These life stages were smaller in diameter than trophont life stages (Table 3.2) and had small amounts of foamy, vacuolated cytoplasm (Figure 3.9). Uninucleate life stages predominated; multinucleated life stages (including vermiform plasmodia within the heart) were occasionally observed (Figure 3.10).

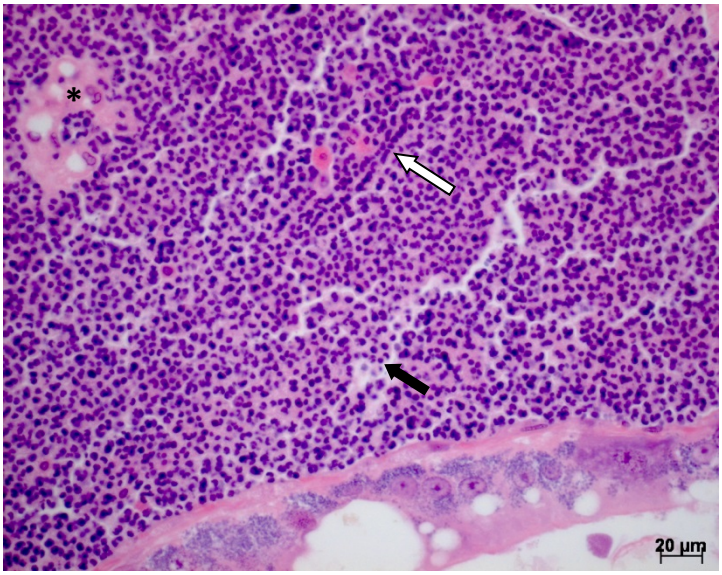

Figure 3.9. Sporoblastic life stages (black arrows) expanding the hepatopancreatic interstitium (snow crab #2010-117). Note occasional multinucleate vermiform plasmodia with nuclear rowing (white arrow) and prominent, enlarged (reactive), perivascular fixed phagocytes (* in top left corner; 400x, H&E).

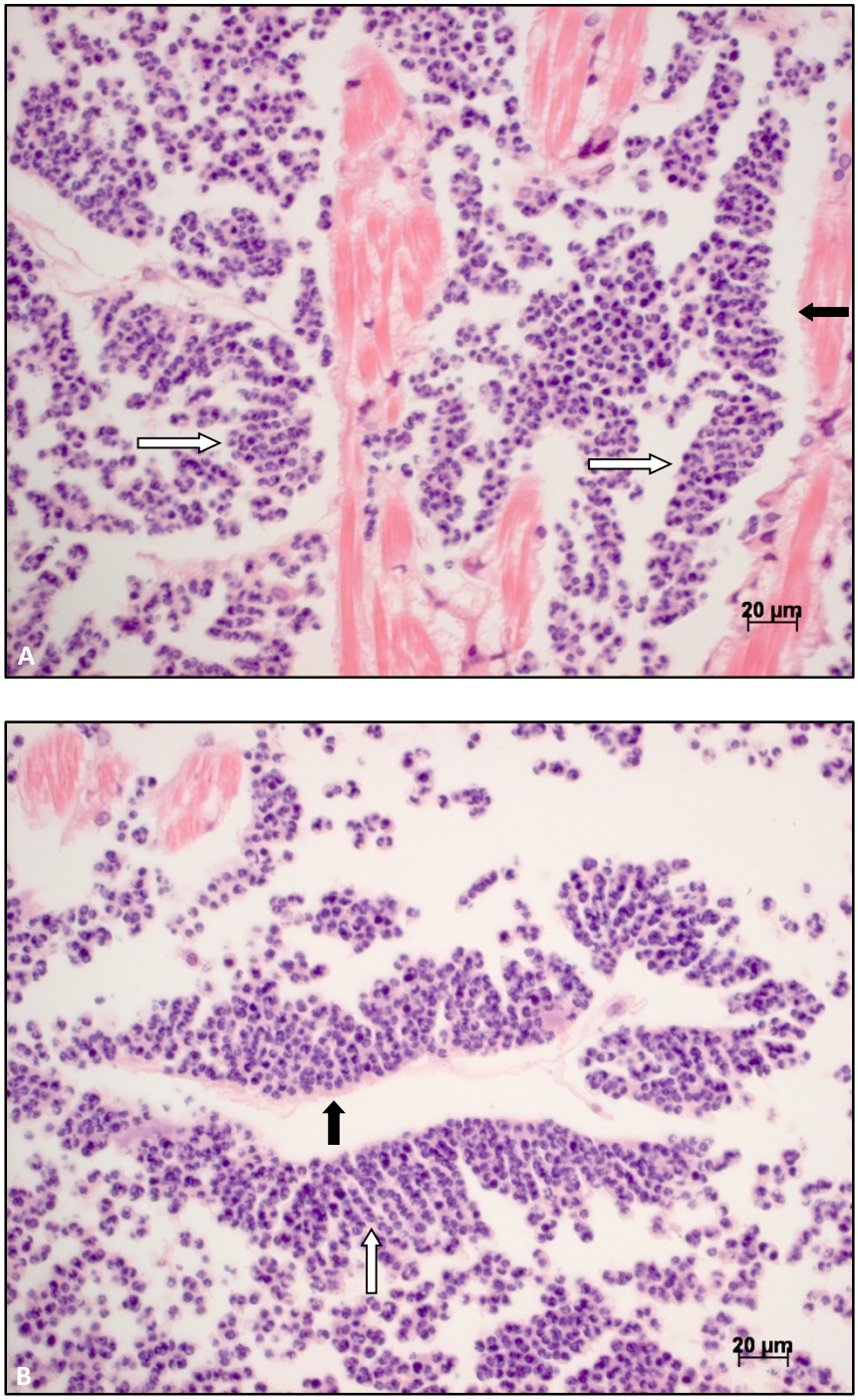

Figure 3.10. Sporoblast attached vermiform plasmodia (white arrows) in the heart (A and B; snow crab #2010-117). Note intimate association of the vermiform plasmodia with cardiomyocyte sarcolemmal surfaces and/or connective tissue surfaces (black arrows; 400x, H&E).

Table 3.2. Cell dimensions of the two different morphologic variants of uninucleate life stages observed. Trophonts were irregularly ovoid with measurements of both width and length while sporoblasts were round with mean and range of cell diameter.

	Trophonts	**Sporoblasts**
Shape	Ovoid	Round
Mean	8.89 x 10.97	5.225
Range	7.737 x 7.895 to 10.955 x 12.258 to 8.539 x 13.869	4.111 to 6.237
n	27	1

3.3.1.2. Histopathologic Changes in Host Tissues

3.3.1.2.1. Hepatopancreas

The hepatopancreatic tubular epithelium in BCD+ snow crabs was commonly pale (rarefied) and swollen with numerous intracytoplasmic vacuoles (hepatocellular hydropic degeneration, presumed) when compared with the hepatopancreatic epithelium of uninfected snow crabs (Figure 3.11). In several of the BCD+ snow crabs (5/28, 17.9%) the hepatopancreas also contained areas with loss of tissue and cellular detail, tissue basophilia, loss of cytoplasmic detail, cellular disruption and loss, and karyolysis (Figure 3.12). This pattern was most commonly observed within the central regions of the hepatopancreatic tissue and was found in animals that died during shipping (post mortem autolysis and/or possible perimortem). The animals with these hepatopancreatic changes had advanced (n=1) or very advanced (n=4) infection intensities and included both female (n=1) and male (n=4) snow crabs (#2010-39, 2010-59, 2010-131, 2011-98, 2011-99).

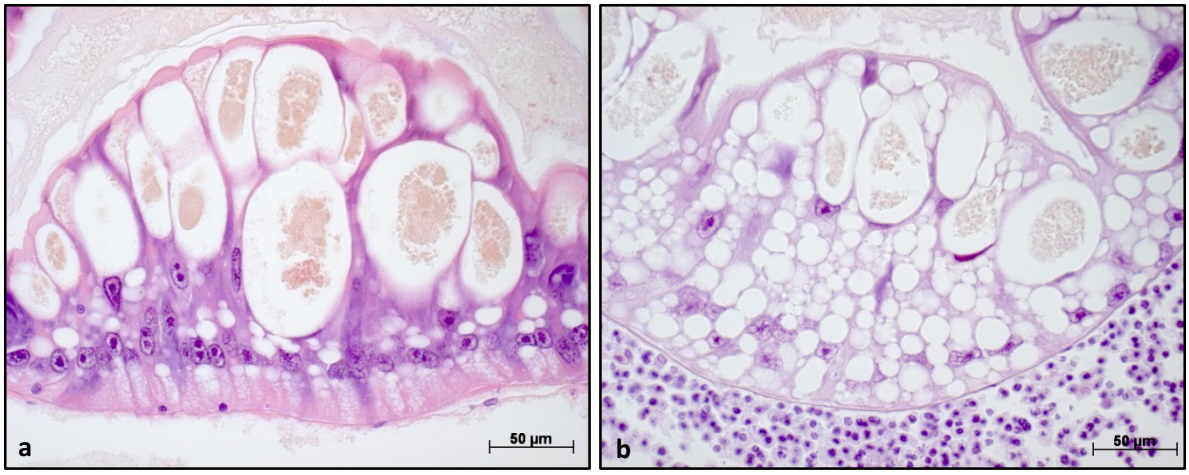

Figure 3.11. Comparison of hepatopancreatic epithelial cytoplasmic appearance by BCD status. **A)** Hepatopancreas from a snow crab without BCD (snow crab #2010-1; 400x, H&E). **B)** Hepatopancreas from a snow crab with BCD (snow crab #2011-67). Note rarefaction of the cytoplasm and prominent cytoplasmic vacuolation (vacuolar degeneration, presumed) of the hepatopancreatic epithelium and the interstitial parasitic infiltration in the BCD+ snow crab (400x, H&E).

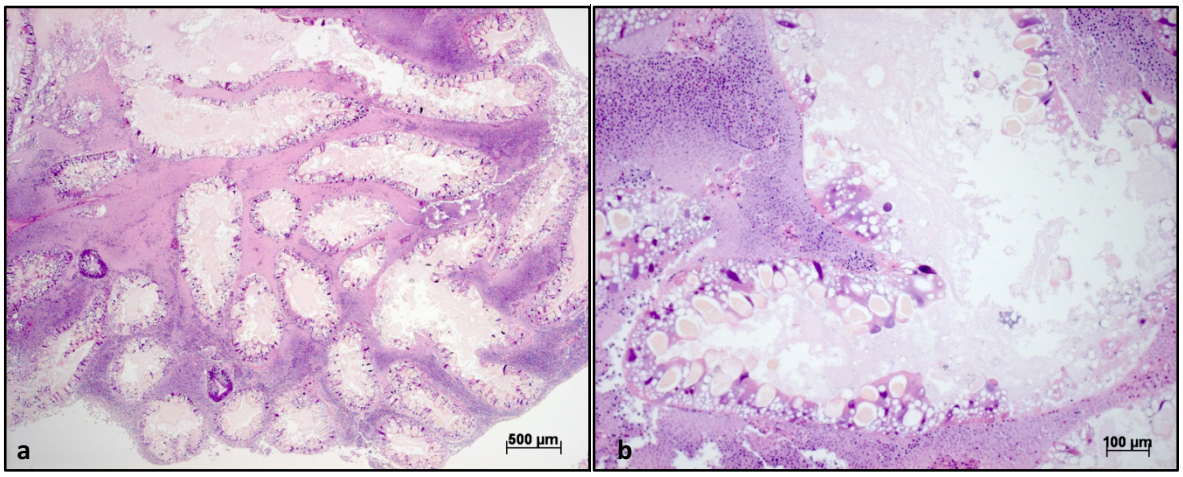

Figure 3.12. Disruption of hepatopancreatic architecture in BCD+ shipping mortalities at progressive levels of magnification (A and B; H&E, 25x and 100x). Note central disruption of architecture with tissue eosinophilia, cytoplasmic disruption and loss, and karyolysis (peracute hepatopancreatic degeneration and necrosis or postmortem autolysis).

3.3.1.2.2. Skeletal Muscle

Occasionally skeletal myofibers were pale in BCD+ shipping mortalities. These pale myofibers did not exhibit myofiber fragmentation or vacuolation (postmortem autolysis or possible perimortem myodegeneration).

3.3.1.2.3. Ovary

Four BCD+ 2010 female snow crabs (2010-106, 2010-106, 2010-120, and 2010-131) were mature and gravid with vitellogenic eggs in their ovaries. The spermathecae of these mature females contained a mixture of sperm packets and bacteria (no definitive evidence of intraluminal parasitic infiltration was observed). Crabs 2010-NS1 and 2011-163 were immature (prepubescent) females. The ova within crab 2010-NS1 were small and very mildly vacuolated (early vitellogenesis, presumed). The ova in the ovary of crab 2010-65 were enlarged and were moderately to markedly vacuolated (ineffective vitellogenesis or possible resorption of vitellogenic lipoproteins) when compared to ovaries of an uninfected non-gravid snow crab (Figure 3.13). The lumina of the spermathecae of these immature females were collapsed, immature, and did not contain sperm packets.

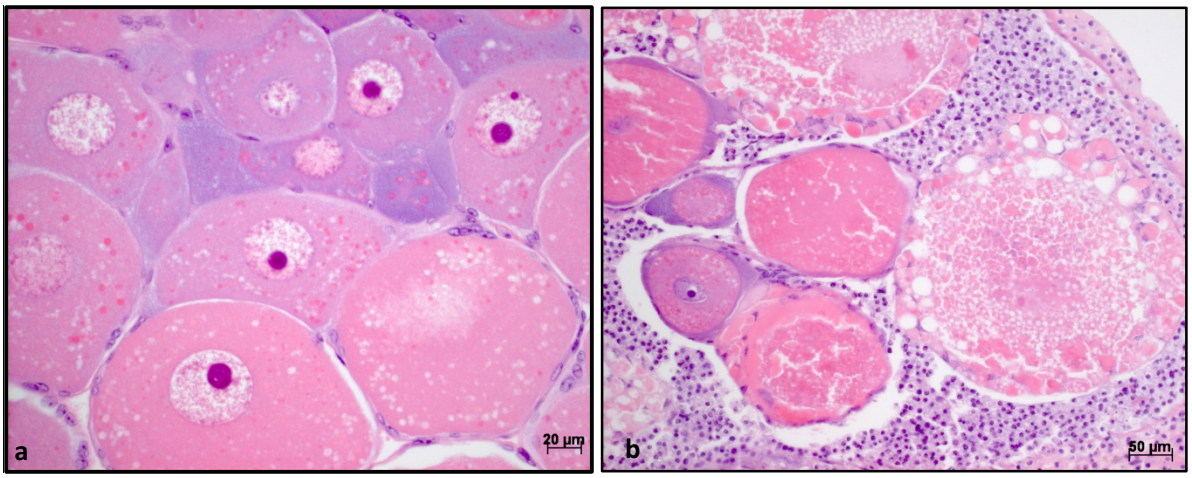

Figure 3.13. Comparison of ovaries from non-gravid females without and with BCD.
A) Ovary of a non-gravid (immature) female without BCD (snow crab #2010-65; 400x, H&E).
B) Ovary of a non-gravid (immature) snow crab with BCD (snow crab #2011-63). Note moth-eaten appearance of ova (degeneration, presumed) and ovarian interstitial infiltration of dinoflagellate parasites (200x, H&E).

3.3.2. Semithin Sections

In semithin sections of the heart, muscle, stomach, midgut, gill, and hepatopancreas, ovary and spermatheca numerous dinoflagellate parasites expanded the interstitial connective tissues and hemal spaces of all tissues examined (data not shown). The parasites were irregularly oval (amoeboid) to vermiform with moderate to abundant amounts of cytoplasm which contained numerous variably sized intracytoplasmic well-defined vacuoles. The cells contained one to several prominent nuclei with moderate anisokaryosis and prominent condensed and darkly staining chromatin characteristic of dinoflagellate endoparasites (dinokaryon). The centers of the semithin sections of the organs were often more pale-staining than the periphery of the sections with increased metachromasia of the intracytoplasmic vacuoles (presumed poor fixation due to inadequate central fixative infiltration). This finding was especially prominent in organs that were lined or partially-lined with chitin, including the stomach, hindgut, and spermatheca. The parasites within the lamellae of the gills stained more darkly than the parasites between the lamellae of the gills (presumed inadequate fixation, possibly due to reduced fixative infiltration due to the chitin lining of the gill lamellae). In the heart, vermiform plasmodia were intimately associated with the cell surface of the cardiac spongy connective tissue/musculature (Figure 3.14).

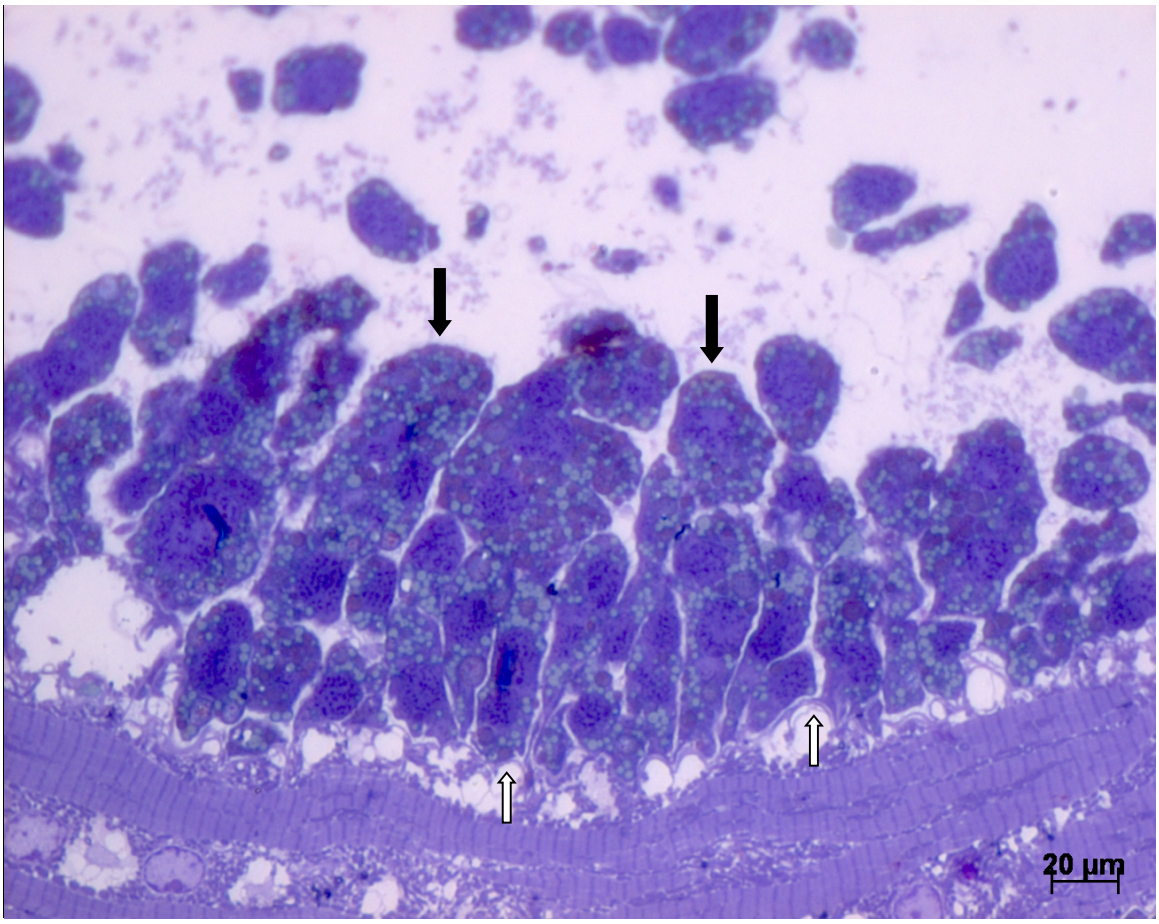

Figure 3.14. Semithin sections of heart from snow crab 2010-NS1. Note attached vermiform plasmodia (black arrows) intimately associated with the sarcolemmal surface of cardiomyocytes (white arrows; Toluidine blue, 1000x).

3.3.3. Transmission Electron Microscopy

Electron microscopic examination of the hepatopancreas, stomach, ovary, spermatheca, and gills revealed infiltration of the interstitial connective tissues and hemal spaces of all organs examined. The parasitic dinoflagellates typically had one to several nuclei (up to five nuclei per cell) with condensed chromatin profiles, abundant intracytoplasmic lipid droplets, lipofuscin-like granules, occasional clear intracytoplasmic membrane-bound vacuoles, small numbers of mitochondria, and a surrounding alveolar membrane with empty amphiesmal vesicles (Figure 3.15). Uninucleate and multinucleate parasites often contained one or several cross-sectional,

longitudinal, or tangential profiles of membrane-bound trichocysts. In the areas interpreted as foci of poor fixation due to inadequate fixative infiltration, the mitochondria were less distinct with occasional slightly swollen cristae, the cytoplasm was more condensed, and the lipid vacuoles often had areas of clearing (presumed incomplete lipid fixation).

In the ovary, sporonts infiltrated and expanded the interstitium between oocytes (Figure 3.16) with a focal site of rupture of an oocyte's limiting membrane. No evidence of intracellular invasion of oocytes was observed, and no vitellogenic eggs, which are characterized by numerous intracytoplasmic lipid vacuoles, were observed. In the spermatheca, the sporonts invaded the interstitium and the lumen of the organ in areas lined by both chitin (ventral spermatheca) and glandular epithelium (dorsal spermatheca). In areas of the spermatheca lined by glandular epithelium, the cells lining the lumen invaded by parasites typically exhibited cellular degeneration with swollen rarefied cytoplasm, loss of cytoplasmic organelles, and swollen nuclei, and exhibited prominent interdigitation of their basal membranes (Figure 3.17).

In the heart, uninucleate and multinucleate plasmodial sporonts were free within the hemal and interstitial spaces of the spongy connective tissue. Vermiform multinucleate plasmodial sporonts were observed in close association with the outer cell membrane (sarcolemma) of the cardiomyocytes and often oriented perpendicularly to the host sarcolemmal surface (Figure 3.18). The vermiform plasmodial life stages had multifocal small cytoplasmic extensions which extended along the extracytoplasmic surface of the heart cell membrane or interdigitated with sarcolemma of the host cardiomyocytes (Figures 3.19, 3.20, and 3.21). Very thin connections

between two parasitic cell bodies were occasionally observed (Figures 3.18 and 3.19). These vermiform life stages had occasional cross-sections or tangential sections of intracytoplasmic trichocysts, indicating that the vermiform plasmodia were sporonts (when trichocysts are used to delineate sporont from trophont life stages; Figures 3.18, 3.19 and 3.20).

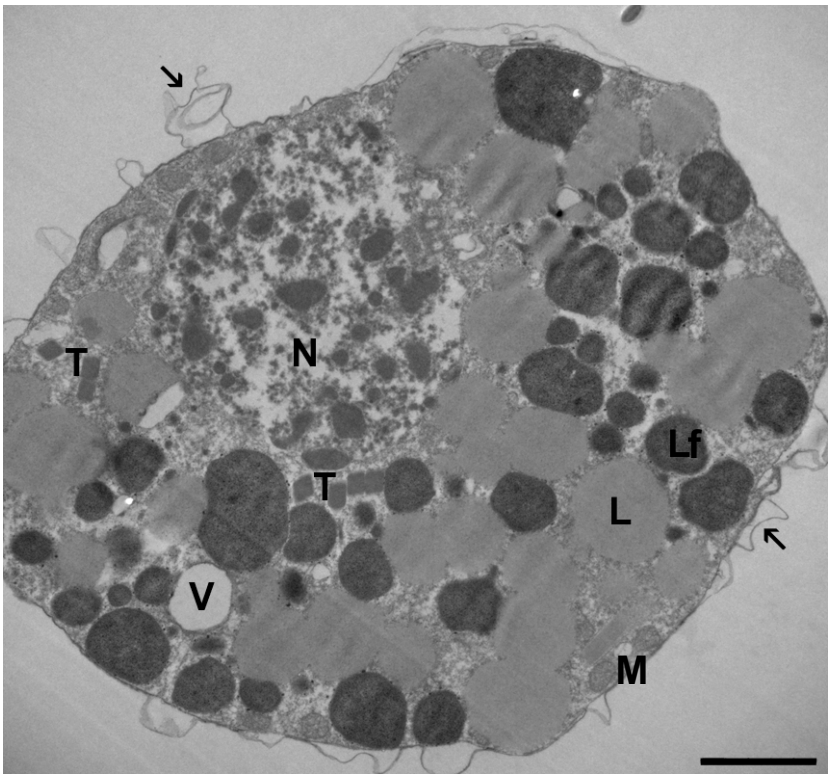

Figure 3.15. *Hematodinium* sp. sporont from snow crab 2010-NS1. Note the presence of intracytoplasmic lipid droplets (L), lipofuscin-like inclusions (Lf), membrane-bound trichocysts (T), mitochondria, (M), vacuoles (V), and a surrounding alveolar membrane (arrows). Parasites typically contained one to five nuclei (N). TEM, scale bar = 2 µm.

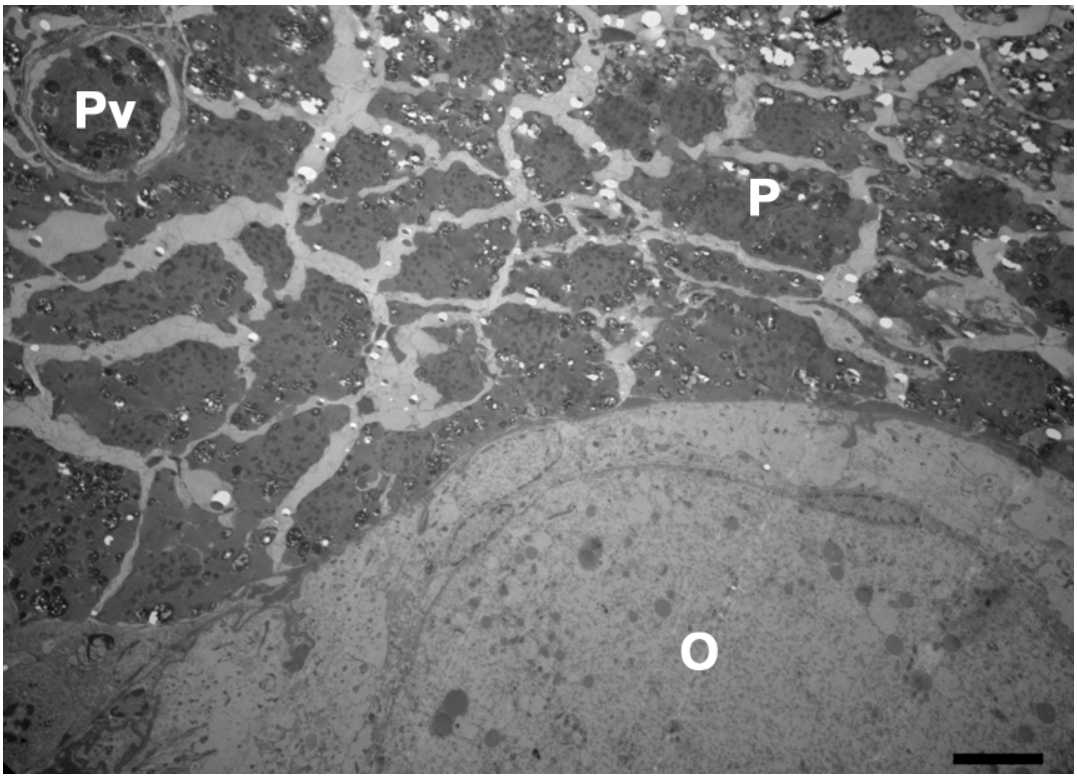

Figure 3.16. Ovary of female crab 2010-NS1. Note the presence of a pre-vitellogenic oocyte (O) and the sheet of uninucleate and multinucleate parasitic plasmodial cells (P) in the ovarian interstitium and within a small-caliber hemolymph vessel (Pv). TEM, scale bar = 10 microns.

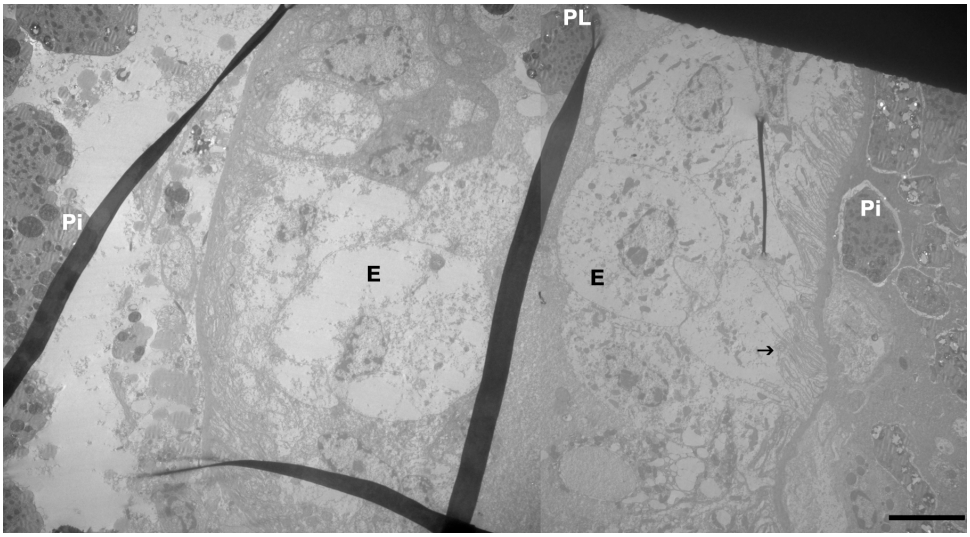

Figure 3.17. Parasitic dinoflagellates within the interstitium and lumen of the spermatheca. The spermatheca was lined by degenerative glandular epithelial cells (E) with parasitic dinoflagellate sporonts in the glandular lumen (PL) and in the surrounding interstitial connective tissue (Pi). Note the prominent interdigitation of basal membranes of the glandular epithelial cells (arrow). TEM, scale bar = 10 microns.

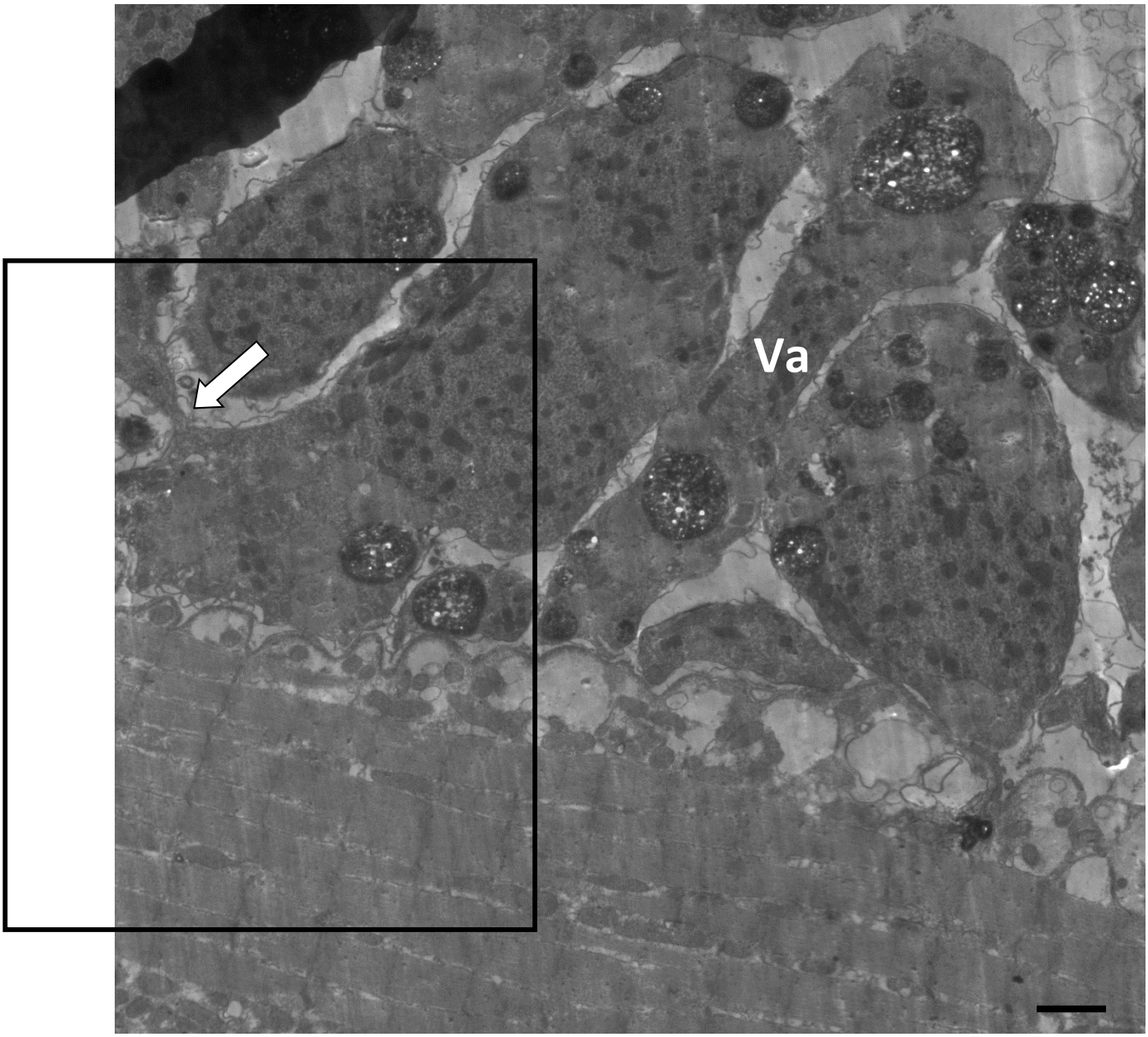

Figure 3.18. Heart of female crab 2010-NS1. Note intimate association of vermiform multinucleate plasmodia (Va) with the outer cell membrane of the cardiomyocyte and the thin cytoplasmic connection (arrow). TEM, scale bar = 2 microns. (Note: Higher magnification of boxed region is pictured in Figure 3.19.)

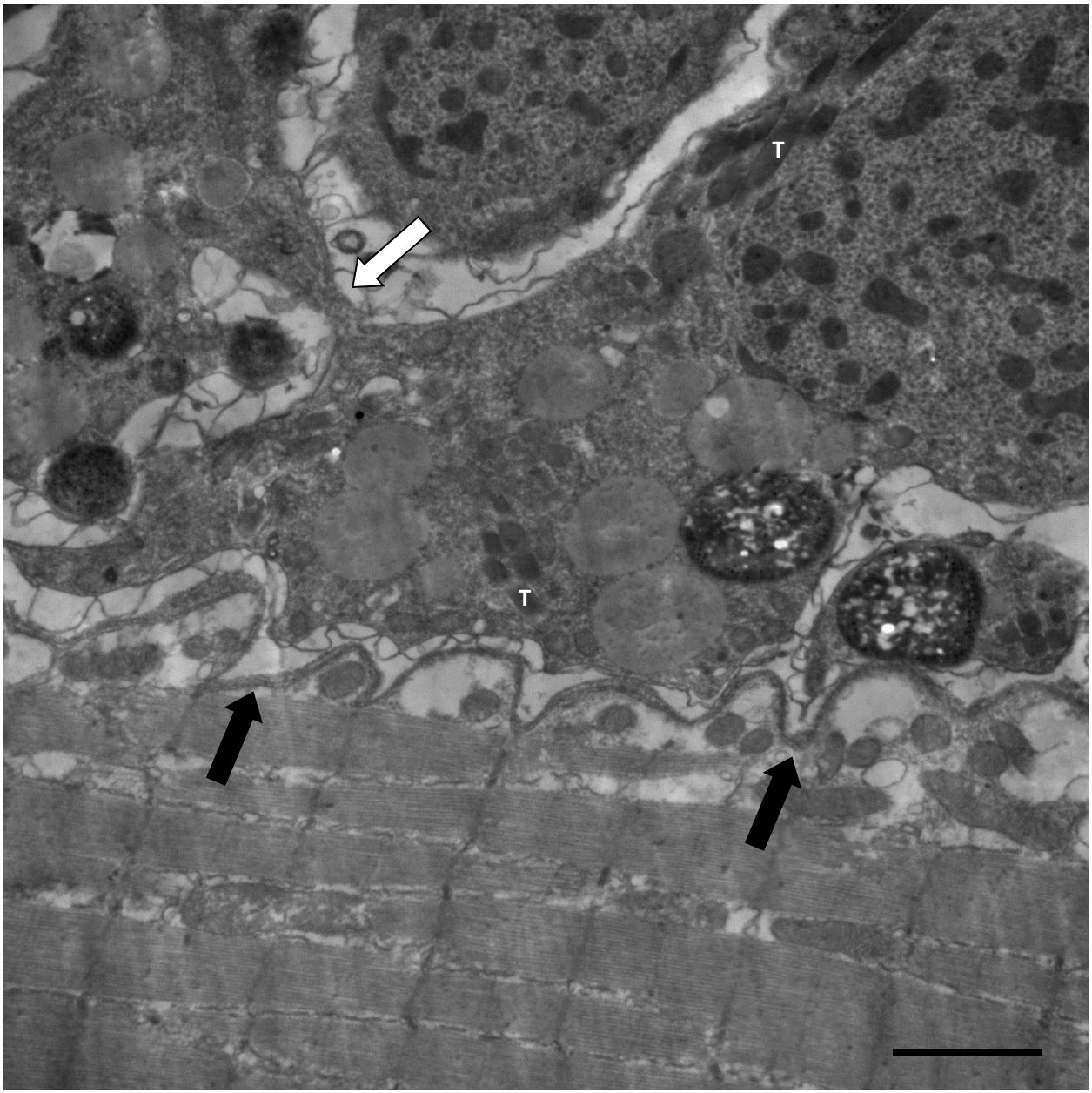

Figure 3.19. Boxed area of Figure 3.18, heart of female crab 2010-NS1. Note intimate association of the outer surface of the amphiesmal membrane of vermiform multinucleate plasmodia with the outer cell membrane of the cardiomyocyte, with interdigitation of the parasites with the undulating surface of the cell membrane (black arrows). Note also a thin cytoplasmic connection between two parasitic masses (possible intercellular connection; white arrow) and intracytoplasmic trichocysts (T). TEM, scale bar = 2 microns.

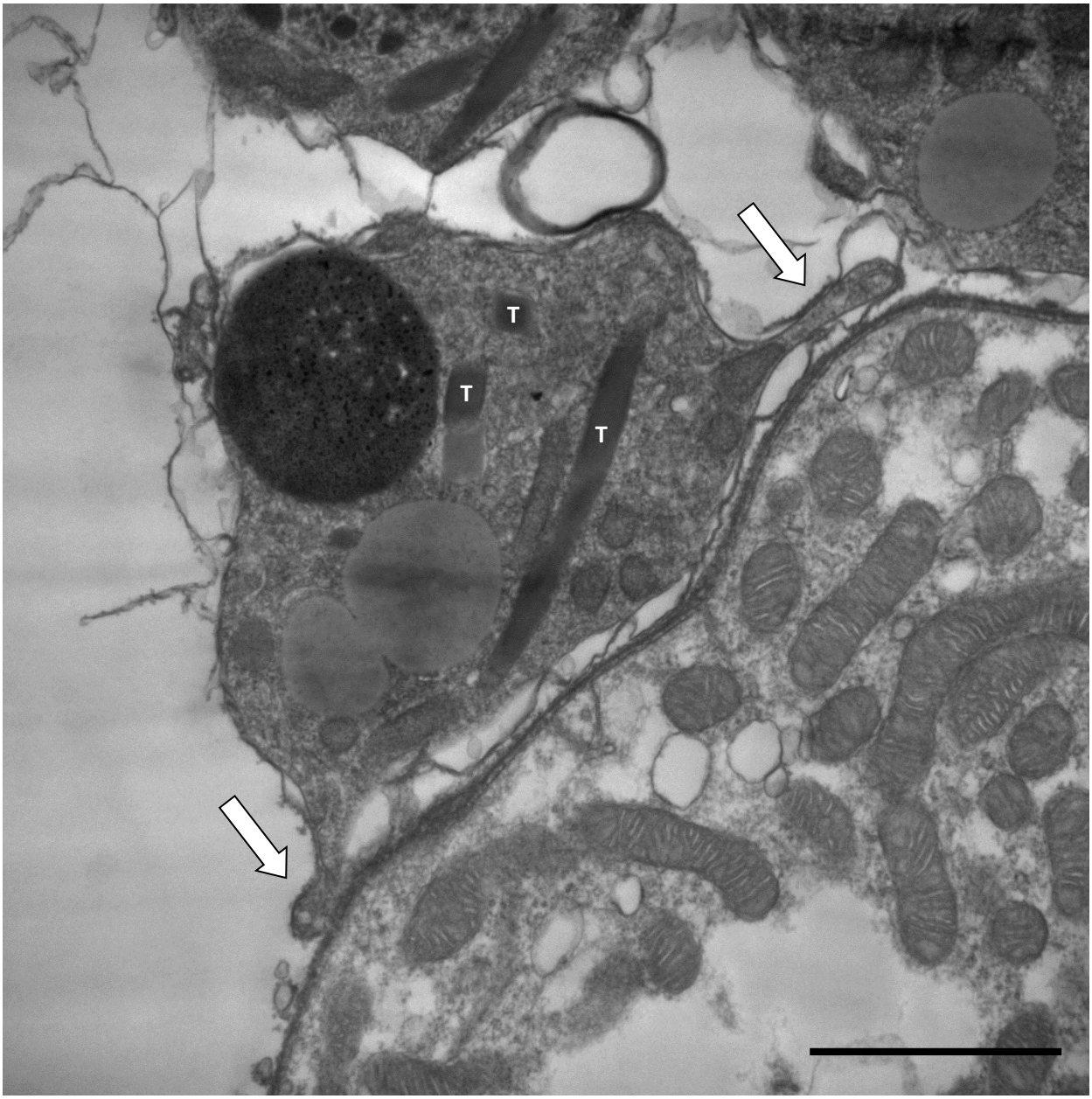

Figure 3.20. Heart of female crab 2010-NS1. Note intimate association of the amphiesmal surface of vermiform multinucleate plasmodia with the outer cell membrane of the cardiomyocyte and thin cytoplasmic extensions along the parasite cell margins (white arrows) and intracytoplasmic trichocysts (T). TEM, scale bar = 2 microns.

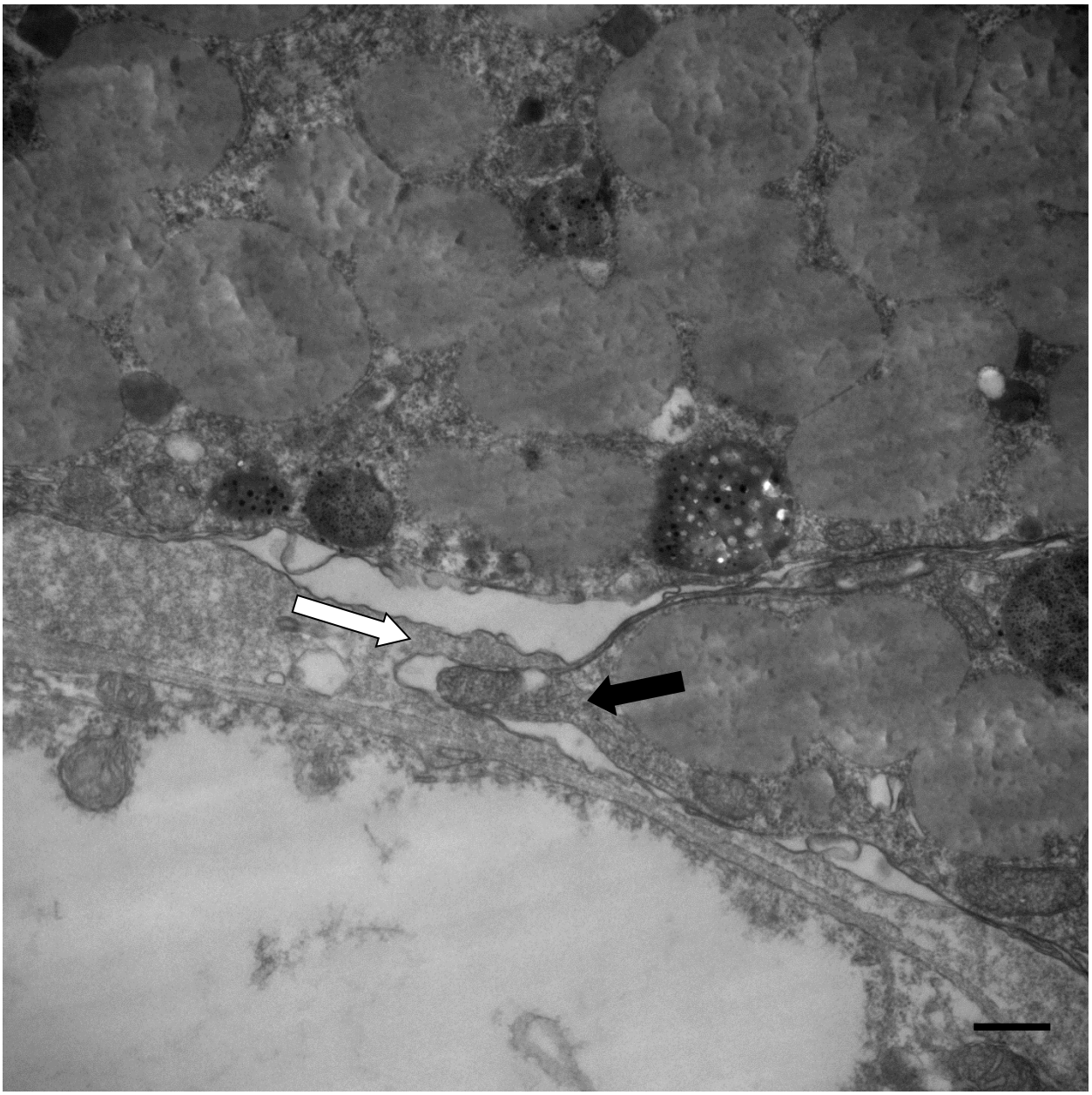

Figure 3.21. Heart of female crab 2010-NS1. Note parasitic cytoplasmic extension interdigitating (black arrow) with host cardiomyocyte plasma membrane (white arrow). TEM, scale bar = 500 nm.

3.4. Discussion

The endoparasitized snow crabs from Newfoundland and Nova Scotia were multisystemically infiltrated by dinoflagellates with light microscopic and ultrastructural features characteristic of the genus *Hematodinium*. The parasitic proliferation infiltrated and expanded the hemal spaces and interstitial connective tissues of the gill, heart, and hepatopancreas, as reported previously by Wheeler et al (2007) in snow crabs off the eastern and northeastern coast of Newfoundland and Labrador. In addition, we also examined the stomach (TEM only), midgut, leg muscle, ovary, and spermatheca and found similar infiltration of parasites in the interstitial hemal spaces of all tissue examined.

In the snow crab with a mild infection the parasitic dinoflagellates had less cytoplasm with increased cytoplasmic basophilia and reduced cytoplasmic vacuolation when compared to parasites observed in heavier (moderate, advanced, and very advanced) infections. An accumulation of cytoplasmic ribosomal and messenger RNA content, protein, and ribosomes results in enhanced cytoplasmic basophilia; a cytoplasmic change which can be observed in proliferating cells (Singer 1954, Goodman et al 1994). The basophilic appearance of the parasitic dinoflagellates in this mild (early) infection may suggest that the cells are rapidly proliferating. This suggestion is supported by the high proportion of multinucleated cells (50%) present in this early stage of the disease. The cytoplasm of parasites in infections with higher intensities was abundant and vacuolated. The vacuolated appearance of cytoplasm in later infections was associated with intracytoplasmic accumulation of vacuoles and lipid droplets

suggestive of nutrient acquisition at the expense of its host (Hudson et al 1993, Taylor and Khan 1995, Appleton and Vickerman 1998, Stentiford and Shields 2005).

In moderate infections the parasitemia was predominated by uninucleate cells. In advanced and very advanced infectious there appeared to be a progressive increase in the proportion of multinucleate life stages. The increase in multinucleate life stages in these advanced stages of disease could be due to a resurgence of proliferation late in the disease or reduced and/or impaired cytokinesis. Cytokinesis is a complex process which involves signal transduction, membrane trafficking, integral-membrane and peripheral cytoskeletal proteins, myosin mechanochemistry and general cellular physiological processes (Robinson and Spudich 2000). Inhibition of parasitic proliferation or cytokinesis may result from general nutrient limitation (Muscatine and Pool 1979). However, an imbalance in specific metabolites, rather than general limitation, may also limit cytokinesis since impaired glycosphingolipid biosynthesis and decreased cellular phosphatidylethanolamine levels have both been reported to induce cytokinesis failure (Emoto and Umeda 2000, Atilla-Glokcumen et al 2011). Alternatively, some parasites (such as *Trypanosoma* sp.) have mechanisms to sense parasite density to limit parasite proliferation to prevent premature host killing (Vassella et al 1997). Quorum sensing bacteria can produce, release, detect, and respond to small hormone-like molecules (autoinducers) to coordinate gene-expression with cell density (Thomas et al 2002, Waters and Bassler 2005). Interestingly synchronous sporulation occurs in *Hematodinium* sp. in Norway lobsters *Nephrops norvegicus,* Atlantic blue crabs *Callinectes sapidus,* tropical mud crabs *Scylla serrata*, and Japanese blue crab *Portunus trituberculatus* suggesting that quorum sensing may

play a role in life stage progression in this parasite (Appleton and Vickerman 1998, Shields and Squyars 2000, Stentiford and Shields 2005, Li et al 2008). Perception of signals from their immediate environment may also impact parasite life stage as a response to the health status of their host; parasite virulence is often higher in hosts which are in poor condition or experiencing stressful conditions (Thomas et al 2002).

Histopathologic examination of crustacean tissues affected by hematodiniosis is characterized by multisystemic interstitial infiltration of parasites. Observations of mild degenerative and atrophic changes are typical for affected snow crabs. In advanced or terminal stages of disease, observed histologic changes in some crustacean hosts were occasionally interpreted as necrosis (see Chapter 1, Table 1.5). One of the most commonly reported histopathologic changes was vacuolation of hepatopancreatic tubular epithelium, a lesion which was also observed in this study. In mammals, hepatocellular vacuolar change is a non-specific finding that is characterized by intracytoplasmic accumulation of glycogen and/or lipid that can be seen secondary to a variety of underlying disease processes including metabolic disorders (Cullen 2009). This suggests that the hepatopancreatic vacuolar change may be of metabolic origin in BCD-affected animals. In previous studies this vacuolation of the hepatic tubular epithelium was associated with an alteration in lipid content and has been attributed to parasite-induced metabolic dysregulation and/or physiological starvation (Meyers *et al* 1987, Stentiford *et al* 2002). In a small number of shipping mortalities with BCD regions of cellular disruption were also observed within the hepatopancreas. These regions may represent perimortem hepatocellular degeneration and necrosis (i.e., hypoxic or ischemic hepatocellular degeneration

and necrosis) or may represent regions of postmortem autolysis. Similarly, a few areas of pallor were observed within skeletal musculature which may represent very mild perimortem myodegeneration (possibly due to perimortem hypoxia) or postmortem autolytic changes in crabs which died during shipping.

Degenerative changes were also observed within the ovary of an immature (prepubescent or pubescent) female snow crab with BCD. This female snow crab was not a shipping mortality thus the ovarian changes are unlikely to represent post-mortem autolysis. The moth-eaten appearance of the ova may indicate impaired vitellogenesis and/or mobilization of vitellogenic proteins from developing ova. This suggests that BCD can impair the reproductive capacity of female snow crabs. In this study the majority (4/6) of affected females were gravid (berried). It is unclear whether these females became infected with *Hematodinium* before or after egg extrusion. However, the apparent degeneration of ova in one of the two non-gravid females suggests that parasitic castration through targeting of reproductive energy and/or generalized nutritional drain may contribute to the impact of BCD on snow crab populations (Lafferty and Kuris 2009). Furthermore, Dawe (2002) reported that BCD was consistently about twice as prevalent in females as in males. Parasitic castration can influence the sex ratio of its host population by affecting the number of females or males or both differentially. If females are preferentially affected in this case, the general sex ratio and consequently the ratio of fertilizable females to sexually active males of their hosts would be more male biased. This could increase the intensity of inter-male competition because fewer receptive females would be available at any one time and ultimately influence the outcome of sexual selection

(Brockerhoff 2004). But, as very few BCD+ female snow crabs were collected in this study, these findings suggestive of possible reproductive impairment should be interpreted with caution.

Reproductive impairment could also impact the spread of hematodiniosis if cannibalism is involved in its transmission. Cannibalism during molting is usually deterred via a combination of pheromones released in urine and reproductive behavior (Hayden et al 2007). The metabolic demands of the disease and direct infiltration of the female reproductive tract may interfere with normal molting and reproductive processes. Thus cannibalism may not be deterred in diseased animals at the time of molting. Furthermore, a recent study in another crustacean species (*Gammarus duebenie celticus*) demonstrated that parasitized individuals were more likely to be cannibalized by both unparasitized and parasitized individuals (MacNeil et al 2003).

The proliferating parasites within interstitial hemal spaces occurred in dense sheets of parasites in the late stages of hematodiniosis, with increased numbers of multinucleate life stages as infection intensity progressed from moderate to very advanced. Multinucleated plasmodia (syncytial) cell masses observed *in vitro* may be exaggerated forms of these dense interstitial parasitic aggregates. *In vivo* the multinucleate plasmodia in hemal spaces most often had amoeboid morphology although vermiform (elongate) plasmodia were also observed. In advanced and very advanced infections vermiform plasmodia could also be seen in intimate association with the cell surfaces in the heart and more rarely along skeletal muscle fibers. Ultrastructural examination of these attached vermiform plasmodia revealed cytoplasmic

extensions which interdigitated with host cell membranes and which occasionally appeared to form connections between parasite cell bodies. These findings suggest that arachnoid sporonts seen *in vitro* may represent exaggerations of attached vermiform plasmodial life stages seen *in vivo*. Attached vermiform plasmodial life stages are seen associated with myofibers (heart and skeletal musculature) in snow crabs but have also been seen in association with hepatopancreatic tubules, antennal gland, midgut, and linings of hemal spaces in various crustacean species infected with *Hematodinium* (Chatton and Poisson 1931, Newman and Johnson 1975, Field et al 1992, Messick 1994 Ryazanova 2010; see Chapter 1, Table 1.3).

Ultrastructurally, the attached vermiform plasmodia contained membrane-bound trichocysts. If trichocysts delineate the trophont and sporont life stages, then the presence of trichocysts indicates that sporont life stages were present in the advanced infections examined by TEM (Appleton and Vickerman, 1998). It is unclear whether attached vermiform plasmodia also form in trophont life stages *in vivo* in snow crabs. Arachnoid trophonts have been described in *in vitro* studies of isolates from Norway lobsters *Nephrops norvegicus* and blue crabs *Callinectes sapidus* (Appleton and Vickerman 1998, Li et al 2011). No arachnoid trophont life stage was found in an *in vitro* study of *Hematodinium* isolated from snow crabs (Gaudet et al 2015).

The histologic and ultrastructural features observed in this study are similar to those reported for *Hematodinium* in other crustacean hosts. Comparison of *in vivo* and *in vitro* life stages of *Hematodinium* isolated from snow crabs suggests that *in vitro* sheet-like and arachnoid plasmodial may represent exaggerations of amoeboid plasmodial and attached vermiform

plasmodial life stages observed *in vivo*. Mild vacuolar (degenerative) changes were observed in the hepatopancreatic epithelium and ova which are most likely secondary to metabolic compromise of the host. No convincing evidence of parasite-induced tissue necrosis or inflammation was observed (see Chapter 5 regarding patterns of inflammation). Degenerative changes within the ova combined with epidemiological data which suggests that females may be predisposed to infection (Dawe 2002) indicate that this disease could have occult effects on female reproductive success and could result in altered sex ratios in infected populations. But, only a small number of BCD+ females were examined in this study and thus this suggestion should be interpreted with caution. Such an impact on the snow crab reproductive biology may alter current population management strategies for the commercial snow crab fishery and thus further study into this issue may be warranted.

3.5. References

Appleton PL, Vickerman K. 1998. *In vitro* cultivation and developmental cycle in culture of a parasitic dinoflagellate (*Hematodinium* sp.) associated with mortality of the Norway lobster (*Nephrops norvegicus*) in British waters. Parasitology 116(2):115-130.

Atilla-Golkcumen GE, Bedigian V, Sasse S, Eggert US. 2011. Inhibition of glycosphingolipid biosynthesis induces cytokinesis failure. J Am Chem Soc 133(26): 10010-10013.

Brockerhoff AM. 2004. Occurrence of the internal parasite *Portunion* sp. (Isopoda: Entoniscidae) and its effect on reproduction in intertidal crabs (Decapoda: Grapsidae) from New Zealand. J Parasitol 90(6):1338-1344.

Chatton É, Poisson R. 1931. Sur l'existence dans le sang des crabes, de péridiniens parasites: *Hematodinium perezi* n.g., n.sp. (Syndinidae). C R Seances Soc Biol Paris 105: 553–557.

Chualáin CN, Robinson M. 2011. Comparison of assessment methods used to diagnose *Hematodinium* sp. infections in *Cancer pagurus*. ICES J Mar Sci 68(3):454-462.

Coffey AH, Li C, Shields JD. 2012. The effect of salinity on experimental infections of a *Hematodinium* sp. in blue crabs, *Callinectes sapidus.* J Parasitol 98(3):536-542.

Cullen JM. 2009. Summary of the World of Small Animal Veterinary Association Standardization Committee Guide to classification of liver disease in dogs and cats. Vet Clin Small Anim 39(3): 395-418.

Dawe EG. 2002. Trends in prevalence of Bitter Crab Disease caused by *Hematodinium* sp. in snow crabs (*Chionoecetes opilio*) throughout the Newfoundland and Labrador continental shelf. *In* Crabs in Cold Water Regions: Biology, Management and Economics. Alaska Sea Grant College Program, AK-SG-02-02:385-400.

Dawe E, Mullowney D, Colbourne E, Han G, Morado JF, Cawthorn R. 2010. Relationship of oceanographic variability with distribution and prevalence of bitter crab syndrome in snow crab (*Chionoecetes opilio*) on the Newfoundland–Labrador shelf. *In:* Biology and management of exploited crab populations under climate change. Alaska Sea Grant College Program, AK-SG-10-01:175-198.

Eaton WD, Love DC, Botelho C, Meyers TR, Imamura K, Koeneman T. 1991. Preliminary results on the seasonality and life cycle of the parasitic dinoflagellate causing Bitter Crab Disease in Alaskan Tanner crabs (*Chionoecetes bairdi*). J Invertebr Pathol 57(3):426-434.

Elner, RW, and Beninger, PG. 1995. Multiple reproductive strategies in snow crab, *Chionoecetes opilio*: physiological pathways and behavioral plasticity. J Exp Mar Biol Ecol 193(1):93–112.

Emoto K, Umeda M. 2000. An essential role for a membrane lipid in cytokinesis: regulation of contractile ring disassembly by redistribution of phosphatidylethanolamine. J Cell Biol 149(6): 1215-1224.

Field RH, Appleton PL. 1995. A *Hematodinium*-like dinoflagellate infection of the Norway lobster *Nephrops norvegicus*: observations on pathology and progression of infection. Dis Aquat Org 22:115–128.

Field RH, Chapman CJ, Taylor AC, Neil DM, Vickerman K. 1992. Infection of the Norway lobster *Nephrops norvegicus* by a *Hematodinium*-like species of dinoflagellate on the west coast of Scotland. Dis Aquat Org 13(1):1-15

Gaudet PH, Cawthorn RJ, Buote MA, Morado JF, Wright GM, Greenwood SJ. 2015. *In vitro* cultivation of *Hematodinium* sp. isolated from Atlantic snow crab, *Chionoecetes opilio:* partial characterization of late developmental stages. Parasitology 142(4): 598-611.

Goodman DG, Maronpot RR, Newberne PM, Popp JA, Square RA. 1994. Proliferative and selected other lesions of the liver in rats. G1-5. *In* Guides for Toxicologic Pathology. STP/ARP/AFIP: Washington, DC.

Hayden D, Jennings A, Müller C, Pascoe D, Bublitz R, Webb H, Breithaupt T, Watkins L, Hardege J. 2007. Sex-specific mediation of foraging in the shore crab, *Carcinus maenas*. Horm Behav 52(2):162–168.

Hudson DA, Hudson NB, Shields JD. 1993. Infection of *Trapezia* spp. (Decapoda: Xanthidae) by *Hematodinium* sp. (Duboscquodinida: Syndinidae): a new family record of infection. J Fish Dis 16(3):273-276.

Hudson D, Shields JD. 1994. *Hematodinium australis* n. sp., a parasitic dinoflagellate of the sand crab *Portunus pelagicus* and mud crab *Scylla serrata* from Moreton Bay, Australia. Dis Aquat Org 19(2):109–119.

Lafferty KD, Kuris M. 2009. Parasitic castration: the evolution and ecology of body snatchers. Trends Parasitol 25(12):564-572.

Li C, Miller TL, Small HJ, Shields JD. 2011. *In vitro* culture and developmental cycle of the parasitic dinoflagellate *Hematodinium* sp. from the blue crab *Callinectes sapidus*. Parasitology 138(14):1924-1934.

MacNeil C, Dick JT, Hatcher MJ, Fielding NJ, Hume KD, Dunn AM. 2003. Parasite transmission and cannibalism in an amphipod (Crustacea). Int J Parasitol 33(8):795-798.

Messick GA. 1994. *Hematodinium perezi* infections in adult and juvenile blue crabs *Callinectes sapidus* from coastal bays of Maryland and Virginia, USA. Dis Aquat Org 19(1):77-82.

Meyers TR, Koeneman TM, Botelho C, Short S. 1987. Bitter crab disease: a fatal dinoflagellate infection and marketing problem for Alaskan Tanner crabs *Chionoecetes bairdi.* Dis Aquat Org 3(3):195–216.

Morado FJ. 2007. Bitter crab syndrome: a major player in the global theater of marine crustacean disease. AFSC Quarterly Report July-September:1-6.

Morado FJ. 2011. Protistan diseases of commercially important crabs: a review. J Invert Pathol 106(1): 27-53.

Mullowney DR, Dawe EG, Morado JF, Cawthorn RJ. 2011. Sources of variability in prevalence and distribution of bitter crab disease in snow crab (*Chionoecetes opilio*) along the northeast coast of Newfoundland. ICES J Mar Sci 68(3):463-71.

Muscatine L, Pool RR. 1979. Regulation of numbers of intracellular algae. Proc R Soc Lond B. 204(1155):131-139.

Newman MW, Johnson CA. 1975. A disease of blue crabs (*Callinectes sapidus*) caused by a parasitic dinoflagellate, *Hematodinium* sp. J Parasitol 61(3):554-557.

Robinson DN, Spudich JA. 2000. Towards a molecular understanding of cytokinesis. Trends Cell Biol 10(6):228-237.

Ryazanova TV. 2008. Bitter Crab Syndrome in Two Species of King Crabs from the Sea of Okhotsk. Russian J Mar Biol 34(6): 411-414.

Ryazanova TV, Eliseikina MG, Kukhlevsky AD, Kharlamenko VI. 2010. *Hematodinium* sp. infection of red *Paralithodes camtschaticus* and blue *Paralithodes platypus* king crabs from the Sea of Okhotsk, Russia. J Invertebr Pathol 105(3):329-334.

Sainte-Marie G, Sainte-Marie B. 1998. Morphology of the spermatheca, oviduct, intermediate chamber, and vagina of the adult snow crab (*Chionoecetes opilio*). Can J Zool 76(8):1589-1604.

Shields JD. 1994. The parasitic dinoflagellates of marine crustaceans. Ann Rev Fish Dis 4:241-271.

Shields JD, Squyars CM. 2000. Mortality and hematology of blue crabs, *Callinectes sapidus*, experimentally infected with the parasitic dinoflagellate *Hematodinium perezi.* Fish Bull (Wash DC) 98(1):139–152.

Shields JD, Taylor DM, Sutton SG, O'Keefe PG, Colbourne E, Hynick E. 2007. Epidemiological determinants in outbreaks of bitter crab disease (*Hematodinium* sp.) in snow crabs *Chionoecetes opilio* from Conception Bay, Newfoundland, Canada. Dis Aquat Org 77(1):61–72.

Shields JD, Taylor DM, Sutton SG, O'Keefe PG, Ings DW, Pardy AL. 2005. Epidemiology of bitter crab disease (*Hematodinium* sp.) in snow crabs *Chionoecetes opilio* from Newfoundland, Canada. Dis Aquat Org 64(3):253–264.

Singer M. 1954. The staining of basophilic components. J Histochem Cytochem 2(5): 322-333.

Small HJ, Shields JD, Reece KS, Bateman K, Stentiford GD. 2012. Morphological and molecular characterization of *Hematodinium perezi* (Dinophyceae: Syndiniales), a dinoflagellate parasite of the harbour crab*, Liocarcinus depurator*. J Eukaryot Microbiol 59(1):54-66.

Stentiford GD, Green M, Bateman K, Small HJ, Neil DM, Feist SW. 2002. Infection by a *Hematodinium*-like parasitic dinoflagellate causes Pink Crab Disease (PCD) in the edible crab *Cancer pagurus*. J Invertebr Pathol. 79(3):179-191.

Stentiford GD, Shields JD. 2005. A review of the parasitic dinoflagellates *Hematodinium* and *Hematodinium*-like infections in marine crustaceans. Dis Aquat Org 66(1):47-70.

Taylor DM, Khan RA. 1995. Observations on the occurrence of *Hematodinium* sp. (Dinoflagellata: Syndinidae), the causative agent of bitter crab disease in Newfoundland snow crab (*Chionoecetes opilio*). J Invertebr Pathol 65(3):283–288.

Thomas F, Brown SP, Sukhdeo M, Renaud F. 2002. Understanding parasite strategies: a state-dependent approach? Trends Parasitol 18(9):387-390.

Tremblay MJ. 1997. Snow crab (*Chionoecetes opilio*) distribution limits and abundance trends on the Scotian Shelf. J Northwest Atl Fish Science 21:7-22.

Waters CM, Bassler BL. 2005. Quorum sensing: cell-to-cell communication in bacteria. Annu Rev Cell Dev Biol 21:319-346.

Wheeler K, Shields JD, Taylor DM. 2007. Pathology of *Hematodinium* infections in snow crabs (*Chionoecetes opilio*) from Newfoundland, Canada. J Invertebr Pathol 95(2):93-100.

Vassela E, Beuner B, Yutzy B, Boshart M. 1997. Differentiation of African trypanosomes is controlled by a density sensing mechanism which signals cell cycle arrest via the cAMP pathway. J Cell Sci. 110(21):2661-2671.

4. INVESTIGATION OF HEMOLYMPH CHANGES ASSOCIATED WITH BITTER CRAB DISEASE IN NEWFOUNDLAND SNOW CRABS, *CHIONOECETES OPILIO*

4.1. **Introduction**

Hematodiniosis is a fatal disease of crustaceans caused by parasitic dinoflagellates of the genus *Hematodinium*. *Hematodinium* sp. infection was first reported off the coast of Europe in common shore crabs *Carcinus maenas* and blue-leg swimming crabs *Liocarcinus depurator* (Chatton and Poisson, 1931). Over forty species of crustaceans have been reported as hosts for *Hematodinium* or *Hematodinium*-like infections with distribution concentrated in the North Pacific and Atlantic oceans, including Atlantic Canadian snow crabs *Chionoecetes opilio* (reviewed in Morado et al 2011). Canada is the world's largest producer of snow crab, accounting for approximately two-thirds of the global supply with 2013 landings of 98,065 tonnes and exports valued at $434.2 million (http://www.dfo-mpo.gc.ca).

Diseased hosts generally appear lethargic and moribund with discolored carapaces and opaque milky hemolymph (Field et al 1992, Meyers et al 1987, Messick 1994, Wheeler et al 2007). In several hosts, including Tanner crabs *Chionoecetes bairdi,* snow crabs *Chionoecetes opilio,* edible crab *Cancer pagurus*, Norway lobsters *Nephrops norvegicus*, and red and blue king crabs *Paralithodes* spp., anecdotal reports indicate that the disease alters the texture and taste of infected meat rendering the product unmarketable (Meyers et al 1987, Love et al 1996, Stentiford et al 2000, Ryazanova 2008, Ryazanova et al 2010). Affected meat has been described as either watery or chalky, and the altered taste is typically described as bitter, astringent, or aspirin-like, and is reflected in one common name of hematodiniosis – Bitter Crab

Disease (BCD). The cause of the bitter taste associated with this disease is not known at present.

Crabs and lobsters infected with *Hematodinium* exhibit hemocytopenia and coagulopathy (Meyers et al 1987, Hudson and Shields 1994, Shields 1994, Field and Appleton 1995, Shields and Squyars 2000, Stentiford et al 2005). The clotting mechanisms may be specifically suppressed or reduced due to hemocytopenia since hyalinocytes regulate coagulation (Shields and Squyars 2000, Stentiford and Shields 2005). Reductions in the hemolymph concentration of hemocyanin, the primary protein in crustacean hemolymph, occur in infected Tanner crabs *Chionoecetes bairdi* and male blue crabs *Callinectes sapidus* (Love et al 1996, Shields et al 2003).

The metabolic demands of the disease process and/or starvation also result in significant reductions in tissue reserves of glycogen in infected crabs and lobsters (Love et al 1996, Stentiford et al 2000, 2001, Shields et al 2003). Altered glycogenesis, alteration of host hormonal regulation, and/or carbohydrate uptake by the parasitic dinoflagellates may also contribute to loss of host glycogen stores (Stentiford et al 2000). In *Chionoecetes opilio*, tissue glycogen has been reported to be depleted by 50%, whereas in *Nephrops norvegicus* the glycogen in the abdominal muscles was reduced by up to 80% and was concomitant with increasing parasite burden (Stentiford et al 2000, Stentiford 2005). In blue crabs *Callinectes sapidus* males were more depleted than females with tissue glycogen depletion of 50% in females and 70% in males (Shields et al 2003).

This study provides a comparison of the hemolymph refractive index (HRI) of Newfoundland snow crabs with and without BCD. HRI is affected by gender, local environment, molt stage, and nutritional condition of the snow crab (see Appendix 7), thus comparisons between genders, collection areas (bays and strata within bays), shell conditions, and glycogen stores were undertaken. Untargeted metabolomic evaluation of BCD+ and BCD- hemolymph was attempted to more fully describe changes in hemolymph metabolites during BCD and to determine potential contributing factors in the bitter taste associated with the disease.

4.2. **Materials and Methods**

4.2.1. **Snow Crab Collection**

Atlantic snow crabs (*C. opilio*) were collected during annual Fall surveys in Notre Dame Bay (NDB) and White Bay (WB), Newfoundland during September in 2010 and 2011. In Notre Dame Bay crabs were caught on the grounds of strata 610 and 611 (200-400 m in depth). In White Bay crabs were caught in strata 614 and 615 (200-400 m in depth) as the very deep stratum 613 (401-500 m). NDB is an open ocean-type environment that becomes deeper with distance from shore while WB is a deep fjord-type environment protected at the mouth by a shallow sill and which is deepest inland (Figure 4.1).

The Fall survey had a target of 8 sets per stratum. Each set included 6 conical crab traps baited with squid. Crabs were sampled from two large-meshed (commercial, 135 mm) and two small-meshed (27 mm) traps. Small-mesh trap positions alternated with those of large-meshed traps

along each long line, and soak times were generally 24 h (weather permitting). Within each crab management area surveyed the depth range and actual area sampled corresponded approximately to the commercial fishery area. Shell condition was classified as soft, new, intermediate, and old (Dawe et al 2009). New-shelled snow crabs were assumed to have molted during the most recent Spring whereas intermediate-shelled crabs were assumed to have molted in the previous year and old-shelled snow crabs two or more years previously (soft-shelled snow crabs were not collected). New-shelled snow crabs were selectively chosen for collection for this study as BCD is typically observed in new-shelled animals (Dawe 2002, Shields et al 2005, 2007, Wheeler et al 2007, Mullowney et al 2011).

Crabs were kept in coolers layered between seawater-soaked burlap, and placed on saltwater ice until reaching shore. On shore, coolers were transported to St. John's, Newfoundland, where they were sent via air cargo to the Atlantic Veterinary College (AVC) at University of Prince Edward Island (UPEI). The interval between snow crab harvest and their arrival at the AVC was usually 24-48 h. Snow crabs were recovered in 34 ppt artificial seawater which was aerated with air stones and maintained at 0-2 °C until processing. The interval between snow crab arrival at AVC and processing ranged from 15 min to ~4 h.

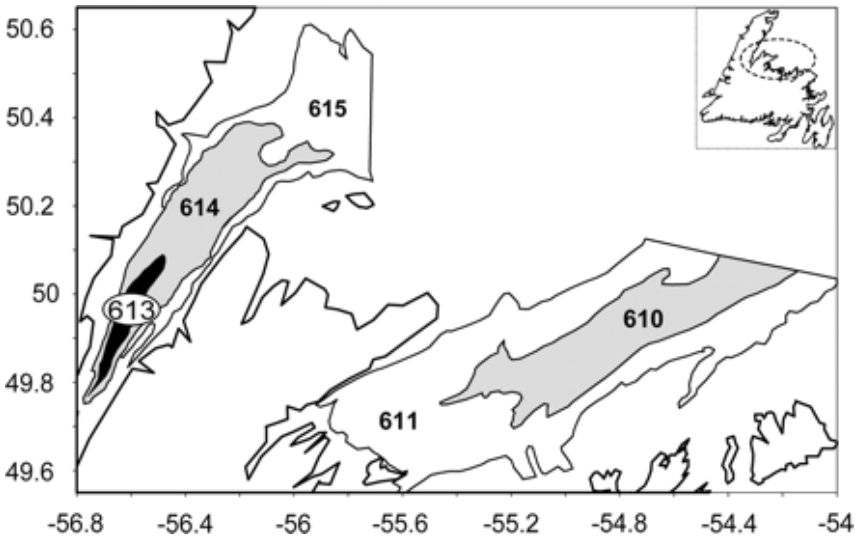

Figure 4.1. Map of the study area showing the depth strata in White Bay (WB) and Notre Dame Bay (NDB). Strata 615, 614, and 613 are in WB, and Strata 611 and 610 in NDB. White strata are 200–300 m, grey strata are 301–400 m, and the black stratum is 401–500 m (from Mullowney et al 2011).

4.2.2. **Snow Crab Processing and Sample Collection**

Crabs were evaluated for gross morphologic evidence of Bitter Crab Disease, which is characterized by an orangish-pink or “cooked” appearance to the carapace and/or white discoloration of arthrodial membranes. All snow crabs that survived shipping to AVC at UPEI and any snow crabs with macroscopic evidence of BCD were processed. In addition, 10 shipping mortalities per shipment (n = 30) were processed from WB.

Each snow crab was photographed (dorsal and ventral digital images), gender was noted and carapace width (mm) was measured. Shell condition category was assessed as new, intermediate, or old hard-shelled by degree of epibiont fouling on the carapace as previously described (see Chapter 2, Table 2.1). Hemolymph from each animal was collected aseptically from the base of the first walking leg using a 3 ml or 5 ml syringe with a 22 gauge needle. For

each animal the gross appearance of the hemolymph was noted and hemolymph refractive index was measured using a digital refractometer (Reichert r^2mini digital refractometer; Reichert Analytical Instruments). A 200 µl sample of hemolymph was placed in a 96-well ethanol block containing 800 µl 100% ethanol per well for DNA extraction. These DNA samples were examined using a polymerase chain reaction (PCR) assay with *Hematodinium*-specific primers (Appendix 1). This assay was used for the molecular detection of *Hematodinium* spp. infection in a larger survey of Newfoundland snow crabs, and was used as a molecular method of disease detection for this project (see Chapter 2). The remaining hemolymph was placed on ice, incubated at 1 °C for ~24 h, pooled in 50 ml Falcon tubes and frozen at -80 °C.

The crab was euthanized via nerve cord disruption via decapitation (i.e., removal of the carapace). Euthanasia via potassium chloride injection resulted in a large streak of tissue disruption and thus this alternative method of euthanasia was not employed (Appendix 2). Upon removal of the carapace, a digital image of the crab's internal organs was taken and tissue samples were collected. The tissue samples collected included: heart, hepatopancreas, gill (1^{st} and 4^{th} gills on the right), gonad, midgut, eyestalks (left and right), a cross-section of the abdomen, and a cross-section of leg (1^{st} merus on the right). The tissues were immediately placed in Davidson's seawater fixative for 24 h (Davidson's seawater fixative was prepared as described in Appendix 3). After 24 h, the tissue samples were transferred into containers of 70% ethanol for storage until routine processing for histology.

4.2.3. **Tissue Trimming and Processing for Histology**

Sections of all soft tissues (heart, hepatopancreas, gill (x2), gonad, and midgut) were trimmed and placed into one cassette per individual snow crab for processing. A second cassette of sections lined by a thick cuticular layer (eyestalk, leg, and abdomen) was also submitted. The eyestalk was bisected along the frontal plane as this plane was found to consistently result in optimal sections of internal neuroendocrine tissues (see Appendix 4).

The blocks of trimmed tissues were processed routinely for histology (Leica processor) and stained with hematoxylin and eosin (H&E). Stained sections were examined on a VistaVision light microscope (VWR) and digital images were captured using an Axioplan 2 imaging microscope with an Axiocam HRc camera and AxioVision 4.8.2.0 software (Zeiss).

4.2.4. **Histologic Examination of H&E Stained Tissue Slides**

Each tissue on each slide was examined in a systematic manner for evidence of *Hematodinium* infection. *Hematodinium* sp. organisms have a characteristic nuclear condensation pattern which makes their nucleus stain more darkly than host hemocytes, and thus are relatively easily identified at low magnification (100x magnification). *Hematodinium* sp. organisms also contain numerous intracellular vacuoles (PAS bodies or accumulation bodies) which contain lipofuscin-like material resulting in the parasitic dinoflagellates having a cytoplasmic vacuolated appearance distinct from the agranular or granular appearance of host hemocytes. If no evidence of infection was observed during the low magnification screening the tissues were screened again at high magnification (400x magnification). Relative abundance of glycogen-containing reserve inclusion (RI) cells was also scored as previously reported (Stentiford and

Fiest 2005). The scoring index ranged from Stage 0 (RI cells absent) through Stage 1 (RI cells present but scarce), Stage 2 (RI cells scattered), Stage 3 (RI cells frequent) to Stage 4 (RI cells abundant and constituting the majority of connective tissue volume). RI scores were completed for both the hepatopancreas and the gut wall. Gut wall RI scores were used for comparisons between groups of snow crabs as they are more representative of body glycogen stores in snow crabs than hepatopancreas RI scores (Appendix 6).

4.2.5. **Sample Preparation for UPLC/HRMS Analysis**

Hemolymph samples (previously frozen at -80 °C) were dried under vacuum using a GeneVac vacuum evaporating system (model: Ez-2 MK2) and extracted using MeOH with 20 min of sonication, incubated at room temperature (~22 °C) for 6 h, then filtered and extracted with MeOH/EtOAc(1:1) with 20 min of sonication and then incubated at room temperature overnight. Extracts were fractionated on Thermo HyperSep C18 Sep Pak columns (500 mg C18, 6 ml column volume) using a vacuum manifold by eluting with the following solvent combinations: 10% MeOH (10 ml, fraction 1), 33% MeOH (5 ml, fraction 2), 66% MeOH (5 ml, fraction 3), 100% MeOH (10 ml, fraction 4), and 1:1 DCM/MeOH (10 ml, fraction 5). The eluents representing fractions 1-5 were retained, concentrated using a GeneVac (model: EZ-2 MK2) evaporating system, and weighed.

The samples were analyzed by UPLC/HRMS using an Orbitrap Velos Exactive system (Thermo Fisher Scientific, Mississauga, ON, Canada) with a Kinetex 1.7 µm C18 100 A 50 x 2.1 mm UPLC column (Phenomenex, Torrance, CA, USA) and eluate was detected by +ESI-HRMS monitoring *m/z* 200-2000 amu with a resolution of 30,000, evaporative light scattering detector (ELSD;

Sedex, Sedere, Alfortville, France) and PDA (200-600 nm). A linear gradient from 95% water/0.1 % FA (solvent A) and 5% ACN/0.1% FA (solvent B) to 100% solvent B over 5 min, followed by 3 min at 100% solvent B and an additional 2 min of re-equilibration with the initial conditions. The mass spectrometer was operated under the following conditions: spray voltage, 3.0 kV; capillary temperature, 320 °C; S-lens RF voltage, 66.0%; maximum injection time (ms), 500; microscans, 3. The system was controlled by XCalibur software modules (ThermoScientific).

4.2.6. **Data Preprocessing and Peak Alignment**

Raw data files generated by the UPLC/HRMS (proprietary format, .RAW) were converted into the open .mzXML format using msconvert (http://proteowizard.sourceforge.net/downloads.shtml) and then imported into MZmine 2 (http://mzmine.github.io/download.html) for preprocessing steps. MZmine 2 is a package which includes several preprocessing modules, including mass detection, chromatogram building, chromatogram deconvolution, deisotoping, peak alignment, and exportation. Mass detection generated a list of masses for each scan in the imported file. This step was accomplished by the exact mass detector with a noise level value (intensity) of 1×10^3 counts s^{-1} (cps). Peaks with intensity below this level were not recognized for further steps, and therefore were not included in the mass list. The exact mass detector searched for all local maxima within the raw spectra, labeling them as candidate ions.

The chromatogram building module takes mass lists generated in the mass detection step and builds a chromatogram for each mass that can be detected continuously over scans. The minimum time span a detected ion must be connected in order for it to be considered as part

of the chromatogram was set at 0.1 min, while the minimum height required for chromatogram inclusion was 1×10^3 cps. Minimum height was setup with a 10% reduction below the mass detection threshold to ensure that the mass detection step is the limiting factor for the selection of ions. For an ion to be considered part of a specific chromatogram, it must be within 0.005 *m/z* units of the *m/z* characteristic of the chromatogram being built.

Chromatogram deconvolution was carried out by noise amplitude algorithm with a minimum peak height of 1.0×10^3, peak duration range was 0.8 min, and amplitude of noise was set at 2.0×10^3. Deisotoping was carried out with a *m/z* tolerance of 0.005 *m/z* units (i.e. to be considered as part of an isotopic pattern, the observed ion must be within 0.005 *m/z* units of the expected location for that isotope), and a retention time tolerance of 0.5 min, and a maximum charge of 2. The most intense isotope was chosen to be representative of the parent molecule. An aligned peak list was generated with *m/z* tolerance of 0.005 *m/z* units (5.0 ppm) with retention time tolerance of 0.5 min. The same charge state was required for alignment. Tentative identification of compounds by MZmine 2 was accomplished via online database searches of the LipidMaps database (http://www.lipidmaps.org), KEGG Compound database (http://www.genome.jp/kegg/compound/), and Human Metabolome Database (http://www.hmdb.ca) using ionizations of [M+H]+ and [M+Na]+ and a m/z tolerance of 0.005 m/z units.

4.2.7. **Statistical Analysis**

Categorical data were analyzed using Pearson Chi-Square Tests or Fisher Exact Tests (the latter used when expected values were <5). Ordinal data were analyzed using Kruskal-Wallis Tests

(adjusted for ties) followed by Mann-Whitney tests (adjusted for ties). Continuous data were analyzed using ANOVA followed by two-way T-tests (means for continuous data are reported a mean ± standard error of the mean). Differences were considered to be statistically significant at p-value < 0.05.

4.3. **Results**

4.3.1. **Collected Snow Crabs**

A total of 316 snow crabs was processed for this study: 142 from NDB in 2010 and 174 from WB in 2011 (Table 4.1). The female snow crabs collected from NDB included a significantly higher proportion of intermediate and old-shelled snow crabs than seen in NDB male snow crabs (Pearson Chi-Square = 12.719, DF =1, p-value = 0.000) while intermediate and old hard-shelled snow crabs were largely excluded from the NDB males and the male and female snow crabs collected from WB (Table 4.1). BCD was only observed in new-shelled snow crabs. BCD was diagnosed via histology in 14/142 NDB and 14/174 WB snow crabs (Table 4.1), with only 2 of the BCD+ snow crabs collected in WB from stratum 613 (Table 4.2). The prevalence of BCD was not significantly different between bays or strata, gender within bays or strata, or gender between bays or strata (data not shown).

Table 4.1. Biological data of snow crabs collected from Notre Dame Bay and White Bay.

	Notre Dame Bay Strata 610/611		**White Bay Strata 613 and 614/615**	
n	142		174	
Gender distribution	57% males (n=61)	43% females (n = 81)	82% males (n=142)	18% females (n=32)
Carapace width Range (mm)	53-103	27-69	46 -108	40-55
Carapace width Mean (mm)	76.3	54.4	78.9	45.9
Shell Condition	60 New-shelled 1 Intermediate	63 New-shelled 17 Intermediate 1 Old-shelled	142 New-shelled	31 New-Shelled 1 Intermediate
Histologic BCD+ (all processed crabs)	16.4% (10/61)	4.9% (4/81)	9.2% (13/142)	3.1% (1/32)
Histologic BCD+ (new-shelled crabs)	16.7% (10/60)	4.9% (4/63)	9.2% (13/142)	3.2% (1/31)
Histologic BCD+ (new-shelled crabs)	11.4% (14/123)		8.1% (14/173)	

Table 4.2. Biological data of snow crabs collected from stratum 613 or strata 614/615 in White Bay.

	White Bay Stratum 613		**White Bay Strata 614/615**	
n	56		118	
Gender distribution	100% males (n=56)	0% females (n=0)	73% males (n=86)	27% females (n=32)
Carapace width Range (mm)	59 -108		46 -107	40-55
Carapace width Mean (mm)	87.1		73.6	45.9
Shell Condition	56 New-shelled		86 New-shelled	31 New-Shelled 1 Intermediate
Histologic BCD+ (all processed crabs)	3.6% (2/56)		12.8% (11/86)	3.1% (1/32)
Histologic BCD+ (new-shelled crabs)	3.6% (2/56)		12.8% (11/86)	3.2% (1/31)
Histologic BCD+ (new-shelled crabs)	3.6% (2/56)		10.2% (12/118)	

4.3.2. **Hemolymph Refractive Index (HRI)**

When the HRI values for all snow crabs were examined together there was an outlier data point. This unusually high HRI value (HRI = 1.362) was the only BCD+ female snow crab collected from WB (snow crab #2011-163). This non-gravid BCD+ female snow crab had reddish-orange hemolymph (Figure 4.2). This was the only BCD+ female that was not gravid. Her HRI value was significantly higher than that of from all snow crabs of all shell conditions and all new-shelled snow crabs (Figure 4.3), all female snow crabs regardless of shell condition (Figure 4.4), and females only from WB (Figure 4.5). A single non-gravid BCD- snow crab was collected from NDB (snow crab #2010-65). The HRI of this non-gravid BCD- snow crab (HRI = 1.3453) was not an outlier data point among the gravid BCD- snow crabs from NDB (Figure 4.5). The outlier data point (BCD+ female snow crab #2011-163 HRI value of 1.362) was removed from the data set for statistical analysis.

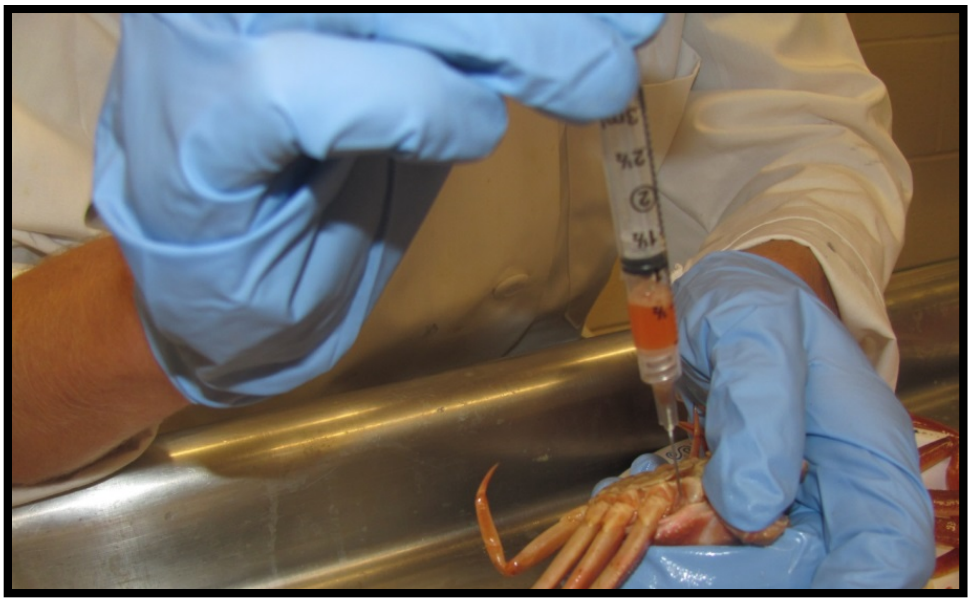

Figure 4.2. Reddish-orange hemolymph sampled from female snow crab with outlier HRI value (snow crab #2011-163).

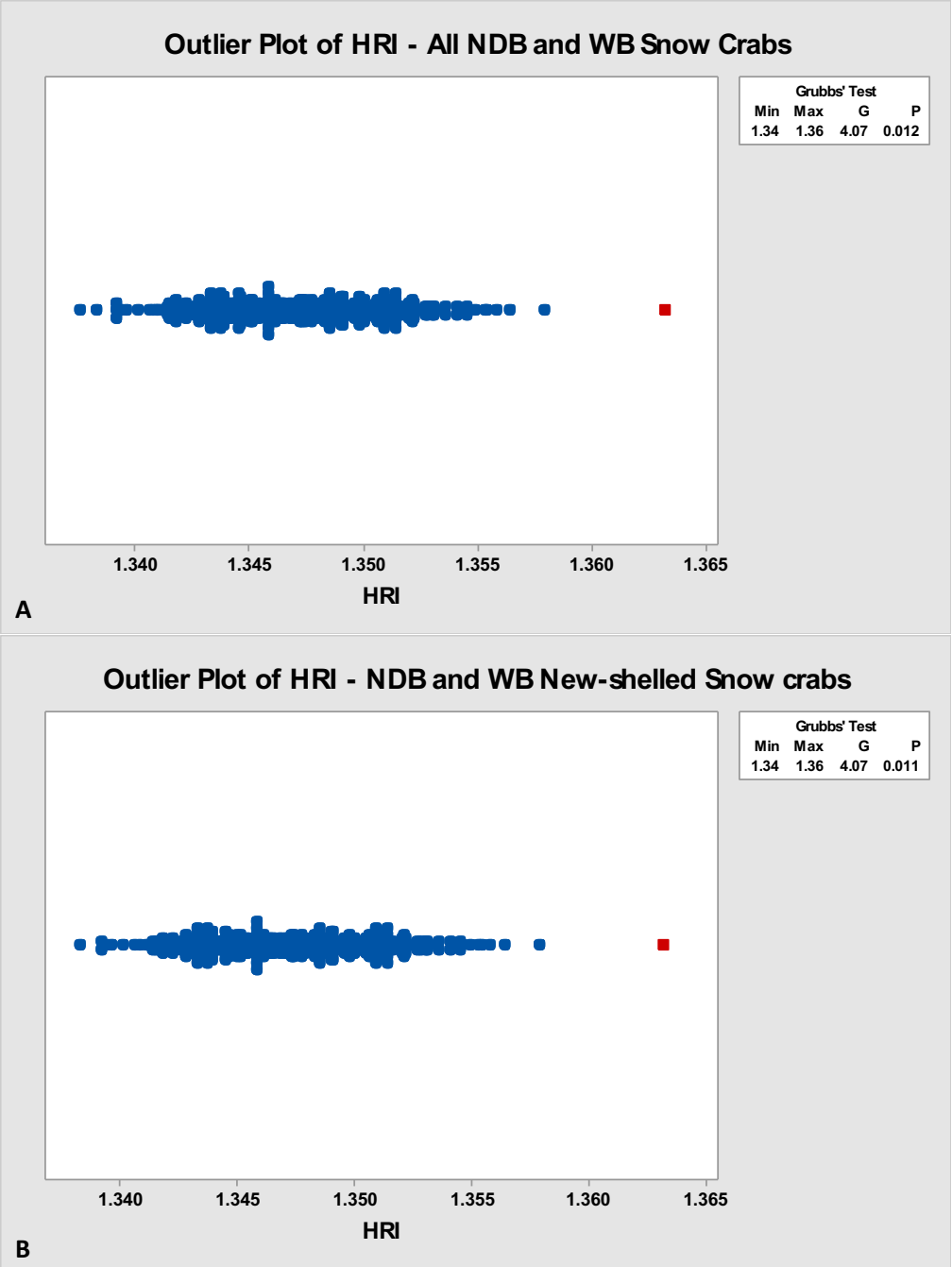

Figure 4.3. Outlier plots of hemolymph refractive index (HRI) for all Notre Dame Bay and White Bay snow crabs (A) and all new-shelled snow crabs (B). Note outlier (red square data point) at HRI value of 1.362 in both plots.

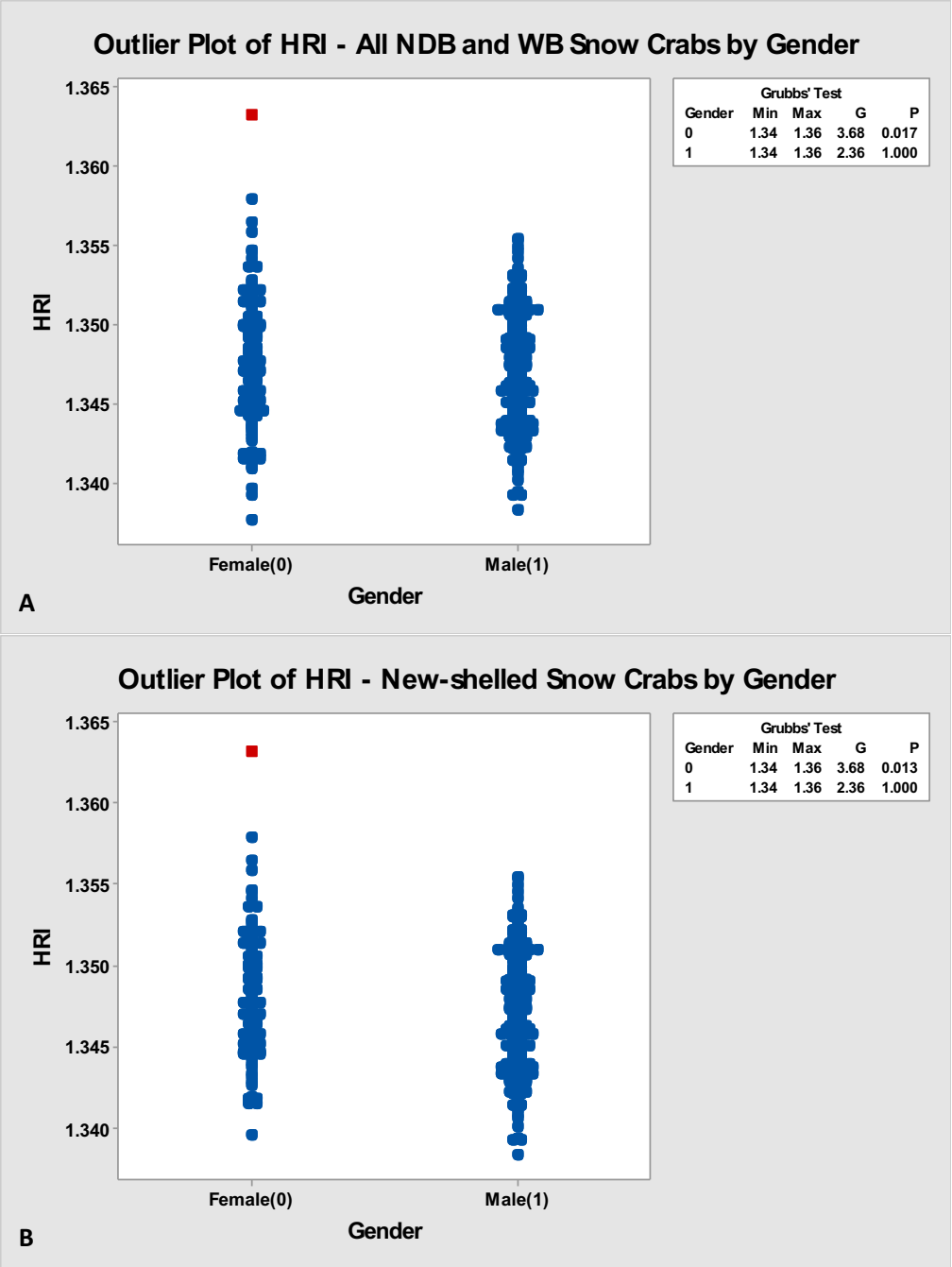

Figure 4.4. Outlier plots of hemolymph refractive index for all Notre Dame Bay (NDB) and White Bay (WB) new-shelled snow crabs (A) and all NDB and WB new-shelled snow crabs by gender (B). Note outlier (red square data point) at HRI value of 1.362 in female new-shelled snow crabs.

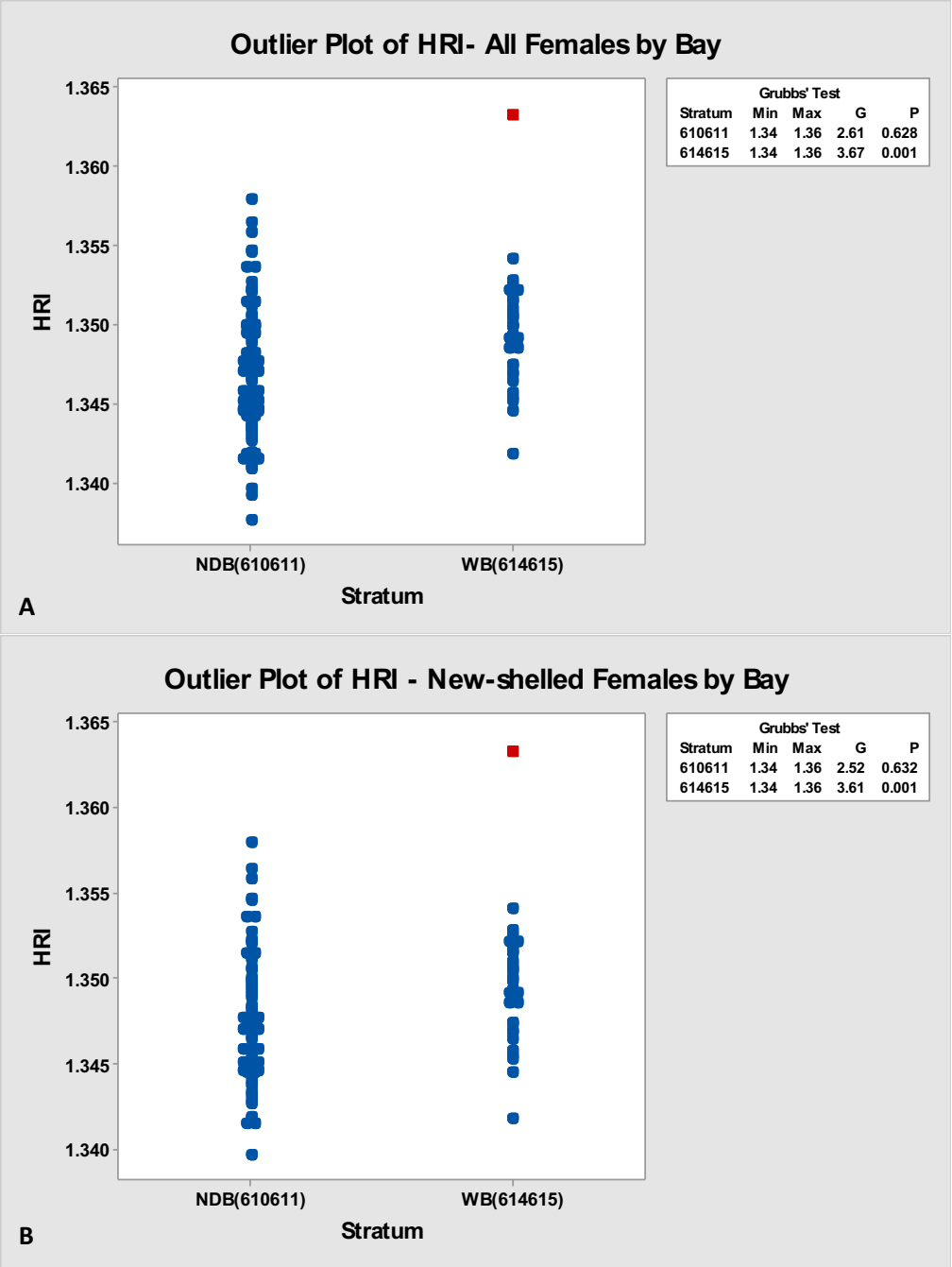

Figure 4.5. Outlier plot of hemolymph refractive index for all females by bay (A) and new-shelled female snow crabs by bay (B). White Bay (WB) collection from strata 614/615 (no female snow crabs were collected from WB stratum 613). Note that there was no outlier within NDB females and the outlier in WB females at a HRI value of 1.362 (red square data point).

4.3.3. **Effect of Shipping Mortality on HRI**

A selection of dead snow crabs was collected from the snow crab shipments from WB. WB BCD- snow crabs that died during shipping had a slightly higher mean HRI (n=26, mean = 1.348823 ± 0.0000573) than all WB BCD- snow crabs that arrived alive after being shipped (n = 134, mean = 1.34882 ± 0.000237); the difference was not statistically significant (two-way T-test: T-value = 1.26, DF = 39, p-value = 0.216).

The shipping mortalities from WB 614/615 had a higher mean HRI (n=16, mean = 1.35023 ± 0.000545 SEM) than the BCD- snow crabs from WB 614/615 that arrived alive (n = 90, mean = 1.34896 ± 0.000296), a difference that was just above the cut-off value for statistical significance (two-sample T-test: T-value = 2.03, DF = 25, p-value = 0.053). Male WB 614/615 new-shelled BCD- snow crabs that died during shipping (n=11, mean = 1.350318 ± 0.000691) had a higher mean HRI than those that arrived alive (n=64, mean = 1.34898 ± 0.000370) but this difference was not statistically significant; two-sample T-test: T-value = 1.71, DF = 16, p-value = 0.107). Similarly, no significant difference was observed between female WB 614/615 new-shelled BCD- snow crabs that died during shipping (n=5, mean = 1.35004 ± 0.000962) and females from that same region that arrived alive (n=26, mean = 1.34890 ± 0.000292; two-sample T-test: T-value = 1.01, DF = 7, p-value = 0.344). There was also no significant difference in mean HRI between snow crabs that died (n=10, mean = 1.34657 ± 0.000813) or survived shipping (n= 44, mean = 1.346075 ± 0.000556) from WB 613 (two-sample T-test: T-value = 0.50, DF = 18, p-value = 0.621). All new-shelled BCD- snow crabs from WB 613 were male snow crabs. Note that although these differences were not statistically significant the trend in all groups

was for higher HRI in animals that died during shipping versus those that arrived alive (Figure 4.6). Shipping mortalities were removed from the data for the following statistical analyses.

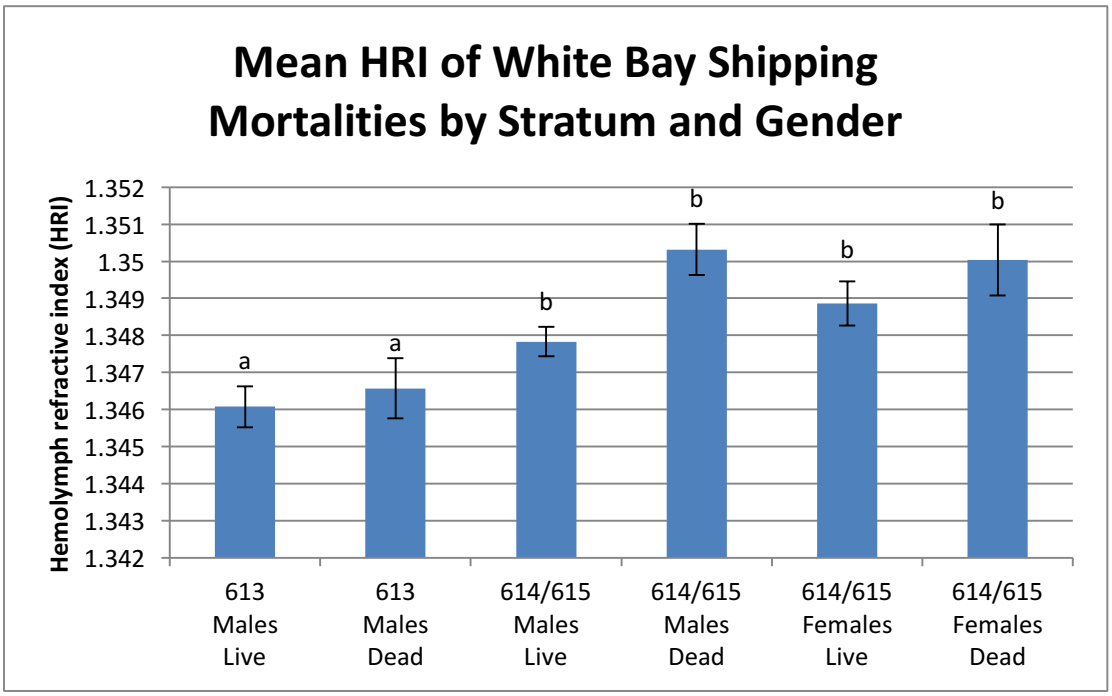

Figure 4.6. Comparison of mean HRI of shipping mortalities (presumed BCD-) and live BCD- snow crabs from White Bay by stratum and gender. Groups with different letters above the data bar were statistically significant ($p<0.05$).

4.3.4. **Bitter Crab Disease and Gut Wall Reserve Inclusion Score**

4.3.4.1. **Gut Wall RI Scores in BCD+ Snow Crabs**

All five female BCD+ crabs had gut wall RI scores of 0 (Table 4.2). The majority of male BCD+ crabs also had a gut wall RI score of 0 (n=21) with two male BCD+ crabs with gut wall RI scores of 2 (Table 4.3).

Table 4.3. Gut wall RI scores in BCD+ snow crabs with collection gender and carapace width, with bay of origin, infection intensity, and gut wall RI score of each diseased crab. Snow crabs with a gut wall RI score greater than zero are indicated in bold.

	Crab ID #	Bay	Gender	Carapace Width (mm)	Infection Intensity	Gut Wall RI Score
1	2010-133	NDB	Female, gravid	49	Moderate	0
2	2010-106	NDB	Female, gravid	56	Moderate	0
3	2011-163	WB	Female	48	Advanced	0
4	2010-120	NDB	Female, gravid	60	Very Advanced	0
5	2010-131	NDB	Female, gravid	60	Very Advanced	0
6	2011-147	WB	Male	67	Mild	0
7	**2011-155**	**NDB**	**Male**	**72**	**Moderate**	**1**
8	2011-156	NDB	Male	85	Moderate	0
9	2010-30	WB	Male	93	Moderate	0
10	2011-63	NDB	Male	65	Advanced	0
11	2011-100	NDB	Male	79	Advanced	0
12	2010-39	WB	Male	80	Advanced	0
13	**2010-60**	**WB**	**Male**	**80**	**Advanced**	**1**
14	2011-61	NDB	Male	80	Advanced	0
15	2011-64	NDB	Male	87	Advanced	0
16	2010-19	WB	Male	90	Advanced	0
17	2011-65	NDB	Male	101	Advanced	0
18	2010-40	WB	Male	54	Very Advanced	0
19	2010-117	WB	Male	65	Very Advanced	0
20	2011-67	NDB	Male	67	Very advanced	0
21	2011-98	NDB	Male	67	Very advanced	0
22	2011-99	NDB	Male	74	Very advanced	0
23	2010-59	WB	Male	75	Very Advanced	0
24	2010-119	WB	Male	78	Very Advanced	0
25	2010-38	WB	Male	83	Very Advanced	0
26	2010-20	WB	Male	96	Very advanced	0
27	2011-62	NDB	Male	99	Very advanced	0
28	2011-66	NDB	Male	107	Very advanced	0

4.3.4.2. **Gut Wall RI Score Comparison By BCD Status**

Median gut wall RI score was significantly lower in BCD+ crabs (n=27, median = 0.000) than BCD- snow crabs (n=262, median = 1.000; Mann-Whitney Test: W = 39701.5, p-value = 0.000; Figure 4.7A). All BCD+ snow crabs were new-shelled. These BCD+ new-shelled snow crabs also had a median gut wall RI score that was significantly lower than in BCD- new-shelled snow crabs

(n=242, median = 1.000; Mann-Whitney Test: W= 34329.0, p-value = 0.000; Figure 4.7B). Furthermore, all BCD+ snow crabs had a higher proportion with a RI score of 0 versus a gut wall score greater than 0 as compared to all BCD- snow crabs (Pearson Chi-Square = 21.344, DF = 1, P-value = 0.000). And, the same was true when comparing BCD+ and BCD- new-shelled snow crabs (Pearson Chi-Square = 22.355, DF = 1, P-value = 0.000). Thus, all further gut wall RI score comparisons were conducted on new-shelled snow crabs due to differences in median RI scores between snow crabs of varying shell conditions (see Appendix 7).

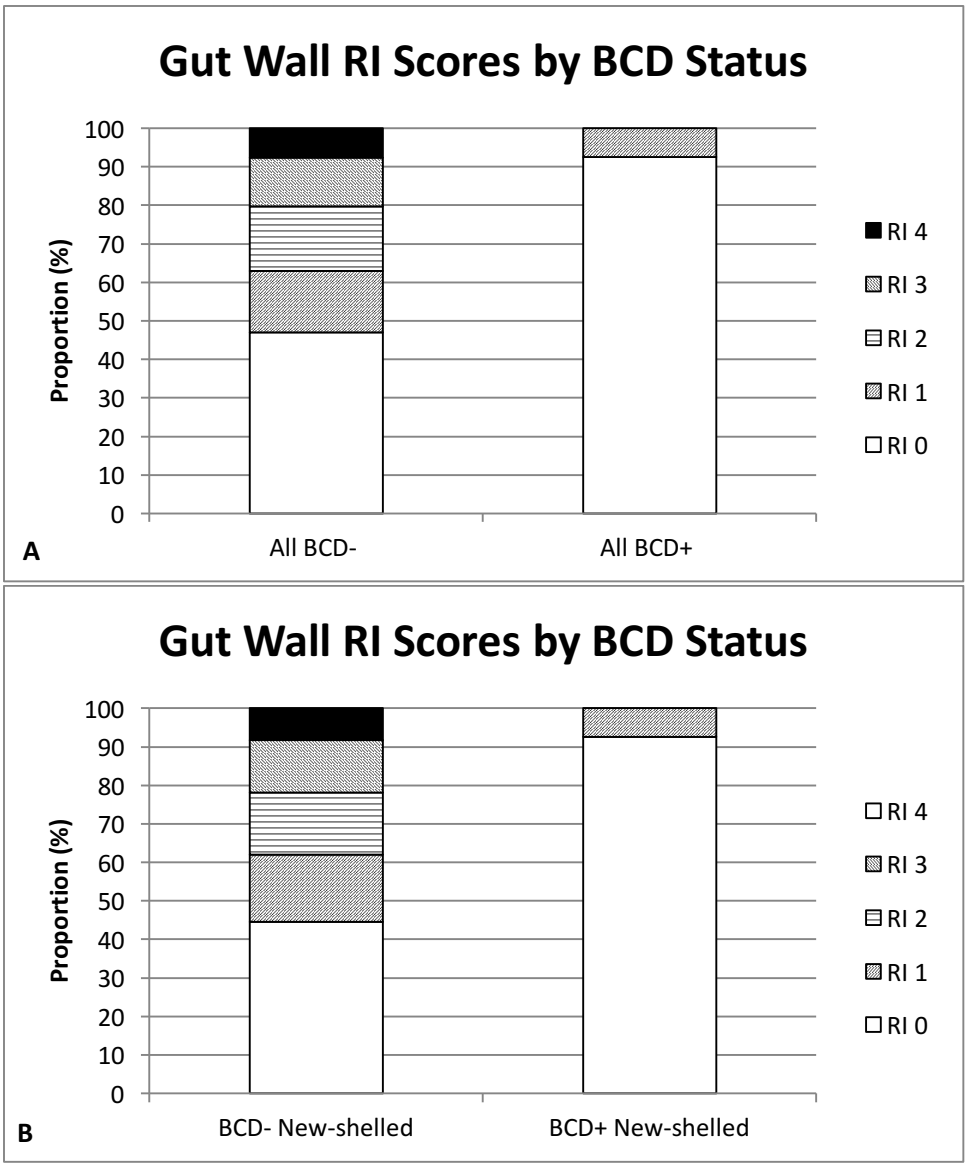

Figure 4.7. Proportions of snow crabs with gut wall reserve inclusion (RI) scores ranging from 0 to 4 in BCD- and BCD+ snow crabs in all snow crabs (A) and new-shelled snow crabs (B).

4.3.4.3. **Gut Wall RI Score Comparison in New-shelled Snow Crabs by BCD Status and Gender**

Median gut wall RI score was significantly lower in BCD- new-shelled females (n=84, median = 0) than in BCD- new-shelled males (n = 158, median = 1; Mann Whitney Test: W= 8304.0, p-value = 0.0001). Median gut wall RI score was significantly lower in BCD+ new-shelled males (n = 23, median = 0) than in BCD- new shelled males (n=158, median = 1; Mann-Whitney Test: W =

1052.0, p-value = 0.000; Figure 4.8). (Note: BCD+ females all had a RI score of 0 – could not complete Mann-Whitney Test or T-test.) The proportions of snow crabs with a gut wall RI score of 0 versus an RI score greater than zero were not significantly different between BCD+ new-shelled female crabs and BCD- new-shelled female crabs (Fisher Exact test p-value = 0.141; Table 4.4). A significantly higher proportion of BCD+ new-shelled male snow crabs had an RI score of 0 than seen in BCD- new-shelled snow crabs (Pearson Chi-Square = 23.095, DF = 1, P-value = 0.000; Table 4.4).

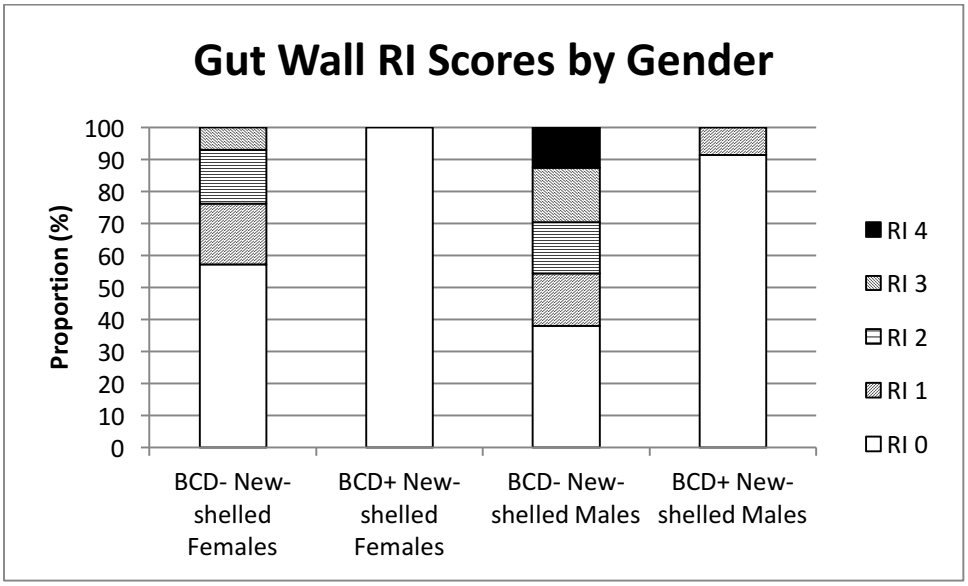

Figure 4.8. Proportions of snow crabs with gut wall reserve inclusion (RI) scores ranging from 0 to 4 in BCD- and BCD+ snow crabs in new-shelled snow crabs by gender.

Table 4.4. Summary of differences in gut wall reserve inclusion (RI) scores by BCD status. Statistically significant differences (p <0.05) are indicated in bold.

		n	Gut Wall RI Score Median Comparisons		Gut Wall RI Score 0 or >0 Proportions		
			Median	Mann-Whitney Test p-value	RI = 0 (n)	RI >0 (n)	Pearson Chi-Square p-value
All	**BCD-**	262	1	**0000**	123	139	**0.000**
	BCD+	27	0		26	2	
New-shelled	**BCD-**	242	1	**0.000**	108	134	**0.000**
	BCD+	27	0		25	2	
New-shelled by Gender	**BCD- Females**	84	0	*	48	36	0.141$^{\perp}$
	BCD+ Females	4	0		4	0	
	BCD- Males	158	1	**0.000**	60	98	**0.000**
	BCD + Males	23	0		21	2	

*All BCD+ female snow crabs have a gut wall RI score of 0 (unable to perform Mann-Whitney Test).
$^{\perp}$Fisher Exact Test used rather than Pearson Chi-Square as some expected cell counts were <5.

4.3.4.4. Gut Wall RI Score Comparison in New-shelled animals by BCD Status, Gender, Bay, and Strata within Bay

All female BCD+ snow crabs (n = 4) had an RI score of 0 (unable to perform Mann-Whitney Test or t-test). Median gut wall RI score was significantly lower in BCD+ male snow crabs in NDB (n=10, median = 0) than in BCD- males in NDB (n = 50, median = 3; Mann-Whitney Test: W = 116.5, p-value = 0.0001). Median gut wall RI score was significantly lower in BCD+ male snow crabs in WB (n=13, median = 0) than in BCD- males in WB (n = 108, median = 1; Mann Whitney Test: W = 446.0, p-value = 0.0018).

The proportions of snow crabs with a gut wall RI score of 0 versus an RI score greater than zero were not significantly different between BCD+ new-shelled female crabs and BCD- new-shelled female crabs in NDB (Fisher Exact Test p-value = 0.115). (Note: The only BCD+ female snow crab

from WB was the excluded outlier.) A significantly higher proportion of BCD+ new-shelled male snow crabs had an RI score of 0 than seen in BCD- new-shelled snow crabs in NDB (Fisher Exact Test p-value 0.000) and in WB (Pearson Chi-Square = 10.266, DF = 1, P-value = 0.001). A significantly higher proportion of snow crabs with a gut wall RI score of 0 were seen in BCD- WB males than in NDB BCD- males (Pearson Chi-square = 8.322, DF = 1, p-value = 0.004; Figure 4.9 and Table 4.5).

All WB 613 male BCD+ snow crabs (n = 4) had an RI score of 0 (unable to perform Mann-Whitney Test or t-test). Median gut wall RI score was significantly lower in BCD+ male snow crabs in WB 614/615 (n=11, median = 0) than in BCD- males in WB 614/615 (n = 64, median = 0.5; Mann-Whitney Test: W = 267.5, p-value = 0.0141; Figure 4.9 and Table 4.5).

The proportions of snow crabs with a gut wall RI score of 0 versus an RI score greater than zero were not significantly different between BCD+ new-shelled male crabs (n=2) and BCD- new-shelled male crabs in WB 613 (Fisher Exact Test p-value = 0.165). A significantly higher proportion of BCD+ new-shelled male snow crabs had an RI score of 0 than seen in BCD- new-shelled snow crabs in WB 614/615 (Fisher Exact Test p-value 0.018).

Median gut wall RI score was significantly higher in BCD – male snow crabs in NDB (n=50, median = 3) than BCD- females in NDB (n = 59, median = 1; Mann-Whitney Test: W = 3516.5, p-value = 0.0000). Median gut wall RI score in NDB BCD- male snow crabs was also higher than in BCD- males in WB (n=108, median =1; Mann-Whitney Test: W = 5128.5, p-value = 0.0000).

Within WB median gut wall RI score was significantly higher in WB 613 BCD- male snow crabs (n = 44, median = 1.5) than in WB 614/615 male snow crabs (n=64, median = 0.5; Mann Whitney Test: W = 2837.5, p-value = 0.0036). Median gut wall RI score in NDB was not significantly different from the median gut wall RI score in WB 613 (Mann Whitney Test W = 2592.5, p-value = 0.0902) but was significantly higher than the median gut wall RI score in WB 614/615 (Mann-Whitney Test W= 3812.0, p-value = 0.0000; Figure 4.10 and Table 4.5).

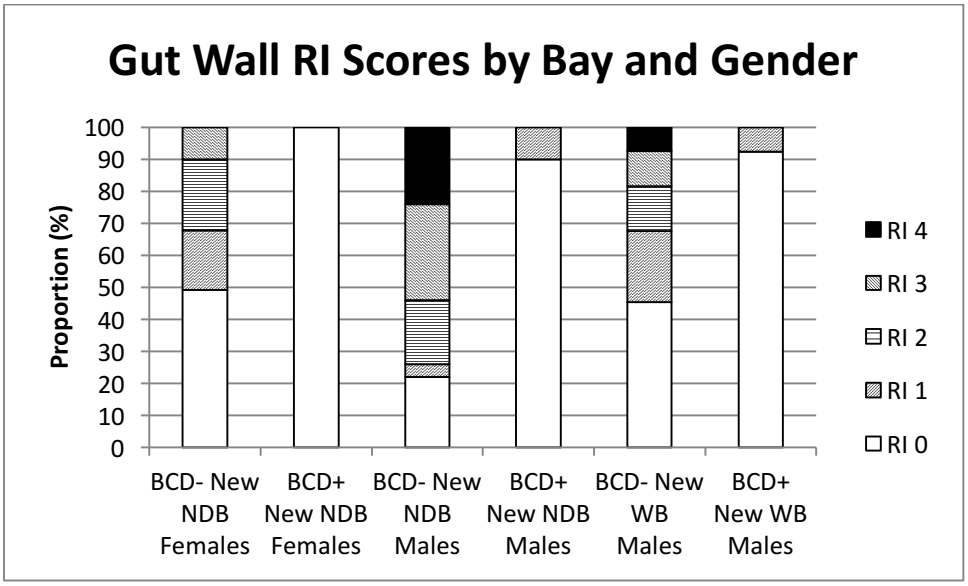

Figure 4.9. Proportions of new-shelled (New) snow crabs with varying gut wall RI scores by BCD status, gender, and bay.

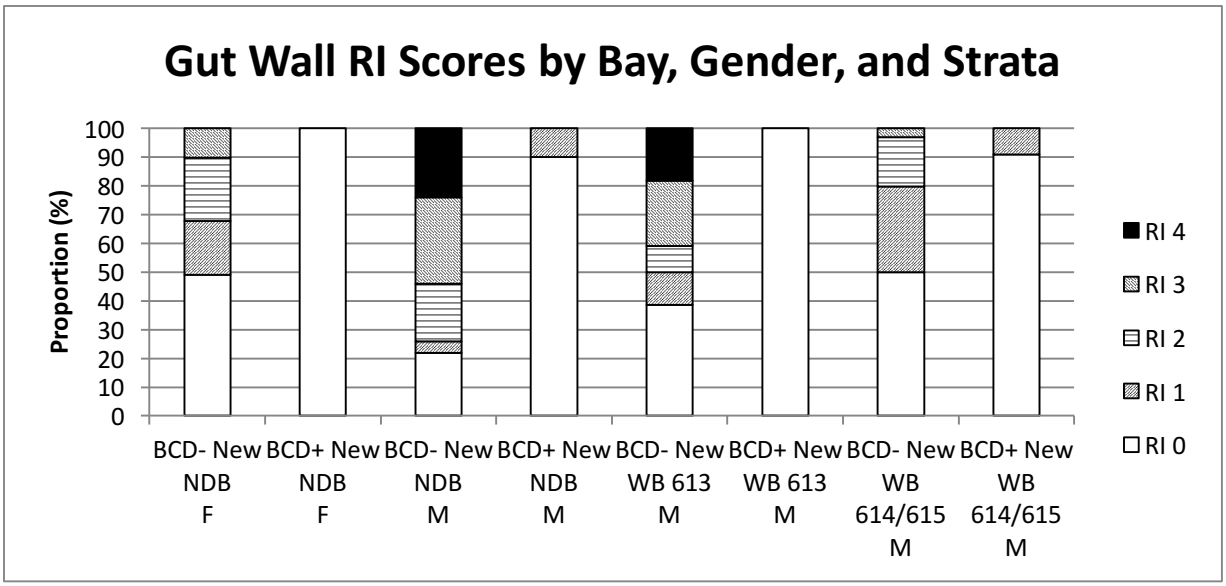

Figure 4.10. Proportions of new-shelled (New) snow crabs with varying gut wall RI scores by BCD status, gender (F = female; M = male), bay, and strata.

Table 4.5. Summary of differences in gut wall RI scores by BCD status in new-shelled snow crabs by gender, bay, and strata within bay. Statistically significant differences ($p<0.05$) are indicated in bold.

		n	Gut Wall RI Score Median Comparisons		Gut Wall RI Score 0 or >0 Proportions		
			Median	Mann-Whitney Test p-value	RI = 0 (n)	RI >0 (n)	Pearson Chi-Square p-value
NDB	**BCD- Females**	59	0	*	29	30	0.115$^{\perp}$
	BCD+ Females	4	0		4	0	
	BCD- Males	50	3	**0.0001**	11	39	**0.000**$^{\perp}$
	BCD+ Males	10	0		9	1	
WB	**BCD- Males**	108	1	**0.0018**	49	59	**0.001**
	BCD+ Males	13	0		12	1	
WB 613	**BCD- Males**	44	1.5	*	17	27	0.165$^{\perp}$
	BCD+ Males	2	0		2	0	
WB 614/615	**BCD- Males**	64	0.5	**0.0121**	32	32	**0.018**$^{\perp}$
	BCD+ Males	11	0		10	1	

*All BCD+ snow crabs had a gut wall RI score of 0 (cannot complete statistical test).

$^{\perp}$Fisher Exact Test used rather than Pearson Chi-Square as some expected cell counts were <5.

4.3.5. **Bitter Crab Disease and Hemolymph Refractive Index**

4.3.5.1. **BCD and HRI in Snow Crabs (All Shell Condition Categories)**

The mean HRI of all BCD+ snow crabs was significantly lower than the mean HRI of all BCD- snow crabs (Figure 4.11). The mean HRI of all BCD+ male snow crabs was significantly lower than the mean HRI of BCD- male snow crabs, but there was no significant difference between mean HRIs in all BCD+ females and all BCD- females (Figure 4.12). There also were differences within bay. All BCD+ female snow crabs were from NDB, and there were no significant differences between the mean HRIs of BCD+ and BCD- females from NDB. BCD+ male snow crabs were found in both NDB and WB and within both strata in WB. There were significant differences between the mean HRIs of BCD+ and BCD - male snow crabs in NDB and WB (Figure 4.13). Within WB there were significant differences in mean HRI by BCD status in strata 614/615 but not in stratum 613 (Figure 4.14).

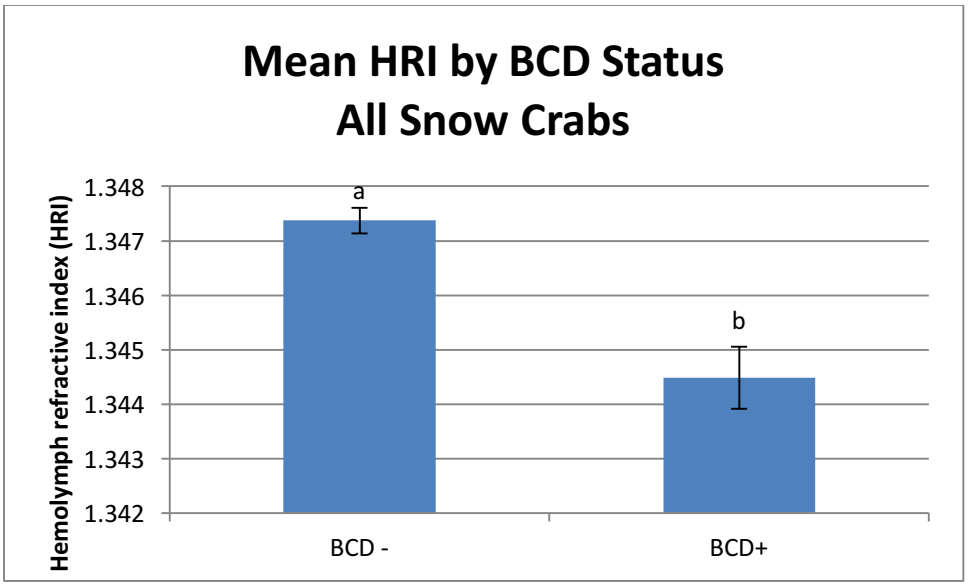

Figure 4.11. Comparison of mean HRI of BCD- and BCD+ snow crabs (mean ± SEM). Mean HRI was significantly lower in BCD+ new-shelled snow crabs (n = 27, mean = 1.34449 ± 0.00057 SEM) than in BCD- new-shelled snow crabs (n=262, mean = 1.34737 ± 0.00024 SEM; two-sample T-test: T-value = -4.66, DF = 35, **p-value = 0.000**). Groups with different letters above the data bar were statistically significant (p <0.05).

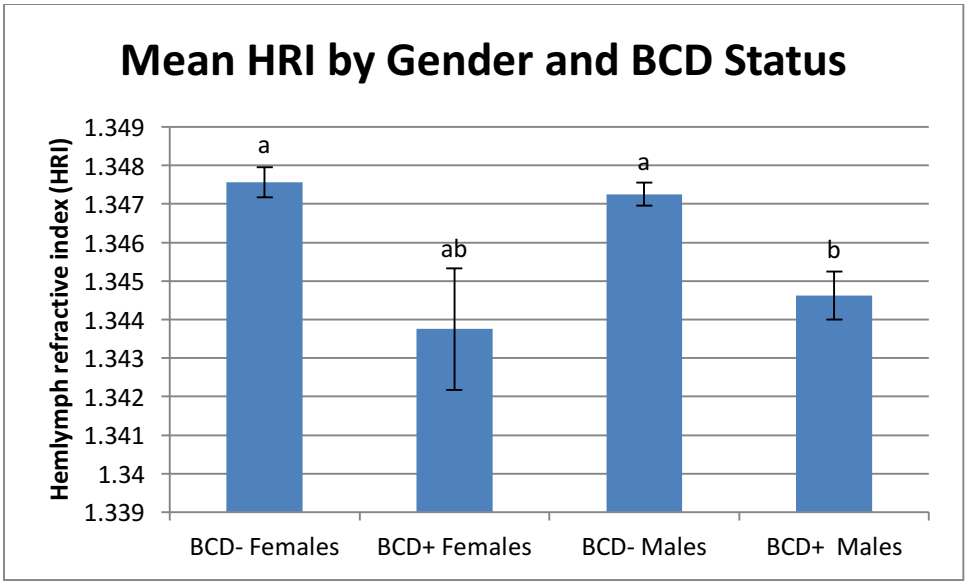

Figure 4.12. Comparison of mean HRIs by gender and BCD status (mean ± SEM). Mean HRI for female BCD+ snow crabs (n=4, mean = 1.34375 ± 0.0016 SEM) was lower than, but not significantly different from, the mean HRI for female BCD- snow crabs (n = 103, mean = 1.34756 ± 0.00039 SEM; two-sample T-test: T-value = -2.35, DF = 3, p-value = 0.101). The mean HRI for male BCD+ snow crabs (n =23, mean = 1.344617 ± 0.00062 SEM) was significantly lower than the mean HRI for male BCD- snow crabs (n = 159, mean = 1.34725 ± 0.00030 SEM; two-sample T-test: T-value = -3.81, DF = 32, **p-value = 0.001**). Groups with different letters above the data bar were statistically significant (p<0.05).

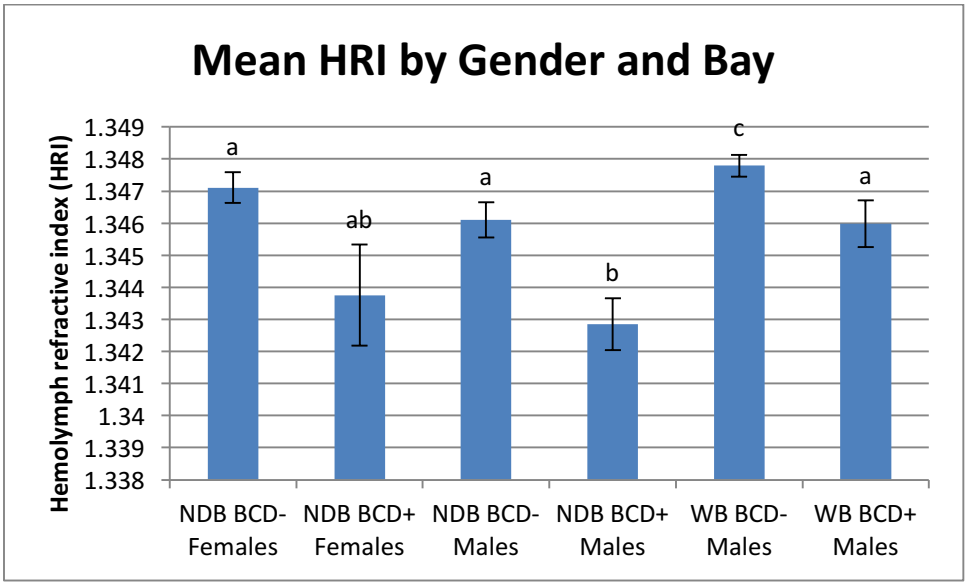

Figure 4.13. Comparison of mean HRIs by gender, BCD status, and bay (mean ± SEM). The mean HRI for female BCD+ snow crabs from NDB (n=4, mean = 1.34375 ± 0.00315 SEM) was not

significantly different from the mean HRI for BCD- snow crabs from NDB (n=77, mean = 1.34711 ± 0.00048; two-sample T-test: T-value = -2.04, DF =3, p-value = 0.134). The mean HRI for male BCD+ snow crabs from NDB (n = 10, mean = 1.34285 ± 0.000813) was significantly lower than the mean for male BCD- snow crabs from NDB (n = 50, mean = 1.34613 ± 0.000561 SEM; two-sample T-test: T-value = -3.32, DF = 18, **p-value = 0.004**). The mean HRI of BCD+ males from WB (n = 13, mean = 1.34598 ± 0.00073 SEM) was lower than the mean HRI of BCD- males from WB (n= 108, mean = 1.34780 ± 0.00034 SEM; two-sample T-test: T-value = -2.26, DF = 17, **p-value = 0.037**). Groups with different letters above the data bar were statistically significant (p<0.05).

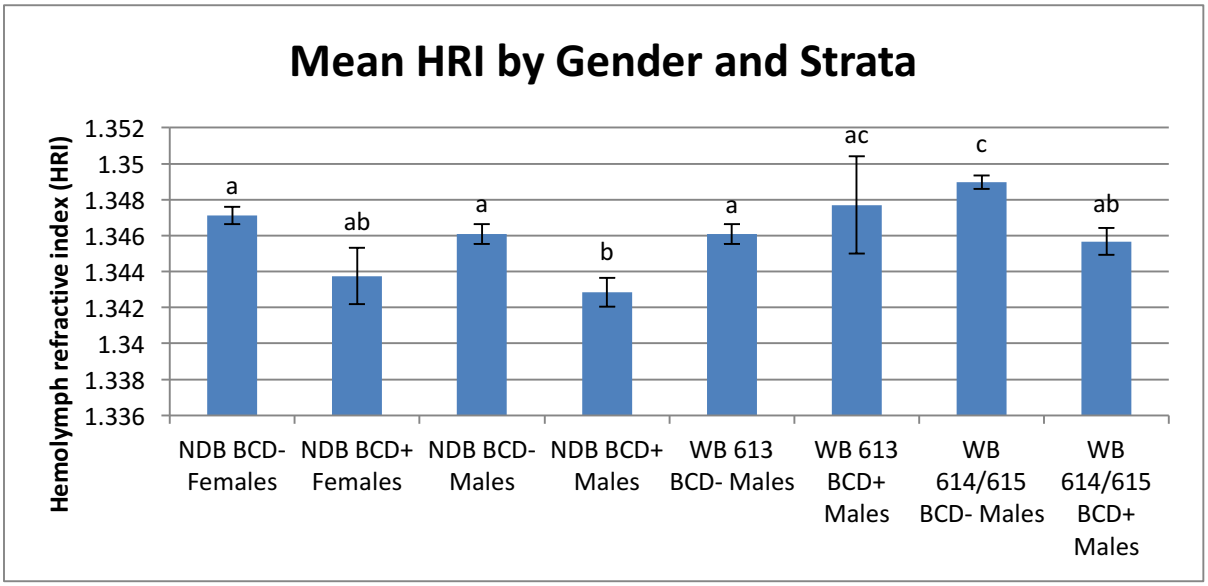

Figure 4.14. Comparison of mean HRIs by gender, BCD status, and strata (mean ± SEM). The results for NDB strata were as indicated above. In WB stratum 613 there was no significant difference between male BCD+ snow crab mean HRI (n = 2, mean = 1.34770 ± 0.0027 SEM) and male BCD- mean HRI (n = 44, mean = 1.34607 ± 0.00056 SEM; two-sample T-test: T-value = 0.59, DF = 1, p=value = 0.661). In WB strata 614/615 male BCD+ snow crabs had a significantly lower mean HRI (n=11, mean = 1.345664 ± 0.000743 SEM) than male BCD- snow crabs (n = 64, mean = 1.34898 ± 0.00037; two-sample T-test: T-value = -3.99, DF = 15, **p-value = 0.001**). Groups with different letters above the data bar were statistically significant (p<0.05).

4.3.5.2. **BCD and HRI in New-shelled Snow Crabs**

The pattern of significance of differences between mean HRIs by BCD status in new-shelled snow crabs was similar to that observed for all snow-crabs. The mean HRI of BCD+ new-shelled snow crabs was significantly lower than the mean HRI of all BCD- new-shelled snow crabs (Figure 4.15). The mean HRI of all BCD+ new-shelled male snow crabs was significantly lower

than the mean HRI of BCD- new-shelled male snow crabs, but there was no significant difference between mean HRIs in BCD+ new-shelled females and BCD- new-shelled females (Figure 4.16). There were also differences within bays. All BCD+ female snow crabs were from NDB, and there were no significant differences between the mean HRIs of BCD+ and BCD- new-shelled females from NDB. BCD+ male snow crabs were found in both NDB and WB and within both strata in WB. There were significant differences between the mean HRIs of BCD+ and BCD – new-shelled male snow crabs in NDB and WB (Figure 4.17). Within WB there were significant differences in mean HRI in new-shelled males by BCD status in strata 614/615 but not in stratum 613 (Figure 4.18).

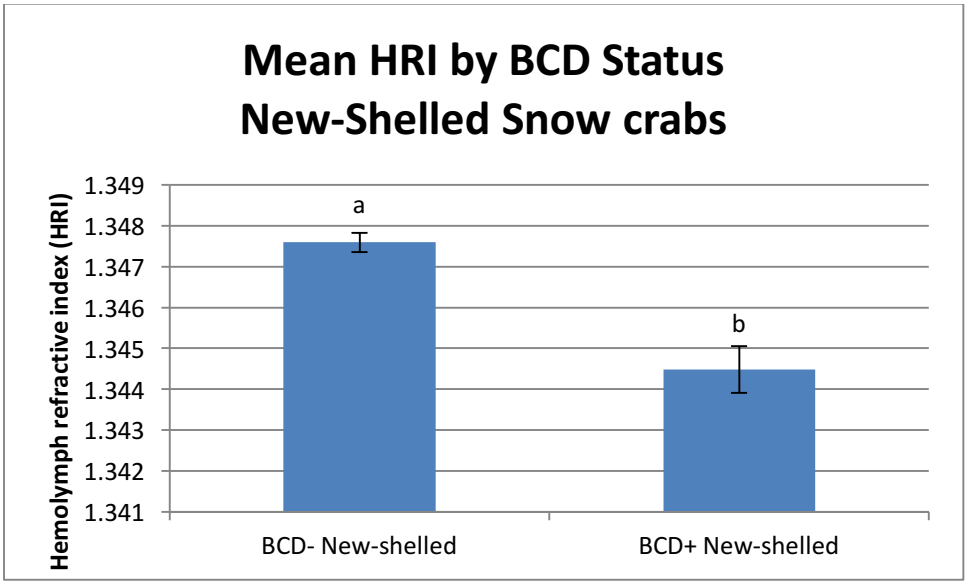

Figure 4.15. Comparison of mean HRI of BCD- new-shelled and BCD+ new-shelled snow crabs (mean ± SEM). The mean HRI of BCD+ new-shelled snow crabs (n = 27, mean = 1.34449 ± 0.00057 SEM) was significantly lower than the mean HRI of BCD- new-shelled snow crabs (n=242, mean = 1.34759 ± 0.00024 SEM; two-sample T-test: T-value = -5.00, DF = 36, **p-value = 0.000**). Groups with different letters above the data bar were statistically significant (p<0.05).

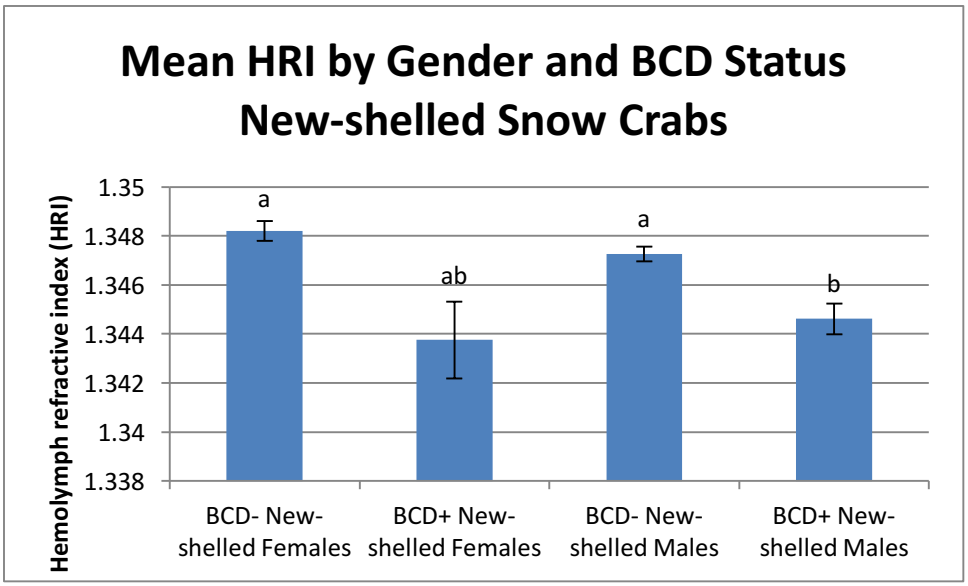

Figure 4.16. Comparison of mean HRIs by gender and BCD status (mean ± SEM). BCD+ new-shelled female snow crabs had a mean HRI (n=4, 1.34375 ± 0.0016 SEM) that was not significantly different from, BCD- new-shelled females from NDB (n=84, mean = 1.34821 ± 0.00041 SEM; two-sample T-test: T-value = -2.74, DF = 3, p-value = 0.071). BCD+ new-shelled male snow crabs had a mean HRI (n = 23, mean = 1.34462 ± 0.00062 SEM) that was lower than the mean HRI of BCD- males from NDB with a gut wall RI score of 0 (n = 158, mean = 1.34727 ± 0.00030 SEM; two-sample T-test: T-value = -3.83, DF = 33, **p-value = 0.001**). Groups with different letters above the data bar were statistically significant (p<0.05).

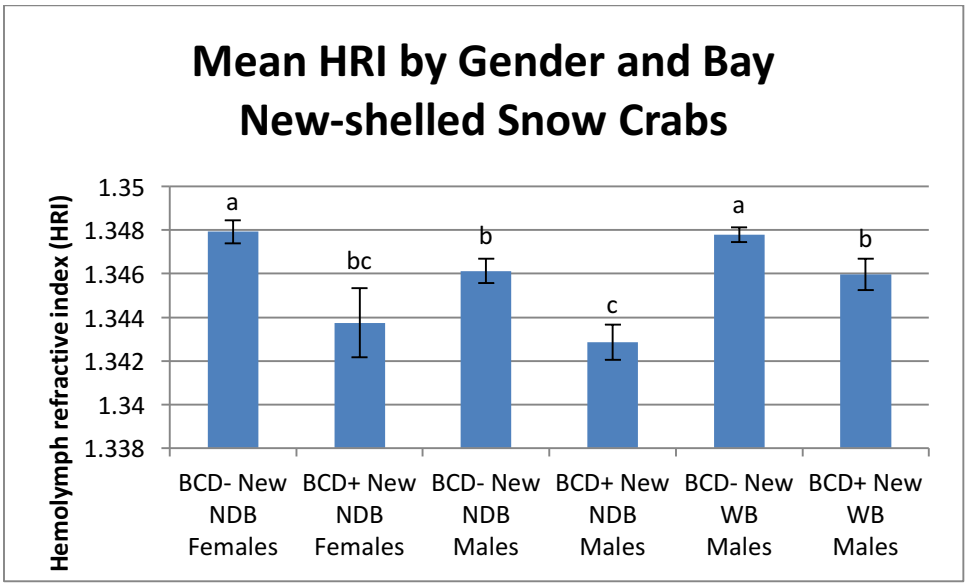

Figure 4.17. Comparison of mean HRIs by gender, BCD status, and bay (mean ± SEM). NDB new-shelled BCD+ new-shelled female snow crabs had a mean HRI (n=4, 1.34375 ± 0.0016 SEM) that was lower than, but not significantly different from, BCD- new-shelled females from NDB (n=59,

mean = 1.34793 ± 0.00052 SEM; two-sample T-test: T-value = -2.52, DF = 3, p-value = 0.086). NDB new-shelled BCD+ male snow crabs had a mean HRI (n = 10, mean = 1.34285 ± 0.00081 SEM) that was lower than the mean HRI of BCD- males from NDB with a gut wall RI score of 0 (n = 50, mean = 1.34613 ± 0.00056 SEM; two-sample T-test: T-value = -3.32, DF = 18, **p-value = 0.004**). The mean HRI of BCD+ new-shelled males from WB (n = 13, mean = 1.34598 ± 0.00073) was lower than the mean HRI of BCD- new-shelled males from WB (n= 108, mean = 1.34780 ± 0.00034; two-sample T-test: T-value = -2.26, DF = 17, **p-value = 0.037**). Groups with different letters above the data bar were statistically significant (p<0.05).

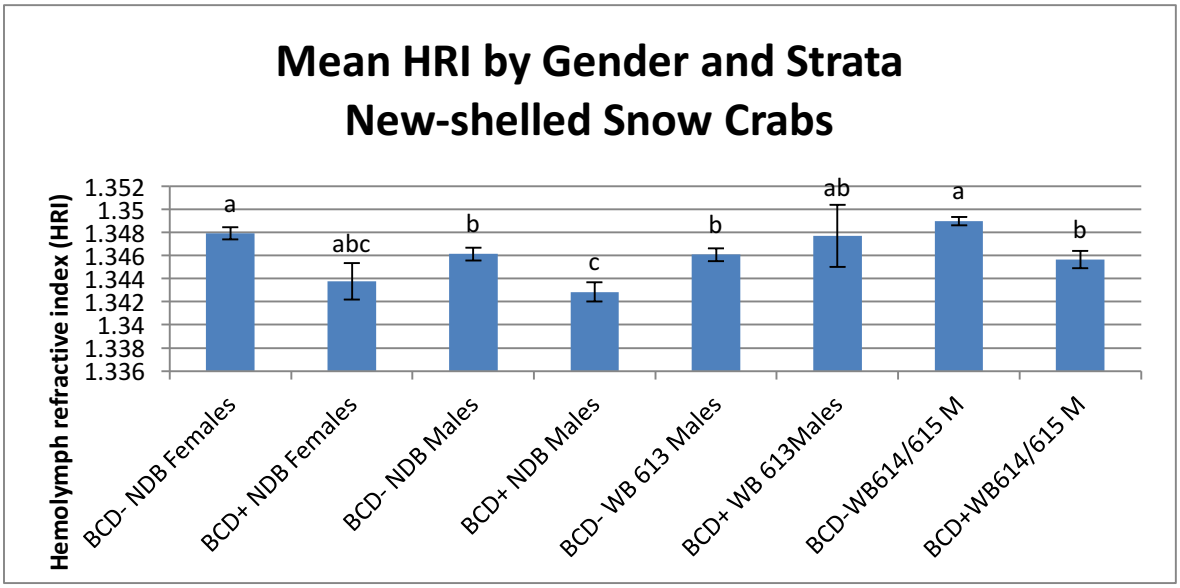

Figure 4.18. Comparison of mean HRIs by strata (mean ± SEM). The results for NDB strata were as indicated above. New-shelled BCD+ new-shelled male snow crabs from WB stratum 613 had a mean HRI (n = 2, mean = 1.34770 ± 0.0027 SEM) not significantly different from the mean HRI in new-shelled BCD- male snow crabs from stratum 613 (n = 44, mean = 1.34607 ± 0.00056 SEM; two-sample T-test: T-value = 0.59, DF = 1, p-value = 0.661). WB BCD+ new-shelled male snow crabs from strata 614/615 had a mean HRI (n=11, mean = 1.345664 ± 0.00074 SEM) that was lower than the mean HRI of new-shelled BCD- male snow crabs from WB 614/615 (n = 64, mean = 1.34898 ± 0.000037 SEM; two-sample T-test: T-value = -3.99, DF = 15, **p-value = 0.001**). Groups with different letters above the data bar were statistically significant (p<0.05).

4.3.6. HRI and Carapace Width

4.3.6.1. HRI and Carapace Width by BCD Status and Gender

(All Shell Condition Categories)

No significant correlation between HRI and carapace width was observed in BCD- or BCD+ snow crabs when all shell conditions and gut wall RI scores were analyzed together. There was no

correlation between HRI and carapace width for both BCD- and BCD+ snow crabs (both genders, all shell condition categories, and all gut wall RI scores). No statistically significant correlation between HRI and carapace width is observed in male or female snow crabs with or without BCD when all shell condition categories and gut wall RI scores are analyzed together. A mild negative correlation was present in BCD- and BCD+ males whereas no correlation was seen in BCD- and BCD+ females (Table 4.6).

Table 4.6. HRI vs carapace width correlations in snow crabs of all shell conditions and RI scores by BCD status with summary of comparisons of mean HRI. Pearson correlations with negative trends (red) and positive trends (green). No statistically significant correlations between HRI and carapace width were observed in these groups of snow crabs. Significant differences in mean HRI between BCD- and BCD+ snow crabs are indicated in bold.

		n	HRI vs Carapace Width		HRI		
			Pearson correlation	Pearson correlation p-value	Mean	Two-sample T-test T-value	Two-sample T-test p-value
All Bays	**BCD-**	262	-0.074	0.231	1.34737	-4.66	**0.000**
	BCD+	27	-0.053	0.793	1.34449		
All Bays By Gender	**BCD- Females**	103	0.050	0.617	1.34756	-2.35	0.101
	BCD+ Females	4	0.036	0.964	1.34375		
	BCD - Males	159	-0.124	0.119	1.34825	-3.81	**0.001**
	BCD+ Males	23	-0.153	0.486	1.34462		

4.3.6.2. HRI and Carapace Width by BCD Status, Gender, & Bay (All Shell Categories)

Female BCD+ snow crabs were only collected in NDB (single WB BCD+ female is the excluded outlier described above). NDB BCD- females had a mild positive correlation between HRI and carapace width while BCD+ snow crab had no correlation between HRI and carapace width. Male snow crabs were collected from both bays. In NDB BCD- snow crabs there was no correlation between HRI and carapace width whereas in BCD+ snow crabs there was a negative

correlation. In WB males there was a negative correlation between HRI and carapace width was present in both BCD- and BCD+ snow crabs. There were also differences within WB collection regions. In WB 613 there was no correlation between HRI and carapace width in BCD- male snow crabs and there were only 2 BCD+ male snow crabs from this stratum. In WB 614/615 there was a positive correlation between HRI and carapace width in BCD- male snow crabs and a negative correlation in BCD+ male snow crabs (Table 4.7).

Table 4.7. Summary of trends observed in HRI vs carapace width correlations seen in snow crabs of all shell conditions and RI scores by bay and BCD status with summary of mean HRI comparisons. Pearson correlations with negative trends (red) and positive trends (green). Statistically significant correlations between HRI and carapace width are indicated in bold. Significant differences in mean HRI between BCD- and BCD+ snow crabs are also indicated in bold.

		n	HRI vs Carapace Width		HRI		
			Pearson correlation	Pearson correlation p-value	Mean	Two-sample T-test T-value	Two-sample T-test p-value
NDB Females	**BCD-**	77	0.171	0.138	1.34711	-2.04	0.134
	BCD+	4	0.036	0.964	1.34375		
NDB Males	**BCD-**	51	-0.080	0.577	1.34613	-3.32	**0.004**
	BCD+	10	-0.222	0.538	1.34285		
WB Males	**BCD -**	108	**-0.206**	**0.032**	1.34780	-2.26	**0.037**
	BCD+	13	-0.208	0.496	1.34598		
WB 613 Males	**BCD -**	44	-0.096	0.536	1.34607	0.59	0.661
	BCD+	2	1	*	1.3477[⊥]		
WB 614/615 Males	**BCD -**	64	0.179	0.156	1.34898	-3.99	**0.001**
	BCD+	11	-0.235	0.487	1.34566		

[⊥]Only a very small amount of hemolymph was extracted from one of these 2 snow crabs (the higher HRI value may be due to a sample collection error).

4.3.6.3. HRI and Carapace Width in New-shelled Snow Crabs by BCD Status and Gender

When new-shelled (rather than all shell categories) snow crabs (with varying gut wall RI scores) were examined, HRI and carapace width were statistically significantly negatively correlated in

BCD- new-shelled snow crabs (Table 4.8). No significant correlation between HRI and carapace width was observed in BCD- or BCD+ new-shelled female snow crabs, and BCD- and BCD+ male snow crabs had negative correlations between HRI and carapace width.

Table 4.8. Summary of trends observed in HRI vs carapace width correlations seen in new-shelled snow crabs with gut wall RI scores 0 through 4. Pearson correlations with negative trends (red) and positive trends (green). Statistically significant correlations between HRI and carapace width are indicated in bold. Significant differences in mean HRI between BCD- and BCD+ snow crabs are indicated in bold.

		n	HRI vs Carapace Width		HRI		
			Pearson correlation	Pearson correlation p-value	Mean	Two-sample T-test T-value	Two-sample T-test p-value
All Bays	**New-shelled BCD-**	242	**-0.143**	**0.027**	1.34759	-5.00	**0.000**
	New-shelled BCD+	27	-0.053	0.793	1.34449		
All Bays By Gender	**New-shelled BCD- Females**	84	0.057	0.607	1.34821	-2.74	0.071
	New-shelled BCD+ Females	4	0.036	0.964	1.34375		
	New-shelled BCD - Males	158	-0.130	0.104	1.34727	-3.83	**0.001**
	New-shelled BCD+ Males	23	-0.153	0.486	1.34462		

4.3.6.4. HRI and Carapace Width in New-shelled Snow Crabs by BCD Status, Gender, and Bay

All BCD+ female snow crabs were collected from NDB. In NDB, BCD- new-shelled female snow crabs had a positive correlation between HRI and carapace width while no correlation was seen in BCD+ new-shelled snow crabs. In NDB new-shelled males no correlation was seen between HRI and carapace width in BCD- snow crabs while negative correlation was seen in BCD+ snow crabs. There was no statistically significant difference between these correlations, but mean HRI was lower in new-shelled NDB BCD+ male snow crabs than in new-shelled NDB BCD- male snow crabs (Table 4.9).

In WB HRI and carapace width were negatively correlated in both BCD- and BCD+ new-shelled male snow crabs. When separated by strata within WB, there was no significant correlation between HRI and carapace width in WB 613 BCD- snow crabs or BCD+ snow crabs (n=2). In WB 614/615 HRI and carapace width were positively correlated in BCD- snow crabs and negatively correlated in BCD+ snow crabs. There was no significant difference between these correlations but mean HRI was significantly lower in new-shelled WB BCD+ male snow crabs from strata 614/615 than in BCD- counterparts (Table 4.9).

Table 4.9. Summary of trends observed in HRI vs carapace width correlations seen in snow crabs of all shell conditions and RI scores by bay and BCD status. Pearson correlations with negative trends (red) and positive trends (green). Statistically significant correlations between HRI and carapace width are indicated in bold. Significant differences in mean HRI between BCD- and BCD+ snow crabs are also indicated in bold.

		n	HRI vs Carapace Width		HRI		
			Pearson correlation	Pearson correlation p-value	Mean	Two-sample T-test T-value	Two-sample T-test p-value
New-shelled NDB Females	BCD-	59	0.122	0.359	1.34793	-2.52	0.086
	BCD+	4	0.036	0.964	1.34375		
New-shelled NDB Males	BCD-	50	-0.088	0.544	1.34613	-3.32	**0.004**
	BCD+	10	-0.222	0.538	1.34285		
New-shelled WB Males	BCD -	108	**-0.206**	**0.032**	1.34780	-2.26	**0.037**
	BCD+	13	-0.208	0.496	1.34598		
New-shelled WB 613 Males	BCD -	44	-0.096	0.536	1.34607	0.59	0.661
	BCD+	2	1	*	1.3477[⊥]		
New-shelled WB 614/615Males	BCD -	64	0.179	0.156	1.34898	-3.99	**0.001**
	BCD+	11	-0.235	0.487	1.34566		

[⊥]Only a very small amount of hemolymph was extracted from one of these 2 snow crabs (the higher HRI value may be due to a sample collection error).

4.3.6.5. HRI and Carapace Width in New-shelled Snow Crabs by BCD Status and Gender in Snow Crabs with the Same Gut Wall RI Score

A significant negative correlation between HRI and carapace width was observed in BCD- new-shelled snow crabs with gut wall RI scores of 0 or 1 (Table 4.10). When the data for animals with these two low RI scores were examined separately the negative trends in correlation were typically observed; the negative correlation was statistically significant in new-shelled BCD- snow crabs with an RI score of 0 but was not significant in new-shelled BCD- snow crabs with an RI score of 1. In contrast, no correlation between HRI and carapace width was observed in BCD+ snow crabs with RI scores of RI 0 or RI 1 (combined or separately).

When the data was separated by gender, no correlation between HRI and carapace was seen in BCD- or BCD+ new-shelled female snow crabs with a gut wall RI score of 0. (Note: All BCD+ female snow crabs had RI scores of 0.) HRI and carapace width were significantly negatively correlated in new-shelled BCD- males with gut wall RI scores of 0 and 1 and a gut wall RI score of 0; there was also negative correlation at a gut wall RI score of 1 but the correlation was not statistically significant. Negative correlations (not statistically significant) were also seen in new-shelled BCD+ snow crabs with gut wall RI scores of 0 and 1 and gut wall RI score of 0. (Note: Only two new-shelled BCD+ snow crabs had gut wall RI scores of 1).

Table 4.10. Summary of trends observed in HRI vs carapace width correlations seen in new-shelled snow crabs with gut wall RI scores 0 through 4. Pearson correlations with negative trends (red) and positive trends (green). Statistically significant correlations between HRI and carapace width are indicated in bold. Significant differences in mean HRI between BCD- and BCD+ snow crabs are also indicated in bold.

			n	HRI vs Carapace Width		HRI		
				Pearson correlation	Pearson correlation p-value	Mean	2-sample T-test T-value	2-sample T-test p-value
All Bays	New-shelled BCD-	RI 0,1	150	**-0.217**	**0.008**	1.34720	-4.23	**0.000**
	New-shelled BCD+	RI 0,1	27	-0.053	0.793	1.34449		
	New-shelled BCD-	RI 0	108	**-0.285**	**0.003**	1.34663	-2.80	**0.008**
	New-shelled BCD+	RI 0	25	-0.060	0.776	1.34473		
	New-shelled BCD-	RI 1	41	-0.188	0.239	1.34860	-12.51	**0.000**
	New-shelled BCD+	RI 1	2	1	*	1.3415		
All Bays Female	New-shelled BCD- Females	RI 0	48	0.057	0.607	1.34706	-2.02	0.137
	New-shelled BCD+ Females	RI 0	4	0.036	0.964	1.34375		
All Bays Male	New-shelled BCD- Males	RI 0,1	86	**-0.348**	**0.001**	1.34699	-3.21	**0.003**
	New-shelled BCD+ Males	RI 0,1	23	-0.153	0.486	1.34462		
	New-shelled BCD- Males	RI 0	60	**-0.394**	**0.002**	1.34628	-1.71	0.094
	New-shelled BCD+ Males	RI 0	21	-0.199	0.387	1.34491		
	New-shelled BCD- Males	RI 1	26	-0.226	0.266	1.34862	-10.91	**0.000**
	New-shelled BCD+ Males	RI 1	2	1	*	1.3415		

4.3.6.6. HRI and Carapace Width in New-shelled Snow Crabs by BCD Status, Gender, and Bay in Snow Crabs with the Same Gut Wall RI Score

When the data by bay and strata were separated, no correlation was seen between HRI and carapace width in NDB new-shelled females. HRI and carapace width was negatively correlated for BCD- and BCD+ NDB new-shelled males with gut wall RI scores of 0 and 1 and gut wall RI scores of 0 (n = 2 and n = 1 for BCD- and BCD+ NDB male snow crabs with gut wall RI scores of 1). Similarly, HRI and carapace width were negatively correlated for BCD- and BCD+ WB snow crabs with gut wall RI scores of 0 and 1, gut wall RI score of 0, or gut wall RI score of 1 (n=1 for WB BCD+ new-shelled male with a gut wall RI score of 1). In WB 613 BCD- new-shelled males with a gut wall RI score of 0 had a negative correlation between HRI and carapace width (n=2 for BCD+). In WB 614/615 HRI and carapace width were positively correlated in BCD- new-shelled male snow crabs while negative correlation was seen in BCD+ new-shelled male snow crabs. Only a single BCD+ snow crab from each NDB and WB 614/615 was collected. The mean HRIs of new-shelled males with gut wall RI scores of 1 from these two regions were not statistically different from one another (two sample T-test: T-value = -1.14, DF = 1, p-value = 0.459). When the data from these two regions were combined there was positive correlation between HRI and carapace width. Differences between mean HRI of BCD- and BCD+ snow crabs with gut wall RI scores of 0 and 1, 0, or 1 were only observed in regions where BCD- snow crabs had positive correlations between HRI and carapace width. All BCD+ new-shelled males from all regions with gut wall RI scores of 0-1 had negative correlations between HRI and carapace width regardless of region of origin (Table 4.11).

Table 4.11. Summary of trends observed in HRI vs carapace width correlations seen in snow crabs of all shell conditions and RI scores by bay and BCD status. Pearson correlations with negative trends (red) and positive trends (green). Statistically significant correlations between HRI and carapace width are indicated in bold. Significant differences in mean HRI between BCD- and BCD+ snow crabs are also indicated in bold.

			n	HRI vs Carapace Width		HRI		
				Pearson correlation	Pearson correlation p-value	Mean	Two-sample T-test T-value	Two-sample T-test p-value
New-shelled NDB Females	BCD-	RI 0	29	0.057	0.768	1.34608	-1.40	0.255
	BCD+	RI 0	4	0.036	0.964	1.34375		
New-shelled NDB Males	BCD-	RI 0,1	13	-0.306	0.309	1.34480	-1.41	0.175
	BCD+	RI 0,1	10	-0.222	0.538	1.34285		
	BCD-	RI 0	11	-0.266	0.430	1.34452	-0.99	0.338
	BCD+	RI 0	9	-0.222	0.565	1.34299		
	BCD-	RI 1	2	-1	*	1.34635	*	*
	BCD+	RI 1	1	*	*	1.3416		
New-shelled WB Males	BCD-	RI 0,1	73	**-0.424**	**0.000**	1.34598	-1.68	0.108
	BCD+	RI 0,1	13	-0.208	0.496	1.34598		
	BCD-	RI 0	49	-0.476	0.001	1.34668	-0.39	0.703
	BCD+	RI 0	12	-0.365	0.244	1.34636		
	BCD-	RI 1	24	-0.361	0.083	1.348808	*	*
	BCD+	RI 1	1	*	*	1.3414		
New-shelled WB 613 Males	BCD-	RI 0	17	-0.389	0.122	1.34358	1.50	0.374
	BCD+	RI 0	2	1	*	1.34770[⊥]		
New-shelled WB614/615Males	BCD-	RI 0,1	51	0.132	0.354	1.34566	-3.70	**0.002**
	BCD+	RI 0,1	11	-0.235	0.487	1.34879		
	BCD-	RI 0	32	0.099	0.591	1.348333	-2.67	**0.015**
	BCD+	RI 0	10	-0.440	0.203	1.34609		
	BCD-	RI 1	19	0.132	0.354	1.34956	*	*
	BCD+	RI 1	1	*	*	1.3414		
New-shelled Males NDB & WB 614615[⊥]	BCD-	RI 1	21	0.169	0.463	1.34925	-12.05	**0.000**
	BCD+	RI 1	2	1	*	1.3415		

[⊥]Only a very small amount of hemolymph was extracted from one of these 2 snow crabs (the higher HRI value may be due to a sample collection error).

[⊥⊥]The mean HRI of BCD- new-shelled males with an RI score of 1 was not significantly different between snow crabs from NDB and WB (two sample T-test: T-value = -1.14, DF = 1, p-value = 0.459).

4.3.7. **General Linear Model**

BCD status was a statistically significant contributing factor in hemolymph refractive index (ANOVA F-value = 14.33, DF = 1, p-value = 0.000). The regression equation for HRI and BCD status was as follows:

HRI = 1.34593 + 0.001442 BCD Status_0 - 0.001442 BCD Status_1

where BCD Status_0 was BCD- and BCD Status_1 was BCD+. BCD status explained less than 5% of the variation in hemolymph refractive index (R^2 = 4.75%, R^2 (adj) = 4.42 %, R^2 (pred) = 3.64%).

When stratum (F-value = 22.69, p-value = 0.000), gut wall reserve inclusion score (F-value = 9.87, p-value = 0.000), BCD status (F-value = 4.24, p-value = 0.041), gender (F-value = 8.36, p-value = 0.004), shell condition (F-value = 3.19, p-value = 0.043), and carapace width (F-value = 0.01, p-value = 0.910), were included in the regression analysis, the contributing factors explained ~25% of the variation in hemolymph refractive index (R^2 = 27.47%, R^2 (adj) = 24.59 %, R^2(pred) = *). Carapace width was not a statistically significant contribution to the model. (Note: Optimal [geometric mean] transformation of carapace width did not alter its contribution to the model, F-value = 9.57, p-value = 0.933.)

When carapace width was removed from the model, the remaining factors of stratum (F-value = 24.76, p-value = 0.000), gender (F-value = 15.98, p-value = 0.000), gut wall reserve inclusion score (F-value = 9.91, p-value = 0.000), BCD status (F-value = 4.26, p-value = 0.040), and shell condition (F-value = 3.22, p-value = 0.041) still explained ~25% of the variation in hemolymph

refractive index (R^2 = 27.47%, R^2 (adj) = 24.86 %, R^2(pred) = *). The regression equation was as follows:

HRI = 1.34629 - 0.000983 Stratum_613 - 0.001166 Stratum_610611 + 0.002149 Stratum_614615
+ 0.001009 Gender_0 - 0.001009 Gender_1
- 0.002227 Gut Wall RI Score_0 - 0.000662 Gut Wall RI Score_1
- 0.000125 Gut Wall RI Score_2 + 0.001384 Gut Wall RI Score_3
+ 0.001630 Gut Wall RI Score_4
+ 0.000755 BCD Status_0 - 0.000755 BCD Status_1
+ 0.00158 Shell Condition_0 - 0.00053 Shell Condition_1 - 0.00106 Shell Condition_2

where the strata from WB (613 and 614/615) and NDB (610/611) were as listed, Gender_0 was female and Gender_1 was male, gut wall RI scores varied from 0 to 4, BCD Status_0 was BCD- and BCD Status_1 was BCD+, Shell Condition_0 was new-shelled, Shell Condition_1 was intermediate, and Shell Condition_2 was old-shelled (Figure 4.19).

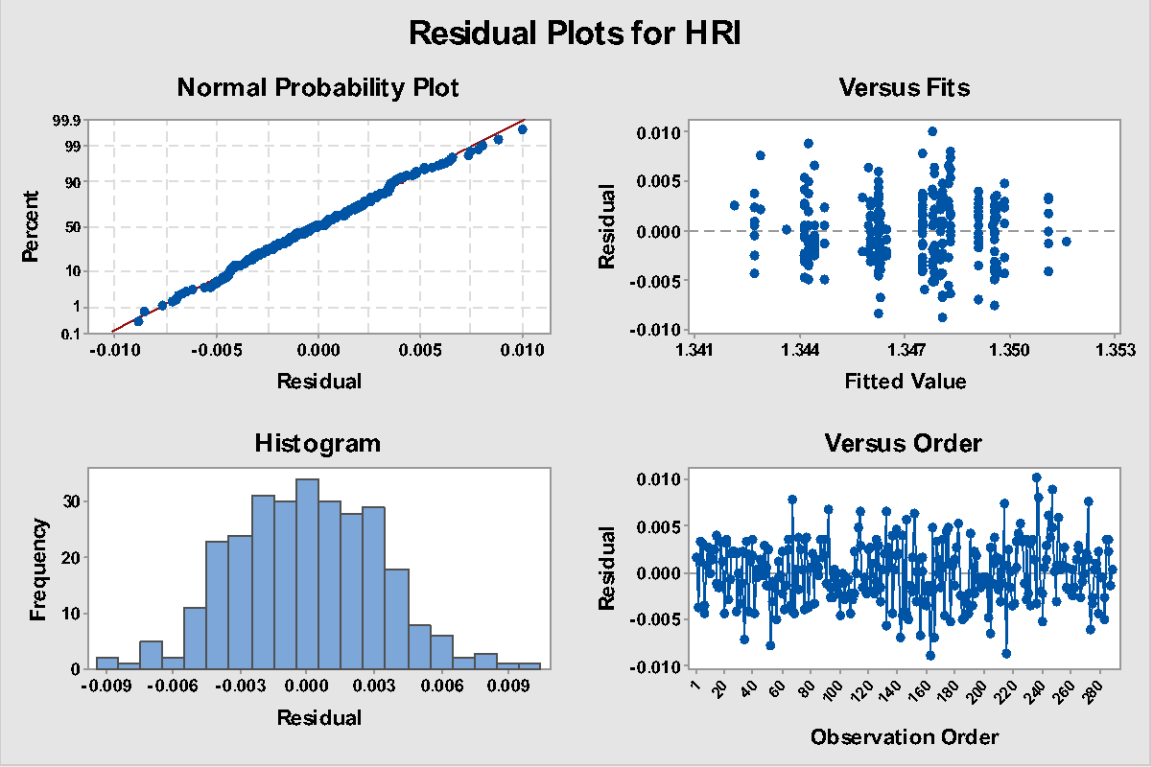

Figure 4.19. Residual plots for general linear model including stratum, gender, gut wall RI score, BCD status, and shell condition.

4.3.8. **Untargeted Metabolomics**

4.3.8.1. **Measured and Estimated HRIs of BCD- and BCD+ Hemolymph Samples**

The mean HRI in the pooled BCD- hemolymph population (n=35, mean = 1.349331 ± 0.000507 SEM) was significantly higher than the mean HRI in the pooled BCD+ hemolymph population (n=9, mean = 1.346189 ± 0.000638 SEM; two-sample T-test: T-value = 3.86, DF = 19, p-value = 0.001). When the volume of hemolymph from each contributing snow crab was considered, the approximate HRI of the BCD- pooled hemolymph sample was 1.349225 and the approximate HRI of the BCD+ pooled hemolymph sample was 1.346498. A sample from a single BCD+ snow crab (HRI = 1.3433) was also compared to the pooled BCD- and BCD+ samples. Hemolymph from this individual was also included in the pooled hemolymph sample (constituted 21.2% of the total pooled volume of BCD+ hemolymph).

4.3.8.2. **RI Scores of snow crabs contributing to BCD- and BCD+ Hemolymph Samples**

The snow crabs in the pooled BCD+ hemolymph sample had a significantly higher proportion of animals with a gut wall RI score of 0 than in the pooled BCD- hemolymph sample (Fisher Exact Test p-value = 0.000; Figure 4.20). No females contributed to the hemolymph in the BCD+ pooled sample. In contrast, six of the 35 snow crabs in the BCD- pooled hemolymph samples were female. On a population level this difference was not statistically significant (Fisher Exact Test p-value = 0.312). In addition, the BCD+ individual hemolymph sample was from a male snow crab.

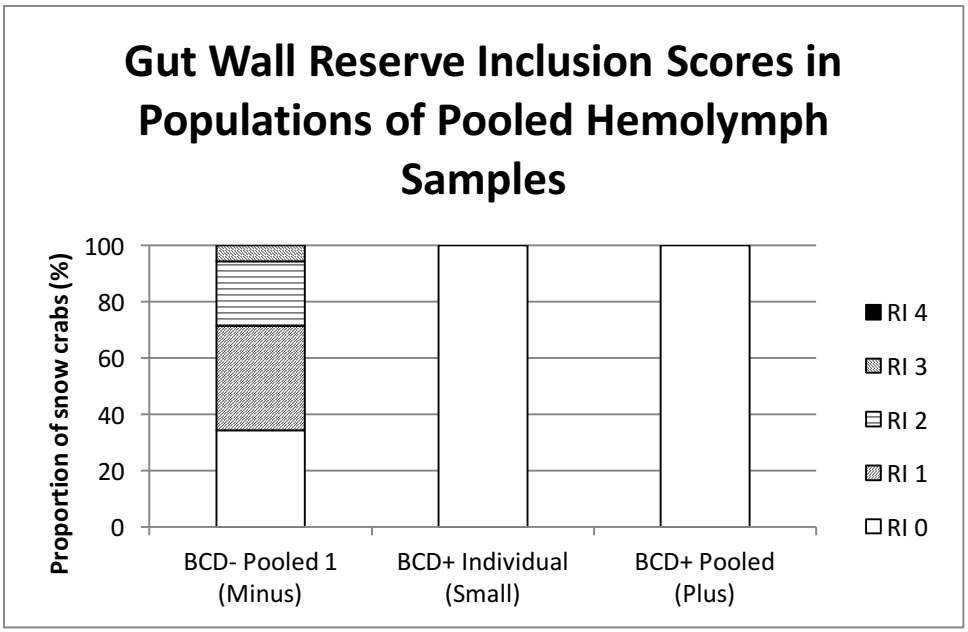

Figure 4.20. Gut wall reserve inclusion (RI) scores in pooled and individual hemolymph samples used for untargeted metabolomics.

4.3.8.3. **Comparison of BCD- and BCD+ Hemolymph Metabolites**

Untargeted metabolomics screening of the BCD+ and BCD- hemolymph samples revealed differences between the BCD- pooled (minus), BCD+ pooled (plus), and BCD+ individual (small) hemolymph samples (Figure 4.21). Evaluation of the aligned peak list generated by MZmine revealed 56 compounds which were present in both the pooled ("Plus") and individual snow crab ("Small") BCD+ pooled hemolymph samples (Figure 4.22). Fourteen of these 56 were also present in the BCD- pooled hemolymph ("Minus") sample (Table 4.12). Identification of peaks using online databases (http://www.lipidmaps.org, http://www.hmdb.ca, http://www.genome.jp/kegg/pathway.html) yielded tentative identifications 5/14 (35.7%) of the compounds in all snow crabs and 36/42 (81.0%) of the BCD-associated compounds (Table 4.13). Seven of the compounds appeared very similar (m/z ratio, retention time, and tentative compound IDs) despite being separated by MZmine data preprocessing and thus may represent

a single compound; this suggests that there were least 35 BCD-associated compounds (Table 4.14). Tentative identification of these compounds found possible compound matches for 29/35 (82.9%) of these BCD-associated compounds and the majority of the compounds were tentatively identified by LC-HRMS as phospholipids (Table 4.14 and Figure 4.23). Thorough evaluation of the BCD- pooled hemolymph ("Minus") peak list generated by MZmine confirmed that none of the 35 (42) BCD-associated compounds were present in the BCD- pooled hemolymph sample (Table 4.15).

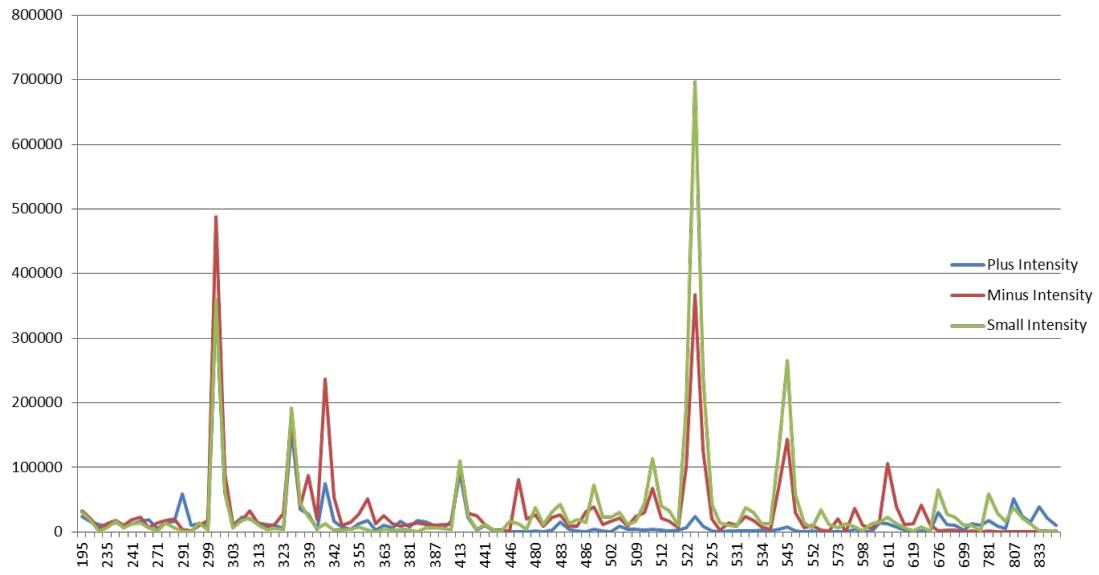

Figure 4.21. Chromatogram of base peak intensity by atomic mass unit (amu) for all three hemolymph samples: BCD+ pooled sample ("Plus" intensity), BCD – pooled sample ("Minus" intensity), and BCD+ individual crab hemolymph sample ("Small" intensity).

ID	Average		Identity	Peak shape	-MINUS-F4.mzXML			-PLUS-F4.mzXML			_SMALL-F4.mzXML		
	m/z	RT			Status	Height	Area	Status	Height	Area	Status	Height	Area
1	522.3554	3.9	LysoPC(18:1(11Z))			3.4E5	2.0E6		1.5E4	8.0E4		5.4E5	3.0E6
2	496.3396	3.8	LysoPC(16:0)			2.5E5	1.4E6		1.7E4	8.4E4		4.8E5	2.7E6
3	723.1846	5.0				2.4E5	9.4E5						
4	469.3650	7.4	24-hydroperoxy-24-vinylcholesterol			2.2E5	1.0E6		2.6E5	1.2E6		4.8E4	2.1E5
5	429.3723	7.4	Cholesteryl acetate			1.8E5	8.2E5		2.4E5	1.1E6		4.3E4	1.9E5
6	544.3370	3.9	PC(O-16:1(11Z)/2:0)			1.4E5	8.1E5					2.2E5	1.1E6
7	518.3214	3.8	PC(O-14:0/2:0)			1.0E5	5.3E5					1.9E5	1.0E6
8	341.1785	4.8				8.0E4	3.8E5		1.0E5	6.1E5		2.5E4	9.7E4
9	579.1653	5.0				7.2E4	2.7E5						
10	494.3239	3.6	PC(16:1(9E)/0:0)			7.0E4	4.3E5					8.7E4	5.1E5
11	341.2084	4.0	9-hydroxy-2Z,5E,7Z,11Z,14Z-Eicosapentaenoic acid			6.9E4	5.4E5		2.0E4	3.6E5			
12	550.3867	4.4	PC(O-18:1(10E)/2:0)			6.6E4	4.1E5					2.1E4	1.1E5
13	542.3238	3.5	PC(20:5(5Z,8Z,11Z,14Z,17Z)/0:0)			5.6E4	3.6E5					1.2E5	8.0E5
14	482.3604	3.9	PC(O-8:0/O-8:0)			4.8E4	2.4E5		1.4E4	7.0E4		6.8E4	3.3E5
15	347.1954	4.8				4.6E4	2.2E5		5.2E4	3.2E5		1.4E4	5.5E4
16	568.3396	3.7	LysoPC(22:6(4Z,7Z,10Z,13Z,16Z,19Z))			4.2E4	2.1E5					7.1E5	3.7E6
17	301.2156	4.2	8,11,14,18-Eicosatetraynoic acid			4.2E4	3.9E5		2.2E3	5.2E3			
18	718.2300	5.0				3.7E4	1.3E5						
19	524.3711	4.3	PC(O-16:0/2:0)			3.7E4	2.2E5					1.5E4	8.9E4
20	367.1943	5.0				3.6E4	1.5E5		8.5E4	4.6E5		2.1E4	8.1E4
21	367.2815	4.7	11,12-dihydroxy arachidic acid			3.6E4	1.4E5		1.1E5	4.6E5			
22	829.5575	8.7				3.5E4	7.4E5						
23	466.3291	4.4	PC(P-15:0/0:0)			3.5E4	1.7E5						
24	464.3131	4.0				3.4E4	1.6E5					2.2E4	1.1E5
25	226.2166	2.8				3.3E4	1.7E5		1.8E4	9.2E4		6.7E4	3.7E5

Figure 4.22. Image of a portion of the aligned peak list generated by MZmine 2. Note that some compounds were in the BCD- pooled hemolymph sample ("Minus"), BCD+ pooled hemolymph sample ("Plus"), and the BCD+ individual hemolymph sample ("Small"). Some compounds were present in 2 of the 3 samples, and other compounds were present in only 1 of the 3 hemolymph samples.

Table 4.12. Compounds that were found in all three hemolymph samples.

	Compound		Compound Peak Height		
	row m/z	**Tentative Identity***	**BCD– Pooled**	**BCD+ Pooled**	**BCD+ Individual**
1	**522.3554**	LysoPC (18:1(11Z)) (or other PCs)	339843.3929	15070.96	535708.3
2	**496.3396**	LysoPC(16:0) (or other PCs)	249070.3969	16562.76	480491.9
3	**469.3650**	24-hydroperoxy-24-vinylcholesterol (other sterol lipids)	221272.158	260999.2	47638.98
4	**429.3723**	Cholesteryl acetate (other sterol lipids, PGs, etc)	182999.1629	238281	43173.62
5	**341.1785**		80136.57589	102673.8	24692.45
6	**482.3604**	PC (O-8:0/O-8:0) or PC(O-16:0/0:0)	47991.10089	14276.07	67810.67
7	**347.1954**		46424.82712	51969.91	13671.28
8	**367.1943**		35975.72405	85385.4	21293.55
9	**226.2166**		33373.7125	18080.18	66977.61
10	**471.3653**		27340.58025	14082.54	70511.59
11	**373.2110**		26708.86652	52077.62	13760.28
12	**529.4073**		26426.34509	13166.24	64372.34
13	**362.2365**		25499.82377	54883.74	16426.4
14	**353.2606**		17919.60505	47812.87	6574.259

*Tentative compound identity was left blank if no match was found for the compound.
LysoPC = Lysophosphatidylcholine, PC = Phosphatidylcholine, PG = phosphatidylglycerol

Table 4.13. BCD-associated compounds.

	Compound		
	row m/z	**Tentative Identity**	**Example Formula (adduct)**
1	435.3441	MG(22:1(13Z)/0:0/0:0)	$C_{25}H_{48}O_4$ (M+Na)
2	407.3129	MG(20:1(11Z)/0:0/0:0)	$C_{23}H_{44}O_4$ (M+Na)
3	379.2815	MG(0:0/18:1(9Z)/0:0)	$C_{21}H_{40}O_4$ (M+Na)
4	635.4648	DG(18:4(6Z,9Z,12Z,15Z)/20:5(5Z,8Z,11Z,14Z,17Z)/0:0)[iso2] Or PA(12:0/19:0) (or other PAs)	$C_{41}H_{62}O_5$ (M+H)
5	637.4807	DG(18:3(9Z,12Z,15Z)/20:5(5Z,8Z, 11Z,14Z,17Z)0:0)[iso2] (or other DGs)	$C_{41}H_{64}O_5$ (M+H)
6	351.2504	MG(16:1(9Z)0:0/0:0)	$C_{19}H_{36}O_4$ (M+Na)
7	788.5613	1(6-[3]-ladderane-hexanoyl)-2-(8-[3]-ladderane-octanyl)-sn-glycerophosphocholine	$C_{46}H_{78}NO_7P$ (M+H)
8	430.3800		
9	856.5772	LacCer(d18:0/14:0)	$C_{44}H_{83}NO_{13}$ (M+Na)
10	399.2504	MG(20:5(5Z, 8Z, 11Z, 14Z,17Z)0:0/0:0)	$C_{23}H_{36}O_4$ (M+Na)
11	637.4807	DG(18:3(9Z,12Z,15Z)/20:5(5Z,8Z,14Z,17Z)0:0)[iso2] (or other DGs)	$C_{41}H_{64}O_5$ (M+H)
12	816.5530	PC(17:2(9Z,12Z)/22:6(4Z,7Z,10Z,13Z,16Z,19Z)) (or other PCs or PEs)	$C_{47}H_{78}NO_8P$ (M+H)
13	425.2659	PA(17:0/0:0)	$C_{20}H_{41}NO_7P$ (M+H)
14	609.4489	DG(18:4(6Z,9Z,12Z,15Z)/18:4(6Z,9Z,12Z,15Z)0:0)	$C_{39}H_{60}O_5$ (M+H)
15	613.4829	DG(18:3(9Z,12Z,15Z)/18:3(9Z,12Z,15Z)0:0) (or other DGs)	$C_{39}H_{64}O_5$ (M+H)
16	816.5509	PC(17:2(9Z,12Z)/22:6(4Z,7Z,10Z, 13Z,16Z,19Z)) (or other PCs or PEs)	$C_{47}H_{78}NO_8P$ (M+H)
17	683.4648	PA(13:0/22:4(7Z,10Z,13Z,16Z) (or other PAs)	$C_{38}H_{67}O_8P$ (M+H)
18	709.4810	1-tetradecanoyl-2-hexadecanoyl-sn-glycero-3-phosphosulfocholine (or PAs or DGs)	$C_{37}H_{73}NO_8PS$ (M+H)
19	860.6198	PC(20:1(11Z)/22:6(4Z,7Z,10Z,13Z,16Z,19Z)) (or other PCs)	$C_{50}H_{86}NO_8P$ (M+H)
20	595.4722	5-methyl-3-{12-[3-(2-{3-[(3Z)-tetradec-3-en-1-yl]oxiran-2-yl}ethyl)oxiran-2-yl]dodecyl}-2,5-dihydrofuran-2-one	$C_{37}H_{64}O_4$ (M+Na)
21	781.5572		
22	597.4876	3-[(15Z,19Z)-11,12-dihydroxydotriaconta-15,19-dien-1-yl]-5-methyl-2,5-dihydrofuran-2-one	$C_{37}H_{66}O_4$ (M+Na)
23	729.5922	SM(d18:1/18:1(9Z)) (or other SMs and PE-Cers)	$C_{41}H_{81}N_2O_6P$ (M+H)
24	339.2890	Glycidyl oleate (glycidyl octadecenoate)	$C_{21}H_{38}O_3$ (M+H)
25	792.5977	GlcCer(d14:1(4E)/24:1(15Z)(2OH))	$C_{44}H_{83}NO_9$ (M+Na)
26	882.6023	PC(22:4(7Z,10Z,13Z,16Z)/22:6(4Z,7Z,10Z,13Z,16Z,19Z)) or PC(22:6(4Z,7Z,10Z,13Z,16Z,19Z)/22:4(7Z,10Z,13Z,16Z))	$C_{52}H_{84}NO_8P$ (M+H)
27	820.5870	PC(17:0/22:6(4Z,7Z,10Z,13Z,16Z,19Z)) (or other PCs or PEs)	$C_{47}H_{82}NO_8P$ (M+H)
28	834.5962	PC(18:0/22:6(4Z,7Z,10Z,13Z,16Z,19Z)) (or other PCs or PEs)	$C_{48}H_{84}NO_8P$ (M+H)

29	828.5554	PC(18:3(6Z,9Z, 12Z)/22:6(4Z,7Z,10Z,13Z,16Z,19Z))	$C_{87}H_{78}NO_8P$ (M+H)
30	828.5548	PC(18:3(6Z,9Z, 12Z)/22:6(4Z,7Z,10Z,13Z,16Z,19Z))	$C_{87}H_{78}NO_8P$ (M+H)
31	832.5875	PC(18:1(11Z)/22:6(4Z,7Z,10Z,13Z,16Z,19Z))	$C_{48}H_{82}NO_8P$ (M+H)
32	807.5764		
33	856.5775	LacCer(d18:0/14:0)	$C_{44}H_{83}NO_{13}$ (M+Na)
34	832.5876	PC(18:1(11Z)/22:6(4Z,7Z,10Z,13Z,16Z,19Z))	$C_{48}H_{82}NO_8P$ (M+H)
35	649.5196	1-(8-[5]-ladderane-octanoyl)-2-(8-[3]ladderane-octanyl)-sn-glycerol	$C_{43}H_{70}O_3$ (M+H)
36	822.6064		
37	804.5530	PC(16:1(9Z)/22:6(4Z,7Z,10Z,13Z,16Z,19Z))	$C_{46}H_{78}NO_8P$ (M+H)
38	755.5407		
39	810.6012	PC(16:0/22:4(7Z,10Z,13Z,16Z))	$C_{46}H_{84}NO_8P$ (M+H)
40	795.5762		
41	729.5923	SM(d18:1/18:1(9Z)	$C_{41}H_{81}N_2O_6P$ (M+H)
42	729.5925	SM(d18:1/18:1(9Z)	$C_{41}H_{81}N_2O_6P$ (M+H)

DG = Diacylglycerol, LacCer = lactosylceramide, GlcCer = glucosylceramide, MG = monoacylglycerol PA = phosphatidic acid, PC = Phosphatidylcholine, PE = Phosphatidylethanolamine; SM = Sphingomyelin.

Table 4.14. BCD-associated compounds organized by m/z ratio with compounds with possible reduplication (indicated in bold).

	Row ID	m/z	Retention Time	PLUS-F4.mzXML Peak m/z	SMALL-F4.mzXML Peak m/z	Compound Category
1	322	339.2890	7.793283	339.289	339.2889	
2	193	351.2504	4.651692	351.2504	351.2503	Monoacylglycerol (MG)
3	187	379.2815	5.148408	379.2815	379.2816	Monoacylglycerol (MG)
4	201	399.2504	4.469567	399.2505	399.2503	Monoacylglycerol (MG)
5	186	407.3129	5.621408	407.313	407.3128	Monoacylglycerol (MG)
6	215	425.2659	4.676533	425.266	425.2658	Monoacylglycerol phosphate (PA)
7	197	430.3800	5.28915	430.38	430.38	
8	185	435.3441	6.213258	435.3441	435.344	Monoacylglycerol (MG)
9	283	595.4722	8.414175	595.4721	595.4722	Fatty alcohol
10	294	597.4876	7.255175	597.4873	597.488	Fatty alcohol
11	239	609.4489	8.323108	609.449	609.4488	Diacylglycerol (DG)
12	242	613.4829	8.414175	613.4827	613.483	Diacylglycerol (DG)
13	188	635.4648	8.414175	635.4649	635.4648	Diacylglycerol (DG) or Diacylglycerolphosphate (PA)
14	**189**	**637.4807**	**7.259308**	**637.4808**	**637.4807**	**Diacylglycerol (DG)**
	204	**637.4807**	**7.768442**	**637.4807**	**637.4807**	
15	398	649.5196	8.40175	649.5194	649.5197	Diradylglycerol (glycerolipid)

16	276	683.4648	7.321392	683.4646	683.465	Diacylglycerolphosphate (PA)
17	277	709.4810	7.6484	709.481	709.4811	Diacylglycerolphosphate (PA)
18	**320**	**729.5922**	**8.778433**	**729.5923**	**729.592**	**Ceramide phosphocholine (SM)**
	450	**729.5923**	**8.550775**	**729.5923**	**729.5923**	
	464	**729.5925**	**8.600442**	**729.5923**	**729.5926**	
19	430	755.5407	8.542492	755.5407	755.5406	
20	286	781.5572	7.039925	781.5573	781.557	
21	196	788.5613	5.944275	788.5609	788.5616	Glycerophosphocholine (PC)
22	328	792.5977	5.600717	792.5953	792.6	Neutral glycosphingolipid
23	443	795.5762	4.631	795.5761	795.5764	
24	423	804.5530	6.532058	804.5511	804.5548	Glycerophosphocholine (PC)
25	377	807.5764	3.976992	807.5765	807.5763	
26	435	810.6012	5.355375	810.6025	810.5999	Glycerophosphocholine (PC)
27	**261**	**816.5509**	**5.065625**	**816.5469**	**816.5548**	**Glycerophosphocholine (PC) or Phosphoethanolamine (PE)**
	206	**816.5530**	**5.464775**	**816.551**	**816.5551**	
28	350	820.5870	6.47805	820.5851	820.5889	Glycerophosphocholine (PC) or Phosphoethanolamine (PE)
29	411	822.6064	5.301567	822.6038	822.609	
30	**367**	**828.5548**	**6.456292**	**828.5543**	**828.5553**	**Glycerophosphocholine (PC)**
	361	**828.5554**	**6.369542**	**828.5537**	**828.557**	
31	**376**	**832.5875**	**6.7419**	**832.5872**	**832.5878**	**Glycerophosphocholine (PC)**
	390	**832.5876**	**6.770875**	**832.5874**	**832.5879**	
32	352	834.5962	5.642108	834.5969	834.5955	Glycerophosphocholine (PC) or Phosphoethanolamine (PE)
33	**198**	**856.5772**	5.456992	**856.5774**	**856.577**	**Neutral glycosphingolipid**
	388	**856.5775**	4.94145	**856.5782**	**856.5767**	
34	282	860.6198	8.728767	860.6207	860.619	Diacylgycerolphosphocholine (PC)
35	336	882.6023	8.745317	882.6032	882.6014	Diacylgycerolphosphocholine (PC)

DG = Diacylglycerol , PA = phosphatidic acid, PC = Phosphatidylcholine, PE = Phosphatidylethanolamine; SM = Sphingomyelin.

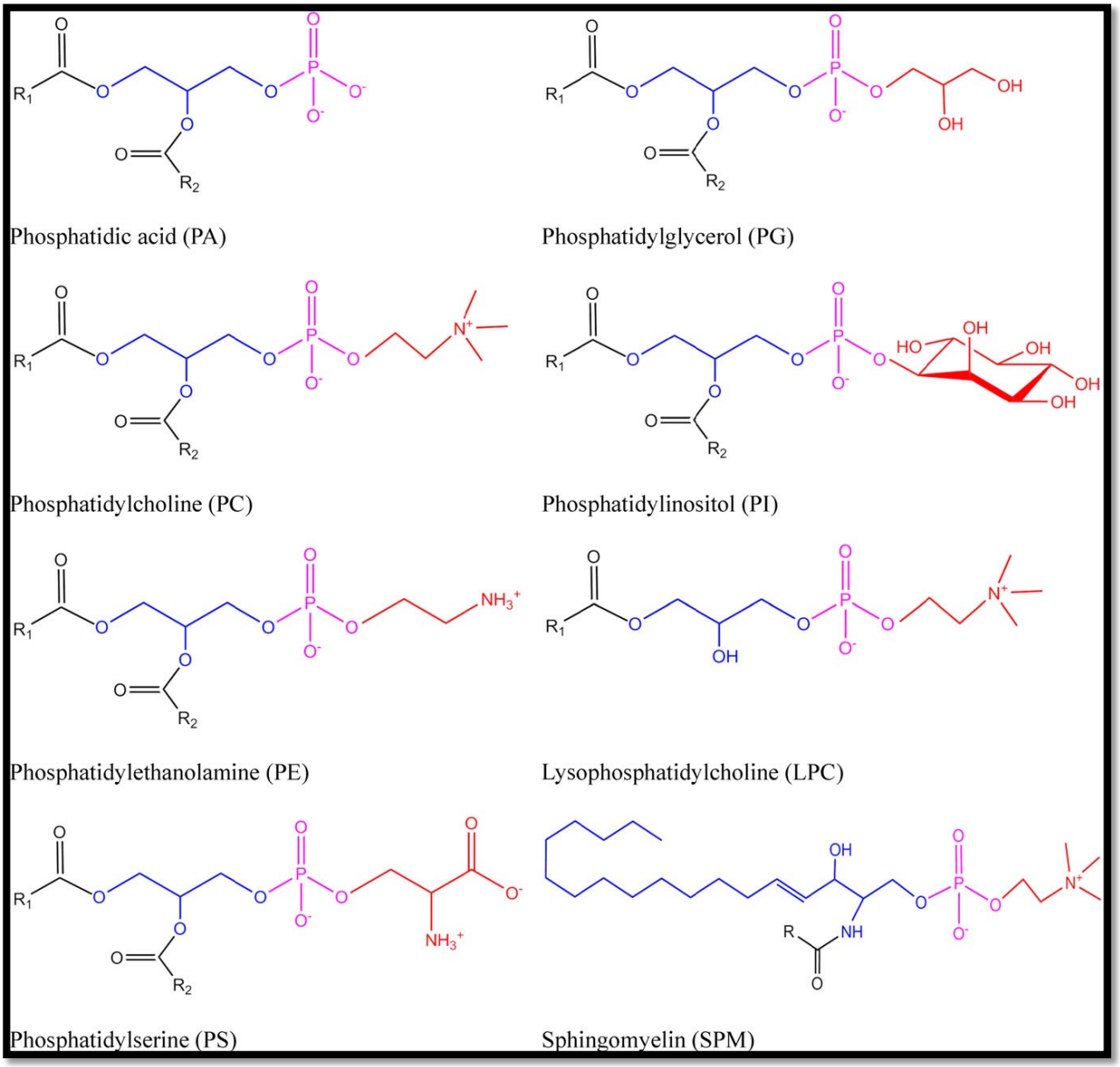

Figure 4.23. Phospholipid structures (from Cui and Decker 2016).

Table 4.15. BCD-associated compounds compared to similar compounds found in the pooled hemolymph sample from snow crabs without BCD ("Minus"). Any compounds within 1 atomic mass unit (amu) of the BCD-associated compounds identified in the BCD- pooled hemolymph sample were listed. Note that no compounds within 0.005 *m/z* of the BCD association compounds were found within the pooled hemolymph sample from BCD- snow crabs.

		BCD-associated compounds				MINUS-F4.mzXML	
	Row ID	**m/z**	**Retention Time**	**PLUS-F4.mzXML Peak m/z**	**SMALL-F4.mzXML Peak m/z**	**Retention time**	**MINUS-F4.mzXML Peak m/z**
1	322	339.2890	7.793283	339.289	339.2889	3.989433	339.1926
						5.363667	339.2868
						3.906633	339.2888
2	193	351.2504	4.651692	351.2504	351.2503		
3	187	379.2815	5.148408	379.2815	379.2816		
4	201	399.2504	4.469567	399.2505	399.2503		
5	186	407.3129	5.621408	407.313	407.3128		
6	215	425.2659	4.676533	425.266	425.2658		
7	197	430.3800	5.28915	430.38	430.38	7.68995	429.3723
						7.4002	429.3724
8	185	435.3441	6.213258	435.3441	435.344		
9	283	595.4722	8.414175	595.4721	595.4722	3.972867	596.3556
10	294	597.4876	7.255175	597.4873	597.488		
11	239	609.4489	8.323108	609.449	609.4488	3.989433	610.3712
12	242	613.4829	8.414175	613.4827	613.483		
13	188	635.4648	8.414175	635.4649	635.4648	4.072217	636.354
14	189	637.4807	7.259308	637.4808	637.4807		
	204	637.4807	7.768442	637.4807	637.4807		
15	398	649.5196	8.40175	649.5194	649.5197		
16	276	683.4648	7.321392	683.4646	683.465		
17	277	709.4810	7.6484	709.481	709.4811		
18	320	729.5922	8.778433	729.5923	729.592	8.410183	730.5392
	450	729.5923	8.550775	729.5923	729.5923		
	464	729.5925	8.600442	729.5923	729.5926		
19	430	755.5407	8.542492	755.5407	755.5406	8.451583	754.5320
						8.054217	754.5397
20	286	781.5572	7.039925	781.5573	781.557		
21	196	788.5613	5.944275	788.5609	788.5616		
22	328	792.5977	5.600717	792.5953	792.6		
23	443	795.5762	4.631	795.5761	795.5764	6.928317	796.5508
						6.886933	796.5510
						6.804133	796.5514
24	423	804.5530	6.532058	804.5511	804.5548	8.782717	805.5569
						8.724767	805.5573

						6.14185	805.5611
25	377	807.5764	3.976992	807.5765	807.5763	8.029383	808.5862
26	435	810.6012	5.355375	810.6025	810.5999		
27	261	816.5509	5.065625	816.5469	816.5548		
	206	816.5530	5.464775	816.551	816.5551		
28	350	820.5870	6.47805	820.5851	820.5889		
29	411	822.6064	5.301567	822.6038	822.609	7.706517	822.566
						7.408483	822.5674
						7.623717	822.5674
						7.2843	822.5679
30	367	828.5548	6.456292	828.5543	828.5553	8.724767	829.5575
	361	828.5554	6.369542	828.5537	828.557		
31	376	832.5875	6.7419	832.5872	832.5878		
	390	832.5876	6.770875	832.5874	832.5879		
32	352	834.5962	5.642108	834.5969	834.5955	6.406767	834.5276
						5.910067	834.5294
						5.463017	834.5306
33	198	856.5772	5.456992	856.5774	856.577		
	388	856.5775	4.94145	856.5782	856.5767		
34	282	860.6198	8.728767	860.6207	860.619	6.679967	860.5428
						6.853817	860.5432
						5.711367	860.5440
						5.645133	860.5449
						5.463017	860.5450
						5.595467	860.5451
35	336	882.6023	8.745317	882.6032	882.6014		

4.4. **Discussion**

Reserve inclusion (RI) cells are large (up to 45 µm diameter) conspicuous cells with abundant amounts of brightly eosinophilic intracytoplasmic material ("inclusions") which are located within the spongy connective tissues of the body of decapod crustaceans (Johnson 1980). RI cells are thought to function in the synthesis and storage of hemocyanin, glycogen, and protein (Johnson 1980). The distribution of RI cells within decapod crustacean connective tissues varies between species (see Appendix 6). RI cells are described as lost or effete in crustaceans with BCD including edible crabs *Cancer pagurus,* blue crabs *Callinectes sapidus,* Norway lobsters

Nephrops norvegicus, and snow crabs *Chionoecetes opilio* and edible crabs *Cancer pagurus* (Stentiford et al 2000, Stentiford et al 2002, Wheeler et al 2007). Spongy connective tissue is a major site of glycogen storage, with glycogen normally being abundant in this tissue except in starving or diseased crabs (Johnson 1980). A reduction and loss of spongy connective tissue in association with BCD has been reported in Norway lobsters *Nephrops norvegicus,* snow crabs *Chionoecetes opilio*, edible crabs *Cancer pagurus,* tropical mud crabs *Scylla serrata,* and white ridgeback prawn *Exopalaemon carinicauda* (Field and Appleton 1995, Stentiford et al 2002, Li et al 2008, Wheeler et al 2007, Xu et al 2010).

In this study, Bitter Crab Disease (BCD) is associated with a reduction in gut wall RI score in all snow crabs when analyzed by gender or region of origin. This reduction in glycogen reserves is statistically significant in most groups examined; however, the difference was not statistically significant when small sample sizes of BCD+ snow crabs were examined (BCD+ new-shelled females, n=4; BCD+ new-shelled males from WB, n=2). RI scores were typically absent in BCD+ snow crabs (26/28 snow crabs) and when present were scarce (2/28). This association of BCD with a low RI score (i.e., low body condition score) may indicate that BCD infection is associated with a reduction of RI cells in snow crabs (i.e., a loss of body glycogen reserves). This is consistent with previous reports of significant reductions in glycogen in infected crustaceans (Love et al 1996, Stentiford et al 2000, 2001, Shields et al 2003). In snow crabs *Chionoecetes opilio* glycogen was depleted by 50%, and in Norway lobsters *Nephrops norvegicus* glycogen in abdominal musculature was reduced by up to 85% and was correlated with parasite burden (Stentiford et al 2000, Shields et al 2003, Stentiford and Shields 2005). In blue crabs *Callinectes*

sapidus males were more depleted than females with tissue glycogen depletion of 50% in females and 70% in males (Shields et al 2003). This decrease in glycogen reserves in BCD-infected crustaceans most likely occurs due to metabolic demands associated with the parasitic infection. Alternatively, crustaceans with low glycogen stores (i.e., poor body conditions) may be predisposed to development of the disease. Glycogen stores were required for maintenance of activity of the prophenoloxidase (proPO) system in amphipods *Gammarus pulex*; the mechanism of action of such glycogen-related immune system impairment is not clear (Cornet et al 2009).

The involvement of proteins in crustacean immune system function is more well-defined. Proteins involved in recognizing foreign glucans include lipopolysaccharide binding protein (LPSBP) and beta-glucan binding protein (BGBP), antimicrobial proteins (such as penaeidins) produced by hemocytes (which are active against gram-positive bacteria), clotting proteins (involved in engulfing foreign invading organisms and preventing hemolymph loss upon wounding), and protein regulators of the proPO system (the proPO activating proteinase cascade, zymogenic serine proteinases, serine proteinase homologs, and pattern recognition proteins; Rosas et al 2004, Cerenius et al 2008, Amparyup et al 2013).

Hemolymph refractive index (HRI) is often assumed to be directly proportional to hemolymph protein levels in crustaceans, and thus is often used as an indicator of nutritional condition with significant reductions in HRI reported in starved crustaceans (Moore et al 2000, Behringer et al 2008). HRI decreases also occur in association with some crustacean diseases. In bumper car

disease (caused by the ciliate *Anophryoides haemophila)* in American lobster there is a decrease in hemolymph refractive index in the presence of parasitemia with moderate to high hemolymph parasite loads (Greenwood et al 2005). Hemolymph of lobsters that are heavily infected with *Anophryoides haemophila* is not cloudy in appearance but can appear scintillating (Greenwood et al 2005). Caribbean spiny lobsters (*Panulirus argus*) infected with *P. argus* Virus 1 (PaV1) have cloudy hemolymph which is macroscopically similar to hemolymph of crustaceans with *Hematodinium* infection (Montgomery-Fullerton et al 2007). This cloudy nature of the hemolymph in PaV1 infection is most likely due to a combination of free virus particles and lytic cellular debris (Shields and Behringer, 2004). Caribbean spiny lobsters with PaV1 infection also have a reduction in hemolymph refractive index that was interpreted as an indicator of reduced nutritional condition and therefore poor physiological condition (Behringer et al 2008).

Infected snow crabs have lower RI scores (glycogen stores) and lower hemolymph protein levels than uninfected snow crabs. This lack of glycogen reserves indicates that these snow crabs were in a state of negative energy balance (i.e., were starving). Such a negative energy balance may be within the normal physiologic range of new-shelled animals because they do not eat for several weeks before and after molting (O'Halloran and O'Dor 1988). This normal physiologic state in new-shelled animals may be masking the negative metabolic effects of BCD in these new-shelled animals. The mean HRI of BCD+ snow crabs with a gut wall RI of 1 or 2 was lower than the mean HRI of BCD- snow crabs with the same gut wall RI. This suggests that BCD infection can be associated with significant reduction of hemolymph proteins/lipoproteins prior

to complete resorption of glycogen stores. However, the presence of the parasites themselves may result in an alteration of the HRI of BCD-infected snow crabs. The shape and size of cells and their intracytoplasmic vacuoles also affect their light scattering properties, indicating that the parasites themselves may also have directly altered the HRI of diseased crabs (Johnsen and Widder 1999). Evaluation of the refractive index of plasma (rather than whole hemolymph) would help to clarify this issue. Furthermore, evaluation of plasma osmolarity/osmolality may also be helpful to determine the effect of parasitemia on host osmotic regulation.

In 2011 some shipping mortality deaths were included in the study. Evaluation of HRI of these uninfected shipping mortalities revealed that the average HRI of dead BCD- animals was not significantly different from the average HRI of animals who were alive during hemolymph collection. In general, the average HRI of dead animals tended to be higher than the average HRI in hemolymph collected from live animals. This slight increase in HRI may have been due to increased hemolymph proteins secondary to post mortem proteolysis: early in the post-mortem process hepatopancreatic autolysis results in release of digestive proteases and rapid proteolysis of myofibrillar proteins (Neil 2012). This indicates that the decrease in BCD+ hemolymph refractive index was not simply due to crab death.

In uninfected snow crabs HRI tended to be positively correlated with carapace width when snow crabs had high RI scores (i.e., were in good body condition) but had no correlation with size or was negatively correlated with size when the snow crab had low RI scores (i.e., were in poor body condition; see Appendix 7). BCD is associated with a loss in body glycogen reserves

and a decrease in mean HRI. BCD was also associated with reductions in the correlation coefficient between HRI and carapace width in all examined groups. This held true when snow crabs with RI scores of 0 without and with BCD are compared. This further supports the suggestion that BCD-infected snow crabs are in poorer nutritional condition than starving snow crabs without BCD.

Metabolomic analysis of pooled snow crab hemolymph revealed a selection of BCD-associated phospholipids that were not present in pooled hemolymph from snow crabs without *Hematodinium* sp. infection. Lipids are essential components of membranes (phospholipids, cholesterol), act as hormones (ecdysone) and antioxidants (tocopherol, pigments), aid in buoyancy (neutral lipids), and storage lipids provide energy for reproduction, escaping predation, migration, and starvation (Lee et al 2006). A recent study examining metabolite profiles of starved *Diporeia* spp. (a Holarctic benthic amphipod) showed that during periods of starvation the macroinvertebrates relied predominantly on glycerophospholipid metabolism and protein-based catabolism for energy production (Maity et al 2012). Whole body lipid decreased by about 50% after 5 days of starvation in penaeid prawns (*Penaeus monodon, P. esculentus and P. semisulcatus*) indicating that these adult crustaceans use stored lipid as an energy source during periods of starvation (Moore et al 2000). Crustaceans can use protein, carbohydrates, or lipids as an energy source during starvation (Sanchez-Paz et al 2006). In some species carbohydrate stores (mainly glycogen) are used first, then lipids and finally protein. In others, glycogen contributes little energy during food deprivation, the metabolic stores being predominantly lipids, proteins, or both. Moreover, some species switch from one stored

metabolite to another as prolonged starvation progresses (reviewed in Hervant et al 1996). Among crustaceans neutral lipids (mainly triglycerides, TG) are preferentially catabolized during starvation while polar lipids (phospholipids and cholesterol) are conserved due to their role as structural components of cell membranes (Heath and Barnes 1970, Fraser 1989, Stuck et al 1996). Triacylglycerol (TAG) is the major depot or storage lipid in animal cells (Lee et al 2006). TAG is catabolized during the early stages of larval development of the American lobster *Homarus americanus* until the energetic demands of growth and metabolism are met from exogenous sources (Fraser 1989). In later stages of larval development (stages IV and V) there is an increased dependence on protein catabolism for energy (Sasaki et al 1986). Instead, lipids serve a storage function with similar patterns seen in adult American lobsters and TAG is catabolized under starvation conditions (Sasaki 1984, Sasaki et al 1986). These findings suggest that the BCD-associated phospholipids may represent metabolites associated with glycerophospholipid metabolism secondary to starvation associated with BCD infection.

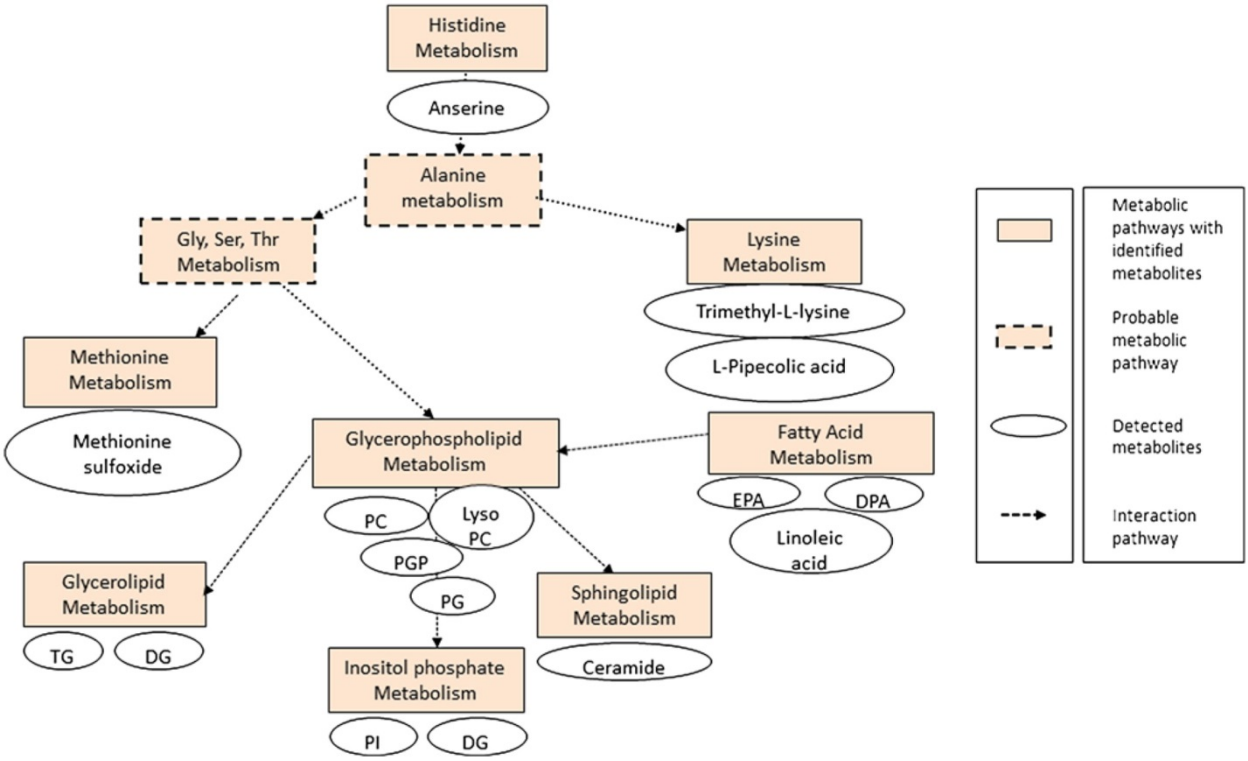

Figure 4.29. Metabolite pathways affected during starvation constructed using canonical biochemical pathways from KEGG. DG = diacylglycerol; DPA = docosapentaenoic acid; EPA = eicosapentaenoic acid; Gly = glycerine; LysoPC = lysophosphatidylcholine; PC = phosphatidylcholine; PG = phosphatidylglycerol; PGP = phosphatidylglycerolphosphate; PI = phosphatidylinositol; Ser = serine; TG = triacylglycerols; Thr = threonine (from Maity et al 2012).

Parasitic acquisition and modification of host lipids may also be contributing to the presence of these BCD-associated lipid metabolites in the hemolymph. Lipids are the main structural elements of biological membranes, serve as signaling molecules within and between cells, and represent a highly efficient store and source of energy and reduction power (Ramakrishnan et al 2013). Lipids are used by pathogens as food or structural building blocks and are also important virulence factors that allow the pathogen to evade immune responses, manipulate host processes, and cause disease (Ramakrishnan et al 2013). Pathogen-derived bioactive lipids can also mediate immune suppression, as is seen with phenolic glycolipids and

lipoarabinomannan in *Mycobacterium tuberculosis* (Ehrt and Schnappinger 2007, Brodsky and Medzhitov 2009). Bioactive lipids are also thought to modulate disease progress in *Trypanosoma cruzi* infections (Machado et al 2011).

Successful replication of protozoan parasites depends on acquiring extracellular and intracellular components from their host or synthesizing them from host-derived precursors (Lund and Chu 2002). As a parasitic infection progresses the total surface area of parasites increases, thus parasites must be able to acquire phospholipids for new cell membranes. Some parasitic protozoans (e.g., *Giardia lamblia, Trichomonas vaginalis, Toxoplasma gondii,* and *Pneumocystis carnii*) rely on their host to provide them with pre-formed phospholipids (Jarroll et al 1989, Smith 1993, Lujan et al 1996, Stevens et al 1997, Kaneshiro 1998, Das et al 2002, Yichoy et al 2011). Other parasitic protozoans (e.g., *Perkinsus marinus, Trypanosoma brucei, Plasmodium knowlesi, Plasmodium falciparum,* and *Leishmania* spp.) can synthesize phospholipids from host-derived precursors (Ancelin and Vial 1986, Smith 1993, Rifkin et al 1995, Lund and Chu 2002). The bloodstream form of *Trypanosoma brucei* acquires most of its lipid precursors from circulating host lipoproteins (van Hellemond and Tielens 2006). Phosphatidylcholine (PC) is the most abundant phospholipid class in many parasitic protozoa including *Trypanosoma* spp. (45-60%), *Leishmania* spp. (30-50%), *Plasmodium* spp. (40-50%), *Toxoplasma gondii* (62%) (Oliveira et al 1977, Beach et al 1979, Wassef et al 1985, Foussard et al 1991, Dechamps et al 2010, Smith and Butikofer 2010). The total phospholipid composition of the bloodstream form of *Trypanosoma brucei* consists primarily of PC and phosphatidylethanolamine (PE), while phosphatidylinositol (PI), Phosphatidylserine (PS), and

cardiolipin (CL) represent minor glycerophospholipid classes in the parasite (Smith and Butikofer 2010). In addition *T. brucei* contain substantial amounts of sphingophospholipids (Smith and Butikofer 2010). The composition of polar lipids in *P. marinus* was predominated by 50% PC, 25% PE, 10% PS/PI, 10% CL and 5% sphingomyelin (Lund and Chu 2002). The phospholipids associated with BCD were predominated by PC and PE, suggesting that the BCD-associated phospholipids may represent parasite-derived phospholipids synthesized from host-derived precursors.

Post-mortem oxidation of host and/or parasitic TAGs and phospholipids may also have contributed to the generation of the BCD-associated metabolites. Phospholipids in muscle are very susceptible to post-mortem lipid oxidation because they are highly unsaturated and within membranes which have a very high surface area (Cui and Decker 2016). Oxidation in meats leads to negative impacts on flavor with increases in "off-flavor" as the ratio of phospholipids to total lipids increases (Wilson et al 1976). Oxidized PCs have been associated with the off-flavor of turkey meat and the bitter taste of soybeans (Sessa et al 1976, Wu and Sheldon 1988). Oxidized PEs, rather than PCs, were thought to be responsible for "off-flavor" from beef and chicken meat (Igene and Pearson 1979). In several hosts, including Tanner crabs *Chionoecetes bairdi,* snow crabs *Chionoecetes opilio,* edible crab *Cancer pagurus*, Norway lobsters *Nephrops norvegicus*, and red and blue king crabs *Paralithodes* spp., anecdotal reports indicate that the disease is associated with a bitter, astringent, or aspirin-like taste of infected meat rendering the product unmarketable (Meyers et al 1987, Love et al 1996, Stentiford et al 2000, Ryazanova 2008, Ryazanova *et al.* 2010). The BCD-associated phospholipids, which include PCs and PEs,

may contribute to the bitter taste reported in this disease. Numerous chemically diverse compounds elicit bitter taste (including hydroxyl fatty acids, fatty acids, amino acids, peptides, amines, azacycloalkanes, N-heterocyclic compounds, amides, ureas, thioureas, carbamides, esters, lactones, carbonyl compounds, phenols and polyphenols, crown ethers, alkaloids, flavonoids and terpenes, methylxanthines, sulfimides, organic and inorganic salts, and metal ions) and thus other bitter tastants may also contribute to the bitter taste of affected snow crabs (Drenowski and Gomez-Carneros 2000, Drenowski 2001, Meyerhof 2005, Maehashi and Huang 2009). For example, alterations in hemolymph free amino acid composition and skeletal muscular free amino acid composition were reported in *Hematodinium*-infected Norway lobsters *Nephrops norvegicus* may affect their flavor (Stentiford et al 1999, 2000). The essential taste components in snow crabs have been listed as a combination of amino acids (alanine, arginine, glutamate, and glycine), nucleic acid-related substances (adenylic acid and guanylic acid), and minerals (sodium, chloride, and potassium) (Hayashi et al 1981). Increased bitterness of snow crab meat synthetic extracts was observed when minerals were omitted as a group or singly (sodium), when amino acids were removed as a group (glycine arginine, alanine, proline, and taurine) or singly (arginine; Hayashi et al, 1981). High hemolymph potassium levels have been reported in Alaskan tanner crabs *Chionoecetes bairdi* (Love et al 1996). Increased potassium (hyperkalemia) could also result in an astringent taste to the meat as the potassium cation tastes bitter at high concentrations (Bartoshuk et al 1988, Saavedra-Garcia et al 2015).

Interestingly, a significant increase in hemolysis was observed in rats fed oxidized phosphatidylcholine for 2 weeks (Al-Orf 2011). Al-Orf (2011) suggested that the pathogenesis of

the hemolysis was oxidative injury to red cell membranes due to formation of covalently linked lipid-protein adducts by phospholipid hydroperoxide, an oxidation product of phosphatidylcholine. This suggests that the BCD-associated phospholipids could also contribute to the pathogenesis of hemocytopenia associated with this disease. Hemolymph lipoproteins are involved in non-self recognition in innate immune responses and hemocyanin-derived phenoloxidase activity can be induced by lipoproteins and/or phospholipids in various arthropod species including decapod crustaceans. Thus, the BCD-associated phospholipids could also be involved in immune system modulation (Sugumaran and Nellaiappan 1991, Hall et al 1995, Coates et al 2011, Schenk et al 2015).

The rapid proliferation of the *Hematodinium* parasites in hemolymph and the parasites high metabolic requirements during growth decrease the hosts protein and carbohydrate reserves, are reported to result in depletion of the hosts metabolic reserves and contribute to host morbidity and eventual mortality (Stentiford et al 2000, 2001, Shields and Squyars 2000, Stentiford and Shields 2005). This study concurs with these findings and indicates that BCD is associated with depletion of protein and carbohydrate metabolic reserves and altered host lipid metabolism. Several BCD-associated phospholipids were identified in this study. These BCD-associated phospholipids could contribute to the bitter taste associated with this disease. Additionally, BCD-associated phospholipids could contribute to the apparent lack of a cellular immune response against *Hematodinium*.

4.5. References

Al-Orf SM. 2011. Effect of oxidized phosphatidylcholine on biomarkers of oxidative stress in rats. Ind J Clin Biochem 26(2):154-160.

Amparyup P, Caroensapsri W, Tassanakajon A. 2013. Prophenoloxidase and its role in shrimp immune responses against major pathogens. Fish Shellfish Immunol 34(4):990-1001.

Ancelin ML, Vial HJ. 1986. Several lines of evidence demonstrating that *Plasmodium falciparum*, a parasitic organism, has distinct enzymes for phosphorylation of choline and ethanolamine. FEBS Lett. 202(2):217–223.

Bartoshuk LM, Rifkin B, Marks LE, Hooper JE. 1988. Bitterness of KCl and benzoate: related to genetic status for sensitivity to PTC/PROP. Chem Senses 13(4):517-528.

Beach DH, Holz GG Jr, Anekwe GE. Lipids of *Leishmania* promastigotes. J Parasitol 65(2):203-216.

Behringer DC, Butler MJ, Shields JD. 2008. Ecological and physiological effects of PaV1 infection on the Caribbean spiny lobster (*Panulirus argus* Latreille). J Exp Mar Biol 359(1):26-33.

Bowes AE, Samad AH, Jiang P, Weaver B, Mellors A. 1993. The acquisition of lysophosphatidylcholine by African trypanosomes. J Biol Chem 268(19):13885-13892.

Brodzky IE, Medzhitov R. 2009. Targeting of immune signaling networks by bacterial pathogens. Nat Cell Biol 11(5):521-526.

Cerenius L, Lee BL, Sŏderhall K. 2008. The proPO-system: pros and cons for its role in invertebrate immunity. Trends Immunol 29(6):263-271.

Chang ES. 1995. Physiological and biochemical changes during the molt cycle in decapod crustaceans: an overview. J Exp Mar Biol Ecol 193:1-14.

Coates CH, Kelly SM, Nairn J. Possible role of phosphatidylserine-hemocyanin interaction in the innate immune response of *Limulus poyphemus.* Dev Comp Immunol 35(2):155-163.

Cornet S, Biard C, Moret Y. 2009. Variation in immune defence among populations of *Gammarus pulex* (Crustacea: Amphipoda). Oecologia 159(2):257-269.

Cui L, Decker EA. 2016 Phospholipids in foods: prooxidants or antioxidants? J Sci Food Agric 96(1):18-31.

Das S, Stevens T, Castillo C, Villasenõr A, Arredondo H, Reddy K. 2002. Lipid metabolism in mucous-dwelling amitochondriate protozoa. Int J Parasitol 32(6):655-675.

Dawe EG. 2002. Trends in prevalence of Bitter Crab Disease caused by *Hematodinium* sp. in snow crabs (*Chionoecetes opilio)* throughout the Newfoundland and Labrador continental shelf. *In* Crabs in Cold Water Regions: Biology, Management and Economics. Alaska Sea Grant College Program, AK-SG-02-02:385-400.

Dechamps S, Shastri S, Wengelnik K, Vial H. 2010. Glycerophospholipid acquisition in *Plasmodium* – a puzzling assembly of biosynthetic pathways. Int J Parasitol 40(12):1347-1365.

Djangmah JS. 1970. The effects of feeding and starvation on copper in the blood and hepatopancreas, and on the blood proteins of *Crangon vulgaris* (Fabricius). Comp Biochem Physiol D 32(4):709-718.

Drewnowski A, Gomez-Carneros C. 2000. Bitter taste, phytonutrients, and the consumer: a review. Am J Clin Nutr 72(6):1424-1435.

Drewnowski A. 2001. The science and complexity of bitter taste. Nutr Rev 59(6):163-169.

Ehrt S, Schnappinger D. 2007. *Mycobacterium tuberculosis* virulence: inside and out. Nat Med 13(3):284-285.

Emoto K, Umeda M. 2000. Regulation of contractile ring disassembly by redistribution of phosphatidylethanolamine. J Cell Biol 49(6):1215-1224.

Ferner RE. 2008. Post-mortem clinical pharmacology. Br J Clin Pharmacol 66(4):430-443.

Field RH and Appleton PL. 1995. A *Hematodinium* -like dinoflagellate infection of the Norway lobster *Nephrops norvegicus*: observations on pathology and progression of infection. Dis Aquat Org 22(2):115-128.

Field RH, Chapman CJ, Taylor AC, Neil DM, Vickerman K. 1992. Infection of the Norway lobster *Nephrops norvegicus* by a *Hematodinium*-like species of dinoflagellate on the west coast of Scotland. Dis Aquat Org 13(1):1-15.

Foussard F, Gallois Y, Girault A, Menez JF. 1991. Lipids and fatty acids of tachyzoites and purified pellicles of *Toxoplasma gondii*. Parasitol Res 77(6):475-477.

Fraser AJ. 1989. Triacylglycerol content as a condition index for fish, bivalve, and crustacean larvae. Can J Fish Aquat Sci 46(11):1868-1873.

Greenwood SJ, Després BM, Cawthorn RJ, Lavallée J, Groman DB, Desbarats A. 2005. Case report: outbreak of bumper car disease caused by *Anophryoides haemophila* in a lobster holding facility in Nova Scotia, Canada. J Aquat Anim Health 17(4):345-352.

Hagerman L. 1983. Haemocyanin concentration of juvenile lobsters (*Homarus gammarus*) in relation to moulting cycle and feeding conditions. Mar Biol 77(1):11-17.

Hall M, vanHeusden MC, Sŏderhall K. 1995. Identification of the major lipoproteins in crayfish hemolymph as proteins involved in immune recognition and clotting. Biochem Biophys Res Comm 216(3):939-946.

Hayashi T, Yamaguchi K, Konosu S. 1981. Sensory analysis of taste-active components in the extract of boiled snow crab meat. J Food Sci 46(2):479-483.

Heath JR, Barnes H. 1970. Some changes in biochemical composition with season and during the moulting cycle of the common shore crab, *Carcinus maenas*. J Exp Mar Biol Ecol 5(3):199-233.

Hervant F, Mathieu J, Barre H. 1999. Comparative study on the metabolic responses of subterranean and surface-dwelling amphipods to long-term starvation and subsequent re-feeding. J Exp Biol 202(24):3587-3595.

Hudson DA and Shields JD. 1994. *Hematodinium australis* n. sp., a parasitic dinoflagellate of the sand crab *Portunus pelagicus* from Moreton Bay, Australia. Dis Aquat Org 19(2):109-119.

Igene JO, Pearson AM. 1979. Role of phospholipids and triglycerides in warmed-over flavor development in meat model systems. J Food Sci 44(5):1285–1290.

Jarroll EL, Manning P, Berrada A, Hare D, Lindmark DG. 1989. Biochemistry and metabolism of *Giardia.* J Protozool 36(2):190-197.

Jiravanichpaisal P, Lee BL, Sőderhall K. 2006. Cell-mediated immunity in arthropods: hematopoiesis, coagulation, melanization and opsonization. Immunobiology 211(4):213-236.

Johansson MW, Keyser P, Sritunyalucksana K, Sőderhall K. 2000. Crustacean hemocytes and hematopoiesis. Aquaculture 191(1-3):45-52.

Johnsen S, Widder EA. 1999. The physical basis of transparency in biological tissue: ultrastructure and the minimization of light scattering. J Theor Biol 199(2):181-198.

Johnson PT. 1980. Histology of the blue crab, *Callinectes sapidus*: a model for the Decapoda. New York, NY: Praeger Publishers.

Kaneshiro ES. 1998. The lipids of *Pneumocystis carinii.* Clin Microbiol Rev 11(1):27–41.

Lee RF, Hagen W, Kattner G. 2006. Lipid storage in marine zooplankton. Mar Ecol Prog Ser 307(1):273-306.

Lee RF, Puppione DL. 1988. Lipoproteins I and II from the hemolymph of the blue crab *Callinectes sapidus*: Lipoprotein II associated with vitellogenesis. J Exp Zool 248(3):278-289.

Li YY, Xia XA, Wu QY, Liu WH, Lin YS. 2008. Infection with *Hematodinium* sp. in mud crabs *Scylla serrata* cultured in low salinity water in southern China. Dis Aquat Org 82(2):145-150.

Love D, Thomas T, Moles A. 1996. Bitter crab hemolymph studies: indications of host physiological condition. High Latitude Crabs: Biology, Management and Economics. Alaska Sea Grant Report, AK-SG-96-02, Alaska Sea Grant Program, University of Alaska, Fairbanks, AK. pp. 549-562.

Lujan HD, Mowatt MR, NashTE. 1996. Lipid requirements and lipid uptake by *Giardia lamblia* trophozoites in culture. J Euk Microbiol 43(3):237–242

Lund ED, Chu FL. 2002. Phospholipid biosynthesis in the oyster protozoan parasite, *Perkinsus marinus*. Mol Biochem Parasitol 121(2):245-253.

Machado FS, Murkherjee S, Weiss LM, Tanowitz HB, Ashton AW. 2011. Bioactive lipids in *Trypanosoma cruzi* infection. Adv Parasitol 76:1-31.

Maehashi K, Huang L. 2009. Bitter peptides and bitter taste receptors. Cell Moll Life Sci 66(10):1661-1671.

Magnum CP, McMahon BR, deFur PL, Whetley MG. 1985. Gas exchange, acid-base balance, and the oxygen supply to tissue during a molt of the blue crab *Callinectes sapidus*. J Crustac Biol 5(2):188-206.

Maity S, Jannasch A, Adamec J, Gribskov M, Nalepa T, Hook T0, Sepulveda MS. 2012. Metabolite profiles in starved *Diporeia* spp. using liquid-chromatography-mass spectrometry (LC-MS) based metabolomics. J Crust Biol 32(2):239-248.

Messick GA. 1994. *Hematodinium perezi* infections in adult and juvenile blue crabs *Callinectes sapidus* from coastal bays of Maryland and Virginia, USA. Dis Aquat Org 19(1):77-82.

Meyerhof W. 2005. Elucidation of mammalian bitter taste. In Reviews of physiology, biochemistry and pharmacology. Springer Berlin Heidelberg, pp. 37-72.

Meyers TR, Koeneman TM, Botelho C, Short S. 1987. Bitter crab disease: A fatal dinoflagellate infection and marketing problem for Alaskan tanner crabs *Chionoecetes bairdi*. Dis Aquat Org 3(3):195-216.

Moore LE, Smith DM, Loneragan NR. 2000. Blood refractive index and whole-body lipid as indicators of nutritional condition for penaeid prawns (Decapoda: Penaeidae). J Exp Mar Biol Ecol 244(1):131-143.

Montgomery-Fullerton MM, Cooper RA, Kauffman KM, Shields JD, Ratzlaff RE. 2007. Detection of *Panulirus argus* Virus 1 in Caribbean spiny lobsters. Dis Aquat Org 76(1):1-6.

Mullowney DR, Dawe EG, Morado JF, Cawthorn RJ. 2011. Sources of variability in prevalence and distribution of bitter crab disease in snow crab (*Chionoecetes opilio*) along the northeast coast of Newfoundland. ICES J Mar Sci 68(3):463-471.

Neil DM. 2012. Ensuring crustacean product quality in the post-harvest phase. J Invert Pathol 110(2): 267-275.

O'Halloran MJ, O'Dor RK. 1988. Molt cycle of male snow crabs, *Chionoecetes opilio*, from observations of external features, setal changes, and feeding behavior. J Crust Biol 8(2):164-176.

Oliveira MM, Timm SL, Costa SC. 1977. Lipid composition of *Trypanosoma cruzi*. Comp Biochem Physiol B 58(2):195-199.

Paterson BD, Davidson GW, Spanoghe PT. 1999. Measuring total protein concentration in blood of the western rock lobster by refractometry. Evans, Louis and Jones, B. (Eds). *In* International Symposium on Lobster Health Management 1999. pp. 110-115.

Ramakrishnan S, Serricchio M, Striepen B, Bütikofer P. 2013. Lipid synthesis in protozoan parasites: a comparison between kinetoplastids and apicomplexans. Prog Lipid Res 52(4):488-512.

Rifkin MR, Strobos CAM, Fairlamb AH. 1995. Specificity of ethanolamine transport and its further metabolism in *Trypanosoma brucei.* J Biol Chem 270(27):16160–16166.

Rosas C, Cooper EL, Pascual C, Brito R, Gelabert R, Moreno T, Miranda G, Sanchez A. 2004. Indicators of physiological and immunological status of *Litopenaeus setiferus* wild populations (Crustacea, Penaeidae). Mar Biol 145(2):401-413.

Ryazanova TV. 2008. Bitter crab syndrome in two species of king crabs from the Sea of Okhotsk. Russian J Mar Biol 34(6):411-414.

Ryazanova TV, Eliseikina MG, Kukhlevsky AD, Kharlamenko VI. 2010. *Hematodinium* sp. infection of red *Paralithodes camtschaticus* and blue *Paralithodes platypus* king crabs from the Sea of Okhotsk, Russia. J Invertebr Pathol 105(3):329-334.

Saavedra-Garcia L, Bernabe-Ortiz A, Gilman RH, Diez-Canseco F, Cárdenas MK, Sacksteder KA, Miranda JJ. 2015. Applying the triangle taste test to assess differences between low sodium salts and common salt: evidence from Peru. PLoS One 10(7):e0134700.

Sanchez-Paz A, Garcia-Carreno FG, Muhlia-Almazan A, Peregrino-Uriarte AB, Hernandez-Lopez J, Yepiz-Plascencia G. 2006. Usage of energy reserves in crustaceans during starvation: Status and future directions. Insect Biochem Mol Biol 36(4):241-249.

Sasaki GC, McDowell Capuzzo J, Biesiot P. 1986. Nutritional and bioenergetics considerations in the development of the American lobster *Homarus americanus*. Can J Fish Aquat Sci 43(11):2311-2319.

Schenk S, Schmidt J, Hoeger U, Decker H. 2015. Lipoprotein-induced phenoloxidase activity in tarantula hemocyanin. Biochim Biophys Acta, Proteins Proteomics. 1854(8):939-949.

Sessa DJ, Warner K, Rackis JJ. 1976. Oxidized phosphatidylcholines from defatted soybean flakes taste bitter. J Agric Food Chem 24(1):16-21.

Shields JD. 1994. The parasitic dinoflagellates of marine crustaceans. Ann Rev Fish Dis 4:241-271.

Shields JD, Scanlon C, Volety A. 2003. Aspects of the pathophysiology of blue crabs, *Callinectes sapidus*, infected with the parasitic dinoflagellate *Hematodinium perezi*. Bull Mar Sci 72(2):519-535.

Shields JD, Squyars CM. 2000. Mortality and hematology of blue crabs, *Callinectes sapidus,* experimentally infected with the parasitic dinoflagellate *Hematodinium perezi*. Fish Bull 98(1):139-152.

Shields JD, Taylor DM, Sutton SG, O'Keefe PG, Ings DW, Pardy AL. 2005. Epidemiology of Bitter Crab Disease (*Hematodinium* sp.) in snow crabs *Chionoecetes opilio* from Newfoundland, Canada. Dis Aquat Org 64(3):253-264.

Shields JD, Taylor DM, O'Keefe PG, Colbourne E, Hynick E. 2007. Epidemiological determinants in outbreaks of Bitter Crab Disease (*Hematodinium* sp.) in snow crabs *Chionoecetes opilio* from Conception Bay, Newfoundland, Canada. Dis Aquat Org 77(1):61-72.

Smith DM, Dall W. 1982. Blood protein, blood volume and extracellular space relationships in two *Penaeus* spp. (Decapoda: Crustacea). J Exp Mar Biol Ecol 63(1):1-15.

Smith JD. 1993. Phospholipid biosynthesis in protozoa. Prog Lipid Res 32(1):47–60.

Smith TK, Butikofer P. 2010. Lipid metabolism in *Trypanosoma brucei*. Mol Biochem Parasitol 172(2):66-79.

Sőderhall K, Cerenius L. 1998. The role of the prophenoloxidase-activating system in invertebrate immunity. Curr Opin Immunol 10(1):23-28.

Spindler-Barth M. 1976. Changes in the chemical composition of the common shore crab, *Carcinus maenas*, during the molting cycle. J Comp Phys B 105:197-205.

Sriket C, Benjakul S, Visessanguan W. 2011. Characterisation of proteolytic enzymes from muscle and hepatopancreas of fresh water prawn (*Macrobrachium rosenbergii*). J Sci Food Agric 91(1):52-59.

Stentiford GD, Chang ES, Chang SA, Neil DM. 2001. Carbohydrate dynamics and the crustacean hyperglycemic hormone (CHH): effects of parasitic infection in Norway lobsters (*Nephrops norvegicus*). Gen Comp Endocrinol 121(1):13-22.

Stentiford GD, Green M, Bateman K, Small HJ, Neil DM, Feist SW. 2002. Infection by a *Hematodinium* -like parasitic dinoflagellate causes Pink Crab Disease (PCD) in the edible crab *Cancer pagurus*. J Invertebr Pathol 79(3):179-191.

Stentiford GD, Neil DM, Coombs GH. 2000. Alterations in the biochemistry and ultrastructure of the deep abdominal flexor muscle of the Norway lobster *Nephrops norvegicus* during infection by a parasitic dinoflagellate of the genus *Hematodinium*. Dis Aquat Org 42(2):133-141.

Stentiford GD, Shields JD. 2005. A review of the parasitic dinoflagellates *Hematodinium* species and *Hematodinium* -like infections in marine crustaceans. Dis Aquat Org 66(1):47-70.

Stevens TL, Gibson GR, Maier AJ, Allison-Ennis M, Das S. 1997. Uptake and cellular localization of exogenous lipids by *Giardia lamblia*, a primitive eukaryote. Exp Parasitol 86(2):133–143.

Stuck KC, Watts SA, Wang SY. 1996. Biochemical responses during starvation and subsequent recovery in postlarval Pacific white shrimp, *Penaeus vannamei*. Mar Biol 125(1):33-45.

Sugumaran M, Nellaiappan K. 1991. Lysolecithin-a potent activator of prophenoloxidase from the hemolymph of the lobster, *Homarus americanus*. Biochem Biophys Res Commun 176(3):1371-1376.

Uglow RF. 1969a. Haemolymph protein concentrations in portunid crabs. I. Studies on adult *Carcinus maenas*. Comp Biochem Physiol 30(6):1083–1090.

Uglow RF. 1969b. Haemolymph protein concentrations in portunid crabs. II. The effects of imposed fasting on *Carcinus maenas*. Comp Biochem Physiol 31(6):959–967.

vanHellemond JJ, Tielens AGM. 2006. Adaptations in the lipid metabolism of the protozoan parasite *Trypanosoma brucei*. FEBS Letters 580(23):551-558.

Wassef MK, Fioretti TB, Dwyer DM. 1985. Lipid analyses of isolated surface membranes of *Leishmania donovani* promastigotes. Lipids 20(2):108-115.

Wheeler K, Shields JD, Taylor DM. 2007. Pathology of *Hematodinium* infections in snow crabs (*Chionoecetes opilio*) from Newfoundland, Canada. J Invertebr Pathol 95(2):93-100.

Wilson BR, Pearson AM, Shorland FB. 1976. Effect of total lipids and phospholipids on warmed-over flavor in red and white muscle from several species as measured by thiobarbituric acid analysis. J Agric Food Chem 24(1):7–11.

Wlodawer P, Wisniewska A. 1965. Lipids in the haemolymph of waxmoth larvae during starvation. J Insect Phys 11(1):11-20.

Wu TC, Sheldon BW. 1988. Influence of phospholipids on the development of oxidized off flavors in cooked turkey rolls. J Food Sci 53(1):55–61.

Xu W, Xie J, Shi H, Li C. 2010. *Hematodinium* infections in cultured ridgetail white prawns, *Exopalaemon carinicauda,* in eastern China. Aquaculture 300(1-4):25-31.

Yichoy M, Duarte TT, De Chatterjee A, Mendez TL, Aguilera KY, Roy D, Roychowdhury S, Aley SB, Das S. 2011. Lipid metabolism in *Giardia*: a post-genomic perspective. Parasitology 138(03):267-278.

5. HISTOPATHOLOGIC SURVEY OF NEWFOUNDLAND SNOW CRABS, *CHIONOECETES OPILIO*: PARASITES, EPIBIONTS, INFLAMMATORY PATTERNS, AND THEIR ASSOCIATIONS WITH BCD.

5.1. Introduction

Snow crab *Chionoecetes opilio* is a subarctic species found in the North Atlantic and North Pacific oceans. Canada is the world's largest producer of snow crab accounting for approximately two-thirds of the global supply with 2013 landings of 98, 065 tonnes and exports valued $434.2 million (http://www.dfo-mpo.gc.ca). Fluctuations in yearly snow crab fishery values are largely due to market fluctuations (such as demand and price) and biotic forces such as synchronous molting events which result in a predomination of recently molted, low-yield male crabs which can result in premature fishery closures (Wheeler et al 2007). Over the last two decades Bitter Crab Disease (BCD) has become endemic in the northern bays of Newfoundland, causing at least three documented disease outbreaks and may have contributed to the declines in snow crab landings in the inshore bays (Shields et al 2005, Shields et al 2007, Wheeler et al 2007).

BCD, caused by parasitic dinoflagellates of the genus *Hematodinium*, is one of the major diseases which affect snow crabs. BCD is a fatal disease of crustaceans which was first reported off the coast of Europe in common shore crabs *Carcinus maenas* and harbour crabs *Liocarcinus depurator* (Chatton and Poisson, 1931). The disease has since been reported in over forty species of crustaceans with a worldwide distribution concentrated in the North Pacific and Atlantic oceans (reviewed in Morado et al 2011). One of the commonly reported features of hematodiniosis is progressive hemocytopenia concomitant with increasing parasite burden

(Field et al 1992, Field and Appleton 1995, Taylor et al 1996, Shields and Squyars 2000, Stentiford and Shields 2005). Hemocytopenia in crustacean hosts has also been observed in other hemocoelic protozoan diseases, including Dungeness crabs *Cancer magister* infected with the parasitic ciliate *Mesanophrys pugettensis* and blue crabs *Callinectes sapidus* infected with the parasitic amoeba *Paramoeba perniciosa* (Johnson 1977, Cain and Morado 2001, Morado 2011). Hemocytopenia is also occasionally reported in crustacean bacterial diseases, such as Aerococcosis (Gaffkemia), caused by *Aerococcus viridans* var *homari*, in American lobsters *Homarus americanus* (Stewart 1984, Battison et al 2004). In these diseases, possible causes of progressive hemocyte depletion have included lysis of host cells after phagocytosis of parasite cells, consumption of hemocytes by invading parasites, disruption of hematopoietic tissue function, or sequestration of hemocytes in host defense reactions which overwhelm the host's immune system (Field and Appleton 1995, Shields and Squyars 2000, Morado 2011, Walker *et al.* 2009).

The two primary defense mechanisms of the crab's innate immune system are the clotting and prophenoloxidase (proPO) systems. The prophenoloxidase activating (proPO) system is an efficient part of the innate immune response and consists of several proteins that are involved in phagocytosis, encapsulation, melanized nodule formation, and cytotoxic reactions (Jiravanichpaisal *et al.* 2006, Vazquez *et al.* 2009). Activation of the proPO system is mediated through the specific recognition of glycosylated pathogen-associated molecular patterns (PAMPs) by crustacean proteins. The proPO system is triggered by the presence of minute amounts of microbial components including as lipopolysaccharides and peptidoglycans from

bacteria, beta-1,3 glucans from fungi, and mannan (Jiravanichpaisal *et al.* 2006, Vazquez *et al.* 2009). The system is composed of pattern-recognition proteins and protein inhibitors, regulatory factors to avoid inappropriate system activation (Jiravanichpaisal *et al.* 2006). The lack of significant inflammation associated with hematodiniosis suggests that this parasite avoids detection by the innate immune system or inhibits activation of the proPO system through unknown mechanisms. The observation of effective encapsulation of fungal co-infections suggests that widespread proPO inhibition is not achieved in affected hosts as the host can produce and release hemocytes in response to other pathogens (Johnson 1986, Stentiford *et al.* 2003). These findings suggest that the crustacean immune systems may not recognize *Hematodinium* as foreign. An absence of recognition of this dinoflagellate pathogen may play a key role in the pathogenesis of hematodiniosis and explain the unchecked parasitic proliferation within the hemolymph and tissues of affected hosts (Stentiford et al, 2003).

In infected Norway lobster *Nephrops norvegicus* and snow crabs *Chionoecetes opilio*, fixed phagocytes in infected hosts appeared activated and enlarged (Field and Appleton 1995, Wheeler *et al.* 2007. This “activation” may have been due to the presence of the parasite, but also may have been in response to secondary invaders or cellular debris arising from the infection. Parasitic dinoflagellates have been observed invading between activated fixed phagocytes and parasitic debris has been seen within fixed phagocytes (Field and Appleton, 1995). Similarly, hemocytic aggregates, encapsulations, and melanized nodules were occasionally seen in infected hosts although definitive evidence of parasitic dinoflagellates was never documented within these immune reactions (see Chapter 1, Tables 1.4 and 1.5). Thus, it

remains unclear whether those cellular aggregates represent immune responses in early stages of *Hematodinium* sp. infections or responses to previous or concurrent infections by other pathogens. Pathogen-pathogen interactions may also influence disease course, expression, severity, and transmission (Cattadori et al 2008, Singer 2010). Interactions between pathogens within the same host can be positive or negative. Positive co-infection interactions can include enhancement of both disease transmission and progression, known in human medicine as syndemism (Cattadori et al 2008). Thus, secondary invaders may alter the course of disease and may hasten the demise of impaired hosts (Sheppard et al 2003).

In additional to BCD, the other main disease observed in snow crabs is shell disease. The two main forms of shell disease in snow crabs are black spot (or brown, rust, or burn spot) caused by chitinolytic bacteria and black mat syndrome caused by the ascomycete fungus *Trichomaris invadens* on the exterior carapace (Kon et al 2011). Milky hemolymph syndrome, caused by an intranuclear bacilliform virus, has also recently been reported in snow crabs *Chionoecetes opilio* from the Sea of Japan (Kon et al 2011). In addition to pathogenic organisms, snow crabs are also typically colonized by a wide range of fouling organisms. The fouling community of snow crabs includes over 20 families of sessile invertebrates including polychaetes (spirorbid and serpulid worms), turbellarian worms, amphipods, bryozoans, hydrozoans, bivalves, barnacles, and leeches (Brattey et al 1985, Hooper 1986, Steele et al 1986, Savoie et al 2007). Some of these organisms were major fouling agents (present on more than 50% of snow crabs) while others were minor contributors to fouling communities (present on less than 10% of snow crab; Savoie et al 2007).

This study provides a histologic survey of snow crabs *Chionoecetes opilio* from 3 bays along the northern coasts of Newfoundland. This histologic survey documents the prevalence of epibiotic fouling communities present on snow crabs, parasites within snow crabs, and histopathologic lesions observed within snow crab tissues. This study compares prevalence data from three bays (Bonavista Bay, Notre Dame Bay, and White Bay) and shallow and deep regions within two of those bays (Bonavista Bay and White Bay). Evaluation for possible associations between commensal and parasitic organs with observed patterns of inflammation were also investigated.

5.2. **Materials and Methods**

5.2.1. **Snow Crab Collection**

Atlantic snow crabs (*C. opilio*) were collected during DFO annual Fall surveys in Notre Dame Bay and White Bay, Newfoundland during September 2010 and 2011. In Notre Dame Bay, crabs were caught by pot trap on the grounds of strata 610 and 611 (200-400 m in depth). In Notre Dame Bay, stratum 611 was shallow (200-300m) and stratum 610 was deep (301-400 m). Deep stratum 610 was missed in 2011 due to inclement weather. Water temperatures for strata 610 and 611 range between -1°C and 3°C in early Fall (Mullowney et al 2011). In White Bay, crabs were caught by pot trap on the grounds of stratum 614 (300-401 m in depth). The water temperatures for stratum 614 normally ranged between 0-1°C in early Fall (Mullowney et al 2011). The salinity in these bays ranges from 31-35 ppt, with BCD-positive crabs typically not

found in regions with salinity <33 ppt (Dawe et al 2010). In Bonavista Bay, crabs were caught by pot trap on the grounds of stratum 796 (300-401 m in depth).

For all of these regions traps were separated by 45 m within each fleet and were baited using squid and/or mackerel. Soak time was usually about 24 h, depending on weather conditions. Within each crab management area surveyed, the depth range and actual area sampled corresponded approximately to the commercial fishery area. Minimum depth for sampling was 170 m for all survey areas. The survey has consistently occurred in September and occupies 5 of the inshore Fall multi-species survey strata with a target of 8 sets per stratum. Each set includes 6 traps, with crabs sampled from two large-meshed (commercial, 135 mm) and two small-meshed (27 mm) traps.

The final sample collections were from Bonavista Bay within Terra Nova Park by a DFO collaborator (Jan Negrin). These snow crabs were collected from a single experimental small-meshed trap (27 mm) at shallow depths (up to 100 m depth). This region was sampled during the Summer of 2011 once per month for 3 months.

For all samples crabs were kept in coolers layered between seawater soaked burlap, and placed above saltwater ice until reaching shore. On shore, coolers were transported to St. John's, Newfoundland, where they were sent via air cargo to the Atlantic Veterinary College (AVC) at University of Prince Edward Island (UPEI). The interval between snow crab harvest and their arrival at the AVC was usually 24-48 h. After the first shipment (100% mortality, see below)

snow crabs were recovered in 34 ppt artificial seawater which was aerated with air stones and maintained at 0-2 °C until processing. The interval between snow crab arrival at AVC and processing ranged from 15 min to ~4 h. A histopathologic survey of green crabs (*Carcinus maenas*) collected by Dr. Pedro Quijon in the Biology Department at UPEI was also performed (Appendix 8).

5.2.2. **Snow Crab Processing and Sample Collection**

Each snow crab was photographed (dorsal and ventral digital images), gender was noted and recorded, and carapace width (mm) was measured and recorded. Hemolymph from each animal was collected aseptically from the base of the first walking leg using a 3 ml or 5 ml syringe with a 22 gauge needle. For each animal the gross appearance of the hemolymph was noted, hemolymph refractive index was measured using digital refractometer (Reichert r^2mini digital refractometer; Reichert Analytical Instruments), and two direct smears of hemolymph were made on glass slides. Air-dried smears were later stained with Wright-Giemsa in a Hema-Tek 1000 automated slide stainer (Miles Scientific). In addition, a 200 µl sample of hemolymph was placed in an ethanol block (96 well block) containing 800 µl 100% ethanol per well for DNA extraction. These DNA samples were examined using a polymerase chain reaction (PCR) assay with *Hematodinium*-specific primers (Appendix 1). This assay was used for the molecular detection of *Hematodinium* sp. infection in a larger survey of Newfoundland snow crabs, and was used as a molecular method of disease detection for this project.

Crabs were evaluated for gross morphologic evidence of Bitter Crab Disease which is characterized by an orangish-pink or "cooked" appearance to the carapace and/or white discoloration of their arthrodial membranes. Crabs with macroscopic evidence of BCD were exsanguinated, with the remaining hemolymph stored on ice and used for the *in vitro* cultivation portion of this project conducted by Mr. Peter Gaudet (MSc project). The crab was then humanely euthanized via nerve cord disruption via decapitation (i.e., removal of the carapace) as it was previously determined that euthanasia via potassium chloride injection resulted in a large streak of tissue disruption (Appendix 2). After removal of the carapace, a digital image of the crab's internal organs was taken and tissue samples were collected. The tissue samples collected included: heart, hepatopancreas, gill (1^{st} and 4^{th} gills on the right), gonad, midgut, eyestalks (left and right), a cross-section of the abdomen, and a cross-section of leg (1^{st} merus on the right). The tissues were immediately placed in Davidson's seawater fixative for 24 h. (Davidson's seawater fixative was prepared as described in Appendix 3.) After 24 h the tissue samples were transferred into containers of 70% ethanol for storage until routine processing for histology.

5.2.3. **Tissue Trimming and Processing**

Sections of all soft tissues (heart, hepatopancreas, gill (x2), gonad, and midgut) were trimmed and placed into one cassette per individual snow crab for processing. A second cassette of sections lined by a thick cuticular layer (eyestalk, leg, and abdomen) was also processed. The eyestalk was bisected along the frontal plane as this plane was found to consistently result in optimal sections of internal neuroendocrine tissues (Appendix 4). The blocks of trimmed tissues

were processed routinely for histology (Leica processor) and stained with hematoxylin and eosin (H&E). In 2010, the tissue sections were all placed in a single large holding container until processing. Tissue sections were collected from this container daily until all blocks were processed. In 2011, all samples from animals with macroscopic evidence of BCD were placed in a separate holding container that was not submitted until all other blocks were processed and slides were prepared and delivered. Then, the samples known to contain dinoflagellates were processed separately. This additional step was instituted after a tissue processing trial undertaken to mimic the conditions of 2010 indicated that a single large holding container can introduce cross-contamination of snow crab tissues with *Hematodinium* (Appendix 5)**.**

5.2.4. **Histologic Examination of Tissue Sections**

Each tissue on each slide was examined systematically for evidence of *Hematodinium* infection. *Hematodinium* sp. organisms have a characteristic nuclear chromatin condensation pattern which makes their nucleus stain more darkly than host hemocytes, and thus are relatively easily identified at low magnification (100x magnification, 10x objective). *Hematodinium* sp. organisms also contain numerous intracellular vacuoles (PAS bodies or accumulation bodies) which contain lipofuscin-like material resulting in the parasitic dinoflagellates having a cytoplasmic vacuolated appearance distinct from the agranular or granular appearance of host hemocytes. If no evidence of infection was observed during the screening at 100x magnification, the tissues were screened again at high magnification (400x magnification, 40x objective). Degree of bacterial gill fouling (minimal, mild, moderate, or marked) was noted. The sections were then screened for histologic evidence of gill fouling, carapace fouling (eyestalk,

leg, and abdominal cross sections), and histopathologic changes within soft tissues. Relative abundance of glycogen-containing reserve inclusion (RI) cells was also scored as previously reported (Stentiford and Fiest, 2005). The scoring index ranged from Stage 0 (RI cells absent) through Stage 1 (RI cells present but scarce), Stage 2 (RI cells scattered), Stage 3 (RI cells frequent) to Stage 4 (RI cells abundant and constituting the majority of connective tissue volume). RI scores were completed for the hepatopancreas and the gut and the highest score for all sections examined was recorded for each tissue.

5.2.5. **Transmission Electron Microscopy**

Transmission electron microscopy (TEM) was pursued to determine the ultrastructural characteristics of a microsporidian parasite found via light microscopy (see results below). Archival heart tissue (previously fixed with Davidson's seawater for 24h and then stored in 70% ethanol) underwent post-fixation in 1% osmium tetroxide dissolved in 70% ethanol at room temperature (~22 EC). After dehydration in an ascending ethanol series followed by propylene oxide, the tissue was embedded in Epon 812/Araldite and placed in a vacuum desiccator overnight to degas. The resin-embedded sample was then placed in Better Equipment for Electron Microscopy, Inc. (BEEM) capsules and polymerized in a 65^{o}C oven for 24 h. Semi-thin (0.5 µm) sections were cut with a Reichert-Jung Ultracut E ultramicrotome, were stained with 1% toluidine blue in 1% sodium tetraborate solution for viewing with a light microscope, and suitable areas were identified for examination under TEM. The blocks were trimmed to <1 mm^2 areas of interest and ultrathin sections (90 nm) of these areas were cut on a Reichert-Jung Ultracut E ultramicrotome, mounted on uncoated 200 supermesh copper grids, and stained

with 5% uranyl acetate in 50% ethanol followed by Sato lead stain. Sections were examined using a Hitachi Bio TEM 7500 transmission electron microscope operated at 80 kV. Images were captured using an Advance Microscopy Techniques (AMT) XR40 side mount digital camera.

5.2.6. **Statistical Analysis**

Categorical data were analyzed using Pearson Chi-Square Tests or Fisher Exact Tests (the latter used when any expected values were <5). Ordinal data were analyzed using Kruskal-Wallis Tests (adjusted for ties) followed by Mann-Whitney tests (adjusted for ties). Differences between bays were considered to be statistically significant at p-value < 0.05.

5.3. **Results**

5.3.1. **Shell Condition**

In 2010 and 2011 a total of 467 snow crabs was shipped from NL to PEI from 3 bays – Bonavista Bay (BB), Notre Dame Bay (NDB) and White Bay (WB) (Table 5.1). The macroscopic epifaunal fouling on the dorsal carapace of snow crabs was composed primarily of spirorbid worms with occasional serpulids and barnacles. This macroscopic fouling was used to determine shell condition category for each snow crab. There were statistically significant differences among the shell conditions of snow crabs collected within the 3 bays (Kruskal-Wallis Test: H = 100.95, DF = 2, P = 0.000). BB had a higher median shell condition than NDB (Mann-Whitney Test (adjusted for ties): W = 21086.0, p-value = 0.0000) and WB (Mann-Whitney Test: W = 26991.0, p-value = 0.0000). NDB had a higher mean shell condition category than WB (Mann-Whitney Test: W = 30406.5, p-value = 0.0000).

Table 5.1. Numbers of male and female snow crabs collected for each shell condition category from Bonavista Bay, Notre Dame Bay, and White Bay, Newfoundland.

	Bonavista Bay		**Notre Dame Bay**		**White Bay**	
n	133		142		192	
Sex Distribution	Male (n=130)	Female (n = 3)	Male (n=61)	Female (n = 81)	Male (n=160)	Female (n=32)
New-shelled	76	1	60	63	160	31
	77		123		191	
Intermediate-shelled	50	1	1	17	0	1
	51		18		1	
Old-shelled	4	1	0	1	0	0
	5		1		0	

5.3.2. **Parasitic infections**

5.3.2.1. Bitter Crab Disease

A total of 29 animals was collected that had histologic evidence of BCD (see Chapter 2). BCD infection was characterized histologically by hemal infiltration and proliferation of parasitic uninucleate and multinucleate plasmodia with condensed chromatin and foamy vacuolated cytoplasm. No BCD+ animals were collected from BB, 14 BCD+ animals were collected from NDB, and 14 BCD+ animals were collected from WB. All BCD+ animals were new-shelled snow crabs (Table 5.2). The new-shelled snow crabs collected from BB had statistically significantly lower prevalence of BCD than the new-shelled snow crabs collected in NDB (Pearson Chi-Square = 9.424, DF = 1, P-Value = 0.002) and WB (Fisher Exact Test p-value = 0.012). There was no statistically significant difference in the prevalence of BCD observed in new-shelled snow crabs in NDB vs WB (Pearson Chi-Square = 1.513, DF = 1, P-Value = 0.219). BCD was seen more frequently in male snow crabs in both NDB and WB but this gender difference in prevalence was not

statistically significant in NDB (Pearson Chi-Square = 3.243, DF = 1, P-Value = 0.072) or WB (Fisher Exact Test p-value = 0.474).

Table 5.2. BCD prevalence in snow crabs from Bonavista Bay, Notre Dame Bay, and White Bay, Newfoundland. Also provided are gender and size distributions of snow crabs from each bay.

	Bonavista Bay		**Notre Dame Bay**		**White Bay**	
n	133		142		192	
Gender distribution	98% males (n=130)	2% females (n = 3)	57% males (n=61)	43% females (n = 81)	81% males (n=160)	19% females (n=32)
Carapace width Range (mm)	60-128	61-75	53-103	27-69	46 -110	40-55
Carapace width Mean (mm)	92.4	68.3	76.3	54.4	80.6	45.9
Histologic BCD+ (all processed)	0% (0/130)	0% (0/3)	16.4% (10/61)	4.9% (4/81)	8.1% (13/160)	3.1% (1/32)
Histologic BCD+ (new-shelled)	0% (0/76)	0% (0/1)	16.7% (10/60)	4.9% (4/63)	8.1% (13/160)	3.1% (1/31)
Histologic BCD+ (new-shelled)	0% (0/77)		11.4% (14/123)		7.3% (14/191)	

5.3.2.2. Microsporidiosis

An unknown microsporidian infection was seen in a single new-shelled male snow crab collected in NDB. Macroscopically, the external surface of snow crab's ventral carapace was dull (rather than iridescent) in appearance (Figure 5.1), the myocardial tissue was tan and with mildly increased tissue opacity, the hepatopancreatic interstitial connective tissue was mildly edematous, and the gills contained pale streaks (Figure 5.2A as compared to Figure 5.2B). Microscopically, clusters of the microsporidian parasites infiltrated the snow crab's hemal spaces multisystemically. The microsporidian parasites were present in the interstitial connective tissues of the hepatopancreas, heart, gonad, midgut and hindgut, gill, abdominal and leg skeletal muscles (Figure 5.3). In the gill the parasites were observed in the primary lamellae but spared the hemal spaces of the secondary lamellae. In the abdominal and leg musculature the parasites invaded the hemal spaces and surrounded, but did not invade,

skeletal myofibers (Figure 5.3F). The parasites occurred singly, in tetrads, and in larger clusters, and occasional larger clusters contained centrally located small, refractile, oval spores (Figure 5.4). An enlarged (karyomegalic) nucleus with peripherally marginated chromatin and a prominent, enlarged nucleolus was often associated with the parasitic clusters (possible host cell nucleus; Figure 5.5). These tetrads and spores were observed ultrastructurally and were surrounded by an outer limiting membrane (presumed sporophorous vesicle) and polar tubes (a characteristic feature of microsporidians) were observed within the spores (Figures 5.6 to 5.8).

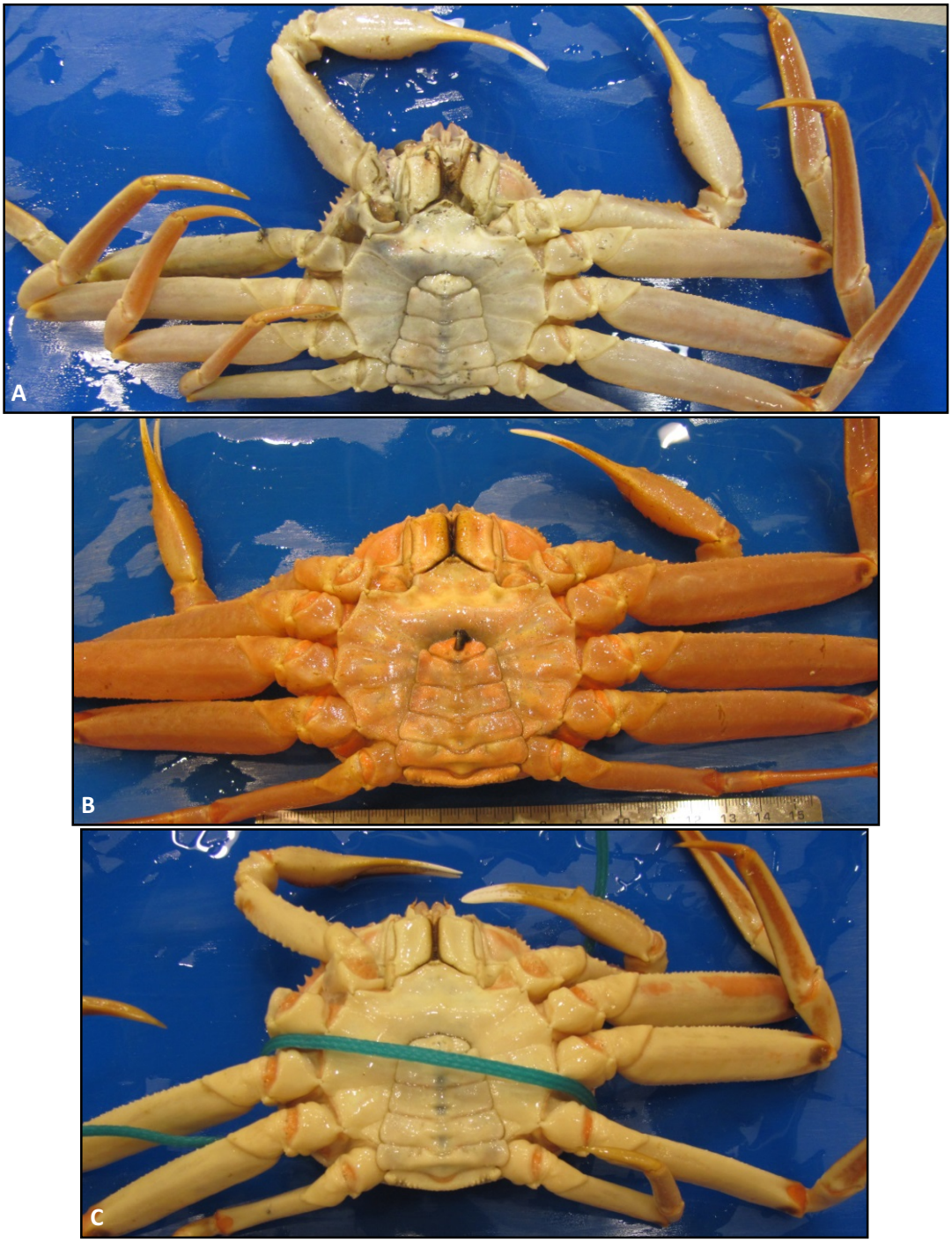

Figure 5.1. Comparison of the external appearance of a snow crab with microsporidiosis to normal snow crab and a snow crab with BCD. **A)** Appearance of the ventral carapace of the snow crab with microsporidiosis (crab 2010-#28). Note dull white appearance of the ventral carapace. **B)** Normal iridescent appearance of the ventral carapace of a snow crab (#2010-30). **C)** Opaque white ventral carapace of a snow crab with BCD (snow crab 2010-20).

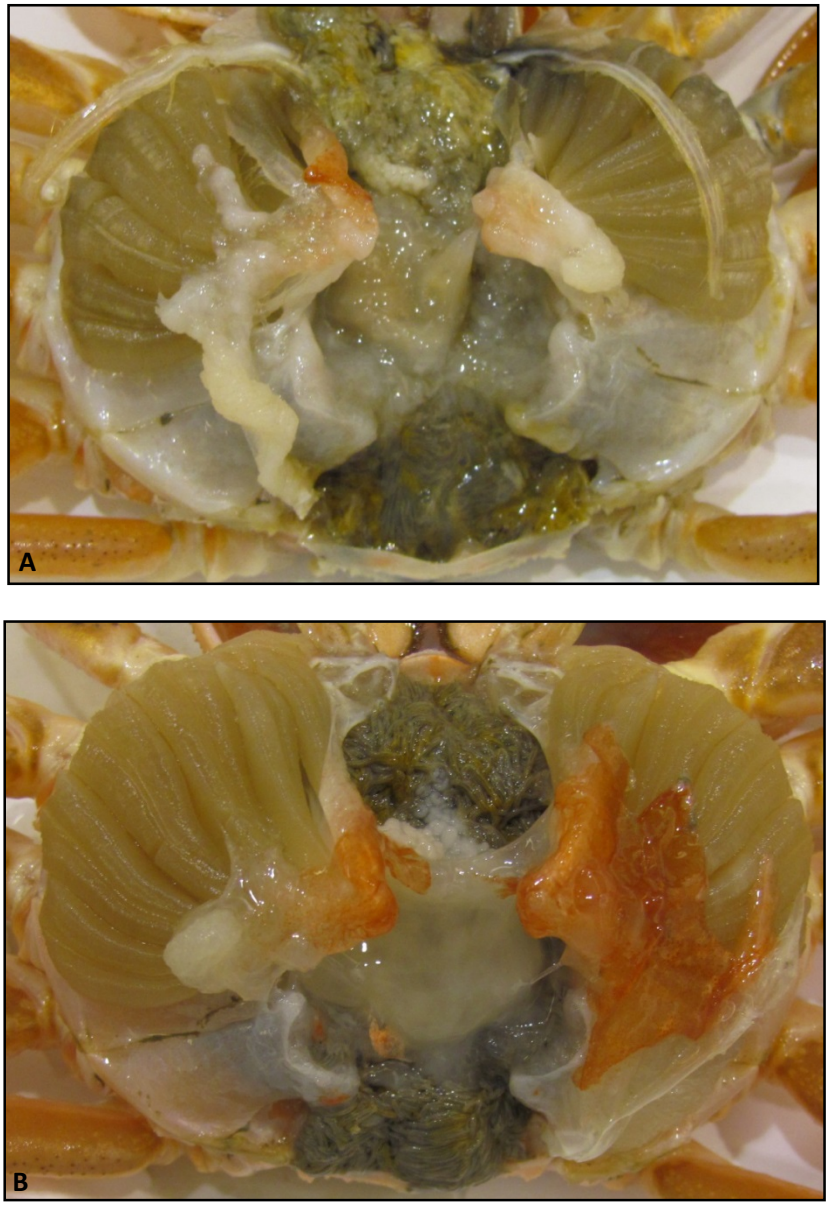

Figure 5.2. Comparison of the appearance of the internal organs of a snow crab with microsporidiosis and the normal appearance of snow crab internal organs. **A)** Appearance of the internal organs of a snow crab with microsporidiosis (snow crab #2010). Note white streaks in primary and secondary gill lamellae, slight cloudiness of the hepatopancreatic interstitial connective tissues, and increased opacity of the heart. **B)** Normal appearance of internal organs of a similarly sized male snow crab.

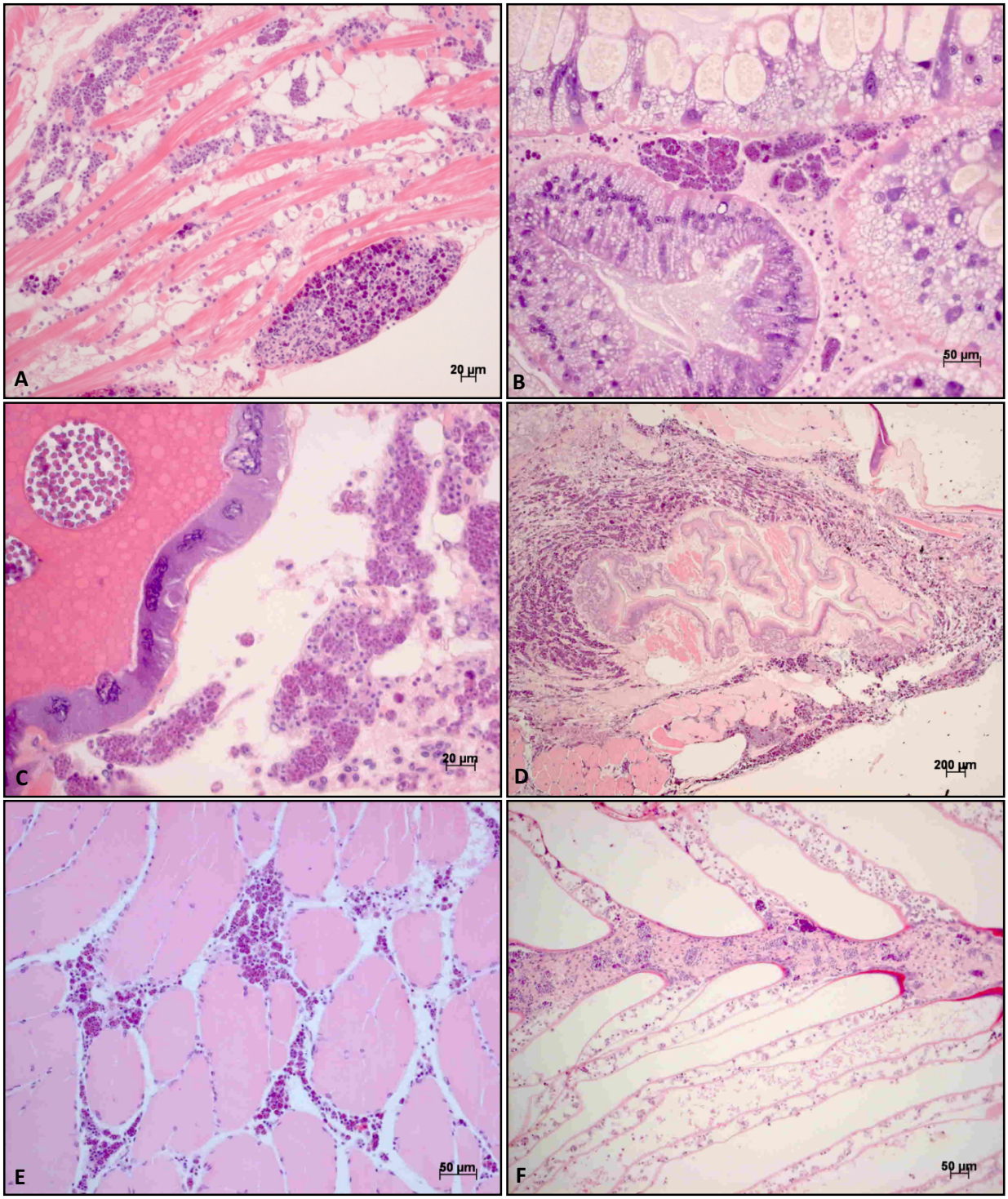

Figure 5.3. Multisystemic interstitial infiltration of the microsporidial parasite. **A)** Interstitial microsporidial infiltration of the heart. Note the hemocytic aggregate with intralesional parasites along the luminal surface of the myocardial lumen (H&E, 200x). **B)** Interstitial microsporidial infiltration of the hepatopancreas (200x, H&E). **C)** Interstitial microsporidial infiltration in the testes (H&E, 400x). **D)** Interstitial microsporidial infiltration in the abdomen surrounding the hindgut and infiltrating between abdominal skeletal muscles (H&E, 25x).

Figure 5.3 (continued). E) Interstitial microsporidial infiltration around skeletal muscles. Note the absence of infiltration into the myofibers and the predominance of small clusters (tetrads) of parasites (H&E, 200x). **F)** Microsporidial infiltration of the primary gill lamellae with sparing of the secondary lamellae (H&E, 100x).

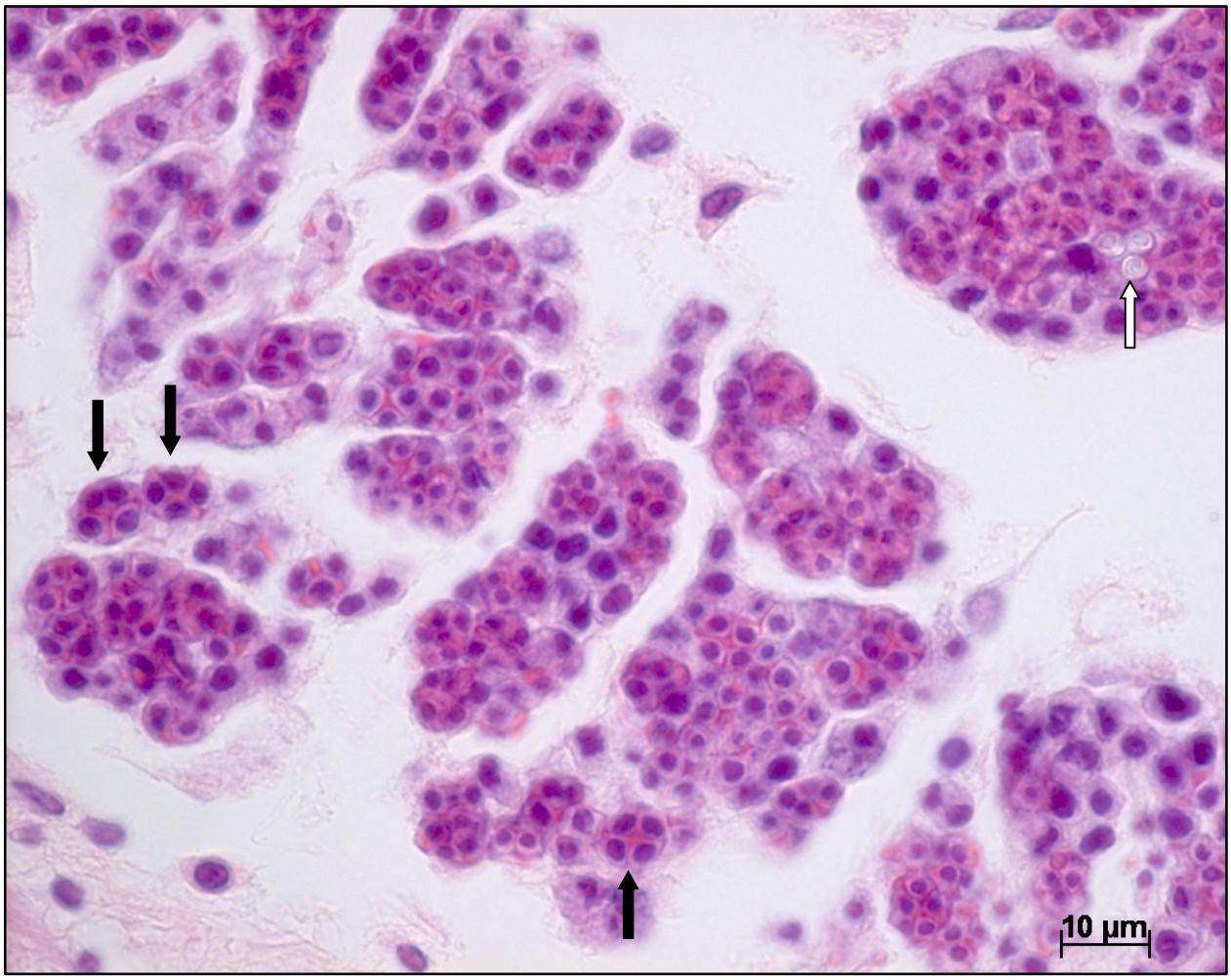

Figure 5.4. Clusters of microsporidial parasites in the interstitial connective tissues of the skeletal musculature. The clusters of parasites were often in tetrads and larger clusters (black arrows). Central clusters of spores were occasionally seen (white arrow; H&E, 1000x)

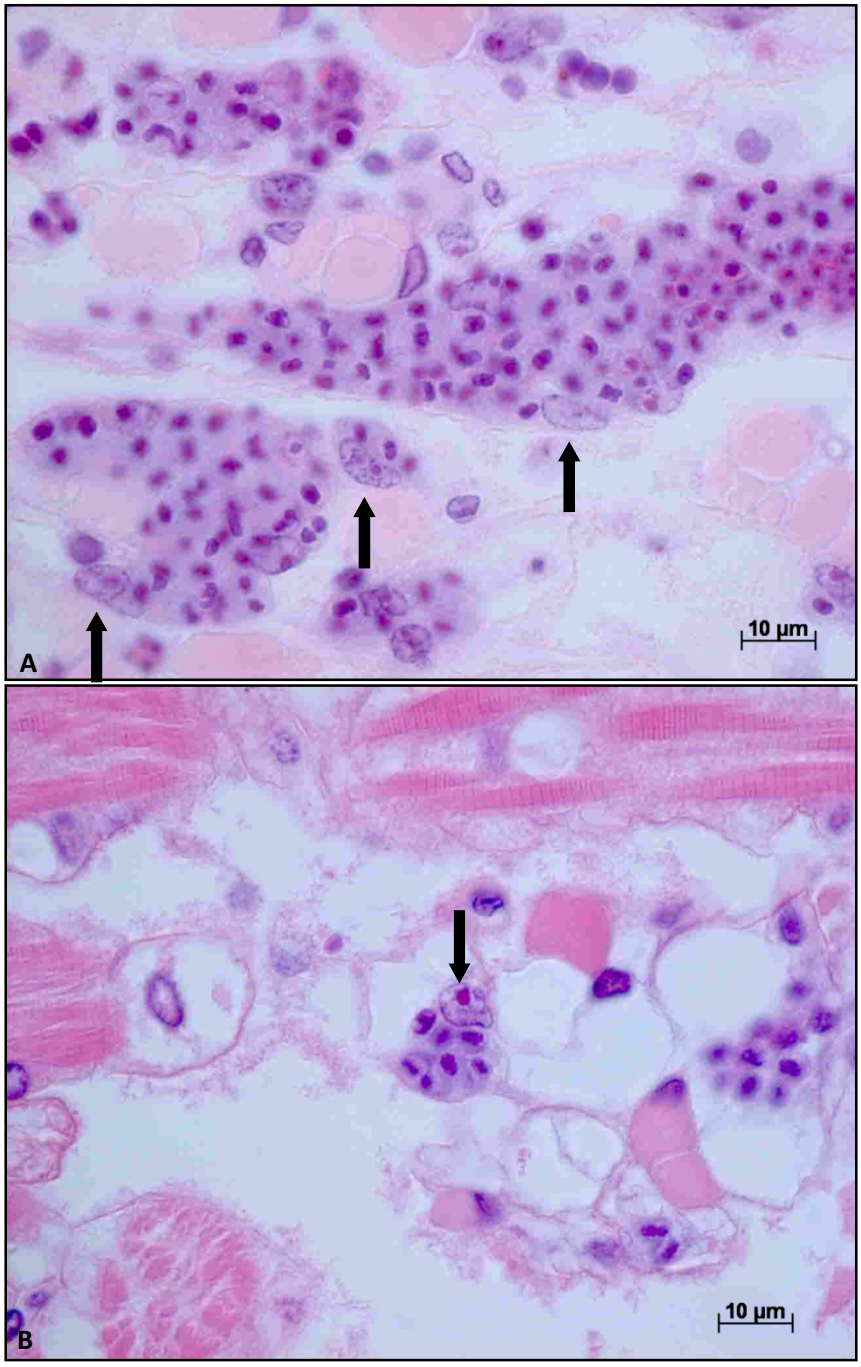

Figure 5.5. Clusters of microsporidial parasites in the interstitial connective tissues of the myocardium. The clusters of parasites were often associated with a peripherally located enlarged (karyomegalic) nucleus with a prominent nucleolus or prominent nucleoli and peripherally marginated chromatin (black arrows). (H&E, 1000x)

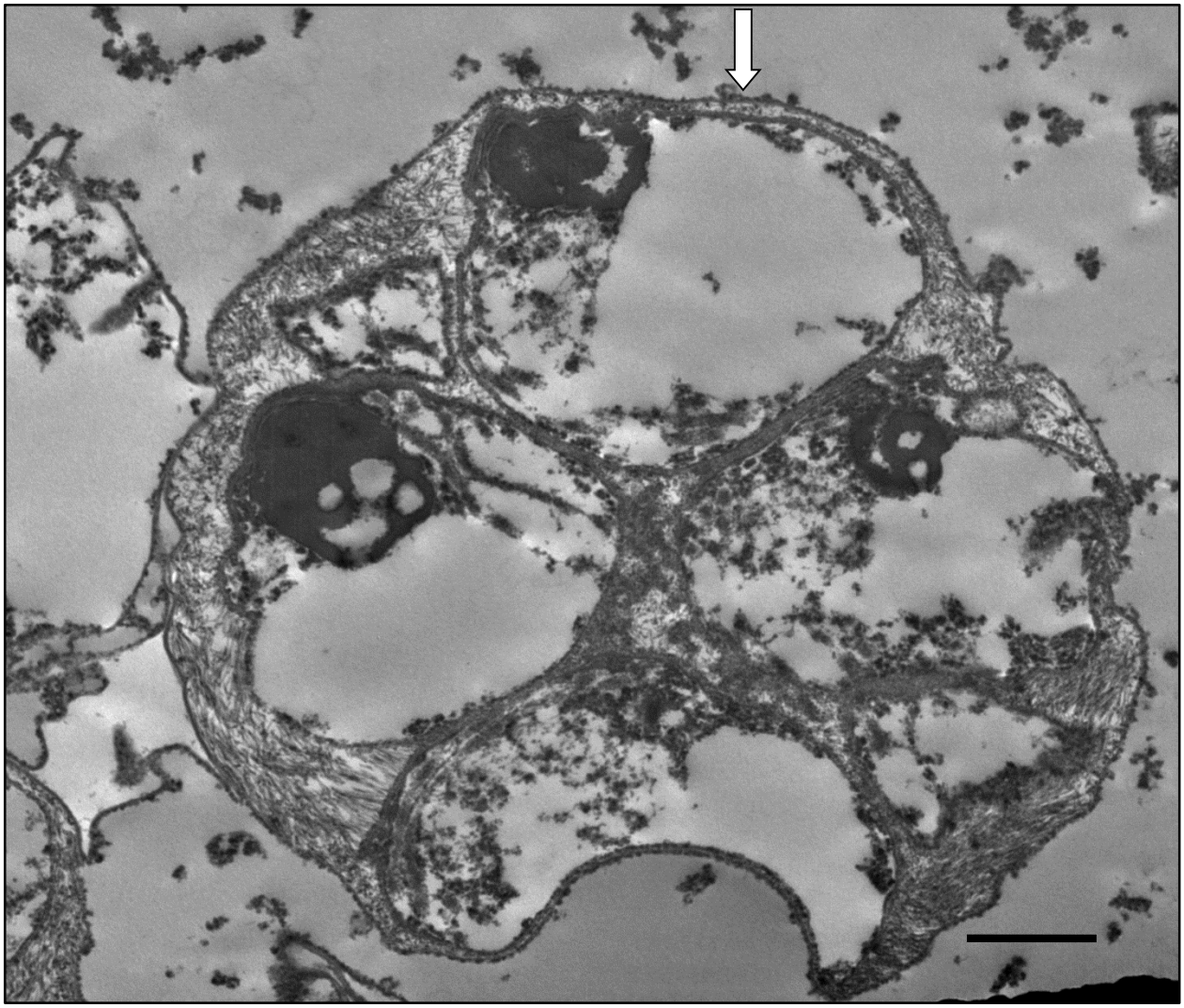

Figure 5.6: Transmission electron microscopic image of a microsporidian tetrad. Note four parasitic cells within an outer limiting membrane (white arrow, sporophorous vesicle or host cell membrane). 10,000x, scale bar = 2 micrometers.

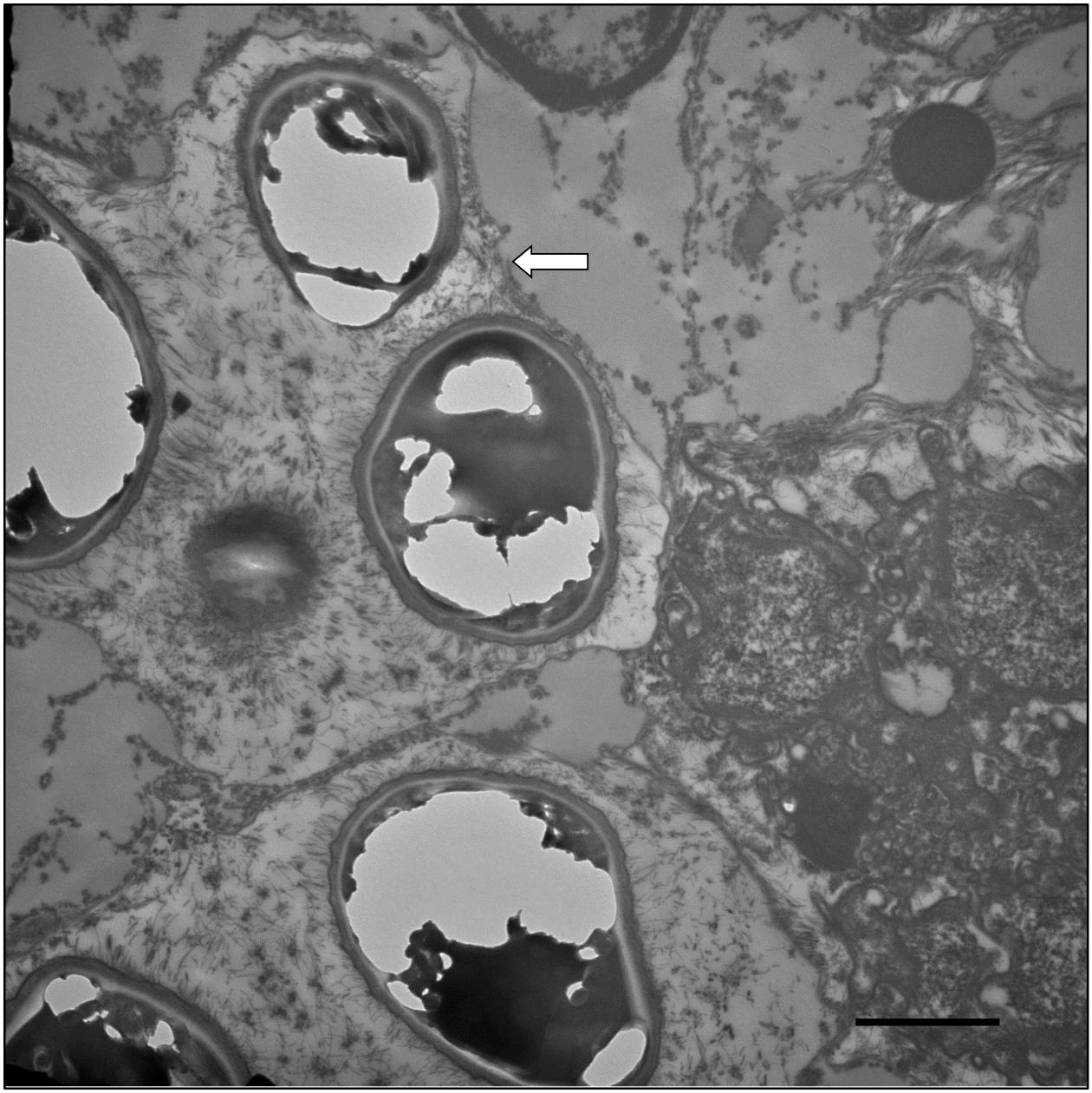

Figure 5.7. Transmission electron microscopic image of microsporidian spores. Note multiple spores within an outer limiting membrane (white arrow, sporophorous vesicle or host cell membrane; 12000x, scale bar = 2 micrometers).

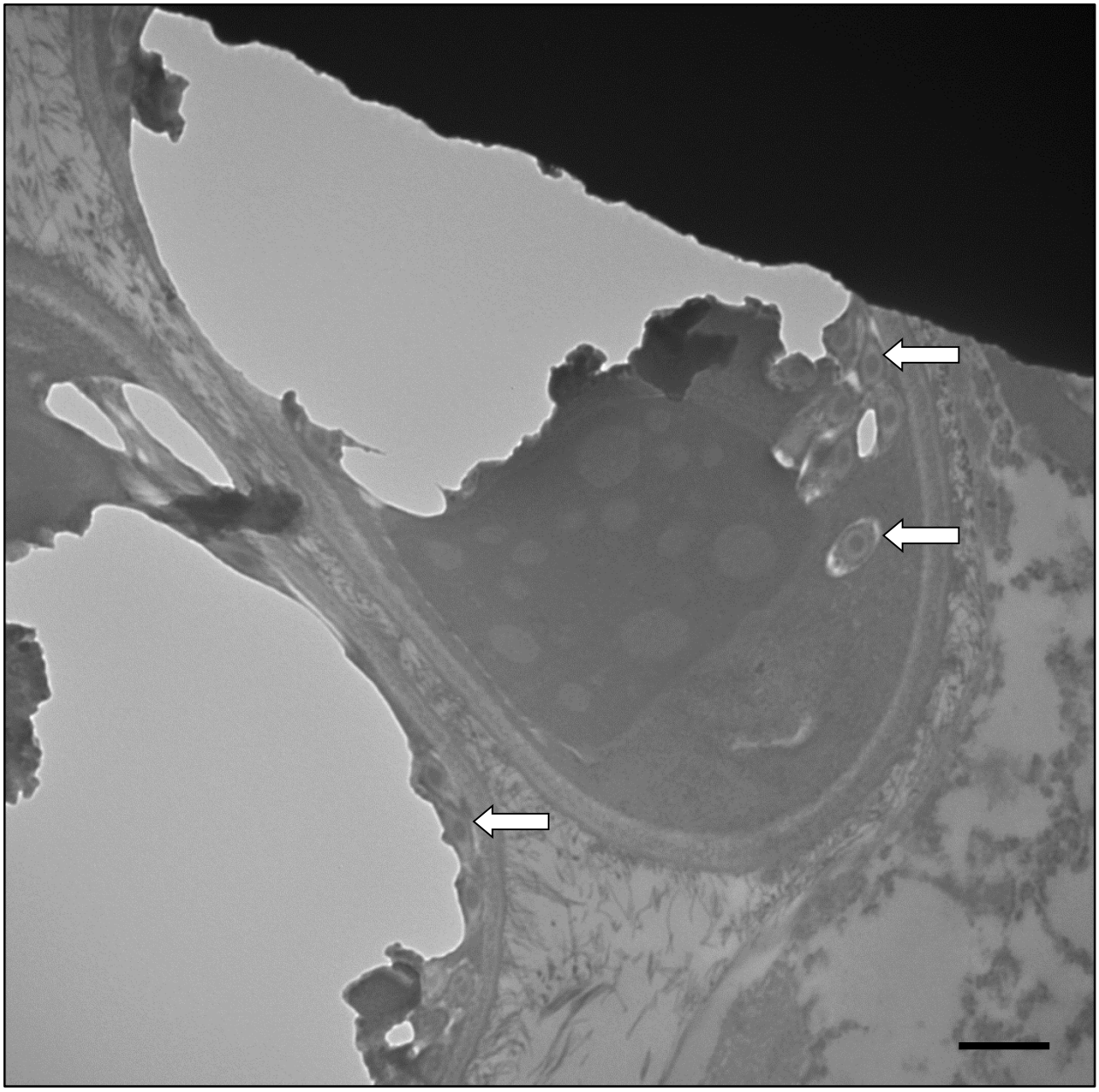

Figure 5.8. Transmission electron microscopic image of microsporidian spores. Note cross-sections and tangential-sections of polar tubes within spores (white arrows, 30,000x, scale bar = 500 nm).

5.3.3. **Epibiota**

5.3.3.1. **Gill Bacterial Fouling**

Examination of the gills revealed gill bacterial fouling that varied in severity from minimal to marked (Figures 5.9 and 5.10). Severity of gill bacterial fouling was significantly different

between bays (Kruskal-Wallis Test: H = 113.66, DF = 2, P = 0.000; Figure 5.18). Gill bacterial fouling was more severe in BB than in NDB (Mann-Whitney Test: W=21755.0, p-value = 0.0000) and WB (Mann-Whitney Test: W=8917.0, p-value = 0.0001), while gill fouling in NDB and WB were not significantly different from one another (Mann-Whitney Test W= 19.0, p-value = 0.8852).

Gill bacterial fouling also varied within bays and strata. In Bonavista Bay snow crabs were collected from a shallow stratum (TN) and a deep stratum (796). Gill bacterial fouling within shallow stratum had a significantly higher median than that observed in the deep stratum (Mann-Whitney Test: W=13535.5, p-value = 0.000; Figure 5.11A). In White Bay, the very deep stratum (Stratum 613) had a significantly lower median of gill bacterial fouling severity median than the median in the combined shallow and deep strata (Strata 614/615; Mann-Whitney Test: W=344.0, p-value = 0.000; Figure 5.11B). (In NDB the snow crabs were all collected as a single group - Strata 610/611.)

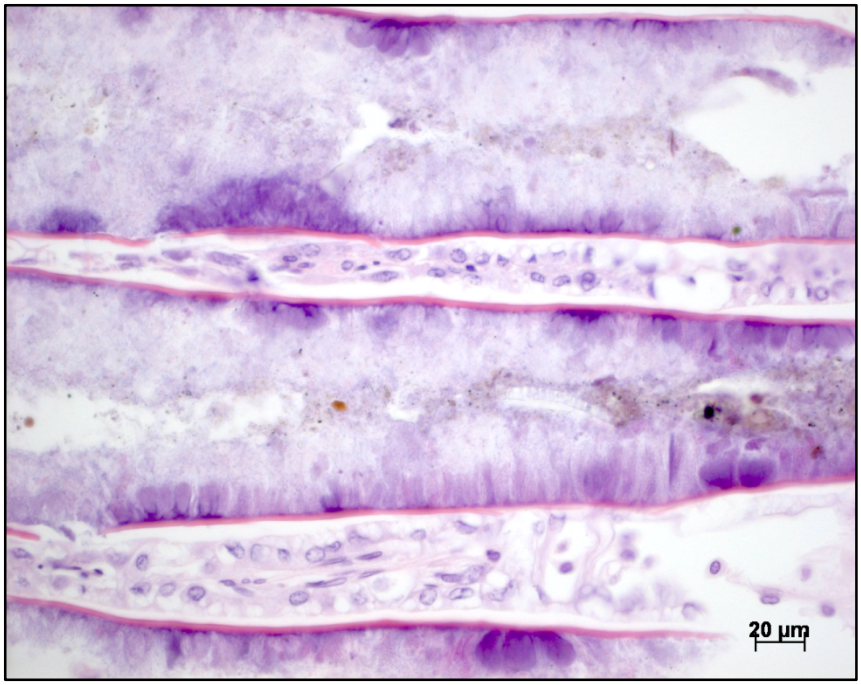

Figure 5.9. Moderate to marked gill bacterial fouling (H&E, 200x).

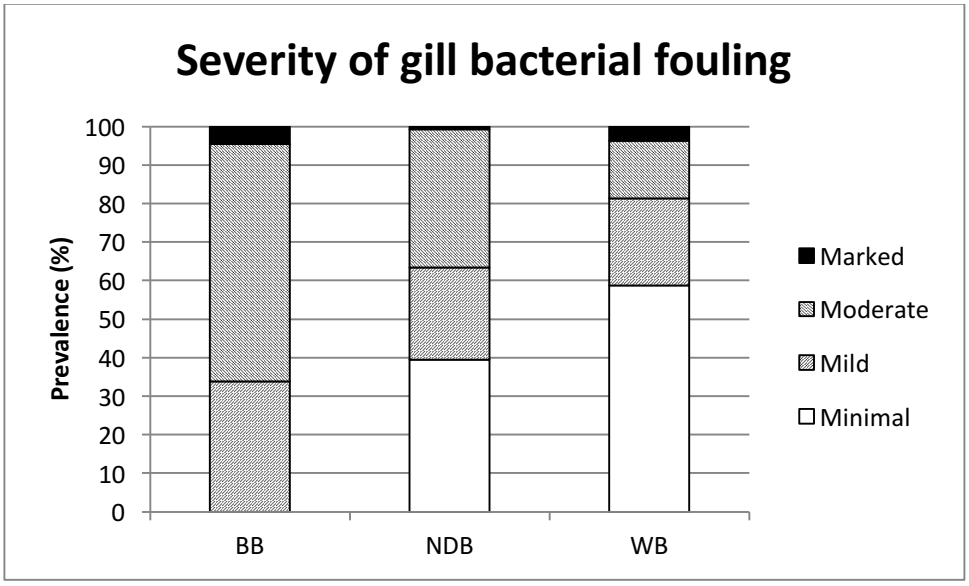

Figure 5.10. Comparison of gill bacterial fouling between bays. Gill bacterial fouling was more severe in Bonavista Bay than in Notre Dame Bay or White Bay.

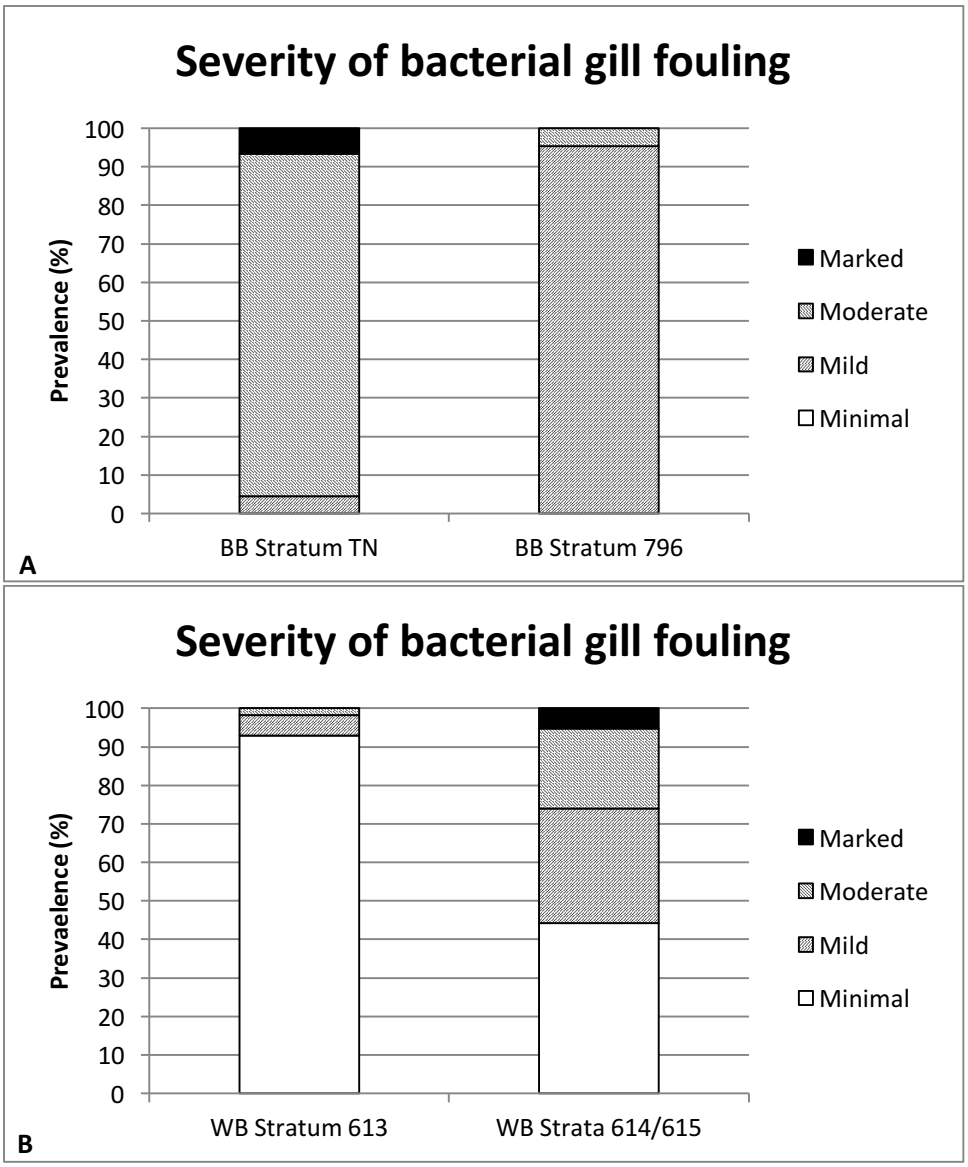

Figure 5.11. Comparison of severity of bacterial gill fouling in strata within Bonavista Bay and White Bay. **A)** The bacterial fouling within Bonavista Bay was more severe in stratum TN (shallow stratum) than in stratum 796 (deep stratum). **B)** The bacterial fouling in White Bay was more severe in strata 614/615 (shallow and deep strata combined) than in stratum 613 (very deep stratum).

5.3.3.2. **Gill Protozoan and Metazoan Epibionts**

Histologic examination of the gills revealed epibiont fouling with amphipods, turbellarian worms, rhabditoid nematodes, and peritrich stalked ciliates (Figure 5.12). The prevalence of

these gill epibionts varied in the populations of snow crabs collected from the three Newfoundland bays. BB had a higher prevalence of amphipods than NDB (Pearson Chi-Square = 94.982, DF = 1, P-Value = 0.000) and WB (Pearson Chi-Square = 95.408, DF = 1, P-Value = 0.000; Table 5.3). BB also had a higher prevalence of peritrich stalked ciliates than NDB (Fisher Exact Test p-value = 0.007) and WB (Fisher Exact Test p-value = 0.010; Table 5.3).

Gill epibiont fouling also varied within bays. In Bonavista Bay, no amphipods were observed in animals collected from stratum 796. All snow crabs collected in stratum 796 were new-shelled animals. When compared to new-shelled animals from BB stratum TN the amphipod prevalence was significantly lower in BB stratum 796 than that observed in BB TN new-shelled snow crabs (Pearson Chi-Square = 46.818, DF = 1, P-Value = 0.000; Table 5.4). There was no significant difference between the prevalence of turbellarian worms (Fisher Exact Test p-value =1.000), rhabditoid nematodes (Fisher Exact Test p-value = 0.192), or peritrich stalked ciliates (Fisher Exact Test p-value = 0.082) in the gills of the snow crabs collected in the two different BB strata (Table 5.4). In White Bay, no amphipods were observed in new-shelled animals collected from stratum 613. When compared to new-shelled animals from WB strata 614/615 the amphipod prevalence was significantly lower in stratum 613 new-shelled animals (Pearson Chi-Square = 9.116, DF = 1, P-Value = 0.003; Table 5.5). There was no significant difference between the prevalence of turbellarian worms (Fisher Exact Test p-value =0.286), rhabditoid nematodes (Fisher Exact Test p-value = 0.325), or peritrich stalked ciliates (Fisher Exact Test p-value = 1.000) in the gills of the snow crabs collected in the two different WB strata (see Table 5.5).

In both bays the amphipod prevalence was higher in the strata with greater severity of gill bacterial fouling. Strata NDB 610/611, WB 614/615 and BB-TN had amphipods. The median gill bacterial fouling severity was significantly higher in snow crabs with amphipods than without amphipods within these strata (Mann-Whitney Test: W=34596.5, p-value = 0.0000). (Note: This was also true within all data (Mann-Whitney Test: W = 64139.0, p-value = 0.0000)). The median gill bacterial fouling severity was also significantly higher in snow crabs with turbellarian worms (strata BBTN, 610/611, 613, and 614/615; Mann-Whitney Test W = 79507.0, p-value = 0.0017) and gill rhabditoid nematodes (strata BBTN, 610-611, and 614/615; Mann-Whitney Test W=59260.5m p-value = 0.0005) than without them. There was no statistically significant association with gill bacterial fouling severity and gill peritrich stalked ciliates (strata BB TN and 614/615; Mann-Whitney Test W = 23416.5, p-value = 0.1701). (Note: If you examine all data together appeared as if peritrich stalked ciliates were associated with bacterial fouling, but this is not the case when the strata were examined independently.)

The prevalence of gill epibionts in histologic sections was largely not significantly different between snow crabs of differing shell categories within each bay. However, BB old-shelled snow crabs had a higher prevalence of turbellarian worms than new-shelled and intermediate-shelled snow crabs (Fisher Exact Test p-values of 0.038 and 0.036, respectively; Table 5.6). NDB intermediate-shelled snow crabs had higher prevalence of amphipods than new-shelled snow crabs (Fisher Exact Test p-value = 0.000; Table 5.7).

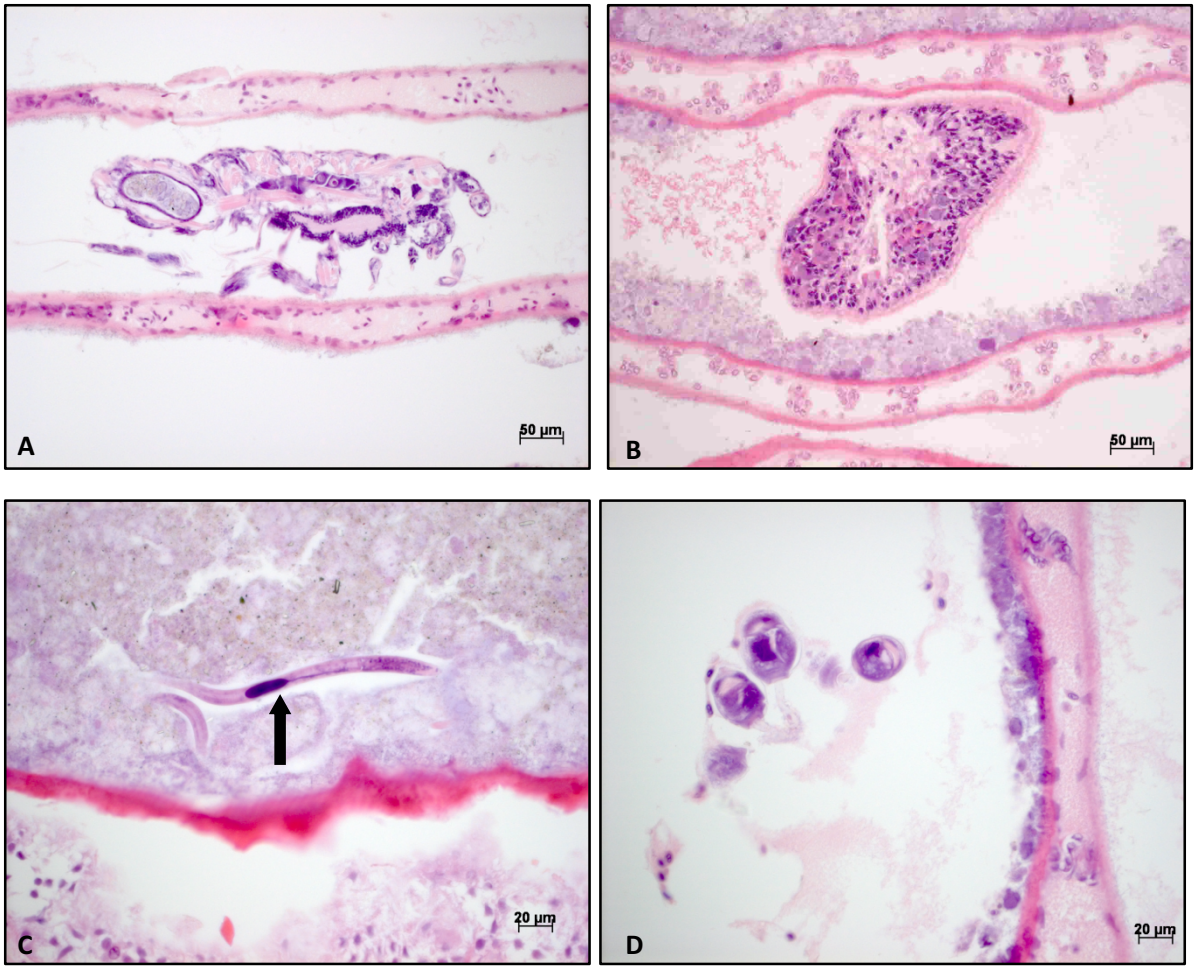

Figure 5.12. Gill protozoan and metazoan epibionts. **A)** Gill amphipods (H&E, 200x). **B)** Gill turbellarian worm (H&E, 200x). **C)** Gill rhabditoid nematodes (H&E, 400x). Note rhabditoid esophagus with corpus leading to a narrow isthmus (black arrow). **D)** Peritrich stalked ciliates (H&E, 400x).

Table 5.3: Prevalence of gill epibionts in snow crabs collected from Bonavista Bay, Notre Dame Bay, and White Bay, Newfoundland.

	BB	NDB	WB	Total
Amphipods	61.7% (82/133)	5.2% (7/134)	10.2% (19/187)	23.8% (108/454)
Turbellarian Worms	4.5% (6/133)	1.5% (2/134)	5.3% (10/187)	4.0% (18/454)
Rhabditoid nematodes	3.0% (4/133)	3.0% (4/134)	2.7% (5/187)	2.9% (13/454)
Peritrich stalked ciliates	5.3% (7/133)	0% (0/134)	0.5% (1/187)	1.8% (8/454)

Table 5.4: Prevalence of gill epibionts in new-shelled snow crabs collected from strata within Bonavista Bay.

	BB Shallow Stratum (TN) New-shelled	BB Deep Stratum (796) New-shelled	p-value
Amphipods	73.5% (25/34)	0 % (0/43)	**0.000**
Turbellarian Worms	2.9% (1/34)	2.3% (1/43)	1.000
Rhabditoid nematodes	5.9% (2/34)	0 % (0/43)	0.192
Peritrich stalked ciliates	8.8% (3/34)	0 % (0/43)	0.082

Table 5.5: Prevalence of gill epibionts in new-shelled snow crabs collected from strata within White Bay.

	WB Shallow Stratum (613) New-shelled	WB Deep Strata (614/615) New-shelled	p-value
Amphipods	0% (0/56)	14.6 % (19/130)	**0.003**
Turbellarian Worms	1.8% (1/56)	0 % (9/130)	0.286
Rhabditoid nematodes	0% (0/56)	0 % (5/130)	0.325
Peritrich stalked ciliates	0% (0/56)	0 % (1/130)	1.000

Table 5.6: Prevalence of gill epibionts in BB stratum TN by shell condition category.

	BB TN New-shelled	BB TN Intermediate	BB TN Old-shelled
Amphipods	73.5% (25/34)	88.2% (45/51)	100% (5/5)
Turbellarian Worms	2.9% (1/34)	3.9% (2/51)	40% (2/5)
Rhabditoid nematodes	5.9% (2/34)	2.0% (1/51)	20% (1/5)
Peritrich stalked ciliates	8.8% (3/34)	7.8% (4/51)	0% (0/5)

Note: BB stratum 796 was composed entirely of new-shelled animals and thus was not included in this comparison.

Table 5.7: Prevalence of gill epibionts in NDB by shell condition category.

	NDB New-Shelled	NDB Intermediate	p-value
Amphipods	6.0 % (7/116)	61.1% (11/18)	**0.000**
Turbellarian Worms	1.7 % (2/116)	5.6% (1/18)	0.354
Rhabditoid nematodes	3.4 % (4/116)	11.1% (2/18)	0.184
Peritrich stalked ciliates	0 % (0/116)	0% (0/18)	1.000

Note: Gill not done (ND) in single NDB old-shelled snow crab.

Table 5.8: Prevalence of gill epibionts in WB Stratum 614/615 by shell condition category.

	WB 614/615 New-Shelled	WB 614/615 Intermediate	p-value
Amphipods	14.6% (19/130)	0% (0/1)	0.679
Turbellarian Worms	6.9% (9/130)	0% (0/1)	0.785
Rhabditoid nematodes	3.8% (5/130)	0% (0/1)	0.842
Peritrich stalked ciliates	0.8% (1/130)	0% (0/1)	0.930

Note: WB stratum 613 was composed entirely of new-shelled animals and thus was not included in this comparison.

5.3.3.3. Cuticular Protozoan and Metazoan Epibionts

Histologic examination of the cuticle over the abdomen and proximal aspect of the merus revealed several epibionts. First, turbellarian worms similar to those observed in the gills were observed on the abdominal carapace. In addition, eggs were occasionally adhered to the abdominal cuticle and transition from an undifferentiated egg mass to a turbellarian juvenile worm was observed within those eggs (Figure 5.13). BB had a higher prevalence of turbellarian worms over its carapace than NDB (Pearson Chi-Square = 12.847, DF = 1, P-Value = 0.000) and WB snow crabs (Pearson Chi-Square = 12.998, DF = 1, P-Value = 0.000; Table 5.9). BB had a lower prevalence of turbellarian eggs than the other two bays; this difference was not statistically significant (Pearson Chi-Square = 5.211, DF = 2, P-Value = 0.074).

Clusters of leech eggs were observed in a few male snow crabs from BB stratum 796 (n=4). Leech eggs were not observed in animals from NDB or WB. The dark brown, oval leech eggs (~1.5 x 1 mm) were found on the ventral aspect of the 1st and/or 2nd merus of the walking legs (Figure 5.14). The prevalence was not statistically significantly higher in BB as compared to NDB (Fisher Exact Test p-value = 0.053). The prevalence in BB was significantly higher than in WB (Fisher Exact Test p-value = 0.027; Table 5.9).

Rhabditoid worms similar to those observed in the gill epibiont fouling were occasionally observed within areas of cuticular erosion (Figure 5.15). Rhabditoid worms were seen within cuticular ulcers only in BB-TN and Strata 610/611 (NDB). There was no significant difference in the prevalence of rhabditoid worms in these two regions (Fisher Exact Test p-value = 0.266). The prevalence in WB was significantly lower than that seen in BB (Fisher Exact Test p-value = 0.011) and was not significantly lower than the prevalence in NDB (Fisher Exact Test p-value = 0.180). The median gill bacterial fouling severity was not significantly different for animals with or without rhabditoid worms within cuticular erosions (W = 24207.5, p-value = 0.1744).

Clusters of larger nematodes worms were observed along the internal surface of the abdominal cuticle in both male and female snow crabs (Figure 5.16). No evidence of egg damage (as could be induced by predation by the nematodes) was observed in gravid female snow crabs. The prevalence of these nematodes was higher in snow crabs collected from NDB than in BB snow crabs (Pearson Chi-Square = 4.890, DF = 1, P-Value = 0.027) and WB snow crabs (Pearson Chi-Square = 15.536, DF = 1, P-Value = 0.000). The median gill bacterial fouling was significantly higher in snow crabs with abdominal nematodes than without abdominal nematodes (Mann Whitney Test: W=71531.5, p-value = 0.0315).

Two types of colonial invertebrate organisms were observed histologically. The first colonial organism observed was a colonial hydrozoan that occurs over the external (ventral) aspect of the abdominal cuticle (Figure 5.17). Snow crabs from BB had a higher prevalence of colonial hydrozoans than NDB (Pearson Chi-Square = 24.880, DF = 1, P-Value = 0.000) and WB Pearson

Chi-Square = 47.723, DF = 1, P-Value = 0.000). The second colonial invertebrate observed was an encrusting bryozoan (Figure 5.18 and 5.19). Snow crabs from BB also had higher prevalence of encrusting bryozoans than NDB (Pearson Chi-Square = 8.076, DF = 1, P-Value = 0.004) although the difference in prevalence was not statistically significant when compared to the prevalence in WB (Pearson Chi-Square = 2.213, DF = 1, P-Value = 0.137). A higher median severity of gill bacterial fouling was seen snow crabs with than without colonial hydrozoans (Mann-Whitney Test: W=65777.5, p-value = 0.0000) and this association also occurred with encrusting bryozoans (Mann-Whitney Test: W=47152.0, p-value = 0.0112).

Significant differences were not observed between BB-TN and BB-796 for the prevalence of turbellarian worms, turbellarian eggs, leech eggs, rhabditoid nematodes within cuticular erosions, or nematodes along the internal abdomen (Table 5.10). Prevalence was higher in the shallower BB stratum (BB-TN) than in the deeper stratum for both the colonial hydrozoan (Pearson Chi-Square = 10.383, DF = 1, p-value = 0.001) and encrusting bryozoan (Pearson Chi-Square = 21.598, DF = 1, P-Value = 0.000). The only significant difference observed between WB 613 and WB 614/615 was in the encrusting bryozoans where the shallow stratum had a significantly higher prevalence than the deep strata (Pearson Chi-Square = 24.474, DF = 1, p-value = 0.000; Table 5.11). Differences in prevalence between additional shipments within bays were also noted (data not shown).

Epibiont prevalence also varied with shell condition category within NL strata (Tables 5.12 – 5.14). The only significant differences in gill cuticular epibiont prevalence with varying shell

condition category were noted in NDB snow crabs. Intermediate-shelled NDB snow crabs had statistically significantly more snow crabs with nematodes along the internal margin of their abdominal cuticle (Fisher's exact two-tailed p-value = 0.001) and more individuals with encrusting bryozoans (Pearson Chi-Square = 5.225, DF = 1, P-Value = 0.022) in histologic sections than new-shelled NDB snow crabs. No significant differences in cuticular epibiont prevalence were observed between old-shelled NDB snow crabs and snow crab with new- or intermediate-categories of shell fouling (old shelled NDB snow crab n=1).

No significant differences were noted in cuticular epibiont prevalence in differing shell condition categories in snow crabs collected within stratum TN in BB or WB (intermediate-shelled WB snow crab n = 1 and no old-shelled snow crabs were collected in WB).

Table 5.9: Comparison of prevalence of cuticular epibionts in snow crabs collected from Bonavista Bay, Notre Dame Bay, and White Bay, Newfoundland.

	BB	NDB	WB	Total
Turbellarian worms	10.5% (14/133)	0.7% (1/142)	1.5% (3/192)	3.8% (18/467)
Turbellarian eggs	3.0% (4/133)	9.9% (14/142)	6.8% (13/192)	6.6% (31/467)
Leech eggs	3.0% (4/133)	0% (0/142)	0% (0/192)	0.6% (3/467)
Rhabditoid nematodes (cuticular ulcers)	3.8% (5/133)	1.4% (2/142)	0% (0/192)	1.5% (7/467)
Nematodes along internal abdomen	6.0% (8/133)	14.1% (20/142)	2.6% (5/192)	7.1% (33/467)
Colonial hydrozoan	24.1% (32/133)	3.5% (5/142)	0.5% (1/192)	8.1% (38/467)
Encrusting bryozoan	59.4% (79/133)	42.2% (60/142)	51.0% (98/192)	50.7% (237/467)

Table 5.10: Comparison of prevalence of cuticular epibionts in snow crabs collected from strata within Bonavista Bay

	BB Shallow Stratum (TN) New-shelled	**BB Deep Stratum (796) New-shelled**	**p-value**
Turbellarian worms	2.9% (1/34)	2.3% (1/43)	1.000
Turbellarian eggs	5.9% (2/34)	4.6% (2/43)	1.000
Leech eggs	0% (0/34)	9.3% (4/43)	0.125
Rhabditoid nematodes (cuticular ulcers)	5.9% (2/34)	0% (0/43)	0.192
Nematodes along internal abdomen	5.9% (2/34)	4.6% (2/43)	1.000
Colonial hydrozoan	32.3% (11/34)	4.6% (2/43)	**0.001**
Encrusting bryozoan	76.5% (26/34)	23.2% (10/43)	**0.000**

Table 5.11: Comparison of prevalence of cuticular epibionts in snow crabs collected from different strata within White Bay.

	WB Stratum 613 New-shelled	**WB Strata 614/615 New-shelled**	**p-value**
Turbellarian worms	0% (0/56)	2.2% (3/135)	0.557
Turbellarian eggs	1.8% (1/56)	8.2% (11/135)	0.186
Leech eggs	0% (0/56)	0% (0/135)	1.000
Rhabditoid nematodes (cuticular ulcers)	0% (0/56)	0% (0/135)	1.000
Nematodes along internal abdomen	0% (0/56)	3.7% (5/135)	0.324
Colonial hydrozoan	0% (0/56)	0.7% (1/135)	1.000
Encrusting bryozoan	78.6% (44/56)	39.3% (53/135)	**0.000**

Table 5.12: Comparison of prevalence of cuticular epibionts in snow crabs collected from Bonavista Bay stratum TN by shell condition category.

	BB TN New-shelled	**BB TN Intermediate**	**BB TN Old-shelled**
Turbellarian worms	2.9% (1/34)	13.7% (7/51)	20% (1/5)
Turbellarian eggs	5.9% (2/34)	0% (0/51)	0% (0/5)
Rhabditoid nematodes (cuticular ulcers)	5.9% (2/34)	5.9% (3/51)	0% (0/5)
Nematodes along internal abdomen	5.9% (2/34)	7.8% (4/51)	0% (0/5)
Leech eggs	0% (0/34)	0% (0/51)	0% (0/5)
Colonial hydrozoan	32.3% (11/34)	47.1% (24/51)	40% (2/5)
Encrusting bryozoan	76.5% (26/34)	78.4% (40/51)	60% (3/5)

Table 5.13: Comparison of prevalence of cuticular epibionts in snow crabs collected from Notre Dame Bay by shell condition category.

	NDB New-Shelled	NDB Intermediate	NDB Old-shelled
Turbellarian worms	0.8% (1/123)	0% (0/18)	0% (0/1)
Turbellarian eggs	8.1% (10/123)	22.2% (4/18)	0% (0/1)
Rhabditoid nematodes (cuticular ulcers)	0.8% (1/123)	5.6% (1/18)	0% (0/1)
Nematodes along internal abdomen	9.8% (12/123)	44.4% (8/18)	0% (0/1)
Leech eggs	0% (0/123)	0% (0/18)	0% (0/1)
Colonial hydrozoan	2.4% (3/123)	11.1% (2/18)	0% (0/1)
Encrusting bryozoan	38.2% (47/123)	66.7% (12/18)	100% (1/1)

Table 5.14: Comparison of prevalence of cuticular epibionts in snow crabs collected from White Bay strata 614/615 by shell condition category.

	WB 614/615 New-Shelled	WB 614/615 Intermediate	p-value
Turbellarian worms	2.2% (3/135)	0% (0/1)	1.000
Turbellarian eggs	8.1% (11/135)	100% (1/1)	0.088
Rhabditoid nematodes (cuticular ulcers)	0% (0/135)	0% (0/1)	1.000
Nematodes along internal abdomen	3.7% (5/135)	0% (0/1)	1.000
Leech eggs	0% (0/135)	0% (0/1)	1.000
Colonial hydrozoan	0.7% (1/135)	0% (0/1)	1.000
Encrusting bryozoan	39.3% (53/135)	100% (1/1)	0.397

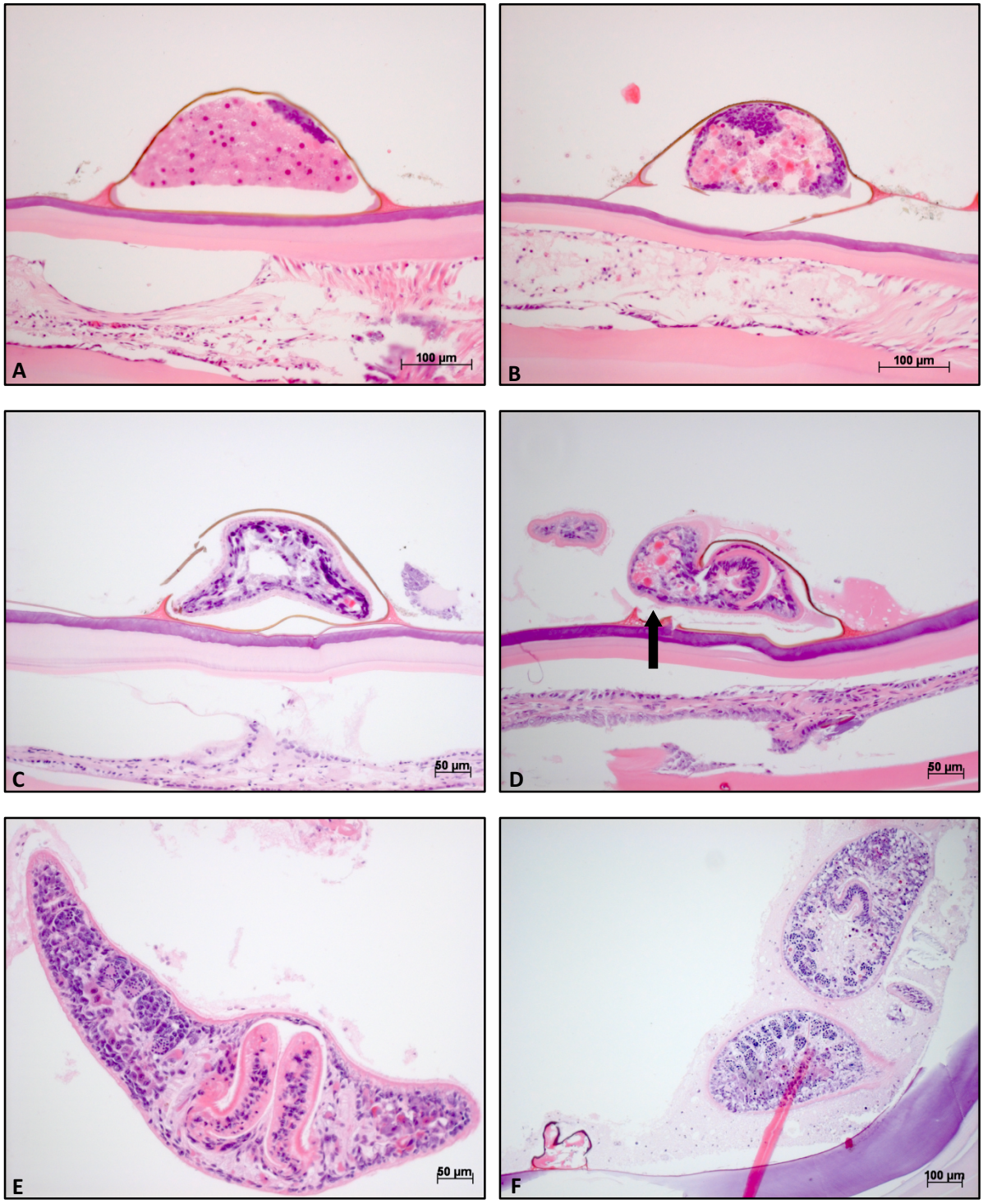

Figure 5.13. Turbellarian life stages on the snow crab abdominal carapace**. A-B)** Eggs on the carapace contained a developing morula (H&E, 200x**). C-D)** Eggs which contained developing or emerging (D, black arrow) juvenile worms (H&E, 200x). **E-F)** Adult turbellarians with reproductive tissue observed over the abdominal carapace (H&E, 200x and 100x, respectively).

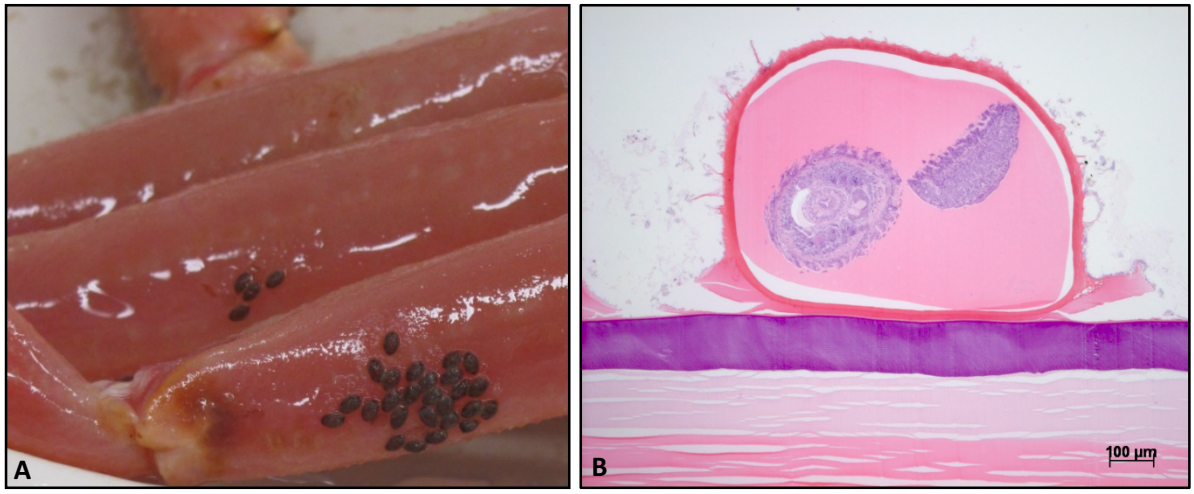

Figure 5.14. Leech eggs. **A)** Macroscopic image of leech eggs on the ventral surface of the merus of the 1st and 2nd walking legs. **B)** Microscopic image of a developing leech within an egg (100x, H&E).

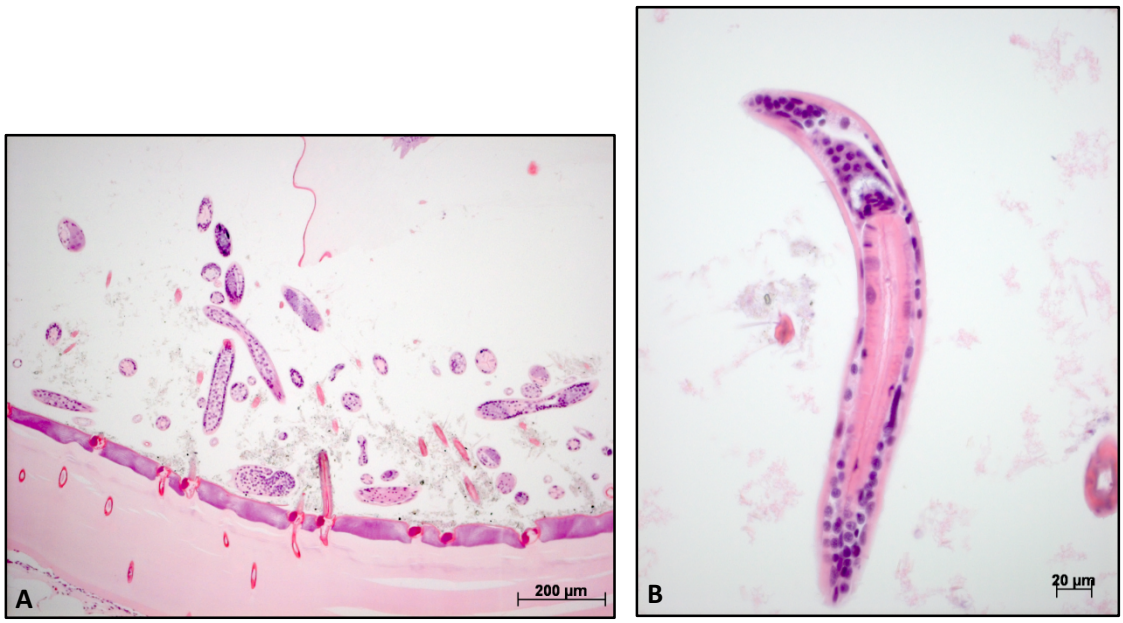

Figure 5.15. Nematodes along the internal margin of the abdominal carapace**. A)** Nematodes admixed with abdominal setae along the internal margin of the abdominal cuticle (H&E, 100x). **B)** Higher magnification of a representative nematode, with an outer cuticle, hypodermal nuclei, and a thick muscular esophagus. No reproductive tissue was observed within the nematodes along the internal margins of the snow crabs' abdomens (H&E, 400x).

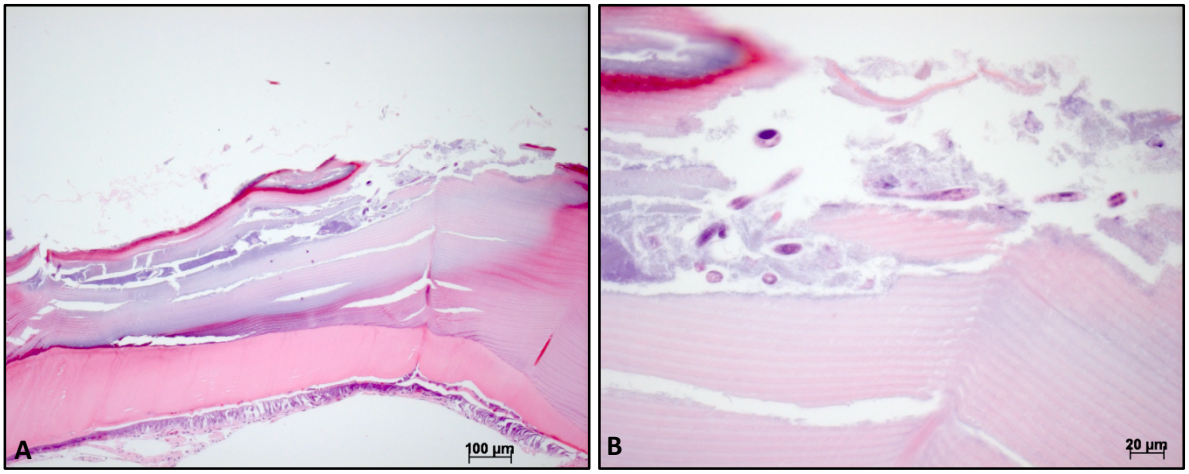

Figure 5.16. Cuticular ulcer with intralesional rhabditoid nematodes at low-power (A; H&E, 100x) and high-power magnification (B; H&E, 400x).

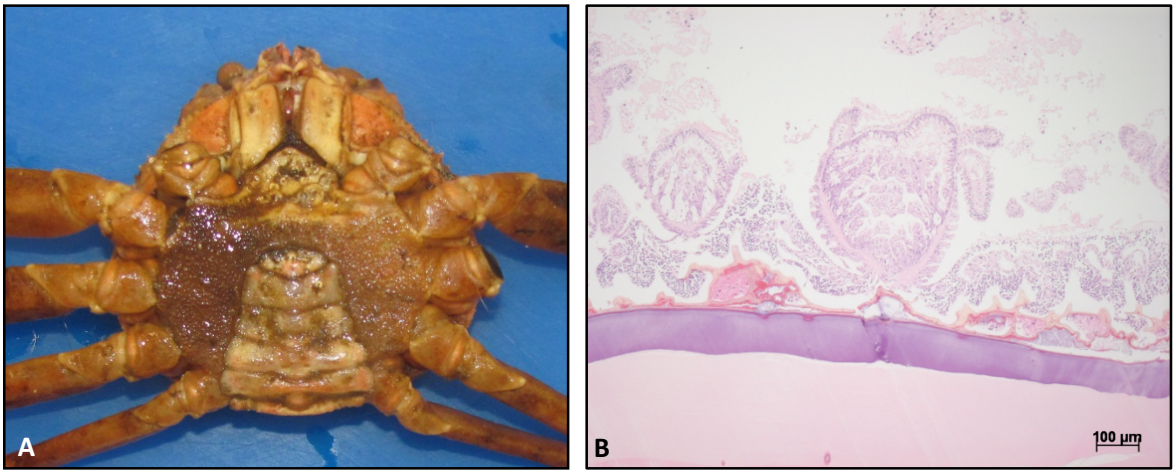

Figure 5.17. Gross (A) and histological appearance (B) of colonial hydrozoan (H&E, 200x). Note the gelatinous gross appearance of the hydrozoan colonies located along the snow crab's ventrum.

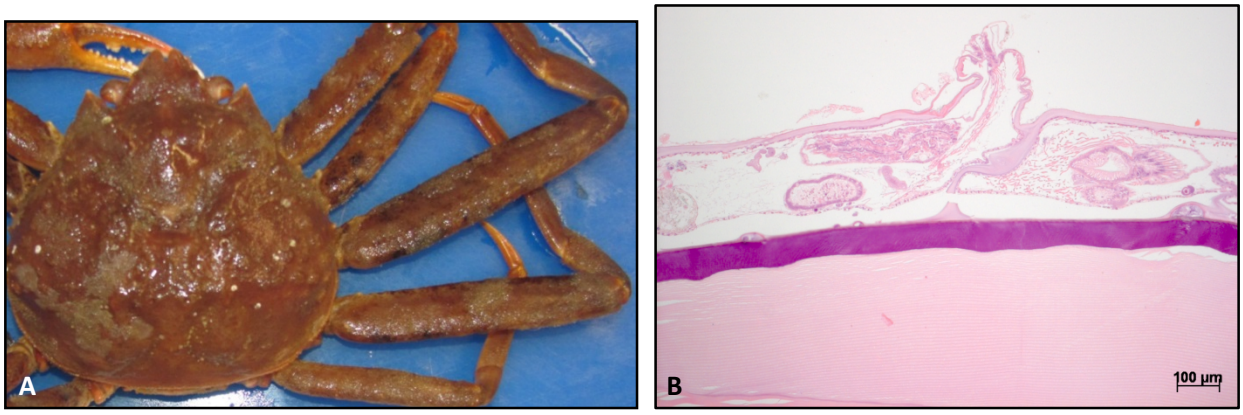

Figure 5.19. Gross (A) and histological appearance (B) of colonial encrusting bryozoan (H&E, 200x). Note the generalized distribution of the encrusting bryozoan on the carapace and legs of the snow crab.

Figure 5.19. Encrusting bryozoan sectioned along the frontal plane. Note polygonal shape of the bryozoan zooids and the longitudinal and tangential sections of retracted lophophores, the bryozoan feeding organ (black arrows; 100x, H&E).

5.3.3.4. **Internal metazoan parasite**

A single cross-section of a platyhelminthes (trematode) worm was observed within a single male (CW=111mm) snow crab (Figure 5.20). The identity (genus/species) of this platyhelminthes worm was unclear.

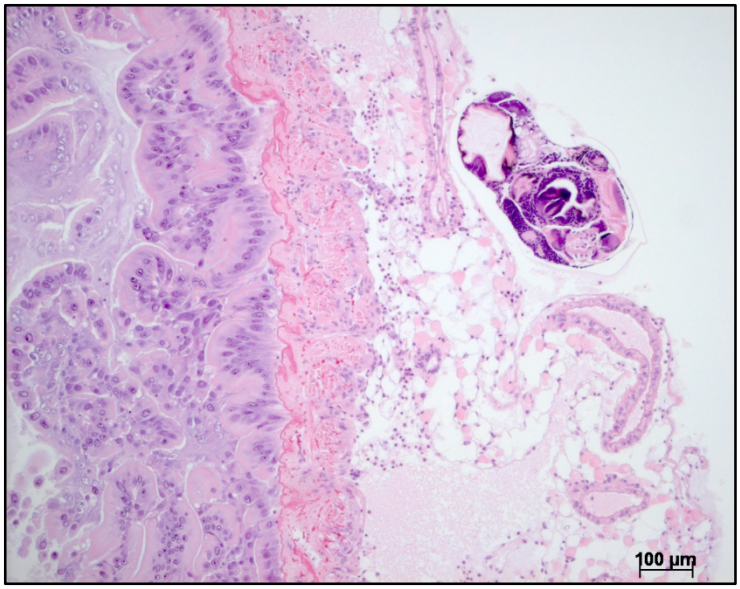

Figure 5.20. Platyhelminthes (trematode) worm observed adjacent to the midgut of a single snow crab (H&E, 100x).

5.3.4. **Inflammatory Patterns**

Two patterns of necrotizing enteritis were observed. The first pattern was necrotizing enteritis in the non-chitinized epithelium of the midgut (Figure 5.21). This pattern of inflammation was uncommon, but was most prevalent in snow crabs collected from BB stratum 796. Second, ulceration of the non-chitinized epithelium at the level of the midgut-hindgut junction was observed (Figure 5.22). This pattern of inflammation was occasionally accompanied by extension of hemocytic inflammation into the underlying tegumental glands as hemocytic aggregates or (more rarely) melanized nodules (Figure 5.23). Occasional randomly scattered hemocytic aggregates and melanized nodules (1 or 2 per animal) were also occasionally noted within tissues and were most commonly observed in the gill (Figure 5.24; Table 5.15). Round structures were seen within a single gill hemocytic nodule (Figure 5.24). Unfortunately, the gill nodule was not present in serial sections of this tissue and TEM of the slice of tissue on the

stained slide did not reveal any foreign organisms (data not shown) suggesting that these structures may have represented rounded-up host hemocytes.

The median severity of midgut necrotizing enteritis in BB snow crabs was significantly higher than that observed in NDB snow crabs (Mann-Whitney Test: W=19873.0, P-value = 0.0000) and WB snow crabs (Mann-Whitney Test: W = 23594.0, p-value = 0.0000; Figure 5.25). The median severity of junctional ulceration in BB snow crabs was significantly higher than that observed in NDB snow crabs (Mann-Whitney Test: W=19765.0, p-value = 0.0005). The difference was not statistically significant when compared to WB snow crabs (Mann-Whitney Test: W=22610.0, p-value = 0.0962; Figure 5.26).

When the shallow (stratum TN) and deep (stratum 796) strata were compared within Bonavista Bay, the prevalence of midgut necrotizing enteritis was much higher in snow crabs collected from stratum 796 than stratum TN (Fisher Exact Test p-value = 0.000; Table 5.16). The single case of necrotizing enteritis in stratum TN was mild with much higher median severity of necrotizing enteritis observed in BB 796 snow crabs (Mann-Whitney Test: W= 5052.0, p-value = 0.0000; Figure 5.27). In contrast, when junctional ulceration was compared between the two strata there was no difference in prevalence (Fisher Exact Test p-value = 1.000; Table 5.16) or severity of junctional ulceration (Mann-Whitney Test: W=6117.0, p-value = 0.5691; Figure 5.28). No significant difference was observed in the prevalence of hemocytic nodules between the two BB strata; a higher prevalence of corneal ulcers was observed in BB TN snow crabs (Fisher Exact Test = 0.034). There was no difference noted in prevalence of the different patterns of

inflammation observed between stratum 613 (shallow) and strata 614/615 in White Bay (Table 5.17). Similarly, there was no difference observed in the severity of necrotizing enteritis or junctional ulceration between the shallow and deep strata (Figures 5.29 and 5.30).

When the prevalence of inflammation was compared between snow crabs with different shell condition categories (new, intermediate, and old shells) were compared, the only difference observed was that the junctional ulcers in BB TN snow crabs tended to be more severe in intermediate-shelled snow crabs than in new-shelled snow crabs; this difference was not statistically significant (Mann-Whitney Test: W=5208.5, p-value = 0.0586; Table 5.18 and Figure 5.31). No significant differences in the prevalence of different patterns of inflammation by shell conditions were observed in BB TN snow crabs, NDB snow crabs, or WB snow crabs (Tables 5.19 and 5.20). No difference was seen in the median severity of junctional ulcers between new-shelled and intermediate-shelled NDB snow crabs (Mann-Whitney Test: W=8690.0, p-value = 0.5723; Figure 5.32).

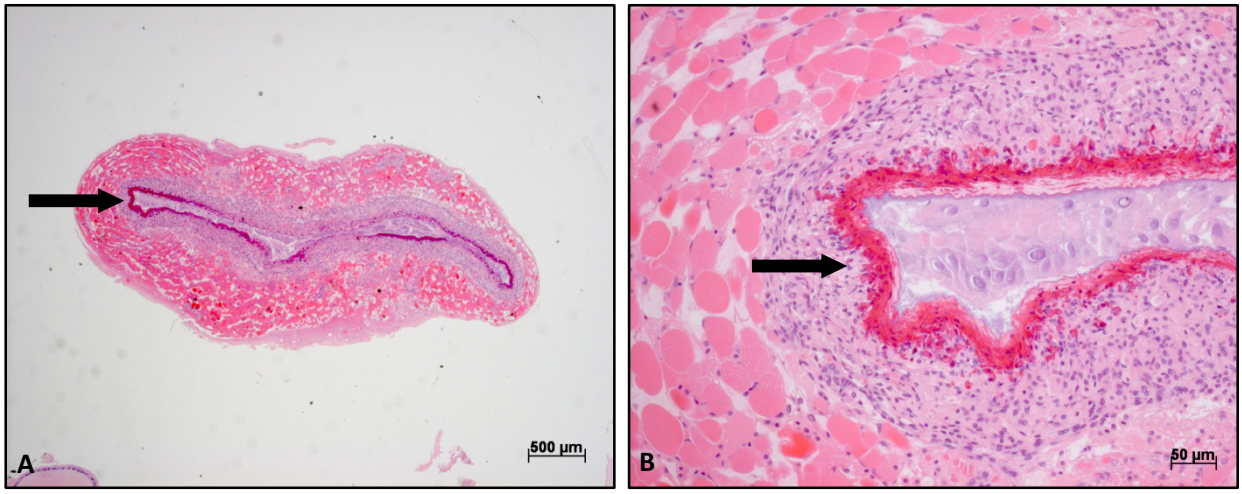

Figure 5.21. Midgut necrotizing enteritis at low (A) and high (B) magnification (H&E, 25x and 200x, H&E). Note the band of brightly eosinophilic infiltrating hemocytes (arrows).

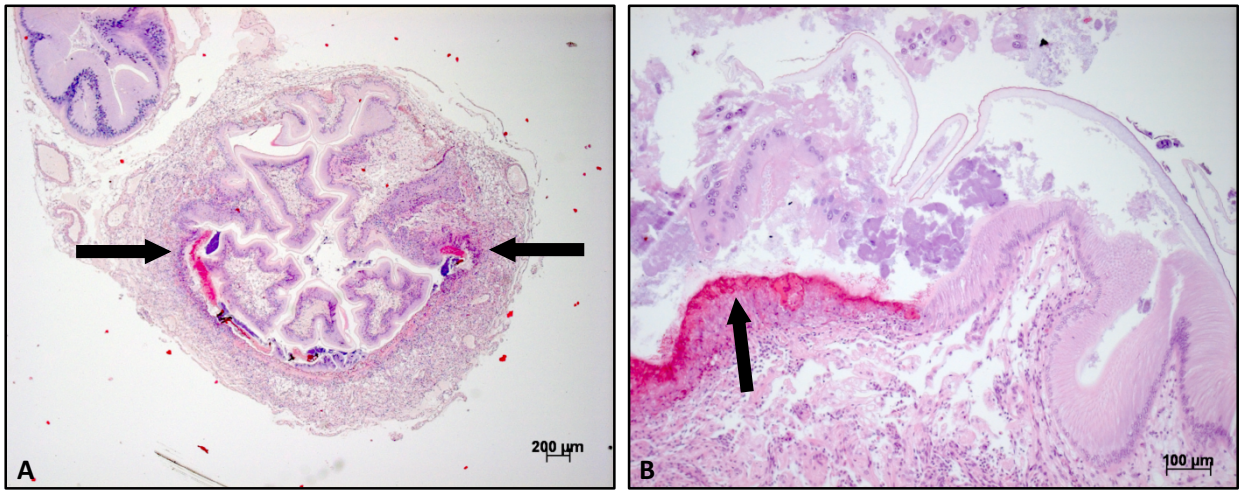

Figure 5.22. Midgut-hindgut junctional ulcerative enteritis at low (A) and high (B) magnification (H&E, 25x and 200x). Note the locally extensive regions of brightly eosinophilic infiltrating hemocytes (arrows).

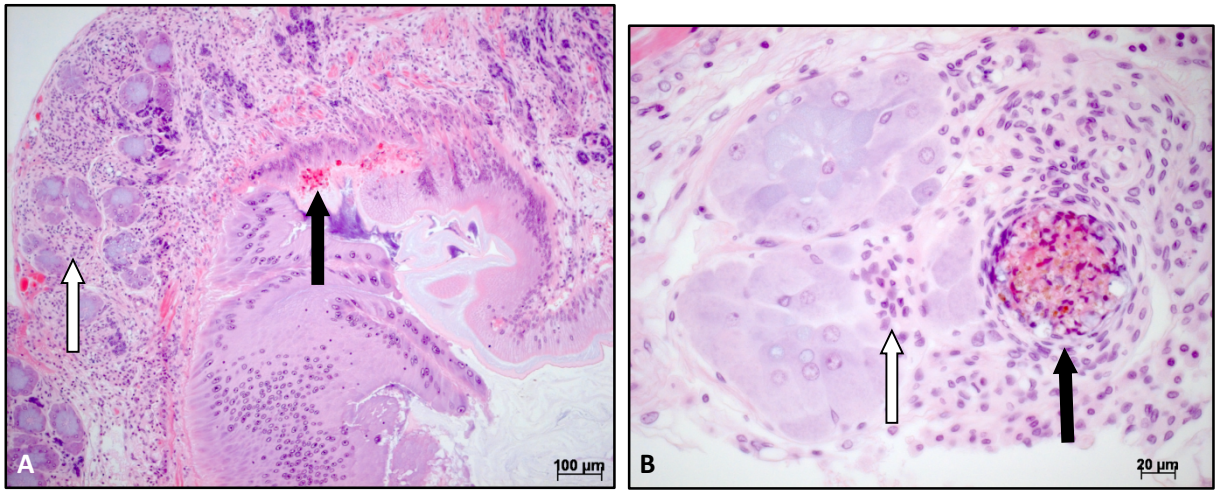

Figure 5.23. Tegumental gland adenitis at low magnification (A) and high magnification (B). **A)** Tegumental gland adenitis (white arrow) with minimal junctional hemocytic infiltration (black arrow; 10x, H&E). **B)** Tegumental adenitis (white arrow) with a melanized nodule (black arrow; 400x, H&E).

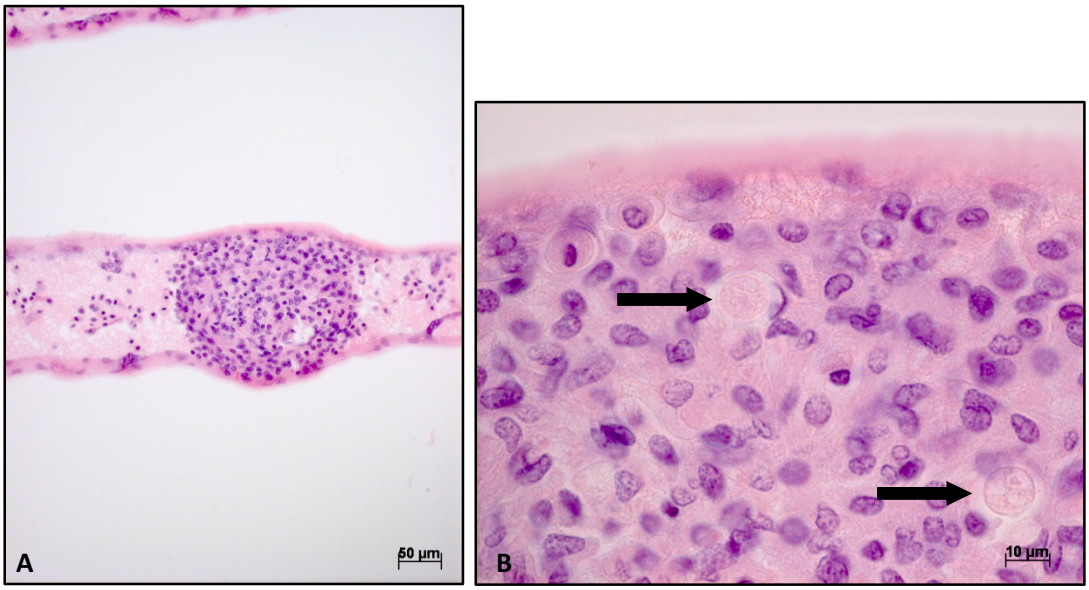

Figure 5.24. Gill hemocytic nodule at low (A) and high (B) magnification (200x and 1000x, H&E). Note intralesional round structures in high magnification (b) photomicrograph (arrows).

Table 5.15: Comparison of prevalence of the different patterns of inflammation in snow crabs collected from Bonavista Bay, Notre Dame Bay, and White Bay.

	BB	NDB	WB	Total
Midgut necrotizing enteritis	10.5% (14/133)	1.4% (2/142)	2.1% (4/192)	4.3% (20/467)
Midgut-hindgut* junction ulcers	49.2% (30/61)	18.0% (11/61)	40.8% (29/71)	32.6% (70/193)
Midgut-hindgut junction tegumental gland adenitis	18.0% (11/61)	36.0% (22/61)	40.8% (29/71)	32.1% (62/193)
Hemocytic aggregates and nodules	7.5% (10/133)	9.2% (13/142)	8.9% (17/192)	8.6% (40/467)
Heart	1.5% (2/133)	4.2% (6/142)	2.6% (5/192)	2.8% (13/467)
Pericardium	0.8% (1/133)	0% (0/142)	1.0% (2/192)	0.6% (3/467)
Hepatopancreas	0.8% (1/133)	0.7% (1/142)	0.5% (1/192)	0.6% (3/467)
Gut wall	0.8% (1/133)	1.4% (2/142)	0% (0/192)	0.4% (2/467)
Gonad	0% (0/133)	1.4% (2/142)	0.5% (1/192)	0.6% (3/467)
Gill	3.8% (5/133)	1.5% (2/134)	4.8% (9/187)	3.5% (16/454)
Corneal ulcers	4.5 %(6/133)	2.1% (3/142)	0% (0/192)	1.9% (9/467)

*Midgut-hindgut junction is not visible in histologic sections for all animals.

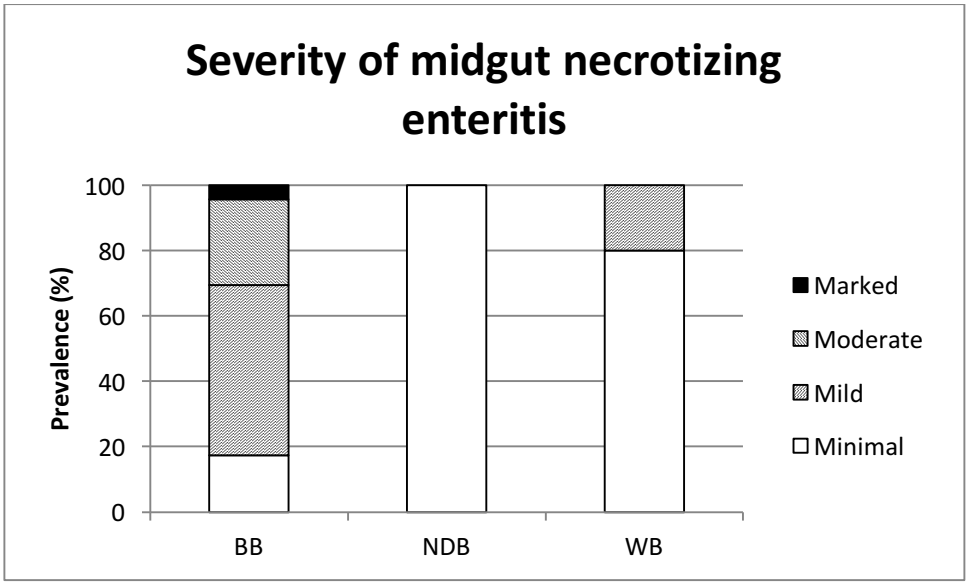

Figure 5.25. Comparison of severity of midgut necrotizing enteritis (when enteritis was present) in snow crabs collected from 3 different Newfoundland bays.

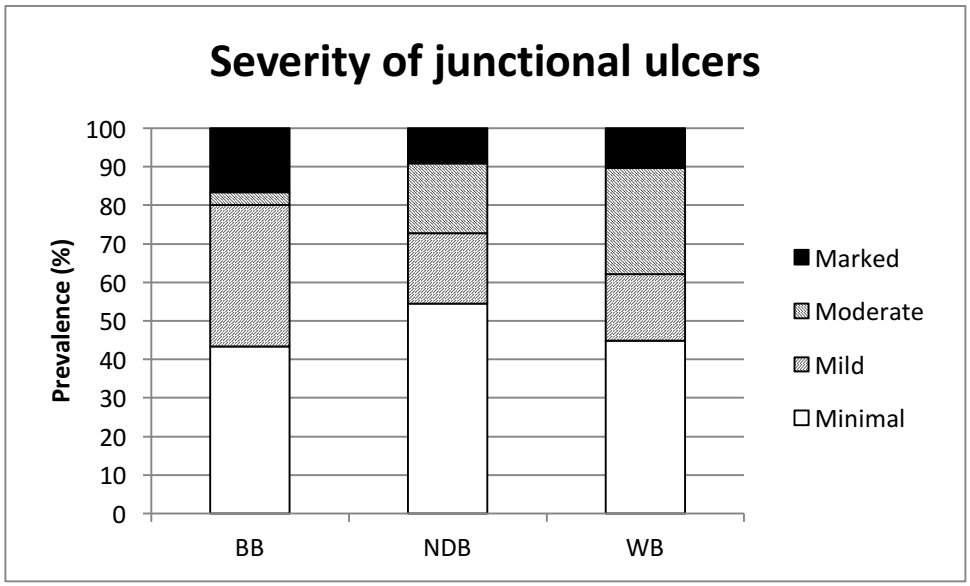

Figure 5.26. Comparison of severity of midgut-hindgut junctional ulcers (when ulcers were present) in snow crabs collected from 3 different Newfoundland bays.

Table 5.16: Comparison of prevalence of the different patterns of inflammation in snow crabs collected from strata within Bonavista Bay.

	BB Shallow Stratum (TN) New-shelled	**BB Deep Stratum (796) New-shelled**	**p-value**
Midgut necrotizing enteritis	2.9% (1/34)	51.2% (22/43)	**0.000**
Midgut-hindgut* junction ulcers	52.9% (9/17)	50% (9/18)	0.862
Midgut-hindgut junction tegumental gland adenitis	17.6% (3/17)	16.7% (3/18)	1.000
Hemocytic aggregates and nodules	8.8% (3/34)	0% (0/43)	0.082
Heart	2.9% (1/34)	0% (0/43)	0.442
Pericardium	0% (0/34)	0% (0/43)	1.000
Hepatopancreas	2.9% (1/34)	0% (0/43)	0.442
Gut wall	0% (0/34)	0% (0/43)	1.000
Gonad	0% (0/34)	0% (0/43)	1.000
Gill	2.9% (1/34)	0% (0/43)	0.442
Corneal ulcers	11.8%(4/34)	0% (0/43)	**0.034**

*Midgut-hindgut junction not visible in histologic sections for all animals.

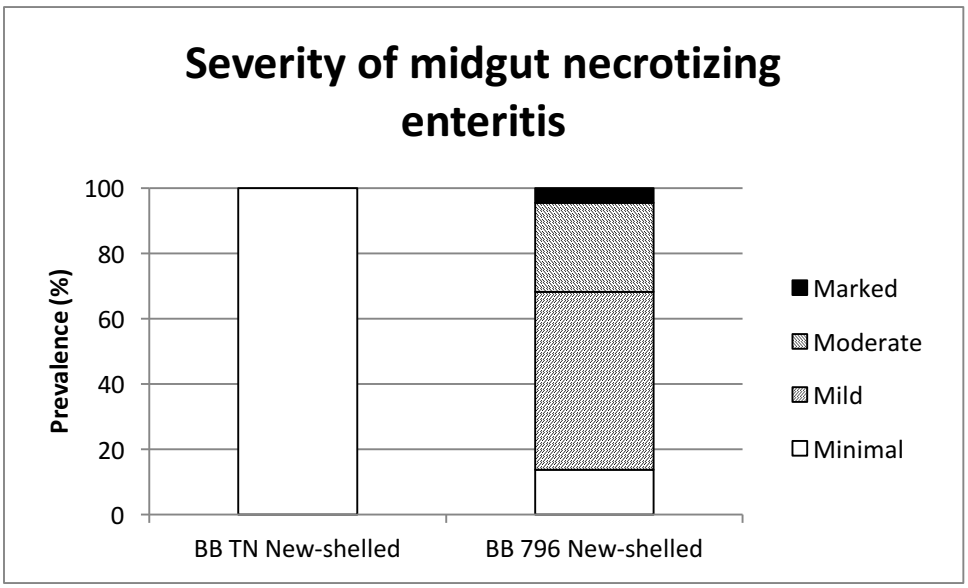

Figure 5.27. Comparison of severity of midgut necrotizing enteritis (when enteritis was present) in snow crabs collected from 2 different strata within Bonavista Bay.

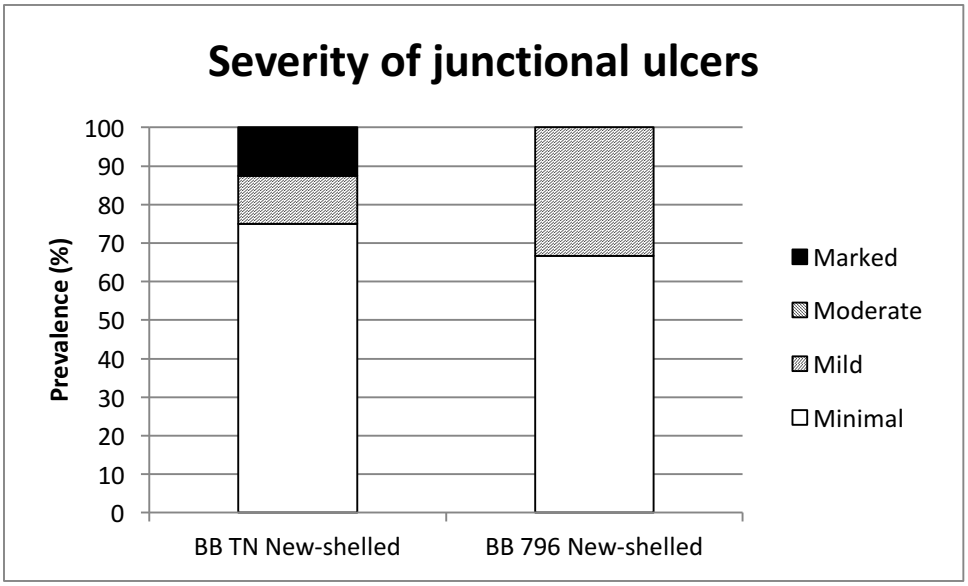

Figure 5.28. Comparison of severity of midgut-hindgut junctional ulcers (when ulcers were present) in snow crabs collected from 2 different strata within Bonavista Bay.

Table 5.17: Comparison of prevalence of the different patterns of inflammation in snow crabs collected from strata within White Bay.

	WB Shallow Stratum (613) New-shelled	WB Deep Strata (614/615) New-shelled	p-value
Midgut necrotizing enteritis	5.4% (3/56)	0.7% (1/135)	0.076
Midgut-hindgut* junction ulcers	30% (9/30)	28.6% (20/70)	0.885
Midgut-hindgut junction tegumental gland adenitis	23.3% (7/30)	31.4% (22/70)	0.414
Hemocytic aggregates and nodules	10.7% (6/56)	8.1% (11/135)	0.583
Heart	3.6% (2/56)	2.2% (3/135)	0.631
Pericardium	1.8% (1/56)	0.7% (1/135)	0.502
Hepatopancreas	0% (0/56)	0.7% (1/135)	1.000
Gut wall	0% (0/56)	0.7% (1/135)	1.000
Gonad	0% (0/56)	0.7% (1/135)	1.000
Gill	7.1% (4/56)	3.7% (5/135)	0.453
Corneal ulcers	0% (0/56)	0% (0/135)	1.000

*Midgut-hindgut junction not visible in histologic sections for all animals.

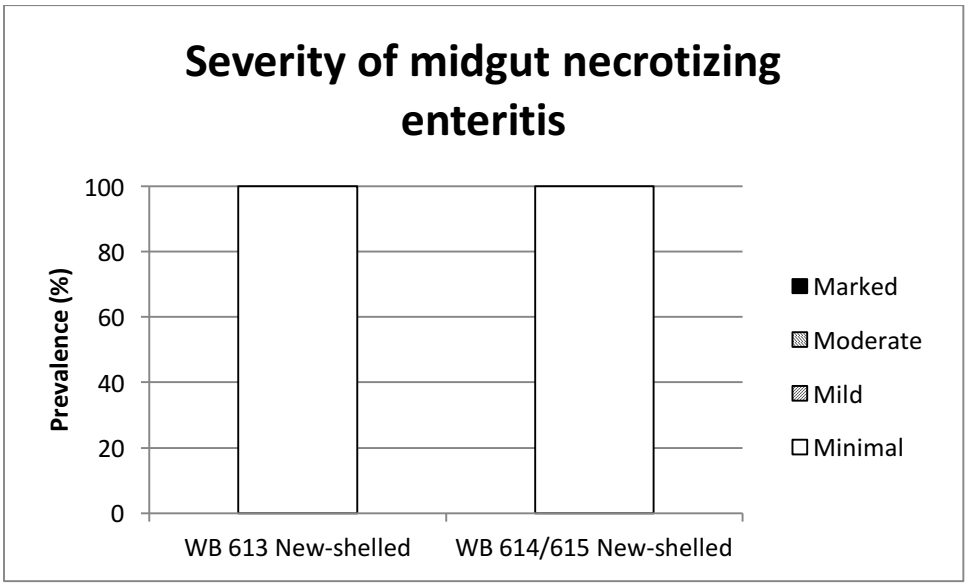

Figure 5.29. Comparison of severity of midgut necrotizing enteritis (when enteritis was present) in snow crabs collected from 2 different strata within White Bay.

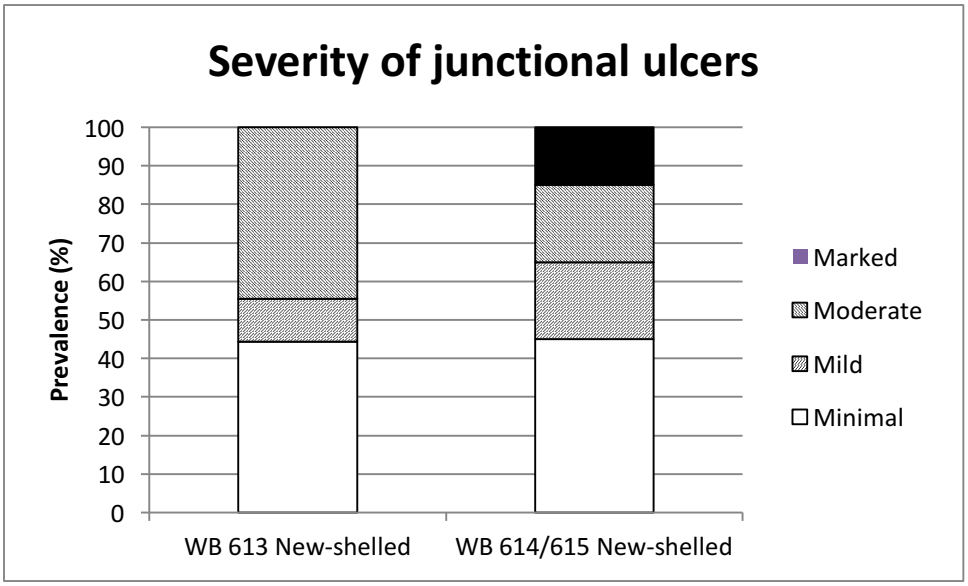

Figure 5.30. Comparison of severity of midgut-hindgut junctional ulcers (when ulcers were present) in snow crabs collected from 2 different strata within White Bay.

Table 5.18: Comparison of prevalence of the different patterns of inflammation in snow crabs collected from Bonavista Bay stratum TN by shell condition category.

	BB TN New-shelled	BB TN Intermediate	BB TN Old-shelled
Midgut necrotizing enteritis	2.9% (1/34)	0% (0/51)	0% (0/5)
Midgut-hindgut* junction ulcers	47.1% (8/17)	54.2% (13/24)	0% (0/2)
Midgut-hindgut junction tegumental gland adenitis	17.6% (3/17)	20.8% (5/24)	0% (0/2))
Hemocytic aggregates and nodules	8.8% (3/34)	11.8% (6/51)	20% (1/5)
Heart	2.9% (1/34)	2.0% (1/51)	0% (0/5)
Pericardium	0% (0/34)	2.0% (1/51)	0% (0/5)
Hepatopancreas	2.9% (1/34)	0% (0/51)	0% (0/5)
Gut wall	0% (0/34)	2.0% (1/51)	0% (0/5)
Gonad	0% (0/34)	0% (0/51)	0% (0/5)
Gill	2.9% (1/34)	5.9% (3/51)	20% (1/5)
Corneal ulcers	11.8% (4/34)	3.9% (2/51)	0% (0/5)

*Midgut-hindgut junction not visible in histologic sections for all animals.

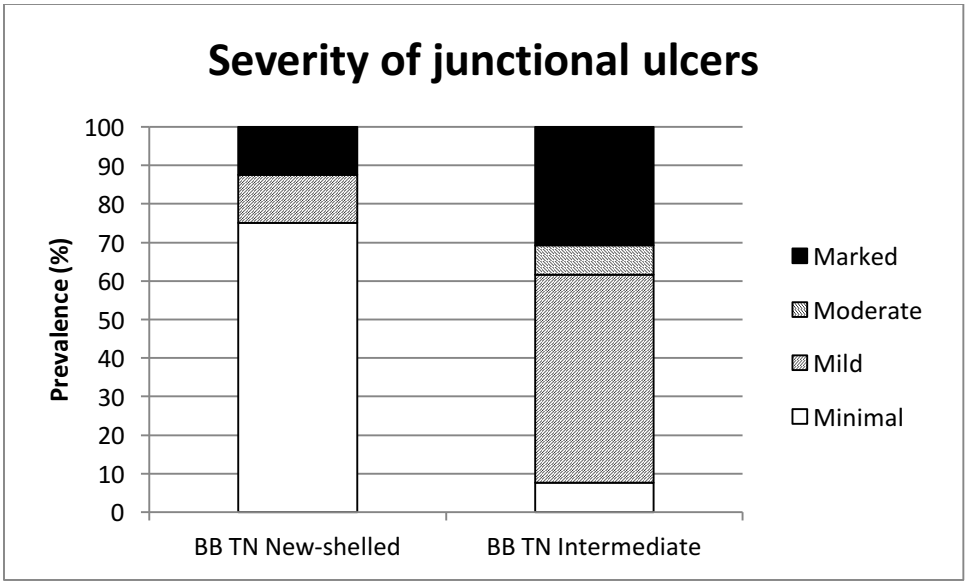

Figure 5.31. Comparison of severity of midgut-hindgut junctional ulcers (when ulcers were present) in snow crabs collected from Bonavista Bay stratum TN by shell condition category.

Table 5.19: Comparison of prevalence of the different patterns of inflammation in snow crabs collected from Notre Dame Bay by shell condition category.

	NDB New-shelled	NDB Intermediate	NDB Old-shelled
Midgut necrotizing enteritis	1.6% (2/123)	0% (0/18)	0% (0/1)
Midgut-hindgut* junction ulcers	16.7% (9/54)	33.3% (2/6)	0% (0/1)
Midgut-hindgut junction tegumental gland adenitis	29.6% (16/54)	83.3% (5/6)	100% (1/1)
Hemocytic aggregates and nodules	8.9% (11/123)	11.1% (2/18)	0% (0/1)
Heart	4.9% (6/123)	0% (0/18)	0% (0/1)
Pericardium	0% (0/123)	0% (0/18)	0% (0/1)
Hepatopancreas	0.8% (1/123)	0% (0/18)	0% (0/1)
Gut wall	1.6% (2/123)	0% (0/18)	0% (0/1)
Gonad	0% (0/123)	11.1% (2/18)	0% (0/1)
Gill	1.6% (2/123)	0% (0/18)	0% (0/1)
Corneal ulcers	2.4% (3/123)	0% (0/18)	0% (0/1)

*Midgut-hindgut junction not visible in histologic sections for all animals.

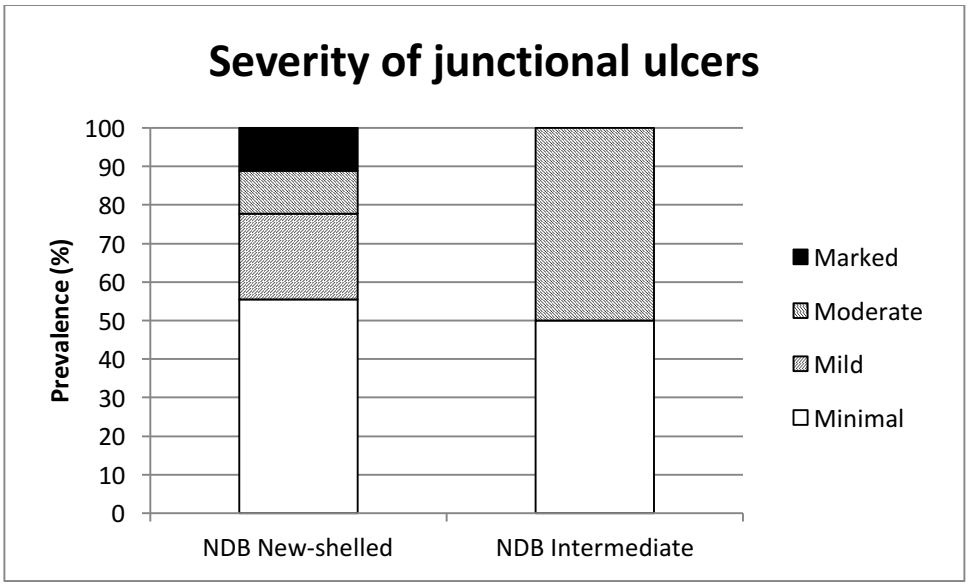

Figure 5.32. Comparison of severity of midgut-hindgut junctional ulcers (when ulcers were present) in snow crabs collected from Notre Dame Bay by shell condition category.

Table 5.20: Comparison of prevalence of the different patterns of inflammation in snow crabs collected from White Bay strata 614/615 by shell condition category.

	WB 614/615 New-Shelled	WB 614/615 Intermediate	p-value
Midgut necrotizing enteritis	0.7% (1/135)	0% (0/1)	1.000
Midgut-hindgut* junction ulcers	28.6% (20/70)	0% (0/1)	1.000
Midgut-hindgut junction tegumental gland adenitis	31.4% (22/70)	0% (0/1)	1.000
Hemocytic aggregates and nodules	8.1% (11/135)	0% (0/1)	1.000
Heart	2.2% (3/135)	0% (0/1)	1.000
Pericardium	0.7% (1/135)	0% (0/1)	1.000
Hepatopancreas	0.7% (1/135)	0% (0/1)	1.000
Gut wall	0.7% (1/135)	0% (0/1)	1.000
Gonad	0.7% (1/135)	0% (0/1)	1.000
Gill	3.7% (5/135)	0% (0/1)	1.000
Corneal ulcers	0% (0/135)	0% (0/1)	1.000

*Midgut-hindgut junction not visible in histologic sections for all animals.

5.3.5. **Interactions Between Epibionts and Inflammatory patterns**

5.3.5.1. **Gill Hemocytic Nodules and Gill Epibionts**

Higher prevalence of hemocytic nodules was observed in animals with gill rhabditoid worms than without them in BB (Mann-Whitney Test: W=8586.5, p-value = 0.0251) and NDB (Mann-Whitney Test: W=9659.0, p-value = 0.0014). No gill hemocytic nodules were observed in animals with gill rhabditoid nematodes in WB (n=5). No difference in the prevalence of hemocytic nodules was observed in snow crabs with or without gill amphipods, gill turbellarian worms, or gill peritrich stalked ciliate was observed. (Note: No gill hemocytic nodules were observed in any animal with gill peritrich stalked ciliates.)

5.3.5.2. **Inflammatory Patterns and Severity of Gill Bacterial Fouling**

Mean severity of gill bacterial fouling was higher in snow crabs with midgut-hindgut junctional ulceration in NDB snow crabs (Kruskal-Wallis Test: H = 4.09, DF = 1, P = 0.043) but not in BB snow crabs (H = 1.98, DF = 2, P = 0.372) or WB snow crabs (H = 1.41, DF = 2, P = 0.494). There was no difference among strata within bays (i.e., BB TN, BB796, WB 613, WB 614/615) when analyzed separately (data not shown). Mean severity of gill bacterial fouling was not different in snow crabs with or without tegumental gland adenitis for snow crabs within any bay (or strata within bays).

Higher mean severity of gill bacterial fouling was seen in snow crabs with midgut necrotizing enteritis in BB (H = 47.28, DF = 1, P = 0.000) when analyzed as a group but not in BB 796 (H = 2.15, DF = 1, P = 0.143). (Note: Gill bacterial severity was the same for all individuals collected

from TN, thus an association between degree of bacterial fouling and inflammatory patterns could not be evaluated.) No difference was noted in snow crabs from NDB or WB (strata 613 and 614/615 analyzed separately or together).

No difference in gill bacterial fouling severity was observed between snow crabs with and without hemocytic aggregates (any tissue location) from any of the 3 bays. Similarly, no significant differences in gill bacterial fouling severity was observed in snow crabs with or without hemocytic aggregates or nodules located in the gill in any of the 3 bays.

5.3.5.3. **Severity of Gill Bacterial Fouling With and Without Gill Epibionts**

Gill bacterial fouling was more severe in snow crabs with amphipods than without amphipods in BB (Kruskal-Wallis Test: H=44.64, DF=1, P=0.000), NDB (Kruskal-Wallis Test: H=23.61, DF=1, P=0.000), and WB (Kruskal-Wallis Test: H=28.55, DF=1, P=0.000). Gill bacterial fouling was more severe in snow crabs with turbellarian worms than without them in WB (Kruskal-Wallis Test: H=15.46, DF=1, P=0.000) but not in BB (Kruskal-Wallis Test: H = 2.99, DF = 1, P = 0.084) or NDB (Kruskal-Wallis Test: H = 0.49, DF = 1, P = 0.485). Gill bacterial fouling was more severe with gill rhabditoid worms than without them in NDB (Kruskal-Wallis Test: H = 8.37, DF = 1, P = 0.004) and WB (Kruskal-Wallis Test: H = 10.68, DF = 1, P = 0.001) but not in BB (Kruskal-Wallis Test: H = 1.45, DF = 1, P = 0.228). No significant difference in gill bacterial fouling severity was seen in association with peritrich stalked ciliates.

5.3.6. **Interactions between BCD and Epibionts**

5.3.6.1. **Interactions between BCD and Gill Bacterial Fouling**

Gill bacterial fouling tended to be less severe in BCD+ snow crabs than in BCD- snow crabs, although the difference was just above the cut-off value for statistical significance (Kruskal-Wallis Test: H = 3.53, DF = 1, P = 0.060; Mann-Whitney Test W = 42263.5, p-value = 0.0603; Figure 5.33). When the data from the separate Newfoundland bays was examined gill bacterial fouling was less severe in BCD+ new-shelled snow crabs than in BCD- new-shelled snow crabs in NDB (Mann-Whitney Test: W=6270.0, p-value = 0.0060; Figure 5.34). In WB stratum 614/615 the median bacterial gill fouling was lower in BCD+ than in BCD- snow crabs; the difference was just above the cut-off value for statistical significance (Mann-Whitney Test: W=5848.0, p-value = 0.0503; Figure 5.35). In WB stratum 613 (the very deep stratum) median bacterial gill fouling severity was significantly more severe in BCD+ snow crabs (n=2) than in BCD- snow crabs (Mann-Whitney Test: W=1515.5, p-value = 0.0229; Figure 5.36).

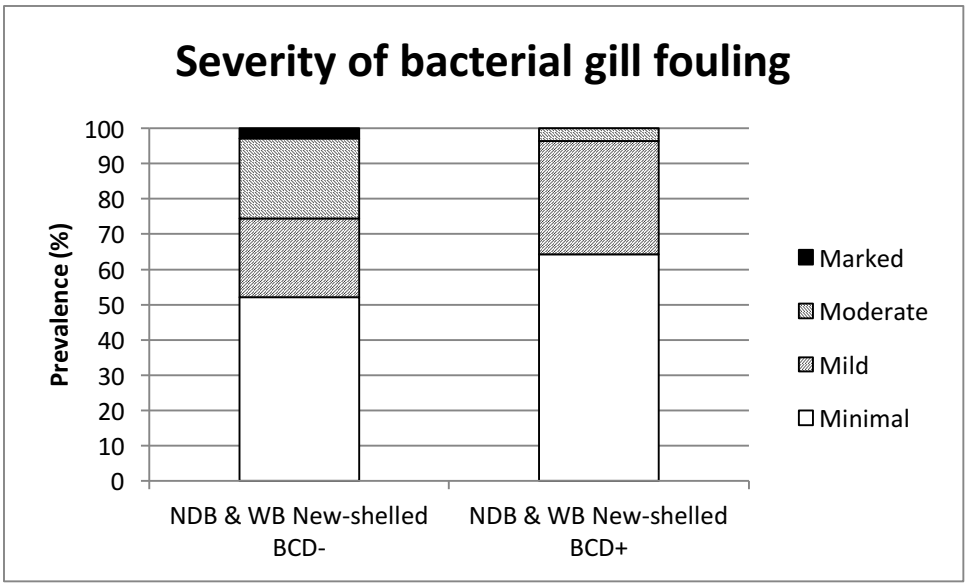

Figure 5.33. Comparison of severity of gill bacterial fouling by BCD status.

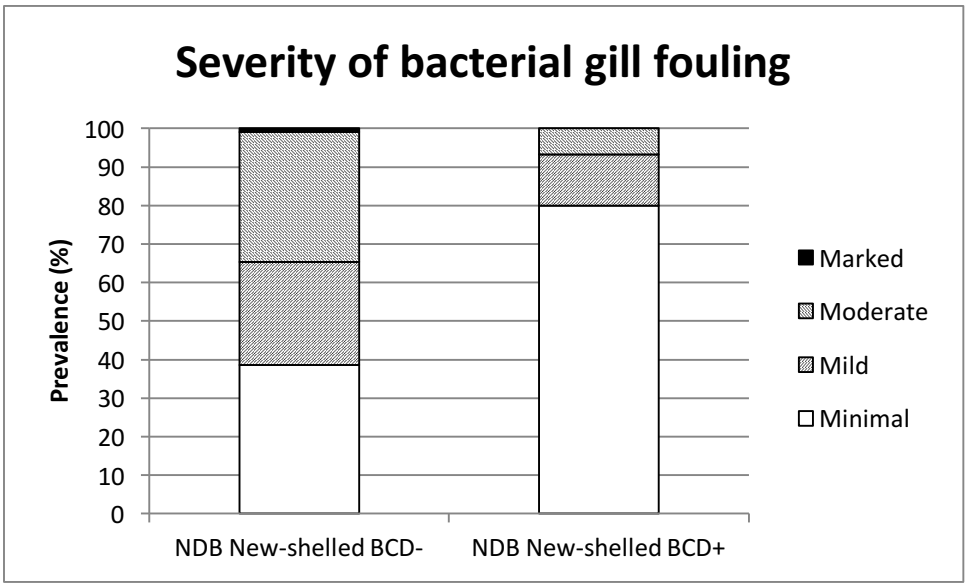

Figure 5.34. Comparison of severity of gill bacterial fouling by BCD status in NDB.

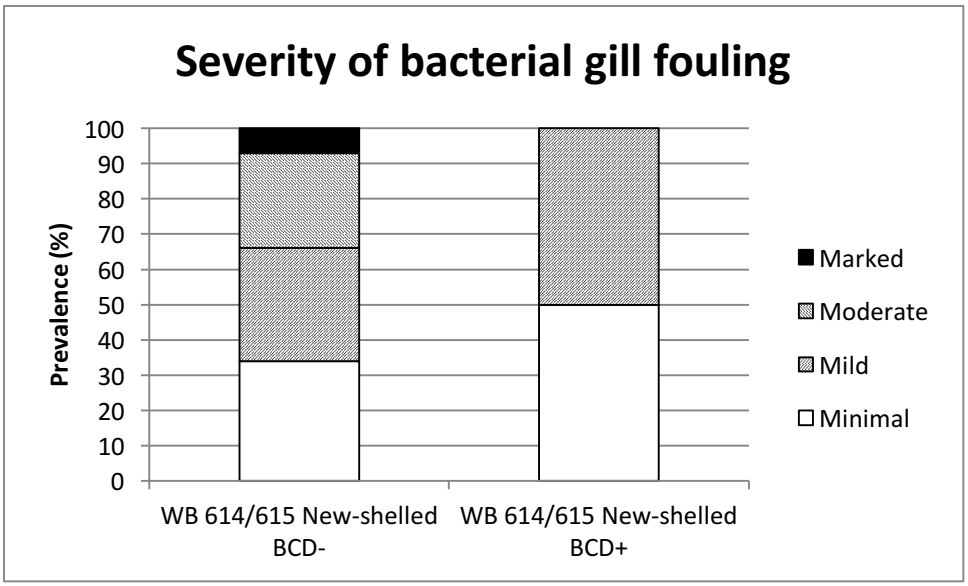

Figure 5.35. Comparison of severity of gill bacterial fouling by BCD status in WB strata 614/615.

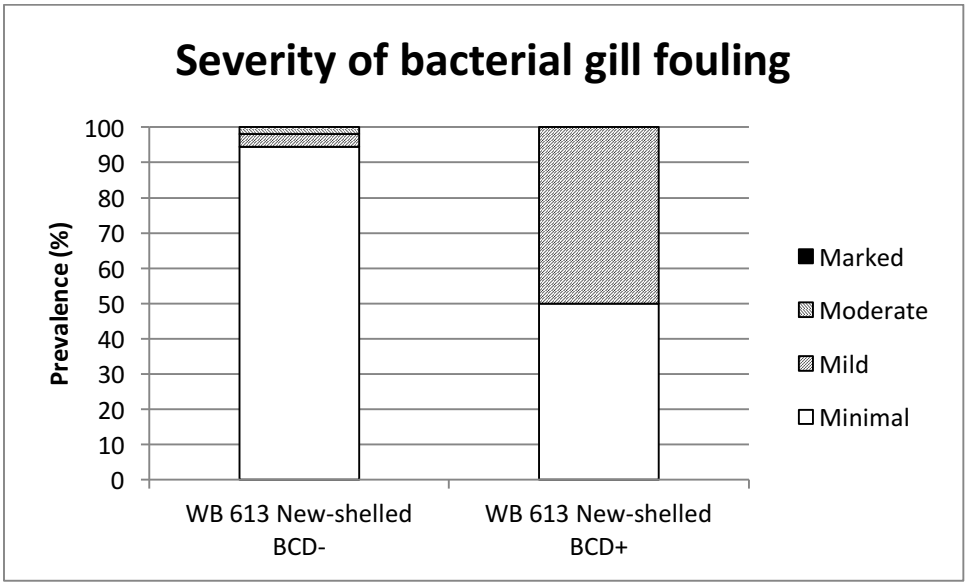

Figure 5.36. Comparison of severity of gill bacterial fouling by BCD status in WB stratum 613.

5.3.6.2. **Interactions Between BCD and Protozoan & Metazoan Epibionts**

There was no significant difference between gill or cuticular epibiont prevalence in BCD- and BCD+ snow crabs in individual bays or in the combined data (Tables 5.21-5.28).

Table 5.21. Comparison of prevalence of gill epibionts in new-shelled snow crabs collected from Notre Dame Bay without and with BCD.

	NDB New-Shelled BCD-	NDB New-Shelled BCD+	p-value
Amphipods	6.0 % (7/101)	0% (0/14)	0.595
Turbellarian Worms	1.7 % (2/101)	0% (0/14)	1.000
Rhabditoid nematodes	3.4 % (4/101)	0% (0/14)	1.000
Peritrich stalked ciliates	0 % (0/101)	0% (0/14)	1.000

Table 5.22. Comparison of prevalence of gill epibionts in new-shelled snow crabs collected from White Bay Stratum 613 without and with BCD.

	WB Stratum 613 New-shelled BCD-	WB Stratum 613 New-shelled BCD+	p-value
Amphipods	0% (0/54)	0% (0/2)	1.000
Turbellarian Worms	1.8% (1/54)	0% (0/2)	1.000
Rhabditoid nematodes	0% (0/54)	0% (0/2)	1.000
Peritrich stalked ciliates	0% (0/54)	0% (0/2)	1.000

Table 5.23. Comparison of prevalence of gill epibionts in new-shelled snow crabs collected from White Bay Strata 614/615 without and with BCD.

	WB Strata 614/615 New-shelled BCD-	WB Strata 614/615 New-shelled BCD+	p-value
Amphipods	14.6 % (18/123)	8.3% (1/12)	1.000
Turbellarian Worms	6.5 % (8/123)	8.3% (1/12)	0.579
Rhabditoid nematodes	4.1 % (5/123)	0% (0/12)	0.461
Peritrich stalked ciliates	0.8 % (1/123)	0% (0/12)	0.170

Table 5.24. Comparison of prevalence of gill epibionts in new-shelled snow crabs collected from White Bay and Notre Dame Bay (combined) without and with BCD.

	NDB & WB New-shelled BCD-	NDB & WB New-shelled BCD+	p-value
Amphipods	9.0% (25/278)	3.6% (1/28)	0.489
Turbellarian Worms	4.0% (11/278)	3.6% (1/28)	1.000
Rhabditoid nematodes	3.2% (9/278)	0% (0/28)	1.000
Peritrich stalked ciliates	0.4% (1/278)	0% (0/28)	1.000

Table 5.25. Comparison of prevalence of carapace epibionts in new-shelled snow crabs collected from Notre Dame Bay without and with BCD.

	NDB New-Shelled BCD-	NDB New-Shelled BCD+	p-value
Turbellarian worms	0.8% (1/108)	0% (0/14)	1.000
Turbellarian eggs	8.1% (10/108)	0% (0/14)	0.603
Rhabditoid nematodes in cuticular ulcers	0.8% (1/108)	0% (0/14)	1.000
Nematodes along internal surface of abdomen	9.8% (12/108)	14.3% (2/14)	
Leech eggs	0% (0/108)	0% (0/14)	1.000
Colonial hydrozoan	2.4% (3/108)	0% (0/14)	1.000
Encrusting bryozoan	38.2% (47/108)	28.6% (4/14)	0.286

Table 5.26. Comparison of prevalence of carapace epibionts in new-shelled snow crabs collected from White Bay Stratum 613 without and with BCD.

	WB Stratum 613 New-Shelled BCD-	WB Stratum 613 New-Shelled BCD+	p-value
Turbellarian worms	0% (0/54)	0% (0/2)	1.000
Turbellarian eggs	1.8% (1/54)	0% (0/2)	1.000
Rhabditoid nematodes in cuticular ulcers	0% (0/54)	0% (0/2)	1.000
Nematodes along internal surface of abdomen	0% (0/54)	0% (0/2)	1.000
Leech eggs	0% (0/54)	0% (0/2)	1.000
Colonial hydrozoan	0% (0/54)	0% (0/2)	1.000
Encrusting bryozoan	79.6% (43/54)	50% (1/2)	0.386

Table 5.27. Comparison of prevalence of carapace epibionts in new-shelled snow crabs collected from White Bay Strata 614/615 without and with BCD.

	WB Strata 614/615 New-Shelled BCD-	WB Strata 614/615 New-Shelled BCD+	p-value
Turbellarian worms	2.4% (3/123)	0% (0/12)	1.000
Turbellarian eggs	8.9% (11/123)	8.3% (1/12)	1.000
Rhabditoid nematodes in cuticular ulcers	0% (0/123)	0% (0/12)	1.000
Nematodes along internal surface of abdomen	4.1% (5/123)	8.3% (1/12)	0.434
Leech eggs	0% (0/123)	0% (0/12)	1.000
Colonial hydrozoan	0.7% (1/123)	0% (0/12)	1.000
Encrusting bryozoan	37.4% (46/123)	58.3% (7/12)	0.216

Table 5.28. Comparison of prevalence of carapace epibionts in new-shelled snow crabs collected from White Bay and Notre Dame Bay (combined) without and with BCD.

	NDB & WB New-Shelled BCD-	NDB & WB New-Shelled BCD+	p-value
Turbellarian worms	1.4% (4/285)	0% (0/28)	1.000
Turbellarian eggs	7.7% (22/285)	3.6% (1/28)	0.706
Rhabditoid nematodes in cuticular ulcers	0.4% (1/285)	0% (0/28)	1.000
Nematodes along internal surface of abdomen	6.0% (17/285)	7.1% (2/28)	0.682
Leech eggs	0% (0/285)	0% (0/28)	1.000
Colonial hydrozoan	1.4% (4/285)	0% (0/28)	1.000
Encrusting bryozoan	47.7% (136/285)	42.9% (12/28)	0.623

5.3.7. **Interactions Between BCD and Inflammatory Patterns**

There were no significant differences in the prevalence of the observed inflammatory patterns in BCD- and BCD+ new-shelled snow crabs from NDB or WB (Tables 5.29-5.31). When the data for both bays were combined, BCD- snow crabs had higher prevalence of ulcers at the midgut-hindgut junction than BCD+ snow crabs (Fisher Exact Test p-value = 0.039). No significant differences were observed in the other patterns of inflammation (Table 5.32).

Table 5.29. Comparison of prevalence of inflammatory patterns in new-shelled snow crabs from Notre Dame Bay without and with BCD.

	NDB New-Shelled BCD-	NDB New-Shelled BCD+	p-value
Midgut necrotizing enteritis	1.8% (2/109)	0% (0/14)	1.000
Midgut-hindgut* junction ulcers	19.6% (9/46)	0% (0/8)	0.326
Midgut-hindgut junction tegumental gland adenitis	32.6% (15/46)	12.5% (1/8)	0.411
Hemocytic aggregates and nodules	10.1% (11/109)	14.3% (2/14)	0.643
Heart	4.6% (5/109)	7.1% (1/14)	0.523
Pericardium	0% (0/109)	0% (0/14)	1.000
Hepatopancreas	0.9% (1/109)	0% (0/14)	1.000
Gut wall	0.9% (1/109)	7.1% (1/14)	0.216
Gonad	1.8% (2/109)	0% (0/14)	1.000
Gill	1.8% (2/109)	0% (0/14)	1.000
Corneal ulcers	1.8% (2/109)	7.1% (1/14)	0.306

*Midgut-hindgut junction not visible in histologic sections for all animals.

Table 5.30. Comparison of prevalence of inflammatory patterns in new-shelled snow crabs from White Bay Stratum 613 without and with BCD.

	WB Stratum 613 New-shelled BCD-	WB Stratum 613 New-shelled BCD+	p-value
Midgut necrotizing enteritis	5.6% (3/54)	0% (0/2)	1.000
Midgut-hindgut* junction ulcers	31.0% (9/29)	0% (0/1)	1.000
Midgut-hindgut junction tegumental gland adenitis	24.1% (7/29)	0% (0/1)	1.000
Hemocytic aggregates and nodules	11.1% (6/54)	0% (0/2)	1.000
Heart	0% (0/54)	0% (0/2)	1.000
Pericardium	1.9% (1/54)	0% (0/2)	1.000
Hepatopancreas	0% (0/54)	0% (0/2)	1.000
Gut wall	0% (0/54)	0% (0/2)	1.000
Gonad	0% (0/54)	0% (0/2)	1.000
Gill	7.4% (4/54)	0% (0/2)	1.000
Corneal ulcers	0% (0/54)	0% (0/2)	1.000

*Midgut-hindgut junction not visible in histologic sections for all animals.

Table 5.31. Comparison of prevalence of inflammatory patterns in new-shelled snow crabs from White Bay Strata 614/615 without and with BCD.

	WB Strata 614/615 New-shelled BCD-	WB Strata 614/615 New-shelled BCD+	p-value
Midgut necrotizing enteritis	0.8% (1/123)	0% (0/12)	1.000
Midgut-hindgut* junction ulcers	29.8% (20/67)	0% (0/3)	0.552
Midgut-hindgut junction tegumental gland adenitis	32.8% (22/67)	0% (0/3)	0.547
Hemocytic aggregates and nodules	8.1% (10/123)	8.3% (1/12)	1.000
Heart	2.4% (3/123)	0% (0/12)	1.000
Pericardium	0.8% (1/123)	0% (0/12)	1.000
Hepatopancreas	0.8% (1/123)	0% (0/12)	1.000
Gut wall	0.8% (1/123)	0% (0/12)	1.000
Gonad	0.8% (1/123)	0% (0/12)	1.000
Gill	3.3% (4/123)	8.3% (1/12)	0.377
Corneal ulcers	0% (0/123)	0% (0/12)	1.000

*Midgut-hindgut junction not visible in histologic sections for all animals.
(2 hemocytic nodules were in same individual)

Table 5.32. Comparison of prevalence of inflammatory patterns in new-shelled snow crabs from Notre Dame Bay and White Bay (combined) without and with BCD.

	NDB & WB New-Shelled BCD-	NDB &WB New-Shelled BCD+	p-value
Midgut necrotizing enteritis	2.1% (6/286)	0% (0/28)	1.000
Midgut-hindgut* junction ulcers	26.8% (38/142)	0% (0/12)	**0.039**
Midgut-hindgut junction tegumental gland adenitis	31.0% (44/142)	8.3% (1/12)	0.182
Hemocytic aggregates and nodules	9.4% (27/286)	10.7% (3/28)	0.740
Heart	2.8% (8/286)	3.6% (1/28)	0.573
Pericardium	0.7% (2/286)	0% (0/28)	1.000
Hepatopancreas	0.7% (2/286)	0% (0/28)	1.000
Gut wall	0.7% (2/286)	3.6% (1/28)	0.245
Gonad	1.0% (3/286)	0% (0/28)	1.000
Gill	3.5% (10/286)	3.6% (1/28)	1.000
Corneal ulcers	0.7% (2/286)	3.6% (1/28)	0.245

*Midgut-hindgut junction not visible in histologic sections for all animals.

5.4. **Discussion**

5.4.1. **Microsporidiosis**

Microsporidia are intracellular parasites which are common pathogens of decapod crustaceans (Ryazanova and Eliseikina 2010). Almost half of the known microsporidian genera infect aquatic hosts with ~50 genera that infect aquatic arthropods (Stentiford et al 2013, Wang et al 2013). Most major organ and tissue systems can be parasitized, although in many cases infection is restricted to one organ, tissue, or even cell type (Stentiford et al 2013). These parasites are obligate intracellular parasites, replication may take place within the host cell's cytoplasm or nucleoplasm, and hypertrophy of the infected host cells is common (Stentiford et al 2013). The microsporidian parasite was apparently associated with hypertrophied host nuclei suggesting that the parasite is intracytoplasmic in nature. The cell line infected by the parasite is unclear; the parasites are not associated with epithelial cells (such as hepatopancreatic epithelium), gonadal tissue, or skeletal muscle cells, common infection sites in microsporidial infections in crustacean hosts (Ryazanova and Eliseikina 2010, Stentiford et al 2013, Wang et al 2013). The multisystemic nature and interstitial location of the infection indicates that connective tissues and fixed phagocytes may be likely considerations. Microsporidial spore shape varies among genera including spherical, oval, pyriform, lanceolate, rod-shaped, lageniform (flask-shaped), and horseshoe-shaped appearances (Larsson 1999). The spores in this microsporidial infection appear round to ovoid; contraction artifact due to ethanol fixation may have altered the shape of the spores. The histologic and electron microscopic features of this microsporidian parasite are similar (but not identical) to those recently described for red and blue king crabs *Paralithodes camtschaticus* and *P. platypus* infected with *Thelohania* (Ryazanova and Eliseikina

2010). The microsporidial infection in red and blue king crabs infects connective tissues while sparing musculature and contains up to 8 spores within sporophorous vesicles. However, the microsporidian infection in red and blue king crabs resulted in formation of xenomas, a feature not observed in this snow crab microsporidial infection. Unfortunately, fixation with Davidson's seawater fixative followed by storage of the tissue in 70% ethanol resulted in fixation artifacts (cell shrinkage, condensation of membranes, loss of cytoplasmic detail, vacuolation and loss of cytoplasmic organelles, and tissue holes) that resulted in poor quality transmission electron micrographs of the microsporidian life stages. Within the poor-quality images, the parasitic spores contained tangential and cross-sections of polar tubes, a highly specialized extrusive structure that is important for host invasion by microsporidians (Morado 2011). With the exceptions of BCD and microsporidiosis, no histologic evidence of any other systemic protozoal, bacterial, fungal, or viral disease (such as intranuclear bacilliform virus) was observed.

5.4.2. **Epibiota**

Histologic evaluation of Newfoundland snow crabs revealed various epibionts on snow crab gills and carapace. The most prevalent gill metazoan epibionts were amphipods. Colonization of crab gills may be beneficial for epibiont species, enhancing food acquisition, increasing their mobility, and reducing the risk of predation (Wahl 1989, McGaw 2006, Fernandez-Leborans 2010, Dvoretsky and Dvoretsky 2013). Gill epibionts may reduce respiratory efficiency of host crabs (Gannon and Wheatley 1992, Dvoretsky and Dvoretsky, 2013). Two species of corophid amphipods occur in snow crabs: *Gammaropsis inaequistylus* and *Ischyrocerus commensalis*

(Steele et al 1986). Most specimens of *G. inaequistylus* were found in the marginal groove at the lower edge of the carapace with fewer below the eye socket and on the large chelae (Steele et al 1986). No anatomic location for *I. commensalis* was noted (Steele et al 1986). In red king crab *Paralithodes camtschaticus, I. commensalis* amphipods were located on the limbs, gills, and mouth part apparatus (Dvoretsky et al 2007). Juvenile amphipods were more common in the gills and the gills closest to the mouthparts were most commonly affected (Dvoretsky et al 2007, Dvoretsky and Dvoretsky 2009). The identity of these amphipods is uncertain; their location in the gills suggests that they are most likely *I. commensalis*. Gill amphipods were more likely to be seen in gills with heavier degrees of bacterial fouling in this study. Host mucus secretions enriched with microorganisms and detritus are a high-quality source of food for amphipods, and thus the higher microbial load may attract more amphipods (Briggs 1976, 1977, Gotto 1979, Vader 1983). Amphipods can perceive host species through olfactory means via semiochemicals (Williams and Moore 1985). Detection of mucus and arthropodin (the aqueous extract of arthropod cuticle) are thought to play a role in semiochemical detection of arthropods by amphipods; microbial factors could also release detected substances (Williams and Moore 1985). Alternatively, amphipods could augment microbial growth via release of their waste products into the gill environment. Feeding on host tissues has also been reported for lysianassid amphipods (genus *Acidostoma*) in sea anemones (Vader 1983).

The second epibionts observed on snow crab gills were the turbellarians. Three species of turbellarian worms have been described in snow crab *Chionoecetes opilio* from eastern Canada: *Ectocotyla hirudo*, *E. multitesticulata* and *E. pagurus* (Fleming et al 1981, Brattey and Elner

1985). *Ectocotyla* spp. are ectocommensals that appear to have a direct life cycle (Fleming et al 1981). Similar to the case in amphipods gill bacterial fouling was more severe in snow crabs with turbellarians (1 out of the 3 bays). As mentioned above, this may indicate that the microbes are an attractive source of nutrition or that waste products from the turbellarian worms enhance local microbial growth.

Peritrich stalked ciliates were also observed in small numbers of snow crabs. Peritrich stalked ciliates are also ectocommensals but in high infection intensities can be implicated in disease (Shields and Overstreet 2003). The genera *Epistylus* and *Lagenophrys* occur on marine brachyuran crabs (Couch 1966, Shields and Overstreet 2003). No difference in gill bacterial fouling severity is seen in association with peritrich stalked ciliates.

Small rhabditoid nematodes were observed in association with gill fouling and in areas of cuticular ulceration. These small rhabditoid nematodes may represent bacterial-feeding larvae which have infested microbial-rich areas in the fouled gills and shell ulcers containing chitinolytic bacteria. Rhabditoid nematodes can also liberate bacteria on which they feed from their gut (with their waste products) into the local environment altering the local microbial environment (Morley 2010). Thus, the positive association between gill fouling and rhabditoid nematodes may be a cause and effect relationship or may reflect a synergistic relationship between the epibionts. Interestingly, prevalence of gill hemocytic nodules was higher in animals with rhabditoid worms than without them. No similar association is noted for any of the other gill epibionts. This suggests that rhabditoid worms may induce focal gill damage and

thus result in local inflammation, indicating that these worms may be parasites rather than commensal organisms. While rhabditoid worms were occasionally observed within cuticular ulcers admixed within intralesional bacteria, no fungal hyphae were observed in any histologic sections examined. The shell disease known as black spot (or brown, rust, or burn spot), which is caused by chitinolytic bacteria, and black mat syndrome (BMS) caused by the ascomycete fungus *Trichomaris invadens* are two of the major diseases in snow crabs (Kon *et al.* 2011). While shell ulcers with intralesional chitinolytic bacteria were observed, no shell lesions invaded by fungal hyphal structures (i.e., lesions of black mat syndrome) were observed. Similarly, Benhalima et al (1998) did not see fungal hyphae within exoskeletal lesions in snow crab from the southern Gulf of St. Lawrence.

The leech eggs cocoons are most likely from the marine piscicolid leech *Johanssonia arctica.* *Johanssonia arctica* has been reported on snow crabs *Chionoecetes opilio* in the northwestern Atlantic coast of North America, including the northern bays of Newfoundland (Meyer and Kahn 1979, Kahn 1982). The adult leech feeds on the blood of several species of marine fishes (including Atlantic cod *Gadus morhua* and American plaice *Hippoglossoides platessoides*) and leaves the fish host to lay its eggs on a hard substrate including the carapace of crabs (Kahn 1982). *Johanssonia arctica* are most commonly found attached to recently molted (soft-shelled) crabs (Khan 1982). This leech is a vector for several blood parasites of marine fish including a trypanosome *Trypanosoma murmanensis,* a hemogregarine *Haemogregarina uncinata,* and a piroplasm *Haemohormidinium beckeri* (reviewed in Khan 1982). Although *J. arctica* could represent a potential vector for *Hematodinium* infection, this is unlikely because snow crabs are

used strictly as a substrate for egg deposition and no feeding from crab hemolymph occurs (Khan 1982).

The identity of the juvenile nematodes along the internal margin of the abdomen is unclear. These nematodes may represent early life stages of nematode parasites of crabs (such as *Nectonema* spp.) or crab-eating hosts (such as the ascaridoid worms *Hysterothylacium aduncum* and the seal worm *Pseudoterranova decipiens*), parasites which have been reported to infect decapod crustaceans (Brattey et al 1981, McClelland 1990, Marcogliese 1993, Marcogliese 1996). Crabs act as paratenic hosts, hosts in which development does not occur but which may be an essential link in the completion of the parasite's life cycle in the definitive host (Palm 1999, Shields and Overstreet 2003). Nemertean worms are another possibility considered in this case given the nematode's abdominal location. Nemertean worms (such as *Carcinonemertes* spp.) are egg predators which have the potential to cause significant egg mortality in decapod crustacean hosts (reviewed in Kuris and Wickham 1987). But, no evidence of egg predation (such as degenerative eggs) was observed in association with the abdominal nematodes in this study (n=16 gravid females with abdominal nematodes). Furthermore, the histologic appearance of the organisms was not consistent with that of a nemertean.

Several encrusting bryozoans were observed on the Newfoundland snow crabs. The most commonly observed encrusting bryozoan is consistent with *Alcyonidium* spp. which has been reported as common on Atlantic Canadian snow crabs (Hooper 1986, Savoie et al 2007). *Alcyonidium* spp. is an encrusting-type bryozoan with gelatinous colonies which form into

whitish or brownish crusts. Zooids are hexagonal or irregularly polygonal in shape. Epibiont fouling with *Alcyonidium* showed similarly high prevalence levels in tanner crabs *Chionoecetes bairdi* off Kodiak Island, Alaska (Dick et al 1998). Other genera of bryozoans (such as *Hippothoa*) have also been reported as epibionts on snow crabs (Savoie et al 2007). The histologic appearance of the gelatinous epibiont along the ventral abdomen of snow crabs is most consistent with a hydrozoan. The identity of the colonial hydrozoan is unclear but may be *Hydractinia*. The hydrozoan *Hydractinia* has been reported on snow crabs (Hooper 1986). The microscopic appearance of this hydrozoan is similar to that described for *Hydractinia* (Di Camillo et al 2008).

5.4.3. **Midgut-hindgut Junctional Ulcers and Midgut Necrotizing Enteritis**

Two patterns of necrotizing and ulcerative enteritis were observed in snow crabs: focal ulcers at the level of the midgut-hindgut junction and more extensive areas of necrotizing enteritis in the non-chitinized midgut epithelium. Necrotizing and ulcerative enteritis occurs in penaeid shrimp *Penaeus monodon, Fenneropenaeus (P.) penicillatus, Litopenaeus (P.) stylirostris,* and *L. (P.) vannamei* and in American lobsters *Homarus americanus* (Lightner 1978, 1996, Lightner et al 1987, Battison et al 2008). Hemocytic enteritis in penaeid shrimp is a form of necrotizing and ulcerative enteritis which affects the non-chitinized enteric mucosa. This lesion has been associated with blue-green algae related to red tides (with possible exotoxin involvement), some forms of Gram-negative bacteria (including *Vibrio*), and with heavy metal pollutants (Lightner 1978, 1996, Battison et al 2008, Frias-Espericueta et al 2008). In the American lobster necrotizing enteritis affected non-chitinized epithelium of the midgut which, in the provided

figures, was located just proximal to the midgut-hindgut junction (Battison et al 2008). The cause of the necrotizing enteritis in the American lobster was undetermined; however, a species of *Vibrio* was isolated from the affected individual that was not cultured from unaffected animals (Battison et al 2008). *Vibrio* bacteria can be normal flora within crustaceans and can also be pathogenic with virulence factors including a variety of exotoxins (including proteases and chitinases) that can act locally or enter the blood stream and attack distant organs or tissues (reviewed in Aguirre-Guzman et al 2004).

The snow crabs in this study were captured in Newfoundland with air exposure (emersion) during shipment. Emersion in crustaceans results in hypoxia, hypercapnia, and metabolic acidosis. Hypercapnic hypoxia impairs the crab's ability to remove culturable bacteria from its hemolymph and decreases the activity of phenoloxidase, an enzyme critical in the innate immune response in crustaceans (Tanner et al 2006). Hypoxic stress in crustaceans is associated with increased susceptibility to infection with *Vibrio alginolyticus* in *Penaeus stylirostris*, *Vibrio campbellii* in *Callinectes sapidus, Vibrio parahaemolyticus* in *Litopenaeus vannamei* and *Palaemonetes pugio, and Enterococcus* in *Macrobrachium rosenbergii* (Le Moullac et al 1998, Mikulski et al 2000, Cheng et al 2002). Significant decreases in total hemocyte counts occurred in penaeid shrimp held under hypoxia (*Penaeus stylirostris*) and hypercapnic hypoxia which likely contributes to this reduced bacterial clearance (*Litopenaeus vannamei;* Le Moullac et al 1998, Mikulski et al 2000). Their studies indicate that emersion may have predisposed snow crabs in the present study to opportunistic bacterial enteritis. Higher mean bacterial gill fouling was seen in snow crabs with midgut necrotizing enteritis in Bonavista Bay. In contrast, this

association was not seen in snow crabs from BB 796 when analyzed separately from BB TN snow crabs or from snow crabs collected from Notre Dame Bay or White Bay. Thus, heavy bacterial gill fouling does not appear to be a consistent risk factor for development of necrotizing enteritis in snow crabs.

Hypoxia and emersion in crabs have shown differential partitioning of cardiac output between arterial distribution systems via neural and/or neurohumoral stimulation of innervated muscular cardio-arterial valves at the base of each arterial tree (Airriess and McMahon 1996, McMahon 2001, Chung and Zmora 2008). In periods of hypoxia hemolymph flow is increased in the anterior aorta which gives rise to the optic arteries and supplies hemolymph to the supraesophageal ganglion (brain) and neuroendocrine organs, a response which may be important in the release and distribution of crustacean hyperglycemic hormone (CHH) in animals exposed to environmental stress (Airriess and McMahon 1996, Webster 1996, McGaw and Reiber 2002, Chung and Zmora 2008). This increase in hemolymph flow towards the anterior region of the crab is accompanied by substantial declines in hemolymph through the anterolateral arteries, hepatic arteries, and sternal arteries which shunts hemolymph away from the viscera (Airriess and McMahon 1996, McMahon 2001, McGaw and Reiber 2002). In decapod crustaceans the midgut is supplied by hemolymph by the pyloric hepatic artery, a side-branch off the paired hepatic arteries, and the hindgut has collateral circulation supplied by the posterior artery, posterior lateral arteries, and inferior abdominal artery (McGaw and Reiber 2002). This reduction of hemolymph flow in the viscera may compound the effects of hypoxia on visceral tissues (Airiess and McMahon 1996, McMahon 2001).

In humans reduced mucosal blood flow (hypoxemia/ischemia) is considered to be one of the factors which contribute to stress-related mucosal disease (SRMD), although progression of the disease also requires luminal acid (Ali and Harty 2009, Marik 2010). SRMD is a common complication in critically ill patients, which varies from stress-related injury to stress ulcerations (Stollman and Metz 2005, Ali and Harty 2009, Malfertheiner et al 2009, Marik 2010, Monnig and Prittie 2011). Stress-related injury is typified by diffuse, superficial mucosal erosions that are unlikely to result in gastrointestinal bleeding associated with hemodynamic compromise while stress ulcers extend deeper into the submucosa and are more focal (Monnig and Prittie 2011). Under hypoxic-ischemic conditions reactive oxygen species (ROS) are rapidly and continuously produced and are an important element in the development and progression of epithelial necrosis and ulceration (Das et al 1997, Ali and Harty 2009). Overproduction of ROS results in oxidative damage including lipid peroxidation, protein oxidation, and DNA damage which can lead to cell death (Ali and Harty 2009). ROS can also act as second messengers and activate diverse redox-sensitive signaling transduction pathways resulting in tissue inflammation and injury (Ali and Harty 2009, Valko et al 2007). In humans the most significant effect of ROS on signaling pathways has been observed in the mitogen-activated protein kinase (MAPK) pathways (Valko et al 2007). MAPK pathways are found in arthropods including crustaceans and are involved in innate immunity (Shi et al 2012, Yang et al 2012, Cui et al 2013, He et al 2013, Yan et al 2013, De Coninck et al 2014, Shilo 2014). More specifically, oxidative stress (induced by UV-B radiation) resulted in p38 MAPK phosphorylation and increased p53 expression in the benthic copepod *Tigriopus japonicus* (Kim et al 2015). This suggests that the

two patterns of necroulcerative enteritis seen in snow crab may be comparable to the two patterns of stress-related mucosal disease in humans.

Some species of invertebrates (i.e., intertidal animals) undergo rapid transition between hypoxia and hyperoxia without any damage. In Pacific white shrimp, changes in antioxidant enzyme activities (such as superoxide dismutase, glutathione peroxidase, and catalase) have been observed in response to hypoxia-reoxygenation and may be crucial to avoid oxidative damage (Parrilla-Taylor and Savin 2011). Hypoxia tolerance among crustacean species appears to be closely correlated with activity and metabolic rate, and is impacted by the frequency and duration of hypoxic exposure the animal typically encounters in its natural habitat (Stickle et al 1989). Hypoxia tolerance has not been investigated in snow crabs; they are found in a deep, cold water environment suggesting that their hypoxic tolerance may not be high. Snow crab energetic requirements were within the same range for shallow-water crabs when compared at similar temperatures, suggesting that snow crabs do not have a low metabolic rate (Foyle et al 1989). Thus, hypoxia/ischemia and/or re-oxygenation (re-perfusion) injury may have contributed to the development of the necroulcerative lesions observed in this study.

While hypoxemia/ischemia likely plays a role in the development of SRMD, the pathogenesis of stress ulceration is multifactorial. Alterations in gastric acid, mucosal blood flow, mucus layer, protein synthesis, bicarbonate and prostaglandin secretion, and/or epithelial cell renewal are all postulated to alter the gastric mucosal barrier leading to back diffusion of acid leading to mucosal damage and ulceration (Marik 2010). *Helicobacter pylori* (the infectious cause of the

majority of human gastric ulcers) also plays a role in some cases (Marik 2010). Disruption of mucosal blood flow plays a significant role in ulcers in the glandular mucosa of horses. The etiology of gastric ulceration in horses is also multifactorial, with stress (including transport stress), stall confinement, exercise type, exercise intensity, diet type, and diet frequency (i.e., intermittent feeding) all suggested to be contributing factors (Hammond et al 1986, Andrews and Nadeau 1999, Martineau et al 2009). The pathophysiology of equine gastric ulceration involves an imbalance between aggressive (HCl, pepsin) and defensive factors (Martineau et al 2009). Volatile fatty acids (fermentation by-products of resident bacteria), because of their high lipid solubility at stomach pH ≤ 4.0, diffuse into the non-glandular mucosal cells, acidifying the cell and damaging chloride-dependent sodium transport, resulting in cell swelling, necrosis, and ulceration (Andrews and Nadeau 1999, Andrews et al, 2005, Martineau et al 2009). Non-glandular squamous mucosa is predisposed to acid injury because it lacks substantial protective mucus and bicarbonate layers (Ross et al 1981, Murray 1992, Videla and Andrews 2009). In the horse, the layered epithelium of the squamous mucosa forms a physical barrier to acid (HCl and organic acids) diffusion (Andrews et al 2005). The cuticular lining of the snow crab's hindgut most likely performs a similar physical barrier function. Post-molt weakening of such a barrier function could predispose this junctional location to acid injury. The majority (80%) of equine gastric ulcers occurs in the non-glandular (squamous) region of the stomach and these ulcers are often located along the margo plicatus, the junction of the non-glandular and glandular regions of the stomach (Hammond et al 1986, Sandin et al 2000, Luthersson et al 2009, Videla and Andrews 2009). Interestingly, the junction of non-chitinized mucosa and chitinized-mucosa

is similarly affected in snow crabs. This suggests that transitional regions within mucosal epithelium are predisposed to hypoxic and/or acid-induced mucosal injury.

5.4.4. **Hemocytic Nodules and Corneal Ulcers**

Foci of hemocytic inflammation including hemocytic aggregates and larger hemocytic nodules were occasionally observed within snow crab tissues. These foci of inflammation were randomly distributed and etiologic agents were not seen within them. The only hemocytic aggregate with a visible intralesional etiologic agent was a hemocytic aggregate along the luminal surface of the heart in the snow crab with microsporidiosis (Figure 5.24). A hemocytic nodule in the gill (Figure 5.43) had some intralesional structures (Figure 5.34) that may have been degenerated hemocytes or a possible etiologic agent; unfortunately further attempts to examine the lesion (special staining with PAS and GMS and transmission electron microscopy) were unsuccessful (data not shown). The shallow stratum (stratum TN) in Bonavista Bay had higher prevalence of corneal ulcers than those seen in the deeper region of that bay (stratum 796) but the TN had a higher prevalence of corneal ulcers than BB 796. The reason for this higher rate of corneal ulceration in the shallow region of the bay is unclear. However, BB TN had the most severe bacterial gill fouling suggesting that higher bacterial fouling in this region may contribute to the pathogenesis of these lesions.

5.4.5. **Prevalence of Epibiota and Inflammation with BCD**

Gill bacterial fouling tended to be less severe in BCD+ snow crabs than in BCD- snow crabs. Starvation in snow crabs is associated with a reduction in both glycogen stores and hemolymph

proteins (Chapter 4). This metabolic impairment of the diseased crustacean hosts may result in an altered gill microenvironment resulting in reduced gill bacterial fouling.

There was no significant difference in the prevalence of intestinal inflammation (midgut-hindgut junctional ulcers or midgut necrotizing enteritis) or in the prevalence of hemocytic aggregates between BCD- and BCD+ snow crabs. When the data from both bays that contain cases of BCD were combined, higher prevalence of one pattern of inflammation (midgut-hindgut junctional ulcers) was seen in snow crabs without BCD. This coincides with previous reports that BCD does not induce an inflammatory response in snow crabs (reviewed in Stentiford and Shields 2005).

A common feature of hematodiniosis is progressive hemocytopenia concomitant with increasing parasite burden (Field et al 1992, Filed and Appleton 1995, Taylor et al 1996, Shields and Squyars 2000, Stentiford and Shields 2005). Hemocytopenia in crustacean hosts develops in other hemocoelic protozoan and bacterial diseases (Johnson 1977, Stewart 1984, Cain and Morado 2001, Battison 2004, Morado 2011). In those diseases, possible causes of progressive hemocyte depletion have included lysis of host cells after phagocytosis of parasite cells, consumption of hemocytes by the invading cells, possible disruption of hematopoietic tissue function, or sequestration of hemocytes in host defense reactions which overwhelms the host's immune system (Field and Appleton 1995, Walker et al. 2009, Morado 2011). The mechanism by which hemocytopenia is produced in *Hematodinium*-associated disease is unknown. Mitotic activity in hematopoietic tissue with concurrent hemocytopenia occurs in Norway lobsters

Nephrops norvegicus and red and blue king crabs *Paralithodes* spp. (Field and Appleton 1995, Ryazanova 2008). However, the authors did not specify whether hematopoiesis in these crabs appeared orderly and complete or whether the stages present exhibited evidence of maturation arrest (i.e., incomplete differentiation) which could indicate ineffective hematopoiesis (Lin and Sőderhall 2011). Ineffective hematopoiesis contributes to the pathogenesis of human malarial anemia (Perkins et al 2011, Awandare et al 2011, Panichakul et al 2012). Host metabolic exhaustion due to parasitic acquisition of host resources is another possible cause of the profound hemocytopenia (Rowley et al 2015).

The two primary defense mechanisms of the crab's innate immune system are the clotting and prophenoloxidase (proPO) systems. Impaired clotting ability is often observed in BCD (Hudson and Shields 1994, Meyers et al 1987, Shields and Squyars 2000). Hemolymph clotting is an important component of the innate immune system which overlaps the humoral/cellular boundary and involves a combination of soluble and cell-derived factors (Jiravanichpaisal et al 2006). In decapod crustaceans, clotting consists of polymerization of large circulating clottable proteins into long, branched chains to form a gel. The polymerization is mediated by a transglutaminase released from hemocytes or tissues upon injury. Transglutaminases are calcium-dependent enzymes which can form covalent bonds between the side chains of free lysine and glutamine residues on the clottable proteins (Fuller and Doolittle 1971, Sritunyalucksana and Sőderhall 2000, Kollman and Quispe 2005, Jiravanichpaisal et al 2006). The hemocytopenia associated with hematodiniosis may impair coagulation in affected

crustaceans via lack of transglutaminase release due to marked reduction in circulating hemocytes.

The prophenoloxidase activating (proPO) system is an efficient component of the innate immune response and comprises several proteins involved in phagocytosis, encapsulation, melanized nodule formation, and cytotoxic reactions (Jiravanichpaisal et al 2006, Vazquez et al 2009). Activation of the proPO system is apparently mediated through the specific recognition of glycosylated pathogen-associated molecular patterns (PAMPs). The proPO system is triggered by the presence of minute amounts of microbial components such as lipopolysaccharides and peptidoglycans from bacteria, beta-1,3 glucans from fungi, and mannan (Jiravanichpaisal et al 2006, Vazquez et al 2009). The system is composed of pattern-recognition proteins and protein inhibitors, regulatory factors to avoid inappropriate system activation (Jiravanichpaisal et al 2006). The lack of significant inflammation associated with hematodiniosis suggests that this parasite avoids detection by the innate immune system or inhibits activation of the proPO system through unknown mechanisms (Stentiford et al 2003, Stentiford and Shields 2005, Rowley et al 2015). Extracellular protozoan parasites can evade the innate immune response by antigen-based strategies (mimicry, masking, variation and sharing of parasite antigens), eliminating their protein coat, anti-immune mechanisms, immunosuppression, immunomodulation, exploitation of the host immune reaction, and fast development (i.e., the parasites proliferate faster than the development of a host defense response; Zambrano-Villa et al 2002, Sitjà-Bobadilla 2008). The observation of effective encapsulation of fungal and bacterial co-infections suggests that widespread proPO inhibition is

not achieved in affected hosts as the host can produce and release hemocytes in response to other pathogens (Johnson 1986, Stentiford et al 2003, Rowley et al 2015). These findings suggest that generalized immunosuppression is unlikely (Rowley et al 2015). The crustacean immune systems may not recognize *Hematodinium* as foreign. An absence of recognition of this dinoflagellate pathogen may play a key role in the pathogenesis of hematodiniosis and account for the unchecked parasitic proliferation within the hemolymph and tissues of affected hosts (Stentiford et al 2003).

In BCD-infected Norway lobster *Nephrops norvegicus* and snow crabs *Chionoecetes opilio* (Field and Appleton 1995), fixed phagocytes in infected hosts appeared activated and enlarged (Field and Appleton 1995, Wheeler et al 2007). This "activation" may reflect the presence of the parasite, but also may be in response to secondary invaders or cellular debris arising from the parasitic infection. Similarly, hemocytic aggregates, encapsulations, and melanized nodules were occasionally seen in infected hosts, although definitive evidence of parasitic dinoflagellates was never documented within those immune reactions (Tables 1.5 and 1.6). Thus, it is uncertain whether observed cellular aggregates represent immune responses in early stages of *Hematodinium* sp. infections or responses to previous or concurrent infections by other pathogens. In this study there was no significant difference in the prevalence of hemocytic aggregates between *Hematodinium* infected snow crabs and uninfected snow crabs. This suggests that the hemocytic aggregates observed in snow crabs are most likely background lesions unrelated to *Hematodinium* infection, and supports the hypothesis proposed by Rowley

and others (2015) that *Hematodinium* circumvents the cellular immune defense reactions in some crustacean hosts.

5.5. References

Aguirre-Guzman G, Mejia Ruiz H, Ascencio F. 2004. A review of extracellular virulence product of *Vibrio* species important in diseases of cultivated shrimp. Aquac Res 35(15):1395-1404.

Andrews FM, Buchanan BR, Elliot SB, Clariday NA, Edwards LG. 2005. Gastric ulcers in horses. J. Anim. Sci. 83(E. Suppl.):E18–E21.

Airriess CN, McMahon BF. 1996. Short-term emersion affects cardiac function and regional hemolymph distribution in the crab *Cancer magister*. J Exp Biol 199(3):569-578.

Ali T, Harty RF. 2009. Stress-induced ulcer bleeding in critically ill patients. Gastroenterol Clin N Am 38(2):245-265.

Andrews FM, Buchanan BR, Elliot SB, Clariday NA, Edwards LH. 2005. Gastric ulcers in horses1. J Anim Sci 83:E18-21.

Andrews FM, Nadeau JA. 1999. Clinical syndromes of gastric ulceration in foals and mature horses. Equine Vet J 31(S29):30-33.

Awandare GA, Kempaiah P, Ochiel DO, Piazza P, Keller CC, Perkins DJ. 2011. Mechanisms of erythropoiesis inhibition by malarial pigment and malaria-induced proinflammatory mediators in an in vitro model. Am J Hematol 86(2):155-62.

Battison AL, Cawthorn RJ, Horney BS. 2004. Response of American lobsters *Homarus americanus* to infection with a field isolate of *Aerococcus viridans* var. *homari* (Gaffkemia). Dis Aquat Org 61(3):263-268.

Battison AL, Després BM, Greenwood SJ. 2008. Ulcerative enteritis in *Homarus americanus*: case report and molecular characterization of intestinal aerobic bacteria of apparently healthy lobsters in live storage. J Invertebr Pathol 99(2):129-135.

Benhalima K, Moriyasu M, Wade E, Hébert M. 1998. Exoskeletal lesions in the male snow crab Chionoecetes opilio (Brachyura: Majidae) in the southern Gulf of St. Lawrence. Can J Zool 76(4):601-8.

Brattey J, Elner RW, Uhazy LS, Bagnall AE. 1985. Metazoan parasites and commensals of five crab (Brachyura) species from eastern Canada. Can J Zool 63(9):2224-2229.

Briggs RP. 1976. Biology of *Paranthessius anemoniae* in association with anemone hosts. J Mar Biol Assoc U.K. 56(04):917-24.

Briggs RP. 1977. Structural observations on the alimentary canal of *Paranthessius anemoniae*, a copepod associate of the snakelocks anemone *Ammonia sulcata*. J Zool 182(3):353-68.

Cain TA, Morado JF. 2001. Changes in total hemocyte and differential counts in Dungeness crabs infected with *Mesanophrys pugettensis*, a marine facultative parasitic ciliate. J Aquat Anim Health 13(4):310-9.

Cattadori IM, Boag B, Hudson PJ. 2008. Parasite co-infection and interaction as drivers of host heterogeneity. Int J Parasitol 38(3):371-80.

Chatton É, Poisson R. 1931. Sur l'existence dans le sang des crabes, de péridiniens parasites: *Hematodinium perezi* n.g., n.sp. (Syndinidae). C R Seances Soc Biol Paris 105:553–557.

Cheng W, Liu CH, Hsu JP, Chen JC. 2002. Effect of hypoxia on the immune response of giant freshwater prawn *Macrobrachium rosenbergii* and its susceptibility to pathogen *Enterococcus*. Fish Shellfish Immunol 13(5):351-365.

Chung JS, Zmora N. 2008. Functional studies of crustacean hyperglycemic hormones (CHHs) of the blue crab, *Callinectes sapidus*–the expression and release of CHH in eyestalk and pericardial organ in response to environmental stress. FEBS J 275(4):693-704.

Couch JA. 1966. Two peritrichous ciliates from the gills of the blue crab. Chesapeake Sci 7(3):171-3.

Cui Z, Li X, Liu Y, Song C, Hui M, Shi G, Luo D, Li Y. 2013. Transcriptome profiling analysis on whole bodies of microbial challenged *Eriocheir sinensis* larvae for immune gene identification and SNP development. PLoS One. 8(12):e82156.

Dawe E, Mullowney D, Colbourne E, Han G, Morado JF, Cawthorn R. 2010. Relationship of oceanographic variability with distribution and prevalence of bitter crab syndrome in snow crab (*Chionoecetes opilio*) on the Newfoundland–Labrador shelf. *In:* Biology and management of exploited crab populations under climate change. Alaska Sea Grant College Program, AK-SG-10-01:175-198.

Das D, Bandyopadhyay D, Bhattacharjee M, Banerjee R. 1997. Hydroxyl radical is the major causative factor in stress-induced gastric ulceration. Free Radic Biol Med 23(1):8-18.

De Coninck DIM, Asselman J, Glaholt S, Janssen CR, Colbourne JK, Shaw JR, De Schamphelaere KAC. 2014. Genome-wide transcription profiles reveal genotype-dependent responses of biological pathways and gene-families in *Daphnia* exposed to single and mixed stressors. Environ Sci Technol 48(6):3513-3522.

Di Camillo C, Bo M, Puce S, Tazioli S, Froglia C, Bavestrello G. 2008. The epibiontic assemblage of *Geryon longipes* (Crustacea: Decapoda: Geryonidae) from the Southern Adriatic Sea. Ital J Zool 75(1):29-35.

Dick MH, Donaldson WE, Vining IW. 1998. Epibionts of the tanner crab *Chionoecetes bairdi* in the region of Kodiak Island, Alaska. J Crust Biol 18(3):51-528.

Dunn PH, Young CM. 2014. Larval settlement of the nemertean egg predator *Carcinonemertes errans* on the Dungeness crab, *Metacarcinus magister.* Invertebr Biol 133(3):201–212.

Dvoretsky AG, Kuz'min SA, Matishov GG. 2007. The biology of the amphipod *Ischyrocerus commensalis* and its symbiotic relationships with the red king crab in Barents Sea. Doklady Akademii Nauk 417(3):424-426.

Dvoretsky AG, Dvoretsky VG. 2009. Distribution of amphipods *Ischyrocerus* on the red king crab, *Paralithodes camtschaticus*: possible interactions with the host in the Barents Sea. Estuar Coast Shelf Sci 82(3):390-396.

Dvoretsky AG, Dvoretsky VG. 2013. Copepods associated with the red king crab *Paralithodes camtschaticus* (Tilesius, 1815) in the Barents Sea. Zool Stud 30 52:17.

Fernandez-Leborans G. 2010. Epibiosis in Crustacea: an overview. Crustaceana 83(5):549.

Field RH, Appleton PL. 1995. A *Hematodinium* -like dinoflagellate infection of the Norway lobster *Nephrops norvegicus*: Observations on pathology and progression of infection. Dis Aquat Org 22(2):115-128.

Field RH, Chapman CJ, Taylor AC, Neil DM, Vickerman K. 1992. Infection of the Norway lobster *Nephrops norvegicus* by a *Hematodinium*-like species of dinoflagellate on the west coast of Scotland. Dis Aquat Org 13(1):1-15.

Fleming LC, Burt MDB, Bacon GB. 1981. On some commensal Turbellaria on the Canadian east coast. Hydrobiologia 84(1):131-137.

Foyle TP, O'Dor RK, Elner RW. 1989. Energetically defining the thermal limits of the snow crab. J Exp Biol 145(1):371-393.

Frías-Espericueta MG, Abad-Rosales S, Nevárez-Velázquez AC, Osuna-López I, Páez-Osuna F, Lozano-Olvera R, Voltolina D. 2008. Histological effects of a combination of heavy metals on Pacific white shrimp *Litopenaeus vannamei* juveniles. Aquat Toxicol 89(3):152-157.

Fuller GM, Doolittle RF. 1971. Invertebrate fibrinogen. II. Transformation of lobster fibrinogen into fibrin. Biochemistry-US 10(8):1311-1315.

Gannon AT, Wheatly MG. 1992. Physiological effects of an ectocommensal gill barnacle, *Octolasmis muelleri*, on gas exchange in the blue crab Callinectes sapidus. J Crust Biol 12(1):11-18.

Gotto RV. 1979. The association of copepods with marine invertebrates. Adv Mar Biol 16:1-09.

Hammond CG, Mason DK, Watkins KL. 1986. Gastric ulceration in mature Thoroughbred horses. Equine Vet J 18(4):284-287.

He S, Qian Z, Yang J, Wang X, Mi X, Liu Y, Hou F, Liu Q. 2013. Molecular characterization of a p38 MAPK from *Litopenaeus vannamei* and its expression during the molt cycle and following pathogen infection. Dev Comp Immunol 41(2):217-221.

Hooper RG. 1986. A spring breeding migration of the snow crab, *Chionoecetes opilio* (O. Fabr.), into shallow water in Newfoundland. Crustaceana 500(3):257-264.

Hudson DA, Shields JD. 1994. *Hematodinium australis* n. sp., a parasitic dinoflagellate of the sand crab *Portunus pelagicus* from Moreton Bay, Australia. Dis Aquat Org 19(2):109-119.

Jiravanichpaisal P, Lee BL, Söderhäll K. 2006. Cell-mediated immunity in arthropods: hematopoiesis, coagulation, melanization and opsonization. Immunobiology 211(4): 213-236.

Johnson PT. 1986. Parasites of benthic amphipods: dinoflagellates (Duboscquodinida: Syndinidae). Fish Bull 84(3):605-614.

Khan RA. 1977. Susceptibility of marine fish to trypanosomes. Can J Zool 55:1235-1241.

Khan RA. 1982. Biology of the marine piscicolid leech *Johanssonia arctica* (Johansson) from Newfoundland. Proc Helminthol Soc Wash 49(2):266-78.

Kim BM, Rhee JS, Lee KW, Kim MJ, Shin KH, Lee SJ, Lee YM, Lee JS. 2015. UV-B radiation-induced oxidative stress and p38 signaling pathway involvement in the benthic copepod *Tigriopus japonicas*. Comp Biochem Phys C 167:15-23.

Kollman JM, Quispe J. 2005. The 17Å structure of the 420kDa lobster clottable protein by single particle reconstruction from cryoelectron micrographs. J Struct Biol 151(3):306-314.

Kon T, Isshiki T, Mihadai T, Honma Y. 2011. Milky hemolymph syndrome associated within an intranuclear bacilliform virus in snow crab *Chionoecetes opilio* from the Sea of Japan. Fish Sci 77(6):99-1007.

Kuris AM, Wickham DE. 1987. Effect of nemertean egg predators on crustaceans. Bull Mar Sci 41(2):151-164.

Larssen JIR. 1999. Identification of microsporidia. Acta Protozool 38:161-197.

Le Moullac GL, Soyez C, Saulnier D, Asnquer D, Avarre JC, Levy P. 1988. Effect of hypoxic stress on the immune response and the resistance to vibriosis of the shrimp *Penaeus stylirostris*. Fish Shellfish Immunol 8(8):621-629.

Lightner DV. 1978. Possible toxic effects of the marine blue-green alga, *Spirulina subsalsa*, on the blue shrimp, *Penaeus stylirostris*. J Invert Pathol 32(2):139-150.

Lightner DV. 1996. A handbook of shrimp pathology and diagnostic procedures for diseases of cultured penaeid shrimp. World Aquaculture Society, Louisiana.

Lightner DV, Hendrick RP, Fryer JL, Chen SN, Liao IC, Kou GH. 1987. A survey of cultured penaeid shrimp in Taiwan for viral and other important diseases. Fish Pathol 22(3):127-140.

Lin X, Söderhäll I. 2011. Crustacean hematopoiesis and the astakine cytokines. Blood 117(24):6417-6424.

Luthersson N, Nielsen K, Harris P, Parkin TD. 2009. The prevalence and anatomical distribution of equine gastric ulceration syndrome (EGUS) in 201 horses in Denmark. Equine Vet J 41(7):619-624.

Malfertheiner P, Chan FK, McColl KE. 2009. Peptic ulcer disease. Lancet 374(9699):1449-1461.

Marcogliese DJ. 1993. Larval parasitic nematodes infecting marine crustaceans in eastern Canada. 1. Sable Island, Nova Scotia. J Helminthol Soc Wash 60(1):96-99.

Marcogliese DJ. 1996. Larval parasitic nematodes infecting marine crustaceans in eastern Canada. 3. *Hysterothylacium aduncum*. J Helminthol Soc Wash 63(1):12-18.

Marik PE. 2010. Stress ulcer prophylaxis in the new millennium! ICU Director 1(1):12-16.

Martineau H, Thompson H, Taylor D. 2009. Pathology of gastritis and gastric ulceration in the horse. Part 1: Range of lesions present in 21 mature individuals. Equine Vet J 41(7):638.

McClelland G. 1990. Larval sealworm (*Pseudoterranova decipiens*) infections in benthic macrofauna. Can Bull Fish Aquat Sci 222:47-65.

McGaw IJ. 2006. Epibionts of sympatric species of *Cancer* crabs in Barkley Sound, British Columbia. J Crust Biol 26(1):85-93.

McGaw IJ, Reiber CL. 2002. Cardiovascular system of the blue crab *Callinectes sapidus*. J Morphology 251(1):1-21.

McMahon BR. 2001. Respiratory and circulatory compensation to hypoxia in crustaceans. Resp Physiol 128(3):349-64.

Meyer MC, Khan RA. 1979. Taxonomy biology, and occurrence of some marine leeches in Newfoundland waters. Proc Helminthol Soc Wash 46(2):254-64.

Meyers TR, Koeneman TM, Botelho C, Short S. 1987. Bitter crab disease: a fatal dinoflagellate infection and marketing problem for Alaskan tanner crabs *Chionoecetes bairdi*. Dis Aquat Org 3(3):195-216.

Mikulski CM, Burnett LE, Burnett KG. 2000. The effects of hypercapnic hypoxia on the survival of shrimp challenged with *Vibrio parahaemolyticus*. J Shellfish Res 19(1):310-311.

Monnig AA, Prittie JE. 2011. A review of stress-related mucosal disease. J Vet Emerg Crit Care 21(5):484-495.

Morado JF. 2011. Protistan diseases of commercially important crabs: a review. J Invert Path 106(1):27-53.

Morley NJ. 2010. Aquatic molluscs as auxiliary hosts for terrestrial nematode pathogens: implications for pathogen transmission in a changing climate. Parasitol 137(7):1041-1056.

Mullowney DR, Dawe EG, Morado JF, Cawthorn RJ. 2011. Sources of variability in prevalence and distribution of bitter crab disease in snow crab (*Chionoecetes opilio)* along the northeast coast of Newfoundland. ICES J Mar Sci 68(3):463-471.

Murray MJ. 1992. Aetiopathogenesis and treatment of peptic ulcer in the horse: a comparative review. Equine Vet J 24(S13):63-74.

Palm HW. 1999. Ecology of *Pseudoterranove decipiens* (Krabbe, 1878) (Nematoda: Anisakidae) from Antarctic waters. Parasitol Res 85(8-9):638-646.

Panichakul T, Payuhakrit W, Panburana P, Wongborisuth C, Hongeng S, Udomsangpetch R. 2012. Suppression of erythroid development in vitro by *Plasmodium vivax*. Malar J 11:173.

Parrilla-Taylor DP, Zenteno-Savín T. 2011. Antioxidant enzyme activities in Pacific white shrimp (*Litopenaeus vannamei*) in response to environmental hypoxia and reoxygenation. Aquaculture 318(3):379-83.

Perkins DJ, Were T, Davenport GC, Kempaiah P, Hittner JB, Ong'echa JM. 2011. Severe malarial anemia: innate immunity and pathogenesis. Int J Biol Sci 7(9):1427.

Ross IN, Bahari HM, Turneberg LA. 1981. The pH gradient across mucus adherent to rat fundic mucosa *in vivo* and the effect of potential damaging agents. Gastroenterology 81(4):713-718.

Rowley AF, Smith AL, Davies CE. 2015. How does the dinoflagellate parasite *Hematodinium* outsmart the immune system of its crustacean hosts? PLoS Pathog 11(5):e1004724.

Ryazanova TV. 2008. Bitter Crab Syndrome in two species of king crabs from the Sea of Okhotsk. Russian J Mar Biol 34(6):411-414.

Ryazanova TV, Eliseikina MG. 2010. Microsporidia of the genera *Thelohania* (Thelohaniidae) and *Ameson* (Pereziidae) in two species of lithodid crabs from the Sea of Okhotsk. Russ J Mar Biol 36(6):435-442.

Sandeman A. 1967. The vascular circulation in the brain, optic lobes, and thoracic ganglia of the crab *Carcinus*. Proc R Soc Lond B Biol Sci 168(1010):82-90.

Sandin A, Skidell J, Haggstrom J, Nilsson G. 2000. Postmortem findings of gastric ulcers in Swedish horses older than age one year: a retrospective study of 3715 horses (1924-1996). Equine Vet J 32(1):36-42.

Savoie L, Miron G, Biron M. 2007. Fouling community of the snow crab *Chionoecetes opilio* in Atlantic Canada. J Crust Biol 27(1):30-36.

Sheppard M, Walker A, Frischer ME, Lee RF. 2003. Histopathology and prevalence of the parasitic dinoflagellate, *Hematodinium* sp., in crabs (*Callinectes sapidus, Callinectes similis, Neopanope sayi, Libinia emarginata, Menippe mercenaria*) from a Georgia estuary. J Shellfish Res 22(3):873-880.

Shi H, Yan X, Xu X, Ruan L. 2012. Molecular cloning and characterization of a cDNA encoding extracellular signal-related kinase from *Litopenaeus vannamei*. Fish Shellfish Immunol 33(4):813-820.

Shields JD, Squyars CM. 2000. Mortality and hematology of blue crabs, *Callinectes sapidus,* experimentally infected with the parasitic dinoflagellate *Hematodinium perezi*. Fish Bull 98(1):139-152.

Shields JD, Overstreet RM. 2003. The Blue Crab: Diseases, parasites, and other symbionts. Faculty Publications from the Harold W. Manter Laboratory of Parasitology. Paper 426. Retrieved from http://digitalcommons.unl.edu/parasitologyfacpubs/426.

Shields JD, Taylor DM, Sutton SG, O'Keefe PG, Ings DW, Pardy AL. 2005. Epidemiology of Bitter Crab Disease (*Hematodinium* sp.) in snow crabs *Chionoecetes opilio* from Newfoundland, Canada. Dis Aquat Org 64(3):253-264.

Shields JD, Taylor DM, O'Keefe PG, Colbourne E, Hynick E. 2007. Epidemiological determinants in outbreaks of Bitter Crab Disease (*Hematodinium* sp.) in snow crabs *Chionoecetes opilio* from Conception Bay, Newfoundland, Canada. Dis Aquat Org 77(1):61-72.

Shilo BZ. 2014. The regulation and functions of MAPK pathways in *Drosophila*. Methods 68(1):515-519.

Singer M. 2010. Pathogen-pathogen interaction: a syndemic model of complex biosocial processes in disease. Virulence 1(1):10-18.

Sitjà-Bobadilla A. 2008. Living off a fish: a trade-off between parasites and the immune system. Fish Shellfish Immun 25(4):358-372.

Sritunyalucksana K, Söderhäll K. 2000. The proPO and clotting system in crustaceans. Aquaculture 191(1):53-69.

Steele DH, Hooper RG, Keats D. 1986. Two corophorid amphipods commensal on spider crabs in Newfoundland. J Crust Biol 6(1):119-124.

Stentiford GD, Evans M, Bateman K, Feist SW. 2003. Co-infection by a yeast-like organism in *Hematodinium*-infected European edible crabs *Cancer pagurus* and velvet swimming crabs *Necora puber* from the English Channel. Dis Aquat Org 54(3):195-202.

Stentiford GD, Feist SW, Stone DM, Bateman KS, Dunn AM. 2013. Microsporidia: diverse, dynamic, and emergent pathogens in aquatic systems. Trends Parasitol 29(11):567-578.

Stentiford GD, Shields JD. 2005. A review of the parasitic dinoflagellates *Hematodinium* species and *Hematodinium* -like infections in marine crustaceans. Dis Aquat Org 66(1):47-70.

Stewart JE. 1984. Lobster Diseases. Helgoläinder Meeresunters 37: 243-254.

Stickel WB, Kapper MA, Liu LL, Gnaiger E, Want SY. 1989. Metabolic adaptations of several species of crustaceans and molluscs to hypoxia: tolerance and microcalorimetric studies. Biol Bull 177(2):303-312.

Stollman N, Metz DC. 2005. Pathophysiology and prophylaxis of stress ulcer in intensive care unit patients. J Crit Care 20(1):35-45.

Tanner CA, Burnett LE, Burnett KG. 2006. The effects of hypoxia and pH on phenoloxidase activity in the Atlantic blue crab, *Callinectes sapidus.* Comp Biochem Phys 144(2):218-223.

Taylor AC, Field RH, Parslow-Williams PJ. 1996. The effects of *Hematodinium* sp.-infection on aspects of respiratory physiology of the Norway lobster, *Nephrops norvegicus* (L.). J Exp Mar Biol Ecol 207(1): 217-228.

Vader W. 1983. Associations between amphipods (Crustacea: Amphipoda) and sea anemones (Anthozoa, Actinaria). Papers from the Conference on the Biology and Evolution of Crustacea. Australian Museum Memoir 18:141-153.

Valko M, Leibfritz D, Moncol J, Cronin MTD, Mazur M, Telser J. 2007. Free radicals and antioxidants in normal physiological functions and human disease. Int J Biochem Cell Biol 39(1):44-84.

Vazquez L, Alpuche J, Maldonado G, Agundis C, Pereyra-Morales A, Zenteno E. 2009. Review: immunity mechanisms in crustaceans. Innate Immun 15(3):179-188.

Videla R., Andrews FM. 2009. New perspectives in equine gastric ulcer syndrome. Vet Clin Equine 25(2):283-301.

Wahl M. 1989. Marine epibiosis. I. Fouling and antifouling: some basic aspects. Mar Ecol Prog Ser 58:175-89.

Walker AN, Lee RF, Frischer ME. 2009. Transmission of the parasitic dinoflagellate *Hematodinium* sp. infection in blue crabs *Callinectes sapidus* by cannibalism. Dis Aquat Org 85(3):193-197.

Wang TC, Nai YS, Wang CY, Solter LF, Hsu HC, Wang CH, Lo CF. 2013. A new microsporidian, *Triwangia caridinae* gen. nov., sp. nov. parasitizing fresh water shrimp, *Caridina formosae* (Decapoda: Atyidae) in Taiwan. J Invert Pathol 112(3):281-293.

Webster SG. 1996. Measurement of crustacean hyperglycaemic hormone levels in the edible crab *Cancer pagurus* during emersion stress. J Exp Biol 199(7):1579-1585.

Wheeler K, Shields JD, Taylor DM. 2007. Pathology of *Hematodinium* infections in snow crabs (*Chionoecetes opilio*) from Newfoundland, Canada. J Invertebr Pathol 95(2):93-100.

Wickham DE. 1979. Predation by the nemertean *Carcinonemertes errans* on eggs of the Dungeness crab *Cancer magister.* Mar Biol 55(1):45–53.

Wickham DE. 1980. Aspects of the life history of *Carcinonemertes errans* (Nemertea: Carcinonemertidae), an egg predator of the crab *Cancer magister.* Biol Bull 159(1):247–257.

Williams DD, Moore KA. 1985. The role of semiochemicals in benthic community relationships of the lotic amphipod *Gammarus pseudolimnaeus*: a laboratory analysis. OIKOS 44: 280-286.

Yan H, Zhang 2, Li CZ, Chen YH, Chen YG, Weng SP. 2013. Molecular characterization and function of a p38 MAPK gene from *Litopenaeus vannamei*. Fish Shellfish Immunol 34(6):1421-1431.

Yang L, Liu X, Huang J, Yang Q, Qui L, Liu W, Jiang S. 2012. Molecular characterization and expression profile of MAP2K1ip1/MP1 gene from tiger shrimp, *Penaeus monodon*. Mol Biol Rep 39(5):5811-5818.

Zambrano-Villa S, Rosales-Borjas D, Carrero JC, Ortiz-Ortiz L. 2002. How protozoan parasites evade the immune response. Trends Parasitol 18(6):272-278.

http://www.dfo-mpo.gc.ca/fm-gp/sustainable-durable/fisheries-peches/snow-crab-eng.htm

6. General Discussion

6.1. Diagnostic Testing For BCD

In advanced stages of hematodiniosis, affected hosts are often externally recognized by discoloration of the carapace. In snow crabs BCD is associated with pinkish-orange discoloration of the carapace and an opaque white appearance to the ventrum. This characteristic macroscopic appearance of BCD has been used as a means of estimating disease prevalence in the field via diagnosis by visual exam. In this study diagnosis by visual exam had excellent specificity (100%) with no disease-free animals mistakenly classified as having BCD (i.e., animals diagnosed by visual as having BCD always had the disease). The sensitivity of the test is not as robust (85.7%) due to false negative test results (i.e., some BCD+ snow crabs were mistakenly classified as BCD-). False negative test results associated with diagnosis by visual exam were often early infections with mild to moderate infection intensities. This indicates that there are subclinical infections at the time of the Fall surveys in Newfoundland which are missed by diagnosis via visual exam, confirming that disease prevalence data from this diagnosis method underestimates BCD prevalence in Newfoundland snow crabs. In this study these subclinical BCD infections represented 14.3 to 21.4% of *Hematodinium* sp. infections and were associated with a 1.25 – 1.76% underestimation of BCD prevalence. This underestimation of BCD prevalence by macroscopic diagnosis is consistent with previous reports of this diagnostic technique (Pestal et al 2003, Dawe et al 2010, Mullowney et al 2011, Mullowney et al 2014). While visual exam underestimates disease prevalence, it is considered representative of disease trends within Newfoundland snow crab populations (Mullowney et al 2011, Mullowney et al 2014).

Furthermore, a single non-gravid female with BCD did not have macroscopic discoloration of the carapace despite having advanced infection intensity: the immature female had late-stage BCD but did not have an opaque appearance to her ventrum. Instead of having "milky" hemolymph, this snow crab had opaque reddish-orange hemolymph. This reddish-orange discoloration may have been due to altered hemolymph lipoproteins and/or carotenoids associated with vitellogenesis and/or ovarian degeneration. This finding may suggest that the macroscopic changes typical of BCD could be masked in prepubescent/pubescent female snow crabs, which may also contribute to underestimations of BCD prevalence by diagnosis via visual examination. The sensitivity and specificity of diagnosis by PCR assay were equivalent to that of diagnosis by visual exam. Molecular diagnosis by PCR assay also missed the subclinical infections that were missed by visual examination in this study. These false negative tests may have been due to insufficient amounts of template DNA in the tested hemolymph samples. Modifying the PCR protocol (i.e., increasing the amount of hemolymph sampled) for screening of subclinical snow crabs (particularly in female snow crabs) may be one approach for increasing the sensitivity of diagnosis by PCR assay.

6.2. Comparison of *In Vivo* and *In Vitro* Life Stages of BCD

Microscopic examination of BCD-infected snow crabs revealed multisystemic infiltration of hemal spaces and interstitial connective tissues as reported previously (see Chapter 1, Table 1.6). In this study multisystemic infiltration of hemal spaces and interstitial connective tissues was evident even in the earliest infection observed with mild infection intensity. The

hepatopancreas may be the initial site of infection in some crustacean hosts; it is often the most severely affected tissue (Stentiford et al 2002). However, no preferential tissue tropism (i.e., no evidence of differential infection intensity based on tissue location) was observed in this study.

In the mildest case of BCD, the morphologic appearance of the parasites was different than in more advanced stages of the disease. In the early stage of the disease the parasites had smaller amounts of cytoplasm that was basophilic rather than vacuolated in appearance. This basophilic cytoplasmic appearance is most likely due to cytoplasmic ribosomal and messenger RNA content, protein, and ribosomes associated with cellular proliferation (Singer 1954, Goodman et al 1994). These early stages also had a high proportion (50%) of multinucleate cells, consistent with a replicating parasitic population. In snow crabs with moderate infection intensities, uninucleated stages predominated while in more intense infections (advanced and very advanced infections) the parasitic populations had increasing proportions of multinucleate cells. This increase in multinucleation in the late stages of the disease may represent progressive increase in parasite proliferation in late BCD. Such a surge in proliferation could be induced by perception of unfavorable environmental conditions and/or quorum sensing in the *Hematodinium* parasites (Thomas et al 2002, Waters and Bassler 2005). Alternatively, the increased multinucleation may be an indicator of reduced or impaired cytokinesis in late BCD. The latter could occur due to generalized nutrient limitation associated with depletion of host metabolic reserves (Muscatine and Pool 1979). Specific alterations in hemolymph lipid

metabolites could also impair cytokinesis (Emoto and Umeda 2000, Atilla-Glokcumen et al 2011).

Light microscopic and electron microscopic examination of parasitic life stages revealed amoeboid life stages that varied from uninucleate to multinucleate. In addition, vermiform (elongate) life stages were also observed. These vermiform life stages were often intimately associated with the sarcolemmal surface of cardiomyocytes, skeletal myocytes (in the abdomen, leg, and eyestalk), and/or connective tissue surfaces. Similar attached vermiform life stages have been described in other host species, associated with the surfaces of hepatopancreatic tubules, hemal spaces, midgut, and antennal gland tissues; attached vermiform plasmodia have not been reported in association with tissue surfaces in either the gonad or the gill (Table 1.4). Ultrastructurally, these vermiform plasmodia have cytoplasmic extensions which interdigitate with host cell membranes and which appear to attach parasitic cell bodies to one another. These findings suggest that *in vitro* arachnoid sporont life stages may represent exaggerations of *in vivo* attached vermiform plasmodia (Appleton and Vickerman 1998, Li et al 2011, Gaudet et al 2015).

6.3. Hemolymph Alterations in BCD

Hemolymph refractive index (HRI) is often assumed to be directly proportional to hemolymph protein levels in crustaceans, and thus is often used as an indicator of nutritional condition with significant reductions in HRI reported in starved crustaceans (Smith and Dall 1982, Moore et al 2000, Behringer et al 2008). Decreases in HRI are seen in association with some diseases

(bumper car disease in American lobster, *P. argus* virus 1 in Caribbean spiny lobsters) and with starvation in crustacean hosts (Djangmah 1970, Dall 1974, Smith and Dall 1982, Moore et al 2000, Greenwood et al 2005, Montgomery-Fullerton et al 2007, Behringer et al 2008). Mean HRI was significantly lower in BCD+ snow crabs than in BCD- snow crabs, indicating that the infected snow crabs were in poorer nutritional condition than uninfected snow crabs. BCD+ snow crabs also have significantly lower gut wall RI scores, an index of total body glycogen stores (Stentiford and Feist 2005). Mean HRI of BCD+ snow crabs was either not significantly different from or lower than the mean HRI of uninfected new-shelled snow crabs with similar glycogen reserves (gut wall RI scores of 0 or 1). These findings suggest that BCD is associated with a significant metabolic drain on their hosts' protein and glycogen stores. The metabolic demand of the rapidly proliferating parasites likely depletes host protein constituents and contributes to host morbidity (Stentiford et al 2000, 2001, Shields et al 2003). The metabolic demands of the proliferating parasites are exacerbated by cessation of feeding (starvation) associated with morbidity (Uglow 1969a,b, Stewart et al 1972,Taylor et al 1996, Stentiford et al 2000, Stentiford and Shields 2005). However, poor body condition could also be a predisposing host factor in the development of BCD rather than just a result of the disease. Low protein and glycogen stores could predispose crustaceans to developing disease due to interactions of these stores with crustacean innate immune function. Glycogen stores are required for maintenance of activity of the prophenoloxidase (proPO) system in amphipods *Gammarus pulex* (Cornet et al 2009). Proteins are important on many levels in the crustacean immune system involving pathogen recognition (lipopolysaccharide binding protein and the beta-glucan binding protein), antimicrobial proteins (such as penaeidins), clotting proteins, and the proPO activating

proteinase cascade (Rosas al 2004, Cerenius et al 2008, Amparyup et al 2013). In humans, malnutrition impairs elements of both adaptive and innate immunity important in defense against parasitic infections, although evidence of increased incidence of severity of parasitic infections in malnourished humans is limited (Hughes and Kelly 2006). Malnutrition can either increase or decrease the severity of a parasitic disease depending on the complex interactions between the nutritional status of the host, the functions of the immune system, and the nature of the parasitic infection (Beisel 1982). Because of their bulk, some parasites require sizeable quantities of nutrients which must be obtained from the same sources available to host cells leading to progressive host malnutrition and immune system impairment (Beisel 1982). Host metabolic exhaustion due to parasitic acquisition of host resources may contribute to the development of profound hemocytopenia in hosts with BCD (Rowley et al 2015).

In addition to depletion of body stores of protein and glycogen, BCD also alters lipid metabolism within infected hosts. Untargeted metabolomics evaluation of BCD-infected hemolymph revealed at least 35 BCD-associated metabolites, the majority of which were glycerophospholipid metabolites. Altered glycerophospholipid metabolism in infected hosts may result from negative energy balance (i.e., starvation) associated with the parasitic disease. Successful replication of protozoan parasites depends on acquiring extracellular and intracellular components from their host or synthesizing them from host-derived precursors (Lund and Chu 2002). As a parasitic infection progresses, the total surface area of parasites increases; thus parasites must be able to acquire phospholipids for new cell membranes. Some parasitic protozoans (such as *Giardia lamblia, Trichomonas vaginalis, Toxoplasma gondii,* and

Pneumocystis carnii) rely on their host to provide them with pre-formed phospholipids while other parasitic protozoans (*Perkinsus marinum, Trypanosoma brucei, Plasmodium knowlesi, Plasmodium falciparum,* and *Leishmania* spp.) can synthesize phospholipids from host-derived precursors (Ancelin and Vial 1986, Jarroll et al 1989, Smith 1993, Rifkin et al 1995, Lujan et al 1996, Stevens et al 1997, Kaneshiro 1998, Lund and Chu 2002). The bloodstream form of *Trypanosoma brucei* acquires most of its lipid precursors from circulating host lipoproteins (van Hellemond and Tielens 2006). Thus, these BCD-associated phospholipids may represent parasitic phospholipids rather than host phospholipids. Such parasitic phospholipids would be derived from parasitic acquisition of host lipids and/or synthesis from host precursors indicating that host lipid metabolism has been altered by the disease. These BCD-associated glycerophospholipid metabolites may contribute to the bitter taste reported to be associated with *Hematodinium* infected crustacean meat. Bitter taste perception is complex and numerous compounds can be bitter tastants, suggesting that alterations in many factors (electrolytes, free fatty acids, amino acids and peptides) could contribute to the bitter taste associated with BCD. Furthermore, BCD-associated metabolites could include immunomodulatory lipids similar to those which have been reported in other pathogens including *Mycobacterium tuberculosis* and *Trypanosoma cruzi* (Ehrt and Schnappinger 2007, Brodsky and Medzhitov 2009, Machado et al 2011).

6.4. BCD and Inflammation

Histopathologic survey of Newfoundland snow crabs revealed no evidence of a gender or size effect on BCD prevalence in this study. This is in contrast to previous studies which indicated

that disease prevalence was highest in intermediate-sized animals and that females consistently had prevalence levels twice that of males (Dawe 2002, Mullowney et al 2011). The prevalence data in this study should be interpreted with caution because the snow crab collections for this study were convenience samples and did not include many new-shelled females or small- and intermediate-sized snow crabs of either gender, resulting in both gender and size biases in our study.

Prevalence of gill and cuticular epibionts was generally not effected by BCD status. The one exception to this was reduced severity of gill bacterial fouling in BCD+ snow crabs. This reduction in gill microbial fouling may be due to the metabolic effects of the disease. As discussed above, BCD is associated with reductions of both glycogen and protein stores which could alter the gill microenvironment and limit nutritional bioavailability to gill microflora.

Prevalence of inflammation was also not impacted by BCD status. This indicates that there was no increase in any pattern of inflammation observed in snow crabs in association with *Hematodinium* sp. infection. The only difference observed between BCD- and BCD+ snow crabs was lower prevalence of midgut-hindgut junctional ulcers in BCD+ snow crabs, suggesting that BCD may reduce the potential for inflammation rather than induce it. Occasional hemocytic aggregates or nodules in animals with *Hematodinium* have been described elsewhere, although dinoflagellate parasites were not found within these inflammatory foci. The prevalence data in this study suggests that these hemocytic lesions are background lesions within crustaceans (i.e., are not induced by BCD) and supports the hypothesis that *Hematodinium* avoids induction of the cellular immune response in some infected crustacean hosts.

6.5. Conclusions

This study confirms that BCD is associated with alterations in protein, glycogen, and lipid metabolism consistent with parasite-associated negative energy balance (i.e., starvation) in affected snow crabs. Histologic examination of BCD infected snow crabs revealed vacuolar degeneration in hepatopancreatic epithelium but no definitive evidence of parasite-associated inflammation or tissue necrosis. These findings indicate that the main pathologic effects of BCD are metabolic in nature. Altered lipid metabolism in *Hematodinium*-infected host is associated with generation of at least 35 BCD-associated metabolites. These BCD-associated glycerophospholipid metabolites may contribute to the bitter taste associated with infected meat and may include immunomodulatory lipids. Evaluation of *Hematodinium* sp. lipid fractions for immunomodulatory activity may be warranted. The lack of co-infections in BCD infected snow crabs despite marked hemocytopenia suggests that evaluation of parasite fractions for antimicrobial activity should also be pursued.

Diagnosis of BCD by visual exam and by PCR underestimated disease prevalence due to misclassification of snow crabs with early stage disease (mild and moderate intensity infections) as BCD-negative. In addition, BCD infection in a non-gravid female snow crab was masked by hemolymph discoloration that was most likely a result of altered host hemolymph lipoproteins (and/or carotenoids). Degenerative changes within the ova of this non-gravid female combined

with epidemiological data which suggests that females may be predisposed to infection (Dawe 2002) indicate that it is possible that this disease could have occult effects on female reproductive success. Further investigation of this possibility may be warranted. Subclinical infections represented 14.3-21.4% of the BCD infections in the Fall in this study, but it is unclear if this accurately reflects true natural disease distribution in Newfoundland snow crabs. Evaluation of large snow crabs collected at other time points during the year (Winter, Spring, and Summer) for histologic evidence of subclinical BCD infections may also be warranted.

Evaluation of prevalence of inflammatory lesions within animals with and without BCD indicates that there is no significant increase in any pattern of inflammation observed in association with BCD. This supports the hypothesis that *Hematodinium* avoids induction of the innate immune system of crustaceans affected by BCD. Investigation of the mechanism of *Hematodinium* immune system evasion is recommended to further our understanding of host-pathogen interactions in BCD. Such research has the potential to lead to development of novel immunotherapeutic agents for protozoal diseases.

6.6. References

Amparyup P, Caroensapsri W, Tassanakajon A. 2013. Prophenoloxidase and its role in shrimp immune responses against major pathogens. Fish Shellfish Immunol 34(4):990-1001.

Ancelin ML, Vial HJ. 1986. Several lines of evidence demonstrating that *Plasmodium falciparum*, a parasitic organism, has distinct enzymes for phosphorylation of choline and ethanolamine. FEBS Lett 202(2):217–223.

Appleton PL, Vickerman K. 1998. *In vitro* cultivation and developmental cycle in culture of a parasitic dinoflagellate (*Hematodinium* sp.) associated with mortality of the Norway lobster (*Nephrops norvegicus*) in British waters. Parasitol 116(2):115-130.

Atilla-Golkcumen GE, Bedigian V, Sasse S, Eggert US. 2011. Inhibition of glycosphingolipid biosynthesis induces cytokinesis failure. J Am Chem Soc 133(26): 10010-10013.

Behringer DC, Butler MJ, Shields JD. 2008. Ecological and physiological effects of PaV1 infection on the Caribbean spiny lobster (*Panulirus argus* Latreille). J Exp Mar Biol 359(1):26-33.

Beisel WR. 1982. Synergism and antagonism of parasitic diseases and malnutrition. Rev Infect Dis. 4(4): 746-750.

Brodzky IE, Medzhitov R. 2009. Targeting of immune signaling networks by bacterial pathogens. Nat Cell Biol 11(5):521-526.

Cerenius L, Lee BL, Söderhall K. 2008. The proPO-system: pros and cons for its role in invertebrate immunity. Trends Immunol 29(6): 263-271.

Cornet S, Biard C, Moret Y. 2009. Variation in immune defence among populations of *Gammarus pulex* (Crustacea: Amphipoda). Oecologia 159(2):257-269.

Dall W. 1974. Indices of nutritional state in the western rock lobster, *Panulirus longipes* (Milne Edwards). I. Blood and tissue constituents and water content. J Exp Mar Biol Ecol 16:167-180.

Dawe EG. 2002. Trends in prevalence of Bitter Crab Disease caused by *Hematodinium* sp. in snow crabs (*Chionoecetes opilio*) throughout the Newfoundland and Labrador continental shelf. *In* Crabs in Cold Water Regions: Biology, Management and Economics. Alaska Sea Grant College Program, AK-SG-02-02:385-400.

Dawe E, Mullowney D, Colbourne E, Han G, Morado JF, Cawthorn R. 2010. Relationship of oceanographic variability with distribution and prevalence of bitter crab syndrome in snow crab (*Chionoecetes opilio*) on the Newfoundland–Labrador shelf. *In:* Biology and management of exploited crab populations under climate change. Alaska Sea Grant College Program, AK-SG-10-01:175-198.

Djangmah JS. 1970. The effects of feeding and starvation on copper in the blood and hepatopancreas, and on the blood proteins of *Crangon vulgaris* (Fabricius). Comp Biochem Physiol D 32(4):709-718.

Ehrt S, Schnappinger D. 2007. *Mycobacterium tuberculosis* virulence: inside and out. Nat Med 13(3):284-285.

Emoto K, Umeda M. 2000. Regulation of contractile ring disassembly by redistribution of phosphatidylethanolamine. J Cell Biol 49(6):1215-1224.

Gaudet PH, Cawthorn RJ, Buote MA, Morado JF, Wright GM, Greenwood SJ. 2015. *In vitro* cultivation of *Hematodinium* sp. isolated from Atlantic snow crab, *Chionoecetes opilio:* partial characterization of late developmental stages. Parasitol 142(4):598-611.

Goodman DG, Maronpot RR, Newberne PM, Popp JA, Square RA. 1994. Proliferative and selected other lesions of the liver in rats. G1-5. *In* Guides for Toxicologic Pathology. STP/ARP/AFIP: Washington, DC.

Greenwood SJ, Després BM, Cawthorn RJ, Lavallée J, Groman DB, Desbarats A. 2005. Case report: outbreak of bumper car disease caused by *Anophryoides haemophila* in a lobster holding facility in Nova Scotia, Canada. J Aquat Anim Health 17(4):345-352.

Hughes S, Kelly P. 2006. Interactions of malnutrition and immune impairment, with specific reference to immunity against parasites. Parasit Immunol 28(11):577-588.

Jarroll EL, Manning P, Berrada A, Hare D, Lindmark DG. 1989. Biochemistry and metabolism of *Giardia.* J Protozool 36(2):190-197.

Kaneshiro ES. 1998. The lipids of *Pneumocystis carinii.* Clin Microbiol Rev 11(1):27–41.

Li C, Miller TL, Small HJ, Shields JD. 2011. In vitro culture and developmental cycle of the parasitic dinoflagellate *Hematodinium* sp. from the blue crab *Callinectes sapidus*. Parasitology 138(14):1924-1934.

Lujan HD, Mowatt MR, NashTE. 1996. Lipid requirements and lipid uptake by *Giardia lamblia* trophozoites in culture. J Euk Microbiol 43(3):237-242

Lund ED, Chu FL. 2002. Phospholipid biosynthesis in the oyster protozoan parasite, *Perkinsus marinus*. Mol Biochem Parasitol 121(2):245-53.

Machado FS, Murkherjee S, Weiss LM, Tanowitz HB, Ashton AW. 2011. Bioactive lipids in *Trypanosoma cruzi* infection. Adv Parasitol 76:1-31.

Moore LE, Smith DM, Loneragan NR. 2000. Blood refractive index and whole-body lipid as indicators of nutritional condition for penaeid prawns (Decapoda: Penaeidae). J Exp Mar Biol Ecol 244(1):131-143.

Montgomery-Fullerton MM, Cooper RA, Kauffman KM, Shields JD, Ratzlaff RE. 2007. Detection of *Panulirus argus* Virus 1 in Caribbean spiny lobsters. Dis Aquat Org 76(1):1-6.

Mullowney DR, Dawe EG, Morado JF, Cawthorn RJ. 2011. Sources of variability in prevalence and distribution of bitter crab disease in snow crab (*Chionoecetes opilio*) along the northeast coast of Newfoundland. ICES J Mar Sci 68(3):463-471.

Mullowney DRJ, Dawe DG, Colbourne EG, Rose GA. 2014. A review of factors contributing to the decline of Newfoundland and Labrador snow crab (*Chionoecetes opilio*). Rev Fish Biol Fisheries 24(2):639-657.

Muscatine L, Pool RR. 1979. Regulation of numbers of intracellular algae. Proc R Soc Lond B. 204(1155):131-139.

Rifkin MR, Strobos CAM, Fairlamb AH. 1995. Specificity of ethanolamine transport and its further metabolism in *Trypanosoma brucei.* J Biol Chem 270(27):16160–16166.

Rosas C, Cooper EL, Pascual C, Brito R, Gelabert R, Moreno T, Miranda G, Sanchez A. 2004. Indicators of physiological and immunological status of *Litopenaeus setiferus* wild populations (Crustacea, Penaeidae). Mar Biol 145(2):401-413.

Shields JD, Scanlon C, Volety A. 2003. Aspects of the pathophysiology of blue crabs, *Callinectes sapidus*, infected with the parasitic dinoflagellate *Hematodinium perezi*. Bull Mar Sci 72(2):519-535.

Singer M. 1954. The staining of basophilic components. J Histochem Cytochem 2(5):322-333.

Smith DM, Dall W. 1982. Blood protein, blood volume and extracellular space relationships in two *Penaeus* spp. (Decapoda: Crustacea). J Exp Mar Biol Ecol. 63(1):1-15.

Smith JD. 1993. Phospholipid biosynthesis in protozoa. Prog Lipid Res 32(1):47–60.

Stentiford GD, Chang ES, Chang SA, Neil DM. 2001. Carbohydrate dynamics and the crustacean hyperglycemic hormone (CHH): Effects of parasitic infection in Norway lobsters (*Nephrops norvegicus*). Gen Comp Endocrinol 121(1):13-22.

Stentiford GD, Feist SW. 2005. A histopathological survey of shore crab (*Carcinus maenas*) and brown shrimp (*Crangon crangon*) from six estuaries in the United Kingdom. J Invert Pathol 88(2):136–146.

Stentiford GD, Green M, Bateman K, Small HJ, Neil DM, Feist SW. 2002. Infection by a *Hematodinium* -like parasitic dinoflagellate causes Pink Crab Disease (PCD) in the edible crab *Cancer pagurus*. J Invertebr Pathol 79(3):179-191.

Stentiford GD, Neil DM, Coombs GH. 2000. Alterations in the biochemistry and ultrastructure of the deep abdominal flexor muscle of the Norway lobster *Nephrops norvegicus* during infection by a parasitic dinoflagellate of the genus *Hematodinium*. Dis Aquat Org 42(2):133-141.

Stentiford GD, Shields JD. 2005. A review of the parasitic dinoflagellates *Hematodinium* species and *Hematodinium* -like infections in marine crustaceans. Dis Aquat Org 66(1):47-70.

Stevens TL, Gibson GR, Maier AJ, Allison-Ennis M, Das S. 1997. Uptake and cellular localization of exogenous lipids by *Giardia lamblia*, a primitive eukaryote. Exp Parasitol 86(2):133-143.

Stewart JE, Zwicker BM, Arie B, Horner GW. 1972. Food and starvation as factors affecting the time to death of the lobster *Homarus americanus* infected with *Gaffkya homari*. J Fish Res Board Can 29(4):461–464.

Taylor AC, Field RH, Parslow-Williams PJ. 1996. The effects of *Hematodinium* sp.-infection on aspects of respiratory physiology of the Norway lobster, *Nephrops norvegicus* (L.). J Exp Mar Biol Ecol 207(1): 217-228.

Thomas F, Brown SP, Sukhdeo M, Renaud F. 2002. Understanding parasite strategies: a state-dependent approach? Trends Parasitol 18(9):387-390.

Uglow RF. 1969a. Haemolymph protein concentrations in portunid crabs. I. Studies on adult *Carcinus maenas*. Comp Biochem Physiol 30(6):1083–1090

Uglow RF. 1969b. Haemolymph protein concentrations in portunid crabs. II. The effects of imposed fasting on *Carcinus maenas*. Comp Biochem Physiol 31(6):959–967

van Hellemond JJ, Tielens AGM. 2006. Adaptations in the lipid metabolism of the protozoan parasite *Trypanosoma brucei*. FEBS Letters 580(23):551-558.

Waters CM, Bassler BL. 2005. Quorum sensing: cell-to-cell communication in bacteria. Annu Rev Cell Dev Biol 21:319-346.

Appendix 1: BCD Polymerase Chain Reaction (PCR) Assay Protocol

Modified BCD version of Ivanova 96 well Plate Extraction Protocol

Pre-DNA Extraction:

Note: The night before extraction: check wells to see if the EtOH has evaporated and if so then top them up to original 1 ml volume. Place sample plate on its side in a shaking incubator overnight (shake, no heat). ***Add a known positive blood sample to B10 of the plate.**

Day 1:

1. Vortex plate and transfer 150 µl blood-EtOH into 0.2ml strip tubes for lysis. (**Cut ends off tips to assist in pipetting chunky blood**)
2. Cover tubes and centrifuge for 3 min at 2000Hg to pellet blood. Removing only one strip of tubes at a time, pour off ethanol onto thick paper towel. Let the residue evaporate for 30 m to 1 h in the 56°C incubator
3. Recap original sample plate with new caps to prevent cross contamination.
4. Combine 5 ml of Insect Lysis buffer per plate and 0.5 ml of Proteinase K (20mg/ml) in a sterile container. Add 50 µl of Lysis mix to each well of blood. Cap and vigorously vortex to mix in lysis mix.
5. Incubate at 56°C overnight (24 h incubation gives better yield).

Day 2:

1. Centrifuge at 1500 g for 2 min to remove condensation from strip caps.
2. Add 100 µl of Binding Mix to each sample and shake vigorously for 10-15 sec. Centrifuge at 1000Hg for 2 min.
3. Transfer lysate (about 150 µl) to the wells of the glass fiber (PALL2) plate on top of the square-well block and seal plate.
4. Centrifuge at 600Hg for 7 min to bind DNA.
5. First Wash: Add 180 µl of Protein Wash Buffer to each well and seal with a new cover. Centrifuge at 6000 g for 5 min.
6. Second Wash **(2X)**: Add 750 µl of Wash Buffer to each well and seal with new cover. Centrifuge at 6000Hg for 7 min. **Repeat this step twice.**
7. Open sealing cover, close it and centrifuge at 6000Hg for 5 min to completely remove the Wash Buffer.
8. Remove cover and place plate on the lid of a tip box. Incubate at 56°C for 30 min to evaporate residual EtOH. . **Aliquot nuclease free water into 15ml sterile tube. Aliquot 10xTE buffer into 1.5 ml sterile tube. Place both aliquots in incubator with plates.**
9. Position PALL 2 collar on the collection microplate and place the glass fiber plate on top. Dispense 50 µl of preheated (56°C) ddH_2O onto the membrane of each well and incubate at RT for 2 min. Seal plate
10. Place assembled plates on a clean square-well block to prevent cracking and centrifuge at 6000Hg for 5 min to collect DNA elute. Remove and discard PALL plate.

11. Add 5.5 µl of 10X TE buffer to each sample. Label plate with Sample plate ID, date and Initials both on plate and foil. Cover plate and store at -20°C or proceed directly with PCR reaction.

Stock Solutions:

Solution	Components	Final Volume
1M Tris-HCl, pH 8.0:	Tris base 60.57 g HCl	500 ml
1M Tris-HCl, pH 7.4:	Tris base 60.57 g HCl	500 ml
0.1M Tris-HCl, pH6.4: (adjust pH with HCL to 6.4-6.5)	Tris base 6.06 g	500 ml
1M NaCl:	NaCl 29.22 g	500 ml
0.5M EDTA pH 8.0:	EDTA 93.05 g NaOH ~10.0 g	500 ml

(NOTE: Vigorously mix on a stirrer with heat. The disodium salt will not go into solution until the pH is approx. 8.0 by the addition of NaOH).

Proteinase K:	100 mg	5 ml

Reconstitute to a final volume of 5ml in Molecular grade Nuclease Free water (Qiagen).

Aliquot by 0.5 ml. Store at -20°C.

- Wash all lab ware with ELIMINase and rinse with dH_20. Filter buffers through 0.2 µm filter into a clean bottle. Make smaller working volume aliquots (eg.100 ml). Store stock solutions and working aliquots at 4°C, unless otherwise stated.

Working Solutions for DNA Extraction:

Buffer	Vol. of stock	Initial stock conc.	Final Volume
Insect Lysis Buffer:			
700 mM GuSCN	16.5 g		200 ml
30 mM EDTA	12 ml	**0.5M EDTA, pH 8.0**	
30 mM Tris-HCl	6 ml	**1M Tris-HCl, pH 8.0**	
0.5% Triton X-100	1 ml		
5% TWEEN 20	10 ml		

NOTE: Vigorously mix on a stirrer with heat.

Binding Buffer:			
6 M GuSCN	354.6 g		500 ml

20 mM EDTA	20 ml	**0.5M EDTA, pH 8.0**	
10 mM Tris-HCl	50 ml	**0.1M Tris-HCl, pH 6.4**	
4% Triton X	20 ml		

NOTE: Vigorously mix on a stirrer with heat. If any recrystallization occurs, then pre-warm at 56°C to dissolve before use.

Wash Buffer:

60% EtOH	300 ml	**100% EtOH**	500 ml
50 mM NaCl	25 ml	**1 M NaCl**	
10 mM Tris-HCl	5 ml	**1 M Tris-HCl, pH 7.4**	
0.5 mM EDTA	0.5 ml	**0.5M EDTA, pH 8.0**	
Sterile water	169.5 ml		

NOTE: mix well, store at -20°C.

Binding Mix:

Binding buffer	50 ml	100 ml
100% EtOH	48 ml	
Sterile water	2 ml	

Protein Wash Buffer:

Binding buffer	26 ml	100 ml
100% EtOH	67.2 ml	
Sterile water	6.8 ml	

NOTE: Stable at room temperature for about 1 week, discard if crystallization occurs.

*Make sure that there are two empty wells left for the controls; discard any liquids that may have eluted into the wells.

PCR:

-Use 6 µl of DNA template or control.

Three controls: negative (water)
positive DNA (validate the PCR reaction)
positive blood (validate the DNA extraction)

Circle the control wells on the PCR plate.

ITSR1:

Per 25 µl reaction.	106 reactions for 96 well plate
12.5 µl Master mix	1325 µl Master Mix
5.51 µl Sterile water	584.1 µl Sterile water
0.54 µl Primer ITSR1 (10 µM)	57.24 µl Primer ITSR1 (10 µM)
0.45 µl Primer Hemat-F-1487(10 µM)	47.7 µl Primer Hemat-F-1487 (10 µM)
6.0 µl DNA	+6 µl DNA per well

25.0 µl

ITSR1 – 5’-CTAGTCATACGTTTGAAGAAAGCC-3’ Small et al (2007)
Tm=58.4°C (as per Sigma Genosys)

Hemat-F-1487 – 5’ CCTGGCTCGATAGAGTTG-3’ Gruebl et al (2002)
Tm= 76.9°C (as per Sigma Genosys)

Profile for ITSR1 locus
1 min @ 95°C
20 s @ 94°C
30 s @ 57°C } 35 cycles
30 s @ 72°C
7 min @ 72°C
Always use a heated lid with this protocol.

Short term storage at 4°C or long term storage at -20°C.

*Use 1% agarose gel and load 8.5 µl of each PCR reaction with 3 µl of loading buffer (total volume of 20 µl). Use a microplate as a loading plate to mix the loading buffer with the samples.
* Run gel at 150V (constant voltage) for 45 min.

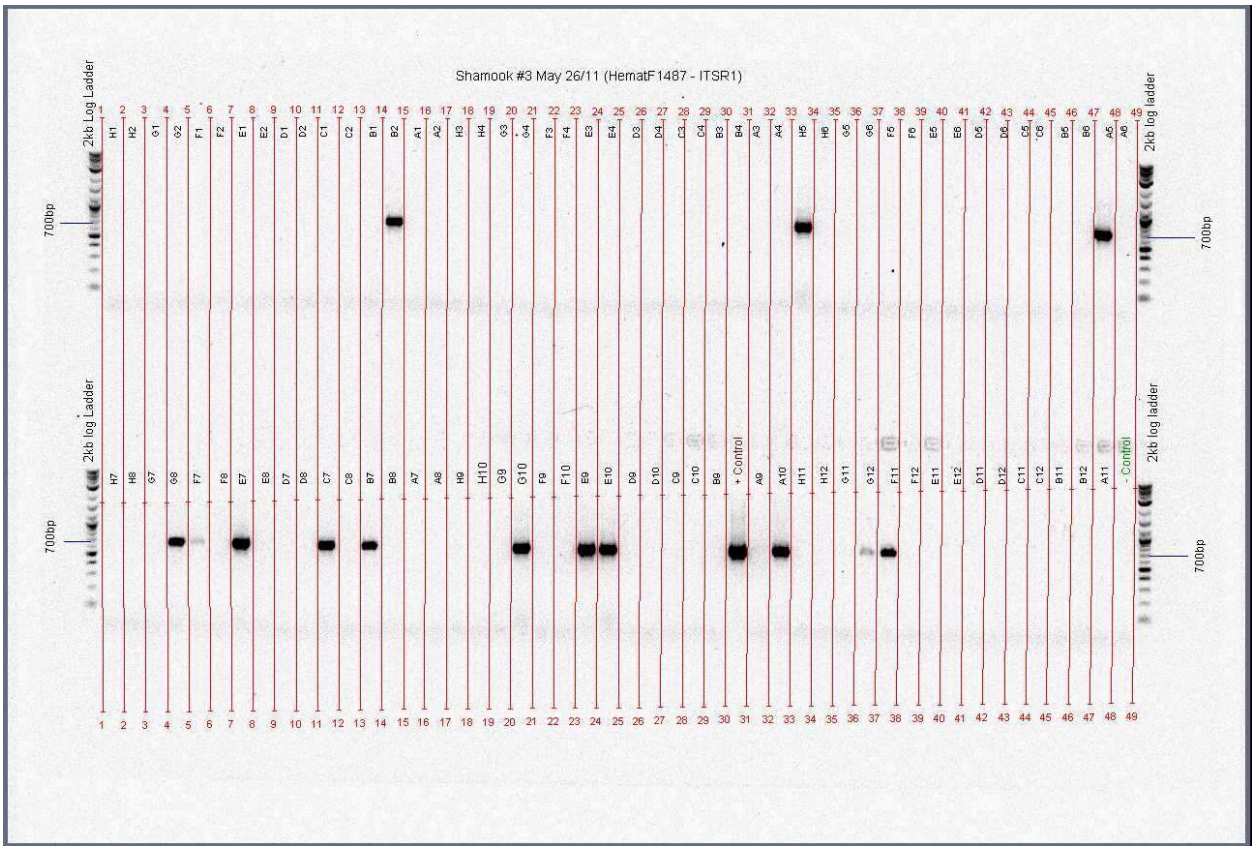

Figure A1.1. Sample plate Shamook #3 from 2008. Amplicon was approximately 700 bp. Positive and Negative controls in lanes B10 and A12 respectively. Marker lane was 2 kb log ladder.

References:

Gruebl T, Frischer ME, Sheppard M, Neumann M, Maurer A, Lee RF. 2002. Development of an 18S rRNA gene-targeted PCR based diagnostic for the blue crab parasite *Hematodinium* sp. Dis Aquat Org 49:61–70.

Small HJ, Shields JD, Hudson KL, Reece KS. 2007. Molecular detection of *Hematodinium* sp. infecting the blue crab, *Callinectes sapidus.* J Shellfish Res 26:131–139.

Appendix 2 – Potassium Chloride (KCl) Euthanasia Trial

A.2.1. Introduction

Injectable potassium chloride (KCl) is an effective, rapid, reliable, and safe method of euthanasia that has been reported as a viable means of humane euthanasia in American lobsters *Homarus americanus* (Battison et al 2000). A small trial was performed to determine if potassium chloride (KCl) solution would be a viable alternative method for humane euthanasia in snow crabs.

A.2.2. Materials and Methods:

Snow crabs (~30-50 mm carapace width) were euthanized using 0.25 ml (250 µl) of 330 mg/ml KCl. The solution was prepared from reagent grade KCl (Fischer Scientific, Nepean, Ontario, Canada) and sterile distilled water. The solution was cold-filtered (0.2 µm filter) under vacuum and placed in a 45 ºC warm water bath for 30 min to ensure complete dissolution. The KCl solution was injected at the posterior suture line. Completion of euthanasia via KCl overdose may require 30-60 sec. After euthanasia is complete, the suture line was then incised with a single-edged razor blade and the carapace was removed from the snow crabs. This method of euthanasia was compared to euthanasia by decapitation procedure (i.e., removal of the carapace) which was sufficient for rapid euthanasia on its own.

A.2.3. Results:

Snow crabs injected with KCl solution died rapidly (typically within 30-60 sec) as indicated externally by cessation of mouth movements and internally by cessation of beating of the heart. Euthanasia via KCl solution resulted in formation of a streak of cellular disruption within the snow crab's internal tissues.

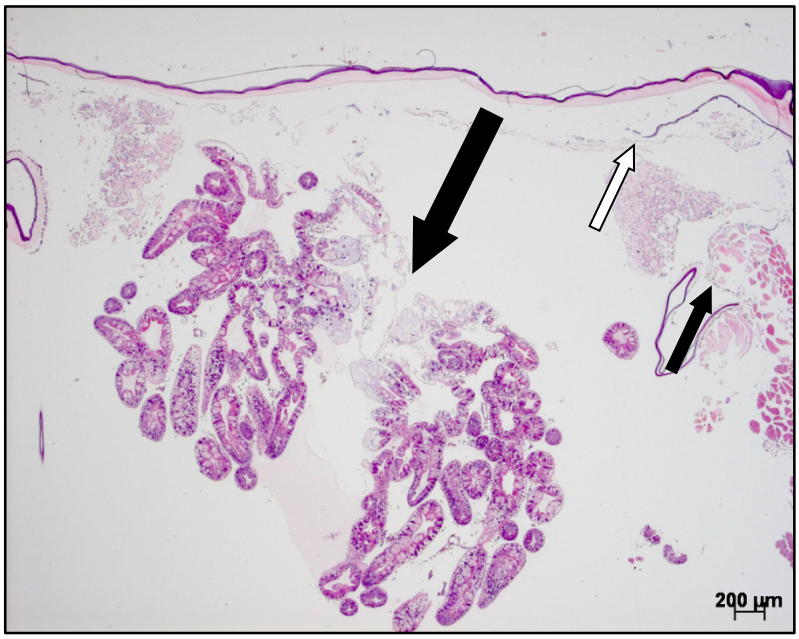

Figure A2.1. Streak of cellular degeneration and necrosis in hepatopancreas (large black arrow), adjacent abdominal skeletal muscle (short black arrow), and cuticular epithelium (white arrow; H&E, 25x).

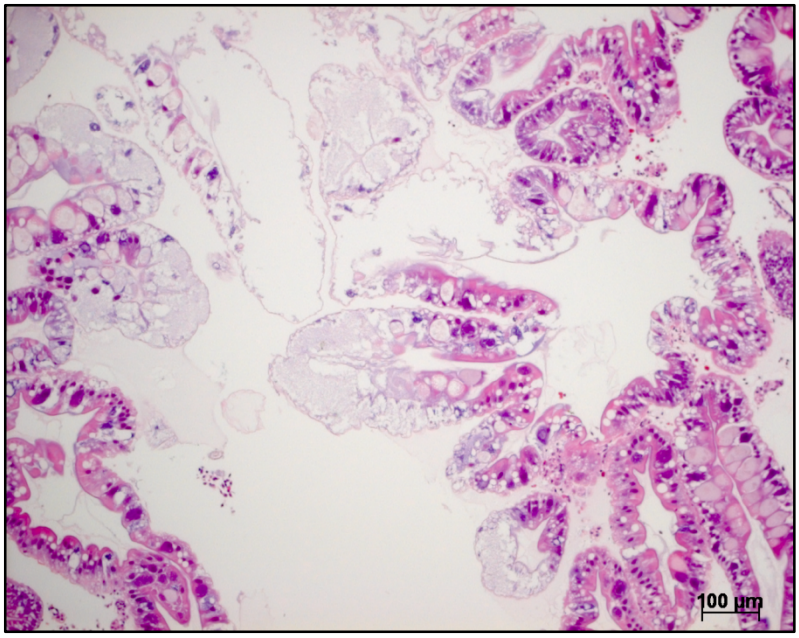

Figure A2.2. Streak of cellular degeneration and necrosis in hepatopancreas. Note central region of hepatopancreatic cellular degeneration and necrosis with cytoplasmic swelling, rarefaction, and basophilia with nuclear condensation or karyolysis (H&E, 100x).

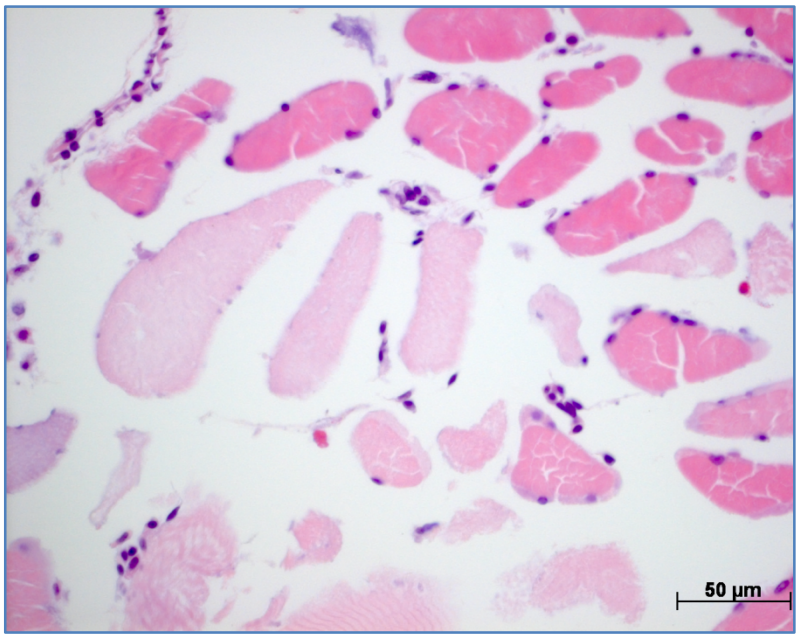

Figure A2.3. Myodegeneration in abdominal skeletal musculature. Abdominal skeletal myofibers were locally extensively pale and swollen (no vacuolar degeneration or fragmentation was observed; H&E, 400x).

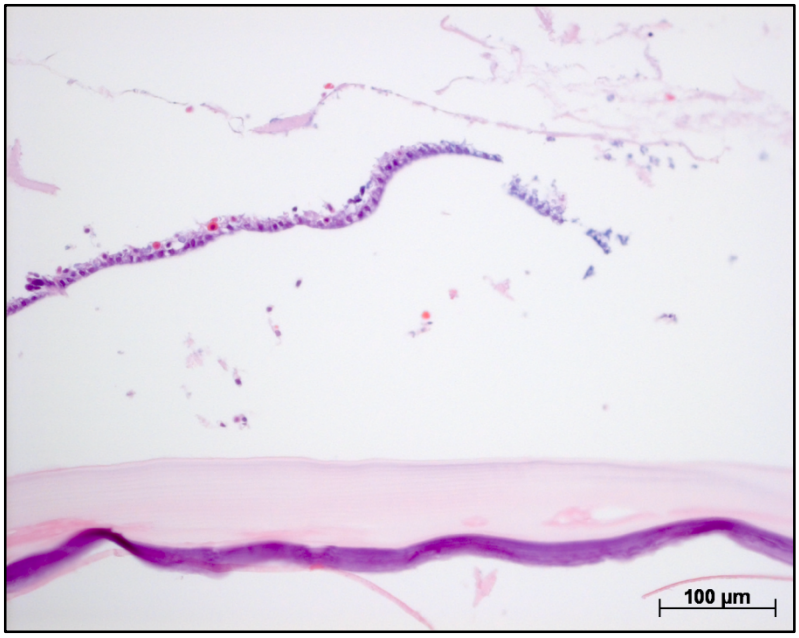

Figure A2.4. Region of cuticular epithelial degeneration and necrosis. Note transition from intact cuticular epithelium (right) to degenerative epithelium (left) with cytoplasmic swelling, pallor, and basophilia (H&E, 200x).

A.2.4. Discussion:

Potassium chloride solution injection was a rapid (30-60 sec) and effective means of euthanasia in the snow crab. However, the potassium chloride solution resulted in a streak of cellular disruption in the snow crab's tissues including the hepatopancreas, skeletal musculature, and cuticular epithelium. In American lobsters the only histologic lesion noted as an artifact of euthanasia via KCl was mild to moderate, multifocal, skeletal muscular degeneration at the injection site (Battison et al 2000). The lesion was characterized by cell swelling, loss of contraction bands, and occasional mild cytoplasmic vacuolation. This cellular disruption may be due to the hypertonic nature of the potassium chloride solution as the measured osmolarity of the solution has been reported to be 8,800 mOsm/kg on dilution (Battison et al 2000). In American lobsters the KCl solution is injected into a hemolymph sinus at the base of the walking

leg that communicated with the sternal sinus. This caudal location of the KCl injection as compared to more cranial location of the internal organs may have spared the lobster's vital organs from cellular degeneration. In snow crabs, the bases of the walking legs are immediately adjacent to the crab's vital organs. Thus, proximity to the injection site to the crab's internal organs may have resulted in this species difference. Thus, while potassium chloride solution is a viable alternative to humane euthanasia in snow crabs, this method of euthanasia is not applicable for studies which include tissue collections as significant cellular disruption occurs within the snow crabs' tissues.

A.2.5. Reference:

Battison A, MacMillan R, MacKenzie A, Rose P, Cawthorn R. 2000. Use of injectable potassium chloride for euthanasia of American Lobsters. Comp Med 50(5):545-550.

Appendix 3: Standard Operating Protocol for the preparation of Davidson's Seawater Fixative

Davidson's Seawater Fixative:

Stock Solution

Filtered sea water	3340 ml
95% Ethanol	3330 ml
36 - 40% Formaldehyde	2220 ml
Glycerin	1110 ml

Working Solution

Stock solution	720 ml
Glacial acetic acid	80 ml

Davidson's Seawater Fixative (by volume ratios):

Stock Solution

Filtered sea water	3340 ml	3 parts
95% Ethanol	3330 ml	3 parts
36 - 40% Formaldehyde	2220 ml	2 parts
Glycerin	1110 ml	1 parts
Total:		**9 parts**

Working Solution

Stock solution 720ml	9 parts
Glacial acetic acid 80ml	1 part
Total:	**10 parts**

Example:

Reagent	**Ratio**	**Amount (for example)**
Filtered sea water	3 parts	**30 ml**
95-100% Ethanol	3 parts	**30 ml**
36-40% Formaldehyde	2 parts	**20 ml**
Glycerin (Glycerol)	1 parts	**10 ml**
Glacial acetic acid*	1 parts	**10 ml**
Total	**10 parts**	**100 ml (1 necropsy container)**

*** Add glacial acetic acid extemporaneously (immediately before use).**

Note: Long-term stability of stock solution is unclear from the literature (may be stable for days to weeks or even months).

Use of Davidson's Seawater Fixative: Fix sample for 24 h in Davidson's-Seawater Fixative then transfer for storage into 50-70% ethanol for storage.

Reference: http://www.crustaceancrl.eu/sops%5C2013.pdf

Appendix 4: Eyestalk Sectioning Pilot Study

A.4.1. Introduction:

Bitter Crab Disease (BCD) is an emerging disease in decapod crustaceans. To date over 40 species of crustaceans have been reported to be infected by *Hematodinium* species world-wide, primarily in the North Pacific and Atlantic Oceans, including several commercially important decapods such as snow crabs (*Chionoecetes opilio*). Infections of *Hematodinium* spp. are fatal in every host species. However, it is unclear whether parasitemia in BCD occurs early in the disease process or only manifests in late stages of disease. Histologic examination of internal organs of snow crabs collected from bays (Bonavista Bay, Notre Dame Bay, and White Bay) along the northern coast of Newfoundland were examined via histology to determine the tissue distribution of early *Hematodinium* sp. infection. Additional to internal organs (gill, hepatopancreas, heart, midgut, and gonad) tissues lined by chitin (eyestalk, leg, and abdomen) were also examined. Preliminary examination of sections of the eyestalks (n=10) revealed rare clusters of the dinoflagellate parasites in 90% (9/10) of the eyestalks examined. A small trial was performed to determine the optimal method of longitudinal sectioning (midsagittal or frontal plane) snow crab eyestalks for evaluation of *Hematodinium* sp. infection in the early stages of BCD.

A.4.2. Materials and Methods:

Snow crabs (n=10, ~40-60 mm carapace width) collected from Quebec (a region thought to be BCD-free) were humanely euthanized via decapitation. Complete necropsies were performed with routine tissue collection (gill, heart, hepatopancreas, midgut, gonad, leg, abdominal cross-section, and both eyestalks). The eyestalks were placed in individually-labeled cassettes marked with the side of origin (left or right) of the eyestalk. The tissue samples were fixed in Davidson's Seawater fixative for 24 h then transferred into 70% ethanol for storage until processing. The tissues were trimmed routinely with the exception of the eyestalks. Each eye was trimmed in longitudinal section on either the mid-sagittal (median) plane or frontal plane. For 5 crabs the left eye was sectioned along the mid-sagittal plane and the right eye was sectioned along the frontal plane (Figure 4A.1). For the remaining 5 crabs the left eye was sectioned along the frontal plane and the right eye along the mid-sagittal plane. The eyestalks were examined histologically for orientation of anatomic structures to determine the optimal plane of sectioning.

Figure A4.1: Macroscopic appearance of longitudinal sections of the eyestalk along the mid-sagittal (top) and frontal (bottom) planes.

A.4.3. Results:

Comparison of the sections of eyestalk trimmed mid-sagittal plane versus the frontal plane revealed that the sections cut along the frontal plane yielded optimal cross sections of the x-organ-sinus gland tract and/or optic lobe peduncle (lamina ganglionaris, medulla externa, medulla interna and medulla terminalis). All four ganglia were often present in one of the two histologic sections examined (Figure A4.2) or the four ganglia were divided between the two halves of the eyestalk. In most mid-sagittal sections of eyestalks, only a small portion of the optic lobe peduncle (i.e. one or two ganglia) was observed (Figure A4.3A). More rarely the midsagittal sections contained an elongate tangential section of the ganglia (Figure A4.3B).

Figure A4.2. Eyestalk of *Chionoecetes opilio*: frontal plane long-section. The eyestalk ganglia were surrounded by connective tissue and hemal spaces. The four ganglia were the lamina ganglionaris (LG), medulla externa (ME), medulla interna (MI), and medulla terminalis (MT) which terminated in the optic tract (ot). The retinal basement membrane is indicated by the solid arrow (H&E, 25x).

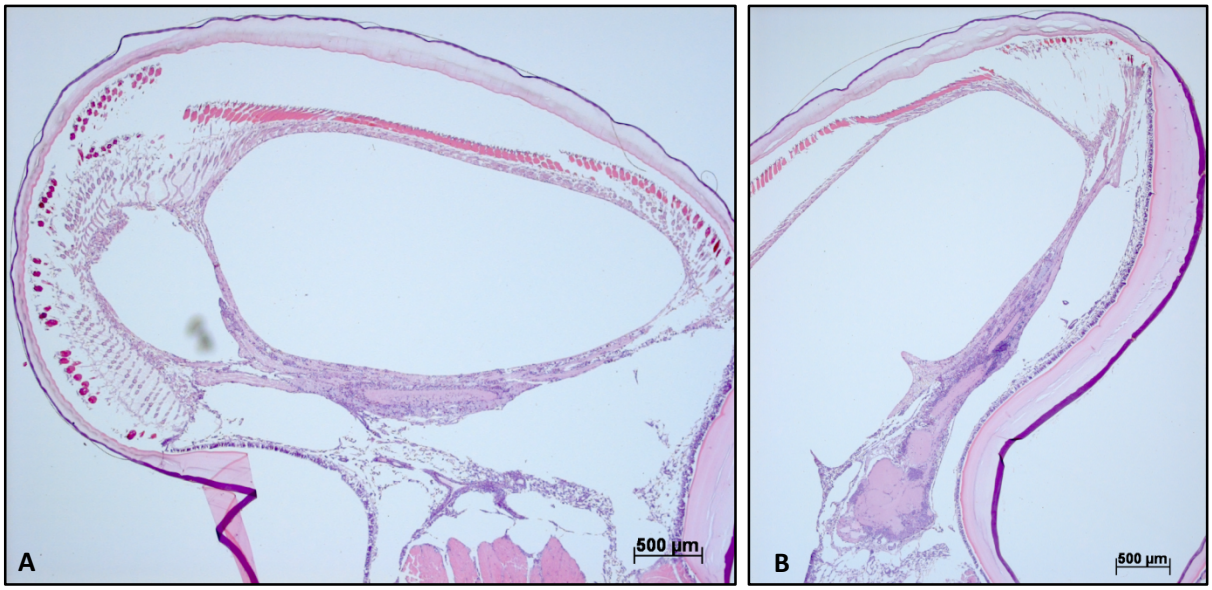

Figure A4.3. Eyestalk of *Chionoecetes opilio:* mid-sagittal long-sections with only the lamina ganglionaris present (A) and an elongate tangential section of the ganglia (B; H&E, 25x).

A.4.4. Discussion:

Eyestalk anatomy varies with species of crustacean examined. The eyestalks of most decapod crustaceans contain the optic lobe peduncle, which contains four distinct ganglia: the lamina ganglionaris, medulla externa, medulla interna, and medulla terminalis (Maynard et al 1968, Adiyodi and Adiyodi 1970, Blaustein et al 1988). The anatomic locations of the eyestalk structures vary among species (Figures A4.4 – A4.7). For example, the medulla interna of *Panulirus argus* (Figures A4.4 and A4.6a) is in a more ventral and proximal position than in *Procambarus clarkii* (Figure A4.6b). Consequently, when viewed from the transverse aspect, the shape of the distal region of the medulla terminalis in *P. argus* is spherical rather than columnar as seen in in *P. clarkii* (Blaustein et al 1988). This anatomic variation results in species

differences in histologic appearance of the ganglia when sectioned along different body planes (Figure A4.7). For snow crabs, sections of the eyestalk cut along the frontal plane yielded optimal cross sections of the x-organ-sinus gland tract and/or optic lobe peduncle (lamina ganglionaris, medulla externa, medulla interna and medulla terminalis) while mid-sagittal eyestalk sections contained smaller visible portions of the eyestalk ganglia.

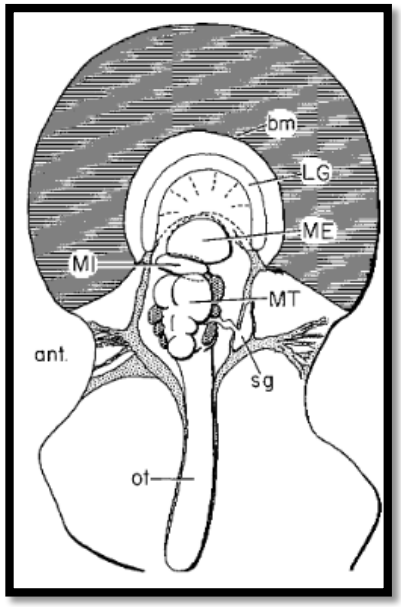

Figure A4.4. Eyestalk of *Panulirus argus* viewed from above. The eyestalk ganglia are surrounded by connective tissue (lightly stippled) which is attached laterally to the sides of the eyestalk. The medulla terminalis (MT), an olfactory ganglion, contains clumps of neuron cell bodies (heavily stippled). Neuron cell bodies associated with the three optic ganglia, lamina ganglionaris (LG), medulla externa (ME), and medulla interna (MI) are not shown. The sinus gland (sg), optic tract (ot), and basement membrane of the retinal layer (bm) are also noted (from Maynard and Yager 1968).

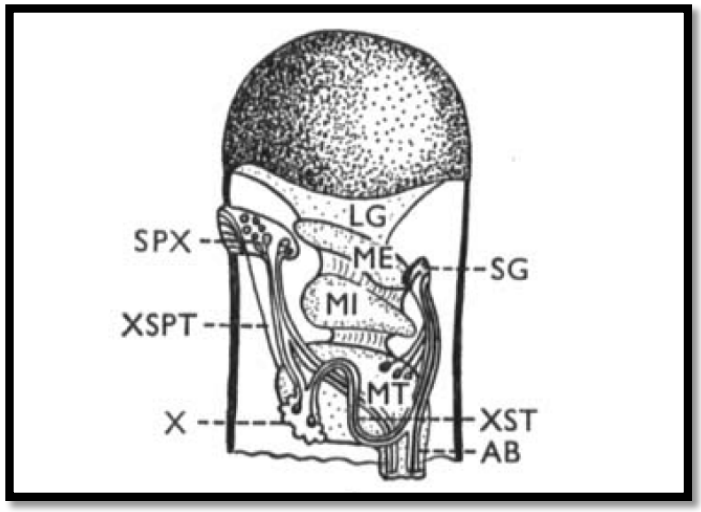

Figure A4.5: Eyestalk of *Lysmata seticaudata* showing pars ganglionaris X-organ (X), sensory pore X-organ (SPX), sinus gland (SG), the X-organ-sinus gland tract (XST), and the X-organ-sensory pore tract (XSPT). AB, axonal tract of brain neurosecretory cells. LG, ME, MI and MT represent respectively the lamina ganglionaris, medulla externa, medulla interna and medulla terminalis, all parts of the optic lobe peduncle. (from Carlisle 1953, as reported in Adiyodi and Adiyodi 1970).

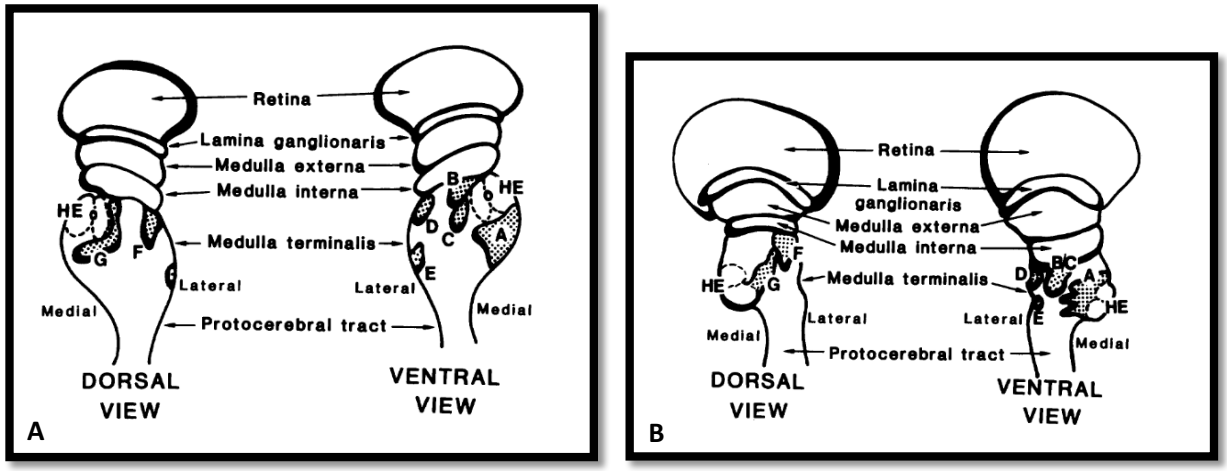

Figure A4.6a and A4.6b: Eyestalks of *P. clarkii* (A) and *P. argus* (B; From Blaustein et al 1988).

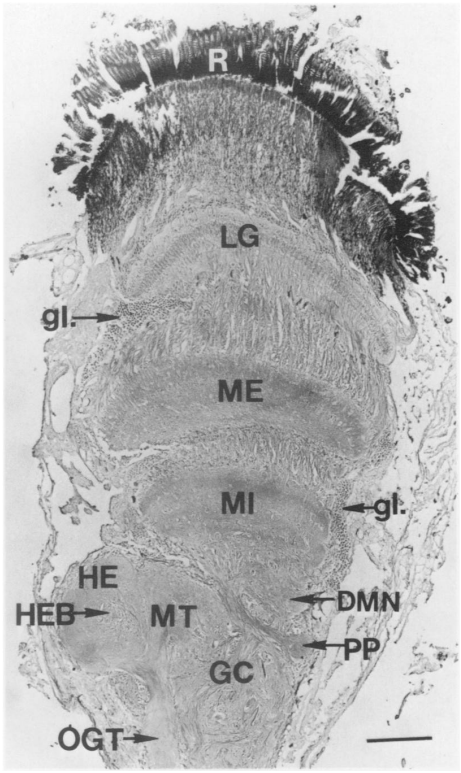

Figure A4.7. Horizontal section of the four eyestalk ganglia of *Procambarus clarkii*. LG, lamina ganglionaris (lamina); ME, medulla externa (medulla); MI, medulla interna (lobula); MT, medulla terminalis. Note chiasmata among the three distal ganglia. OGT, olfactory-globular tract; HE, hemiellipsoid body; HEB, hemiellipsoid bundle; GC, glomeruli centrales; R, retina; gl., small globuli cells; PP, proximal promontory of the diamedullary neuropile (DMN). (Silver stain, 7 #m.) Scale bar = 175 µm (From Blaustein et al 1988).

A.4.5. References:

Adiyodi KG, Adiyodi RG. 1970. Endocrine control of reproduction in decapod crustacean. Biol Rev 45:121-165.

Blaustein DB, Dreby CD, Simmons RB, Beall AC. 1988. Structure of the brain and medulla terminalis of the spiny lobster *Panulirus argus* and the crayfish *Procambarus clarkia*, with an emphasis on olfactory centers. J Crust Biol. 8(4):493-519.

Maynard DM, Yager JG. 1968. Function of an eyestalk ganglion, the medulla terminalis, in olfactory integration in the lobster *Panulirus argus*. Z Vgl Physiol 59:241-249.

Appendix 5: Tissue Cross-contamination Trial

A.5.1. Introduction:

Bitter Crab Disease (BCD) is an emerging disease in decapod crustaceans. To date over 40 species of crustaceans have been reported to be infected by *Hematodinium* species world-wide, primarily in the North Pacific and Atlantic Oceans, including several commercially important decapods such as snow crabs (*Chionoecetes opilio*, reviewed in Morado 2011). Infections of *Hematodinium* spp. are fatal in every host species. However, it is unclear whether parasitemia in BCD occurs early in the disease process or only manifests in late stages of disease. Histologic examination of internal organs of snow crabs collected from bays (Bonavista Bay, Notre Dame Bay, and White Bay) along the northern coast of Newfoundland were examined via histology to determine the tissue distribution of early *Hematodinium* sp. infection. Additional to internal organs (gill, hepatopancreas, heart, midgut, and gonad) several tissues lined by chitin (eyestalk, leg, and abdomen) were also examined. Preliminary examination of histologic tissue sections revealed high prevalence (88%) of very light *Hematodinium* sp. infections in Newfoundland snow crabs. This very high prevalence level was unexpected and thus cross-contamination of tissues was suspected. The most likely point of cross-contamination of the tissues was co-mingling of cassettes of trimmed tissues from BCD- and BCD+ snow crabs. Thus, a small trial was pursued to determine if cross-contamination could be induced by co-mingling of cassettes with tissues from BCD+ snow crabs.

A.5.2. Materials and Methods:

Tissue samples collected from Newfoundland snow crabs in 2010, which were fixed in Davidson's Seawater fixative and stored in 70% ethanol, were used for this trial. Two replicates of tissues from each of 16 ($1/10^{th}$ of the sampled population, n=160) snow crabs were trimmed from each snow crab. The trimmed tissues were: heart, gill, gonad, hepatopancreas, midgut, and eyestalk (sections of leg and abdomen were not used for this trial). Only a single eyestalk remained for each snow crab and half was placed in each cassette. The tissues were trimmed routinely and placed into tissue cassettes. One replicate of tissue cassettes (n=16) was placed in a fixative container (70% ethanol) with a histologic cassette of tissues from a BCD+ snow crab. The second replicate of tissues n=16) was placed in a fixative container (70% ethanol) and was not co-mingled with a BCD+ tissue cassette.

A.5.3. Results:

Rare clusters and individual *Hematodinium* sp. parasites were observed in 13/16 (81.25%) of the sets of tissues from cassettes which were co-mingled with a cassette containing BCD+ tissues. No *Hematodinium* sp. parasites were observed in the tissue sections from cassettes where there was no co-mingling with infected crab tissues. The *Hematodinium* sp. parasites were typically associated with the hepatopancreas (n=8) and/or gonad (n = 5), with fewer parasites associated with the midgut (n=2), gill (n=1), and eyestalk (n=1). (Note: Parasites were found in several locations in an individual crab's tissue.) Furthermore, precipitation of hemolymph contents (hemocytes and/or parasites) was seen along the basal margin of

containers of fixed tissues in both uninfected snow crabs and in BCD-infected snow crabs (Figure A5.1).

Figure A5.1. Snow crab tissues in Davidson's Seawater fixative. These snow crabs were from Bonavista Bay, a region from which no BCD+ snow crabs were collected. Note the white precipitate (presumably fixed hemocytes) along the basal margin of all four of the containers of fixed tissues.

A.5.4. Discussion:

Decapod crustaceans possess a condensed muscular heart which pumps hemolymph through complex arterial systems that perfuse the tissues via a network of small-caliber vessels which are functionally equivalent to the capillaries of closed circulatory systems (McMahon and Burnett 1990). The hemolymph then flows over the tissues in sinuses and lacunar spaces (McMahon and Burnett, McGaw 2005). The presence of sinuses, rather than a complete series of veins, defines the circulatory system as open (McGaw 2005). In these sinuses and lacunar spaces the hemolymph passes through tissues directly in passages unbounded by vascular walls (McMahon 2001). The presence of hemolymph in these unbounded sinuses and lacunar spaces

within the snow crab tissue sections allowed precipitation of hemolymph contents (hemocytes and/or parasites) from the unbounded vascular spaces within snow crab tissues into the surrounding environment (i.e., the container of Davidson's Seawater fixative and/or 70% ethanol). This precipitation from infected tissues most likely caused cross-contamination of tissue sections within histologic cassettes when the cassettes were co-mingled in a holding container prior to tissue processing. Avoidance of co-mingling by use of separate holding containers for snow crabs that had macroscopic evidence suggestive of BCD eliminated this problem in year 2 of the study.

A.5.5. References:

McGaw IJ. 2005. The decapod crustacean circulatory system: a case that is neither open nor closed. Microsc Microanal 11:18-36.

McMahon BR, Burnett LE. 1990. The crustacean open circulatory system: a reexamination. Physiol Zool 63(1):35-71.

McMahon BR. 2001. Control of cardiovascular function and its evolution in crustacean. J Exp Biol 204:923-932.

Morado JF. 2011. Protistan diseases of commercially important crabs: a review. J Invert Pathol 106:27-53.

Appendix 6: Evaluation of the use of hepatopancreatic and gut wall reserve inclusion scores as indicators of total body glycogen stores in Atlantic Canadian green crabs, *Carcinus maenas,* and Atlantic Canadian snow crabs, *Chionoecetes opilio*

A.6.1. Introduction

Snow crabs *Chionoecetes opilio* are marine crustaceans found in the North Atlantic and North Pacific oceans. Canada is the world's largest producer of snow crab accounting for ~ two-thirds of the global supply (total landings in 2013 of 98,065 tonnes); snow crab is the second most valuable Canadian fishery export product (exports valued at $434.2 million in 2013; www.dfo-mpo.gc.ca). After the collapse of the cod fishery in the early 1990s, groundfish have been replaced by shellfish; the snow crab fishery is considered to be a lynchpin of Newfoundland's rural economy (Shrank 2005, Hermann and Greenberg 2007, Davis and Korneski 2012, Mullowney et al 2011).

The European green crab *Carcinus maenas* was originally distributed along the eastern Atlantic coast from Norway to Mauritania, including southern Iceland; however, this invasive species is now found on the east coast of Canada (Audet et al 2003). This non-indigenous (invasive) species has important impacts on bivalves, and could impact native populations via predation, competition, and/or habitat disruption. There is great potential to negatively impact local bivalve aquaculture industries (Miron et al 2005, Pickering and Quijon 2011, Malyshev and Quijon 2011).

Reserve inclusion (RI) cells are cells within the spongy connective tissue of crustaceans containing eosinophilic reserve materials (Johnson 1980). RI cells function in the synthesis and storage of hemocyanin, glycogen, and protein (Johnson, 1980). The concentration of glycogen

in abdominal muscle is the best nutritional index for the Hawaiian spiny lobster *Panulirus marginatus* (Parrish and Martinelli-Liedtke 1999). Stentiford and Feist (2005) utilized relative abundance of RI cells in histologic sections of connective tissues of the hepatopancreas as a body condition assessment tool in European green crab *Carcinus maenas* and was used to compare populations of the crab in several UK estuarine sites. The application of RI score as an indicator of total body glycogen reserves was evaluated in Newfoundland snow crabs *Chionoecetes opilio* with comparisons to a local (invasive) population of European green crabs *Carcinus maenas.*

A.6.2. Materials and Methods

A.6.2.1. Crab collection

Atlantic snow crabs (*C. opilio*) were collected during annual Fall surveys in Notre Dame Bay (NDB) and White Bay (WB), Newfoundland during September in 2010 and 2011. In Notre Dame Bay crabs were caught on the grounds of strata 610 and 611 (200-400 m in depth). In White Bay crabs were caught in strata 614 and 615 (200-400 m in depth) as the very deep stratum 613 (401-500m). NDB is an open ocean-type environment that becomes deeper with distance from shore while WB is a deep fjord-type environment protected at the mouth by a shallow sill and which is deepest inland.

The Fall survey had a target of 8 sets per stratum. Each set included 6 conical crab traps baited with squid. Crabs were sampled from two large-meshed (commercial, 135 mm) and two small-

meshed (27 mm) traps. Small-mesh trap positions alternated with those of large-meshed traps along each long line, and soak times were generally 24 h (weather permitting). Within each crab management area surveyed the depth range and actual area sampled corresponded approximately to the commercial fishery area.

Shell condition was classified as soft, new, intermediate and old (Dawe et al 2009). New-shelled snow crabs are assumed to have molted during the most recent Spring whereas intermediate-shelled crabs are assumed to have molted in the previous year and old-shelled snow crabs two or more years previously (soft-shelled snow crabs were not collected). New-shelled snow crabs were selectively chosen for collection for this study as BCD is typically observed in new-shelled animals (Dawe 2002; Shields et al 2005, 2007; Wheeler et al 2007, Mullowney et al 2011).

Crabs were kept in coolers layered between seawater soaked burlap, and placed above saltwater ice until reaching shore. On shore, coolers were transported to St. John's, Newfoundland, where they were sent via air cargo to the Atlantic Veterinary College (AVC) at University of Prince Edward Island (UPEI). The interval between snow crab harvest and their arrival at the AVC was usually 24-48 h. Snow crabs were recovered in 34 ppt artificial seawater which was aerated with air stones and maintained at 0-2 °C until processing. The interval between snow crab arrival at AVC and processing ranged from 15 min to ~4 h.

In Bonavista Bay snow crabs were collected on the ground from stratum 796 (200-400 m depth) in the Fall survey in August 2010. These snow crabs were recovered in tanks of recirculating

seawater for 48-72 h prior to processing. During this time the seawater chillers failed and thus the snow crabs were maintained at ambient temperature. In addition, snow crabs from Bonavista Bay were also collected by a DFO collaborator from shallow waters (50-100 m depth) in Terra Nova National Park (stratum TN).

Green crabs (*Carcinus maenas*) were collected by Dr. Quijon in the Biology Department at UPEI for use in studies investigating the impact of this invasive species on local ecosystem components. The green crabs were collected monthly in 3 consecutive months (May, June, and July) in the North River, PE in experimental traps set at ~ 1.5-2.5 m depth. The green crabs were delivered to the AVC in coolers and processed immediately.

A.6.2.2. Snow crab processing and sample collection

For each crab, gender was noted and carapace width (mm) was measured, and each was humanely euthanized via nerve cord disruption via decapitation (i.e., removal of the carapace). However, euthanasia via decapitation (used for snow crabs) was not sufficient to disrupt the ventral nerve cord in green crabs. After decapitation (removal of the carapace) in green crab completion of severance of the ventral nerve cord via manual fracturing of the sternum along the medial sternal groove was necessary. After removal of the carapace a necropsy was performed and tissue samples were collected. These included: heart, hepatopancreas, gill (1^{st} and 4^{th} gills on the right), gonad, midgut, eyestalks (left and right), a cross-section of the abdomen, and a cross-section of leg (1^{st} merus on the right). The tissues were immediately placed in Davidson's seawater fixative (Appendix 3) for 24 h. After 24 h, the tissue samples

were transferred into containers of 70% ethanol for storage until routine processing for histology.

A.6.2.3. Tissue trimming and processing for histology

Sections of all soft tissues (heart, hepatopancreas, gill, gonad, and midgut) were trimmed and placed into one cassette per individual crab for processing. A second cassette of sections lined by a thick cuticular layer (eyestalk, leg, and abdomen) was also submitted for each crab. The eyestalk was bisected along the frontal plane as this plane was found to consistently result in optimal sections of internal neuroendocrine tissues (Appendix 4). The blocks of trimmed tissues were processed routinely for histology (Leica processor) and stained with hematoxylin and eosin (H&E). Stained sections were examined on a VistaVision light microscope (VWR) and digital images were captured using an Axioplan 2 imaging microscope with an Axiocam HRc camera and AxioVision 4.8.2.0 software (Zeiss).

A.6.2.4. Reserve Inclusion (RI) Scores

Each tissue on each slide was examined systematically. Relative abundance of glycogen-containing reserve inclusion (RI) cells was scored as previously reported (Stentiford and Fiest, 2005). The scoring index ranged from Stage 0 (RI cells absent) through Stage 1 (RI cells present but scarce), Stage 2 (RI cells scattered), Stage 3 (RI cells frequent) to Stage 4 (RI cells abundant and constituting the majority of connective tissue volume). RI scores were completed for both the hepatopancreas and the gut wall. Evaluations of all sections of hepatopancreas and gut wall

(midgut and hindgut), respectively, were examined to determine an overall RI score for each tissue.

A.6.3. Results

A.6.3.1. Collection Data

A total of 395 snow crabs from 3 Newfoundland bays and 25 green crabs from PEI was collected (Note: Only live BCD- snow crabs from WB/NDB were included in this study. Table A6.1).

Table A6.1. Biological data of collected NL snow crabs and PEI green crabs.

	Green Crab		**Snow Crab – NDB**		**Snow Crab - WB**		**Snow Crab - BB**	
n	25		128		134		133	
Sex Distribution	60% male (n=15)	40% female (n = 10)	39.8% male (n=51)	60.2% female (n=77)	82.9% male (n=108)	17.1% female (n=26)	97.7% male (n=130)	2.3% female (n=3)
Carapace width Range (mm)	51-90	36-57	53 -103	27-69	46 -108	40-55	60-128	61-75
Carapace width Mean (mm)	62.9	50.3	75.6	54.3	79.4	45.5	92.4	68.3

A.6.3.2. Tissue distribution of glycogen reserves

In PEI green crabs, RI cells were observed in the spongy connective tissues of the hepatopancreas, gut wall, and gonad (Figure A6.1). RI cells were not observed in the gill or heart of green crabs (Figure A6.2). In snow crabs RI cells were observed in the spongy connective tissues of the gut wall, hepatopancreas, heart, and gonad (Figures A6.3 through A6.5). RI cells were seen in the heart of snow crabs with abundant RI cells in spongy connective tissues of at other body sites (Figure A6.4). RI cells were not observed in snow crab gills. The

difference between RI cell abundance in poor condition snow crabs (RI score 0) and snow crabs in excellent condition (RI score 4) was particularly striking in abdominal cross-sections (Figures A6.6 and A6.7).

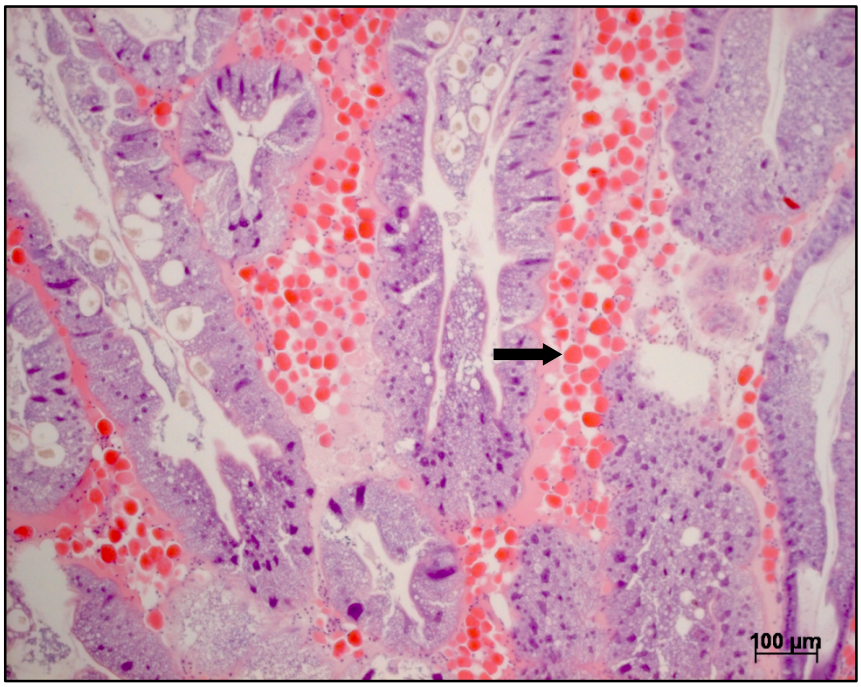

Figure A6.1. Hepatopancreas of a green crab with HP and gut wall RI scores of 4 (100x, H&E). Note the abundant numbers of RI cells (arrow), the conspicuous brightly eosinophilic globoid cells within the interstitial connective tissues.

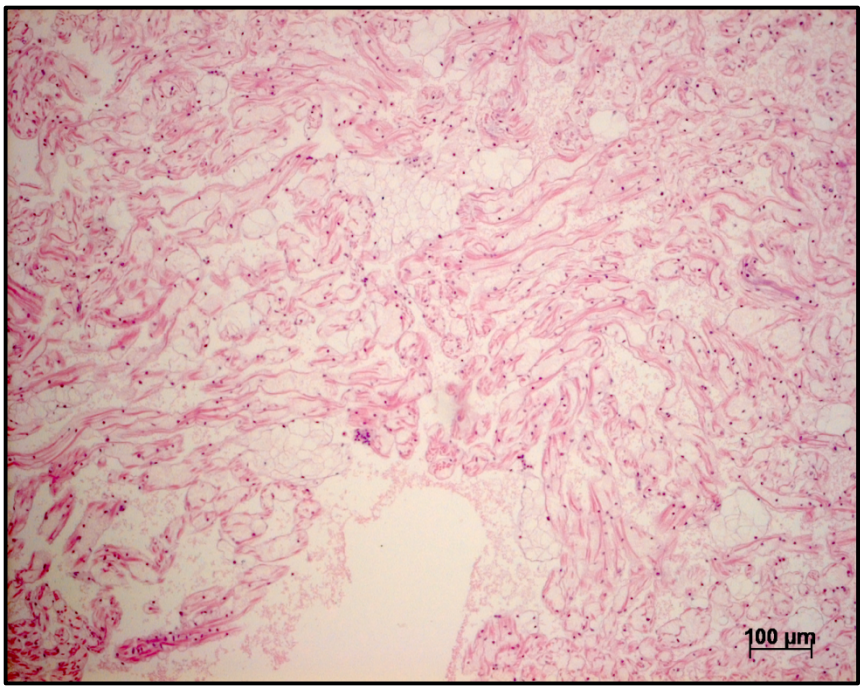

Figure A6.2. Heart of a green crab (same crab as above) with HP and gut wall RI scores of 4 (100x, H&E). Note the diffuse lack of RI cells within the cardiac tissue.

Figure A6.3. Hindgut wall of a snow crab with a gut wall RI score of 4 (100x, H&E). Note the abundant numbers of RI cells (arrow) in the mural connective tissues.

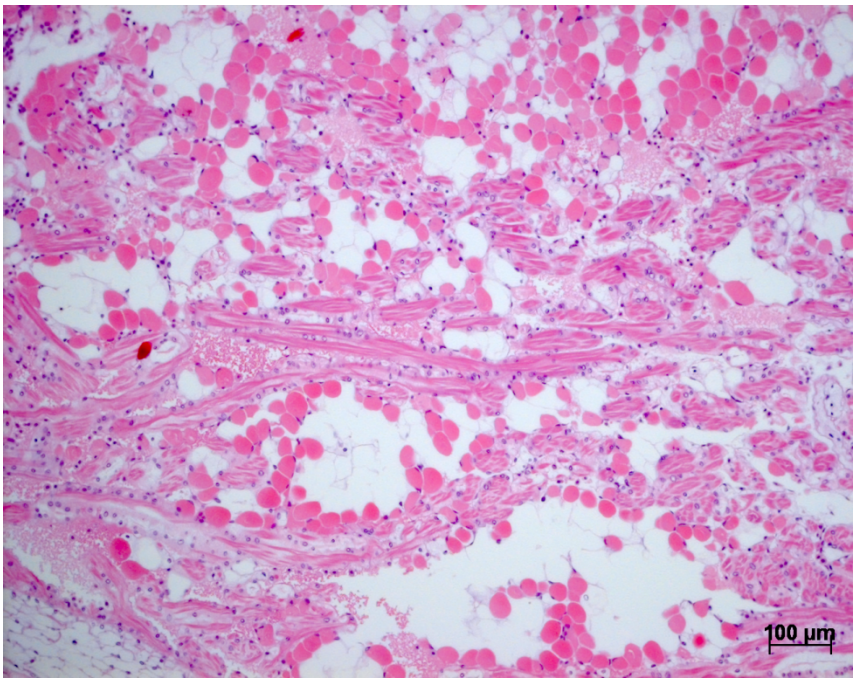

Figure A6.4. Heart of a snow crab (same snow crab as above) with a gut wall RI score of 4 (100x, H&E). Note the abundant numbers of RI cells (arrow) within the spongy cardiac tissue.

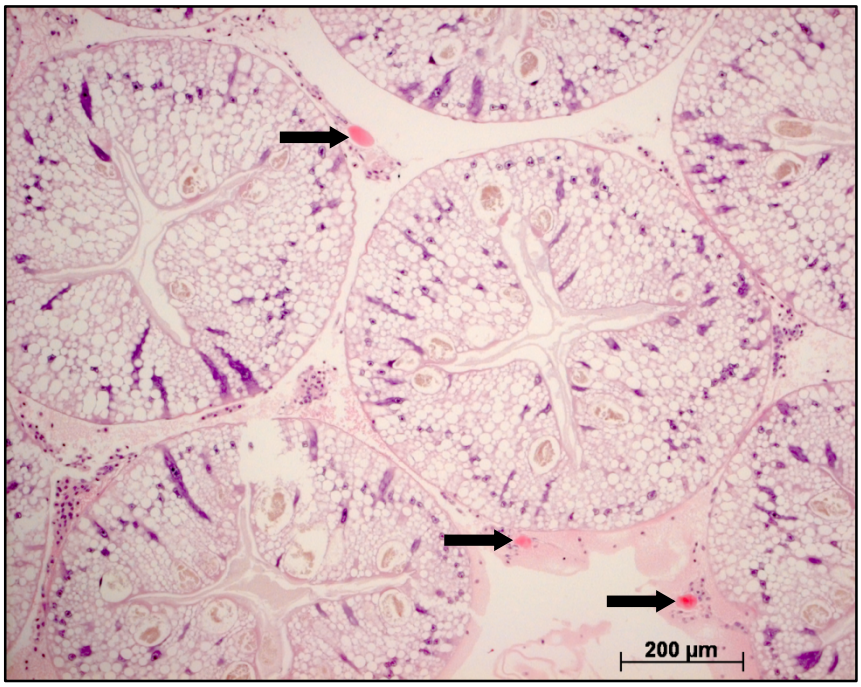

Figure A6.5. Hepatopancreas of a snow crab (same snow crab as above) with a gut wall RI score of 4 (100x, H&E). RI cells (arrows) were sparse in the hepatopancreatic connective tissues.

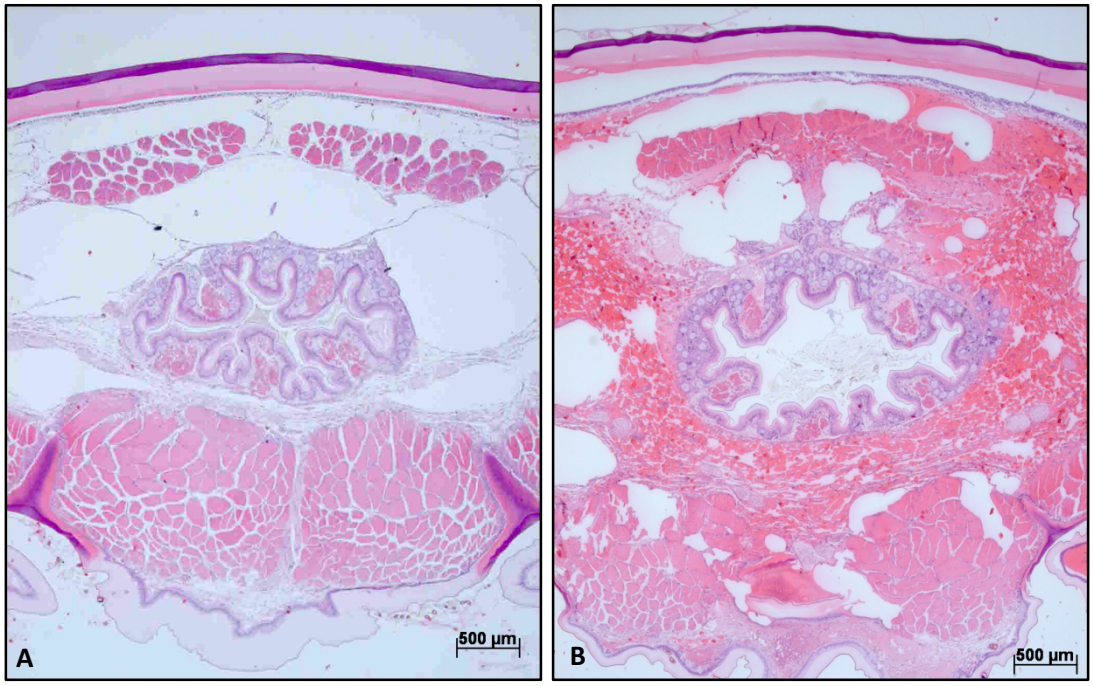

Figure A6.6. Abdominal cross section of a snow crab with a gut wall RI score of 0 (A) and a snow crab with a gut wall RI score of 4 (B). Note the lack of RI cells in connective tissues surrounding the hindgut with a gut wall RI score of 0 (A)and the abundant RI cells expanding the connective tissues surrounding the hindgut with a gut wall RI score of 4 (B; 25x, H&E).

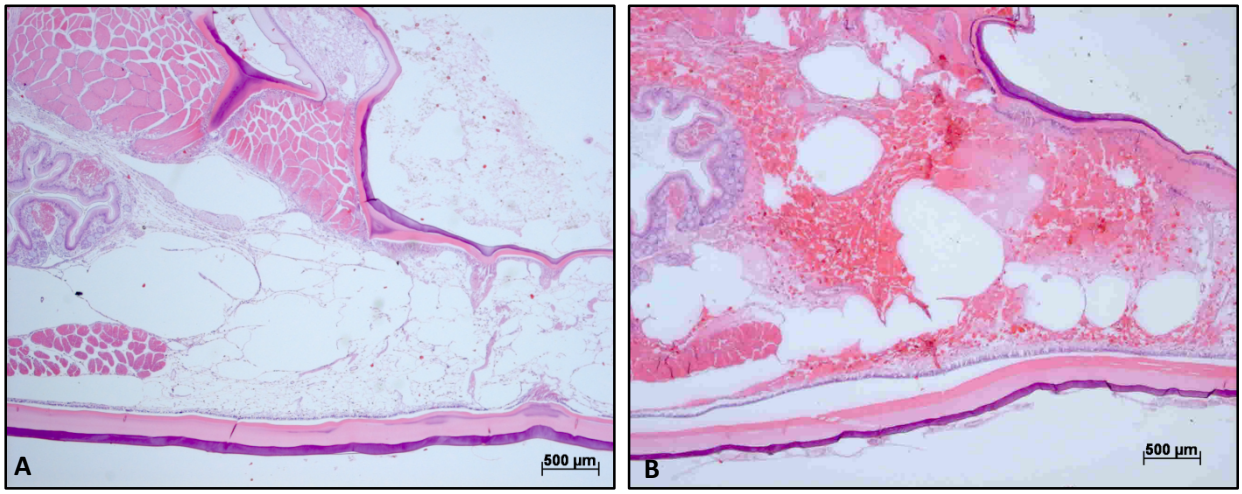

Figure A6.7. Abdominal cross section of snow crabs with a gut wall RI score of 0 (A) and a gut wall RI score of 4 (B). Note the lack of RI cells in connective tissues surrounding the hindgut in the snow crab with a gut wall RI score of 0 (A) and the abundant RI cells expanding the connective tissues surrounding the hindgut in the snow crab with a gut wall RI score of 4 (B; 25x, H&E).

A.6.3.3. Comparison of hepatopancreas and gut wall reserve inclusion scores

In PEI green crabs, HP and gut wall RI scores both ranged from 0 (absent) to 4 (very abundant). In green crabs there was no significant difference in median RI score when HP RI scores (n=25, median =1) and gut wall RI scores (n=25, median =1) were compared (Mann-Whitney Test: W=638.5, p-value = 0.9918). In green crabs there was no significant difference in mean RI score when HP RI scores (n = 25, mean = 1.36 ± 0.28 SEM) and gut wall RI scores (n=25, mean = 1.36 ± 0.29 SEM; two-sample T-test: T-value = 0.00, DF = 47, p-value = 1.000; Figure A6.10) were compared.

In Newfoundland snow crabs, HP RI scores ranged from 0 to 2 (frequent) while gut wall RI scores ranged from 0 to 4. In snow crabs from NDB the median HP RI score (n=128, median = 0) was significantly lower than the median gut wall RI score (n=128, median = 1; Mann Whitney Test W=13196.0, **p-value = 0.0000**; Figure A6.11). In snow crabs from WB the median HP RI score (n=134, median = 0) was significantly lower than the median gut wall RI score (n=134, median = 0; Mann Whitney Test W=14591.0, **p-value = 0.0000**; Figure A6.12). Similarly, in snow crabs from BB the HP RI scores (n-133, median = 0) were significantly lower than the gut wall RI scores (n= 133, median = 0, Mann Whitney Test W=18557.5, **p-value = 0.0182**; Figure A6.13).

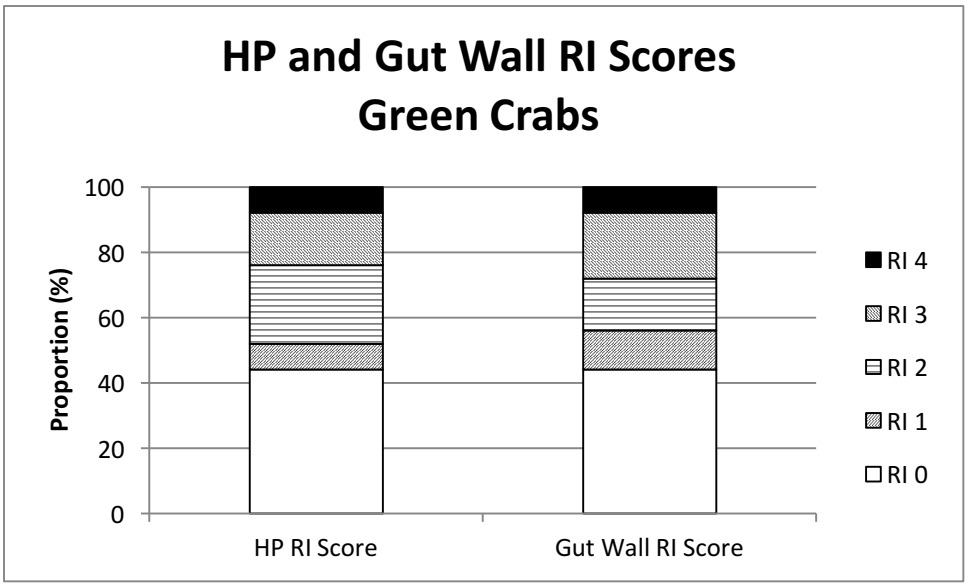

Figure A6.10. Proportions of snow crabs with hepatopancreas (HP) and gut wall (RI) scores from 0 through 4 in PEI green crabs.

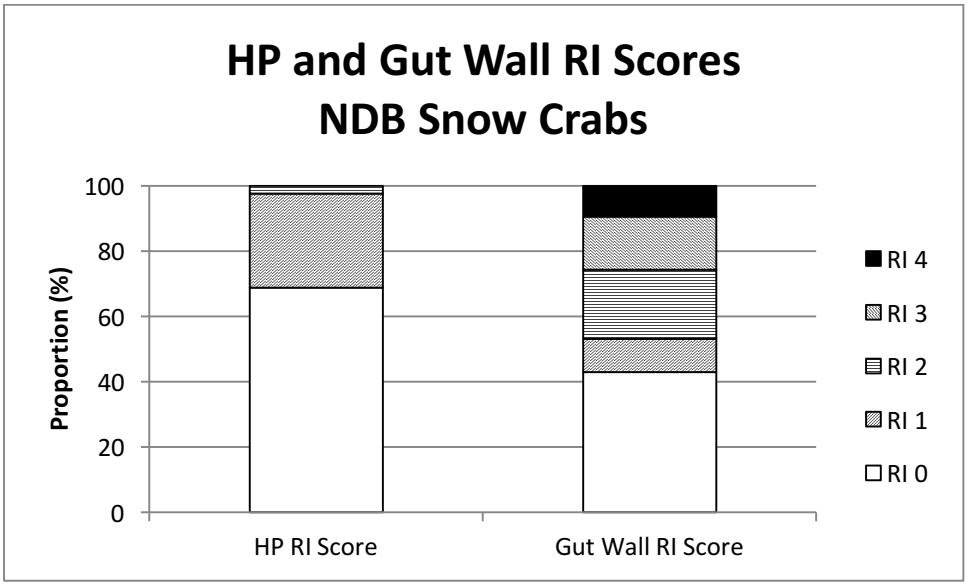

Figure A6.11. Proportions of snow crabs with hepatopancreas (HP) and gut wall (RI) scores from 0 through 4 in snow crabs collected from Notre Dame Bay (NDB), Newfoundland.

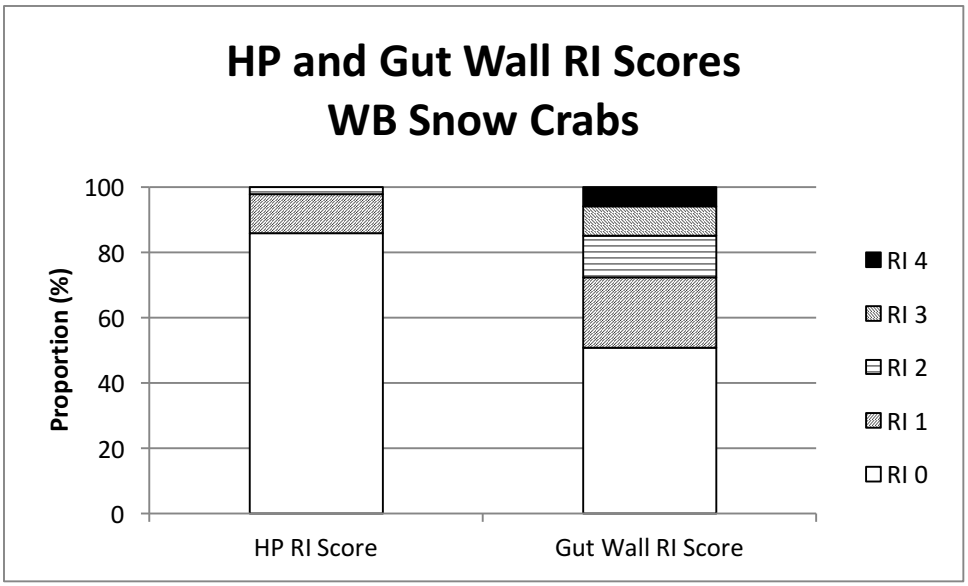

Figure A6.12. Proportions of snow crabs with hepatopancreas (HP) and gut wall (RI) scores from 0 through 4 in snow crabs collected from White Bay (WB), Newfoundland.

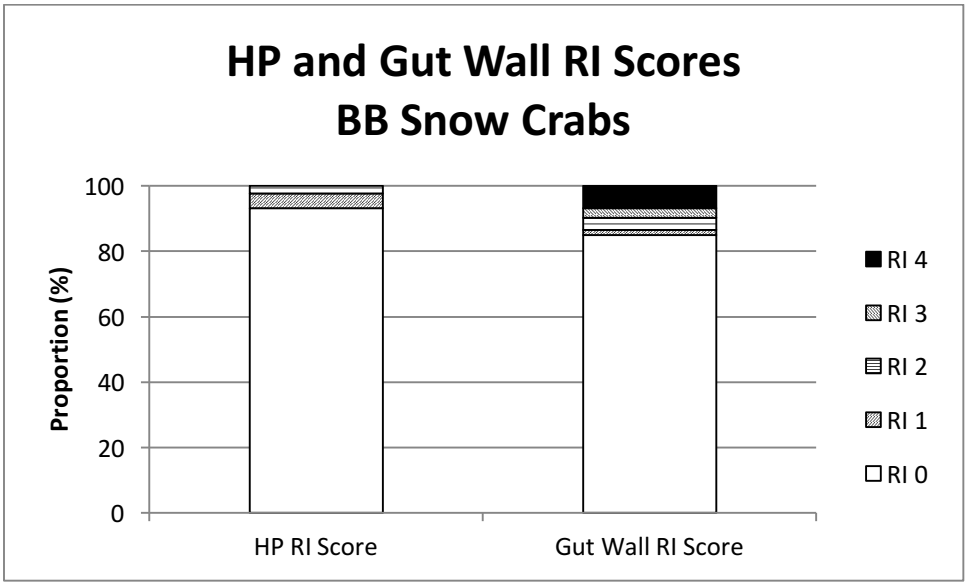

Figure A6.13. Proportions of snow crabs with hepatopancreas (HP) and gut wall (RI) scores from 0 through 4 in snow crabs collected from Bonavista Bay (BB), Newfoundland.

A.6.3.4. Correlations between hepatopancreas and gut wall RI scores

In PEI green crab, HP and gut wall RI scores exhibited strong positive correlation that was just above the cut-off level for statistical significance (Spearman rho correlation = 0.872, p-value =

0.054; Figure A6.14). In Newfoundland snow crabs from NDB, HP and gut wall RI scores exhibited statistically significant positive correlation from WB (Spearman rho correlation = 0.535 **p-value = 0.000;** Figure A6.15), NDB (Spearman rho correlation = 0.744, **p-value = 0.000;** Figure A6.16), and BB (Spearman rho correlation = 0.700, **p-value = 0.000;** Figure A6.17). In PEI green crabs, individuals with a HP RI score of 0 also had a gut wall RI score of 0. In Newfoundland snow crabs, individuals with a HP RI score of 0 had gut wall RI scores that ranged from 0-2 (NDB) and 0-3 (WB and BB).

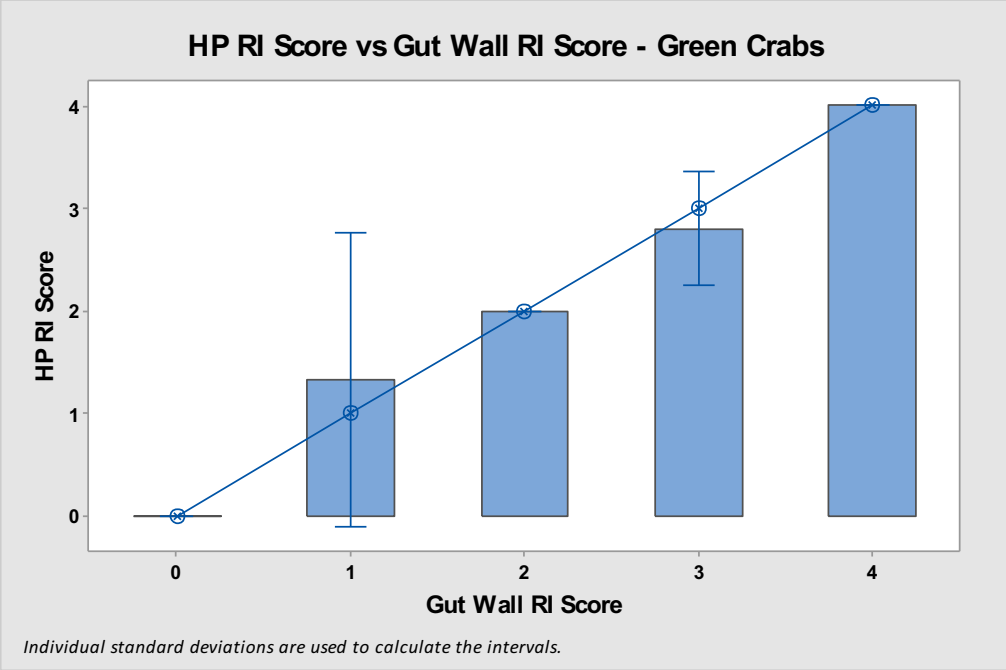

Figure A6.14. Chart of HP RI score gut wall RI score (open circles = median) in PEI green crabs (Spearman rho correlation = 0.872, p-value = 0.054).

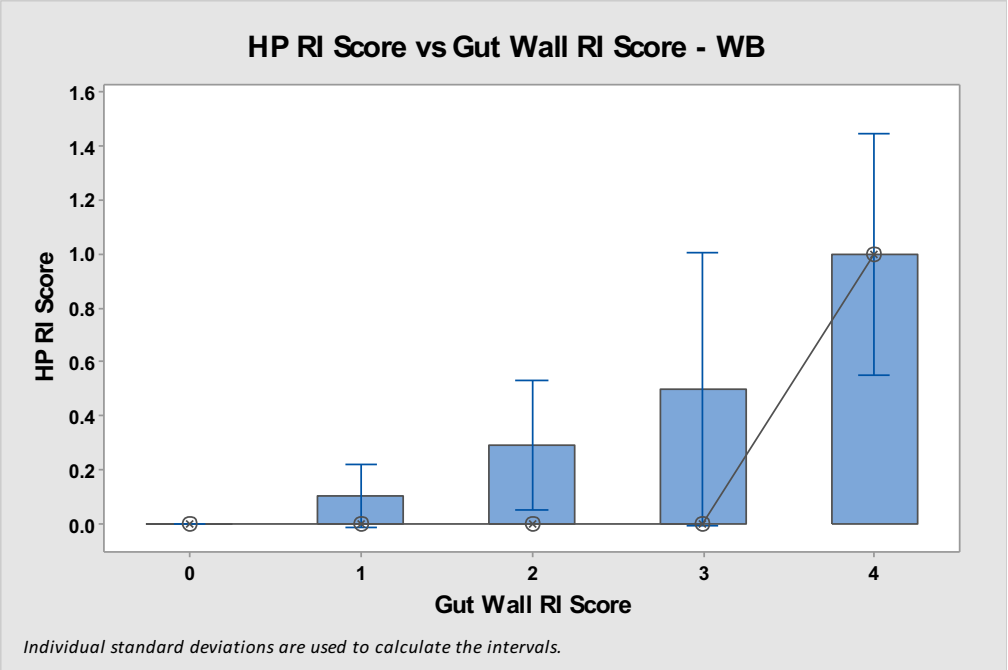

Figure A6.15. Chart of HP RI score versus gut wall RI score (open circles = median) in Newfoundland snow crabs from White Bay (Spearman rho correlation = 0.535 **p-value = 0.000**).

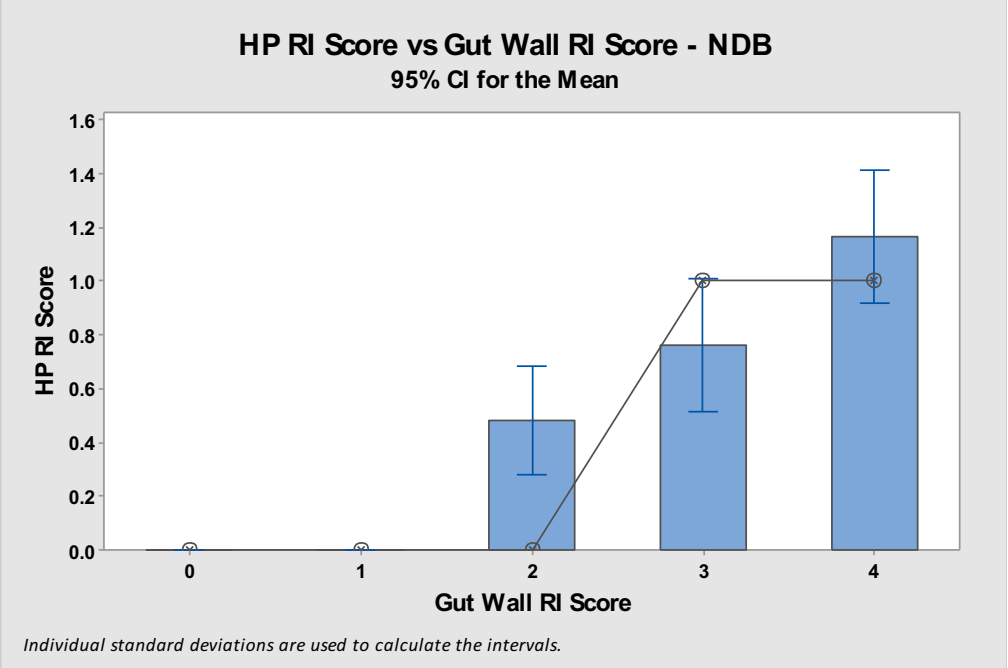

Figure A6.16. Chart of HP RI score by gut wall RI score (open circles = median) in Newfoundland snow crabs from Notre Dame Bay (Spearman rho correlation = 0.744, **p-value = 0.000**).

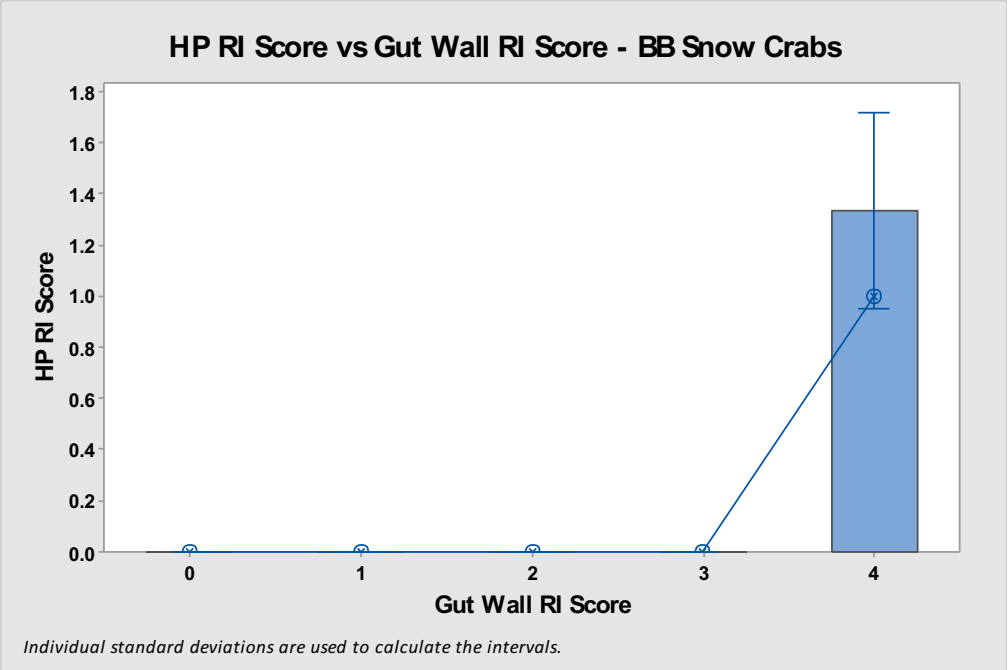

Figure A6.17. Chart of HP RI score versus gut wall RI score (open circles = median) in Newfoundland snow crabs from Bonavista Bay (Spearman rho correlation = 0.700, **p-value = 0.000**).

A.6.4. Discussion

Decapod crustacean reserve inclusion (RI) cells are round to oval cells within the spongy connective tissue which have eosinophilic intracytoplasmic inclusions containing reserve materials (Johnson 1980). RI cells apparently function in the synthesis and storage of hemocyanin, glycogen, and protein, and these reserves are often depleted during molting and/or periods of starvation (Johnson 1980). A historical study on shore crab *Carcinus maenas* stated that RI cells were common in well-fed crabs and absent in starving crabs (Cuénot 1893). Relative abundance of RI cells in histologic sections of connective tissues of the hepatopancreas has been suggested as a tool for grading overall body condition score in shore crab *Carcinus maenas* (Stentiford and Feist 2005). Stentiford and Feist (2005) noted significant differences between RI scores between UK estuarine sites. They also noted reduced RI cell abundance in

shore crabs *Carcinus maenas* with parasitic infection by the parasitic Rhizocephalan barnacle *Sacculina carcini* (Stentiford and Feist 2005).

In PEI green crabs, hepatopancreas RI scores were not significantly different from RI scores obtained from the gut wall. Apparently RI scores obtained from both tissue locations are equally representative of total body glycogen reserves. However, in Newfoundland snow crabs the RI score obtained from the hepatopancreas was significantly lower than the RI score obtained from evaluation of the gut wall in snow crab populations from 3 different bays along the northern coast of Newfoundland. In BB snow crabs, RI cells were absent in the hepatopancreatic interstitial connective tissues in animals which had scattered, frequent, or abundant RI cells in the gut wall. Hepatopancreatic RI cells were consistently seen only in snow crabs with abundant (NDB and WB) or very abundant (BB) numbers of RI cells in the gut wall. This suggests that gut wall RI score is a better measure of total body glycogen reserves than HP RI score in snow crabs.

Interestingly, snow crabs in good body condition in this study often contained RI cells within their myocardium; RI cells were not observed in the myocardium of green crabs. The American lobster *Homarus americanus* has RIs associated with the spongy connective tissue and the myocardium of the heart (Johnson 1980). In contrast, Johnson (1980) did not observe RI cells in the hearts of blue crabs *Callinectes sapidus*. These findings indicate that tissue sites of glycogen storage vary among crustacean species and consideration for such species differences should

be made prior to application of RI scores as an indicator of glycogen reserves in a given crustacean species.

The RI score of snow crabs varied somewhat (± 1 RI score, data not shown) within the midgut and hindgut histologic sections examined. The interstitial connective tissues surrounding the hindgut wall of the hindgut in cross-sections of the abdomen consistently appeared to be representative of total body RI stores (personal observation). This suggests that ante-mortem evaluation of this region could be useful in determining the body condition score of snow crabs. For example, ultrasonographic evaluation of abdominal gut wall thickness and/or echogenicity may be able to distinguish between snow crabs with low and high levels of RI cells since high-frequency transducers provide good image resolution and allow the depiction of details of <1 mm (Filipucci et al 2006). Increased echogenicity of the liver is associated with glycogen storage in dogs (Kishani et al 2001) and humans (Pozzato et al 2001). This suggests that glycogen could alter the echogenicity of spongy connective tissues in crustacean hosts. Such ante-mortem evaluation for glycogen stores could aid in selection of snow crabs with high glycogen stores for live-shipment to reduce the likelihood of shipping mortality.

A.6.5. References

Audet D, Davis DS, Miron G, Moriyasu M, Benhalmia K, Campbell R. 2003. Geographical expansion of a nonindigenous crab, *Carcinus maenas* (L.), along the Nova Scotian shore into the southeastern Gulf of St. Lawrence, Canada. J Shellfish Res. 22(1):255-262. Retrieved from https://archive.org.

Cuenet L. 1893. Etudes physiologiques sur les Crustaces Decapodes. Arch Zool Exp Gen (Ser 4) 3:1-116. Retrieved from http://books.google.com.

Davis R, Korneski K. 2012. In a pinch: snow crab and the politics of crisis in Newfoundland. Labour 69(1):119-145.

Dawe EG. 2002. Trends in prevalence of Bitter Crab Disease caused by *Hematodinium* sp. in snow crabs (*Chionoecetes opilio)* throughout the Newfoundland and Labrador continental shelf. *In* Crabs in Cold Water Regions: Biology, Management and Economics. Alaska Sea Grant College Program, AK-SG-02-02:385-400.

Filippucci E, Iagnocco A, Meenagh G, Riente L, Delle Sedie A, Bombardieri S, Valesini G, Grassi W. 2006. Ultrasound imaging for the rheumatologist. Clin Exp Rheumatol. 24(1):1-5.

Herrmann M, Greenberg J. 2007. The demand and allocation of Alaskan and Canadian snow crab. Can J Abr Econ 55(1):27-48.

Johnson PT. 1980. Histology of the blue crab, *Callinectes sapidus.* A model for the Decapoda. New York, New York: Praeger Publishers.

Kishnani PS, Faulkner E, VanCamp S, Jackson M, Brown T, Boney A, Koeberl D, Chen YT. 2001. Canine model and genomic structural organization of glycogen storage disease type Ia (GSD Ia). Vet Pathol. 38(1):83-91.

Malyshev A, Quijon PA. 2011. Disruption of essential habitat by a coastal invader: new evidence of the effects of green crabs on eelgrass beds. ICES J Mar Sci. 68(9):1852-1856.

Miron G, Audet D, Landry T, Moriyasu M. 2005. Predation potential of the invasive green crab (*Carcinus maenas*) and other common predators on commercial bivalve species found on Prince Edward Island. 24(2):579-586.

Mullowney DR, Dawe EG, Morado JF, Cawthorn RJ. 2011. Sources of variability in prevalence and distribution of bitter crab disease in snow crab (*Chionoecetes opilio*) along the northeast coast of Newfoundland. ICES J Mar Sci 68(3):463-471.

Parrish FA, Martinelli-Liedtke TL. Some preliminary findings on the nutritional status of the Hawaiian spiny lobster (*Panulirus marginatus*). Pac Sci 53:361-366.

Pickering T, Quijon PA. 2011. Potential effects of a non-indigenous predator in its expanded range: assessing green crab, *Carcinus maenas*, prey preference in a productive coastal area of Atlantic Canada. Mar Biol 158:2065-2078.

Pozzato C, Botta A, Melgara C, Fiori L, Giannì ML, Riva E. 2001. Sonographic findings in type I glycogen storage disease. J Clin Ultrasound. 29(8):456-461.

Shrank WE. 2005. The Newfoundland fishery: ten years after the moratorium. Mar Policy 29:407-420.

Shields JD, Taylor DM, O'Keefe PG, Colbourne E, Hynick E. 2007. Epidemiological determinants in outbreaks of Bitter Crab Disease (*Hematodinium* sp.) in snow crabs *Chionoecetes opilio* from Conception Bay, Newfoundland, Canada. Dis Aquat Org 77(1):61-72.

Shields JD, Taylor DM, Sutton SG, O'Keefe PG, Ings DW, Pardy AL. 2005. Epidemiology of Bitter Crab Disease (*Hematodinium* sp.) in snow crabs *Chionoecetes opilio* from Newfoundland, Canada. Dis Aquat Org 64(3):253-264.

Stentiford GD, Feist SW. 2005. A histopathological survey of shore crab (*Carcinus maenas*) and brown shrimp (*Crangon crangon*) from six estuaries in the United Kingdom. J Invert Path 88:136-146.

Wheeler K, Shields JD, Taylor DM. 2007. Pathology of *Hematodinium* infections in snow crabs (*Chionoecetes opilio*) from Newfoundland, Canada. J Invertebr Pathol 95(2):93-100.

http://www.dfo-mpo.gc.ca/fm-gp/sustainable-durable/fisheries-peches/snow-crab-eng.htm

Appendix 7: Evaluation of hemolymph refractive index (HRI) in Atlantic Canadian snow crabs: determination of effects of gender, region of origin, glycogen reserves, and molt stage on HRI.

A.7.1. Introduction

Hemolymph refractive index (HRI) is often assumed to be directly proportional to hemolymph protein levels in crustaceans and thus is often used as an indicator of nutritional condition (Stewart et al 1967, Stewart and Li 1969, Busselen 1970, Dall 1974, Smith and Dall 1982, Behringer et al 2008). Variation in hemolymph hemocyanin and protein levels may also depend on blood volume and osmotic conditions, the type and quality of food in the diet, nutritional state, and molt stage of the crustacean (Busselen 1970, Dall 1974, Spindler-Barth 1976, Truchot 1978, Boone and Schoffeniels 1979, Hagerman 1983, Magnum et al 1985, Chan et al 1988, Chen and Cheng 1993, Chang 1995, Chen and Chia 1997, Terwilliger 1999, Paterson et al 2001).

Body glycogen stores are also used as an index of condition in crustaceans. The concentration of glycogen in abdominal muscle has been reported to be the best nutritional index for the Hawaiian spiny lobster *Panulirus marginatus* (Parrish and Martinelli-Liedtke 1999). Stentiford and Feist (2005) utilized relative abundance of RI cells in histologic sections of connective tissues of the hepatopancreas as a body condition assessment tool in European green crab *Carcinus maenas* and was used to compare populations of the crab in several UK estuarine sites. Reserve inclusion (RI) cells are cells within the spongy connective tissue containing eosinophilic reserve materials which thought to function in the synthesis and storage of hemocyanin, glycogen, and protein (Johnson 1980).

Snow crab hemolymph refractive index (HRI) in snow crabs without Bitter Crab Disease (BCD) was evaluated to determine if gender, bay of collection, glycogen reserve stores (RI score), and molt stage (shell condition category) have significant effects on HRI in snow crabs.

A.7.2. Materials and Methods

A.7.2.1. Snow crab collections

Atlantic snow crabs (*C. opilio*) were collected during annual Fall surveys in Notre Dame Bay and White Bay, Newfoundland during September 2010 and 2011. In Notre Dame Bay, crabs were caught by pot trap on the grounds of strata 610 and 611 (200-400 m in depth). In Notre Dame Bay, stratum 611 is shallow (200-300m) and stratum 610 is deep (301-400 m). Deep stratum 610 was missed in 2011 due to inclement weather. Water temperatures for strata 610 and 611 range between -1°C and 3°C in early Fall (Mullowney et al 2011). In White Bay, crabs were caught by pot trap on the grounds of stratum 614 (300-401 m in depth). The water temperatures for stratum 614 normally ranged between 0-1°C in early Fall (Mullowney et al 2011). The salinity in these bays ranges from 31-35 ppt, with BCD-positive crabs typically not found in regions with salinity <33 ppt (Dawe et al, 2010).

Traps were separated by 45 m within each fleet and were baited using squid and/or mackerel. Soak time was usually about 24 hours, depending on weather conditions. Within each crab management area surveyed, the depth range and actual area sampled corresponded approximately to the commercial fishery area. Minimum depth for sampling was 170 m for all survey areas. The survey has consistently occurred in September and occupies 5 of the inshore

Fall multi-species survey strata with a target of 8 sets per stratum. Each set includes 6 traps, with crabs sampled from two large-meshed (commercial, 135 mm) and two small-meshed (27 mm) traps.

Crabs were kept in coolers layered between seawater soaked burlap, and placed above saltwater ice until reaching shore. On shore, coolers were transported to St. John's, Newfoundland, where they were sent via air cargo to the Atlantic Veterinary College (AVC) at University of Prince Edward Island (UPEI). The interval between snow crab harvest and their arrival at the AVC was usually 24-48 h. After the first shipment (100% mortality, see below) snow crabs were recovered in 34 ppt artificial seawater which was aerated with air stones and maintained at 0-2 °C until processing. The interval between snow crab arrival at AVC and processing ranged from 15 min to ~4 h. In 2010 the snow crabs were shipped in 5 separate shipments while in 2011 there were 3 shipments of snow crabs.

A.7.2.2. Snow crab processing and sample collection

Each snow crab was photographed (dorsal and ventral digital images), gender was noted and recorded, and carapace width (mm) was measured and recorded. Hemolymph from each animal was collected aseptically from the base of the first walking leg using a 3 ml or 5 ml syringe with a 22 gauge needle. For each animal the gross appearance of the hemolymph was noted, hemolymph refractive index was measured using digital refractometer (Reichert r^2mini digital refractometer; Reichert Analytical Instruments) and the measured value was recorded.

The crab was then humanely euthanized via nerve cord disruption via decapitation (i.e., removal of the carapace) as it was previously determined that euthanasia via potassium chloride injection resulted in a large streak of tissue disruption (Appendix 2). Upon removal of the carapace, a digital image of the crab's internal organs was taken and tissue samples were collected. The tissue samples collected included: heart, hepatopancreas, gill (1^{st} and 4^{th} gills on the right), gonad, midgut, eyestalks (left and right), a cross-section of the abdomen, and a cross-section of leg (1^{st} merus on the right). The tissues were immediately placed in Davidson's seawater fixative (Appendix 3) for 24 h. After 24 h, the tissue samples were transferred into containers of 70% ethanol for storage until routine processing for histology.

A.7.2.3. Tissue trimming and processing for histology

Sections of all soft tissues (heart, hepatopancreas, gill (x2), gonad, and midgut) were trimmed and placed into one cassette per individual snow crab for processing. A second cassette of sections lined by a thick cuticular layer (eyestalk, leg, and abdomen) was also submitted. The eyestalk was bisected along the frontal plane as this plane was found to consistently result in optimal sections of internal neuroendocrine tissues (Appendix 4). Stained sections were examined on a VistaVision light microscope (VWR) and digital images were captured using an Axioplan 2 imaging microscope with an Axiocam HRc camera and AxioVision 4.8.2.0 software (Zeiss).

A.7.2.4. Histologic examination of H&E stained tissue slides

Each tissue on each slide was examined systematically for evidence of Hematodinium infection (see Chapters for results on BCD+ snow crabs). Degree of bacterial gill fouling (minimal, mild, moderate, or marked) was noted. The histologic sections were then screened for histologic evidence of gill fouling, carapace fouling (eyestalk, leg, and abdominal cross sections), and histopathologic changes within soft tissues (see Chapter 3). Relative abundance of glycogen-containing reserve inclusion (RI) cells was also scored as previously reported (Stentiford and Fiest 2005). The scoring index ranged from Stage 0 (RI cells absent) through Stage 1 (RI cells present but scarce), Stage 2 (RI cells scattered), Stage 3 (RI cells frequent) to Stage 4 (RI cells abundant and constituting the majority of connective tissue volume). RI scores were completed for the hepatopancreas and the gut, and the RI score for the gut was chosen as most representative of total body RI stores (see Appendix 6).

A.7.3. Results

A.7.3.1. Collected snow crabs

A total of 306 BCD- snow crabs was shipped to AVC in this two-year study (Table 1). All 128 BCD- snow crabs from NDB were shipped in year 2010. Almost all BCD- snow crabs from WB were shipped in year 2011 (n=160) while a small subset was shipped in year 2010 (n=18). The NDB female snow crabs in 2010 included a significantly higher proportion of intermediate- and old-shelled snow crabs (Pearson Chi-Square = 11.132, DF = 1, P-Value = 0.001) than in the NDB males while intermediate-and old-shelled crabs were largely excluded from the sampled populations of WB snow crabs (Tables A7.1 and A7.2). All of the BCD- female snow crabs

collected were gravid (mature and berried) with the exception of a single non-gravid (immature) new-shelled female from NDB.

Table A7.1. Biological data of snow crabs collected from Notre Dame Bay and White Bay.

	Notre Dame Bay		**White Bay**	
n	128		178	
Gender distribution	39.8% males (n=51)	60.2% females (n = 77)	82.6% males (n=147)	17.4% females (n=31)
Carapace width Range (mm)	53-103	27-69	46 -110	40-55
Carapace width Mean (mm)	76.3	55.0	80.6	45.9
Shell Condition	50 New-shelled 1 Intermediate	59 New-shelled 17 Intermediate 1 Old-shelled	147 New-shelled	30 New-Shelled 1 Intermediate

Table A7.2. Biological data of snow crabs collected from White bay stratum 613 and strata 614/615.

	White Bay Stratum 613		**White Bay Strata 614/615**	
n	54		124	
Gender distribution	100% males (n=56)	0% females (n=0)	75% males (n=93)	25% females (n=31)
Carapace width Range (mm)	59 -108		46 -107	40-55
Carapace width Mean (mm)	87.1		80.6	45.9
Shell Condition	56 New-shelled		147 New-shelled	30 New-Shelled 1 Intermediate

A.7.3.2. Shell Condition and RI Score

A.7.3.2.1. Shell Condition and RI Score: All BCD- Snow crabs

Shell condition category was negatively correlated with gut wall reserve inclusion score (Spearman rho correlation = -0.274, **p-value = 0.000**). The mean gut wall RI score was higher in new-shelled animals (n=286, median = 1) than intermediate-shelled animals (n=19, median = 0;

Mann-Whitney Test: W = 44516.5, **p-value = 0.0297;** Figure A7.1). The only old-shelled animal had a gut wall RI score of 0.

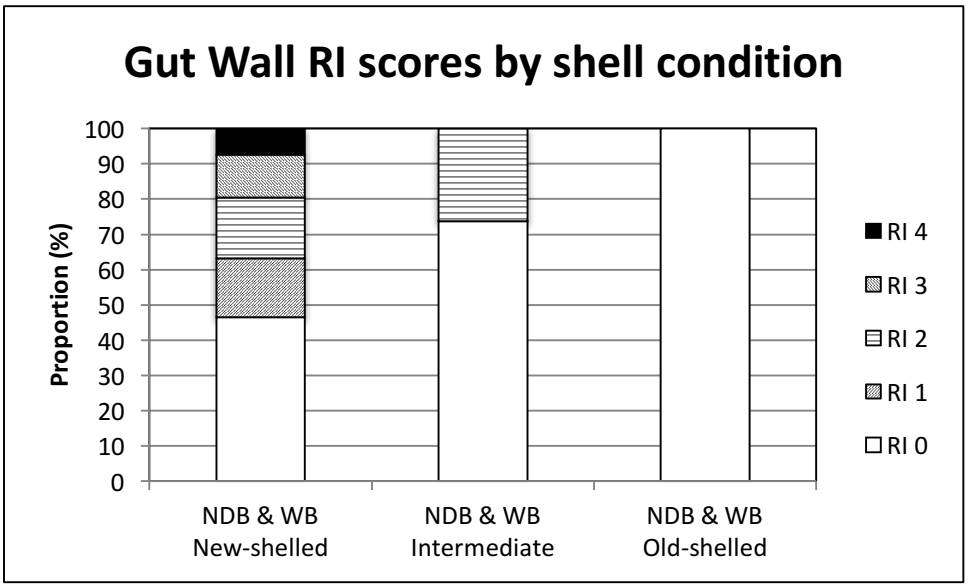

Figure A7.1. Chart of gut wall gut wall reserve inclusion (RI) scores in all new-shelled snow crabs.

A.7.3.2.2. Shell Condition and RI Score: BCD- Snow Crabs by Gender and Shell Condition

Median gut wall RI score was not significantly different between new-shelled (n=89, median =0) and intermediate-shelled (n=18, median = 0) female snow crabs (Mann-Whitney Test W = 4898.0, p-value = 0.3868; Figure A7.2). The only old-shelled female snow crab had a gut wall RI score of 0. In the male snow crabs, all animals were new-shelled except a single intermediate-shelled snow crab with a gut wall RI score of 0. Male new-shelled snow crabs had a higher median gut wall RI score (n = 197, median = 1) than female new-shelled snow crabs (n = 89, median = 0, Mann-Whitney Test W = 30368.5, p-value = 0.0006; Figure A7.3).

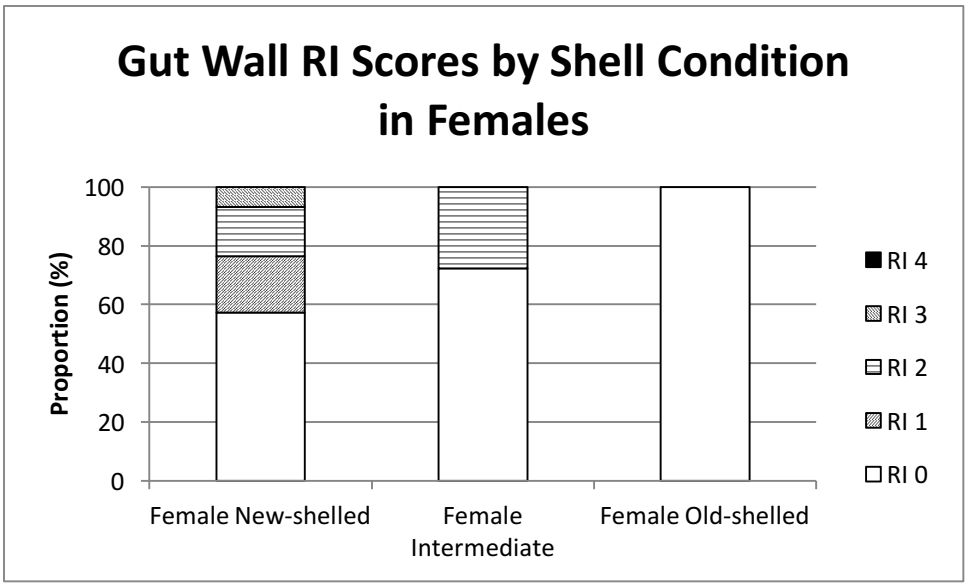

Figure A7.2. Chart of gut wall gut wall reserve inclusion (RI) scores in female snow crabs by shell condition.

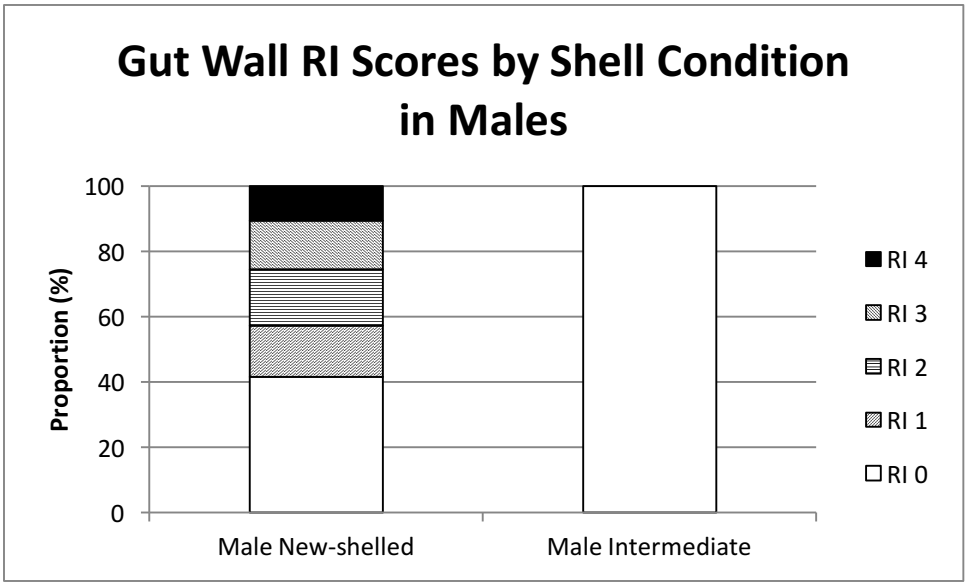

Figure A7.3. Chart of gut wall gut wall reserve inclusion (RI) scores in male snow crabs by shell condition.

A.7.3.2.3. Shell Condition and RI Score: New-shelled BCD- snow crabs by gender, shell condition, bay and strata

The median gut wall RI score was higher in new-shelled animals from NDB (n = 109, median = 2) than intermediate-shelled animals (n = 18, median = 0; Mann-Whitney Test W=7419.0, **p-value = 0.0013;** Figure A7.4). The only old-shelled animal had a gut wall RI score of 0. Female new-shelled snow crabs from NDB had a higher median gut wall RI score (median = 1) than intermediate-shelled females (median = 0) but the difference was not statistically significant (Mann-Whitney Test W = 2398.5, p-value = 0.0810; Figure A7.5). The only old-shelled female snow crab had a gut wall RI score of 0. In the male snow crabs, all animals were new-shelled except a single intermediate-shelled snow crab with a gut wall RI score of 0. Male new-shelled snow crabs from NDB had a higher median gut wall RI score (n=50, median = 3) than female new-shelled snow crabs from NDB (n = 59, median = 1; Mann-Whitney Test: W = 3516.5, **p-value = 0.000;** Figure A7.6).

The median gut wall RI score in WB new-shelled snow crabs was 1 while the single intermediate-shelled snow crab collected in WB had a gut wall RI score of 2 (Figure A7.7). Male new-shelled snow crabs from WB had a higher median gut wall RI score (n = 147, median = 1) than female new-shelled snow crabs (n = 30, median = 0; Mann-Whitney Test: **p-value = 0.0035;** Figure A7.8). The only intermediate shelled snow crab collected in WB was a female with a gut wall RI score of 2. No female snow crabs were collected from WB stratum 613. Male new-shelled snow crabs from stratum 613 had a higher median gut wall RI score (n = 54, median = 1) than male new-shelled snow crabs from strata 614/615 (n = 93, median = 0; Mann-

Whitney Test: W = 4686.0, **p-value = 0.0030**). New-shelled snow crabs from NDB had a higher median gut wall RI score (n= 50, median = 3) than new-shelled male snow crabs from WB stratum 613 (Mann Whitney Test: W= 2968.5, **p-value = 0.0214**) and WB strata 614/615 (Mann-Whitney Test: W=4938.0, **p-value = 0.0000;** Figure A7.9).

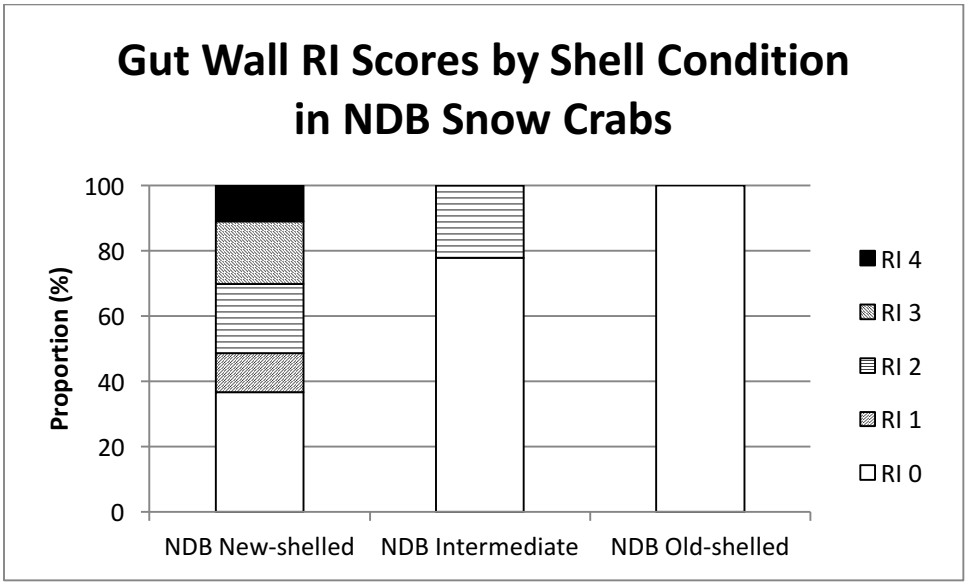

Figure A7.4. Chart of gut wall gut wall reserve inclusion (RI) scores in NDB snow crabs.

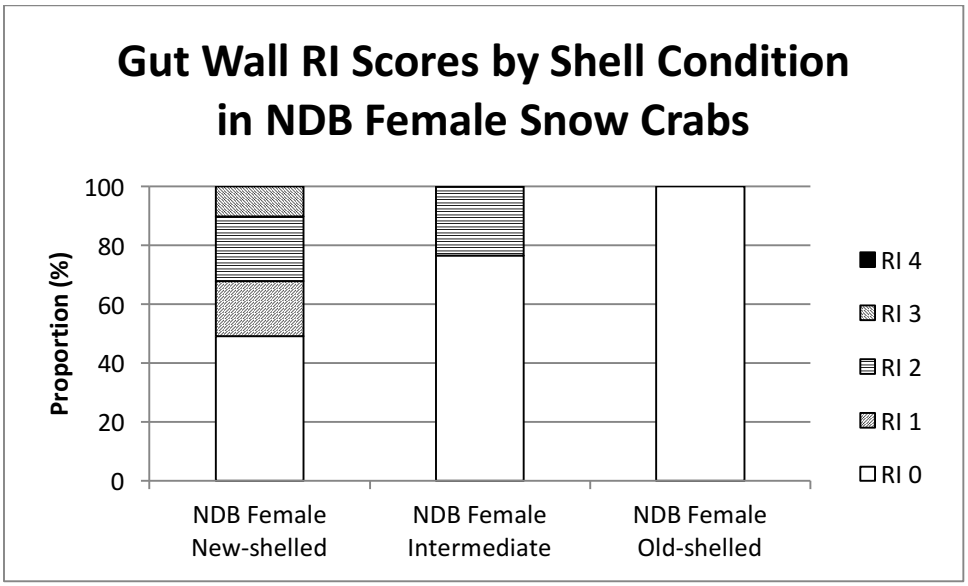

Figure A7.5. Chart of gut wall gut wall reserve inclusion (RI) scores in NDB female snow crabs.

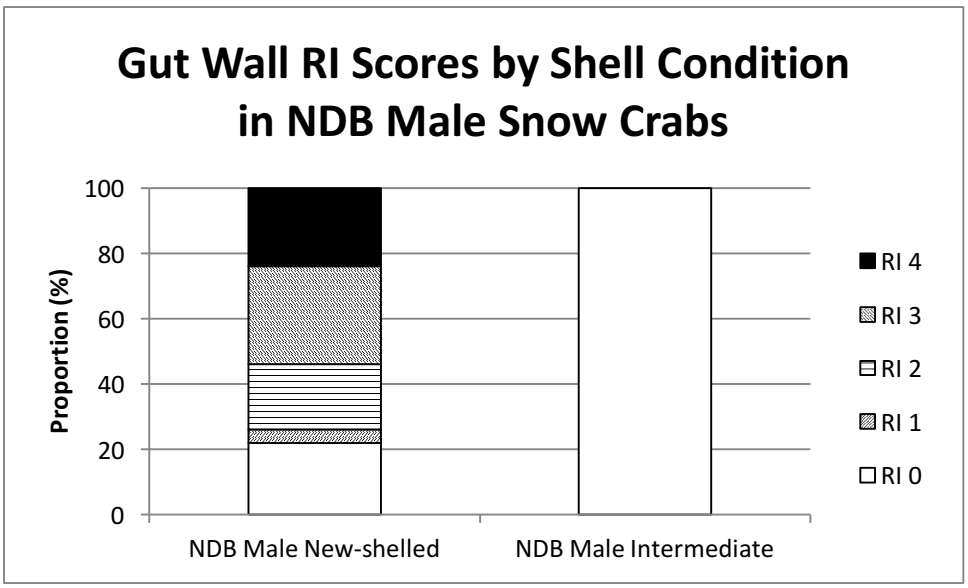

Figure A7.6. Chart of gut wall gut wall reserve inclusion (RI) scores in NDB male snow crabs.

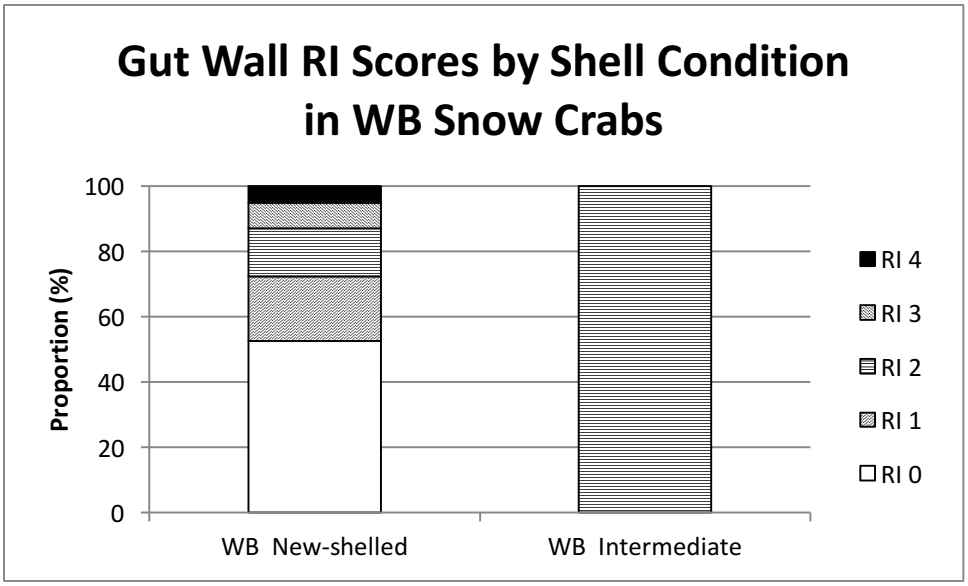

Figure A7.7. Chart of gut wall gut wall reserve inclusion (RI) scores in WB snow crabs.

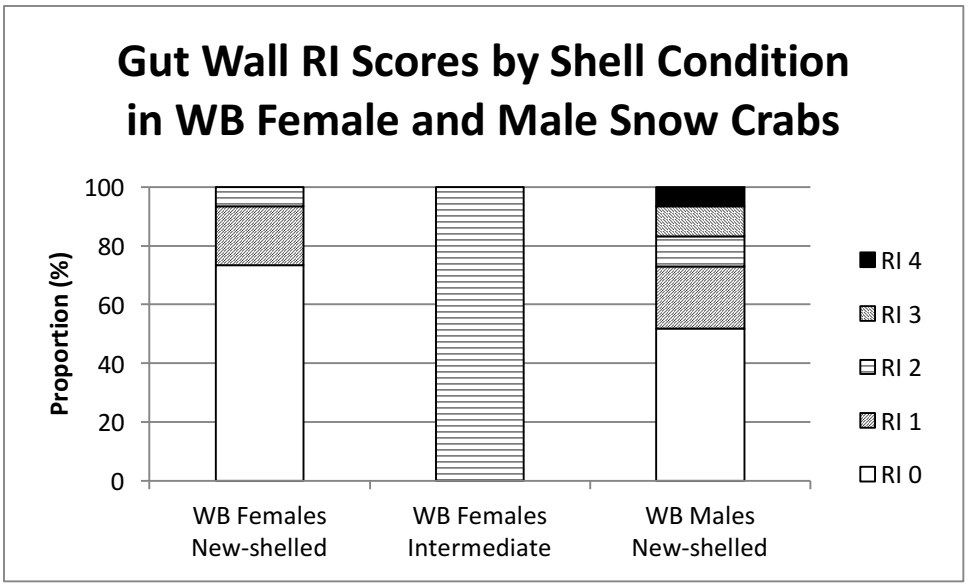

Figure A7.8. Chart of gut wall gut wall reserve inclusion (RI) scores in WB female and male snow crabs.

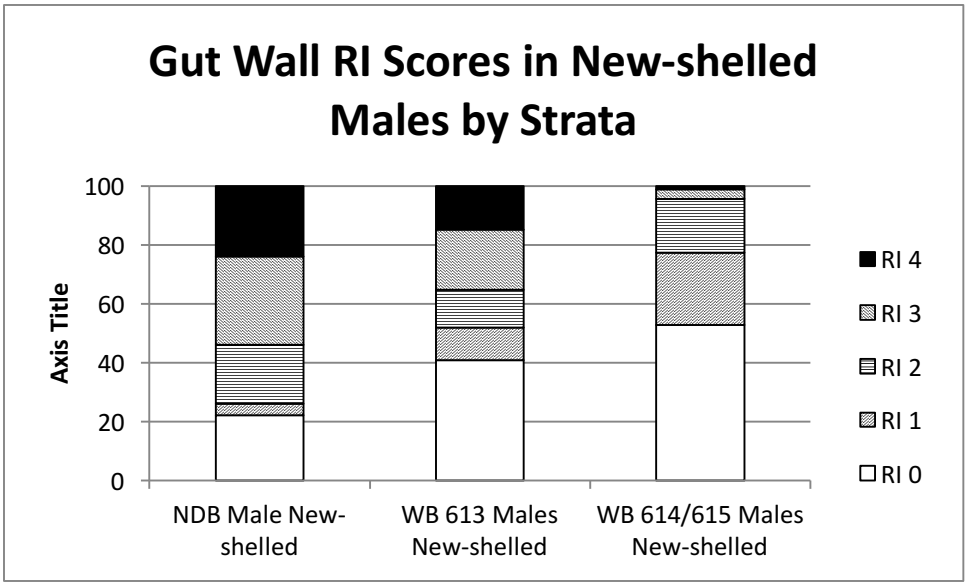

Figure A7.9. Chart of gut wall gut wall reserve inclusion (RI) scores in NDB and WB new-shelled male snow crabs by strata.

A.7.3.2.4. Shell Condition and RI Score: NDB and WB Comparisons

Snow crabs from NDB (all shell conditions) had a higher median gut wall RI score (n = 128, median = 1) than snow crabs from WB (all shell conditions, n = 178, median = 0; Mann-Whitney

Test W = 21554.5, **p-value = 0.0076**). New-shelled snow crabs from NDB had a higher median gut wall RI score (n = 109, mean = 2) than new-shelled snow crabs from WB (n = 177, median = 0; Mann-Whitney Test W = 17985.5, **p-value = 0.0003**).

New-shelled female snow crabs from NDB had a higher median gut wall RI score (n = 59, median = 1) than new-shelled female snow crabs from WB (n = 30, median = 0; Mann-Whitney Test W = 2921.0, **p-value = 0.010**). New-shelled male snow crabs from NDB had a higher median gut wall RI score (n = 50, median = 3) than new-shelled male snow crabs from WB (n = 147, median = 1; Mann-Whitney Test: W = 6631.5, **p-value = 0.000**) whether the snow crabs are from stratum 613(Mann-Whitney Test: W = 2968.5, **p-value = 0.0214**) or from strata 614/615 (Mann-Whitney Test: W = 4938.0, **p-value = 0.000;** Figure A7.10).

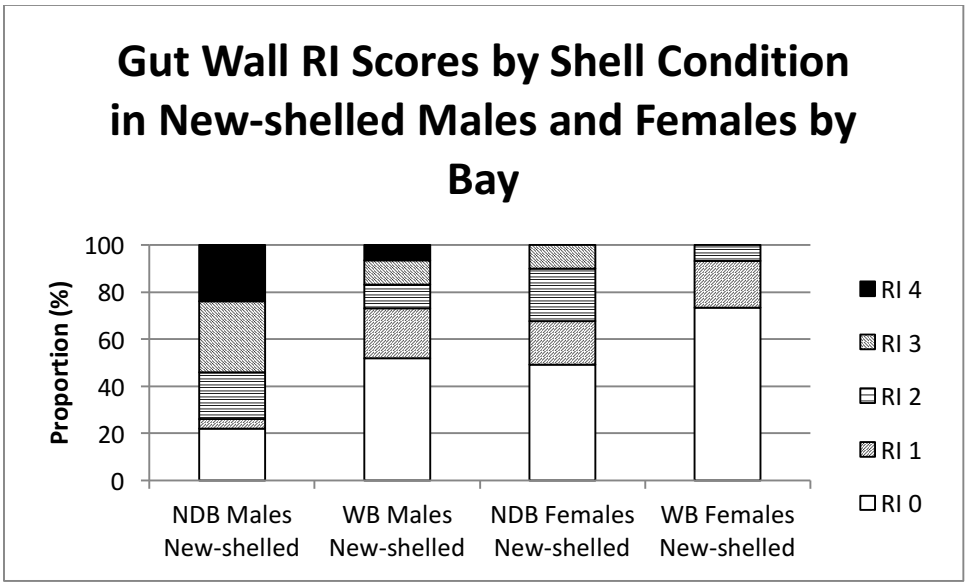

Figure A7.10. Chart of gut wall gut wall reserve inclusion (RI) scores in NDB and WB new-shelled snow crabs by gender

A.7.3.2.5. Shell Condition Category and Hemolymph Refractive Index (HRI)

A.7.3.2.5.1. Shell Condition Category and HRI: All BCD- Snow crabs

New-shelled snow crabs had higher mean HRI (n = 286, mean = 1.34746 ± 0.00022) than intermediate-shelled snow crabs (n = 19, mean = 1.34475 ± 0.00087; two sample T-test: T-value = 3.00, DF = 20, **p-value = 0.007**; Figure A7.11). The single old-shelled snow crab had a HRI of 1.3436.

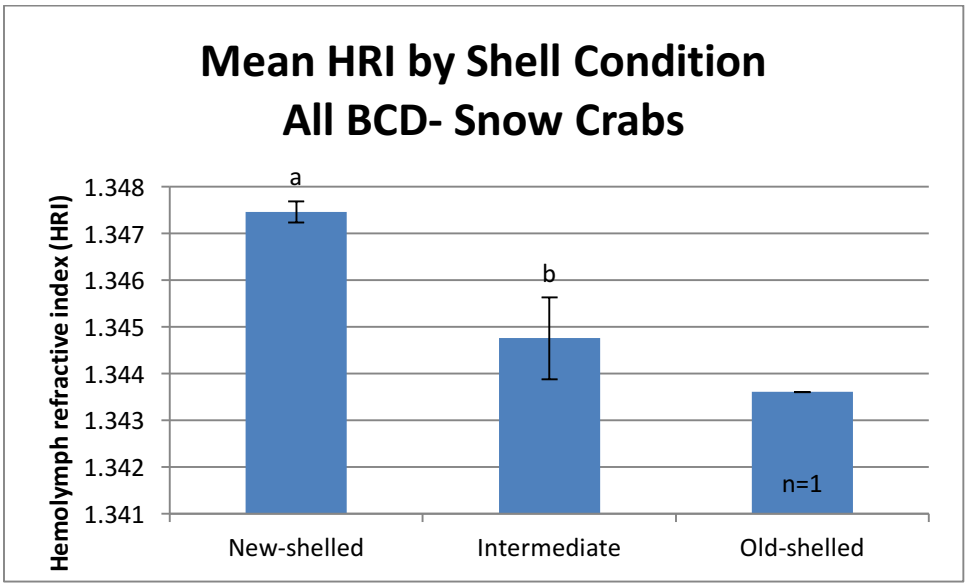

Figure A7.11. Comparison of mean HRI scores in snow crabs by shell condition category. Groups with different letters above the data bar were statistically significant ($p<0.05$).

A.7.3.2.5.2. Shell Condition Category and HRI by Gender

New-shelled female snow crabs had higher mean HRI (n = 89, mean = 1.34831 ± 0.00039) than intermediate-shelled female snow crabs (n = 18, mean = 1.34476 ± 0.00092; two-sample T-test: T-value = 3.54, DF = 23, **p-value = 0.002**). New-shelled female snow crabs also had a higher mean HRI than new-shelled male snow crabs (n = 197, mean = 1.34708 ± 0.00027; two-sample

T-test: T-value = 2.60, DF = 173, **p-value = 0.010**). The single intermediate-shelled male snow crab had a HRI of 1.3446 (Figure A7.12).

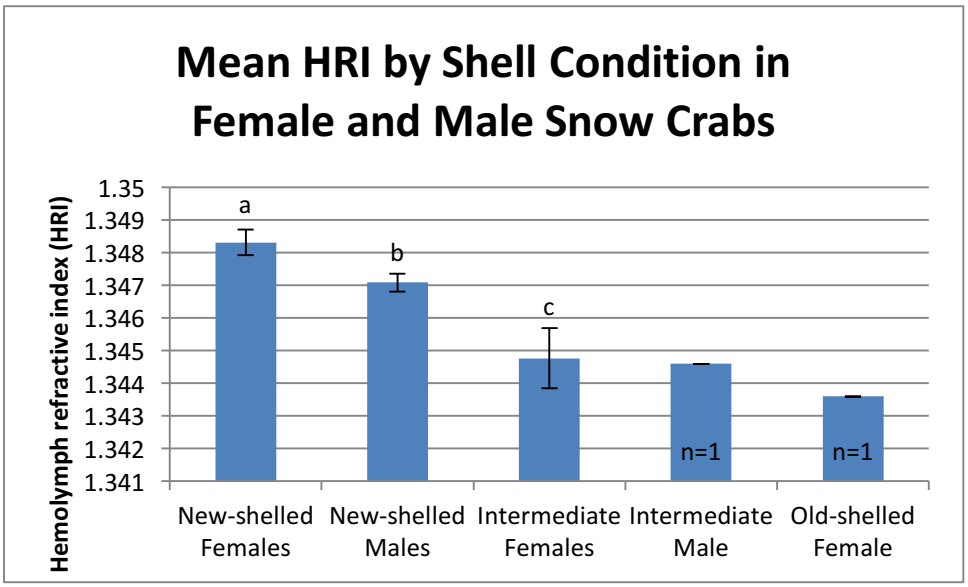

Figure A7.12. Comparison of mean HRI scores in snow crabs by shell condition category and gender. Groups with different letters above the data bar were statistically significant ($p<0.05$).

A.7.3.2.5.3. Shell Condition Category and HRI: By Gender and Bay

Shell condition was negatively correlated with hemolymph refractive index (Pearson correlation = -0.155, p-value = 0.005; Spearman Rho correlation = -0.147, p-value = 0.007). New-shelled female snow crabs from NDB had a higher mean HRI (n = 59, mean = 1.34793 ± 0.00052 SEM) than intermediate-shelled females from NDB (n = 17, mean = 1.34446 ± 0.00093; two-sample T-test: T-value = 3.26, DF = 27, **p-value = 0.003**). New-shelled female snow crabs from NDB had a higher mean HRI than new-shelled male snow crabs from NDB (n = 50, mean = 1.34613 ± 0.00056; two-sample T-test: T-value = 2.35, DF = 104, **p-value = 0.021**). The single old-shelled female snow crab from NDB had a HRI of 1.3436 and the single intermediate-shelled male snow crab from NDB has a HRI of 1.3446.

New-shelled female snow crabs from WB had a higher mean HRI (n = 30, mean = 1.34906 ± 0.00052 SEM) than new-shelled male snow crabs from WB (n = 147, mean = 1.34740 ± 0.00030 SEM; two-sample T-test: T-value = 2.75, DF = 50**, p-value = 0.008**). The single intermediate-shelled female snow crab from WB had a HRI of 1.3499.

WB new-shelled female snow crabs had a slightly higher mean HRI than new-shelled female NDB snow crabs but the difference was not statistically significant (two-sample T-test: T-value = 1.53, DF = 77, p-value = 0.129). WB new-shelled male snow crabs had a higher mean HRI than NDB new-shelled male snow crabs (two-sample T-test: T-value = 2.00, DF = 79**, p-value = 0.049;** Figure A7.13).

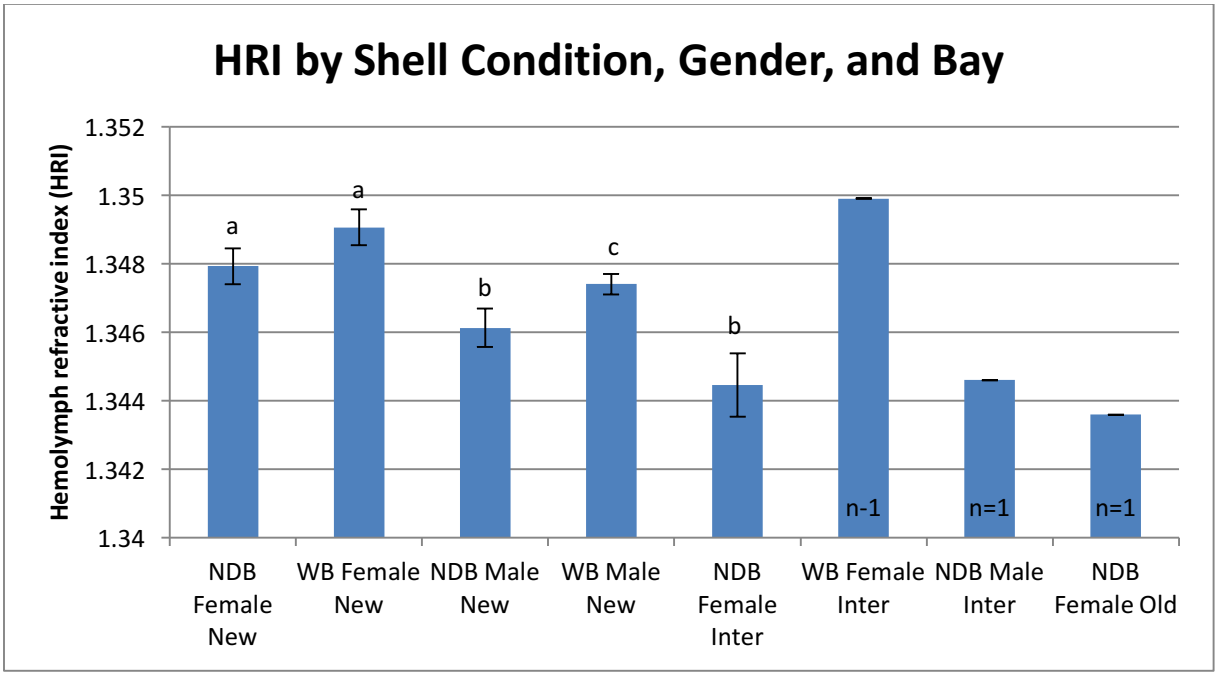

Figure A7.13. Comparison of mean HRI scores in snow crabs by shell condition category, gender, and bay. Groups with different letters above the data bar were statistically significant ($p<0.05$).

There were also differences within strata within WB. Male new-shelled snow crabs from WB strata 614/615 had a higher mean HRI (n = 93, mean = 1.34812 ± 0.00037 SEM) than new-shelled male snow crabs from WB stratum 613 (n = 54, mean = 1.34617 ± 0.00048 SEM; two-sample T-test: T-value = 3.25, DF = 112, **p-value = 0.002**). The mean HRI of new-shelled male snow crabs from WB stratum 613 was not significantly different from the mean HRI of new-shelled male snow crabs from NDB (two-sample T-test: T-value = 0.05, DF = 97, p-value = 0.960) while the mean HRI of new-shelled male snow crabs from WB strata 614/615 was higher than in new-shelled male snow crabs from NDB (two sample T-test: T-value = 2.97, DF = 91, **p-value = 0.004;** Figure A7.14).

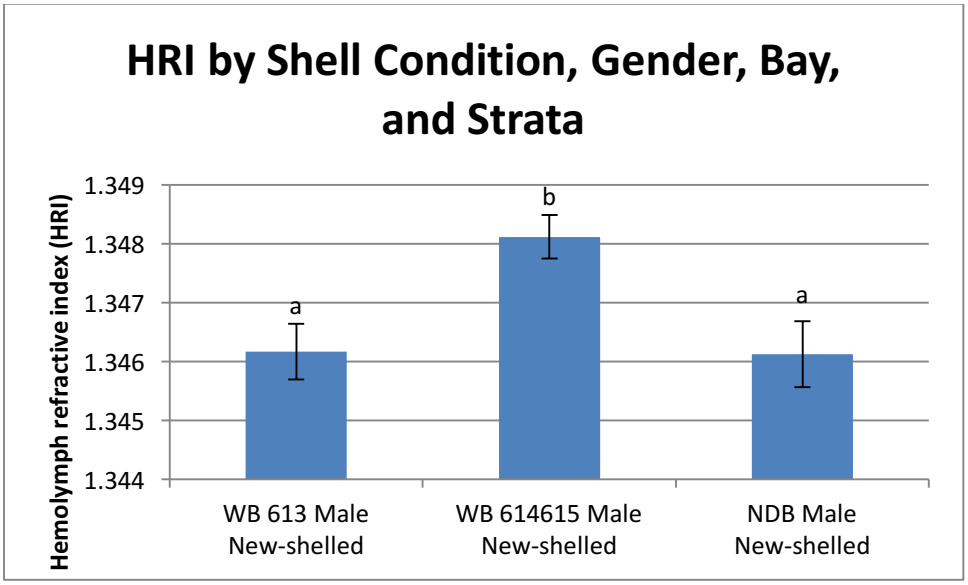

Figure A7.14. Comparison of mean HRI scores in snow crabs by shell condition category, gender, and WB strata. Groups with different letters above the data bar were statistically significant (p<0.05).

A.7.3.2.6. RI Score and HRI

A.7.3.2.6.1. RI Score and HRI: All BCD- Snow Crabs

Gut wall RI score was positively correlated with gut wall RI Score when examined in snow crabs of all shell categories (Spearman rho correlation = 0.225, **p-value = 0.000**; Pearson correlation = 0.193, **p-value = 0.000**). Snow crabs with a gut wall RI score of 0 had a mean HRI (n = 148, mean = 1.34639 ± 0.00030 SEM) that was significantly lower than animals with a gut wall RI score of 1 (n=48, 1.34843 ±0.00051 SEM; two-sample T-test: T-value = -3.45, DF = 81**, p-value = 0.001**), RI score of 2 (n=54, mean = 1.34775 ±0. 00054 SEM; two-sample T-test: T-value = -2.19, DF = 86, **p-value = 0.031**), and RI score of 3 (n = 35, mean = 1.34829 ± 0.00062 SEM; two-sample T-test: T-value = -2.74, DF = 50, **p-value = 0.008**). The mean HRI of snow crabs with a gut wall RI score of 0 was lower than that of snow crabs with a gut wall RI score of 4 (mean = 1.34805 ± 0.0099 SEM) but this difference was not statistically significant (two-way T-test: T-value = -1.61, DF = 23, p-value = 0.122). Mean HRI was not significantly different in animals with gut wall RI values from 1 to 4 (one-way ANOVA F-value = 0.29, DF = 3, p-value = 0.830; Figure A7.15).

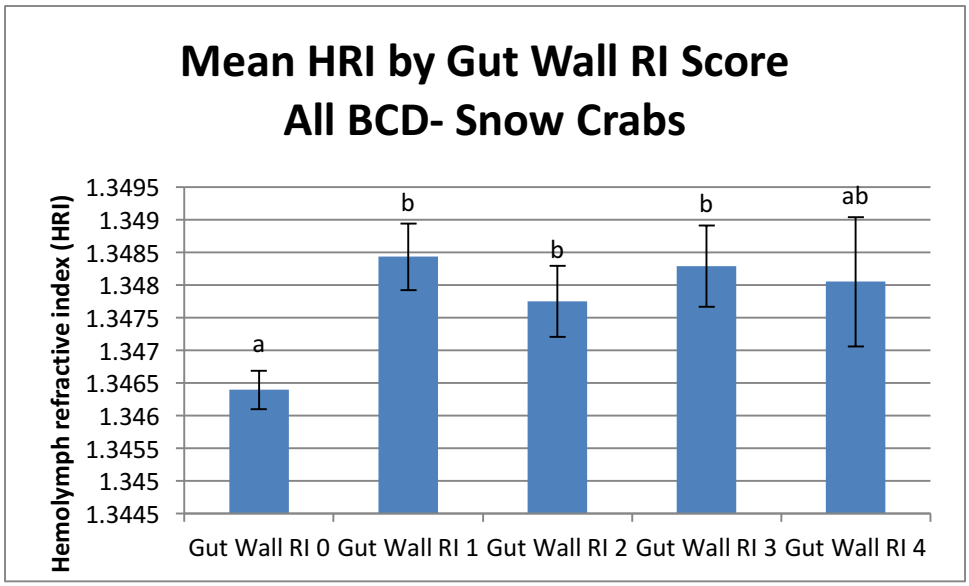

Figure A7.15. Comparison of mean HRI scores in snow crabs by gut wall RI score. Groups with different letters above the data bar were statistically significant ($p<0.05$).

A.7.3.2.6.2. RI Score and HRI: New-shelled BCD- snow crabs

Gut wall RI score was positively correlated with gut wall RI Score when examined in new-shelled snow crabs (Spearman rho correlation = 0.174, **p-value = 0.003**; Pearson correlation = 0.153, **p-value = 0.009**). New-shelled now crabs with a gut wall RI score of 0 (n=133, mean = 1.34667 ± 0.00031) had a mean HRI that was significantly lower than animals with a gut wall RI score of 1 (n=48, mean = 1.34843 ± 0.00051 SEM; two-sample T-test: T-value = -2.95, DF = 84, **p-value = 0.004**) and RI score of 3 (n=35, mean = 1.34829 ± 0.062 SEM; two-sample T-test: T-value= -2.33, DF = 52, **p-value = 0.024**). The mean HRI of snow crabs with a gut wall RI score of 0 was lower than, but not significantly different from, the mean HRI of snow crabs with a gut wall RI score of 2 (n=49, mean = 1.34783 ± 0.00056 SEM; two-sample T-test: T-value = -1.83, DF = 79, 9-value = 0.070) and an RI score of 4 (two-way T-test: T-value = -1.33, DF = 24, p-value = 0.194). Mean HRI

was not significantly different in new-shelled animals with gut wall RI values from 1 to 4 (one-way ANOVA F-value = 0.22, DF = 3, P-value = 0.885; Figure A7.16).

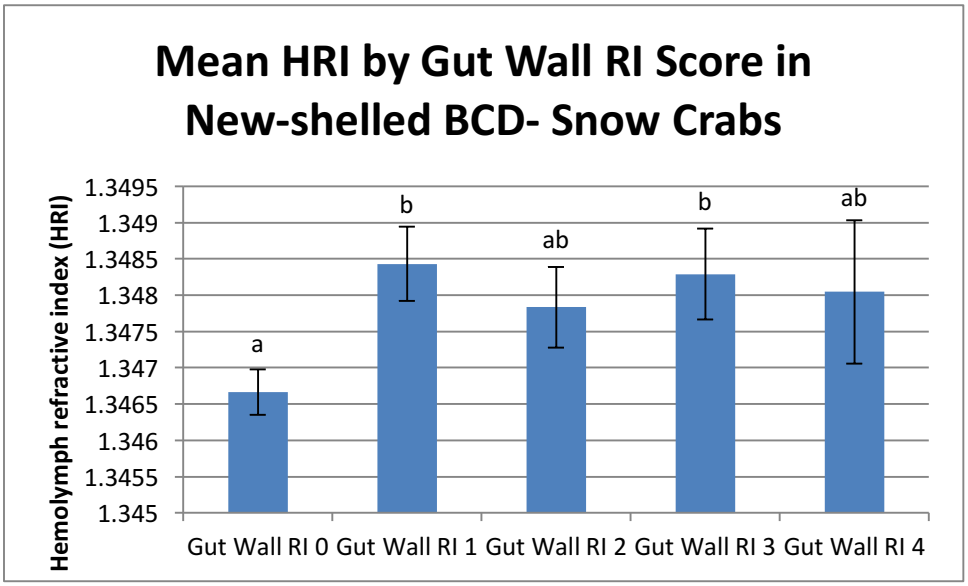

Figure A7.16. Comparison of mean HRI scores in new-shelled snow crabs by gut wall RI score. Groups with different letters above the data bar were statistically significant ($p<0.05$).

A.7.3.2.6.3. RI score and HRI by Gender

Female snow crabs (all shell conditions) with a gut wall RI score of 0 have a mean HRI (n= 65, mean = 1.34646 ± 0.00041) that was significantly lower than animals with a gut wall RI score of 1 (n = 17, mean = 1.34900 ± 0.00099; two-sample T-test: T-value = -2.37, DF = 21, **p-value = 0.027**), RI score of 2 (n = 20, mean = 1.34971 ± 0.00099; two-sample T-test: T-value = -3.04, DF = 26, **p-value = 0.005**), and RI score of 3 (n = 6, mean = 1.35037 ± 0.0015; two-sample T-test: T-value = -2.59, DF = 5, **p-value = 0.049**). Mean HRI was not significantly different in female snow crabs with gut wall RI scores from 1 to 3 (one-way ANOVA F-value = 0.27, DF = 2, P-value = 0.762; Figure A7.17). (Note: No female snow crabs had a gut wall RI Score of 4.) Mean HRI was

not significantly different for male snow crabs with a gut wall RI scores from 0 to 4 (one-way ANOVA F-value = 2.25, DF = 4, P-value = 0.065; Figure A7.18).

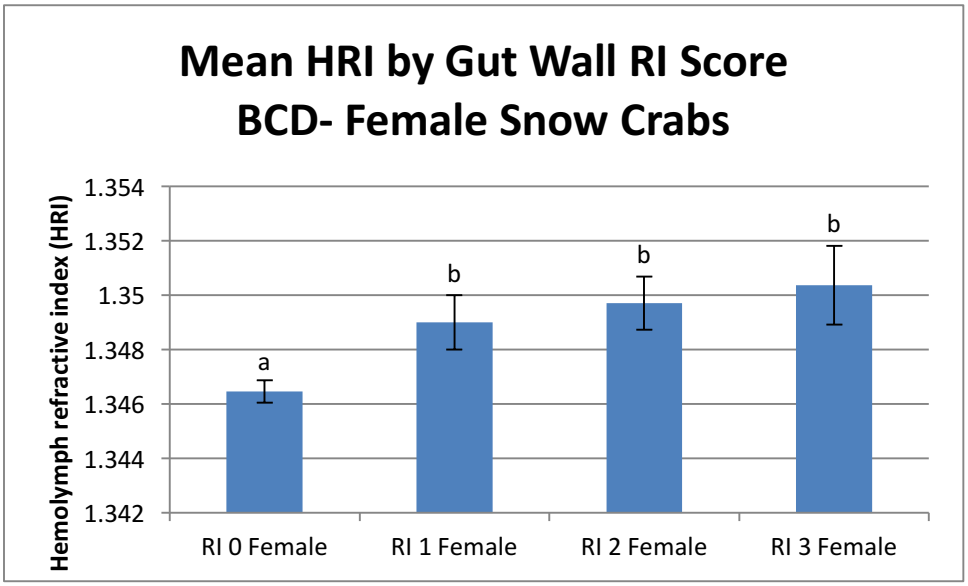

Figure A7.17. Comparison of mean HRI scores in female snow crabs by gut wall RI score. Groups with different letters above the data bar were statistically significant (p<0.05).

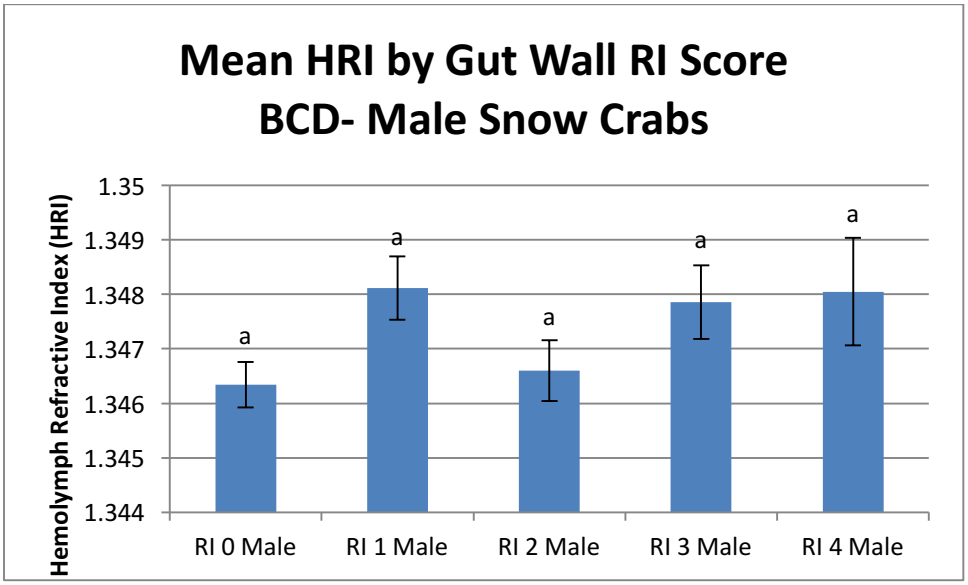

Figure A7.18. Comparison of mean HRI scores in male snow crabs by gut wall RI score. Groups with different letters above the data bar were statistically significant (p<0.05).

A.7.3.2.6.4. RI Score and HRI: New-shelled by Gender

New-shelled female snow crabs with a gut wall RI score of 0 (n = 51, mean = 1.34715 ± 0.00043) had a mean HRI that was lower than, but not significantly different from, new-shelled female snow crabs with a gut wall RI score of 1 (n = 17, mean = 1.34900 ± 0.00099; two-sample T-test: T-value = -1.71, DF = 22, p-value = 0.101) or a gut wall RI score of 3 (n = 6, mean = 1.35037 ± 0.0015; two-sample T-test: T-value = -2.12, DF = 5, p-value = 0.088) but which was significantly lower than new-shelled female snow crabs with a RI score of 2 (n = 15, mean = 1.35064 ± 0.00098; two-sample T-test: T-value = -3.24, DF = 19, **p-value = 0.004**). Mean HRI was not significantly different in female snow crabs with gut wall RI scores from 1 to 3 (one-way ANOVA F-value = 0.76, DF = 2, P-value = 0.474; Figure A7.19). (Note: No female snow crabs had a gut wall RI Score of 4.) Mean HRI is not significantly different for male snow crabs with a gut wall RI scores from 0 to 4 (one-way ANOVA F-value = 2.19, DF = 4, P-value = 0.072; Figure A7.20).

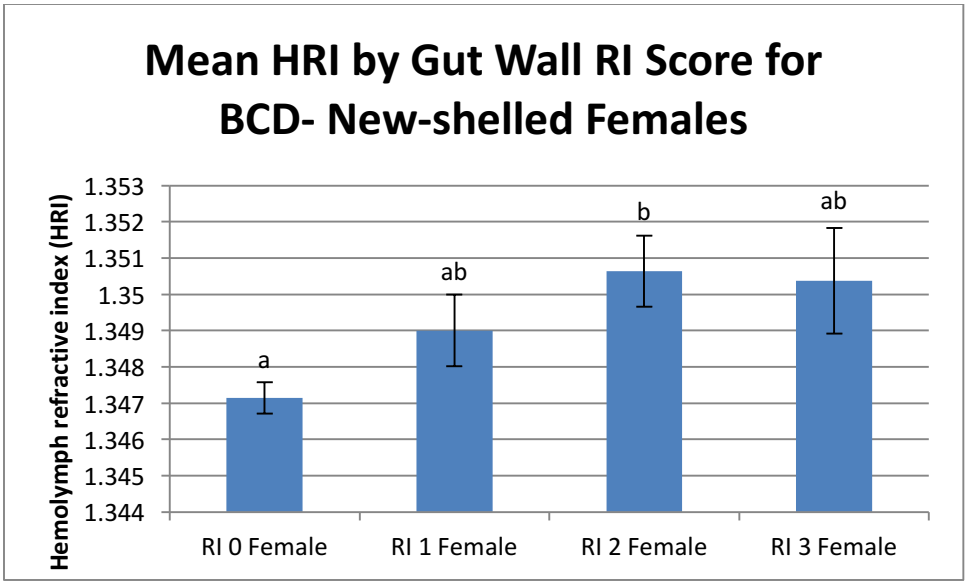

Figure A7.19. Comparison of mean HRI scores in new-shelled female snow crabs by gut wall RI score. Groups with different letters above the data bar were statistically significant (p<0.05).

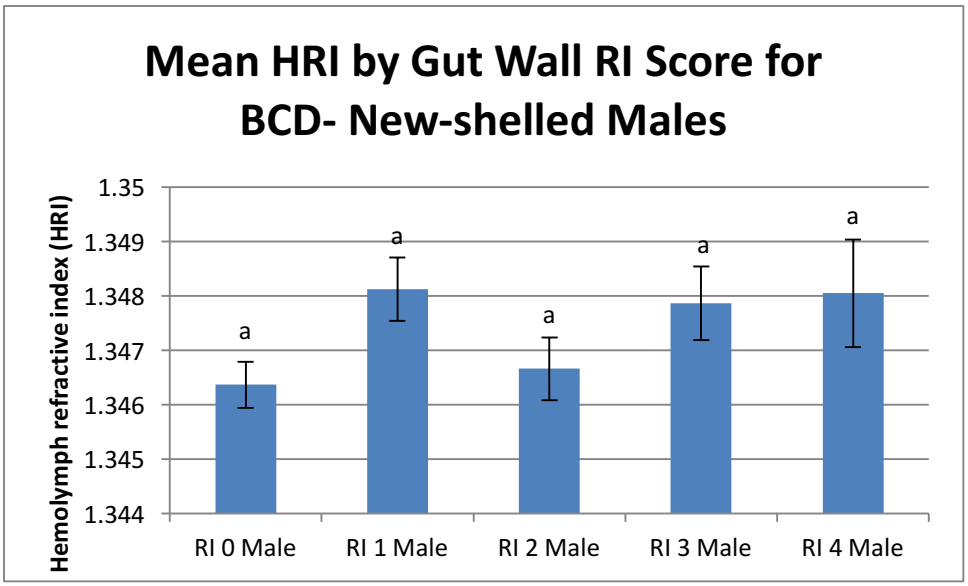

Figure A7.20. Comparison of mean HRI scores in new-shelled male snow crabs by gut wall RI score. Groups with different letters above the data bar were statistically significant ($p<0.05$).

A.7.3.2.6.5. RI Score and HRI: New-shelled by gender and bay

New-shelled female snow crabs from WB with RI scores from 0 to 2 did not have significantly different mean HRIs from one another (one-way ANOVA F-value = 1.38, DF = 2, p-value = 0.267). New-shelled female snow crabs from NDB with a RI score of 0 had lower mean HRI (n = 43, mean = 1.34538 ± 0.00046 SEM) than new-shelled female snow crabs from NDB with a RI score of 2 (n = 17, mean = 1.34952 ± 0.00477 SEM; two-sample T-test, T-value = -3.33, DF = 21, **p-value = 0.003**) and a RI score of 3 (n = 6, mean = 1.35037 ± 0.00356 SEM; two-sample T-test: T-value = -3.57, DF = 6, **p-value = 0.017**). The mean HRI of new-shelled female snow crabs from NDB with a RI score of 0 was also lower than new-shelled female snow crabs with a RI score of 1 (n = 11, mean = 1.34835 ± 0.0014) but the difference was not statistically significant (two-sample T-test: T-value = -2.04, DF = 12, p-value = 0.063). New-shelled female snow crabs from NDB with RI scores of 1 to 3 did not have significantly different mean HRIs from one another (one-way ANOVA F-value = 0.43, DF = 2, p-value = 0.657).

New-shelled female snow crabs with a gut wall RI score of 0 from WB had a higher mean HRI (n = 22, mean = 1.34856 ± 0.00061 SEM) than new-shelled female snow crabs with a gut wall RI score of 0 from NDB (n = 43, mean = 1.34538 ± 0.00046 SEM; two-sample T-test: T-value = 4.17, DF = 45, **p-value = 0.000**). Mean HRI did not significantly differ between bays for RI Score of 1 (two-sample T-Test T-value = 1.00, DF = 14, p-value = 0.336) or RI score of 2 (two-sample T-test: T-value = 0.94, DF = 16, p-value = 0.360; Figure A7.21).

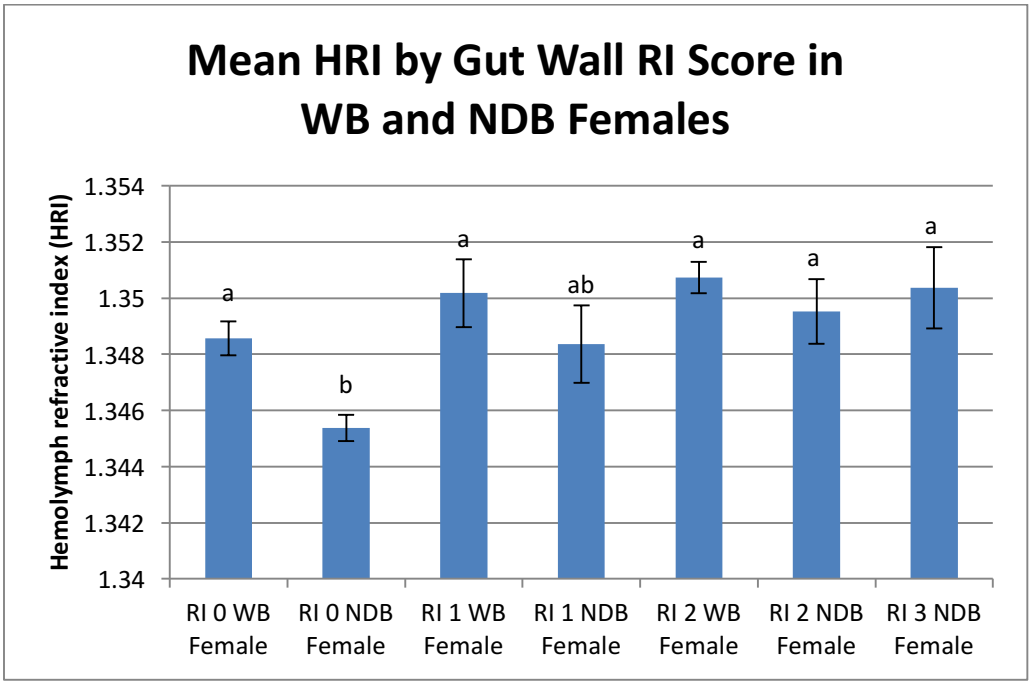

Figure A7.21. Comparison of mean HRI scores in new-shelled female snow crabs by gut wall RI score and bay. Groups with different letters above the data bar were statistically significant ($p<0.05$).

New-shelled male snow crabs from WB with RI scores from 0 to 4 did not have significantly different mean HRIs from one another when the data from the shallow and deep strata were analyzed together (one-way ANOVA F-value = 2.14, DF = 4, p-value = 0.079). And, new-shelled

male snow crabs from NDB with RI scores from 0 to 4 did not have significantly different mean HRIs from one another (one-way ANOVA F-value = 1.43, DF = 4, p-value = 0.239). But, when WB and NDB are analyzed together they were significantly different from one another (one-way ANOVA F-value = 2.16, DF = 9, **p-value = 0.027**). New-shelled males from WB with RI scores of 0 to 4 and new-shelled males from NDB with RI scores of 1 to 4 were not significantly different from each other (one-way ANOVA F-value = 1.68, DF = 9, p-value = 0.107). New-shelled males from NDB with a RI score of 0 had significantly lower mean HRI than new-shelled male snow crabs from WB with a RI score of 1 (two-sample T-test T-value = -2.86, DF = 117, **p-value = 0.011**), RI score of 2 (two-sample T-test T-value = -2.13, DF = 18, **p-value = 0.048**), RI score of 3 (two-sample T-test T-value = -2.40, DF = 23, **p-value = 0.025**), and RI score of 4 (two-sample T-test T-value = -2.84, DF = 17, **p-value = 0.011;** Figure A7.22).

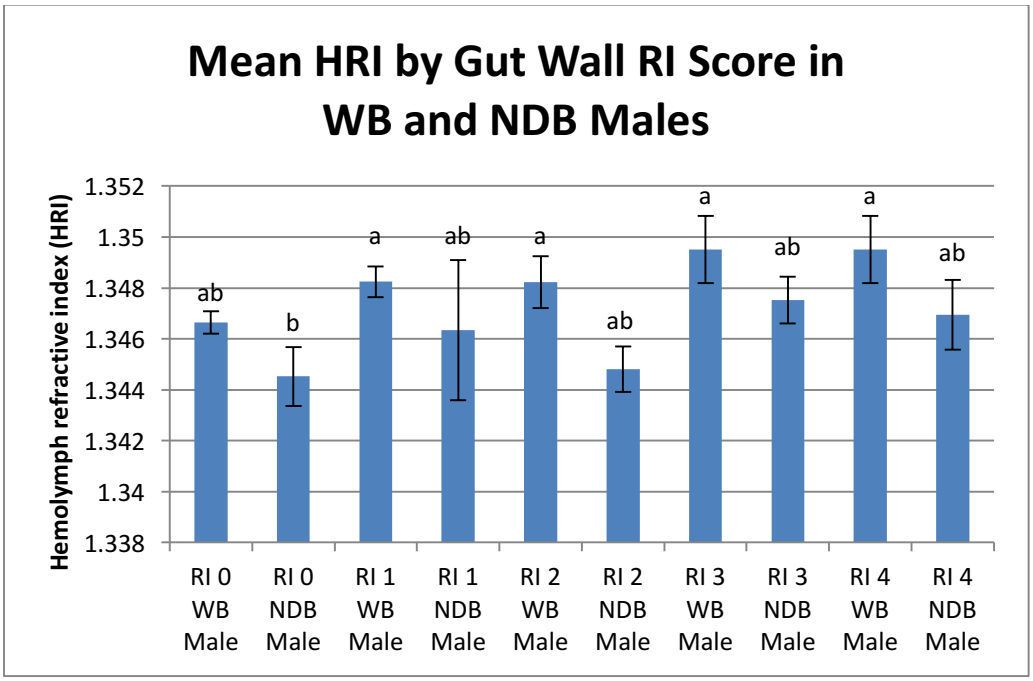

Figure A7.22. Comparison of mean HRI scores in new-shelled male snow crabs by gut wall RI score and bay. Groups with different letters above the data bar were statistically significant ($p<0.05$).

New-shelled male snow crabs from WB with RI scores from 0 to 4 did not have significantly different mean HRIs from one another when the data from the shallow and deep strata are analyzed together (one-way ANOVA F-value = 2.14, DF = 4, p-value = 0.079). Mean HRI did not differ significantly for new-shelled male snow crabs from strata 614/615 with RI scores of 0 to 4 (one-way ANOVA F-value = 0.60, DF = 4, p-value = 0.661). But, in stratum 613 new-shelled male snow crabs with a RI score of 0 had lower mean HRI (n = 22, mean = 1.34412 ± 0.00055 SEM) than new-shelled male snow crabs with a RI score of 2 (n = 7, mean = 1.34590 ± 0.00052 SEM; two-sample T-test: T-value = -2.36, DF = 19, **p-value = 0.029**), a RI score of 3 (n = 11, mean = 1.34780 ± 0.00091; two-sample T-test: T-value = -3.47, DF = 17, **p-value = 0.003**), and a RI score of 4 (n = 8, mean = 1.34995 ± 0.0014; two-sample T-test: T-value = -3.83, DF = 9, **p-value = 0.004**). New-shelled male snow crabs from stratum 613 with a RI score of 0 also had a lower mean HRI than those with a RI score of 1 (n = 6, mean = 1.34593 ± 0.0014 SEM) but the difference was not significant (two-way T-test: T-value = -1.22, DF = 6, p-value = 0.268). New-shelled male snow crabs from stratum 613 with a RI score of 0 also had lower mean HRI than new-shelled male snow crabs from strata 614/615 with an RI score of 0 (n = 49, mean = 1.34778 ± 0.0052 SEM; two-sample T-test: T-value = -4.83, DF = 56, **p-value = 0.000**), RI score of 1 (n = 23, mean = 1.34884 ± 0.00298 SEM; two-sample T-test: R-value = -5.70, DF = 42, **p-value = 0.000**), RI score of 2 (n=17, mean = 1.34794 ± 0.00087 SEM; two-sample T-test: T-value = -3.72, DF = 27, **p-value = 0.001**), and RI score of 3 (n = 11, mean = 1.34780 ± 0.00091 SEM; two-sample T-test: T-value = -3.47, DF = 17, **p-value = 0.003**). There was only a single new-shelled snow crab with a gut wall RI score of 4 (mean = 1.346 ± 0). Mean HRI did not significantly differ for new-

shelled male snow crabs from stratum 613 with RI scores of 1 to 4 (one-way ANOVA F-value = 2.81, DF = 3, p-value = 0.058; Figures A7.23 and A7.24).

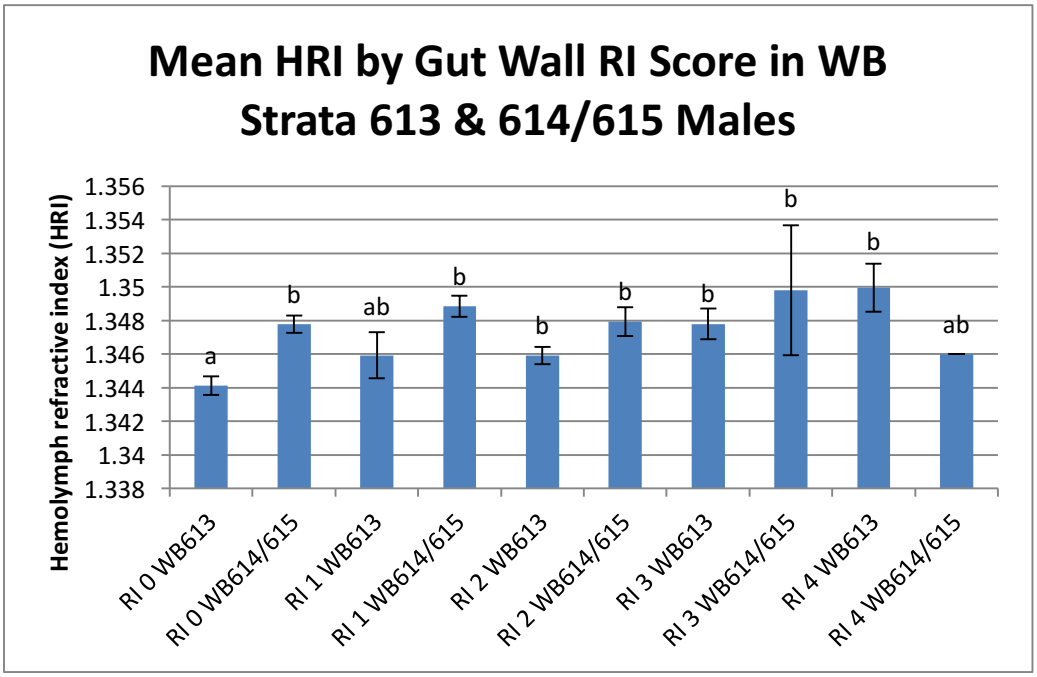

Figure A7.23. Comparison of mean HRI scores in new-shelled male snow crabs by gut wall RI score and strata within WB. Groups with different letters above the data bar were statistically significant (p<0.05).

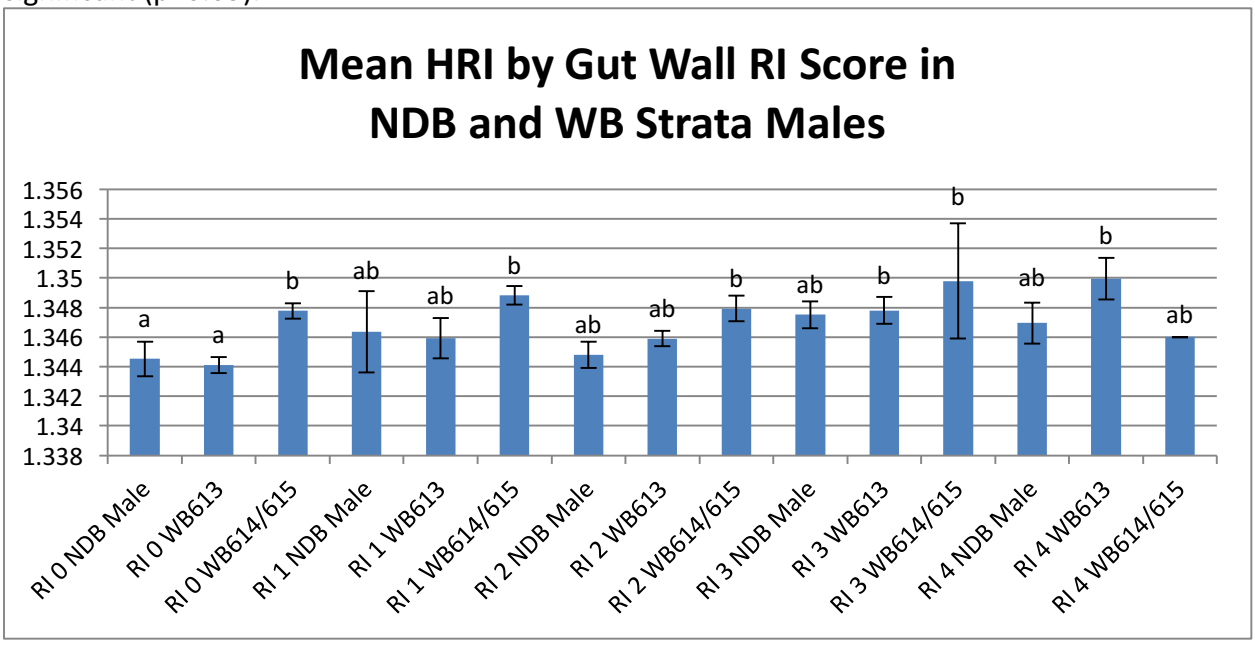

Figure A7.24. Comparison of mean HRI scores in new-shelled male snow crabs by gut wall RI score and strata within WB and NDB. Groups with different letters above the data bar were statistically significant (p<0.05).

A.7.3.2.6.6. Hemolymph refractive index (HRI) and Carapace Width

A.7.3.2.6.6.1. HRI and Carapace Width: All BCD- Snow crabs

When all snow crabs are grouped together there was no statistically significant correlation between HRI and carapace width but the general trend is a slight negative association between HRI and carapace width (Figure A7.25 and Table A7.3). When separated by gender, bay or strata there were also no statistically significant correlations between HRI and carapace width (Figures A7.26 to A7.29 and Table A7.3). In male snow crabs the trend was a mild negative correlation between HRI and carapace width, while in female snow crabs there was a very slight trend of positive correlation. Within bays, NDB male snow crabs showed a negative correlation and NDB females showed slight positive correlation (Figure A7.27). WB 613 males also show a negative correlation between HRI and carapace width (Figure A7.29). But, in WB 614/615 positive correlations were seen in both males and females (Figure A7.28).

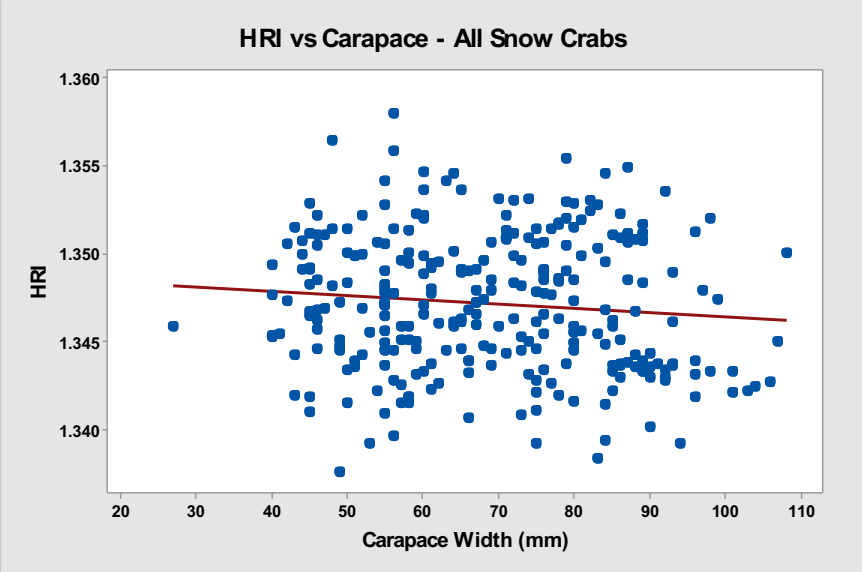

Figure A7.25. Scatterplot of hemolymph refractive index (HRI) and carapace width (mm) for all BCD- snow crabs (excluding shipping mortalities). No significant correlation between HRI and carapace width was observed (n=262, Pearson correlation = -0.074, p-value = 0.231).

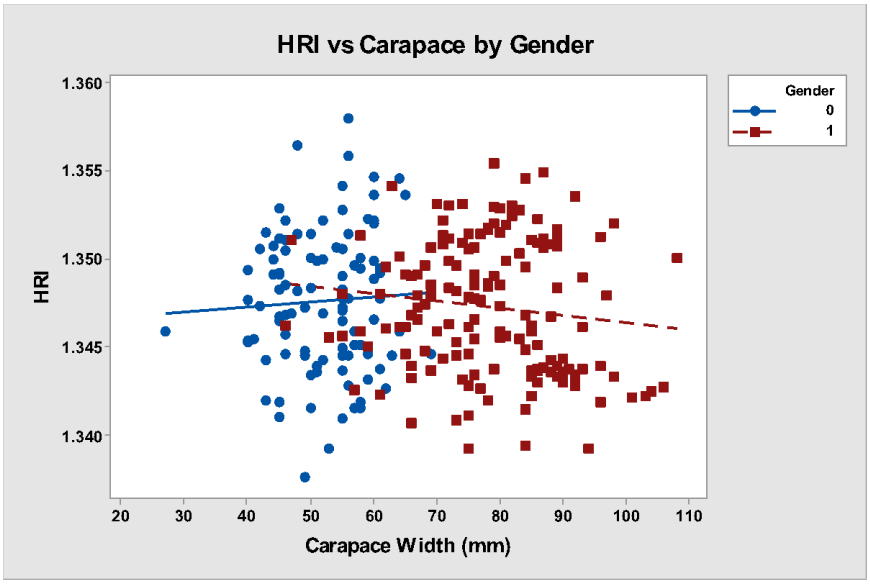

Figure A7.26. Scatterplot of hemolymph refractive index (HRI) and carapace width (mm) for snow crabs by gender (excluding shipping mortalities). Female snow crabs (Gender "0") had no significant correlation between HRI and carapace width (n = 103, Pearson correlation = 0.050, p-value = 0.617). Male snow crabs (Gender "1") had a negative correlation between HRI and carapace width (n = 159, Pearson correlation = -0.124, p-value = 0.119).

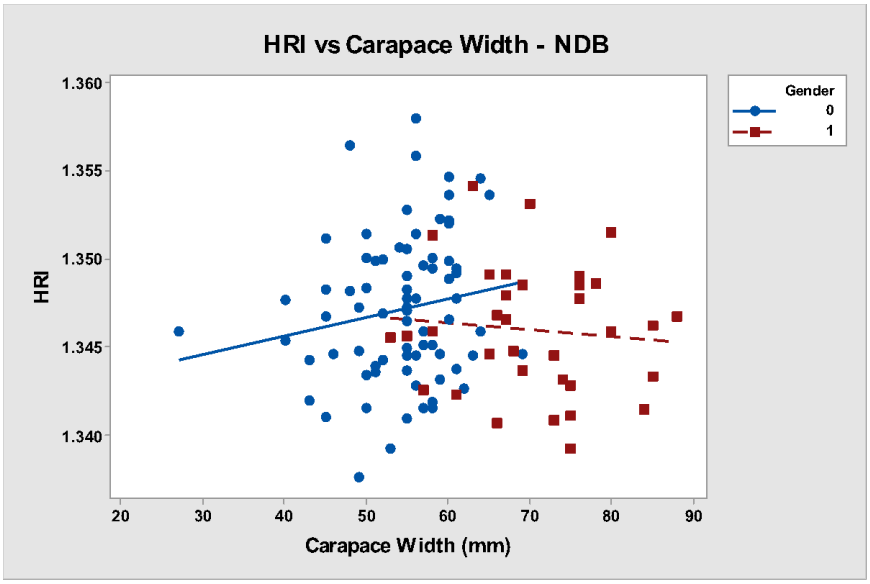

Figure A7.27. Scatterplot of hemolymph refractive index (HRI) and carapace width (mm) for snow crabs by gender in Notre Dame Bay (no shipping mortalities collected from this bay). In NDB female (n=77, Pearson correlation = 0.171, p-value = 0.138) and male (n=51, Pearson correlation = -0.80, p-value = 0.577) snow crabs no significant correlation between HRI and carapace width was observed.

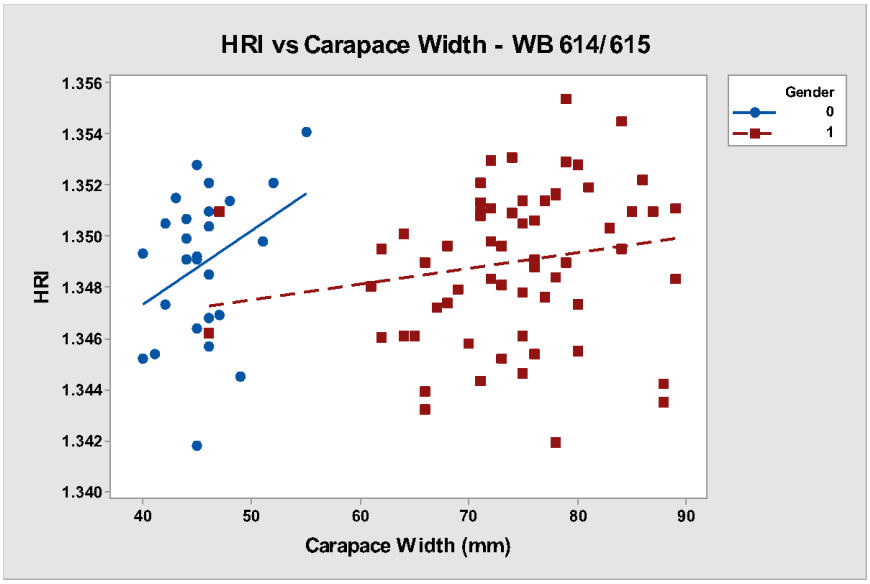

Figure A7.28. Scatterplot of hemolymph refractive index (HRI) and carapace width (mm) for snow crabs by gender in White Bay strata 614/615 (excluding shipping mortalities). In WB 614/615 female snow crabs there was a positive correlation between HRI and carapace width (n=26, Pearson correlation = 0.349, p-value = 0.080). In WB 614/615 male snow crabs there was no significant correlation (n=64, Pearson correlation = 0.179, p-value = 0.156). No significant difference was observed between the mean HRI of WB614/615 females (n=26, mean = 1.34890 ± 0.00057 SEM) and males (n=64, mean = 1.34898 ± 0.00037 SEM; two-sample T-test: T-value = -0.11, DF = 47, p-value = 0.914).

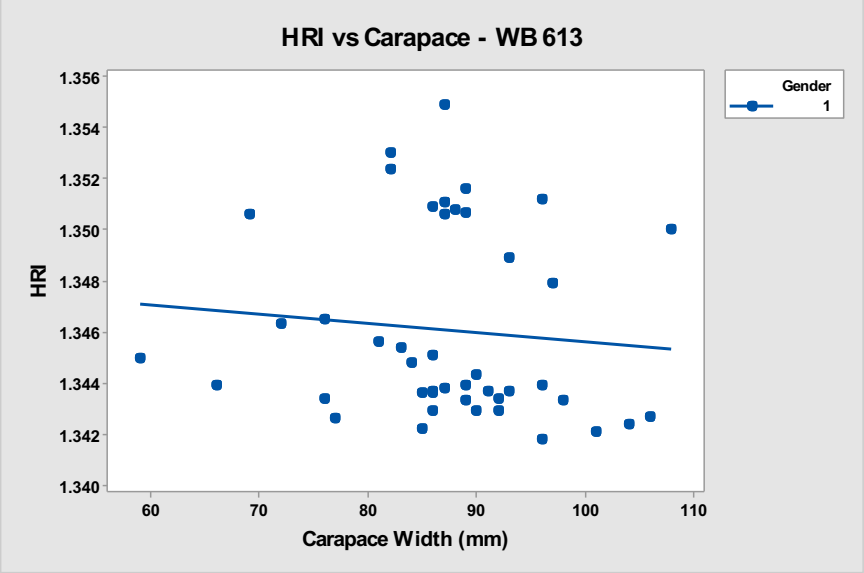

Figure A7.29. Scatterplot of hemolymph refractive index (HRI) and carapace width (mm) for snow crabs by gender in WB stratum 613 (no females were collected from this this stratum, and shipping mortalities were excluded). No significant correlation between HRI and carapace width was observed (n=44, Pearson correlation = -0.096, p-value = 0.536).

Table A7.3. Summary of trends observed in HRI vs carapace width correlations seen in snow crabs of all shell conditions and RI scores. Pearson correlations with negative trends (red) and positive trends (green). No statistically significant correlations between HRI and carapace width or significant differences in mean HRI between genders were observed in these groups of snow crabs.

		n	HRI vs Carapace Width		HRI		
			Pearson correlation	Pearson correlation p-value	Mean	Two-sample T-test T-value	Two-sample T-test p-value
All Bays	All Snow Crabs	262	-0.074	0.231	1.34737	N/A	N/A
	All Females	103	0.505	0.617	1.34756	0.63	0.531
	All Males	159	-0.124	0.199	1.34725		
NDB	NDB Females	77	0.171	0.138	1.34711	1.49	0.142
	NDB Males	51	-0.080	0.577	1.34594		
WB	WB 614/615 Females	26	0.349	0.080	1.34890	-0.11	0.914
	WB 614/615 Males	64	0.179	0.156	1.34898		
	WB 613 Males	44	-0.096	0.536	1.34608	N/A	N/A

A.7.3.2.6.6.2. HRI and Carapace Width: By Gut Wall RI Score

In female snow crabs there were no significant correlations between HRI and carapace width (Figures A7.30 and A7.31, Table A7.4). However, HRI and carapace width were negatively correlated at low gut wall RI scores (0 and 1) and positively correlated at high gut wall RI scores (2 and 3). In male snow crabs HRI and carapace width were also negatively correlated at low gut wall RI scores (0, 1, and 2) and positive correlated at high gut wall RI scores (3 and 4). The correlations between HRI and carapace width in male snow crabs were statistically significant in snow crabs with a gut wall RI score of 0 (negative correlation) and a gut wall RI score of 4 (positive correlation; Figures A7.32 and A7.33). In both male and female BCD- snow crabs mean HRI was lower at gut wall RI scores of 0 than in gut wall RI scores above 0 (Table A7.4).

When separated by bay and strata no statistically significant correlations between HRI and carapace width were observed (Figures A7.34-A7.43; Tables A7.5 and A7.6). In female snow crabs from NDB HRI and carapace width were not correlated at a gut wall RI score of 0, negatively correlated at a gut wall RI score of 1, and positively correlated at gut wall RI scores of 2 and 3. Mean HRI was significantly lower in NDB females with a gut wall RI score of 0 than in NDB females with gut wall RI scores 2 or 3. In female snow crabs from WB 614/615 HRI and carapace width were positively correlated at RI scores of 0 and 1 (only 2 snow crabs had a gut wall RI score of 2). Mean HRI did not vary significantly with gut wall RI score in WB 614/615 females.

In male snow crabs from NDB HRI and carapace width were negatively correlated at low gut wall RI scores (0-2), no correlation at gut wall RI score 3, and positive correlation gut wall RI scores 4. No significant difference was seen between mean HRI with varying gut wall RI score in NDB males. In male snow crabs from WB 613 HRI and carapace width were negatively correlated at low gut wall RI scores 0 and 1, not significantly correlated and gut wall RI score 2, and positively correlated at gut wall RI scores 3 and 4. Mean HRI was significantly lower in snow crabs with a gut wall RI score of 0 than in snow crabs with gut wall RI scores of 3 and 4 in WB 613 males. In male snow crabs from WB 614/615 HRI and carapace width were not correlated, and there was no significant difference in mean HRI with varying gut wall RI score.

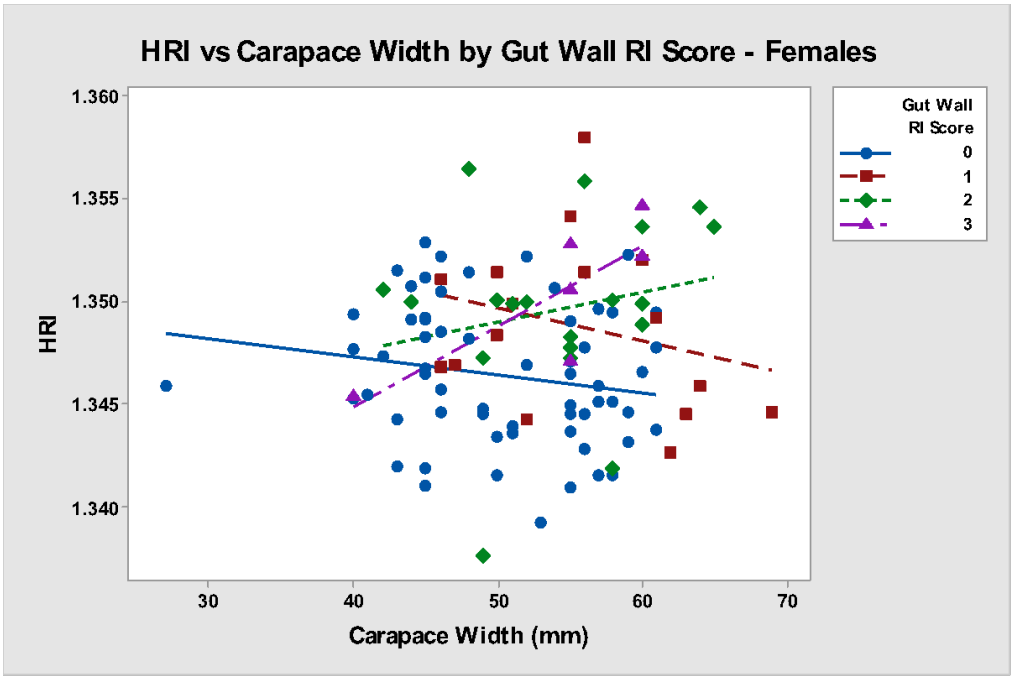

Figure A7.30. Scatterplot of HRI versus carapace width by gut wall reserve inclusion (RI) score in female snow crabs excluding shipping mortalities. No statistically significant correlations between HRI and carapace width were observed. At a gut wall RI score of 0 (n=62, Pearson correlation = -0.183, p-value = 0.155) and 1 (n=16, Pearson correlation = -0.277, p-value = 0.299) there were trends of negative association, while at gut wall RI scores of 2 (n=19, Pearson correlation = 0.204, p-value = 0.401) and 3 (n=6, Pearson correlation = 0.808, p-value = 0.052) the trends were of positive correlation between HRI and carapace width.

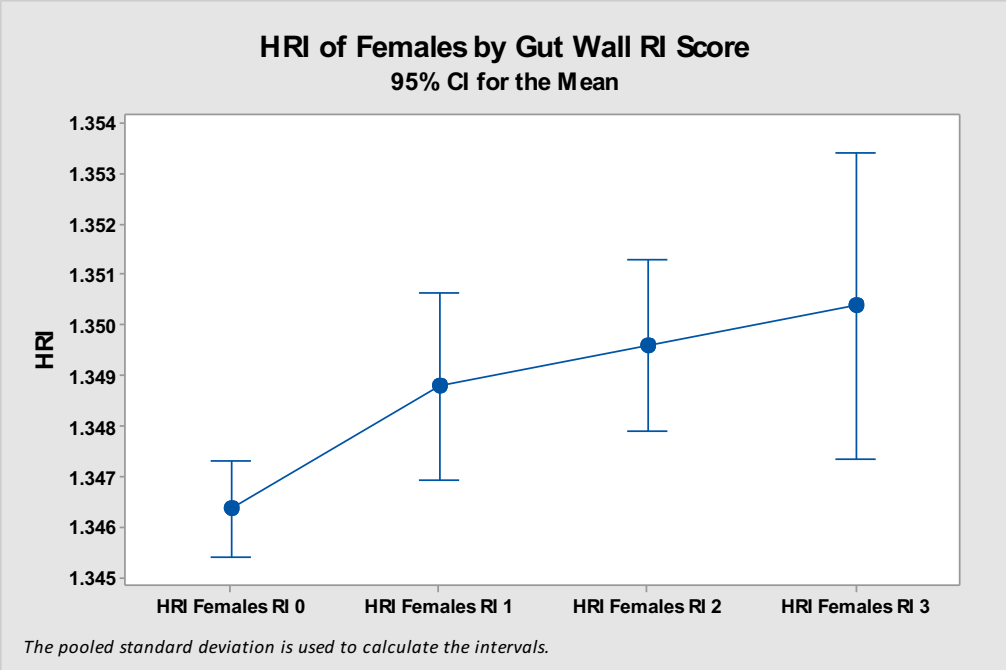

Figure A7.31. Interval plot of mean HRI by gut wall RI score in BCD- female snow crabs. Mean HRI at RI 0 (mean = 1.34635 ± 0.00043) was significantly lower than mean HRI at RI 1 (mean = 1.34878 ± 0.0010; two-sample T-test: T-value = -2.19, DF = 20, **p-value = 0.041**), RI 2 (mean = 1.34959 ± 0.0010; two –sample T-test: T-value = -2.90, DF = 24, **p-value = 0.008**), and RI 3 (mean = 1.35037 ± 0.0015; two-sample T-test: T-value = -2.65, DF = 5, **p-value = 0.045**). Mean HRI for RI scores 1 through 3 were not significantly different from one another (one-way ANOVA: F-value = 0.35, DF = 2, p-value = 0.709).

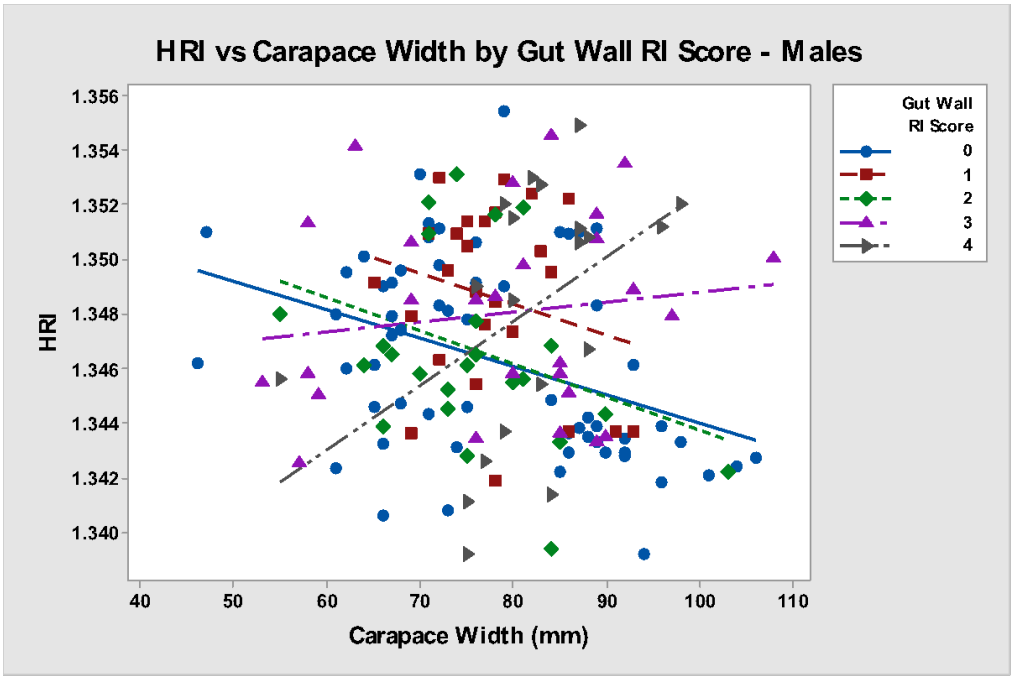

Figure A7.32. Scatterplot of HRI versus carapace width by gut wall RI scores for male snow crabs (excluding shipping mortalities). Male snow crabs had a negative correlation between HRI and carapace width at gut wall RI scores of 0 (n = 66, Pearson correlation = -0.364, **p-value = 0.003**). At gut wall RI scores of 1 (n = 27, Pearson correlation = -0.266, p-value = 0.179), 2 (n = 28, Pearson correlation = -0.299, p-value = 0.122), and 3 (n = 28, Pearson correlation = 0.130, p-value = 0.510) no statistically significant correlations were observed. At a gut wall RI score of 4 HRI and carapace width were positively correlated (n = 20, Pearson correlation = 0.457, **p-value = 0.043**).

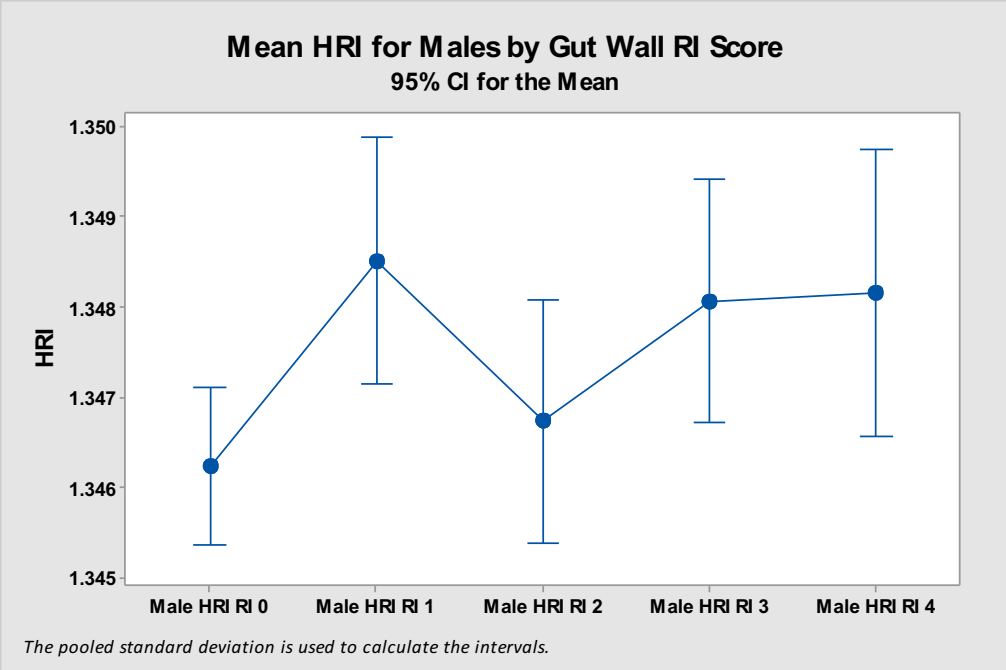

Figure A7.33. Interval plot of mean HRI by gut wall RI score in BCD- male snow crabs. Mean HRI for males with a gut wall RI score of 0 (mean = 1.34623 ± 0.00044) was significantly lower than mean HRI for males with a gut wall RI score of 1 (mean = 1.34851 ± 0.00063; two-sample T-test: T-value = -2.96, DF = 52, **p-value = 0.005**) and 3 (mean = 1.34806 ± 0.00067 SEM; two-sample T-test: T-value = -2.29, DF = 51, **p-value = 0.026**), but was not statistically different from the mean HRI of male snow crabs with a gut wall RI of 1 (n = 2, mean = 1.34673 ± 0.00061; two-sample T-test: T-value = -0.66, DF = 55, p-value = 0.514) and 4 (n = 20, mean = 1.34815 ± 0.0010 SEM, two-sample T-test: T-value = -1.71, DF = 26, p-value = 0.100). Mean HRI for RI scores 1 through 4 were not significantly different from one another (one-way ANOVA: F-value = 1.27, DF = 3, p-value = 0.290).

Table A7.4. Summary of trends observed in correlations between HRI vs carapace width in female and male snow BCD- crabs of all shell conditions with varying RI scores. Pearson correlations with negative trends (red) and positive trends (green). Statistically significant correlations between HRI and carapace width are indicated in bold. Significant differences in mean HRI between gut wall RI scores within gender are also indicated in bold.

	Gut Wall RI Score	n	HRI vs Carapace Width		HRI			
			Pearson correlation	Pearson correlation p-value	Mean	ANOVA p-value		Two-sample T-test Groups: p-value
All Females	0	62	-0.183	0.155	1.34635	**0.001**		RI 0 & RI 1: **0.041**
	1	16	-0.277	0.299	1.34878		0.709	RI 0 & RI 2: **0.008**
	2	19	0.204	0.401	1.34959			RI 0 & RI 3: **0.045**
	3	6	0.808	0.052	1.35037			
All Males	0	66	**-0.364**	**0.003**	1.34626	**0.022**		RI 0 & RI 1: **0.005**
	1	27	-0.266	0.179	1.34851		0.290	RI 0 & RI 2: 0.514
	2	28	-0.299	0.122	1.34673			RI 0 & RI 3: **0.026**
	3	28	0.130	0.510	1.34806			RI 0 & RI 4: 0.100
	4	20	**0.457**	**0.043**	1.34815			

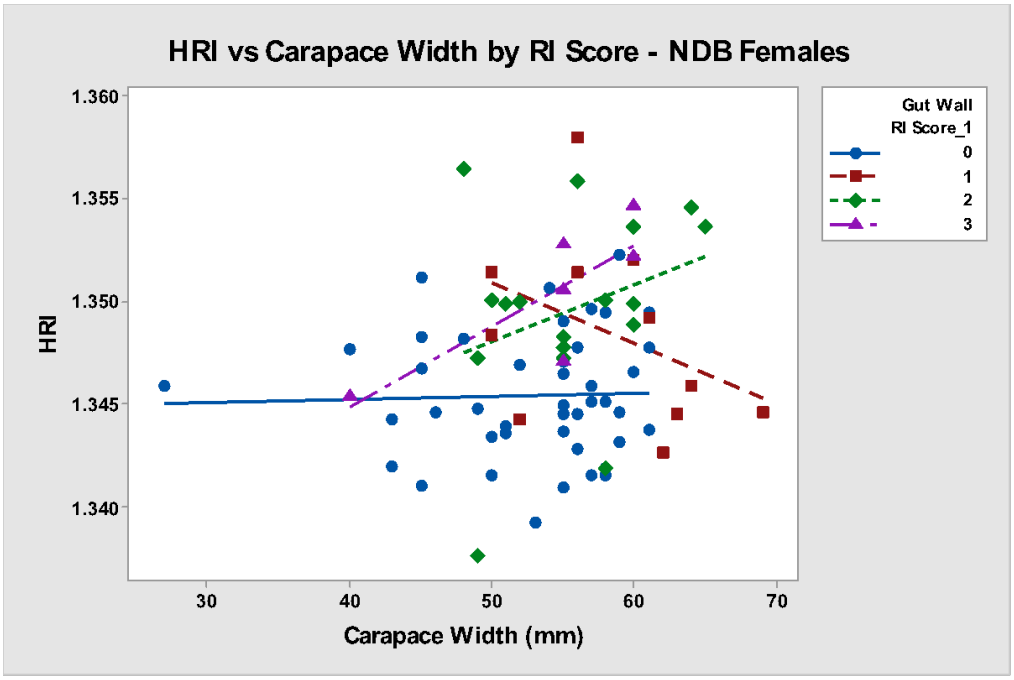

Figure A7.34. Scatterplot of HRI versus carapace width by gut wall reserve inclusion (RI) score in female snow crabs from NDB. No statistically significant correlations between HRI and carapace width were observed. At a gut wall RI score of 0 (n = 43, Pearson correlation = 0.035, p-value = 0.826) there was a very slight positive trend, a negative trend at a gut wall score of 1 (n = 11, Pearson correlation = -0.401, p-value = 0.222), and trends of positive correlation at gut wall scores of 2 (n = 17, Pearson correlation = 0.302, p-value = 0.238) and 3 (n = 6, Pearson correlation = 0.808, p-value = 0.052).

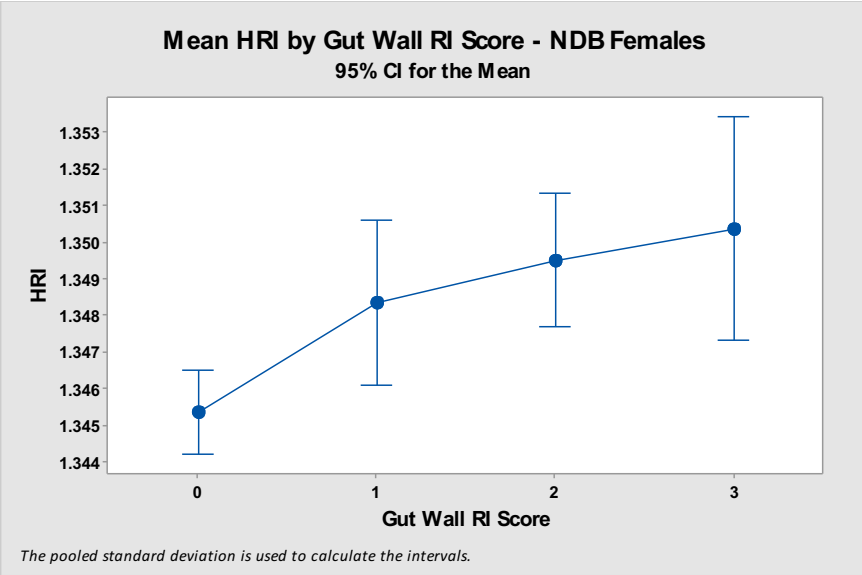

Figure A7.35. Interval plot of mean HRI by gut wall RI scores in NDB female snow crabs (no NDB female snow crabs had a gut wall RI score of 4). Mean HRI in NDB females significantly varied by gut wall RI score (one-way ANOVA: F-value = 7.32, DF = 3, p-value = 0.000). Mean HRI of NDB females with a gut wall RI of 0 (n=43, mean = 1.34538 ± 0.00046) was significantly lower than those with a gut wall RI score of 2 (n=17, mean = 1.34952 ± 0.0012; two-sample T-test: T-value = -3.33, DF = 21, p-value = 0.003) and 3 (n=6, mean = 1.35037 ± 0.0015; two-sample T-test: T-value = -3.27, DF = 6, p-value = 0.017) but was not significantly lower than NDB females with a gut wall RI score of 1 (n = 11, mean = 1.34835 ± 0.0014; two-sample T-test: T-value = -2.04, DF = 12, p-value = 0.063). Mean HRI did not vary significantly among NDB females with gut wall RI scores 1 through 3 (one-way ANOVA: F-value = 0.43, DF = 2, p-value = 0.657).

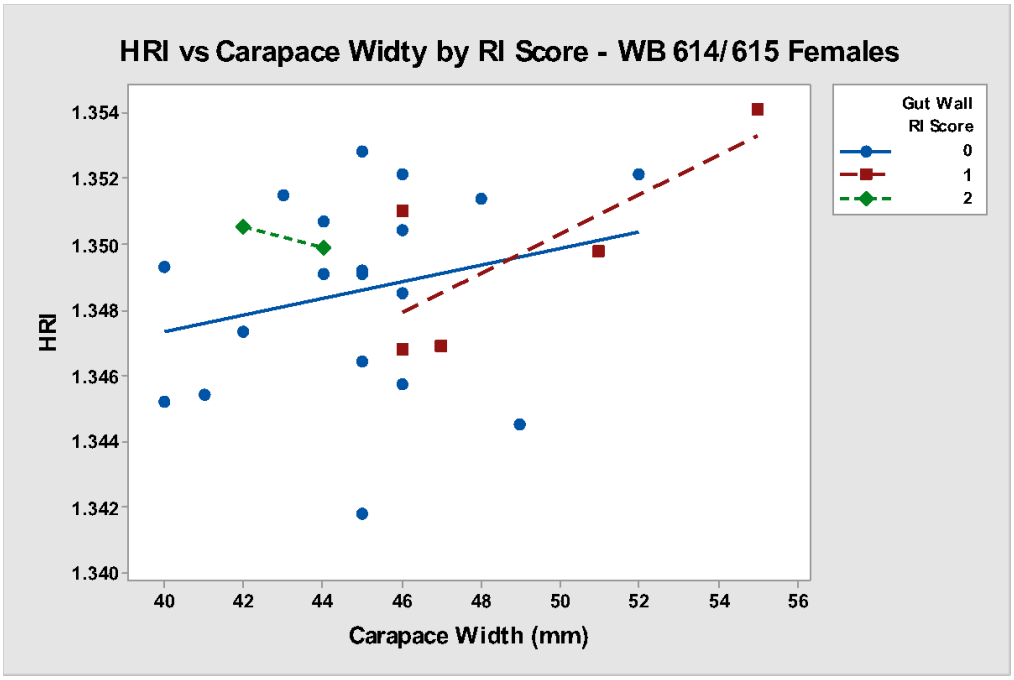

Figure A7.36. Scatterplot of HRI versus carapace width by gut wall reserve inclusion (RI) score in female BCD- snow crabs from WB 614/615 excluding shipping mortalities. No statistically significant correlations between HRI and carapace width were observed. At a gut wall RI scores of 0 (n = 19, Pearson correlation = 0.249, p-value = 0.305) and 1 (n = 5, Pearson correlation = 0.769, p-value = 0.128) there were positive trends of association. There were only 2 female BCD- snow crabs from WB 614/615 with a gut wall RI score of 2 (n = 2, Pearson correlation = -1.000, p-value = *).

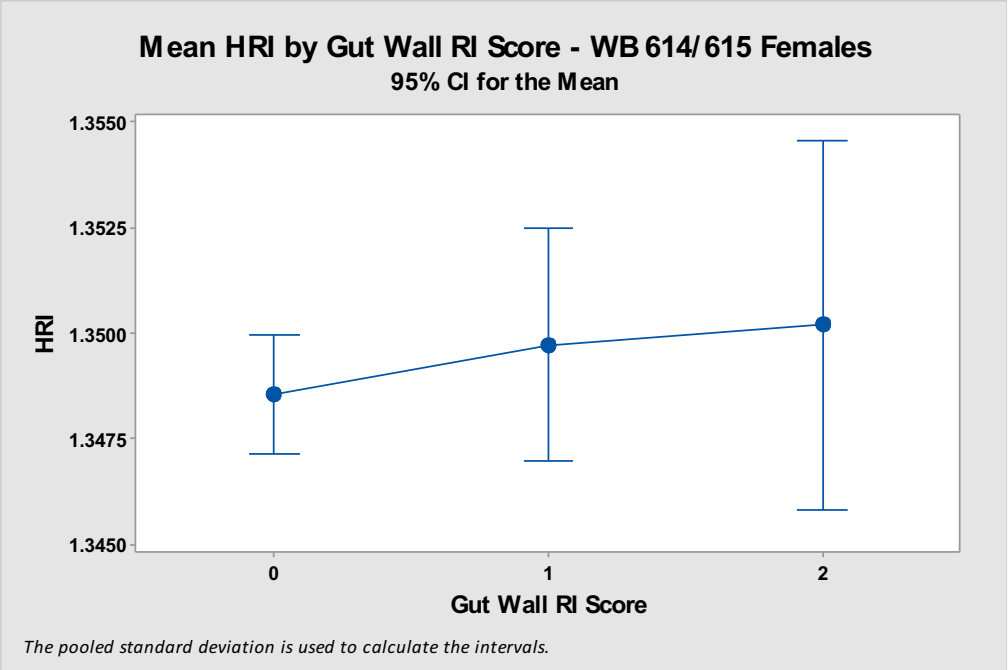

Figure A7.37. Interval plot of mean HRI by gut wall RI score in WB strata 614/615 female snow crabs (no WB 614/615 females had gut wall RI scores of 3 or 4). Mean HRI in WB 614/615 females did not significantly vary by gut wall RI score (one-way ANOVA: F-value = 0.51, DF = 2, p-value = 0.608).

Table A7.5. Summary of trends observed in correlations between HRI vs carapace width in female snow crabs of all shell conditions with varying RI scores by bay. Pearson correlations with negative trends (red) and positive trends (green). Statistically significant correlations between HRI and carapace width are indicated in bold. Significant differences in mean HRI between gut wall RI scores within gender are also indicated in bold.

	Gut Wall RI Score	n	HRI vs Carapace Width		HRI			
			Pearson correlation	Pearson correlation p-value	Mean	ANOVA p-value		Two-sample T-test Groups: p-value
NDB 610/611 Females	0	43	0.035	0.826	1.34538	**0.000**		RI 0 & RI 1: 0.063
	1	11	-0.401	0.222	1.34835		0.657	RI 0 & RI 2: **0.003**
	2	17	0.302	0.238	1.34952			RI 0 & RI 3: **0.017**
	3	6	0.808	0.052	1.35037			
WB 614/615 Females	0	19	0.249	0.305	1.34853	0.608		N/A
	1	5	0.769	0.128	1.34972			
	2	2	1	*	1.35020			

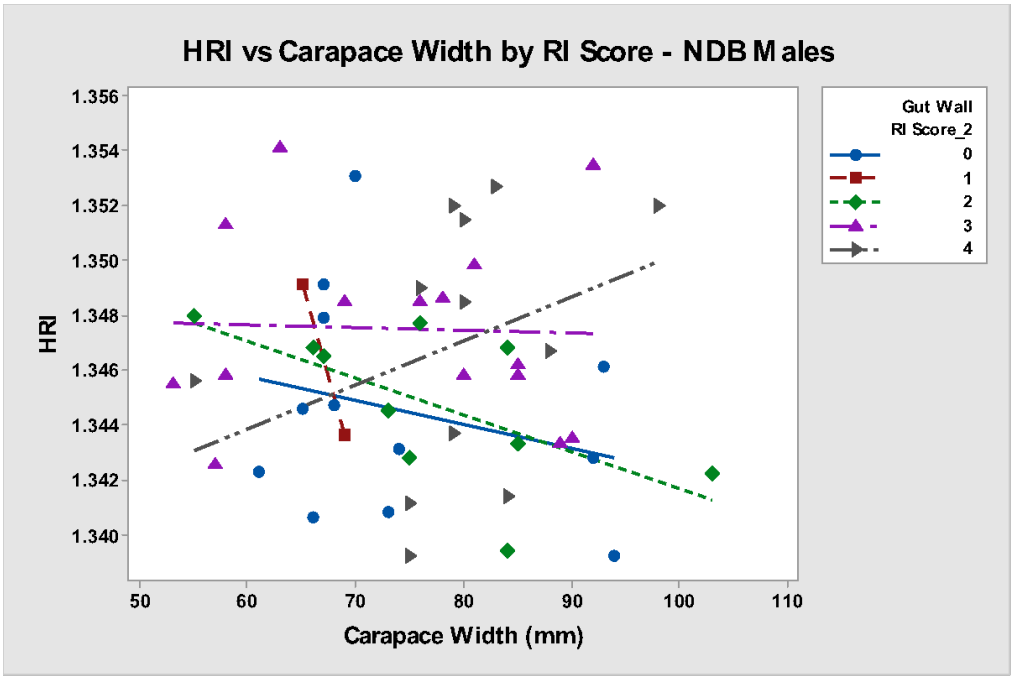

Figure A7.38. Scatterplot of HRI versus carapace width by gut wall reserve inclusion (RI) score in male BCD - snow crabs from NDB. No statistically significant correlations between HRI and carapace width were observed. A t a gut wall RI score of 0 (n = 12, Pearson correlation = -0.259, p-value = 0.416), 1 (n = 2, Pearson correlation = -1.000, p-value = *), 2 (n = 10, Pearson correlation = -0.628, p-value = 0.052) and 3 (n = 15, Pearson correlation = -0.036, p-value = 0.899) there were trends of negative correlation and a trend of positive correlation at a gut wall RI score of 4 (n = 12, Pearson correlation = 0.336, p-value = 0.286).

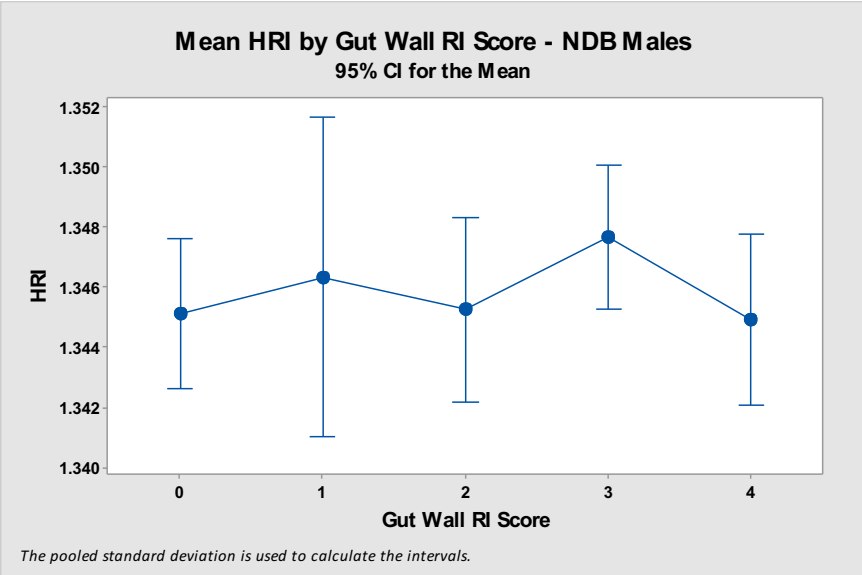

Figure A7.39. Mean HRI in NDB males did not significantly vary by gut wall RI score (one-way ANOVA: F-value = 0.85, DF = 4, p-value = 0.505).

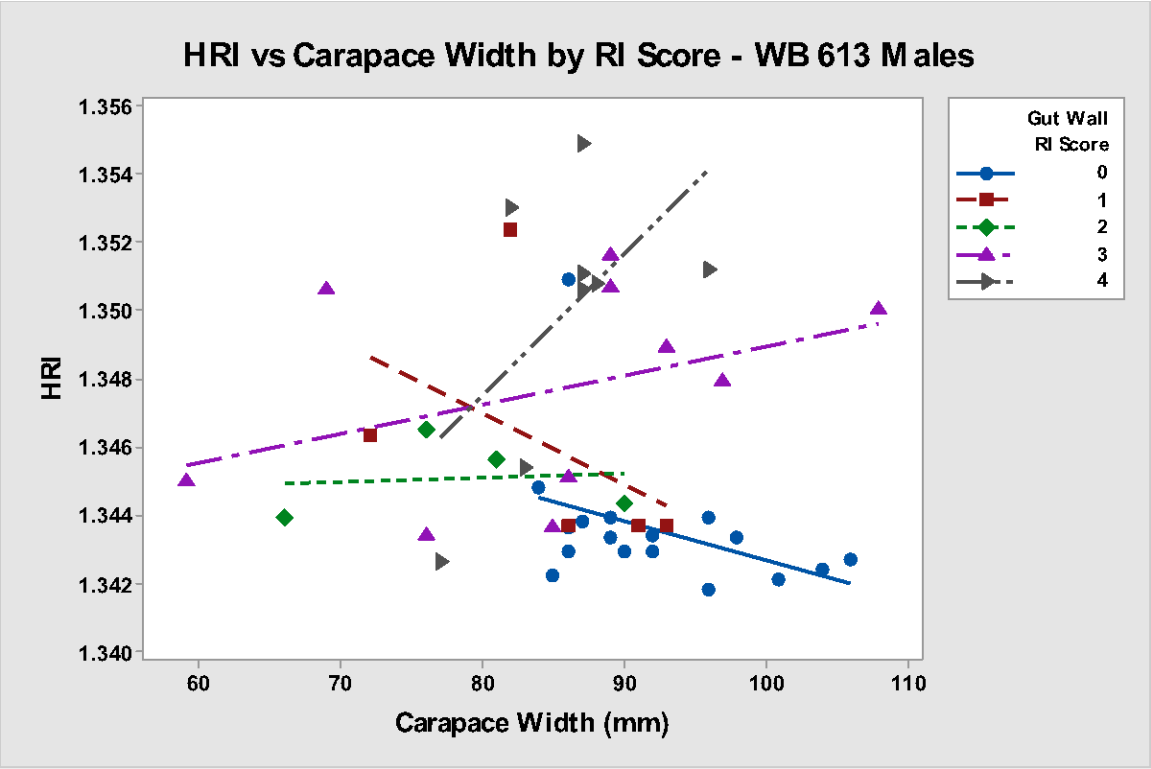

Figure A7.40. Scatterplot of HRI versus carapace width by gut wall reserve inclusion (RI) score in male BCD - snow crabs from WB stratum 613 excluding shipping mortalities. No statistically significant correlations between HRI and carapace width were observed. Negative correlation trends were observed gut wall RI scores of 0 (n = 17, Pearson correlation = -0.389, p-value = 0.122) and 1 (n = 5, Pearson correlation = -0.458, p-value = 0.438) while positive correlation trends were noted at gut wall RI scores of 2 (n = 4, Pearson correlation = 0.098, p-value = 0.902), 3 (n = 10, Pearson correlation = 0.383 p-value = 0.274) and 4 (n = 8, Pearson correlation = 0.572, p-value = 0.138).

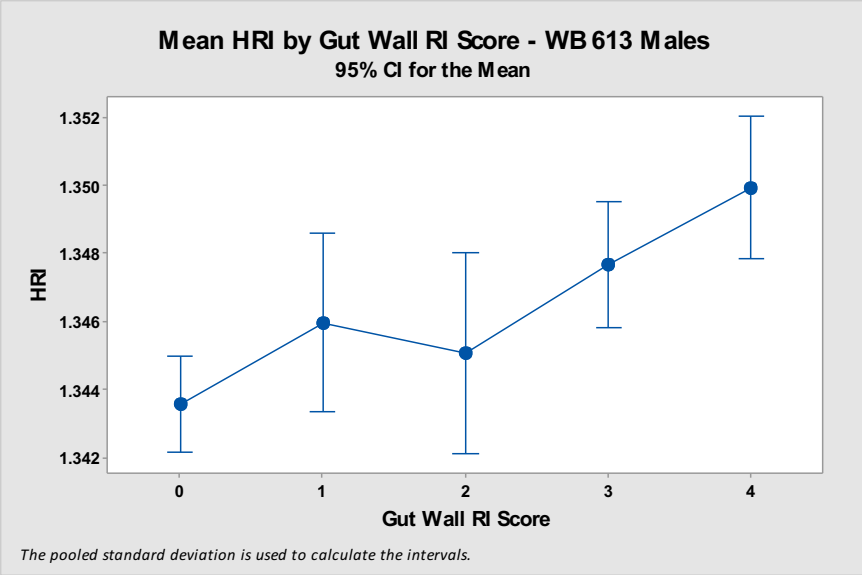

Figure A7.41. Mean HRI in WB 613 males varied by gut wall RI score (one-way ANOVA: F-value = 7.59, DF = 4, p-value = 0.000). Mean HRI of WB 613 male snow crabs with a gut wall RI score of 0 (n=17, mean = 1.34358 ± 0.00049) was significantly lower than snow crabs with a gut wall RI score of 3 (n=10, mean = 1.34768 ± 0.0099; two-sample T-test: T-value = -3.70, DF = 13, p-value = 0.003) and 4 (n=8, mean = 1.34995 ± 0.0014 SEM; two-sample T-test: T-value = -4.25, DF = 8, p-value = 0.003) but was not significantly different from animals with a gut wall RI score of 1 (n=5, mean = 1.34596 ± 0.0017; two-sample T-test: T-value = -1.36, DF = 4, p-value = 0.247) or 2 (n=4, mean = 1.34508 ± 0.00060; two-sample T-test: T-value = -1.93, DF = 7, p-value = 0.095). Mean HRI in WB 613 males did not vary significantly among snow crabs with gut wall RI scores from 1 to 4 (one-way ANOVA: F-value = 2.43, DF =34, p-value = 0.091).

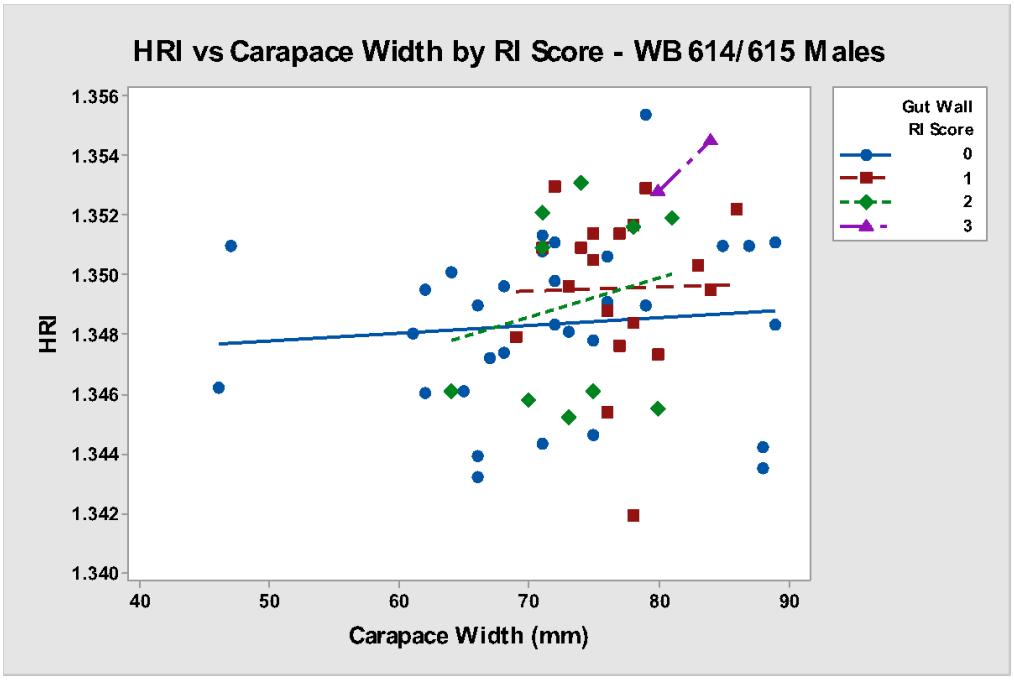

Figure A7.42. Scatterplot of HRI versus carapace width by gut wall reserve inclusion (RI) score in male BCD - snow crabs from WB strata 614/615 excluding shipping mortalities. No statistically significant correlations between HRI and carapace width were observed. At a gut wall RI scores of 0 (n = 32, Pearson correlation = 0.099, p-value = 0.591) and 1 (n = 19, Pearson correlation = 0.020 p-value = 0.937) there were slight positive trends of correlation and a positive correlation trend at a gut wall RI score of 2 (n = 13, Pearson correlation = 0.071, p-value = 0.818). Only 2 male BCD- snow crabs had a gut wall RI score of 3 (n = 2, Pearson correlation = 1.000, p-value = *) and only no male BCD- snow crab from WB 614/615 had a gut wall RI score of 4.

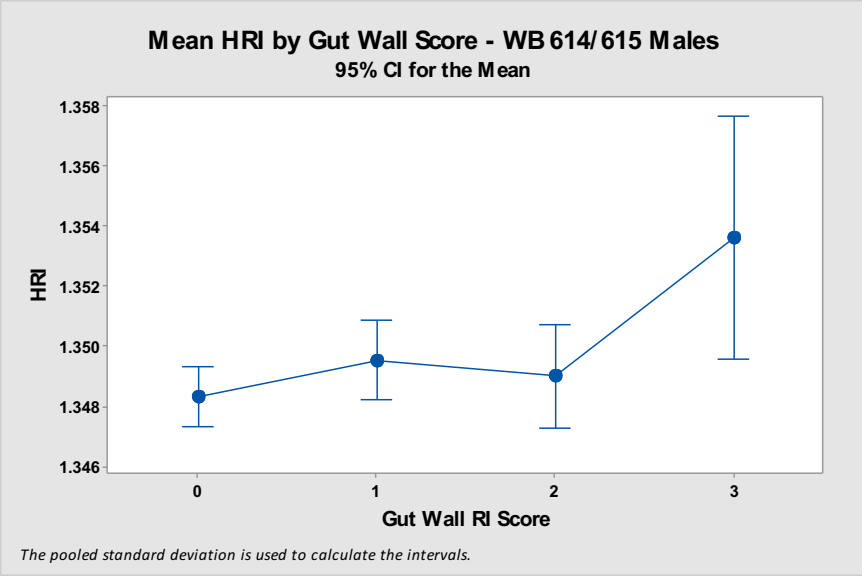

Figure A7.43. Mean HRI in WB 614/615 males did not significantly vary by gut wall RI score (one-way ANOVA: F-value = 2.59, DF = 3, p-value = 0.061).

Table A7.6. Summary of trends observed in correlations between HRI vs carapace width in male snow crabs of all shell conditions with varying RI scores by bay and strata within WB. Pearson correlations with negative trends (red) and positive trends (green). Statistically significant correlations between HRI and carapace width were not observed. Significant differences in mean HRI between gut wall RI scores within gender are indicated in bold.

	Gut Wall RI Score	n	HRI vs Carapace Width		HRI			
			Pearson correlation	Pearson correlation p-value	Mean	ANOVA p-value		Two-sample T-test Groups: p-value
NDB 610/611 Males	0	12	-0.259	0.416	1.344525	0.505		N/A
	1	2	-1	*	1.34635			
	2	10	-0.628	0.052	1.34480			
	3	15	0.036	0.899	1.34751			
	4	12	0.336	0.286	1.34695			
WB 613 Males	0	17	-0.389	0.122	1.34358	**0.000**		RI 0 & RI 1: 0.247
	1	5	-0.458	0.438	1.34596		0.091	RI 0 & RI 2: 0.095
	2	4	0.098	0.902	1.34508			RI 0 & RI 3: **0.003**
	3	10	0.383	0.274	1.34768			RI 0 & RI 4: **0.003**
	4	8	0.572	0.138	1.34995			
WB 614/615 Males	0	32	0.099	0.591	1.34833	0.061		N/A
	1	19	0.020	0.937	1.34956			
	2	13	0.071	0.818	1.34906			
	3	2	1	*	1.35365			

A.7.4. Discussion

The level of body glycogen stores has been suggested as index of condition in crustaceans. The concentration of glycogen in abdominal muscle has been reported to be the best nutritional index for the Hawaiian spiny lobster *Panulirus marginatus* (Parrish and Martinelli-Liedtke 1999). Stentiford and Feist (2005) utilized relative abundance of RI cells in histologic sections of connective tissues of the hepatopancreas as a body condition assessment tool in European green crab *Carcinus maenas* and was used to compare populations of the crab in several UK estuarine sites. Reserve inclusion (RI) cells are cells within the spongy connective tissue containing eosinophilic reserve materials which thought to function in the synthesis and storage of hemocyanin, glycogen, and protein (Johnson 1980).

In this study gut wall reserve inclusion score was negatively correlated with shell condition category: new-shelled snow crabs had higher levels of glycogen storage than intermediate or old-shelled snow crabs. This finding was somewhat unexpected as snow crabs are reported to stop feeding 3-6 weeks before molt and not feed for 3-4 weeks after molt suggesting, an extended period of anorexia would suggest that glycogen stores would be depleted during molting (O'Halloran and O'Dor 1988). But, higher glycogen stores in new-shelled animals may suggest that snow crabs with low glycogen reserves are less likely to molt than those with higher glycogen stores. Intermolt crabs are reported to have lower glycogen stores than molting crabs (Heath and Barnes 1970). Furthermore, in this study intermediate and old-shelled snow crabs collected in this study were almost all gravid females and female snow crabs had lower glycogen RI stores than males in general. One possible reason for this gender difference in glycogen reserves may be glycogen reserve depletion due to reproductive energetic expenditures. The investment per brood in dry weight terms in free-living brachyuran crabs ranges from 3-21% with a mean of about 11 % (Hartnoll 2006). Other gender and/or sized-based impacts on diet or competition for food could also be contribute to this gender-effect on glycogen stores, but no differences in diet components were detected between snow crabs of different gender, size, or shell condition inn one study on snow crabs from Bonne Bay, Newfoundland (Wieczorek and Hooper 1995). Rather than size or gender, prey availability and food preferences were the important factors influencing in the diet of Newfoundland snow crabs with the foraging strategy of snow crabs being a combination of opportunistic feeding behavior in the case of some highly available food (fish bait and polychaetes) and selective

feeding in the case of less abundant food items (sponges, *Yoldia* spp. clams, brittle stars and basket stars, and small gastropods; Wieczorek and Hooper 1995).

New-shelled male snow crabs from NDB had a higher median gut wall reserve inclusion score than similar snow crabs from WB 613 and both of those regions had higher scores than WB 614/615. This suggests that snow crabs collected from NDB in 2010 were in better body condition than those collected from WB. This difference may be a year-effect and/or a region-effect, suggesting that the ocean shelf-type environment of Notre Dame Bay may a nutritionally superior environment than the fjord-type environment of White Bay. New-shelled male snow crabs from WB 613 (very deep stratum) had higher reserve inclusion scores than new-shelled male snow crabs from the combined strata of 614 (deep) and 615 (shallow). These snow crabs were collected in the same year (2011) within less than a week of one another and thus this difference appears to be regional. This suggests that snow crabs in the very deep stratum were in better body condition than in the more shallow regions of White Bay in 2011, suggesting that the very deep waters of stratum 613 may be a nutritionally superior environment to the shallower waters of strata 614/615 within White Bay.

Blood refractive index is often assumed to be directly proportional to hemolymph protein levels in crustaceans, and thus is also often used as an indicator of nutritional condition (Stewart and Li 1969, Smith and Dall 1982, Moore 2000, Behringer et al 2008). Hemocyanin, a respiratory pigment, is the main hemolymph protein in crustacean representing 60–93%, 64–84%, 81–88% and 60–77% of total protein in the hemolymph of the bay shrimp *Crangon vulgaris*, Japanese

tiger prawn *Marsupenaeus (Penaeus) japonicus*, tropical mud crab *Scylla serrata*, and giant river prawn *Macrobrachium rosenbergii*, respectively (Djangmah, 1970; Chen and Cheng, 1993; Chen and Chia, 1997; Cheng et al, 2001). Djangmah (1970) suggested that decreases of hemolymph hemocyanin levels during starvation may indicate that hemocyanin is used as a food reserve. For example, hemolymph refractive index (HRI) was significantly reduced in starved penaeid shrimp as compared to fed penaeid shrimp, with significant difference between fed and starved prawn after 12 hours (Moore et al 2000). The decrease in HRI may reflect decrease protein stores within hemolymph but a dilution effect may also contribute due to increased blood volume due to muscle catabolism (Dall 1974, Smith and Dall 1982, Moore 2000). Aside from being an index of condition protein concentration in the hemolymph of crustaceans also varies with the molt cycle, generally being lowest during post-molt and highest pre-molt, a factor which needs to be taken into account when interpreting why a given crustacean has low or high protein level (Dall 1974, Paterson et al 2001).

Shell condition category negatively associated with hemolymph refractive index in this data set similar to the trend seen with RI score mentioned above. But, again, the older shell categories were predominated by gravid females. Thus, while these negative associations with shell condition category are evident in gravid females there were too few male snow crabs with intermediate and old shell conditions to draw meaningful conclusions about correlations of shell condition with either gut wall RI score or HRI in male snow crabs. In crustaceans, hemolymph protein and hemocyanin levels are generally lower in the post-molt stage than during the premolt stage due to water uptake during ecdysis (Busselen 1970, Bursey and Lane

1971, Truchot 1978, Hagerman 1983, Chan et al 1988, Mercaldo-Allen 1991, Chen and Cheng 1993, Chen and Chia 1997, Cheng et al 2002). Intermolt hemolymph protein levels can be lower or higher than those seen in post-molt (Chan et al 1988, Chen and Cheng 1993, Chen and Chia 1997, Cheng et al 2002).

Generally, females had higher mean HRI than males. Female crustaceans have vitellogenesis-associated hemolymph lipoproteins which may contribute to this gender difference in HRI (Lee and Puppione 1988.) New-shelled male snow crabs from WB 614/615 had significantly lower mean hemolymph refractive index than new-shelled male snow crabs from either WB stratum 613 or NDB. If gut wall RI score is used as a nutritional index to compare snow crabs between regions it would indicate that snow crabs from WB 614/615 were in poorer body condition than snow crabs from NDB or WB 613. But, if mean HRI is used as a conditional index it would indicate the WB 614/615 snow crabs were in better body condition than NDB or WB 613 snow crabs. Variation in hemolymph hemocyanin and protein levels may also depend on blood volume and osmotic conditions and thus can vary between environmental locations (Boone and Schoffeniels, 1979). This suggests that HRI may not be as robust of a nutritional index as gut wall RI score and HRI may not be useful for comparison of nutritional index between regions. These conflicting results may reflect differences in the diet within snow crab populations in these regions as hemocyanin levels in decapod crustaceans vary with the quality of the food eaten (Busselen 1970, Djangmah 1970, Hagerman 1983). Snow crabs in WB 614/615 may have a high-protein, low-carbohydrate diet which results in high protein hemolymph stores and low tissue glycogen stores, while snow crabs in the other 2 regions have a lower-protein, higher

carbohydrate diet resulting in low hemolymph protein stores (lower mean HRI) and higher tissue glycogen stores. This suggests that the overall condition status of snow crabs may be better assessed by evaluating gut wall RI score and HRI rather than either measure alone.

A.7.5. References

Balazs GH, Olbrich SE, Tumbleson, M.E. 1974. Serum constituents of the Malaysian prawn (*Macrobrachium rosenbergii*) and pink shrimp (*Penaeus marginatus*). Aquaculture 3:147-157.

Behringer DC, Butler MJ, Shields JD. 2008. Ecological and physiological effects of PaV1 infection on the Caribbean spiny lobster *Panulirus argus* Latreille). J Exp Mar Biol Ecol. 359(1):23-33.

Boone WR, Schoffeniels E. 1979. Hemocyanin synthesis during hypo-osmotic stress in the shore crab *Carcinus maenas* (L.). Comp Biochem Physiol Part B 63(2):207-214.

Bursey CR, Lane CE. 1971. Ionic and protein concentration changes during the molt cycle of *Penaeus duorarum*. Comp. Biochem. Physiol. 40A:155-162.

Busselen P. 1970. Effects of moulting cycle and nutritional conditions on haemolymph proteins in *Carcinus maenas*. Comp Biochem Physiol 37(1):73-83.

Castell JD, Budson SD. 1974. Lobster nutrition: The effect on *Homarus americanus* of dietary protein levels. J Fish Res Board Canada. 31(8):1363-1370.

Chan SM, Rankin SM, Keeley LL. 1988. Characterization of the molt stages in *Penaeus vannamei*: setogenesis and hemolymph levels of total protein, ecdysteroids, and glucose. Biol Bull 175:185-192

Chang ES. 1995. Physiological and biochemical changes during the molt cycle in decapod crustaceans: an overview. J Exp Mar Biol Ecol 193:1-14.

Chen JC, Cheng SY. 1993. Studies on haemocyanin and haemolymph protein levels of *Penaeus japonicus* based on sex, size and moulting cycle. Comp Biochem Physiol B 106:293–296.

Chen JC, Chia PG., 1997. Oxyhemocyanin, protein, osmolality and electrolyte levels in the hemolymph of *Scylla serrata* in relation to size and molt cycle. J Exp Mar Biol Ecol 217:93–105.

Cheng W, Liu CH, Cheng CH, Chen JC. 2001. Hemolymph oxyhemocyanin, protein, osmolality and electrolyte levels of *Macrobrachium rosenbergii* in relation to size and molt stage. Aquaculture 198: 387-400

Cheng W, Liu CH, Fan DF, Chen JC. 2002. Hemolymph oxyhemocyanin, protein, osmolality and electrolyte levels of whiteleg shrimp *Litopenaeus vannamei* in relation to size and molt stage. Aquaculture 211:325-339.

Dall W. 1974. Indices of nutritional state in the western rock lobster, *Panulirus longipes* (Milne Edwards). I. Blood and tissue constituents and water content. J Exp Mar Biol Ecol 16:167-180.

Dawe E, Mullowney D, Colbourne E, Han G, Morado JF, Cawthorn R. 2010. Relationship of oceanographic variability with distribution and prevalence of bitter crab syndrome in snow crab (*Chionoecetes opilio*) on the Newfoundland–Labrador shelf. *In:* Biology and management of exploited crab populations under climate change. Alaska Sea Grant College Program, AK-SG-10-01:175-198.

Djangmah JS. 1970. The effects of feeding and starvation on copper in the blood and hepatopancreas, and on blood proteins of *Crangon vulgaris* (Fabricius). Comp Biochem Physiol 32:709-731.

Ferner RE. 2008. Post-mortem clinical pharmacology. Br J Clin Pharmacol. 66(4):430-443.

Ferraris RP, Parado-Estepa FD, Ladja JM. 1986. Effect of salinity on the osmotic, chloride, total protein and calcium concentrations in the hemolymph of the prawn *Penaeus monodon* (Fabricius). Comp Biochem Physiol A 83:701-708.

Hagerman L. 1983. Haemocyanin concentration of juvenile lobster (*Homarus gammarus*) in relation to moulting cycle and feeding conditions. Mar Biol 77:11-17.

Hartnoll RG. 2006. Reproductive investment in Brachyura. Hydrobiologia 557:31-40.

Heath JR, Barnes H. 1970. Some changes in biochemical composition with season and during the moulting cycle of the common shore crab, Carcinus maenas (L.). J Exp Mar Biol Ecol 5(3):199-233.

Johnson PT. 1980. Histology of the blue crab, *Callinectes sapidus*: a model for the Decapoda. New York, NY: Praeger Publishers.

Lee RF, Puppione DL. 1988. Lipoproteins I and II from the hemolymph of the blue crab *Callinectes sapidus*: Lipoprotein II associated with vitellogenesis. J Exp Zool 248 (3):278-289.

Mangum CP, McMahon BR, Wheatly MG. 1985. Gas exchange, acid-base balance, and the oxygen supply to the tissues during a molt of the blue crab *Callinectes sapidus*. J Crust Biol 5(2):188-206.

Mercaldo-Allen R. 1991. Changes in the blood chemistry of the American lobster, *Homarus americanus*, H. Milne Edwards, 1837, over the molt cycle. J Shellfish Res 10(1):147-156.

Moore LE, Smith DM, Loneragan NR. 2000. Blood refractive index and whole-body lipid content as indicators of nutritional condition for penaeid prawns (Decapoda: Penaeidae). J Exp Mar Biol Ecol 244(1):131-143.

Mullowney DR, Dawe EG, Morado JF, Cawthorn RJ. 2011. Sources of variability in prevalence and distribution of bitter crab disease in snow crab (*Chionoecetes opilio*) along the northeast coast of Newfoundland. ICES J Mar Sci 68(3):463-471.

Neil DM. 2012. Ensuring crustacean product quality in the post-harvest phase. J Invert Pathol 110:267-75.

O'Halloran MJ, O'Dor RK. 1988. Molt cycle of male snow crabs *Chionoecetes opilio*, from observations of external features, setal changes, and feeding behavior. J Crust Biol 82(2):164-176.

Parrish FA, Martinelli-Liedtke TL. 1999. Some preliminary findings on the nutritional status of the Hawaiian spiny lobster (*Panulirus marginatus*). Pac Sci 53(4):361.

Paterson BD, Davidson GW, Spanoghe PT. 2001. Measuring total protein concentration in blood of the western rock lobster by refractrometry. Evans, Louis and Jones, B. (Eds). *In* International Symposium on Lobster Health Management, 19-21 September, 1999: International Symposium on Lobster Health Management. Adelaide.

Smith DM, Dall W. 1982. Blood protein, blood volume and extracellular space relationships in two *Penaeus* spp. (Decapoda: Crustacea). J Exp Mar Biol Ecol 63(1):1-15.

Spindler-Barth M. 1976. Changes in the chemical composition of the common shore crab, *Carcinus maenas*, during the molting cycle. J Comp Phys B 105:197-205.

Sriket C, Benjakul S, Visessanguan W. 2011. Characterisation of proteolytic enzymes from muscle and hepatopancreas of fresh water prawn (*Macrobrachium rosenbergii*). J Sci Food Agric 91(1):52-59.

Stentiford GD, Feist SW, Stone DM, Bateman KS, Dunn AM. 2013. Microsporidia: diverse, dynamic, and emergent pathogens in aquatic systems. Trends Parasitol 29(11):567-578.

Stewart JE, Cornick JW, Dingle JR. 1967. An electronic method for counting lobster (*Homarus americanus* Milne Edwards) hemocytes and the influence of diet on hemocyte numbers and hemolymph proteins. Can J Zool 5(3):291-304.

Stewart JE, Li MF. 1969. A study of lobster (*Homarus americanus*) ecology using serum protein concentration as an index. Can J Zool 47(1):21-28.

Stewart JE, Zwicker BM, Arie B, Horner GW. 1972. Food and starvation as factors affecting the time to death of the lobster *Homarus americanus* infected with *Gaffkya homari*. J Fish Res Board Can 29(4):461–464.

Terwilliger NB. 1999. Hemolymph proteins and molting in crustaceans and insects. Am Zoologist 39(3):589-599.

Truchot JP. 1978. Variations de la concentration sanguine d'hemocyanin fonctionelle au cours du cycle d'intermue chez le crabe *Carcinus maenas* (L.). Arch Zool Exp Gen 119:265–282.

Vazquez-Boucard CG, Moureau CE, Ceccaldi H. 1985. Etude preliminaire des variations circadiennes des proteines de l'hemolymphe de *Penaeus japonicus* Bate. J Exp Biol Ecol 85:123–133.

Wieczorek SK, Hooper RG. 1995. Relationship between diet and food availability in the snow crab *Chionoecetes opilio* (O. Fabricius) in Bonne Bay, Newfoundland. J Crust Biol 15(2):236-247.

Appendix 8: Histologic Survey of PEI Green Crabs, *Carcinus maenas*.

A.8.1. Introduction

BCD is an emerging disease in decapod crustaceans. BCD was first described in European green crabs (also known as common shore crab) *Carcinus maenas* and blue-leg swimming crabs *Liocarcinus depurator* off the coast of France (Chatton and Poisson 1931). Since that time the infection has been reported in over forty species of crustaceans primarily in the North Pacific and Atlantic Oceans (reviewed in Morado 2011). Infections of *Hematodinium* spp. are thought to be fatal in virtually every host species. Histologic evaluation of European green crab *Carcinus maenas* off the coast of PEI was pursued to determine if this locally invasive species is a possible disease reservoir in Atlantic Canada.

A.8.2. Materials and Methods

Green crabs (*Carcinus maenas*) were collected by Dr. Quijon in the Biology Department at UPEI for use in studies investigating the impact of this invasive species on local ecosystem components. The green crabs were collected monthly in 3 consecutive months (May, June, and July) in the North River, PE in experimental traps set at ~ 1.5-2.5 m depth. The snow crabs were delivered to the AVC in coolers by hand and processed immediately.

For each crab gender was noted, carapace width (mm) was measured, and was humanely euthanized via nerve cord disruption via decapitation (i.e., removal of the carapace). However, euthanasia via decapitation (used for snow crabs) was not sufficient to disrupt the ventral nerve cord in green crabs. After decapitation (removal of the carapace) in green crab it was necessary

to complete the severance of the ventral nerve cord via manual fracturing of the sternum along the medial sternal groove. Upon removal of the carapace a necropsy was performed and tissue samples were collected. The tissue samples collected included: heart, hepatopancreas, gill (1st and 4th gills on the right), gonad, midgut, eyestalks (left and right), a cross-section of the abdomen, and a cross-section of leg (1st merus on the right). The tissues were immediately placed in Davidson's seawater fixative (Appendix 3) for 24 h. After 24 h, the tissue samples were transferred into containers of 70% ethanol for storage until routine processing for histology.

Sections of all soft tissues (heart, hepatopancreas, gill, gonad, and midgut) were trimmed and placed into one cassette per individual crab for processing. A second cassette of sections lined by a thick cuticular layer (eyestalk, leg, and abdomen) was also submitted for each crab. The eyestalk was bisected along the frontal plane as this plane was found to consistently result in optimal sections of internal neuroendocrine tissues (Appendix 4). The blocks of trimmed tissues were processed routinely for histology (Leica processor) and stained with hematoxylin and eosin (H&E). Digital photomicrographs were captured using

Each tissue on each slide was examined systematically. Relative abundance of glycogen-containing reserve inclusion (RI) cells was also scored as previously reported (Stentiford and Fiest, 2005). The scoring index ranged from Stage 0 (RI cells absent) through Stage 1 (RI cells present but scarce), Stage 2 (RI cells scattered), Stage 3 (RI cells frequent) to Stage 4 (RI cells abundant and constituting the majority of connective tissue volume). RI scores were completed

for both the hepatopancreas and the gut wall. Evaluations of sections of hepatopancreas and gut wall (midgut and hindgut) were examined to determine a representative RI score for each crab (Appendix 6).

A.8.3. Results

Histologic screening of PEI green crabs did not reveal any significant disease processes. *Hematodinium* sp. infections were not observed. Histologic evaluation of the gills revealed occasional peritrich stalked ciliates on the gills of 12/25 (48%) of the green crabs (Figure A8.1). The peritrich stalked ciliates were accompanied by minimal to mild gill bacterial fouling. Evaluation of the carapace revealed a small amount of algal growth in 10/25 (40%) of the green crabs and heavy algal growth in 2 green crabs (8%; Figure A8.2A). The carapace of green crabs with heavier algal growth was discolored brown (Figure A8.2B). No other epibionts, parasites, or disease processes were observed.

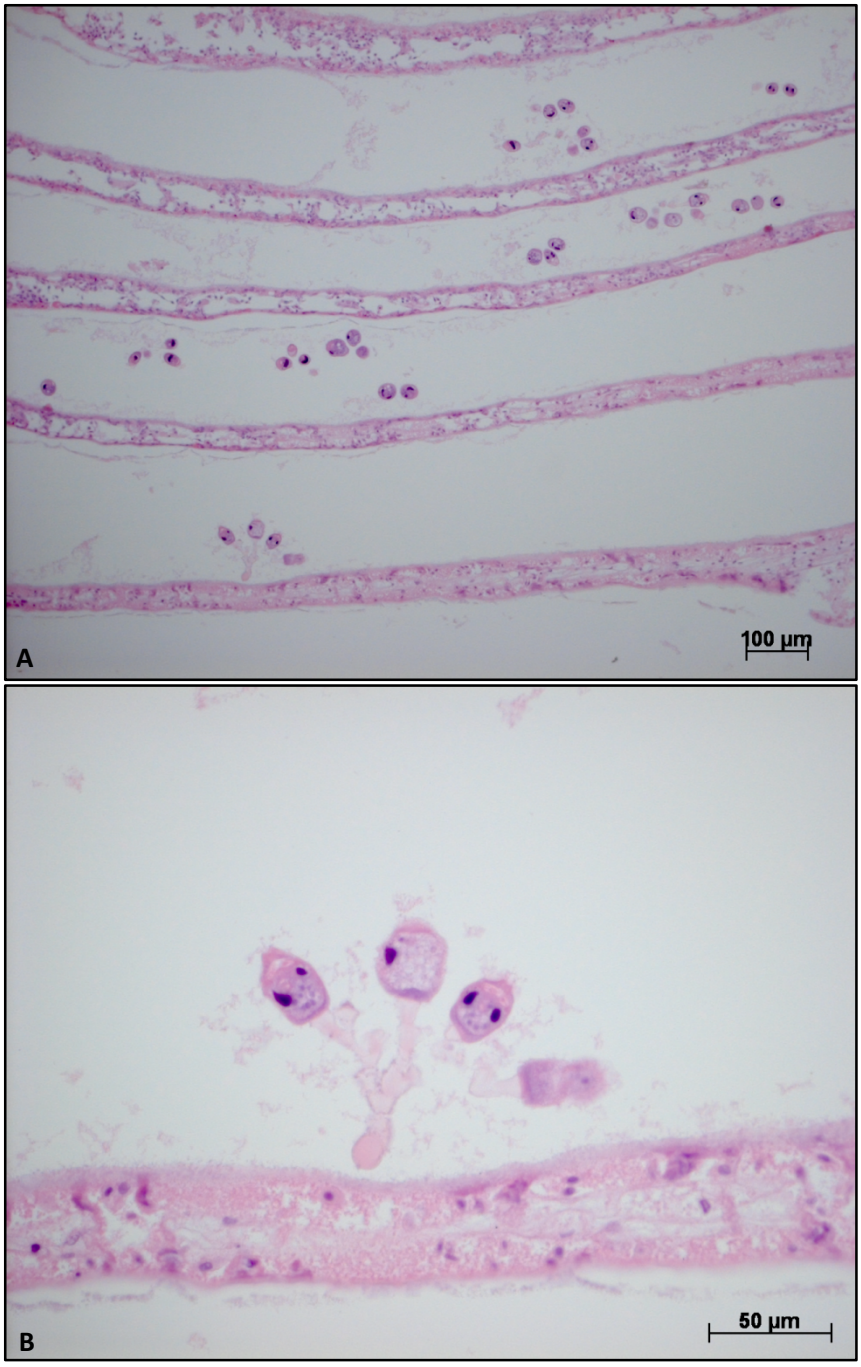

Figure A8.1: The green crab's gills had minimal to mild bacterial fouling and occasional peritrich stalked ciliates (H&E, 25x and 400x).

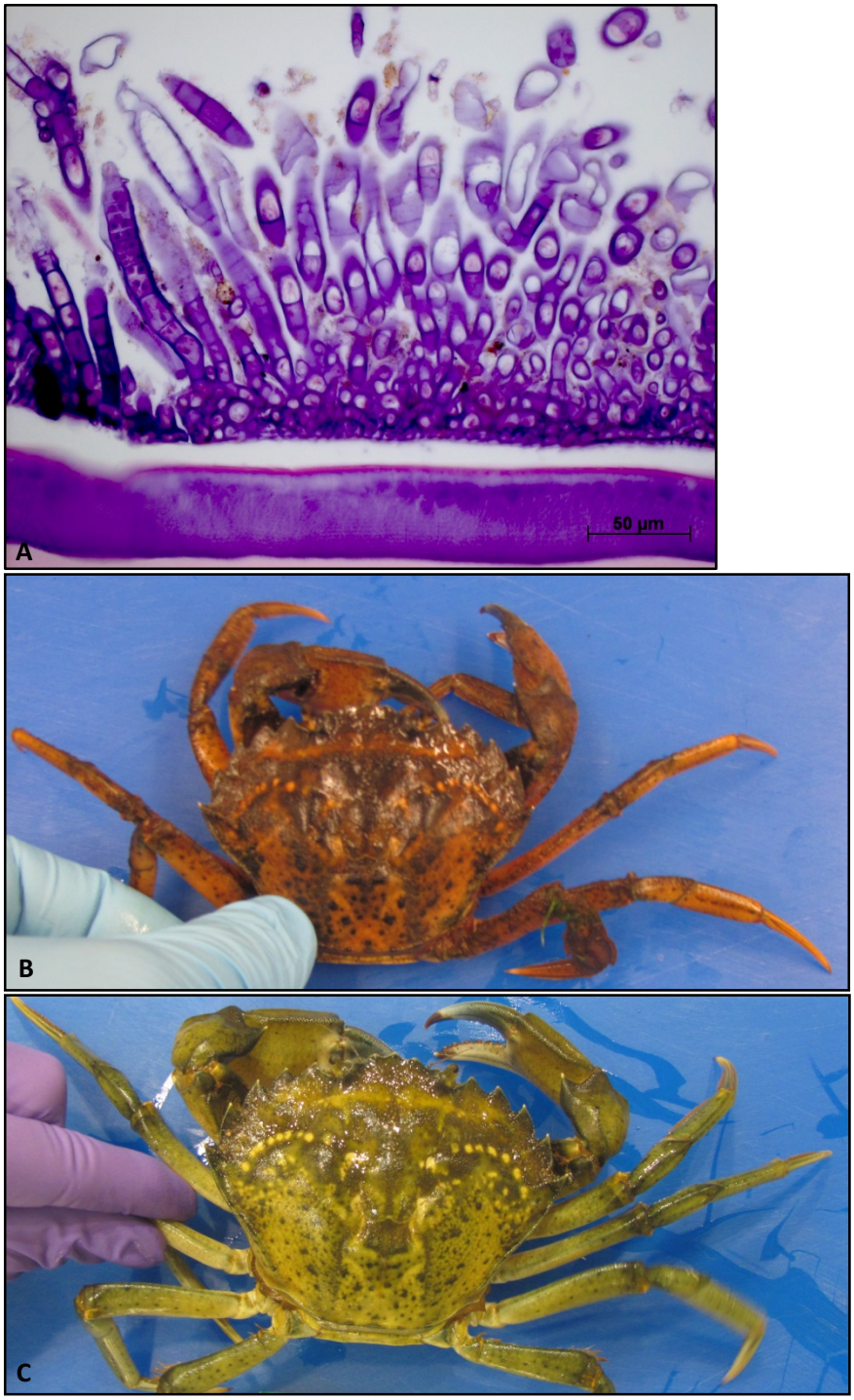

Figure A8.2. Carapace epifaunal algal growth. Heavy growth of the algae (A) on the green crabs' carapace histologically was associated with brown carapace discoloration of the crab's carapace macroscopically (B). A green crab's typical gross appearance without heavy algal growth (C) is shown for comparison.

A.8.4. Discussion

Histologic evaluation of PEI green crabs (2=25) did not reveal evidence of *Hematodinium* infection. The sample size examined was very small and prevalence of BCD in affected populations is often low. Thus, the absence of detection of disease in this group of green crabs does not imply that PEI green crabs are not infected by this disease. It is interesting to note that no significant infectious disease processes were observed in this small group of crabs. Brattey et al (1985) noted that green crabs from Atlantic Canada lacked most of the parasites and symbionts found associated with green crabs in Europe. Similarly, Torchin et al (2001) found that parasite load in green crabs was significantly higher in their native habitat (96%) than in invaded habitats (8%). This reduced parasite load in non-native habitats may partly explain why the green crab is such a successful invasive species (Torchin 2001).

Parasitic infections with *Microphallus* (Platyhelminthes, Digenea) and *Polymorphus* (Acanthocephala, Palaeacanthocephala) have been reported in green crabs in Atlantic Canada (Brattey et al 1985). Crabs are the intermediate hosts for these parasites while their definitive hosts are native marine and coastal bird species (Brattey et al 1985, Ching 1989, Galaktionov et al 2012). *Microphallus* adult worms are normally found in the gut as parasites of gulls and terns while the larval forms (sporocysts and cercariae) develop in a mud snail *Hydrobia ulvae* (Saville and Irwin 2005). *Hydrobia ulvae* is a littoral macrofaunal invertebrate, but the green crabs in this study were collected from an estuarine environment. Thus, lack of exposure to *Microphallus* cercariae due to local environment (rather than larger region of origin) may explain the lack of *Microphallus* metacercariae in this study. In one study prevalence of

Microphallus metacercariae in two other Atlantic Canadian sites was reported to be 40% (Halifax, NS) and 93.5% (St. Andrews, NB; Brattey et al 1985). In contrast, the crab is the only intermediate host for *Polymorphus (Profilicollis)* with diving and eider ducks the definitive hosts (Ching 1989). The prevalence of *Polymorphus* sp. was much lower at these same sites, 0% (Halifax, NS) and 9.7% (St. Andrews, NB) and thus would have been easily missed by the small sample size in this study (Brattey et al 1985).

Most marine dispersal stages (planktonic larvae) of sessile invertebrates are generalists in regards to substrate type (Wahl and Mark 1999). In the aquatic realm many species have adopted this mode of life for at least part of their life cycle, including may bacteria, many protozoa, many diatoms, most macroalgae, all sponges, most cnidarians, many molluscs, some rotifers, most bryozoans, most phoronids, many brachiopods, many tube-building polychaetes, some echinoderms, a few crustaceans, some hemichordates, and all ascidians (Wahl and Mark 1999). The lack of surface epibionts in the green crabs may be due to low species diversity in the local environment. It could also be impacted by periodic emergence and burrowing behavior which shields crabs from planktonic settlers, damages or removes soft-bodied settlers, or exposes settlers to more or different predators (infauna; Wahl et al 1998). The only epibiont noted in histologic sections examined was microalgal growth. Interestingly, even when there was carapace algal growth the algae never extended over the cornea of the eye. This is unlike the case in snow crabs where bryozoan epibionts did occasionally extend over the cornea (data

not shown). The microtopography of the eye of *Carcinus maenas* could have antifouling and/or fouling-release potential (Greco et al 2013).

A.8.5. References:

Brattey J, Elner RW, Uhazy LS, Bagnall AE. 1985. Metazoan parasites and commensals of five crab (Brachyura) species from eastern Canada. Can J Zool 63:2224-2229.

Chatton É, Poisson R. 1931. Sur l'existence dans le sang des crabes, de péridiniens parasites: *Hematodinium perezi* n.g., n.sp. (Syndinidae). CR Soc Biol Fil 105:553–557.

Ching HL. 1989. *Profilicollis botulus* (van Cleave 1916) from diving ducks and shore crabs of British Columbia. J Parasitol 75(1):33-37.

Galaktionov KV, Blasco-Costa I, Olson PD. 2012. Life cycles, molecular phylogeny and historical biogeography of the 'pygmaeus' microphallids (Digenea: Microphallidae): widespread parasite of marine and coastal birds in the Holarctic. Parasitol 139:1346-1360.

Greco G, Svaldo Lanero T, Torrassa S, Young R, Vassalli M, Cavaliere A, Rolandi R, Pelucchi E, Faimali M, Davenport J. 2013. Microtopography of the eye surface of the crab *Carcinus maenas*: an atomic force microscope study suggesting a possible antifouling potential. J R Soc Interface 10(84):20130122.

Morado FJ. 2011. Protistan diseases of commercially important crabs: A review. J Invert Pathol 106: 27-53.

Saville DH, Irwin SW. 2005. A study of the mechanisms by which the cercariae of *Microphallus primas* (Jag, 1909) Stunkard, 1957 penetrate the shore crab, *Carcinus maenas* (L). Parasitol 131(4):521-529.

Torchin ME, Lafferty KD, Kuris AM. 2001. Release from parasites as natural enemies: increased performance of a globally introduced marine crab. Biol Invas 3:333-345.

Wahl M, Kroger K, Lenz M. 1998. Non-toxic protection against epibiosis. Biofouling 12(1-3):205-226.

Wahl M, Mark O. 1999. The predominantly facultative nature of epibiosis: experimental and observational evidence. Mar Ecol Prog Ser 187: 59-66.